Investigation of Structure-Reactivity Relationships of Arylpalladium Complexes in Transmetalations with Arylzinc Reagents

and

Palladium-Catalyzed Directed Halogenations of Bipyridine *N*-Oxides

and

Mechanistic Investigations of the Direct Arylation of Pyridine *N*-Oxides with Bromoarenes

Inaugural-Dissertation

to obtain the academic degree

Doctor rerum naturalium (Dr. rer. nat.)

submitted to the Department of Biology, Chemistry and Pharmacy

of Freie Universität Berlin

by

SINA PATRICIA ZUCKER

2016

The current work was conducted under supervision of Prof. Dr. C. Christoph Tzschucke in the time from October 2012 to October 2016 at the Institut für Chemie und Biochemie of the Freie Universität Berlin.

1st Reviewer: Prof. Dr. C. Christoph Tzschucke

2nd Reviewer: Prof. Dr. Christoph Schalley

date of defence: 9th of January 2017

Acknowledgements

Abstract

Investigation of Structure-Reactivity Relationships of Arylpalladium Complexes in Transmetalations with Arylzinc Reagents
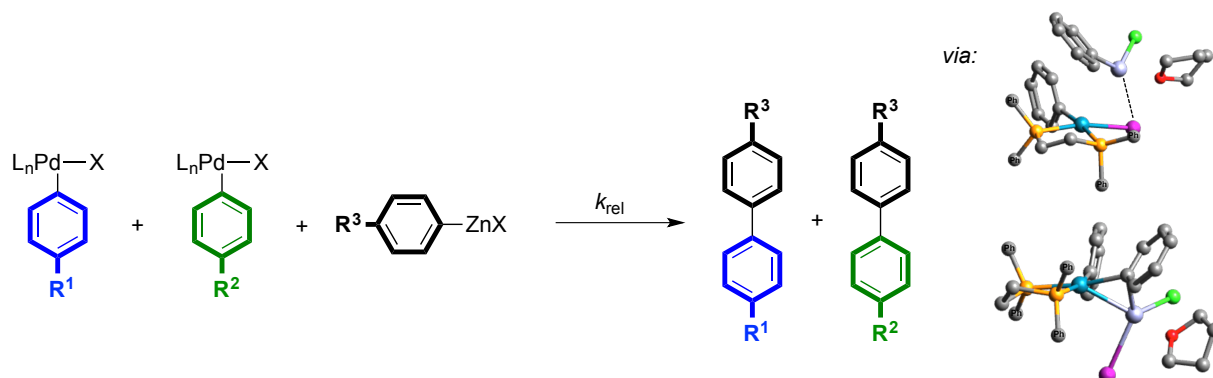
Competition experiments with isolated, differently substituted arylpalladium complexes and arylzinc reagents have been performed to investigate the electronic influences of the arylpalladium intermediate on the transmetallation in Negishi cross-coupling reactions, which is the least understood step, compared to other transmetalations in related cross-coupling reactions (e.g. Suzuki, Stille, Sonogashira etc.). In transmetalation experiments with competing complexes *cis*-[(dppe)Pd(Ar)I] and different arylzinc halides the reactions were faster the more electron-donating the substituent, which resulted in negative Hammett reaction constants ρ_{obs}. The Hammett constant becomes more negative with more Lewis acidic arylzinc reagents (except with diphenylzinc), but becomes less negative (approaching zero) with an excess of $ZnCl_2$, while addition of LiCl did not affected the Hammett constant. Interestingly, if tmeda was added, the Hammett constant was less negative, however addition of dppe ligand resulted in a slightly more negative value. Using other bisphosphine-ligated arylpalladium complexes (PPh$_3$, dppf, dppe), the Hammett constant becomes less negative with increasing steric demand of the phosphine ligand (cone and bite angle), as well as for the corresponding bromide complexes. In contrast, using T-shaped and coordinatively unsaturated complexes [(P^{t}Bu)$_3$Pd(Ar)Br], a positive Hammett parameter was obtained. Competition experiments with competing ester-substituted arylpalladium bromide complexes, coordinated by different phosphine ligands, imply the following reactivity trend regarding the nature of the phosphine: P^{t}Bu$_3$ > XPhos > PPh$_3$ > dppe > P(*o*-tol)$_3$ > dppf. The observed reactivity trends indicate an associative ligand substitution, which proceeds via an intermediate adduct of the complex and the arylzinc reagents. DFT calculations suggest a three-membered cyclic intermediate, which is formed after passing intermediate structures with weak interactions between zinc and the halide ligand of the palladium complex. These calculated interactions are stronger for arylpalladium complexes with electron-donating substituents, which is in agreement with the experimentally observed reactivity trends.

Palladium-Catalyzed Directed Halogenations of Bipyridine *N*-Oxides

Although many procedures have been reported for transition metal-catalyzed directed *ortho*-halogenations of benzenes using different nitrogen- and oxygen-containing directing groups, examples for halogenations of heteroarenes are rare. In particular 2,2′-bipyridines are challenging substrates, because a stabile, unreactive *N,N′*-chelate complex would be formed with the transition metal. To circumvent the undesired catalyst binding, we masked one pyridyl nitrogen as an *N*-oxide, while the second pyridyl nitrogen directs the catalyst for C-H bond cleavage at the C3 position. Using *N*-halosuccinimides (NXS) as halogen source, C3-brominated and chlorinated bipyridine *N*-oxides were obtained in high yields and regioselectivity. The regioselectivity changed when using C6′-substituted bipyridine *N*-oxides to give C3′-halogenated products. Here, the coordination of the catalyst to the pyridyl ring is sterically unfavored, allowing the weaker *N*-oxide coordination to direct the functionalization. Mechanistic investigations with isolated dinuclear cyclometalated palladium(II) intermediates support a Pd(II)/Pd(III) catalytic cycle previously proposed for related halogenations. The halogenated products can be easily deoxygenated by using PX_3 or used as versatile synthetic intermediates. For instance, using 6-methyl-3-bromobipyridine *N*-oxide, the Caerulomycins **G** (15% over 6 steps form 2-picoline *N*–oxide) and Caerulomycinonitrile **C** (5.4% over 8 steps) could be synthesized for the first time, besides Caerulomycin **C** (7.8% over 8 steps). The main advantage of the syntheses is that it avoids lithiation/halogenation sequences, which are typically involved in reported syntheses of Caerulomycin **C**.

Mechanistic Investigations of the Direct Arylation of Pyridine *N*-Oxides

with Bromoarenes

The palladium-catalyzed direct arylation of pyridine *N*-oxides with 2-bromopyridine provides bipyridine *N*-oxides typically in lower yields compared to the corresponding reactions using bromobenzenes as electrophiles. Because this observation cannot be explained by the findings of previous mechanistic investigations, which concern the reactions with bromobenzenes, we performed additional mechanistic experiments. The results revealed that the catalyst (resting state) decomposes faster in arylations with bromopyridine, which is due to disproportionation of the pyridylpalladium(II) intermediate resulting in 2,2′-bipyridine. The pyridylpalladium(II) complex was identified as a phosphine-free pyridyl-bridged dimer ligated by an additional 2-bromopyridine. The poor thermal stability of this intermediate is the reason for the low yields in the arylation reactions, because (1.) this process irreversibly consumes the limiting substrate, and (2.) thereby formed 2,2′-bipyridine inhibits the active catalyst for C-H bond activation by blocking the required vacant coordination site. Initial attempts to find reaction conditions, which suppress the undesired side reaction, showed that lowering the reaction temperature from 120 °C to 80 °C leads to improved yields, however, requires longer reaction times.

VIII

Zusammenfassung

Untersuchung von Struktur-Reaktivitäts-Beziehungen von Arylpalladiumkomplexen in Transmetallierungen mit Arylzinkreagenzien
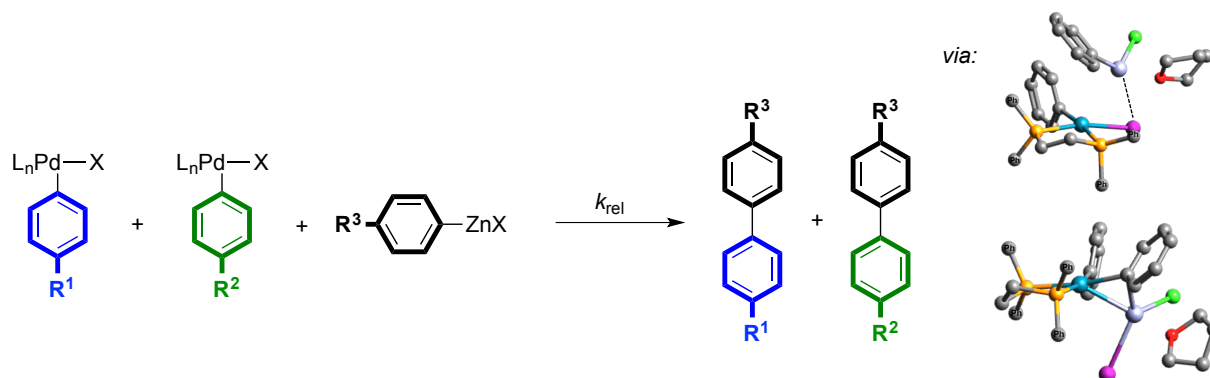
Konkurrenzexperimente mit isolierten, unterschiedlich substituierten Arylpalladiumkomplexen und Arylzinkreagenzien wurden durchgeführt, um die elektronischen Einflüsse des Arylpalladiumintermediats in der Transmetallierung der Negishi-Kreuzkupplungsreaktion, welche im Vergleich zu Transmetallierungen ähnlicher Kreuzkupplungsreaktionen (z. B. Suzuki, Stille, Sonogashira usw.) der am wenigsten verstandene Schritt ist, zu untersuchen. In Transmetallierungsexperimenten mit konkurrierenden Komplexen *cis*-[(dppe)Pd(Ar)I] und unterschiedlichen Arylzinkhalogeniden waren die Reaktionen mit elektronenschiebenden Substituenten schneller, was sich durch eine negative Hammettreaktionskonstante ausdrückte. Die Hammettkonstante wurde negativer mit Lewis-saureren Arylzinkreagenzien (mit Ausnahme von Diphenylzinc), aber wurde weniger negativ (gegen null strebend) mit einem Überschuss von $ZnCl_2$, während die Zugabe von LiCl die Hammettkonstante nicht beeinflusste. Interessanterweise war die Hammettkonstante weniger negativ wenn tmeda hinzugefügt wurde, jedoch führte die Zugabe von dppe zu einem etwas negativeren Wert. Mit anderen bisphosphinkoordinierten Arylpalladiumkomplexen (PPh_3, dppf, dppe) wurde die Hammettkonstante weniger negativ mit zunehmenden sterischen Anspruch des Phosphinliganden (Kegel- und Bisswinkel), sowie auch für die entsprechenden Bromidkomplexe. Im Gegensatz dazu, mit T-förmigen und koordinativ ungesättigten Komplexen [(P^{t}Bu)$_3$Pd(Ar)Br] wurde eine positive Hammettkonstante erhalten. Konkurrenzexperimente mit konkurrierenden, estersubstituierten Arylpalladiumkomplexen mit unterschiedlichen Phosphinliganden zeigten den folgenden Reaktivitätstrend betreffend der Natur des Phosphinliganden: P^{t}Bu$_3$ > XPhos > PPh_3 > dppe > P(*o*-tol)$_3$ > dppf. Die beobachteten Reaktivitätstrends deuten auf einen assoziativen Ligandenaustausch, welcher über ein intermediäres Addukt des Komplexes und des Arylzinkreagenzes verläuft. DFT-Berechnungen ergaben ein dreigliedrig zyklisches Intermediat, welches beim Durchlaufen intermediärer Strukturen mit schwachen Wechselwirkungen zwischen Zink und dem Halogenidliganden des Palladiumkomplexes gebildet wird. Diese berechneten Wechselwirkungen sind stärker für Arylpalladiumkomplexe mit

elektronenschiebenden Substituenten, was in Übereinstimmung mit den experimentell beobachteten Reaktivitättrends ist.

Palladiumkatylisierte dirigierte Halogenierungen von Bipyridin-*N*-Oxiden

Obwoh viele Vorschriften für übergangsmetallkatalysierte dirigierte *ortho*-Halogenierungen von Benzolen mit unterschiedlichen stickstoff- und sauerstoffhaltigen dirigierenden Gruppen berichtet worden sind, sind Beispiele für Halogenierungen von Heteroaromaten selten. Insbesondere sind 2,2′-Bipyridine anspruchsvolle Substarte, weil ein stabiler, unreaktiver *N,N′*-Chelatkomplex mit dem Übergangsmetall gebildet würde. Um die ungewünschte Katalysatorbindung zu umgehen, haben wir einen Pyridylring als *N*-Oxid maskiert, während der zweite Pyridylring den Katalysator für die C-H-Bindungsspaltung in die C3-Position dirigiert. Mit *N*-Halosuccinimiden (NXS) als Halogenquelle wurden C3-bromierte und -chlorierte Bipyridin-*N*-oxide in hohen Ausbeuten und Regioselektivitäten erhalten. Die Regioselektivität änderte sich mit C6′-substituierten Bipyridin-*N*-oxiden und gab C3′-halogenierte Produkte. Hier ist die Koordination des Katalysators am Pyridylring sterisch ungünstig, was die Bindung am schwächer koordinierenden *N*-Oxid ermöglicht, um die Funktionalisierung zu dirigieren. Mechanistische Untersuchungen mit isolierten zweikernigen cyclometallierten Palladium(II)-intermediaten unterstützen einen Pd(II)/Pd(III)-Katalysezyklus, welcher zuvor für verwandte Halogenierungen vorgeschlagen wurde. Die halogenierten Produkte können einfach deoxygeniert werden mit PX$_3$ oder als vielfältig synthetisches Intermediat verwendet werden. Zum Beispiel konnten mit 6-Methyl-3-brombipyridin-*N*-oxid das Caerulomycin **G** (15% über 6 Stufen vom 2-Picolin-*N*-oxid) und Caerulomycinonitril **C** (5.4% über 8 Stufen) zum ersten Mal synthetisiert werden, sowie auch Caerulomycin **C** (7.8% über 8 Stufen). Die hauptsächliche Herausforderung der Synthesen war die Vermeidung von Lithiierung/Halogenierungssequenzen, welche typisch für die existierenden Synthesen für Caerulomycin **C** sind.

Mechanistische Untersuchungen der Direkten Arylierung von Pyridin-*N*-Oxiden mit Bromaromaten

Die palladiumkatalysierte direkten Arylierung von Pyridin-*N*-oxiden mit 2-Brompyridin ergeben Biypridin-*N*-oxide typischerweise in niedrigeren Ausbeuten im Vergleich zu den entsprechenden Reaktionen mit Brombenzolen als Elektrophile. Weil diese Beobachtung nicht mit den Befunden früherer mechanistischer Untersuchungen erklärt werden kann, führten wir zusätzliche mechanistische Experimente durch. Die Ergebnisse deckten auf, dass der Katalysator (-ruhezustand) schneller zerfällt in Arylierungen mit Brompyridin aufgrund der Disproportionierung des Pyridylpalladium(II)-intermediates, was in 2,2′-Bipyridin resultiert. Der Pyridylpalladium(II)complex wurde als phosphinfreies pyridylverbrückendes Dimer, was mit einem zusätzlichen 2-Brompyridin koordiniert ist, identifiziert. Die niedrigere thermische Stabilität dieses Intermediates ist der Grund für die

niedrigen Ausbeuten der Arylierungsreaktionen, weil (1.) dieser Prozess irreversibel das limitierende Substrat verbraucht, und (2.) das dabei gebildete 2,2′-Bipyridin den aktiven Katalysator bei der C-H-Bindungsaktivierung durch Blockierung der erforderlichen freien Koordinationsstelle inhibiert. Erste Versuche Reaktionsbedingungen zu finden, welche die unerwünschte Nebenreaktion unterdrücken, zeigten, dass eine Verringerung der Reaktionstemperatur von 120 °C auf 80 °C zu verbesserten Ausbeuten führt, jedoch längere Reaktionszeiten erfordert.

Table of Contents

(contains NMR spectra of new compounds, Cartesian coordinates of calculated structures, and atomic coordinates of crystal structures)

Abbreviations

Ac	acetyl
approx.	approximately
aq.	aqueous
Ar	aryl
BBP	*n*-butyl benzyl phthalate
bhq	benzo[*h*]quinoline
Bu	butyl
c.m.	complex mixture
Cal. std.	calibration standard
calc.	calculated
cat.	catalytic
CMD	concerted metalation-deprotonation
conc.	concentrated
COSY	correlated spectroscopy
dba	(1*E*, 4*E*)-1,5-diphenylpenta-1,4-dien-3-one
DCM	dichloromethane
decomp.	decomposition
DFT	density functinal theory
DG	directing group
DMA	*N,N*-dimethylacetamide
DMF	*N,N*-dimethylformamide
DMI	1,3-dimethyl-2-imidazolidinone
DMSO	dimethyl sulfoxide
dppe	1,2-bis(diphenylphosphino)ethane
dppf	1,1′-bis(diphenylphosphino)ferrocene
E	electrophile
EDG	electron-donating group
eq.	equation
equiv.	equivalents
ESI	electrospray ionization
Et	ethyl
EWG	electron-withdrawing group
Exp. No.	experimental number
FID	flame ionization detector
FT	fourier transformation

GC	gas chromatography
HMBC	heteronuclear multiple bond correlation
HMQC	heteronuclear multiple quantum coherence
AcOH	acetic acid
HRESI	high resolution electrospray ionization
HSAB	hard and soft acids and bases
i-	*iso-*
IR	infrared spectroscopy
L	ligand
LDA	lithium diisopropylamide
LiHMDS	Lithium bis(trimethylsilyl)amide
lit.	literature
m-	*meta-*
Me	methyl
m.p.	melting point
*m*CPBA	*meta*-Chloroperoxybenzoic acid
MEK	methyl ethyl ketone
n.i.	not investigated
MS	mass spectrometry
NBS	*N*-bromosuccinimide
NCS	*N*-chlorosuccinimide
NHC	*N*-heterocyclic carbene
NMP	N-methyl-2-pyrrolidon
NMR	nuclear magnetic resonance
Nu	nucleophile
NXS	*N*-halosuccinimide
o-	*ortho-*
o.n.	over night
o-tol	*ortho*-tolyl
p-	*para-*
PCM	polarizable continuum model
Ph	phenyl
Piv	pivalyl
ppm	parts per million
quant.	quantitative
r.t.	room temperature
R^2	correlation coefficient
recov.	recovered

XVIII

red.	reducing reagent
R_f	retention factor
S_E2	bimolecular electrophilic substitution
S_EAr	electrophilic aromatic substitution
S_N1	unimolecular nucleophilic substitution
S_N2	bimolecular nucleophilic substitution
Std. dev. (σ)	standard deviation
t	time
t-	*tert*-
TBAB	tetrabutylammonium bromide
TBATB	tetrabutylammonium tribromide
TBHP	*tert*-butyl hydroperoxide
^tBu	*tert*-butyl
TCB	1,3,5-trichlorobenzene
temp.	temperature
TEMPO	2,2,6,6-tetramethylpiperidin-1-yl)oxidanyl
TFA	trifluoroacetic acid
THF	tetrahydrofurane
TLC	thin layer chromatography
TMB	1,3,5-trimethoxybenzene
tmeda	*N*,*N*,*N'*,*N'*-tetramethylethane-1,2-diamine
TMP	2,2,6,6-tetramethylpiperidine
TMS	trimethylsilyl
TOF	time of flight
Tos	*para*-tolylsulfonyl
Tf	trifluoromethylsulfonyl
vac.	vacuum
w/	with
w/o	without
XPhos	2-dicyclohexylphosphino-2',4',6'-triisopropylbiphenyl

1 Investigation of Structure-Reactivity Relationships of Arylpalladium Complexes in Transmetalations with Arylzinc Reagents

1.1 Motivation

The transmetalation is one of the elementary steps in the transition metal-catalyzed cross-coupling reaction of an organic (pseudo)halide with an organometallic reagent, but also a key step in the developing field of bimetallic catalysis for direct couplings via C-H bond activation.[1] The currently accepted mechanism of a palladium-catalyzed cross-coupling reaction consists basically of three elementary steps: (i) oxidative addition of an organic halide or pseudohalide to a palladium(0) species to form an organopalladium(II) intermediate **I-1**, (ii) transmetalation with an organometallic reagent providing a highly reactive diarylpalladium(II) species **I-2**, and (iii) C-C bond-forming reductive elimination, which liberates the product and regenerates the palladium(0) species (scheme 1). While the first and the last step are well understood, the mechanism of the transmetalation remained unclear.
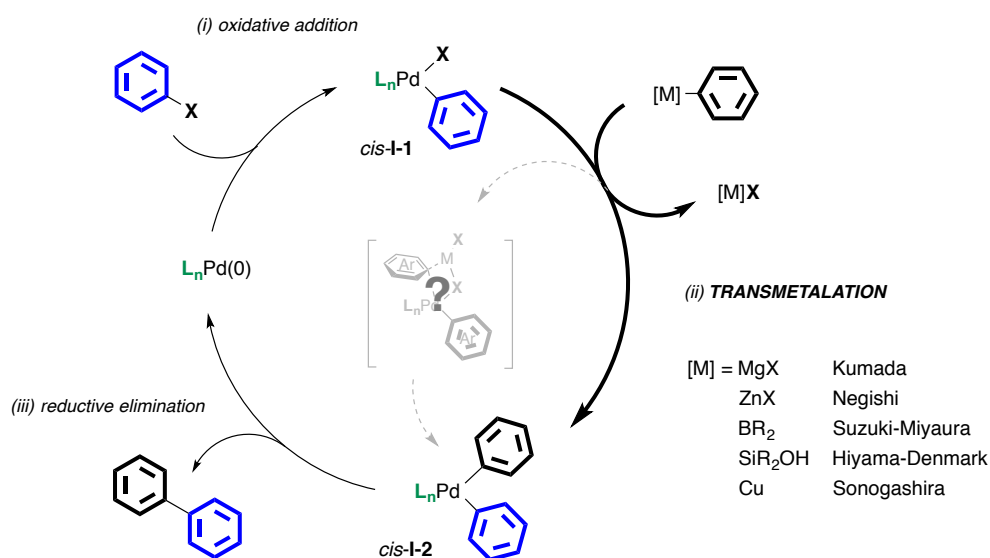
Scheme 1. Simplified mechanism for palladium-catalyzed cross-coupling reactions exemplified for aryl-aryl couplings.

The transmetalation in palladium-catalyzed cross-coupling reactions with less reactive organic nucleophiles, such as organoboron reagents (Suzuki-Miyaura),[2] stannanes (Stille),[3] silanes (Hiyama-Denmark)[4] and *in situ* generated copper(I) acetylides (Sonogashira)[5] has been extensively studied by kinetic measurements of the catalytic and stoichiometric reactions, however, the transmetalation is less studied in reactions with more reactive organozinc (Negishi)[6] or even Grignard reagents (Kumada).

Moreover, the available studies address mainly the reactivity trends of the organometallic reagent, but not include the reactivity manifested on its coupling partner, which is the intermediate **I-1**. The general trend, which was observed for the nucleophile, is that electron-donating substituents enhance the reactivity and therefore accelerate the overall catalytic reaction.[5, 7] Only two studies were reported that comprise also the reactivity trends of the electrophile. Lei and co-workers found that the transmetalation in the Sonogashira coupling is accelerated with more electrophilic aryl iodides, which is the opposite reactivity trend with respect to the nucleophile.[5] Denmark and co-workers performed kinetic measurements on the transmetalation step in stoichiometric reactions of the arylpalladium(II) intermediate **I-1** with silanolates.[7e] They also observed that the transmetalation is faster for more electrophilic palladium(II) centers, which is induced by more electron-withdrawing substituents on the aryl ligand.

The previously observed reactivity trends in the transmetalations basically confirm the expected behavior that increasing electrophilicity of the palladium(II) intermediate **I-1** and increasing nucleophilicity of the organometallic reagent accelerate the reaction. The same electronic trends are expected for the transmetalation in Negishi cross-coupling reactions, if it proceeds via an analogues mechanism. To probe whether there exists mechanistic similarities, we investigate the reactivity of differently substituted arylpalladium(II) intermediates **I-1** in the transmetalation with arylzinc reagents (scheme 2) in competition experiments to obtain relative reaction rates k_{rel}, which can be directly determined by the ratio of the coupled products since the reductive elimination is fast (irreversible) and not product-determining. Rational changing of the reaction parameters, such as addition of additives, variation of the ligands of **I-1**, or the electronic properties of the arylzinc reagent, will result in changes of the Hammett parameters allowing to draw more detailed mechanistic conclusions.
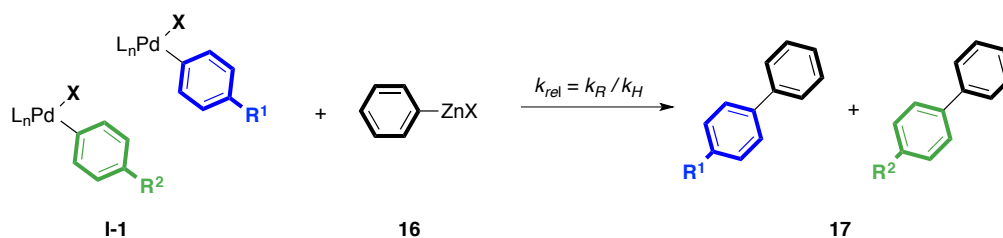
Scheme 2. Principle reaction equation for competition experiments in stoichiometric transmetalation.

1.2 Background

1.2.1 Hammett correlations

The Hammett analysis is a useful tool to evaluate the electronic influences induced by the substituents of an aromatic substrate on the reaction rate for a given set of similar reactions under the same conditions. Hammett observed that the dissociation constants ($pK_a = -\log K_a$) of substituted benzoic acids correlate with the electronic nature of the substituents at the aromatic ring.[8] Moreover, he found that similar relationships exist with reaction rates of many other reaction types involving differently substituted aromatic substrates. This relationship was expressed in a mathematical equation (eq. 1), which is today known as the Hammett equation, where k^R/k^H is the relative reaction rate k_{rel} of the substituted substrate to the unsubstituted substrate, and σ is the substituent dependent parameter, which is derived from the relative dissociation constants of benzoic acids.

(eq. 1)
$$log \left(\frac{k^R}{k^H} \right) = log(k_{rel}) = \rho \cdot \sigma$$

A large set of Hammett substituent parameters σ is now available for many different substituents.[9] The sign and magnitude of the Hammett parameters σ correspond to the electronic influences of the substituents towards the aromatic system. Because, the origin of electronic influences by an individual substituent can be induced by inductive and/or resonance effects, the position relative to the reaction center has an impact on the extant of stabilizing or destabilizing effects. For instance, a carbonyl group releases electron-density from the π-system of the arene by negative mesomeric effect (–M), which builds up a positive charge in the *para* or *ortho* position relative to the carbonyl group by conjugation through the aromatic π-system system. Therefore, the carbonyl group can better stabilize electron-rich reaction centers if it is in *para* or *ortho* position relative to the reaction center. In contrast, stabilizing effects on the transition state by substituents with dominating inductive effects, such as halides or alkyl groups, are more pronounced if the reaction center is in the *meta* position relative to the substituents. To take these effects into account, different sets of Hammett parameters σ have been derived for *meta* (σ_{meta}) and *para* (σ_{para}) substituents. Related σ_{ortho} values play less a role if evaluating purely electronic influences on the reaction rate, because of the additional steric effects of an *ortho* substituent. The Hammett parameters σ values are referenced to the unsubstituted benzoic acid and can have a positive or negative sign. A positive sign expresses an electron-withdrawing influence on the aromatic ring, and a negative sign indicates electron-donating influence. The magnitude of σ implies how strong this electron-withdrawing or -donating effect is.

The proportionality factor, ρ, of the Hammett equation (eq. 1) is also known as the Hammett constant, which is individual for different reactions and displays the sensitivity of a reaction towards the electronic perturbation. Because the reaction constant k_{obs} of an elementary reaction is directly associated with the activation barrier of the transition state $\Delta G^{\ddagger}$ (eq. 2) (with κ transmittance coefficient, k_B Boltzmann constant, h Planck constant, T Temperature, R gas constant, 2.303 conversion factor from ln into log), the Hammett equation can also be expressed as the difference of the activation barriers ($\Delta\Delta G^{\ddagger}$) (eq. 3). Due to this relationship, the Hammett correlation is also referred as the Linear Free Energy Relationship (LFER).

(eq. 2)
$$log(k) = log\left(\kappa\frac{k_B T}{h}\right) + \frac{-\Delta G^{\ddagger}}{2.303RT}$$

(eq. 3)
$$log\left(\frac{k^R}{k^H}\right) = \rho \cdot \sigma = \frac{\Delta G^{\ddagger}(R) - \Delta G^{\ddagger}(H)}{2.303RT} = \frac{-\Delta\Delta G^{\ddagger}}{2.303RT}$$

This mathematical relationship connects the Hammett constant ρ directly with the transition state energy and makes the sign of the Hammett constant ρ diagnostic for a reaction mechanism. A positive ρ value indicates that electron-withdrawing substituents have a stabilizing effect on the transitions state, which is typically achieved by a release of electron density on the reaction center. Correspondingly, a negative ρ value indicates that electron-donating substituents have a stabilizing effect of an electron-poor reaction center in the transition state.

As shown in equation 3, the Hammett constant ρ for one set of reactions is inverse proportional to the temperature T, which means that the magnitude of ρ becomes smaller with increasing temperature. There are also several other dependencies of ρ known,[10] which are not directly revealed by equation 3 and have led to various modifications of the Hammett equation. For instance, the nature of the solvent can have an additional impact on the stabilization of a transition state. This is significant in particular for very polarized transition states, which are better stabilized by solvolysis in polar solvents. A large magnitude of the Hammett constant ρ is characteristic for a highly polarized reaction center in the transition state. This observation was formulated as the Grunwald-Winstein equation (eq. 4), which gives a linear correlation of the relative reaction rates in dependency of the "ionization power of the solvent" Y.[11] The "ionization power of the solvent" (Y) is associated with the solvent's polarity, electrophilicity, nucleophilicity, acidity as well as the polarizability. The proportionality factor m represents the sensitivity of the reaction on the properties of the solvent. A great magnitude of m indicates that highly polarized transition states are formed, such as in the nucleophilic substitution S_N1 reaction, where a fully positive charge is build up.

(eq. 4)
$$log\left(\frac{k^R}{k^H}\right) = m \cdot Y$$

Nevertheless, a small or even zero Hammett constant ρ is not necessarily indicative for a little or no electronic influences on the reaction, in particular if the relative reaction rates were determined by competition experiments, because reactions typically proceed via several steps, and often pre-equilibria are involved, which are also dependent on the electronic nature and are product-determining. For instance if the first step (pre-equilibrium) of a reaction is favored for electron-withdrawing substituents, giving a positive Hammett constant ρ, and the second step is favored by the opposite electronic effect, giving a negative Hammett constant ρ, the magnitude of the actually observed Hammett constant ρ_{obs} value might be small, because it consists of the individual Hammett constant ρ_n of both steps. If the relative reaction rates were determined by absolute reaction rates, only the Hammett constant ρ of the rate-determining step would be obtained. Additionally, if the rate-determining step changes with increasing electron-donating or -withdrawing effects of the substituents, the Hammett plot can be even non-linear and concave-shaped. Those non-linear, concave-shaped Hammett correlations (figure 1) have been reported and were often interpreted as a change in the mechanism.[12] A change of the rate-determining step has been often concluded from a concave downwards Hammett plot, whereas a concave upwards plot has been taken as a change in the mechanism. A continuous change of the slope can also be indicative for a change in the transition state structure (product- or reagent-like).
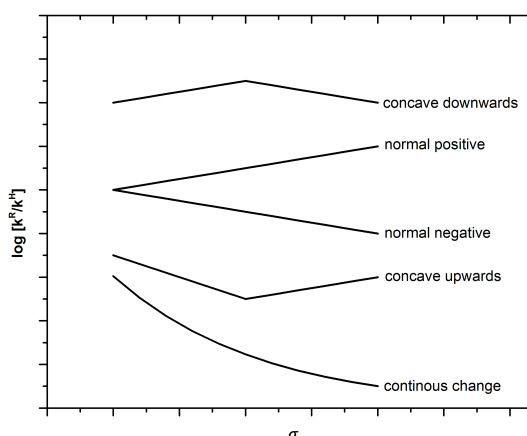
Figure 1. Types of "normal" linear and non-linear Hammett correlations.

The linearity of the Hammett correlation is described by the regression coefficient R^2 and is often taken as a measure how good the logarithm of relative reaction rates correlate with the Hammett substituent parameters σ. An R^2 value close to unity indicates a perfect linear correlation, whereas $R^2 <$ 0.90 suggests a poor correlation. However, the latter case does not necessarily imply a poor

relationship or that the experimental error is large. Initially Brown and co-workers observed that particularly substrates with *para* substituents deviate significantly from the linear regression in cases where the Hammett constant ρ has a large magnitude.[13] They reasoned that transition states, in which a full charge is developed, such as in the electrophilic aromatic substitution (S_EAr), resonance stabilization plays a dominant role. Therefore, substituents with a strong mesomeric effect would lead to a faster (or slower) reaction rate as would be predicted by the Hammett parameter σ. Consequently, they introduced a new set of substituent constants σ^+ and σ^-, which correlate better for reactions where a fully charged transition state is involved.

Data for a Hammett correlation analysis can be obtained by basically two methods. The ratios of the reaction rates k_{rel} can be derived from observed reaction rates k_{obs}, which have to be determined either by monitoring the concentration of the product (or reactant) over a certain time period, or by competition experiments, where two reactants in excess compete for the same substrate. One of the advantages of the competition approach is the smaller volume of data since the final product ratio is directly associated with k_{rel} and does not necessarily require collecting data for the reaction over the time. This approach is robust towards unwanted small changes of the reaction conditions, such as temperature or concentration, which can occur by measuring k_{obs}. Nevertheless, both approaches might provide different mechanistic information. While direct measurements of k_{obs} regards the rate-determining step of the mechanism, the competition experiments give information about all product-determining steps. For instance, the transmetalation of the palladium-catalyzed Stille cross-coupling is usually the slowest and therefore the rate-determining step. Investigation of the electronic influences under catalytic conditions with differently substituted aryl halides by measuring k_{obs} give information about the reactivities of the intermediate **I-1** in transmetalation, however, determination of k_{rel} by competition experiments provides information of the oxidative addition (if irreversible), because the oxidative addition occurs prior the transmetalation and is the first product-determining step, in which the competing aryl halides participate for the first time in the catalytic cycle.

In contrast to the Stille (or Suzuki and Sonogashira) coupling, the transmetalation in the Negishi reaction is typically faster than the preceeding oxidative addition, so that measurements of both, k_{obs} or k_{rel}, under catalytic conditions using differently substituted aryl halides, give information about exclusively the oxidative addition. To address the electronic influences of intermediates **I-1** in the transmetalation step of the Negishi coupling, the reaction between isolated intermediates **I-1** with differently substituted aryl ligands and the arylzinc reagent has to be investigated. However, the transmetalation is too fast to be monitored by standard analytics and would require special techniques (e.g. stopped-flow), therefore, competition experiments is the best choice for this task.

1.2.2   Fundamentals on ligand substitution mechanisms at d^8 metal centers

To discuss the mechanistic aspects of the transmetalations between an organometallic reagent and an arylpalladium(II) complex it is necessary to understand the fundamentals of a ligand substitution. Metal centers with a d^8-electron configuration, such as palladium(II) complexes, usually form $16e^-$ tetra-coordinated square-planar complexes, which can undergo ligand substitution by two different pathways, simply described as an associative (S_N2) or dissociative mechanism (S_N1).[14] The most common mechanism for d^8 metal complexes is the associative pathway and proceeds via rate-determining formation of a transient penta-coordinate square-pyramidal $18e^-$ complex with the nucleophile (Nu) (scheme 3). This complex undergoes a Berry-pseudo rotation, which passes a trigonal-bipyramidal transition state, resulting in a new penta-coordinate complex, where the releasing ligand (X) is now in the apical position. The rate law of this process is dependent on the concentrations of the incoming nucleophile [Nu] and the starting complex [M], but usually independent on the concentration of the releasing ligand [X].
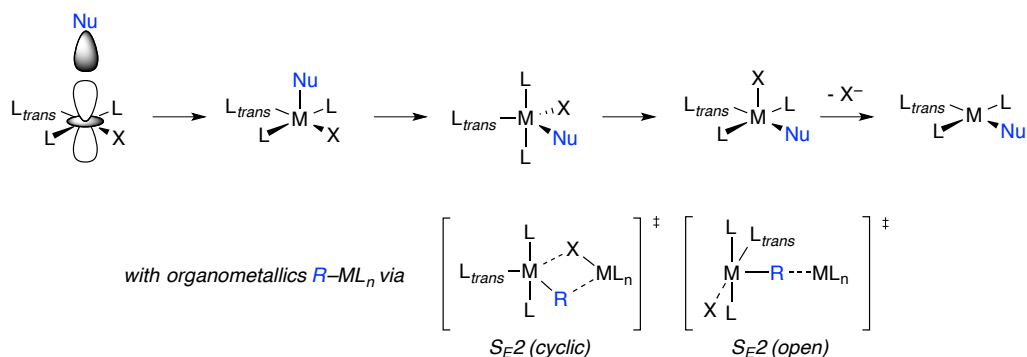
Scheme 3. Associative ligand substitution pathways. Above: nucleophilic substitution (S_N2) and bottom electrophilic substitution (S_E2) via open and cyclic transition states. L_{trans} = ligand with largest *trans* influence. Nu = incoming ligand. X = releasing ligand.

While the associative pathway holds for neutral or anionic nucleophiles, which are fully separated from their counter cation, nucleophiles, which exhibit more covalent bond character, such as organometallic reagents, can add to the electrophilic metal center in a more complex way. Those processes are usually described as a concerted bimolecular electrophilic substitution (S_E2) at carbon and can proceed via an open or cyclic transition state (scheme 3), whereas both follow a second order kinetic making it difficult to kinetically distinguish between them.[14a] However, the use of α-chiral organometallic reagents can be used as indicator, because the open transition state would result in inversion of the configuration, while the cyclic transition state would result in retention. The open transition state can be also considered as an *ipso* substitution at sp²-hybridized carbons via a bridging Wheland-type intermediate (or transition state) if the transferred organic group is an arene. The cyclic

7

transition state is commonly proposed if potentially bridging ligands (e.g. halides, hydroxides or carboxylates) are involved. In absence of bridging ligands (e.g. triflates, tosylates) and in polar solvents, which stabilize a cationic metal center, the ligand substitution proceeds more likely via the open transition state.

The dissociative ligand substitution pathway has been often regarded as less probable since an unfavored T-shaped 14e⁻-complex is formed as intermediate after rate-determining dissociation of ligand X (scheme 4). This dissociative process is often referred to as mononuclear nucleophilic substitution (S_N1), because it follows a first order kinetic, which is independent of the concentration of the incoming nucleophile [Nu]. The dissociative substitutions with d^8-metal complexes plays a role mainly in *cis*/*trans* isomerizations, in particular with complexes bearing strong *trans*-influencing or sterically very demanding ligands, which shield the axial position.[15] It is most likely that a solvent molecule subsequently fills the empty coordination site, in particular if an anionic ligand dissociates and leaves a cationic metal center.[14b] Nevertheless, substitution of a ligand by the solvent might also proceed via an associative mechanism, in which the solvent molecule is the incoming ligand. Because the solvent is in a large excess, the rate law is pseudo zeroth order in solvent molecule and only dependent on the concentration of the starting complex [M], which kinetically pretends a dissociative mechanism.
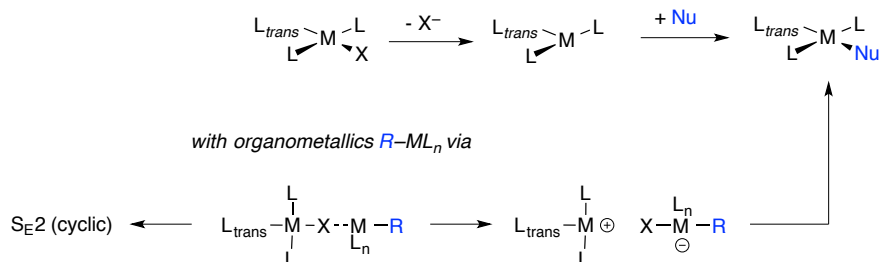
Scheme 4. Dissociative ligand substitution pathway (S_N1) and interchange mechanism (I) with organometallic nucleophiles.

Another variation of the dissociative pathway is possible and is mediated by abstraction of ligand X by the organometallic nucleophile, which can act also as a Lewis acids (LA) (scheme 4).[14a] This process forms initially an adduct of the complex and the Lewis acid with the ligand X as bridging ligand. This adduct might convert into a transient cationic 14e⁻ complex and in an "ate" complex, followed by transfer of the organic residue to the metal complex. However, the initial adduct of complex and organometallic reagent might also form directly a S_E2 cyclic transition state, as in the electrophilic associative ligand substitution mechanism. Because this special case of a dissociative pathway is a bimolecular process, it is impossible to kinetically distinguish from the other associative pathways S_E2.

1.2.3   Transmetalations in cross-coupling reactions

The transmetalation mechanisms have been exhaustively investigated with more stable and less air-sensitive organometallic reagents, such as stannanes[3] and boronic acids.[2] Because the transmetalation is often the rate-determining step in these reactions, kinetic studies under authentic catalytic conditions give directly information about the transmetalation step. To draw reasonable conclusion about the detailed transmetalation mechanism, the configuration of the ligands at starting complex **I-1**, arising from the oxidative addition, and of the product complex **I-2** of the transmetalation have to be considered.

For palladium-catalyzed cross-coupling reactions with non-polar substrates such as organic halides, oxidative addition typically occurs via an associative three-centered transition state forming an organopalladium(II) intermediate *cis*-**I-1** (scheme 1), which is necessarily *cis*-configured due to the concerted nature of the oxidative addition.[16] However, depending on the rate of the subsequent transmetalation the *cis*-complex *cis*-**I-1** can undergo rapid isomerization to the thermodynamically more stable *trans*-complex *trans*-**I-1** (transphobia effect)[17] if non-chelating monodentate (phosphine) ligands are coordinated to *cis*-**I-1**.[16, 18] The isomerization is believed to occur prior to slow transmetalations as in Stille, Suzuki or Sonogashira cross-coupling reactions.[3] Whereas in the Negishi or Kumada coupling reaction, the transmetalation is fast and probably proceeds directly with *cis*-**I-1**. As indicated above, the exchange of the halide ligand of intermediate *cis*- or *trans*-**I-1** by the transferred organic group proceeds under retention of configuration at the metal center. Consequently, the transmetalation with *trans*-**I-1** provides *trans*-**I-2**. Intermediate *trans*-**I-2** has to isomerize to *cis*-**I-2** to undergo reductive elimination, because the concerted nature of the reductive elimination requires that both organic ligands are in *cis*-configuration.[19]

1.2.3.1   *Stille coupling*

The transmetalation in Stille cross-coupling reaction has been extensively investigated with unsaturated organotin compounds and was proposed to proceed via the associative S_E2 mechanism (scheme 5), which passes either a cyclic or open transition state depending on the nature of the leaving group, solvent, ligands, and additives.[3, 20] The cyclic mechanism is more likely for reactions in less polar solvents and with organic halides, which are good bridging ligands. Retention of configuration of the stereocenter in the coupled product from reactions with α chiral alkyltin reagents has been considered as indicative for transmetalations via cyclic transition state.[21] Those reactions have been extensively studied using vinylstannanes, which first substitute one of the neutral ligands (L or S) by coordination of the vinyl π-system to the metal center to give [L(η^2-vinylSnAlk$_3$)Pd(R^1)X] (*trans*-**I-3**)

prior to the actual transmetalation event (scheme 5, pathway A).[22] The exchange of the neutral ligand by the vinylstannane is in accordance with the measured inverse first order dependence in added ligand[23] and with the rate-enhancing effect using labile ligands.[22a, 24] The rate-enhancing effect of copper(I) salts as additives could be traced back to the coordination of copper to excess phosphine ligands to reduce its concentration.[25] The intermediate *trans*-**I-3** converts directly into the T-shaped *cis*-[L(Pd(R^1)(R^2)] (R^2 = vinyl) (*cis*-**I-4**) via a halide- and R^2-bridged bimetallic Pd/Sn transition state (*cyclic*-**TS-1**). This transition state geometry is in agreement with the observed retention of configuration and directly leads to a *cis* configuration at the palladium(II) center necessary for reductive elimination of R^1-R^2. Espinet proposed a similar cyclic transition state, where the ligand dissociation event occurs simultaneously with the coordination of the stannanes via the transition state *cyclic*-**TS-2** (pathway B). The simultaneous ligand exchanges might give a better interpretation for Stille reactions applying saturated alkyltin reagents, because the saturated substrates lack a π-system for coordination. Nevertheless, the retarding effect of added ligand has not been experimentally confirmed in reactions with saturated alkyltin reagents.
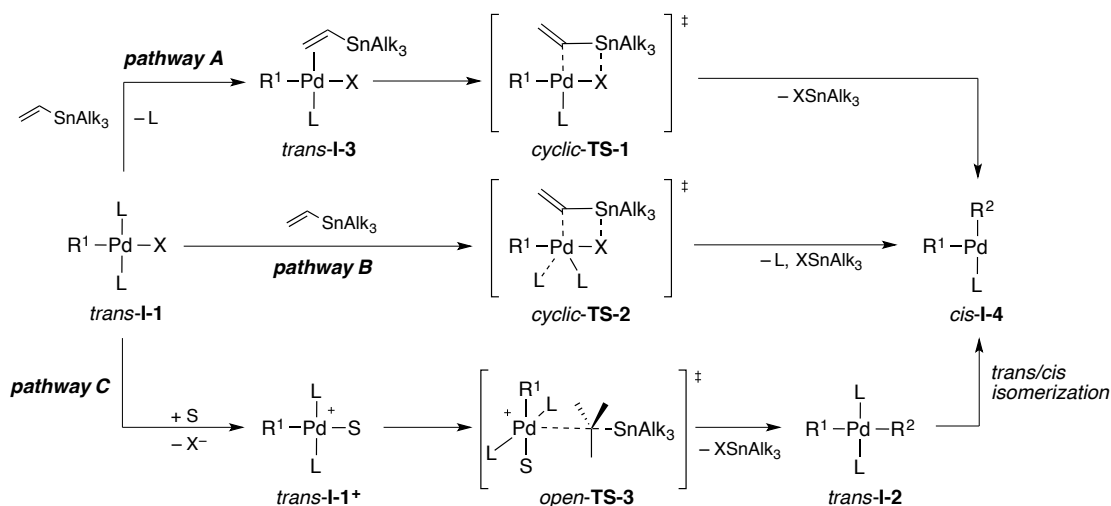
Scheme 5. Proposed transmetalation mechanisms for the Stille cross-coupling reaction.

The mechanism proceeding via open transitions state *open*-**TS-3** (scheme 5, pathway C) involves ionic intermediates and is therefore likely for reactions with organic pseudohalides in polar solvents.[3] Here, the ligand X = OTf of *trans*-**I-1** is substituted by a solvent molecule S (or excess ligand) to form a solvent-stabilized cationic intermediate [L$_2$Pd(R^1)S]$^+$ (*trans*-**I-1$^+$**). The highly electrophilic palladium(II) center is proposed to undergo fast transmetalation via an open square-pyramidal transition state *open*-**TS-3**, where the solvent molecule S is substituted by the organic residue in an electrophilic associative ligand exchange (S$_E$2 open). The resulting intermediate *trans*-[L$_2$Pd(R^1)(R^2)] (*trans*-**I-2**) has to isomerize to *cis*-[L$_2$Pd(R^1)(R^2)] (*cis*-**I-2**) or T-shaped *cis*-**I-4** to undergo the reductive elimination. The mechanism via *open*-**TS-3** was also proposed for reactions with organic halides in

very strong coordinating solvents such as HMPA,[21a] which is able to substitute the halide ligand to give cationic intermediate *trans*-**I-1$^+$**.

The structure-reactivity relationship has been investigated with respect to the electronic properties of the organotin reagent. Early studies by Stille and co-workers of the palladium-catalyzed reaction of benzoyl chloride with differently substituted organotin reagents in CHCl$_3$ revealed that the rate of transmetalation decreases in the order PhC≡C > PrC≡C > PhCH=CH > CH$_2$=CH > Ph > PhCH$_2$ > CH$_3$ > Bu.[21a] The faster reactions with unsaturated substrates is in accordance with a ligand substitution by coordination of the π-system of the organotin reagent prior to transmetalation in a S$_E$2 (cyclic) transmetalation (*cf.* scheme 5, pathway A).[22] The electronic influence of substituents at benzoyltributyltin was also investigated by competition experiments in HMPA and gave a Hammett constant of ρ = +1.2 (R^2 = 0.99) indicating that electron-withdrawing groups accelerate the transmetalation.[21a] Although not further discussed in the literature, this result is surprising, because more nucleophilic benzoyl groups are expected to be transmetalated faster, in particular assuming an one-step transmetalation mechanism proceeding via an open S$_E$2 transition state. Later competition studies of the Pd$_2$dba$_3$/AsPh$_3$-catalyzed coupling reaction of 4-(tri-*tert*-butyl)-1-cyclohexenyl triflate with *para*-substituted phenyltributyltins in NMP provided expectably a negative Hammett constant of ρ = –0.89 (R^2 = 0.946).[7a] The negative Hammett constant ρ implies that a positive charge, which is stabilized by electron-donating substituents, is build up in the transition state. This is in agreement with the proposed S$_E$2 (open) transmetalation mechanism involving a Wheland-type structure.

In addition, the influence of the halide identity of the intermediate *trans*-[L$_2$Pd(R^1)X] has been investigated for cyclic S$_E$2 transmetalation mechanisms on the basis of computational calculations,[3b, 26] and by transmetalation experiments with isolated arylpalladium(II) halide complexes.[22d] It was found that the rate increases using more electronegative organic halides in the order I < Br < Cl. The results were interpreted as the increased driving force for the Sn-X bond formation.[26] An alternative interpretation is that a more electrophilic palladium(II) center with increasing electronegativity of the halide is more reactive towards the organic nucleophile.[22d]

1.2.3.2   *Suzuki-Miyaura reaction*

The transmetalation in Suzuki-Miyaura reactions between organic halides and organic boronic acid derivatives has been extensively investigated.[2, 27] The distinctive characteristic, which differentiates the organoboron from the organotin reagents, is their much higher Lewis acidity. The coupling reactions with organoboron reagents require hydroxide (or fluoride) ions, which are typically generated in

aqueous media usually by inorganic bases, such as carbonates, hydroxides, KO^{t}Bu, K$_3$PO$_4$ or fluorides, to promote the transmetalation. The particular role of the nucleophilic promoter has been mainly the focus of mechanistic investigations, which revealed that the transmetalation proceed via a multi-step mechanism via hydroxide-bridged intermediate *trans*-**I-6** (scheme 6).[28] *Trans*-**I-6** undergoes fast transfer of the organic group from boron to palladium, because the bridging hydroxide brings both reaction center close to each other. A cyclic S$_E$2 transition state has been proposed for the group transfer and is supported by the fact, that Suzuki-Miyaura reactions with α-chiral organoboron reagents usually proceed with retention of configuration (with few special exceptions).[21b, 29] Moreover, it was found that the base has a second role, which is the triggering of the reductive elimination by mediation of the isomerization of *trans*-**I-2** to its *cis* isomer.[30]

Two mechanistic scenarios have been mainly considered for the formation of hydroxide-bridged intermediate *trans*-**I-6**. Pathway A ("oxo-palladium" pathway, scheme 6), the intermediate *trans*-**I-1** is first converted into the hydroxide species *trans*-**I-5**, which then coordinates to the neutral organoboron reagent and forms the bridged intermediate *trans*-**I-6**.[2] Pathway B ("boronate" pathway) involves the reaction of an anionic organoborate species, which exist in the equilibrium with the neutral boron reagent. The formation of a borate species is supposedly preferred, because hydroxide ions are abundant in the reaction medium and boronic acids prefer the coordination of anions since they are Lewis acids.[2] Additionally, the increased nucleophilicity of the borate species is believed to enhance the reactivity towards the electrophilic palladium(II) center to undergo fast associative ligand exchange substitution, by which the halide ligand is substituted with the borate. The actual pathway actually operating under catalytic conditions, however, depends strongly on the nature and strength of base, organoboron reagents and solvent.[2, 31]
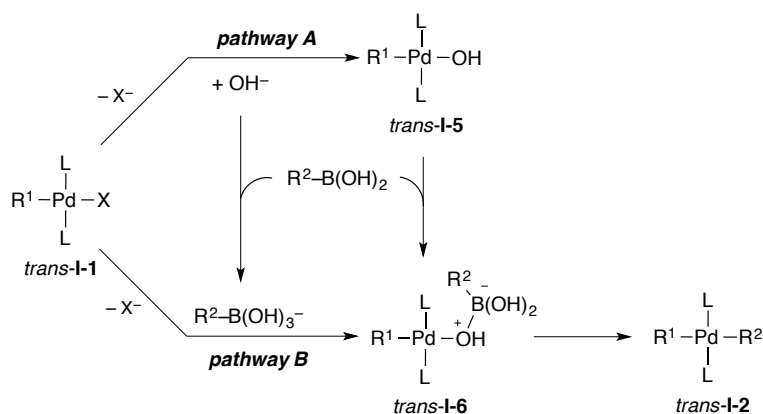
Scheme 6. Mechanistic proposals for the transmetalation in Suzuki cross-couplings.

Suzuki investigated the linear free energy relationship of *para*-substituted phenylboronic acid ester (1,3,2-dioxaborinanes) in the decarboxylative coupling with propargyl carbonates catalyzed by

Pd(PPh$_3$)$_4$ in THF at room temperature.[32] This is one example of a Suzuki(-type) reaction, which proceeds without the need of an external base, because the required bridging ligand, to bring the catalyst and organoboron reagent together, is already supplied by the carbonate. The carbonate form the palladium(II) alkoxide complex upon decarboxylative oxidative addition. Competition experiments with differently *para*-substituted phenylboronic acid ester provided a positive Hammett constant of ρ = +0.73 (R^2 = 0.89), which indicates that more Lewis acidic arylboronic acid esters react faster. Assuming that the formation of intermediate *trans*-**I-6** is irreversible, because subsequent transfer of the organic group from boron to palladium is very fast, the faster reaction of more Lewis acidic boron reagents suggests that the coordination to the alkoxide ligand of the intermediate propargylpalladium(II) alkoxide [L$_n$(Pd)(CR=C=CR$_2$)(OMe)] is product-determining. Moreover, it turned out that more nucleophilic and sterically less hindered alkoxide ligands facilitate coordination the organoboron reagent to the palladium(II) intermediate *trans*-**I-5**. These data imply that the oxo-palladium pathway A is operative under the investigated reaction conditions.

Monteiro and co-workers have investigated the electronic influence of the substrates under different conditions.[7b] The coupling of *para*-substituted phenylboronic acids with vinyl bromide, catalyzed by Pd(OAc)$_2$/PPh$_3$ (1:2, 4 mol%) in the presence of KOH in MeOH at 100 °C, was investigated by competition experiments.[7b] The relative reaction rates gave a negative Hammett constant with a relatively large magnitude of ρ = –1.26 (R^2 = 0.995), which indicates that less Lewis acidic and more electron-rich arylboronic acids react faster in the product-determining step, which is in contrast to Suzuki's data.[32] A similar Hammett constant of ρ = –0.71 (R^2 = 0.921) was determined for the reaction of (*E*)-bromostilbene with *para*-substituted phenylboronic acids at room temperature (but under otherwise same conditions).[7c] The negative Hammett constants ρ indicate that the pathway B (*cf.* scheme 6) is operative, because a more negatively polarized hydroxide ligand at the boronate species, might undergo faster associative ligand exchange reaction with intermediate *trans*-**I-2**.

1.2.3.3   *Hiyama-Denmark couplings*

The Hiyama-Denmark coupling reaction between an organic halide and an organosilanolate is mechanistically related to the Suzuki-Miyaura reaction, and has been applied more and more in organic synthesis due to the stability of the organic nucleophilic coupling partner.[4, 33] The original palladium-catalyzed protocol developed by Hiyama with organosilanes R^{2}Si(Alk)$_2$X required a strong nucleophilic promoter, such as fluoride, hydroxide or alkoxides to form *in situ* an active penta-coordinate silicate species, which transfers the organic moiety to palladium (scheme 7). The organosilane bears usually a halide substituent at the silicon to presumably increase its Lewis acidity

for the activation by the nucleophilic promoter. Extensive investigations by Denmark and co-workers showed that the presence of oxo ligands at the organosilicium reagent increased the efficiency of the coupling reactions, which led to the development of "promoter-free" procedures using organosilanolates $R^2Si(Alk)_2OX$ (X = H, K, Cs).

$$R^2-SiY_3$$
$$\downarrow\, +F^-$$
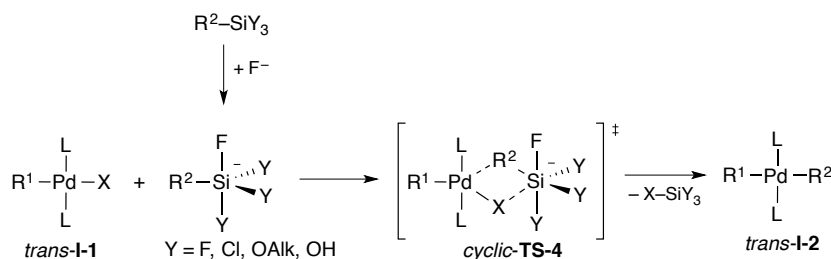
Scheme 7. Mechanism of the transmetalation in fluoride-promoted Hiyama-Denmark couplings.

Mechanistic investigations by Denmark and co-workers on the coupling of aryl halides with alkenyl- and arylsilanols showed that the function of the promoter $KOSiMe_3$ is to deprotonate the silanol, but not necessarily to form a penta-coordinate silicate.[4, 7e, 34] The deprotonated silanolate substitutes the halide ligand of the intermediate *trans*-**I-1** to form a palladium(II) silanolate complex *trans*-**I-7** (scheme 8). Alkenyl- and arylsilanolate complexes could be isolated and characterized for further investigations of stoichiometric reactions of the transmetalation.[34a, 34b, 34d] The corresponding studies revealed that alkenylsilanolate complexes *trans*-**I-7** do not require a promoter to undergo fast transfer of the organic group from silicon to palladium (pathway A). However, using alkenylsilanolates as substrates under catalytic conditions, the mechanism seems to depend on the nature of the counter ion of the silanolate. Denmark and co-workers found that activation of the silanolate takes place with cesium salts (half order in silanolate), but not with the corresponding potassium salts (zero order in silanolate), which was reasoned by the different nucleophilicity of the silanolates. The cesium salt is more nucleophilic and is therefore able to attack another silicon center to form a penta-coordinate silicate. The attack occurs at the silanolate ligand of intermediate *trans*-**I-7** to give a disilanolate complex *trans*-**I-8**, from which eventually transmetalation takes place (pathway B).
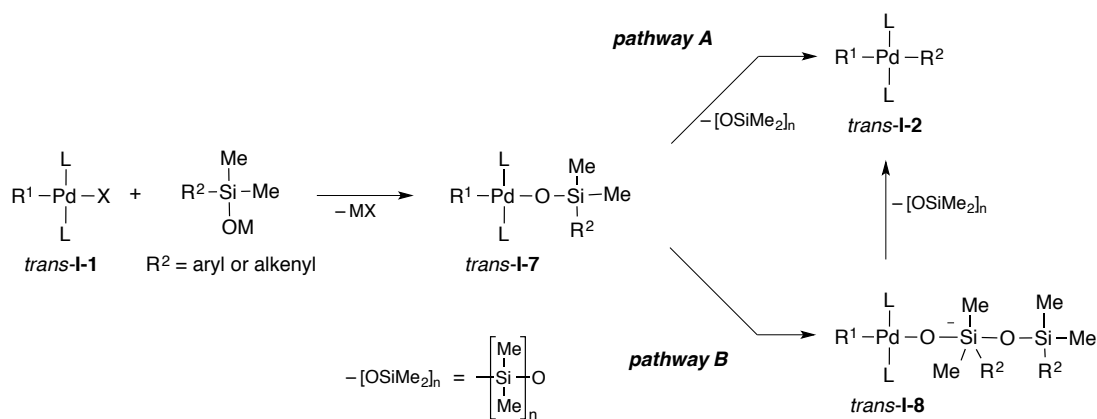
Scheme 8. Mechanism of the transmetalation of the Hiyama-Denmark coupling reaction with silanolates.

The electronic influences of the aryl ligand of intermediate *trans*-**I-7** (L = P^{t}Bu$_3$) on the transmetalation was investigated by Denmark and co-workers in stoichiometric reactions with arylsilanolates (KOSiMe$_2$Ar).[7e] This work is one of three available studies, which give actual information about the electronic influences by the palladium(II) intermediate **I-1** on the transmetalation event in palladium-catalyzed cross-coupling reactions.[5, 7e, 35] For the Hiyama-Denmark transmetalation study, the reaction rates of the decays of complexes **I-7**, bearing differently *para*-substituted aryl ligands, were measured by monitoring by ^{31}P NMR. The results implied that complexes **I-7** with electron-poor aryl ligands react faster than with electron-rich aryl ligands, which would be expected for the transmetalation proceeding via an associative S$_E$2 ligand substitution mechanism. Plotting the reaction rates in terms of Hammett correlation revealed that the electronic effect of the aryl ligand on the transmetalation is relatively small, giving Hammett constants of ρ = +0.49–0.35 (R^2 = 0.90–0.95). The small ρ value suggests that the transmetalation proceeds via a concerted cyclic transition state, where the Si-C and Pd-O bonds are broken simultaneously when the Pd-C bond is formed. In addition, the electronic influences of the aryl group on the silanolate was investigated and showed that more nucleophilic aryl groups transmetalate faster, which resulted in a negative Hammett constant of ρ = –0.50 (R^2 = 0.91). Due to the potential equilibrium between intermediate **I-7** and disilanolate complex **I-8**, the obtained Hammett constant ρ might consist of the individual Hammett constant $\rho_{\pm n}$ values for the formation of **I-8** and the group transfer. To elucidate this, the authors additionally measured the reaction rates at the saturation concentration of the silanolates to ensure that the equilibrium is fully shifted to the side of disilanolate complex **I-8**. The obtained Hammett constant was ρ = –0.80 (R^2 = 0.94), which is higher in magnitude and therefore suggests that the presumed equilibrium exists. These data led to the proposal that the transmetalation in the Hiyama-Denmark coupling with arylsilanolates proceed also via the pathway B (scheme 8) involving an activated anionic palladium(II) intermediate **I-8**.

1.2.3.4   *Sonogashira couplings*

The Sonogashira cross-coupling is different from other cross-couplings in so far, that no isolated organometallic coupling partner is used. The reactive nucleophile is generated *in situ* from copper(I) co-catalyst and a terminal alkyne, which form a copper (I) acetylide with the assistance of an amine base.[36] The modest acidity of the alkyne is believed to be increased by coordination of its π-system to the copper(I) catalyst, which allows facile deprotonation by the excess of base (often used as solvent).[36b]

The first complete kinetic analysis of the Sonogashira reaction was recently reported by Lei and co-workers, who measured the absolute reaction rates of $Pd(PPh_3)_4$/CuI-catalyzed coupling reaction of aryl iodides with arylacetylenes in $^iPr_2NH$ at 0 °C by monitoring with *in situ* IR spectroscopy.[5] The order in reagents were found to be zero in aryl iodide and arylacetylene, but first order in palladium and copper, which suggests the transmetalation as rate-determining step and confirms the co-catalysis by copper(I). The Hammett constant of $\rho = -1.65$ ($R^2 = 0.94$), determined for different *para*-substituted phenylacetylenes, revealed a remarkably strong dependence of the transmetalation rate on the electronic parameters, and suggests that the electron-donating substituents facilitate the transmetalation. This trend has been observed also from studies of other cross-coupling reactions, such as Suzuki-Miyaura, Stille and Hiyama-Denmark reactions.

The fact that the transmetalation is the rate-determining step in the Sonogashira coupling allowed to study also the electronic influences manifested by the aryl ligand of the palladium(II) intermediate *trans*-**I-1** by measuring the reaction rates of the catalytic reactions with differently *para*-substituted aryl iodides.[5] The corresponding Hammett correlation revealed higher reactivity of electron-withdrawing substituents on the aryl iodide. This is the same trend as was observed by Denmark and co-workers in the study of the transmetalation with silanolates,[7e] however, the Sonogashira transmetalation turned out to be more dependent on the electronic effects of the aryl ligand of *trans*-**I-1**, because a relatively large Hammett constant of $\rho = +1.29$ ($R^2 = 0.96$) was found.

Smaller Hammett contants ($\rho = +0.79$–1.12) were observed by Plenio and co-workers, who performed high-throughput experiments of Sonogashira reactions between aryl bromides and phenylacetylene catalyzed by Na_2PdCl_4/CuI in HN^iPr_2 at 80 °C in the presence of trialkylphosphine ligand.[35] The authors determined Hammett constants ρ for reactions in the presence of 17 different trialkylphosphine ligands, of which the bulkiest ligand (Ad_2P^tBu) was found to be more active than the smallest ligand (P^nBu_3). This is surprising expecting the transmetalation to be faster for less sterically crowded palladium(II) center to have space for the transferred organic group. The magnitude of the

Hammett constant ρ increased with decreasing steric bulk of the ligand, which implies that the sensitivity of the transmetalation towards electronic influences increases the less active and smaller the phosphine ligand.

Concerning the nature of the halide on the electrophilic coupling partner, Plenio and co-workers found that the Hammett constant ρ decreases in the order Cl ($\rho = 1.34$) > Br ($\rho = 0.51$) > I ($\rho = 0.38$, at 50 °C).[35a] With the exception of the aryl chlorides, the reactions with the aryl iodides and bromides can be assumed to proceed via rate-determining transmetalation, because the oxidative addition is presumably faster, although the order in reagents were not determined to allow final conclusions about the rate-determining step. Nonetheless, assuming a rate-determining transmetalation, the observed relative reactivities are the result of the different reactivities of the intermediates *trans*-**I-1** with copper(I) acetylide. Moreover, Eyring analysis of the Sonogashira reaction provided the activation enthalpies $\Delta H^{\ddagger}$ for aryl iodides in the range of 48–62 kJ/mol. The activation enthalpies $\Delta H^{\ddagger}$ for aryl bromides were in the range of 54–82 kJ/mol, which is higher than for the reactions with aryl iodides, and therefore mean the transmetalation with intermediate *trans*-**I-1** bearing a bromide ligand is slower compared to *trans*-**I-1** with the iodide ligand.

To propose a detailed mechanism for the transmetalation in Sonogashira couplings, it has to keep in mind that the acetylide group might also be a good ligand for palladium and can therefore coordinate via the π-system of the triple bond prior to transmetalation by a nucleophilic associative ligand substitution of a phosphine ligand (scheme 9) as has been proposed for Stille couplings with vinylstannanes (*cf*. scheme 5, pathway A).[37] The resulting intermediate *trans*-**I-9** features that the acetylide is in close proximity to the palladium center, which would allow a fast Pd-C bond formation. It is possible that the obtained kinetic data by Lei and Plenio reflect rate-determining substitution of one phosphine ligand by the acetylide rather than the actual transmetalation event,[38] which can also explain the observed reactivity trends, as well as the determined reaction orders. Initial coordination of the π-system to *trans*-**I-1**, forming a tetragonal-pyramidal intermediate (*cf*. scheme 3), is typically rate-determining in nucleophilic ligand substitution reactions (S_N2), which is favored for more nucleophilic incoming ligands and electron-deficient metal centers. The resulting intermediate *cis*-**I-9** undergoes transfer of the acetylide from copper to palladium via a cyclic transition state *cyclic*-**TS-5** giving directly *cis*-configured intermediate *cis*-**I-4**, which rapidly reductively eliminates the coupled product.
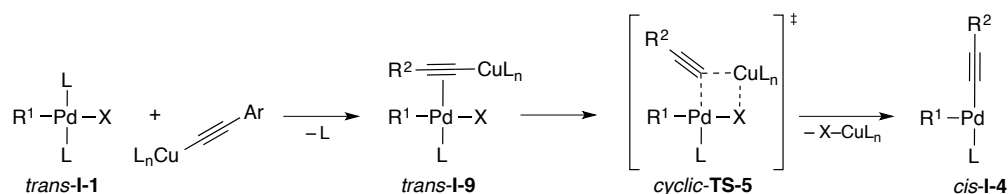
Scheme 9. Mechanism of the transmetalation of the Sonogashira coupling reaction.

1.2.4 Previous mechanistic studies on the transmetalation in Negishi cross-couplings

The transmetalation step in the Negishi cross-coupling reaction is usually faster than the other elementary steps of the catalytic cycle, which complicates kinetic investigations, and is therefore less understood compared to other transmetalations in other cross-coupling reactions.[6] Organozinc halide reagents are used as nucleophile and are Lewis acidic, which enables the coordination of ligands, similar to the organoboron reagents. The nature of the actual organozinc species in solution and in the solid state has been investigated,[39] and is dependent on the preparation procedure. A common method is the transmetalation of the corresponding lithium or Grignard reagent to a zinc halide. However, recent developments by Knochel and co-workers allow even insertion of elemental zinc into the C-X bond of the organic halide in the presence of LiCl.[40] The resulting organozinc reagents are then subsequently used without isolation and purification, simply due to their moisture- and air-sensitive nature. Therefore, the inorganic byproduct (LiX, MgX_2) is usually present in the following coupling reaction and was found to play a crucial role in the activity of the organozinc reagent,[39f, 39h, 41] which has to be considered for mechanistic investigations.

Böhrer and co-workers have studied the formation of higher order zincates in solution by negative mode ESI mass spectroscopy.[39a, 39b] They observed that organozinc reagents, derived from ^{n}BuLi and ZnX_2, as well as from zinc insertion into R-X bonds, in THF form mono- and polynuclear zincates. In the presence of bromide or iodide mononuclear species $BuZnX_2^-$ are favored, whereas with chlorides halide-bridged polynuclear species $Bu_nZn_nX_{n+1}^-$ are preferentially formed.[39b] The reactivity of these mass-isolated zincates towards formic acid in the gas phase decreases in the order $ZnBu_3^- > ZnBu_2Cl^- > ZnBuCl_2^-$.[39a] These zincate species have been found to play a role in alkyl-alkyl cross-couplings with palladium catalysts ligated by NHC ligands.[42][43] The coupling reaction does not take place without the presence of salt additives, but is inhibit by excess of ZnX_2. Mechanistic investigations showed that the concentration of the more reactive zincate $BuZnBr_2^-$, which is more nucleophilic than $BuZnBr$, decreases in the presence of $ZnBr_2$, because it captures the bromide from $BuZnBr_2^-$ to form $ZnBr_3^-$ due to the higher Lewis acidity of $ZnBr_2$ compared to $BuZnBr$.[39h, 44] However, in the presence of LiBr the

concentration of reactive $BuZnBr_2^-$ increases, which explains the need for halide sources for the catalytic coupling reaction to proceed. In addition, it turned out that the concentration of $BuZnBr_2^-$ is also strongly dependent of the nature of solvent. While in unpolar solvents, such as THF, in which the catalytic reaction is slow or even inhibited, the concentration is low, more polar solvents, such as NMP (*N*-methyl-2-pyrrolidone) and DMI (3-dimethyl-2-imidazolidinone), stabilize the anionic charges leading to high the concentration of zincates.[45]

Organ and co-workers investigated the salt effect for the palladium-catalyzed Negishi aryl-aryl coupling with NHC ligands.[41] They observed that the coupling of 4-bromoanisole does not proceed using salt-free PhZnBr, however it does in the presence of LiX, MgX_2, as well as with $ZnBr_2$, which was found to inhibit for related alkyl-alkyl coupling. Moreover, the aryl-aryl coupling takes place even with salt-free Ph_2Zn. Because of the contrasting results with respect to the alkyl-alkyl couplings, the authors concluded that the coupling reaction with arylzinc reagents does not require the formation of higher order zincates. It was concluded that the role of the salt additives in the reaction with PhZnBr is to increase the solvent dielectric to break down aggregates, which are not formed if Ph_2Zn is used. The requirement of salt additives in the palladium-catalyzed alkyl-alkyl Negishi cross-coupling with NHC ligands might also be related to the NHC ligand, because studies by Espinet and co-workers on the transmetalation in stoichiometric reactions between phosphine-ligated *trans*-[$(PR_3)Pd(R^1)Cl$] (R^1 = Ph, Me) and MeZnX (X = Cl, Me) showed that the transmetalation proceed without salt additives.[46]

Lei and co-workers investigated the kinetics of the aryl-aryl Negishi cross-couplings using *in situ* IR spectroscopy. They found that $Pd(OAc)_2$ catalyzes the coupling ArZnCl with aryl iodides at low catalyst loadings (0.1 mol%) within minutes already at 10 °C without the presence of a ligand.[7f] The reaction was zero order in aryl iodide and first order in ArZnCl and $Pd(OAc)_2$, which indicates rate-determining transmetalation. They determined the activation barrier with $\Delta H^{\ddagger}$ = 11.3 kcal/mol by Eyring analysis, which is similar to the barrier ($\Delta H^{\ddagger}$ = 12.3 kcal/mol) determined for the $Pd(OAc)_2$-catalyzed oxidative homocoupling of two arylzinc chlorides with desyl chloride as oxidant, where the transmetalation is rate-determining.[7g] The authors also determined a Hammett constant of $\rho = -1.07$ from observed reaction rates for differently *para*-substituted ArZnCl. This reactivity trend is consistent with the expectation that more electron-rich, i.e. nucleophilic, arylzinc reagents would transfer the aryl group to palladium faster. The Hammett constant ρ is remarkably close to that obtained by Mayr, Knochel and co-workers, who investigated the electronic influences of different arylzinc reagents by competition experiments in the $Pd(PPh_3)_4$-catalyzed Negishi cross-coupling and obtained a Hammett constant of $\rho = -0.98$ (R^2 = 0.97).[7h] They also conducted initial investigations regarding the electronic influence of the aryl ligand of isolated complexes *trans*-[$(PPh_3)_2Pd(Ar)Br$] on the relative rates of competing *para*-tolyl- and *para*-(ethoxycarbonyl)zinc chlorides in stoichiometric

reactions and found that the relative rates k_{Me}/k_{COOEt} increase with increasingly electron-withdrawing substituents on arylpalladium(II) bromide complex.

Despite of previous kinetic investigations, without the knowledge of the reactivity of the intermediate **I-1** in the transmetalation with organozinc reagents it is not as straightforward to predict a mechanism of the aryl transfer mechanism as for other cross-coupling reactions, for which associative ligand substitutions via cyclic or open transition states have been proposed. Assumptions about the preferred mechanism by investigating the stereochemical outcome is complicated, because, α-chiral alkylzinc reagents are less configuration stable than the corresponding tin or boron reagents. Only few examples of stereospecific Negishi couplings are known and typically proceeded via retention of configuration,[21b] which indicates cyclic transition states supported by the fact that bridging halide ligands are abundant under typical reaction conditions. Because of the Lewis acidic nature of arylzinc reagents, a similar mechanism, which has been proposed for the transmetalation in Suzuki-Miyaura reaction, might be possible involving the initial formation of an adduct intermediate similar to *trans*-**I-6** (*cf*. scheme 6) at which the transfer of the organic group from zinc to palladium proceeds directly via a cyclic transition state. However, cationic palladium(II) intermediates of **I-1⁺** were also detected in the transmetalation with $ZnMe_2$ forming the zincate $ZnMe_2X^-$.[46c] Therefore, it is conceivable that a hypothetic halide-bridged adduct of **I-1** and RZnX dissociates to give charged species **I-1⁺** and $RZnX_2^-$. The charged species might recombine to react via cyclic transition state to give intermediate **I-2**, or via a open transmetalation transition state as was proposed for Stille couplings with aryl pseudohalides, which form **I-1⁺** upon oxidative addition.

Although the electronic influence of intermediate **I-1** on the transmetalation have not been directly investigated, studies by Clark and co-workers gave a suggestion. They investigated the steric influence of the phosphine ligands on the transmetalation from PhZnBr to phenylplatinum(II) complexes as model complexes, and monitored the formation of the resulting bisarylplatinum(II) complexes, which do not undergo rapid reductive elimination.[47] Moreover, they used chelating phosphine ligands forming *cis*-complexes, which is probably the configuration of the metal center for the transmetalation in Negishi couplings. Bulky ligands inhibited the aryl transfer, however the bite angle of the ligand plays only a minor role, while the electronic influence induced by the phosphine ligand affected the transmetalation rate directly. Dppe-ligated platinum(II) complex reacted much slower than the structurally equivalent dfppe ligand (1,2-bis(di-pentafluorophenylphosphino)ethane), which is a weaker coordinating ligand due to the electron-withdrawing pentafluorophenyl groups on the phosphine. These observations are consistent with a faster transmetalation from the nucleophilic zinc reagent to more electrophilic metal(II) centers. Moreover, the (dppe)Pt(Ph)Cl reacted faster than the bromide analogue, a trend that was already observed in Stille couplings.[22d]

As already mentioned, mechanistic proposals regarding the transmetalation steps in the Negishi cross-coupling supported by experimental findings do not exists, however previous initial computational studies might give a crude picture. The stoichiometric reaction of a phosphabarrelene-ligated intermediate **I-1**, which is a T-shaped complex and exists in equilibrium with the halide-bridged dimer, was investigated by DFT calculations by Gosmini, Mézailles and co-workers (scheme 10).[48] The coordinatively unsaturated intermediate **I-1** form with ArZnBr a more stable bromide-bridged Pd/Zn dimer **I-10** (ΔG° = –2.8 kcal/mol), which rearranges to an even more stable bromide/aryl-bridged analogue **I-11** (ΔG° = –5.8 kcal/mol). The barrier for the rearrangement was found to be relatively low ($\Delta G^\ddagger$ = +8.1 kcal/mol), but is, among the other calculated ones, the highest activation barrier, which suggests that the rearrangement form **I-10** to **I-11** is rate-limiting.[48] The identification of **I-11** as intermediate is surprising since those halide/aryl-bridged complexes have been proposed rather to be transition states in transmetalations with other organometallic reactions. Finally, the aryl group is completely transferred to palladium in **I-11** by a slightly exothermic process to give intermediate *cis*-**I-4**.
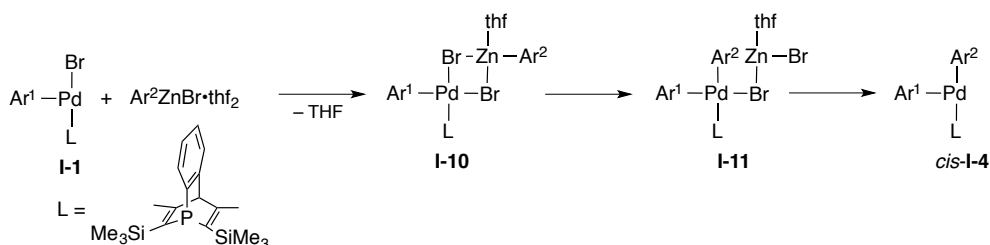
Scheme 10. Calculated transmetalation mechanism in Negishi cross-couplings with coordinatively unsaturated **I-1**.

DFT calculations were also performed by Espinet and co-workers for transmetalations in alkyl-alkyl coupling reactions with coordinatively saturated *trans*-complexes *trans*-**I-1** and ZnMeCl and ZnMe$_2$ (scheme 11).[46b, 46c] The authors found that the organozinc reagents form with *trans*-**I-1** a chloride bridged dimer *trans*-**I-12**, which can dissociate to give THF-stabilized cationic palladium(II) intermediate *trans*-**I-13** and an anionic zincate, from which the transmetalation product *trans*-**I-14** is formed via *cyclic*-**TS-7**. This pathway was computationally found only available for the reaction with ZnMe$_2$, but not with MeZnCl. Alternatively, the intermediate adduct *trans*-**I-12** can undergo direct transmetalation via transition state *cyclic*-**TS-6**, which can be passed with both reagents, MeZnCl and ZnMe$_2$. For all considered pathways, the highest barriers (rate-determining step) were found for the final transfer of the methyl group to the palladium(II) center and are very similar ($\Delta G^\ddagger$ = +10.3 and +10.7 kcal/mol, respectively) for both pathways leading to *trans*-**I-14**. However, in the presence of excess phosphine ligand, the cationic intermediate *trans*-**I-13** undergoes rapid ligand substitution to form a more stable phosphine-stabilized cationic complex, from which transmetalation is unfavored. This fact made it possible to detect those cationic species by NMR. Interestingly, the calculated

transition states (and also some intermediates, which are not shown) feature Pd-Zn bonds, which seem to be unique compared to other transmetalations, such as with stannanes or boronic acid derivatives.

Scheme 11. Calculated transmetalation mechanism in Negishi cross-couplings with *trans*-**I-1**.
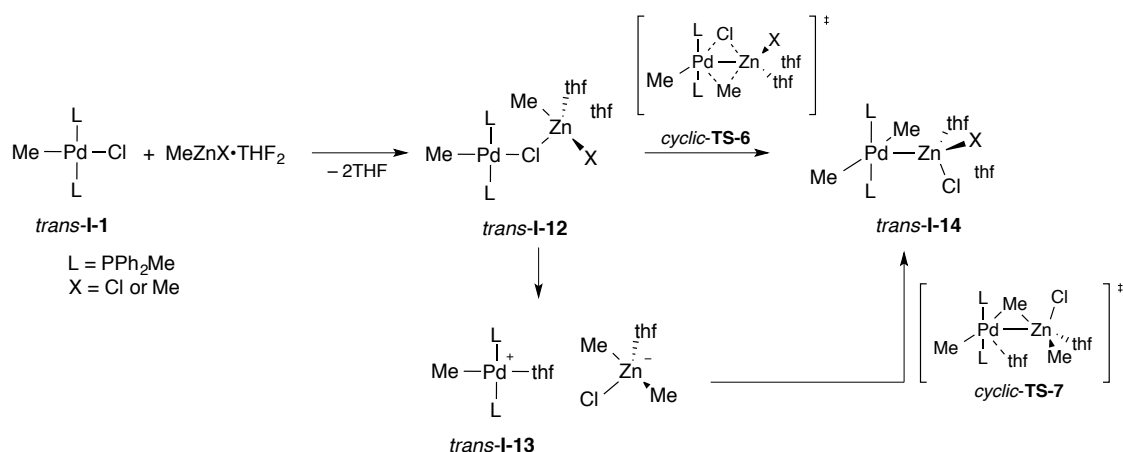
Álvarez, Lera, Aurrecoechea and co-workers performed DFT calculations for the transmetalation with coordinatively saturated PMe$_3$-ligated intermediate *cis*-**I-1** as model complex in the transmetalation with MeZnCl.[49] Interestingly, a three-membered cyclic intermediate **I-15** (scheme 12), which also features a Pd-Zn bond, was found and is energetically more stable than *cis*-**I-1** ($\Delta G^\circ = -1.4$ kcal/mol). The formation of the Pd/Zn hybrid complex **I-15** proceeds via an activation barrier of $\Delta G^\ddagger = +10.4$ kcal/mol, which is lower than for the transfer of the methyl group from zinc to palladium via cyclic transitions state *cyclic*-**TS-8** ($\Delta G^\ddagger = +12.1$ kcal/mol). The product of the transmetalation *cis*-**I-14**, at which the zinc byproduct ZnX$_2$ remains coordinated to the palladium(II) center, exhibits *cis*-configuration to undergo fast reductive elimination. It was further found, as well as previously reported that coordination of zinc to palladium play also a role in reductive elimination and oxidative addition.[49-50] Two other computational studies on the transmetalation in Negishi couplings have been reported, however address special case systems.[51]

Scheme 12. Calculated transmetalation mechanism in Negishi cross-couplings with *cis*-**I-1**.
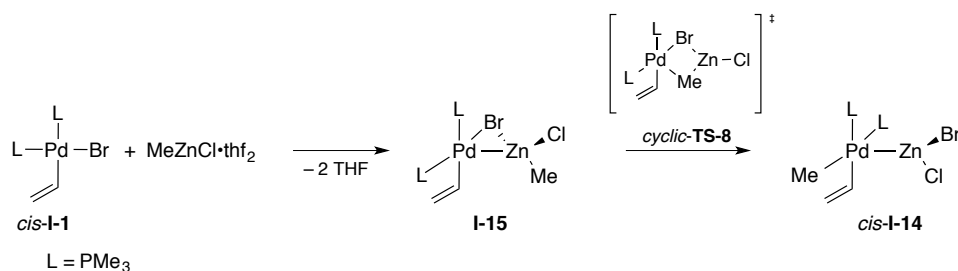
1.3 Results and discussion

1.3.1 Syntheses of arylpalladium complexes

To investigate the transmetalation step in the Negishi cross-coupling reaction, isolated palladium(II) intermediates, which are relevant in catalysis, needed to be prepared. The choice of ligands was made based on their use in cross-coupling reactions.[52] Typically used ligands in palladium-catalyzed cross-couplings are monodentate phosphine ligands, such as PPh_3, $P(o\text{-tol})_3$, P^tBu_3 and ligands of the Buchwald family, of which we chose XPhos, but bidentate bisphosphine ligands, such as dppe and dppf have been proven to be efficient, as well. The simplest and most frequently used ligand is the monodentate ligand PPh_3, which is introduced in the catalytic cross-coupling reactions as $Pd(PPh_3)_4$ or $(PPh_3)_2PdCl_2$. This catalyst (or catalyst precursor) forms *cis*-[$(PPh_3)_2Pd(Ar)X$] intermediates under catalytic conditions upon oxidative addition with an aryl halide. This intermediate isomerizes to its *trans*-isomer, which is assumed to undergo transmetalation with the organometallic coupling partner if the subsequent transmetalation is rate-determining,[16] such as in Suzuki-Miyaura, Stille and Hiyama reactions. However, the transmetalation with organozinc reagents is usually very fast and is assumed to occur with *cis*-[$(PPh_3)_2Pd(Ar)X$] before *cis/trans*-isomerization can occur. However, the isolation of *cis* complexes is complicated, because it isomerizes too quickly to the more stable *trans*-complexes.[16] Therefore, we decided to start our transmetalation study with the structurally most related dppe-ligated complexes **2**, which exhibit the required *cis*-configuration due to the chelating binding mode of the ligand.

To cover a wide range of different electronic properties of the aryl ligand we synthesized a large number of differently *para*-substituted dppe-ligated complexes **2**, of which some have been previously reported and were synthesized by different procedures.[53] We synthesized the dppe-complexes **2** by the procedure reported by Ludwig *et al.* from tmeda-ligated complexes **1**.[53a] The synthesis of tmeda-complexes **1** is based on the known oxidative addition of the *para*-substituted aryl iodides to $Pd_2dba_3 \cdot CHCl_3$ in toluene at 50 °C (table 1).[53d, 54] The reaction time depended strongly on the nature of the aryl iodide, which reacted faster with electron-withdrawing substituents, whereas electron-rich aryl iodides reacted slower. Full conversion of $Pd_2dba_3 \cdot CHCl_3$ was reached within 1 h and could be recognized by the color change of the reaction mixture from deep purple to yellow or orange. After concentration of the reaction solutions, addition of Et_2O and cooling the solution for a short time at –25 °C produced crystalline complexes **1** in high overall yields. The complexes **1a**,[53d] **1d**,[54a] **1f**,[54a] **1g**,[55] **1i**,[56] **1k**,[54] and **1l**[54a] have been previously reported and characterized, whereas **1b**, **1c**, **1e**, **1h**, **1j** and **1m** were synthesized for the first time.

Table 1. Syntheses of bisphosphine-ligated arylpalladium(II) iodide complexes **2** and **3**.
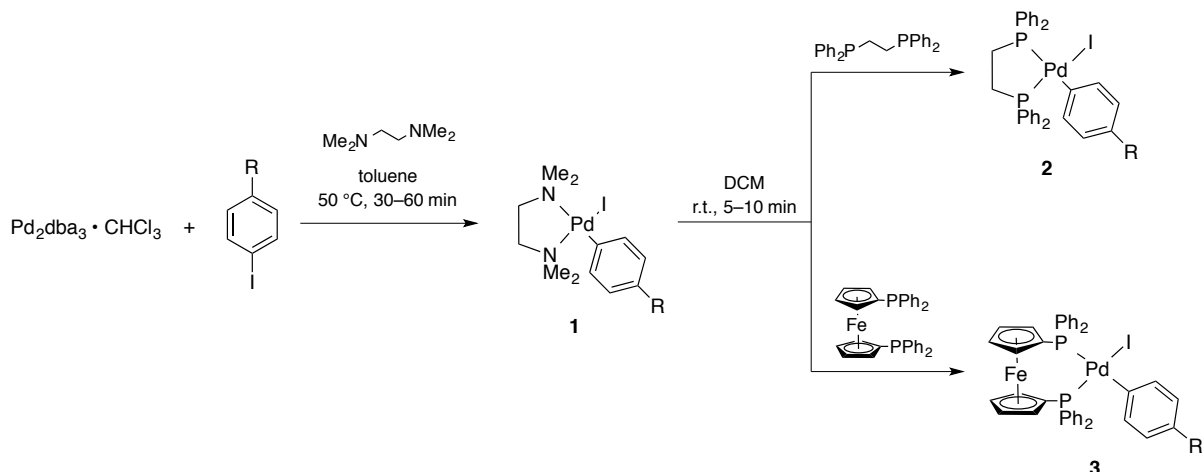
entry	R		**1** yield [%]	**2** yield [%]	**3** yield [%]
1	NMe$_2$	**b**	87	0	–
2	OPh	**c**	74	quant.	–
3	OMe	**d**	89	quant.	81
4	^{t}Bu	**e**	76	93	98
5	Me	**f**	85	quant.	93
6	H	**a**	90	quant.	97
7	F	**g**	99	88	97
8	Cl	**h**	98	42	–
9	CO$_2$Et	**i**	88	98	95
10	CO$_2$Bu	**j**	75	98	–
11	CF$_3$	**k**	82	83	90
12	CN	**l**	86	91	quant.
13	NO$_2$	**m**	99	92	–

Almost all of the prepared tmeda-ligated complexes **1** were successfully converted into the dppe-ligated analogues **2** in very high yields of up to 88%, with the exception of the most electron-rich dimetylamino-substituted complex **1b**, of which the related dppe complex **2b** could not be isolated (table 1). The material, obtained from the attempted synthesis of **1b**, exhibited a complex mixture of signals in the ^{31}P and ^{1}H NMR spectra, which could not be unambiguously assigned to a structure. The methoxy- (**2d**)[53b], methyl- (**2f**)[53b], chloro- (**2h**)[53b] and unsubstituted (**2a**)[53a, 53b] complexes have been reported and characterized, previously. We also prepared analogues dppf-ligated arylpalladium(II) complexes **3** for some of the *para*-substitution patterns in high yields of up to 81% by using identical conditions as for complexes **2**. The complexes **3d**[57], **3f**[53b, 57] and **3k**[54b] have been previously reported by using other procedures, whereas all other complexes **3** in table 1 are new compounds.

We intended to investigate also the reactivities of mono-ligated palladium(II) complexes to compare their reactivities with the reactivities of the bisphosphine complexes **2** and **3** in the transmetalation with arylzinc halides. These complexes are formed with bulky monodentate ligands, such as P(*o*-tol)$_3$, P^{t}Bu$_3$ and XPhos. The P(*o*-tol)$_3$-ligated palladium(II) complexes **5** exist usually as dimers in the solid

state,[58] whereas the P^{t}Bu-ligated analogues **14** are known to form coordinatively unsaturated T-shaped structures.[59] The XPhos-ligated complexes **12,13** have not been reported previously, but related complexes with other Buchwald ligands are described in the literature and their crystal structures show that these complexes exist either as dimers,[60] or as monomers, which are stabilized by coordination of the π system of the biaryl ligand to the vacant coordination site. [61]

The synthesis of P(o-tol)$_3$-ligated palladium(II) complexes **4** by either oxidative addition of the aryl iodide or bromide to Pd$_2$dba$_3$ in the presence of the ligand,[62] or directly to Pd[P(o-tol)$_3$]$_2$ has been previously described.[58, 63] Because the first mentioned approach seemed to us more convenient, we synthesized arylpalladium(II) iodide complex **4a** by oxidative addition of iodobenzene with Pd$_2$dba$_3$·CHCl$_3$ in toluene at room temperature in 86% yield (scheme 13). However, it turned out that **4a** is insoluble in most common organic solvents, and more importantly, it is insoluble in THF, which is the most commonly used solvent in Negishi cross-couplings and therefore considered as solvent for our transmetalation study. This excludes P(o-tol)$_3$-ligated arylpalladium(II) iodide complexes **4** as candidates for our studies.
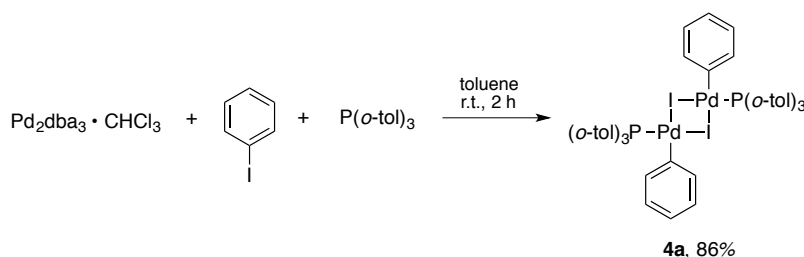
Scheme 13. Syntheses of P(o-tol)$_3$-ligated phenylpalladium(II) iodide complex **4a**.

We synthesized also the bromide analogue **5a**, which behaved similarly to **4a** with respect to its solubility in organic solvents, and excluded them for our study, as well. However it was previously shown that complexes **5** are ideal precursor for the bisphosphine-ligated arylpalladium(II) bromide complexes **6** and **7** (table 2).[64] The complexes **6** and **7** cannot be prepared from the tmeda-ligated precursor like the bisphosphine complexes **2** and **3**, because bromide analogues of **1** are known to be hardly accessible by oxidative addition with the corresponding aryl bromides.[53d] Therefore, we still synthesized the series of P(o-tol)$_3$-ligated dimer complexes **5** with different *para* substituents of the aryl ligand and obtained the products in overall high yields of up to 72%, with the exception of the butyl ester-substituted complex **5j**, which was obtained in only 18%. The reason was the unexpected superior solubility of **5j** even in unpolar solvents that were used to precipitate complexes **5** and remove the dba and the excess ligand. The complexes with the methoxy- (**5d**),[62, 65] methyl- (**5f**),[58, 62] fluoro-(**5g**)[63] and unsubstituted (**5a**)[66] aryl ligands have been previously synthesized, whereas all others of the series of complexes **5** are new compounds.

The P(o-tol)$_3$-ligated complexes **5** were successfully converted into the previously unknown dppe-ligated arylpalladium(II) complexes **6a** and **6i** by simple ligand exchange in DCM at room temperature (table 2). The complex **6i** was obtained in 82% and complex **6a** in 91% yield, however, while complex **6i** is well soluble in organic solvents, the analogous complex **6a** exhibits only moderate solubility in organic solvents and is essentially insoluble in THF. This makes the complexes **6** also unsuitable for the transmetalation studies. However, the related dppf-ligated complex **7a**, which was obtained in 86% according to the same procedure as for **6a**, exhibited good solubility in THF. Therefore, we continued with the syntheses of the other complexes **7** of this series and obtained them in high yields of up to 75%. Most of these complexes have been previously reported,[53f, 64] with the exception of the complexes with methyl- (**7f**) and ester-substituted (**7i**) aryl ligands.

Table 2. Syntheses of P(o-tol)$_3$-ligated dimer complexes **5** and bisphosphine-ligated bromide complexes **6**, **7**.
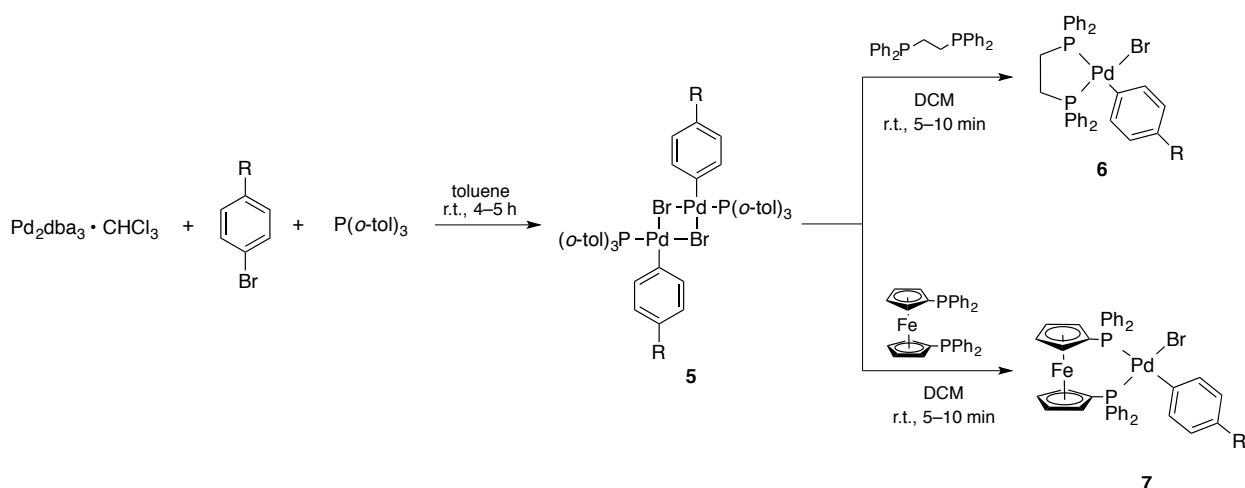
entry	R		5 yield [%]	6 yield [%]	7 yield [%]
1	OMe	**d**	73	–	88
2	^{t}Bu	**e**	–	–	–
3	Me	**f**	63	–	89
4	H	**a**	72	91	86
5	F	**g**	96	–	89
6	CO$_2$Et	**i**	84	82	92
7	CO$_2$Bu	**j**	18	–	–
8	CF$_3$	**k**	82	72^a	75
9	CN	**l**	91	–	96

^{a}Prepared from complex **9k**.

Single crystals suitable for X-ray diffraction analysis for some of the bisphosphine-ligated complexes **2**, **3** and **7** were grown by slow diffusion of Et$_2$O into the saturated DCM solutions. The solid state structures of dppe-ligated complexes **2e** and **2g** exhibit the expected *cis*-configuration as has been reported for related dppe-palladium(II) complexes (figure 2A and B).[53b, 67] The comparison of the bond distances of the ligands to the palladium(II) metal center reveals only minor differences between the

complexes **2e** and **2g** (table 3). The P-Pd bond distances of 2.34 Å *trans* to the aryl ligands are identical for both complexes, which indicates that there is essentially no differentially distinct *trans*-influence of the aryl ligand when changing the electronic properties of the *para*-substituent. The P-Pd bonds *trans* to the iodide ligand are shorter for both complexes and are in the range of 2.23Å for **2e** and 2.25 Å for **2g**. These shorter distances reflect the weaker *trans*-influence of the iodide ligand compared to the stronger σ donor aryl ligands. Similarities in the bond distances were also found for the Pd-I bond distances, which are 2.65 Å for **2e** and 2.64 Å for **2g**, and for the Pd-C bond distances 2.07 Å for **2e** and 2.05 Å for **2g**. Although the differences in the bond distances are small, it can be still recognized that the complex **2e**, with the more electron-rich aryl ligand, exhibits longer bonds of the anionic ligands to palladium, than the complex **2g**. This trend is continued by the comparison of the bond distances of the complex *ortho*-**2d** with the even more electron-donating *ortho*-anisyl ligand, of which the solid state structure was reported previously.[67b]

Table 3. Selected bond distances (Å) and angles (°) of the X-ray structures of bisphosphine-ligated palladium(II) complexes **2**, **3** and **7**. P1 = *trans* to aryl ligand; P2 = *trans* to X.

	2e	2g	*ortho*-2d[67b]	3g	7g	7k[53f]
Pd–P1	2.340	2.340	2.359	2.383	2.379	2.399
Pd–P2	2.232	2.245	2.238	2.281	2.271	2.265
Pd–X	2.653	2.644	2.667	2.751	2.484	2.486
Pd–C	2.067	2.051	2.078	2.058	2.056	2.029
P1–Pd–P2	85.4	86.2	86.3	100.9	101.1	101.4

The solid state structures of dppf-ligated palladium(II) halide complexes **3g** and **7g** are shown in figure 2 (C and D) and exhibit structural characteristics that have been previously reported for related dppf-ligated complexes.[53f, 68] Remarkably, the bond distances to not differ significantly between the iodide complex **3g** and the bromide complex **7g**, as was observed for the solid state structures of dppe-ligated complexes **2** (figure 2A and B), with the exception of the Pd-X bond, which is 0.27 Å longer for the iodide complex **3g** compared to the bromide complex **7g**, as expected.[69] The P-Pd bond distances of dppf-ligated complexes **3g** and **7g** are only slightly longer (0.04–0.05 Å) compared to the dppe-ligated complexes **2**. Comparison of the bond distances for both dppf-ligated bromide complexes **7g** and **7k**, of which the crystal structure was reported previously,[67b] shows similar relations as discussed for the dppe-ligated complexes **2e** and **2g**.

A)

B)

C)

D)
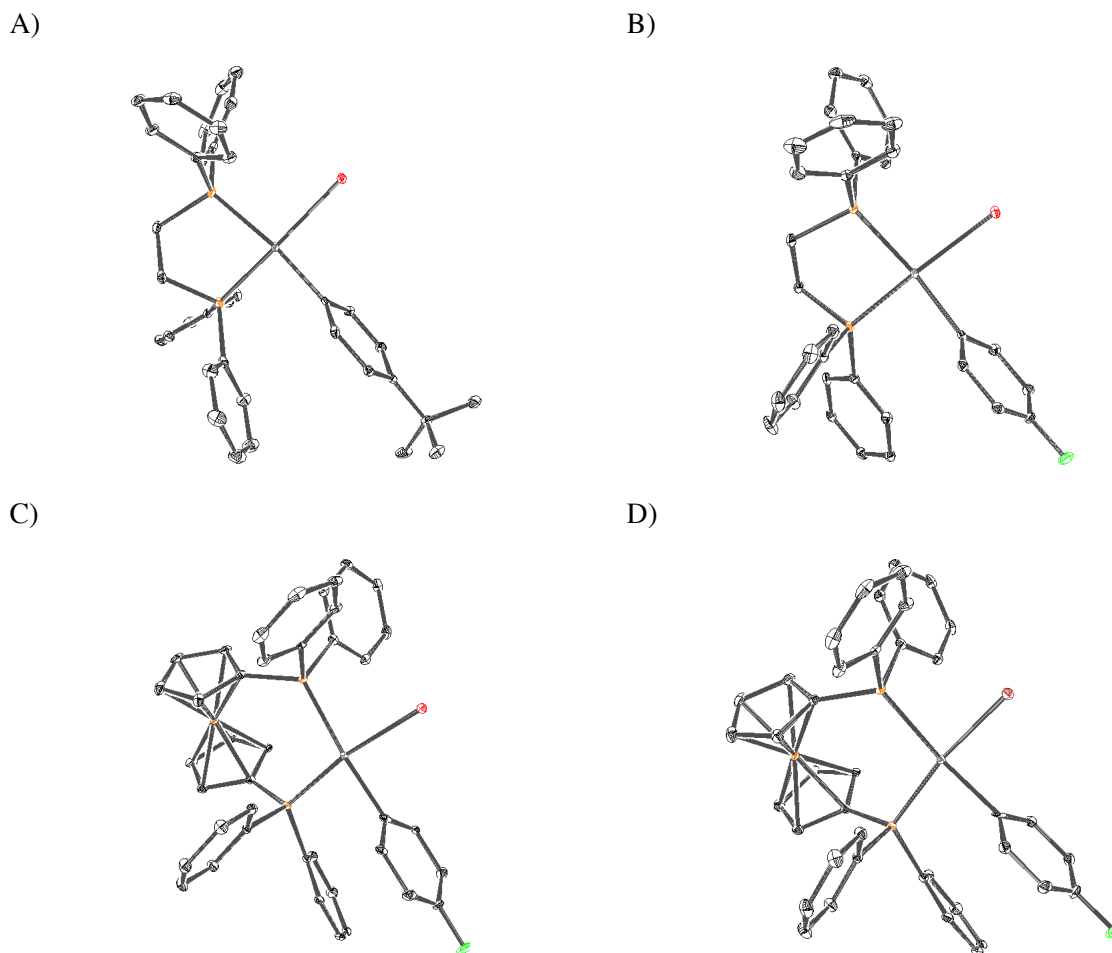
Figure 2. ORTEP 3 diagrams of dppe-ligated arylpalladium(II) iodide complexes **2e** (A) and **2g** (B), as well as dppf-ligated iodide complex **3g** (C) and analogous bromide complex **7g** (D). Thermal ellipsoids are drawn at 30% probability level. Hydrogen atoms were omitted for clarity.

Although the *trans*-configured PPh$_3$-ligated complexes **8** and **9** are not appropriate model complexes for the transmetalation study with arylzinc halides, we are still interested in their reactivity behavior since they are relevant to the slower transmetalations in the Suzuki-Miyaura and Stille reactions. The syntheses of the *trans*-complexes have been reported to proceed by oxidative addition of the aryl halide to Pd(PPh$_3$)$_4$.[53c, 53f, 69-70] Accordingly, we prepared the arylpalladium(II) iodide complexes **8** by reaction of Pd(PPh$_3$)$_4$ with *para*-substituted aryl iodides at room temperature and obtained overall high yields of up to 72% with the exception of the complex **8f**, which was obtained only in 32% yield (table 4). We realized that using toluene as solvent, as reported in the literature, results in lower yields in particular for the reactions with electron-rich aryl iodides, which required also longer reaction times. Nevertheless, the use of THF resulted in higher yields for the iodide complexes **8**. The complexes **8d**,[53c, 70b] **8f**,[53c, 70c] **8a**,[69, 70c] and **8k**[53c] have been previously reported, whereas the other complexes of this series are new compounds.

Table 4. Syntheses of PPh$_3$-ligated *trans*-complexes **8**, **9**.
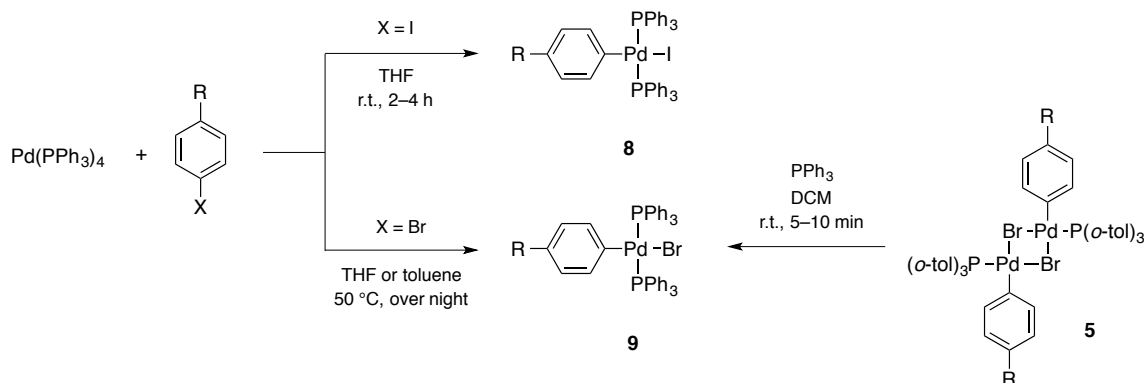
entry	R		8 yield [%]	9 yield [%]
1	OMe	d	86	98[a]
2	^{t}Bu	e	72	13
3	Me	f	34	70[a]
4	H	a	78	70
5	F	g	86	74
6	CO$_2$Et	i	79	83
7	CO$_2$Bu	j	78	99
8	CF$_3$	k	84	54
9	CN	l	86	86

[a]Made from corresponding complexes **5**.

The analogous bromide complexes **9** were obtained by oxidative addition of the corresponding aryl bromides, which required heating and longer reaction times. Complexes **9** with electron-withdrawing substituents (entries 4–9) were obtained in good yields of 54–99%, whereas the electron-rich complexes (entries 2) were obtained only in low yields and exhibited phosphine-containing impurities in significant amounts. Only the methyl-substituted complex **9e** could be satisfactorily purified by recrystallization and was obtained in a low yield of 13%. The observed phosphine signals of the impurities might by unsymmetrical phosphine species, which can be formed by P-C bond-forming reductive elimination of the initially formed arylpalladium(II) bromide complex **9** with the PPh$_3$ ligand yielding a phosphonium salt.[71] Subsequent oxidative addition of the most electron-poor P-C bond forms then a new arylpalladium(II) complex. Since the reductive elimination occurs faster with electron-rich aryl ligands, this side reaction is favored for the complexes with the electron-donating substituents, which is in agreement with our observations. Changing the solvent from toluene to THF, which resulted in improved yields for the analogous iodide complexes **8**, did not lead to higher yields or purer materials. Nevertheless, the complexes **9e** and **9f** could be derived from the corresponding P(*o*-tol)$_3$-ligated complexes **5** in almost quantitative yields. The complexes **9e**,[70d] **9f**,[70b] **9a**,[69, 70b, 70c, 70e] **9k**,[53f, 70b, 72] and **9l**[70b, 70c, 70f] were reported previously, whereas the others were prepared for the first time.

Single crystals suitable for X-ray diffraction analysis could be grown of the PPh$_3$-ligated arylpalladium(II) bromide complexes **9f** and **9g**, which exhibit same structural properties (figure 3) as have been reported for **9a** and **8a**, as well as the analogous chloride and fluoride complexes.[69] The Pd-C bond distance of the methyl-substituted complex **9f** is slightly longer with 2.03 Å compared to the complex **9g** with the fluoro-substituted aryl ligand, which has a Pd-C bond length of 2.01 Å. Comparison of the Pd-C bond distances with the other phosphine complexes **2**, **3** and **7** (*cf.* table 3) reveals that the shortest Pd-C bond for PPh$_3$-ligated complexes **9**. In contrast, the Pd-Br bond distances of 2.54 Å are longer than for dppf-ligated complexes **7**, but are essentially the same for both PPh$_3$-ligated complexes **9f** and **9g**. The longer Pd-Br bond length of complexes **9** versus **7** might be due to a larger *trans* influence of the aryl ligand. The Pd-P bonds are identical for both phosphine ligands and complexes **9f** and **9g** with a length of 2.32 Å, which is also in the same range as for the dppf-ligated complexes **7**.

A)   B)
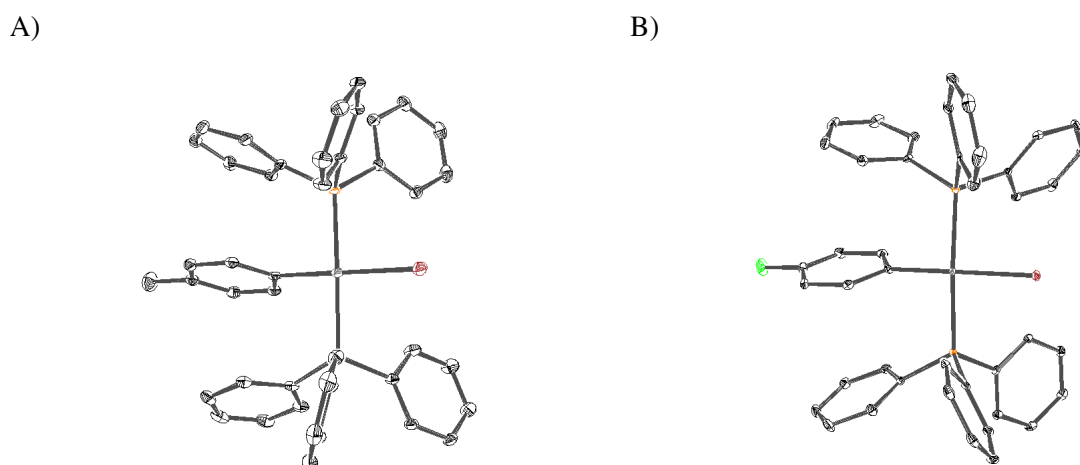
Figure 3. ORTEP 3 diagrams of PPh$_3$-ligated arylpalladium(II) bromide complexes **9f** (A) and **9g** (B). Thermal ellipsoids are drawn at 30% probability level. Hydrogen atoms were omitted for clarity. Selected bond distances (Å) for **9f**: Pd–C 2.034, Pd–Br 2.542, Pd–P 2.323. For **9g**: Pd–C 2.014, Pd–Br 2.535, Pd–P 2.325.

The synthesis of XPhos-ligated arylpalladium(II) complexes has not been described previously, however, was reported for related complexes with other biarylphosphine ligands of the Buchwald's ligand family.[60-61] Initially, we attempted the synthesis of complex **13a** by oxidative addition of bromobenzene to a highly active mono-ligated XPhosPd(0) species, which was shown to be generated *in situ* by treating the Buchwald's *C,N*-cyclometalated precatalyst with a strong base.[61a, 73] The base deprotonates the coordinated amine, which leads to C-N bond-forming reductive elimination of carbazole (scheme 14). This process generates a coordinatively highly unsaturated LPd(0) species, which undergoes rapid oxidative addition even at low temperatures with less reactive chlorobenzene.[73]

This approach seemed to us promising with respect to the synthesis of other difficultly accessible complexes, in particular thermally unstable complexes. However, arylpalladium(II) complexes, derived from the Buchwald's precatalyst, can be coordinated by the deprotonated carbazole byproduct.[61a] To avoid deprotonation of the carbazole, we attached a methyl group to the amine and prepared the *N*-methyl-2-phenylanilin ligand, as well the corresponding cyclometalated palladium(II) complex. The byproduct of the activation is *N*-methylated carbazole, which cannot be further deprotonated and therefore does not coordinate to the desired arylpalladium(II) complex. While this work was in progress, Buchwald and co-workers published the same complex, which is now known as the fourth generation catalyst, and showed that this is a highly active precatalyst in cross-coupling reactions.[74] Nevertheless, the solid-state structure of the Buchwald's precatalyst G4 has not been reported. We could grow crystals of the complex as solvate with benzene, which exhibits a dimer structure with the mesylates as bridging ligands (see Crystallographic Section).

Application of Buchwald's pre-catalyst of the fourth generation G4 in the synthesis of XPhos-ligated arylpalladium(II) complex **13a** was initially successful on a test scale and provided the desired complex in 87% (scheme 15). Increasing the scale of the reaction led to lower yields and to carbazole-contaminated product **13a**, because the byproduct exhibits same solubility behavior as the product, which made the purification difficult. Unfortunately, complex **13a** turned out to be indeed well soluble in most organic solvents, but insoluble in THF, so that it could not be employed in the transmetalation study. We thought, that the analogues iodide complex **12a** might be better soluble, like experienced for the dppe-ligated complexes, of which the iodide complexes **2** are better soluble than the corresponding bromide complexes **6**.
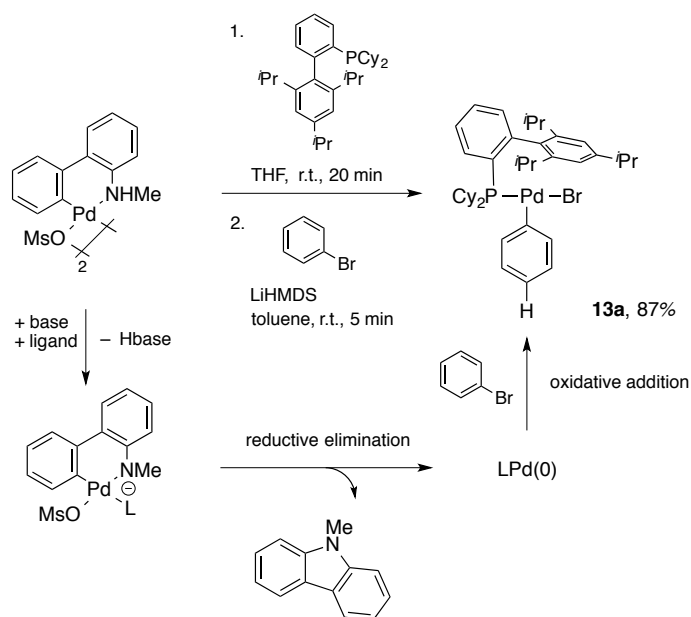
Scheme 14. Synthesis of XPhos-ligated phenylpalladium(II) bromide complex **13a**.

Because of the difficulties with Buchwald's pre-catalyst G4 as the precursor, we sought for an alternative method. A literature search revealed that a pyridine-ligated arylpalladium(II) chloride complex was used as precursor for complexes with very bulky phosphine ligands, which can displace the pyridines.[75] Encourage by this report, we synthesized the analogous dipyridine-ligated phenylpalladium(II) iodide complex **10a**, which was obtained in 89% by oxidative addition of iodobenzene to $Pd_2dba_3 \cdot CHCl_3$ in neat pyridine (scheme 15).[76] Complex **10a** is an air-stable compound, but essentially insoluble in organic solvents. However, the subsequent ligand exchange reaction with XPhos was successfully carried out in DCM by using MeCN as co-solvent and gave presumably desired XPhos-ligated complex **12a** in 70%. Unfortunately, after **12a** was isolated from the reaction mixture, it could not be re-dissolved, which also excludes it from our study.
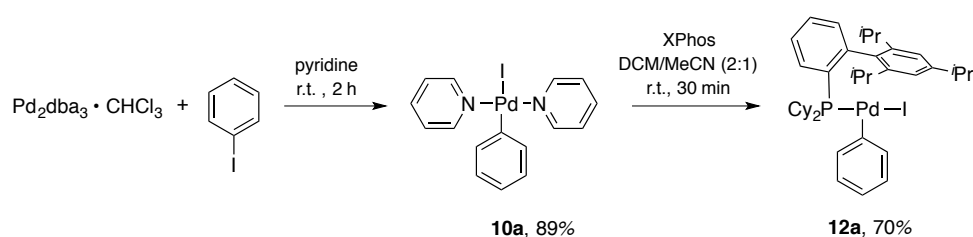
Scheme 15. Syntheses of XPhos-ligated phenylpalladium(II) iodide complex **12a**.

Although the XPhos-ligated bromide complexes could not be used to study electronic influences of the aryl ligand due to their poor solubility, we expected that the ester-substituted analogues **13i** and **13j** are soluble enough to apply them in competition experiments with complexes with different phosphine ligands. Because of the good result using the dipyridine-ligated palladium(II) precursor, we tried to transfer the procedure to the synthesis of bromide complexes **13**. The synthesis of the corresponding precursors **11** using the same procedure as for **10a**, failed. However, addition of P(o-tol)₃ in substoichiometric amounts, as previously reported for the chloride analogue,[75] under otherwise identical conditions provided the complexes **11**. The pyridine-ligated complexes **11** were obtained in moderate yields of 43–55% (scheme 16), which might be improvable if larger amounts of P(o-tol)₃ are employed. Subsequent ligand exchange with XPhos provided the corresponding complexes **13** in high yields of up to 90%. This approach was also applied to the syntheses of the bisphosphine-ligated complexes **6** and **7** giving the products in yields of up to 94%.
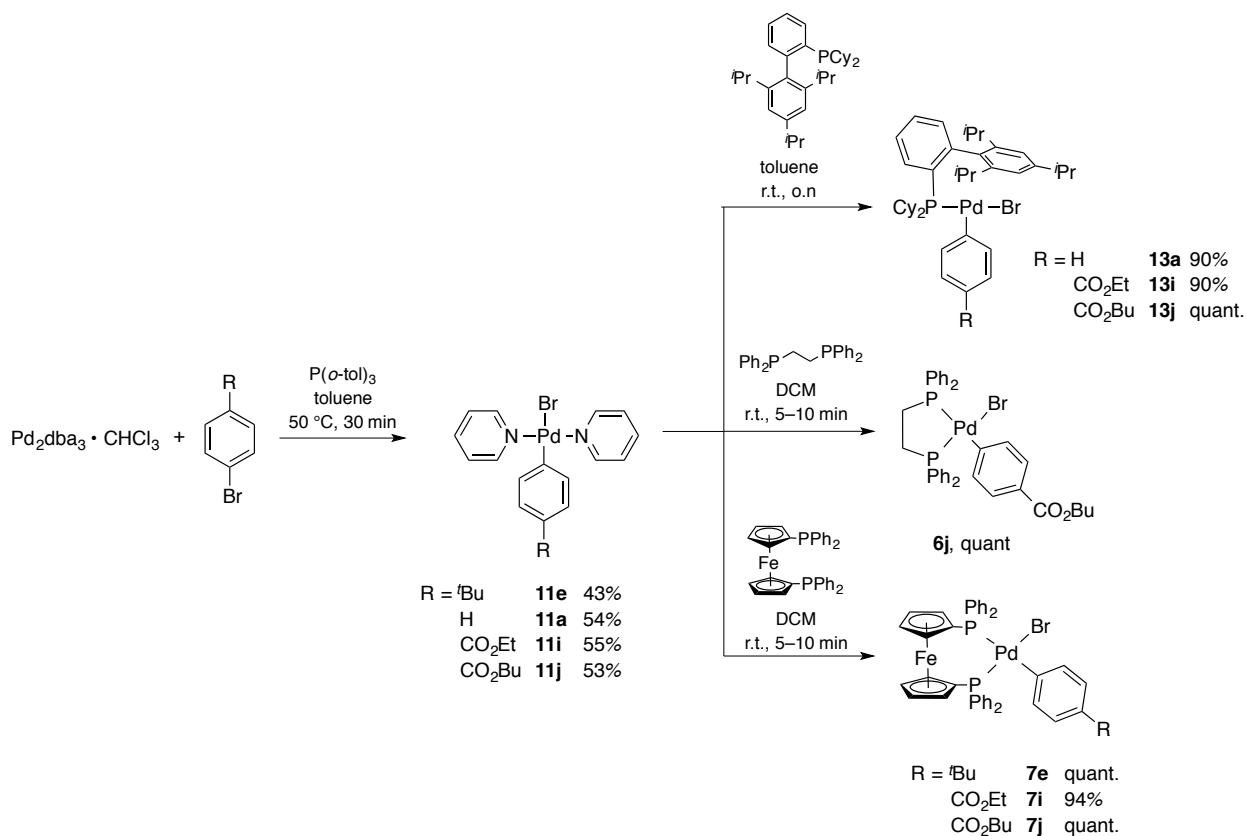
Scheme 16. Syntheses of arylpalladium(II) bromide complexes derived from dipyridine-ligated precursor **11**.
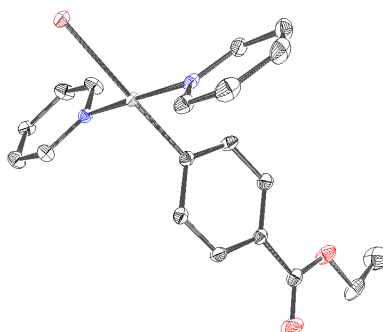
Figure 4. ORTEP 3 diagrams of dipyridine arylpalladium(II) precursor **11i**. Thermal ellipsoids are drawn at 30% probability level. Hydrogen atoms were omitted for clarity. Selected bond distances (Å) and angles (deg): Pd–X 2.545, Pd–C 1.992, Pd–N1 2.026, Pd–N2 2.031.

Single crystals suitable for X-ray diffraction analysis of dipyridine arylpalladium(II) bromide complex **11i** were grown. The solid state structure of **11i** shows the *trans*-configured square-planar complex, where the rings of two pyridine ligands and the aryl ligand are oriented perpendicular to the plane of the complex (figure 4). Only two crystal structures of dipyridine palladium complexes have been reported of the fluoride analogues of **11a** and **11e**, which show that the planes are twisted towards each other,[76a] and is in contrast to the structure of **11i**. With the exception of the Pd-X bond, all Pd-ligand bond distances are similar to those reported for the fluoride complexes and are 1.99 Å for the

Pd-C bond, and 2.03 Å for the Pd-N bonds. As expected, the ester substituent of **11i** is coplanar with

the aryl ring, such that the carbonyl group and the aromatic system are in conjunction.

To have a full set of coordinatively unsaturated arylpalladium(II) complexes for our transmetalation

study, we chose P^{t}Bu$_3$-ligated complexes, which are known to exist as T-shaped monomers[59a] and are

superior soluble in almost all organic solvents due to the very lipophilic and bulky trialkyl phosphine

ligand. Their syntheses have been described analogously to the P(o-tol)$_3$-ligated complexes **5** by

oxidative addition of the aryl bromide to either Pd$_2$dba$_3$ in the presence of P^{t}Bu$_3$ or directly to

Pd(P^{t}Bu$_3$)$_2$.[7e, 59a, 65, 77] We synthesized the complexes **14** from Pd(P^{t}Bu$_3$)$_2$ in the presence of P^{t}Bu$_3$·HBr

in catalytic amounts to facilitate product formations. P^{t}Bu$_3$·HBr was previously shown to be generated

in situ and catalyzes the oxidative addition by formation of L$_2$Pd(H)Br as intermediate, which reacts

faster with the aryl bromide.[78] The desired complexes **14** were isolated in good yields between 57%

and 88%, with the exception of methoxy-substituted complex **14d**, which could be isolated only in a

poor yield of 21% (table 5). Moreover, it turned out that **14d**, as well as the other complexes with

electron-rich aryl ligands (**14e** and **14f**), are only stable in the solid state and decomposed relatively

fast in solution. In addition, the attempted synthesis of the cyano-substituted complex **14l** provided

only a mixture of two complexes (observed by ^{31}P NMR), which might consists of the desired

complex **14l** and presumably a complex, where the 4-bromobenzonitrile coordinates to the vacant

coordination site of complex **14l**. The complexes with methoxy (**14d**),[65] fluoro (**14g**),[59a] and

trifluoromethyl (**14k**)[7e, 77b] substituents, as well as the phenylpalladium(II) complex **14a**[59a] have been

previously reported.

Table 5. Syntheses of P^{t}Bu$_3$-ligated arylpalladium(II) bromide complex **14**.
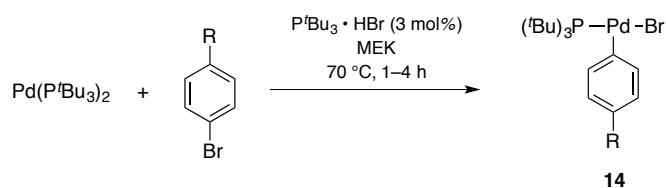
entry	R		yield [%]
1	OMe	**14d**	21
2	^{t}Bu	**14e**	61
3	Me	**14f**	60
4	H	**14a**	80
5	F	**14g**	77
6	CO$_2$Et	**14i**	60
8	CF$_3$	**14k**	57

1.3.2 Syntheses of defined arylzinc reagents

In order to obtain reliable results from our intended transmetalation study, we have to prepare defined arylzinc reagents of known composition. One requirement was that the solution does not contain remaining aryl halide, from which the arylzinc reagents are made. The unreacted aryl halide would react with the palladium(0) species, which is formed after reductive elimination to give a new arylpalladium(II) intermediate. The intermediate can then also undergo competing transmetalation with the arylzinc reagent and would additionaly lead to coupled products of the arylzinc reagent. This would result in errors of the product ratios of the biaryls, which we finally quantify to determine the relative reaction rates. The second requirement is that the arylzinc reagent must not contain any salt impurities, such as LiCl, MgX_2 or ZnX_2, because we also intend to investigate the influences by salt additives on the relative reaction rates and compare the results with the salt-free reaction. The simplest way to realize that is the preparation and isolation of corresponding diarylzinc compounds **15**, which can be converted into the arylzinc halides **16** by mixing them with ZnX_2.

While the unsubstituted diphenylzinc (**15a**) is commercially available, the other substituted diarylzincs **15** had to be prepared. A lot of procedures for the preparation of diverse organozinc reagents has been developed mainly by Knochel and co-workers,[79] however, only few examples for the isolation of **15** can be found in the literature. Hofstee *et al.* prepared the corresponding ditolylzinc compounds by transforming the tolyl bromides into the Grignard reagent and transmetalation to 0.5 equivalents of $ZnCl_2$.[80] The crude product was redissolved in benzene, the insoluble salts were filtered off and the solvent removed. Recrystallization from toluene was reported to provide analytically pure diarylzincs. Attempted synthesis of analogues di-*para*-tolylzinc (**15f**) by this procedure provided also spectroscopically pure product **15f**, however, quantification of the purity by integration of the product signals versus TMB (1,3,5-trimethoxybenzene) as internal standard revealed a purity of only 62%, which indicates the presence of a lot of NMR silent inorganic salt impurities. We additionally attempted precipitation of the inorganic salts from the reaction mixture by addition of dioxane,[81] however the final product was obtained in a low purity of 42%, as well.

Organ and co-workers reported recently that MgX_2 byproduct can be quantitatively removed by cooling the solution to −78 °C and centrifugation, which resulted in a clear salt-free supernatant solution.[41] We followed their procedure with the exception that we filtered off the precipitated salts, however, we could not obtain higher degrees of purity. A similar procedure was reported by Charette and co-workers, who transmetalated the Grignard reagent to $Zn(OMe)_2$ instead of $ZnCl_2$.[82] The formed $Mg(OMe)_2$ was described to be completely insoluble in Et_2O and could be separated from the zinc reagent by centrifugation. However, the claim of a salt-free arylzinc reagent from both procedures,

described by Organ, Charette and their co-workers, was based on a subsequent palladium-catalyzed coupling reaction, which is supposed to be highly affected even in the presence of traces of inorganic salts. They did not isolate the arylzinc compounds to quantify their actual purity.

Therefore, we sought a different procedure to isolate diarylzinc compounds and found that diphenylzinc and some other tolyl- and anisylzinc reagents can be isolated by sublimation.[41, 80] We attempted again the isolation of di-*para*-tolylzinc (**15f**) by sublimation of the product, which finally delivered the pure product **15f** in 31% (scheme 17). We could also isolate pure methoxy-substituted zinc reagent **15d** in a yield of 44%. Encouraged by these results, we attempted also the isolation of diarylzinc reagents **15i** and **15k** with electron-withdrawing substituents, however sublimation resulted in decomposition of the crude products.

R = OMe	**15d**	44%
		(purity: 103%, step 1.: THF, r.t. to 50 °C)
Me	**15f**	31%
		(purity: 111%, step 1: Et$_2$O, r.t.)
CO$_2$Et	**15i**	decomposed
CF$_3$	**15k**	decomposed
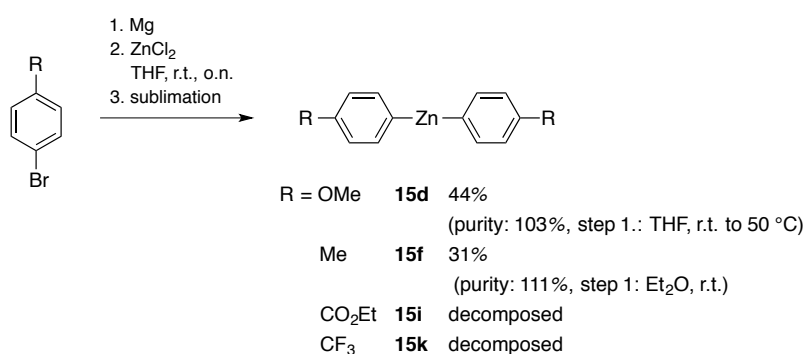
Scheme 17. Syntheses of diarylzinc compounds **15**. Purity was determined by ^{1}H NMR integration of product signals *vs.* TMB as internal standard.

To include also arylzinc reagents with electron-withdrawing *para*-substituents in our study, we finally decided to prepare arylzinc chloride solutions with a known composition. Therefore, we used ^{i}PrMgCl·LiCl, which is also known as "turbo Grignard" and proved to be efficient in the synthesis of even sensitive organozinc reagents.[83] The desired arylzinc reagents are formed by *in situ* formation of the corresponding Grignard at low temperatures of –30 °C from the aryl iodides, and subsequent transmetalation to ZnCl$_2$. The advantage over the classical procedure, which is the formation of the aryl Grignard reagent from the aryl bromide with elemental magnesium at room temperature, is that the low temperatures prevent potential side reactions with electrophilic substituents at the arene. For instance the ester group would react with the Grignard to give the corresponding ketone.

Following this procedure, we synthesized solutions of arylzinc chloride reagents **16** from the corresponding aryl iodides and removed the volatiles to eliminate *iso*-propyl iodide. The residues were redissolved in THF and the concentration was determined by quenching aliquots with iodine and measuring the amount of aryl iodide by GC-FID. To quantify also unreacted aryl iodide, we quenched additional aliquots with methanol and measured the amount of remaining aryl iodide. We found full

conversion and quantitative formation of the desired products **16i** and **16k** with the electron-withdrawing *para*-substituents (scheme 18). Unreacted aryl iodides were observed in cases of the phenylzinc chloride **16a** and reagents with electron-donating substituents **16d** and **16f**. The solvent of these solutions was again removed and the remaining residue washed with pentane to finally eliminate the unreacted aryl iodides. The residues were again redissolved in THF and the concentrations determined by GC-FID, which then showed that the undesired impurities were removed.

R = OMe	**16d**	80%
Me	**16f**	84%
H	**16a**	38%
CO$_2$Et	**16i**	95%
CF$_3$	**16k**	105%
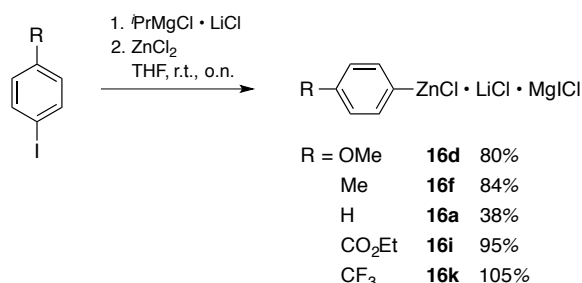
Scheme 18. Preparation of solutions of arylzinc chlorides **16**. Yields are approximated yields.

1.3.3 Development of transmetalation conditions

We intended to start our transmetalation study with PhZnCl (**16a**) and arylpalladium(II) complexes **2**, which have to be in excess to simulate pseudo-zeroth order dependence. To ensure that the unreacted excess of **2** does not undergo side reactions after transmetalation, such as homocoupling in the hot GC injector, remaining complexes **2** have to be quenched for instance by reduction, which would produce volatile arenes that should not overlap with the peaks of biaryl analytes in the GC-FID chromatogram. The reducing reagent must fully convert the aryl ligand of **2** into the corresponding arene and must not react with the attached functional groups. To find a proper quenching procedure for the transmetalation samples, we tested some reducing reagents in the reduction of ester-substituted complex **2j** and quantified the resulting butyl benzoate by GC-FID.

It was reported that Et$_3$SiH reduces aryl iodides in the presence of catalytic amounts of PdCl$_2$,[84] which forms an intermediate arylpalladium(II) complex, which becomes reduced by Et$_3$SiH. Encouraged by this report, we attempted the reduction of **2j** in the presence of Na$_2$CO$_3$, however the conditions provided only 44% of the benzoate (table 6, entry 1). Measurements of the same sample after a longer period (3 h and 5 h) revealed a decrease in the yield, which was due to the formation of methyl benzoate resulting from transesterification with the co-solvent MeOH. MeOH was used as co-solvent to quench possibly unreacted arylzinc reagent in the actual transmetalation samples. A sample without Et$_3$SiH, under otherwise identical conditions (entry 2), showed that transesterfication occurs solely by

reaction with the carbonate base and MeOH. The base was required for the reaction to trap the HI formed by reaction of the byproduct Et_3SiI with the solvents methanol and THF.[85] We also tested $NaBH_4$, as hydride source to reduce **2j**, however, the reaction provided only about 50% yield of the butyl benzoate (entry 3), which is even lower than simple decomposition of **2j** in the solvent mixture (entry 6). Attempts to decompose **2j** in the presence of AcOH, which was thought to protonate the aryl ligand, did not give quantitative yields, neither (entry 5). However, using NH_4HCO_2, which has been applied as hydrogen transfer reagent for the dehalogenation of arenes,[86] provided quantitative yields of the desired benzoate (entry 4).

Table 6. Reduction of arylpalladium(II) complexes **2**.

entry	[red.]	yield[a] [%] of butyl benzoate after		
		1 h	3 h	5 h
1[b]	Et_3SiH, Na_2CO_3	44	10	5
2[b]	Na_2CO_3	21	3	2
3	$NaBH_4$	46	56	49
4	NH_4HCO_2	85	107	102
5	AcOH	11	65	83
6	none	21	60	61

[a]GC yields.
[b]Transesterfication was observed.

To verify that the other arylpalladium(II) complexes **2** with the different substituents are compatible with the reduction conditions, but also with the transmetalation conditions, we performed non-competitive transmetalations experiments using 8 equiv. of each complex **2** with respect to the zinc reagent **16a**. To solutions of the differently substituted complexes **2a–m** in dry THF a stock solution of PhZnCl (**16a**), which was prepared by dissolving Ph_2Zn (**15a**) and $ZnCl_2$ in THF, was added. The reaction solutions were stirred at room temperature for 1 h, before they were quenched with a stock solution of TMB in MeOH and a spatula tip of NH_4HCO_2. After 1 h of additional stirring, the samples were filtered through a small plug of Celite and the filtrates were directly transferred into GC vials. To avoid errors by deviations, caused by different concentrations of the stock solutions or reaction times and temperatures, all reactions were set up at the same time.

Quantification of the biaryl products **17aa–am** by GC-FID revealed that the most electron-withdrawing nitro substituent and the most electron-donating phenyl ether are not compatible with the transmetalation conditions, as judged by the low yields of the coupled products (table 7, entries 1 and 12), whereas the other substituents delivered almost quantitative yields. The exceptions were the ester-

and chloro-substituted complexes **2i** and **2h**, which were reduced in yields of only 75% and 76% (entries 7 and 8). The low yield for the coupling product derived from transmetalation with chloro-substituted complex **2h** was probably due to its low solubility in THF. In case of the ester-substituted complex **2i**, the yields slightly decreased after each measurement (entry 8), which might indicate transesterification of the ethyl benzoate, however, the chromatogram of the sample did not show the formation of methyl benzoate as byproduct.

Table 7. Non-competitive transmetalations of complexes **2** with phenylzinc **16a**.
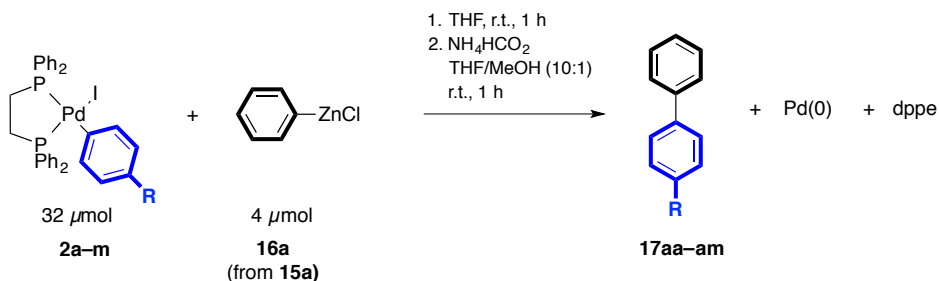
entry	R	2x	1st	2nd	3rd	avg.	Std. dev.
			yield [%] of **17** from measurement No.			
1	OPh	c	18	14	17	16	2
2	OMe	d	99	96	96	97	2
3	^{t}Bu	e	98	97	97	98	1
4	Me	f	96	95	94	95	1
5	H	a	106	103	108	106	3
6	F	g	102	101	98	101	2
7	Cl	h	75	74	76	75	1
8	CO_2Et	i	84	76	69	76	8
9	$CO_2{}^nBu$	j	97	92	97	95	3
10	CF_3	k	93	93	94	93	1
11	CN	l	92	92	92	92	0
12	NO_2	m	19	17	17	18	1

During the progress of our transmetalation study, we also investigated the influence of additives, such as salts or ligands, on the relative reactivities of complexes **2** and recognized that significant matrix contaminations, in particular at higher additive concentrations, resulted in large errors for the quantifications of the biaryls **17** by GC measurements. Therefore, we were seeking for an alternative work-up of the transmetalation samples and found that removal of the solvent in vacuum and re-dissolution of the analytes of interest in pentane or Et$_2$O provided the best results. Because the complexes are typically not soluble in pentane or Et$_2$O, their excess can be eliminated together with the additives by filtration of the re-dissolved sample solutions. To validate this method, three competition experiments between the ester- (**2i**) and the methoxy-substituted (**2d**) complexes with PhZnCl (**16a**) were carried out under authentic transmetalation conditions. Two samples were prepared by the alternative work-up and one sample was reduced by treating the reaction solution with MeOH and NH$_4$HCO$_2$ (table 8). Additionally, a control sample was prepared from the calibration

solution, which contained the biaryls **17ai** and **17ad** and was treated according to the alternative work-up to verify the biaryls are soluble in the unpolar solvents and to exclude any systematic errors.

Table 8. GC results for the validation of the alternative work-up by re-dissolution of transmetalation samples.

measurement	w/ pentane yields [%]		w/ Et$_2$O yields [%]		Cal. std. 5 w/ Et$_2$O recov. **17** [%]		reduction w/ NH$_4$HCO$_2$ yields [%]	
No.	**17ad**	**17ai**	**17ad**	**17ai**	**17ad**	**17ai**	**17ad**	**17ai**
1	75	4	58	0	102	112	87	4
2	81	6	77	11	100	107	71	0
3	79	5	71	9	98	104	76	2
4	80	5	70	8	99	108	95	3
5	75	4	72	8	109	130	93	4
6	81	5	71	8	94	96	66	0
7	79	4	65	0	96	97	76	0
8	84	5	82	12	91	89	98	0
9	77	4	70	7	100	101	72	0
Avg. [%]	**79**	**5**	**71**	**7**	**99**	**105**	**81**	**1**
Std. dev.	3	1	7	4	5	12	12	2
Std. error [%]	1	0	2	1	2	4	4	1

The samples were measured nine times by GC-FID, to identify variations of the results by the instrument. The GC results of the control sample showed full recover of the biaryl analytes **17ad** and **17ai** (table 8, column 4). Nonetheless, the deviations within a series of measurements ranges from 91% to 109% of the recovered biaryl for **17ad** and 89% to 130% for **17ai**, which implies a relatively large instrumental error, however, is still in an acceptable limit of less than 10%. Determining the yields of the corresponding biaryls **17** from the transmetalation samples gave overall much higher yields of the methoxy-substituted biaryl **17ad** than for the ester-substituted **17ai**, indicating faster transmetalation with **2d**. The yield of **17ad** obtained from the sample, which was re-dissolved with pentane (column 2), was 79% with a standard deviation of 3%. This is comparable to the sample, which was quenched by MeOH/NH$_4$CO$_2$H (column 5), and gave 81% yield for **17ad**. The yield of biaryl **17ad** from the sample, which was re-dissolved with Et$_2$O (column 3), was a bit lower with 71%, however comparable with the other samples, with respect to the associated standard deviation of 7%. These results demonstrate, that evaporation of the transmetalation samples in vacuum, and subsequent re-dissolution of the analytes with pentane or Et$_2$O is a viable work-up. Nevertheless, this approach of re-dissolution in pentane was mainly used for experiments at later point in the study.

1.3.4 Reactivity of (dppe)Pd(Ar)I complexes with arylzinc reagents

We started our transmetalation study with *cis*-configured arylpalladium(II) complexes, because isomerization of the *cis* intermediate *cis*-**I-2**, which is the direct outcome of the preceding oxidative addition, to its *trans* isomer *trans*-**I-2** is less probable under catalytic conditions of the Negishi reaction, since the transmetalations with organozinc reagents are probably faster. Dppe-ligated arylpalladium(II) complexes **2** were chosen as model complexes for the investigation of the transmetalation at *cis*-configured complexes. For the transmetalation experiments, all possible combinations of each two differently substituted complexes **2** were investigated in the transmetalation with PhZnCl (**16a**). Substituted complexes **2**, which proved to be unsuitable under the reaction conditions (*cf*. table 7), were excluded from this study. To reduce systematic errors, all combinations (24–27 samples) were set-up and reacted at the same time. One transmetalation set-up was repeated at least one time, however, if the resulting Hammett constants significantly deviated from each other, two additional set-ups were performed.

All possible combinations of differently substituted complexes **2** used for the competition experiments are outlined in table 9. The combination of the complexes **2a/2g** could not be used, because the peaks of the resulting biaryls **17aa** and **17ag** could not be fully separated from each other in the GC. The obtained relative reaction rates $k(R^1)/k(R^2)$ were normalized to $k(R^1)/k(H)$ and corrected to take into account that the ratio of the complexes **2** changes slightly during the course of the reaction (see Mathematical Section 7.1, equations 14–28).[7h] The logarithm of the normalized ratios $k(R^1)/k(H)$ were plotted in terms of a Hammett diagram, which consist of at least 162 data points resulting form three measurements of each individual sample of two transmetalation set-ups. The advantage of the high number of data points is the decrease of the error for the linear regression. Obvious outlying data points were removed from analysis.

Table 9. Possible combinations of complexes **2** for the competition experiments.

	OMe (2d)	*t*Bu (2e)	Me (2f)	F (2g)	CO$_2$Et (2i)	CF$_3$ (2k)	CN (2l)
H (2a)	A1	A2	A3	x	A4	A5	A6
OMe (2d)		B1	B2	B3	B4	B5	B6
*t*Bu (2e)			C1	C2	C3	C4	C5
Me (2f)				D1	D2	D3	D4
F (2g)					E1	E2	E3
CO$_2$Et (2i)						F1	F2
CF$_3$ (2k)							G2

The data from the competition experiments of complexes **2** with PhZnCl (**16a**) gave a good Hammett correlation ($R^2 = 0.96$) with a negative Hammett constant of $\rho = -1.47$ (figure 5), which indicates that the electron-donating substituents on the aryl ligand facilitate the transmetalations. This reactivity trend is surprising, because electron-withdrawing substituents increase the electrophilicity of the palladium(II) center, which should increase the reactivity towards the nucleophile **16a**. Therefore, a positive Hammett constant ρ_{obs} would be expected like it was observed for the transmetalations by Lei and co-workers for Sonogashira couplings[5] and by Denmark and co-workers for the Denmark-Hiyama couplings.[7e] In these studies, the Hammett constants ρ_{obs} were determined by measurements of absolute reaction rates, which provide the reactivity trends for the rate-limiting step. In contrast, competition experiments provide a Hammett constant ρ_{obs}, which consists of the Hammett constants $\rho_{\pm n}$ of all individual steps, in which the electronic properties of the aryl ligand influences the reactivities, until the first irreversible steps. Considering this, the observed negative Hammett constant ρ_{obs}, obtained from the competition experiments with the complexes **2**, suggests that there exists at least one additional step with the opposite reactivity trend prior to the actual aryl transfer event assuming an irreversible reductive elimination.
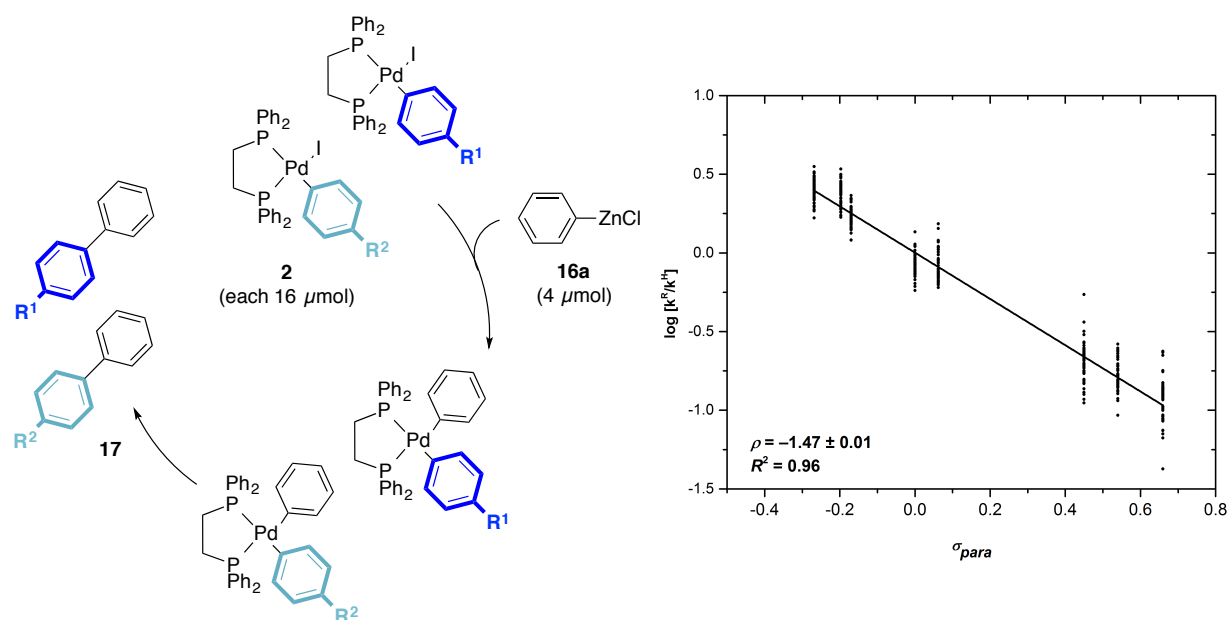
Figure 5. Competition experiments of arylpalladium(II) complexes **2** with PhZnCl (**16a**) and the resulting Hammett plot.

Considering that transmetalations in other cross-coupling reactions have been proposed to proceed via several steps from intermediate **I-1** to **I-2**, at which reductive elimination occurs, it is conceivable that the transmetalation with organozinc reagents also proceeds via a multi step mechanism. Regarding the experimental results from the competition experiments, which suggests that a step, occurring prior to the actual transfer of the aryl group from zinc to palladium, is favored for electron-enriched complexes **2**, one plausible mechanistic scenario might be the formation of a cationic palladium(II) complex

[**2**(thf)]$^+$ (scheme 19, dissociative mechanisms), which is similar to the mechanistic proposal for Stille reactions with organo pseudohalides, but also with organo halides in coordinating solvents (*cf.* pathway C, scheme 5). The dissociation of the halide ligand of complex **2** might be rather an associative ligand substitution with a solvent molecule to give the THF-stabilized cationic complex [**2**(thf)]$^+$ under release of the iodide ligand. Because cationic metal centers are stabilized by electron-donating ligands, the formation of [**2**(thf)]$^+$ would be favored for complexes **2** with electron-donating substituents at the aryl ligand, which would lead to a negative Hammett constant ρ_1.

As already mentioned, the THF-for-halide substitution is an associative ligand substitution, which depends usually on the concentrations of both reactants (**2** and THF, but not **16a**), however, due to the large excess of the solvent (pseudo-zero order), the rate law becomes only dependent in concentration (and nature) of complex **2**. Therefore, the rate law for the formation [**2**(thf)]$^+$ is kinetically indistinguishable from a dissociative ligand exchange, where the iodide ligand first dissociates followed by coordination of the solvent molecule. Due to this kinetic fact, a transmetalation mechanism proceeding via a cationic intermediate [**2**(thf)]$^+$ is only referred to as dissociative mechanism in the following discussion.
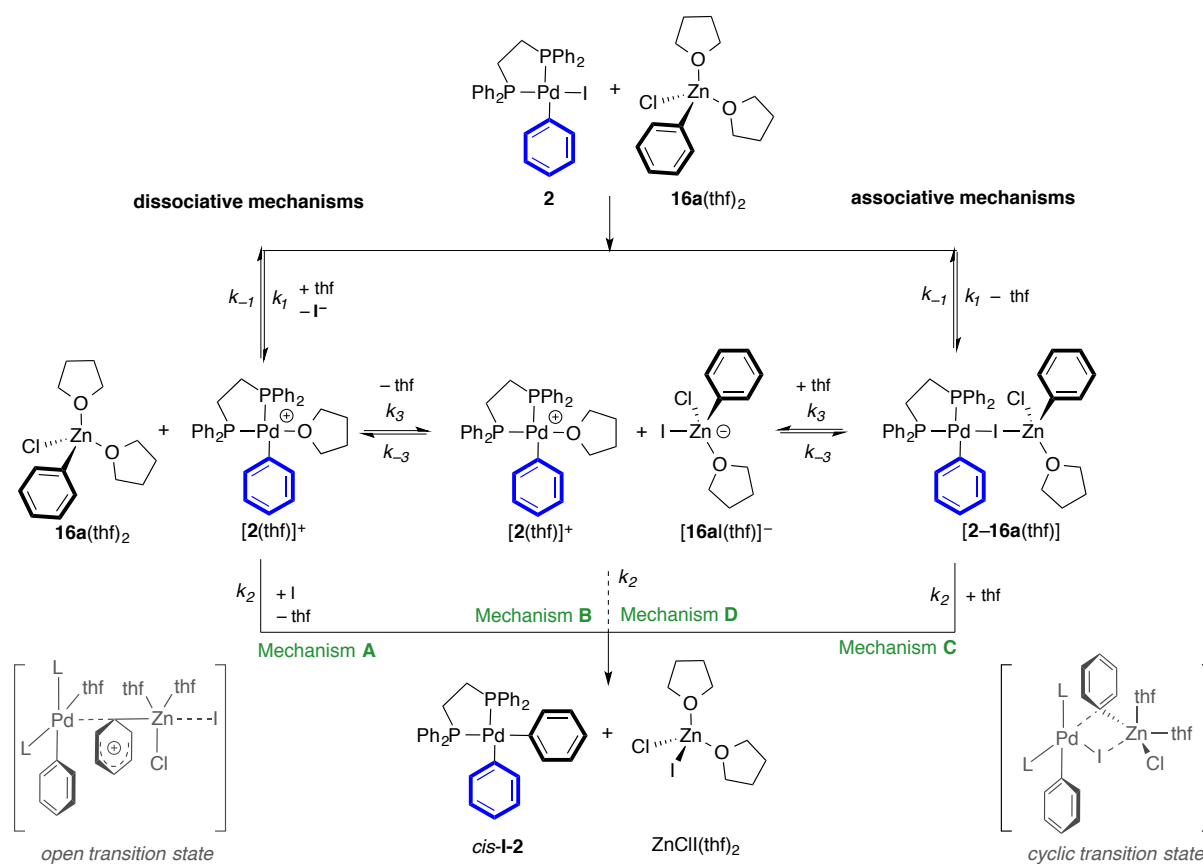
Scheme 19. Conceivable stepwise transmetalation mechanisms.

The cationic species $[2(thf)]^+$ might then undergo transmetalation with arylzinc reagent **16a** via an open transition state (scheme 19, dissociative mechanism A), which can be compared with an electrophilic *ipso* substitution, where the positive charge is delocalized at the transferred aryl group, similar to a Wheland-type intermediate. However, the dissociated free halide ion must be involved in the transition state, so that the aryl transfer is a trimolecular process, otherwise a positively charged zinc species, which is very unlikely, would result. Since it is known, that organozinc reagents form zincates in the presence of halide ions,[39a, 39b] it is more likely that the dissociated halide ligand coordinates to the arylzinc reagent **16a** to form a zincate $[16aX(thf)]^-$ (dissociative mechanism B), which then undergoes the transmetalation with cationic complex $[2(thf)]^+$ via an open transition state.

It is also conceivable that an intermediate Pd/Zn dimer $[2–16a(thf)]$ is formed, where the Lewis acidic zinc(II) center of arylzinc reagent **16a** coordinates to the halide ligand of complex **2** (scheme 19, associative mechanisms). The formation of a halide-bridged intermediate was found by Espinet and co-workers by DFT calculations in the transmetalation of *trans*-**I-1** $L_2Pd(Me)Cl$ with $MeZnCl$ or $ZnMe_2$ to give *trans*-**I-12** (*cf.* scheme 11).[46b, 46c] Analogous hydroxide-bridged intermediates were proposed for the transmetalation in Suzuki reactions, where the boronic acid is bridged with **I-1** via a hydroxide ligand (*cf.* intermediate *trans*-**I-6**, scheme 6). The halide-bridged intermediate $[2–16a(thf)]$ can either directly undergo transmetalation via a cyclic transition state (associative mechanism C), or it dissociates into the ionic intermediates $[2(thf)]^+$ and $[16aX(thf)]^-$ (associative mechanism D), from which the transmetalation occurs via an open transition state.

The mathematical derivations of the observed Hammett constants ρ_{obs} for the possible mechanistic scenarios (table 10, equations 5–12, for details, see Mathematical Section) show that all mechanisms would result in a negative Hammett constant ρ_{obs} from competition experiments with differently substituted arylpalladium(II) complexes **2**, if the individual Hammett constant ρ_2 for the final step, where the aryl group is transferred from zinc to palladium, is not much larger in magnitude (i.e. much more positive) than the Hammett constants for the involved pre-equilibria with $\rho_{\pm 1}$ and $\rho_{\pm 3}$, respectively. However, adopting this assumption to the competition experiments, where two arylzinc reagents **16** compete for complex **2**, the Hammett constant ρ_{obs} would be positive, which is in contrast to previous results by Mayr and co-workers, who studied the relative reactivity of methyl- and ester-substituted arylzinc iodides in competition experiments with triphenylphosphine-ligated *trans* complexes **9**.[7h] These authors found that the magnitude of the Hammett constant ρ_{obs} decreases using a less electrophilic arylpalladium(II) complex **9** (**9l** *p*-CN: $\rho = -0.95$; **9h** *p*-Cl: $\rho = -0.56$). A negative Hammett constant ρ_{obs} is obtained only if the final step with the individual Hammett constant ρ_2, is much larger in magnitude (strongly negative) than for the involved pre-equilibria with $\rho_{\pm 1}$ and $\rho_{\pm 3}$, respectively. The exception is the scenario of the dissociative mechanism, where the aryl transfer

occurs via a trimolecular transition state. Here, the observed Hammett constant ρ_{obs} depends only on the last step, which would have a negative Hammett constant ρ_2 with respect to the arylzinc reagent **16**, since the dissociation of the halide ligand from complex **2** is independent on the arylzinc reagent **16**.

Table 10. Derived equations for observed Hammett constants ρ_{obs} regarding the possible mechanistic scenarios.

	with respect to complex **2** $(\rho_2, \rho_{-1}$ and ρ_{-3} are positive ρ_1 and ρ_3 are negative)		with respect to arylzinc reagent **16** $(\rho_2, \rho_{-1}$ and ρ_{-3} are negative ρ_1 and ρ_3 are positive)	
(dissociative mechanism **A**)	$\rho_2 + \rho_1 - \dfrac{k_{-1}\rho_{-1} + k_2\rho_2[\mathbf{16}]}{k_{-1} + k_2[\mathbf{16}]}$	(eq. 5)	$\rho_2 - \dfrac{k_2\rho_2[\mathbf{16}]}{k_{-1} + k_2[\mathbf{16}]}$	(eq. 9)
(dissociative mechanism **B**)	$\rho_2 + \rho_1 - \dfrac{k_{-1}\rho_{-1} + k_2 K_{\pm 3}\rho_2[\mathbf{16}]}{k_{-1} + k_2 K_{\pm 3}[\mathbf{16}]}$	(eq. 6)	$\rho_2 + \rho_3 - \rho_{-3}$ $- \dfrac{k_2 K_{\pm 3}(\rho_2 + \rho_3 - \rho_{-3})[\mathbf{16}]}{k_{-1} + k_2 K_{\pm 3}[\mathbf{16}]}$	(eq. 10)
(asssociative mechanism **C**)	$\rho_2 + \rho_1 - \dfrac{k_{-1}\rho_{-1} + k_2\rho_2}{k_{-1} + k_2}$	(eq. 7)	$\rho_2 + \rho_1 - \dfrac{k_{-1}\rho_{-1} + k_2\rho_2}{k_{-1} + k_2}$	(eq. 11)
(asssociative mechanism **D**)	$\rho_{\pm 1} + \rho_2 + \rho_3 - \dfrac{k_{-3}\rho_{-3} + k_2\rho_2}{k_{-3} + k_2}$	(eq. 8)	$\rho_{\pm 1} + \rho_2 + \rho_3 - \dfrac{k_{-3}\rho_{-3} + k_2\rho_2}{k_{-3} + k_2}$	(eq. 12)

With $\rho_{\pm 1} = \rho_1 - \rho_{-1}$

To investigate the reactivity trends of the arylzinc reagent **16** in more detail, we also performed the corresponding competition experiments with differently substituted competing arylzinc chlorides **16** and dppe-ligated complexes **2a** and **2d** (scheme 20). Unfortunately, it was impossible to isolate salt-free arylzinc reagents with electron-withdrawing substituents, such as trifluoromethyl or ester groups. Nevertheless, we were able to prepare solutions of differently substituted arylzinc reagents **16** with a defined composition from the corresponding aryl halides by using ^{i}PrMgCl·LiCl. Transmetalation experiments with these solutions provided a Hammett constant of $\rho = -1.13$ ($R^2 = 0.84$) in the reactions with phenyl complex **2a** (figure 6), which is in line with the findings by Mayr and co-workers.[7h] However, in contrast to their results, the competition experiments with less electrophilic arylpalladium(II) complex **2d** provided an even more negative Hammett constant of $\rho = -1.50$ ($R^2 = 0.83$), while Mayr and co-workers observed a less negative value. Although the error of the Hammett correlation is relatively high, which is the result of poorer quantification by GC-FID due to the high salt content of the reaction solutions, the results of the competition experiments clearly show a negative Hammett constant ρ_{obs}, which becomes more negative using the less electrophilic complex **2d**.
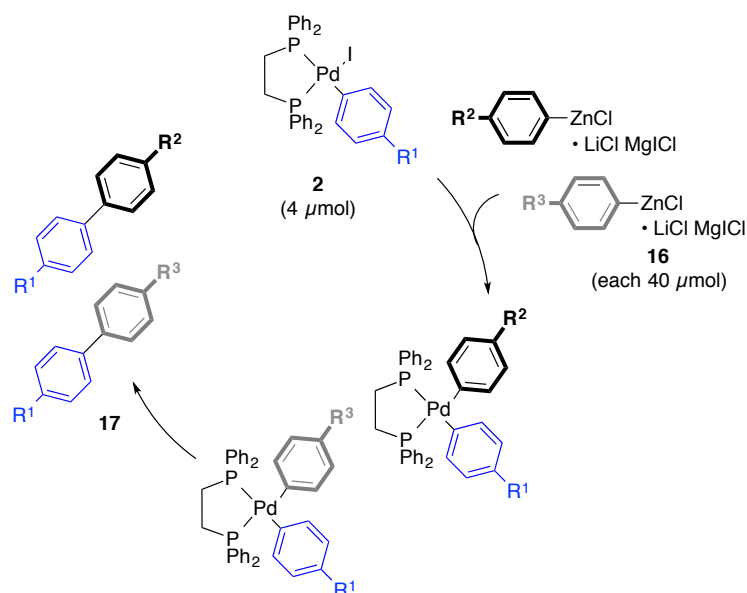
Scheme 20. Competition experiments between differently substituted arylzinc chloride solutions of **16** and complexes **2a** and **2b**.
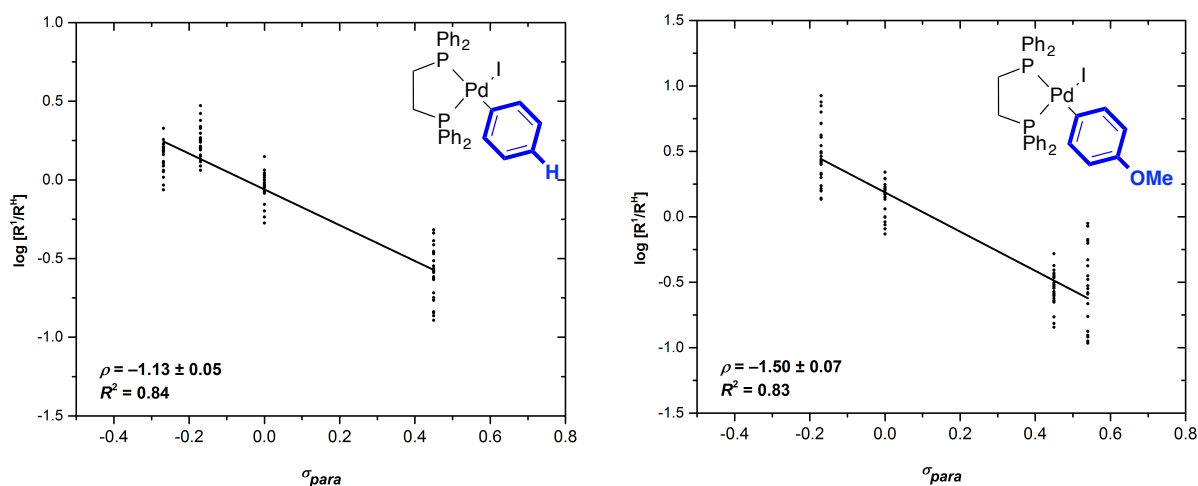
Figure 6. Hammett plots obtained from competition experiments of ArZnCl (**16**) with complexes **2a** and **2d**.

The more negative Hammett constant ρ_{obs}, obtained from competition experiments with the less electrophilic complex **2d**, might be explained by the equations of the expected Hammett constants ρ_{obs} (table 10). All contain a negative term, which consists of a weighted average of the individual Hammett constants ρ_2 (final irreversible step with k_2), and ρ_{-1} or ρ_{-3} (back reaction of the product-leading intermediate into its pre-cursor with k_{-1}, or k_{-3}). In the extreme cases, where either k_2 is much faster than $k_{-1/-3}$, or k_2 is much slower than $k_{-1/-3}$ the observed Hammett constants ρ_{obs} approach the simple sums of the individual Hammett constants $\rho_{\pm n}$ for all conceivable mechanistic scenarios (table 11). Accordingly, if the aryl transfer with k_2 becomes essentially slower in competition experiments with competing arylzinc reagents **16** and more electron-rich complex **2**, the situation $k_2 \gg k_{-1}$ turns into the situation with $k_2 \ll k_{-1}$ and the influence of ρ_2 increases. Besides, to observe a negative Hammett

constant ρ_{obs}, the magnitude of ρ_2 must be much larger (more negative) than ρ_{-1} or ρ_{-3}. Considering this, the Hammett constant ρ_{obs} becomes more negative using less electrophilic arylpalladium(II) complexes, being less reactive in the aryl transfer step.

Table 11. Approximation of observed Hammett constants ρ_{obs}

		with respect to complex **2**		with respect to arylzinc reagent **16**	
		(ρ_2, ρ_{-1} and ρ_{-3} are positive ρ_1 and ρ_3 are negative)		(ρ_2, ρ_{-1} and ρ_{-3} are negative ρ_1 and ρ_3 are positive)	
(dissociative mechanism **A**)	$k_2 \gg k_{-3/-1}$ $k_2 \ll k_{-3/-1}$	ρ_1 $\rho_2 + \rho_{\pm 1}$	(eq. 5)	0 ρ_2	(eq. 9)
(dissociative mechanism **B**)	$k_2 \gg k_{-3/-1}$ $k_2 \ll k_{-3/-1}$	ρ_1 $\rho_2 + \rho_{\pm 1}$	(eq. 6)	0 $\rho_2 + \rho_3 - \rho_{-3}$	(eq. 10)
(asssociative mechanism **C**)	$k_2 \gg k_{-3/-1}$ $k_2 \ll k_{-3/-1}$	ρ_1 $\rho_2 + \rho_{\pm 1}$	(eq. 7)	ρ_1 $\rho_2 + \rho_{\pm 1}$	(eq. 11)
(asssociative mechanism **D**)	$k_2 \gg k_{-3/-1}$ $k_2 \ll k_{-3/-1}$	$\rho_{\pm 1} + \rho_3$ $\rho_2 + \rho_{\pm 1} + \rho_{\pm 3}$	(eq. 8)	$\rho_{\pm 1} + \rho_3$ $\rho_2 + \rho_{\pm 1} + \rho_{\pm 3}$	(eq. 12)

With $\rho_{\pm 1} = \rho_1 - \rho_{-1}$

Applying the same considerations about the observed Hammett constant ρ_{obs}, made for the competition experiments with competing arylzinc reagents **16**, the corresponding competition experiments with competing complexes **2** would result in a less negative Hammett constant ρ_{obs} with a less reactive, more Lewis acidic arylzinc reagent than **16a**, if ρ_2 is larger than $\rho_{\pm 1}$, or $\rho_{\pm 3}$. However, if ρ_2 is smaller, the observed Hammett constants ρ_{obs} becomes more negative. To test this hypothesis, we investigated the influence of the Lewis acidity of the arylzinc reagent on the relative reaction rates of competing complexes **2** in more detail. Therefore, we performed competition experiments with PhZnBr (**18a**), PhZnI (**19a**), Ph$_2$Zn (**15a**) and 4-tolZnCl (**16d**) as nucleophiles. Interestingly, the competition experiments with phenylzinc halides **18a** and **19a** resulted in even more negative Hammett constants ρ_{obs} (figure 7). With PhZnBr (**18a**) a Hammett constant of $\rho = -1.70$ ($R^2 = 0.99$) was obtained, with PhZnI (**19a**) the Hammett constant of $\rho = -1.66$ ($R^2 = 0.95$) was slightly less negative than with **18a**, but equal within the error margin. Nevertheless, the Hammett constants ρ_{obs} seem to correlate with the Lewis acidity of the arylzinc reagent. The Lewis acidity of the corresponding zinc salts ZnX$_2$ were reported to increase in the order ZnCl$_2$ < ZnI$_2$ < ZnBr$_2$.[87] Under the assumption that this trend also holds for the Lewis acidity of the phenylzinc halides, the chloride **16a** is the weakest Lewis acid and the bromide **18a** the strongest one. The same correlation of Lewis acidity of the arylzinc reagent with the Hammett constant ρ_{obs} was also observed with *para*-substituted arylzinc chlorides. Competition

experiments with 4-methoxyphenylzinc chloride (**16d**), which is less Lewis acidic than PhZnCl (**16a**),
because the electron-donating group increases the electron density at the zinc(II) center, resulted in a
Hammett constant of $\rho = -1.26$ ($R^2 = 0.94$) (figure 7), which is less negative than with **16a** (*cf.* figure
5).
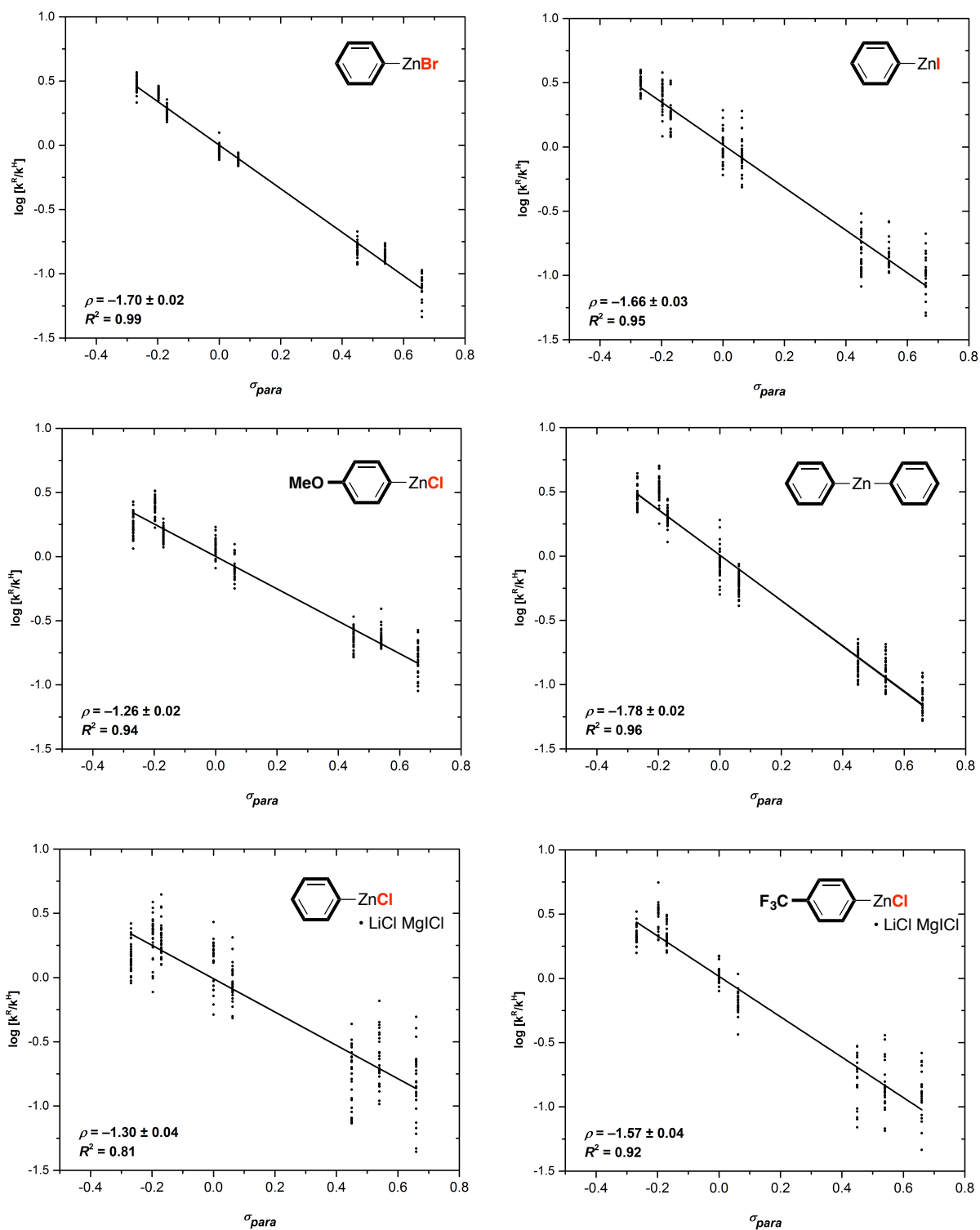
Figure 7. Hammett plots obtained from competition experiments of complexes **2** with other arylzinc reagents.

In addition, we performed the competition experiments with arylzinc reagents with the more Lewis acidic trifluoromethyl-substituted arylzinc reagent **16k** (figure 7), which was prepared as the salt-containing solution, and provided a more negative Hammett constant of $\rho = -1.57$ ($R^2 = 0.92$) compared to **16a**. To properly compare this result with a less Lewis acidic arylzinc reagent, and exclude reactivity influences caused by the salt content of the arylzinc solutions, we performed also the competition experiments with analogously prepared phenylzinc reagent **16a**, which gave a less negative Hammett constant of $\rho = -1.30$ ($R^2 = 0.81$) than with **16k**. These results are also in agreement with the previously made observations that an increased Lewis acidity, which conceivably leads to a slower aryl transfer, results in more negative Hammett constant ρ_{obs}. This clear trend suggests that the magnitude of the Hammett constant ρ_2 of the final aryl transfer with respect to the arylpalladium(II) complex **2** is smaller than ρ_1, which implies that the reactivity of the complexes **2** on the transmetalation is mainly determined by the pre-equilibrium forming the intermediate $[\mathbf{2}(thf)]^+$ or $[\mathbf{2}–\mathbf{16a}(thf)]$. The comparison of the Hammett constants ρ_{obs} for the competition experiments with salt-containing and salt-free solutions of **16a** indicates also that the additional salts (LiX and MgX$_2$) have a significant impact. The Hammett constant ρ_{obs} becomes less negative in the presence of salts (*cf.* figures 5 and 7). Also the quality of the linear regression (expressed with the correlation coefficient R^2) was poorer, which is probably due to the large matrix contamination affecting the quantification by GC-FID.

Surprisingly, the competition experiments with the least Lewis acidic diphenylzinc (**15a**) provided the most negative Hammett constant of $\rho = -1.78$ ($R^2 = 0.96$) in contradiction to the observed trend. Possibly, the electronic influence of the aryl ligand of complexes **2** increases in the actual aryl transfer step, which results in a more positive individual Hammett constant ρ_2. As mentioned above, if the magnitude of ρ_2 is larger than $\rho_{\pm1}$ or $\rho_{\pm3}$, the observed Hammett constant ρ_{obs} becomes more negative. However, it is also possible that the mechanism changes since the steric demand at the zinc(II) center of the diphenylzinc reagent is larger compared to the arylzinc halides.

1.3.5 DFT calculations of transmetalation mechanism

The competition experiments with either competing arylpalladium(II) complexes **2**, or with competing arylzinc reagents **15**–**19** do not allow any conclusions about the exact mechanism. To obtain a more detailed insight into the transmetalation of complexes **2** with arylzinc reagent **16a**, and to identify possible intermediates, we performed DFT calculations using the M06 functional, which has been used for calculations of the Negishi transmetalation by Espinet and co-workers,[46b, 46c] and proven to

provide generally good results for organometallic systems and non-covalent interactions.[88] LanL2DZ

effective core pseudo potentials and basis sets for Pd, Zn, I and Cl and 6-31G(d,p) basis set for C, H,

O and P were used. All calculations were performed with the true dppe-ligated complexes **2** (instead

of smaller model ligands as usually used to save computational cost and time) to ensure most accurate

predictions. Initial calculations with dHpe (= $H_2PCH_2CH_2PH_2$) as smaller model ligand provided

structures, in which interactions of **16a** with the phosphine ligand are predominant. Because those

interactions seemed to us very unlikely with the bulkier dppe ligand, we decided to continue

calculations on the complete complex **2** and the calculation of **16a**(thf) as THF-coordinated tetrahedral

zinc species as it actually exists in solution.[89] Besides the two additional THF molecules, which were

explicitly calculated as ligands to zinc, THF solvation was included for calculations using the

polarizable continuum model (PCM).[90]

Bell-Evans-Polanyi principle   We started with the calculations on the ground state Gibbs free
energies ΔG^0 for the formation of cationic intermediates with the

methyl- ([**2f**(thf)]$^+$) and unsubstituted ([**2a**(thf)]$^+$) aryl ligands. As expected, the THF-stabilized

cationic intermediates [**2**(thf)]$^+$ are less stable by $\approx$ 15 kcal/mol than the neutral complexes **2**, where

[**2f**(thf)]$^+$ is slightly more stable than [**2a**(thf)]$^+$ (figure 8). The lower Gibbs free energy ΔG^0 of

[**2f**(thf)]$^+$ can be rationalized by the more electron-rich aryl substituent, which is able to stabilize the

arising positive charge at the palladium(II) center better than the unsubstituted aryl ligand of [**2a**(thf)]$^+$.

Unfortunately, we were not able to locate the transition state for formation of cationic complexes

[**2**(thf)]$^+$. However, according to the , the relative Gibbs free energy ΔG^0 of [**2f**(thf)]$^+$ and [**2a**(thf)]$^+$

would also qualitatively reflect the relative transition state energy $\Delta G^\ddagger$. Assuming a late transition

state, this allows the prediction that complexes **2** with electron-rich aryl ligands would convert faster

into the cationic intermediate [**2**(thf)]$^+$. Consequently, a negative Hammett constant ρ_1 results for the

dissociation of the halide ligand, and a positive Hammett constant ρ_{-1} for the back reaction to **2** as

expected.

Furthermore, we found that the formation of an arylzincate species [**16I**(thf)]$^-$ is exergonic, as

expected since arylzinc reagents are Lewis acids, and zincates have been previously detected.[39a, 39b]

The calculation of the energy difference between **16a**(thf)$_2$ and [**16aI**(thf)]$^-$ using the standard basis set

and pseudopotential (6-31G** basis set for C, H, and O and LanL2DZ basis set and pseudopotential

for Cl, I and Zn), provided an unrealistic strong negative energy difference of –67.8 kcal/mol relative

to the free iodide ion and **16a**(thf)$_2$. Attempted counter poise correction to account for the different

basis sets was not fruitful and provided also an unrealistic relative energy of –63.7 kcal/mol. However,

using the larger basis set def2QZVP gave a more reasonable energy difference of –6.47 kcal/mol.

Because a large gain of energy is obtained by the complexation of the free halide ion, the mechanistic

scenario of the dissociative mechanism B is more probable than the dissociative mechanism A, where
the final step was considered to be a trimolecular reaction (*cf*. scheme 19).
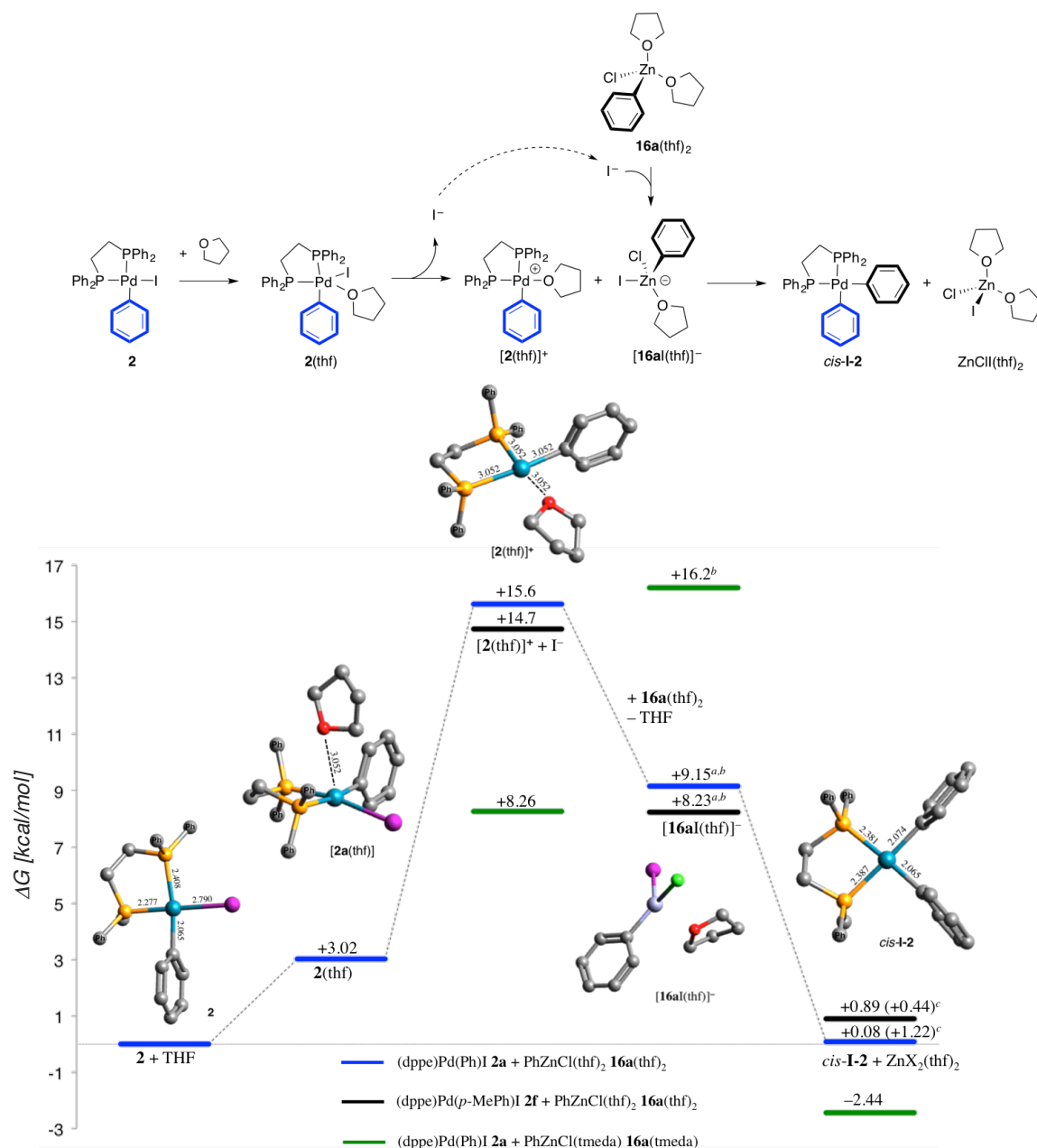
Figure 8. Reaction profile and ground state Gibbs free energies ΔG° [kcal/mol] for calculated intermediates leading to
transmetalation product *cis*-**I-2** via cationic palladium(II) intermediates [**2**(thf)]$^+$. [a]Formation of zincate [**16aI**(thf)]$^-$ using 6-
31G**/LANL2DZ basis sets and pseudopotential $\Delta G^0 = -67.8$ kcal/mol, and using def2QZVP $\Delta G^0 = -6.47$ kcal/mol.
[b]Zincate formation calculated using def2QZVP. [c]*Cis*-**I-2** resulting from transmetalation with **16d**(thf)$_2$. Hydrogen atoms were
omitted for clarity. Ph = phenyl.

The formation of diarylpalladium(II) intermediate *cis*-**I-2** from [**2**(thf)]$^+$ and [**16aI**(thf)]$^-$ was calculated
to be an exergonic process, and is more exergonic for the phenylpalladium(II) intermediate [**2a**(thf)]$^+$
($\Delta G^0 = -9.07$ kcal/mol relative to *cis*-**I-2a**) than for the less electrophilic intermediate [**2f**(thf)]$^+$ ($\Delta G^0 =$

–7.37 kcal/mol relative to *cis*-**I-2f**). Consequently, a positive Hammett constant ρ_2 with respect to complexes **2** would result considering the Bell-Evans-Polanyi principle. In addition, the magnitude of the Hammett constant ρ_2 is probably larger than ρ_1, because the energy difference between the differently substituted intermediates *cis*-**I-2** relative to the previous intermediates [**2**(thf)]$^+$ and [**16aI**(thf)]$^-$ is larger ($\Delta\Delta G_R^0 = 1.70$ kcal/mol) than for formation of the cationic species [**2**(thf)]$^+$ ($\Delta\Delta G_R^0 = 0.90$ kcal/mol) relative to the starting complexes **2**. In this case (according to equation 6, tables 10 and 11) a negative Hammett constant ρ_{obs} is observed if the formation of *cis*-**I-2** with k_2 is much faster than the dissociation of the iodide from [**16I**(thf)]$^-$ with k_{-3} ($k_2 \gg k_{-3}$). Because the aryl transfer is a relatively strongly exergonic process (*cf*. figure 8), it is very likely that k_2 is the fastest step. Therefore, the calculated relative energies are in accordance with the experimental findings from the competition experiments.

Moreover, we found that the aryl transfer between the more nucleophilic anisylzinc reagent [**16dI**(thf)]$^-$ with phenyl complex [**2a**(thf)]$^+$ is thermodynamically less favored ($\Delta\Delta G_R^0 = +1.14$ kcal/mol) than with [**16aI**(thf)]$^-$, however with tolyl complex [**2f**(thf)]$^+$ more favored ($\Delta\Delta G_R^0 = -0.45$ kcal/mol) (figure 8). As a consequence, the magnitude of the Hammett constant ρ_2 (positive sign) decreases and becomes smaller in the transmetalation with [**16dI**(thf)]$^-$ compared to the transmetalation with [**16aI**(thf)]$^-$. Consequently, the observed Hammett constant ρ_{obs} becomes more negative using less Lewis acidic anisylzinc reagent **16d**(thf)$_2$, which is in agreement with the experimental findings (*cf*. figure 7).

Interestingly, if the halide ligand is not displaced by the THF solvent, but by an amine ligand instead (in figure 8 calculated with tmeda), the resulting cationic species [**2**(tmeda)]$^+$ becomes more stable, because the more basic ligand can stabilize the cationic palladium(II) center better than the less electron-donating ether ligand. However the formation of the corresponding tmeda-ligated zincate becomes a less favored endergonic process, while the zincate formation was exergonic with the THF-coordinated arylzinc reagent **16a**(thf)$_2$. Consequently, the final formation of diarylpalladium(II) intermediate *cis*-**I-2** becomes very strongly exergonic ($\Delta G^0 = -18.6$ kcal/mol). Notably, if there were no additional tmeda ligand present, and the halide ligand from complex **2** is displaced by the solvent only, the Gibbs free energy for the charged intermediates [**2a**(thf)]$^+$ and [**16aI**(temda)]$^-$ would be 23.5 kcal/mol higher in energy compared to the reactants **2a** and **16a**(tmeda). Due to this high energy, the transmetalation with **16a**(tmeda) would not proceed by a dissociative mechanism in the absence of excess tmeda ligand at room temperature.
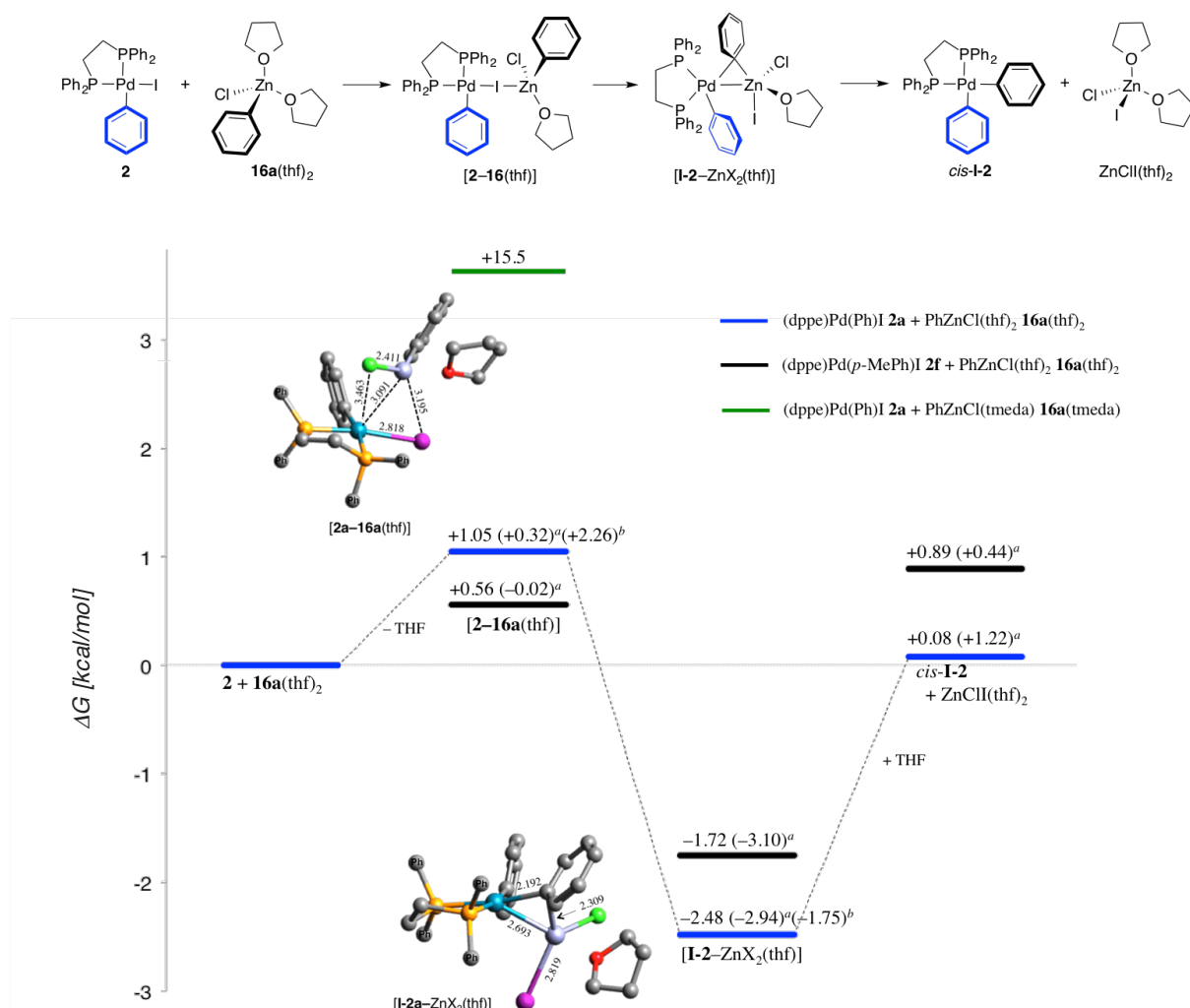
Figure 9. Ground state Gibbs free energies $\Delta G°$ [kcal/mol] for computed intermediates leading to transmetalation product *cis*-**I-2** via the associative mechanism. [a] Energies refer to transmetalation with **16d**(thf)$_2$. [b] Energies refer to transmetalation with **19a**(thf)$_2$ Hydrogen atoms were omitted for clarity. Ph = phenyl.

We also investigated the formation of the putative intermediate [**2**–**16**(thf)], and found indeed an adduct of arylpalladium(II) complex **2a** and arylzinc reagent **16a**(thf)$_2$, which coordinates to the iodide ligand of **2a** (figure 9) similar to the intermediate structure found be Espinet and co-workers.[46c] The distance of the Zn-I bond for intermediate [**2a**–**16a**(thf)$_2$] is 3.168 Å, which is slightly smaller than the sum of the corresponding van-der-Waals radii (3.37 Å), but not longer than a typical Zn-I bond (2.73 Å in compound **19a**(thf)$_2$, 2.71 Å in [**16a**I(thf)]$^-$). Therefore, strong interactions, which mainly determine the relative reactivity of complexes **2** in the formation of [**2a**–**16a**(thf)$_2$], can be assumed. The Gibbs free energy calculated for intermediate [**2a**–**16a**(thf)$_2$] is $\Delta G^0 = +1.05$ kcal/mol, which is much lower than for the formation of the cationic intermediate [**2a**(thf)]$^+$ ($\Delta G^0 = +15.6$ kcal/mol) in the dissociative mechanism, and therefore, more probable to occur. However, if the arylzinc reagent is chelated by tmeda, the Gibbs free energy of the adduct increases significantly to $\Delta G^0 = +15.5$ kcal, which is likely due to the change of the binding mode of the tmeda ligand from η^2 in **16a**(tmeda) to

unfavored η^1 in [**2a**–**16a**(tmeda)]. Subsequent dissociation into the charged species [**2a**(tmeda)]$^+$ and [**16a**I(tmeda)]$^-$ would be a thermodynamically neutral process if mediated by tmeda, but mediated by THF, which would form [**2a**(thf)]$^+$ and [**16a**I(tmeda)]$^-$, a very endergonic process ($\Delta G^0 = +23.6$ kcal/mol, *cf*. figure 8), which makes it very unlikely to occur at room temperature.

Dissociation of the THF-coordinated intermediate adduct [**2a**–**16a**(thf)] into the cationic complex [**2a**(thf)]$^+$ and zincate species [**16a**I(thf)]$^-$ (*cf*. scheme 19, associative mechanism D) is also an endergonic process with $\Delta G^0 = +8.10$ kcal/mol (*cf*. figure 8). Attempts to locate a transition state for a subsequent concerted aryl transfer from adduct [**2a**–**16a**(thf)] to form *cis*-**I-2** failed. However, a thermodynamically more stable structure [**I-2**–ZnX$_2$(thf)] ($\Delta G^0 = -2.48$ kcal/mol) with a Pd-Zn bond (Pd-Zn distance: 2.693 Å, sum of van-der-Waals radii: 3.02 Å) and a bridging aryl ligand was found instead (figure 9). The iodide ligand of complex **2** is already fully transferred to zinc. Similar intermediates have been previously found by DFT calculations of transmetalations between phosphine-ligated palladium(II) complexes and alkylzinc reagents being formed in exergonic processes.[46b, 46c, 49]

The calculated intermediates along the transmetalation pathway in figure 9 correspond to the associative mechanism D (*cf*. scheme 19), where the adduct [**2**–**16**(thf)] eventually passes an additional intermediate, here [**I-2**–ZnX$_2$(thf)] instead of the charged species [**2**(thf)]$^+$ and [**16**I(thf)]$^-$, before the diarylpalladium(II) intermediate *cis*-**I-2** is irreversibly formed and undergoes product-forming reductive elimination. Considering equation 8 (table 10), we can estimate the expected Hammett constant ρ_{obs} for this mechanism. Therefore, we additionally calculated the corresponding Gibbs free energies ΔG^0 for the intermediates and products resulting from transmetalation with less electrophilic tolylpalladium(II) complex **2f** and phenylzinc chloride **16a**(thf)$_2$. Again, the corresponding transition states could unfortunately not be located, which might be due to the large number of possible conformations of all flexible groups, in particular the THF ligand coordinated to zinc. Nevertheless, with respect to the Bell-Evans-Polanyi principle, approximated relative rate constants can be estimated by the relative Gibbs free energies ΔG^0.

As expected, the formation of the intermediate adduct [**2**–**16a**(thf)] is thermodynamically more favored for the less electrophilic tolylpalladium(II) complex **2f** than for the corresponding phenyl complex **2a** ($\Delta\Delta G_R^0 = +0.49$ kcal/mol), which results in a negative individual Hammett constant ρ_1. However, the formation of the aryl-bridged intermediate [**I-2**–ZnX$_2$(thf)] (figure 9) is thermo-dynamically less favored for tolyl complex **2f** ($\Delta G^0 = -2.28$ kcal/mol) than for the phenyl complex **2a** ($\Delta G^0 = -3.53$ kcal/mol) providing a positive Hammett constant ρ_3, which has probably a smaller magnitude than ρ_1. Interestingly, the formation of intermediate *cis*-**I-2** is an endergonic process, which

is energetically almost equal for both differently substituted intermediates [**I-2**–ZnX$_2$(thf)] (with **2a** ΔG^0 = +2.56 kcal/mol; with **2f** ΔG^0 = +2.61 kcal/mol). Therefore, the Hammett constant ρ_2 is only slightly positive, but probably close to zero. With these approximations, a negative Hammett constant ρ_{obs} is estimated, which is in accordance with the experimental results.

To approximate a Hammett constant ρ_{obs} for the competition experiments, where two differently substituted arylzinc reagents **16** compete for one arylpalladium(II) complex **2**, we also calculated the corresponding intermediates resulting from transmetalation with less Lewis acidic zinc reagent **16d**(thf)$_2$. Interestingly, the first intermediate [**2**–**16d**(thf)] becomes even more stable with both complexes **2a** and **2f** compared to adduct with more Lewis acidic arylzinc reagent **16a**(thf)$_2$ (figure 9). This trend might be surprising at first, because intuitively stronger Lewis acids would form stronger acid-base adducts. However the trend might be rationalized considering that Lewis acid-base adducts are more stable between soft bases and soft acids, or hard bases and hard acids, respectively. Basically, zinc(II) centers are classified as borderline acids between soft and hard acids, and is a hard acid with respect to the soft basic iodide ligand. The less Lewis acidic anisylzinc reagent **16d**(thf)$_2$ is a softer acid than **16a**(thf)$_2$, because the methoxy substituent makes the aryl ligand electron-rich, which in turn donates more electron density to the zinc(II) center becoming more polarizable and less charged. Therefore, the more electron-rich zinc(II) center becomes not only less Lewis acidic compared to **16a**(thf)$_2$, it also becomes softer in terms of the HSAB concept. The softer zinc(II) center forms stronger bonds to the iodide ligand, which is essentially a soft base, in particular if coordinated in complex **2a**. To verify this trend, we also calculated the Gibbs free energy for the adduct [**2a**–**19a**(thf)] formed with the strong Lewis acidic, and therefore harder phenylzinc iodide **19a**(thf)$_2$. According to the HSAB concept, the adduct [**2a**–**19a**(thf)] would be less stable compared to [**2a**–**16a**(thf)]. Indeed, [**2a**–**19a**(thf)] was found to be 1.21 kcal/mol higher in energy than [**2a**–**16a**(thf)]. The HSAB concept can also be applied to explain the reactivity trend for the formation of intermediate adduct [**2**–**16a**(thf)] using differently substituted complexes **2**. In the complexes **2** with electron-rich aryl ligands the iodide ligand is less strongly bound to the palladium(II) center (*cf*. table 3), and therefore the soft basic ligand becomes slightly harder and therefore forms stronger bonds to the harder zinc(II) center.

The Hammett constant ρ_1 with respect to the arylzinc reagent **16**(thf)$_2$ is predicted to be negative. The conversion of [**2a**–**16a**(thf)] into the aryl-bridged intermediate [**I-2**–ZnX$_2$(thf)] becomes thermodynamically more favored with phenylzinc reagent **16a**(thf)$_2$ (ΔG^0 = –3.53 kcal/mol) than with **16d** (ΔG^0 = –3.26 kcal/mol), which results in a positive Hammett constant ρ_3 being smaller in magnitude ($\Delta\Delta G_R^0$ = +0.27 kcal/mol) than ρ_1 ($\Delta\Delta G_R^0$ = +0.73 kcal/mol). The endergonic conversion of [**I-2**–ZnX$_2$(thf)] into the diarylpalladium(II) complex *cis*-**I-2** becomes relatively strongly endergonic with

the electron-rich reagent **16d**(thf)$_2$ (ΔG^0 = +4.16 kcal/mol) compared to phenylzinc reagent **16a**(thf)$_2$ (ΔG^0 = +2.56 kcal/mol) resulting in a positive Hammett constant ρ_2. Overall, the signs of the individual Hammett constants $\rho_{\pm n}$ with respect to the arylzinc reagent **16**(thf)$_2$ are essentially the same as with respect to the arylpalladium(II) complex **2**. Consequently, the expected Hammett constant ρ_{obs} is negative, as well, which is also in agreement with the experimental results.

Comparison of the Hammett constants ρ_{obs}, predicted based on computational results for the competition of arylzinc reagents **16**(thf) in transmetalation with complex **2a**, and the one of corresponding experiments with complex **2f**, reveals that all individual Hammett constants $\rho_{\pm n}$, and therefore also the observed Hammett constant ρ_{obs}, become more negative using less electrophilic complexes **2**, which is in agreement with the experimental results (*cf.* figure 7). However, more negative individual Hammett constants $\rho_{\pm n}$ are also found for the competition experiments of competing complexes **2**. The individual and observed Hammett constants $\rho_{\pm n}$ and ρ_{obs} become also negative going to the less Lewis acidic arylzinc reagent **16d**(thf)$_2$, which is in disagreement with the experimental results (*cf.* figure 7). Here, the observed Hammett constant ρ_{obs} became less negative with decreasing Lewis acidity of the arylzinc reagent.

Probably the prediction of the individual Hammett constants $\rho_{\pm n}$ is poor on the basis of the Gibbs free energies ΔG^0. The development of the observed Hammett constant strongly depends on the relative magnitudes of the individual Hammett constants $\rho_{\pm n}$. Moreover, we wondered if additional species, which would not lead the product, could be accessible. Indeed, another conformer of the intermediate [**2a**–**16a**(thf)] was found to be slightly more stable (figure 10). While in [**2a**–**16a**(thf)] the aryl ring bound to the zinc(II) center is positioned close to the palladium(II) center, in the conformer [**2a**–**16a′**(thf)] the aryl ring points away from the palladium(II) center. Besides the zinc-iodide interaction, which appears to be weaker (Zn-I bond: 3.273 Å) than in [**2a**–**16a**(thf)], a Pd-Zn bond is present. Although the additional equilibrium, which forms [**2**–**16′**(thf)], consumes the reactants **2** and **16**(thf)$_2$, the observed Hammett constant ρ_{obs} should not be affected, because the derivative of the rate law is independent on the concentrations of the limiting reagent (**16**(thf)$_2$ in experiments with competing **2**, and **2** in experiments with competing **16**(thf)$_2$), since it is not in a competing situation, and the competing reagents, which are in large excess (pseudo-zero order). Interestingly, we calculated that the reaction with the byproduct ZnX$_2$(thf)$_2$ forms an adduct [**2a**–ZnX$_2$(thf)], which is significantly more stable (with ZnCl$_2$(thf)$_2$: ΔG^0 = −2.15 kcal/mol) than [**2a**–**16a**(thf)] or [**2a**–**16a′**(thf)].
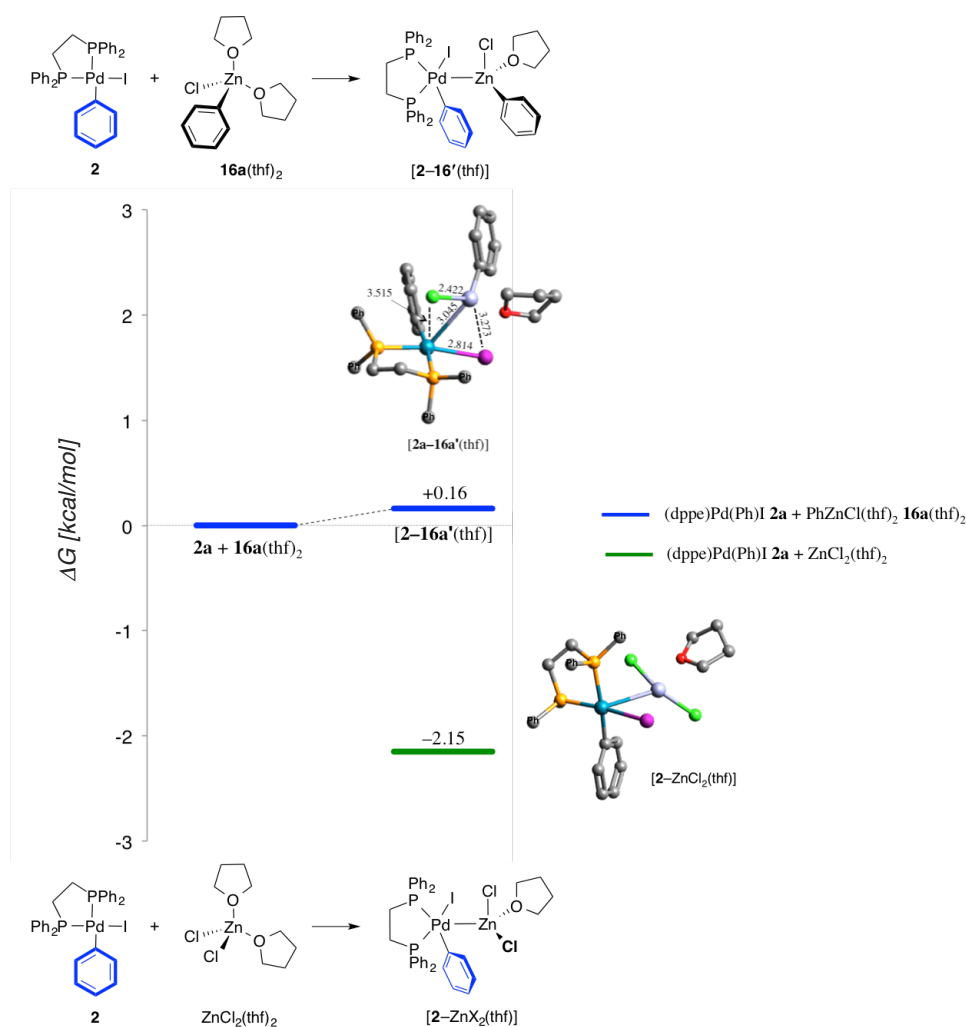
Figure 10. Ground state Gibbs free energies ΔG° [kcal/mol] for computed intermediates, which do not lead to transmetalation product *cis*-**I-2**. Hydrogen atoms were omitted for clarity. Ph = phenyl.

1.3.6 Influence of salts and ligands

Although the DFT calculations suggest that the transmetalation between dppe-ligated arylpalladium(II) complexes proceed via an associative mechanism rather than a dissociative mechanism, the comparison of the approximated Hammett constants ρ_{obs} of DFT calculations with the experimental findings indicate a dissociative mechanism involving cationic intermediate $[\mathbf{2}(thf)]^{+}$ and zincate species $[\mathbf{16}I(thf)]^{-}$. To distinguish between the two mechanistic scenarios, we performed competition experiments of competing complexes **2** with phenylzinc reagent **16a** in the presence of one equivalent LiCl. As the equations 6 and 8 show, the Hammett constant ρ_{obs} depends on the concentration of **16** only for the dissociative mechanism. The Hammett constant ρ_{obs} of the associative mechanism is independent on the concentration of reactants or intermediates. Consequently, the addition of halide ions does not affect the observed Hammett constant ρ_{obs} in this case. For the dissociative mechanism,

however, additional halide ions increase the concentration of the zincate $[\mathbf{16}\text{X(thf)}]^-$, while the concentration of $\mathbf{16a}$ decreases. If the Hammett constant for the product forming step ρ_2 has a larger absolute value than $\rho_{\pm 1}$ for the pre-equilibrium forming cationic intermediate $[\mathbf{2}\text{(thf)}]^+$ (as predicted by DFT calculations), the Hammett constant ρ_{obs} becomes more negative. If the magnitude of ρ_2 is smaller than $\rho_{\pm 1}$, ρ_{obs} becomes more positive. In other words, in case of a dissociative mechanism, addition of LiCl should affect the observed Hammett constant ρ_{obs}.

Figure 11. Hammett plot from competition experiments of complexes **2** with PhZnCl (**16a**) in the presence of 1 equiv. LiCl.

In the competition experiment with one equivalent LiCl with respect to phenylzinc reagent **16a** was added. Larger amounts were not applied to avoid influencing the result by interaction of the Lewis acidic lithium cation with complex **2**. Nevertheless, one equivalent of LiCl would be enough to cause detectable changes of the observed Hammett constant ρ_{obs} if the transmetalation proceeded via a dissociative mechanism. In the event, however, the competition experiment provided a Hammett constant of $\rho = -1.44$ ($R^2 = 0.96$) (figure 11), which is indistinguishable from the value obtained from the competition experiment without LiCl ($\rho = -1.47$; *cf.* figure 5). This result suggests that the dissociative mechanism is not operating.

The DFT calculations showed that the byproduct ZnX_2 of the transmetalation might form a more stable adduct with the complexes **2** (with $K_{\pm 4}$) than the arylzinc reagent (*cf.* figure 10). Because the complexes **2** are in large excess in the competition experiments, the influence of this unproductive equilibrium on the observed Hammett constant ρ_{obs} is negligible. However, if the amount of ZnX_2 is large, the complexes **2** are reversibly consumed, and the ratio of two competing complexes **2** in the competition experiments cannot be considered to be 1:1 anymore. As a result, the Hammett constant of the additional equilibrium with $K_{\pm 4}$ contributes a positive value to the observed Hammett constant

ρ_{obs} (equation 13). The extent of this positive contribution depends on the amount of the added ZnX_2, and can be expressed as a factor f, which is zero if no ZnX_2 is added and –1 for large amounts (for details, see Mathematical Section). Consequently, the competition experiments with competing complexes **2** should provide a more positive Hammett constant ρ_{obs} in the presence of ZnX_2 (with $\rho_{\pm4}$ is negative as for the formation of adduct [**2**–**16**(thf)] with $\rho_{\pm1}$). Likewise, the presence of other Lewis acidic salts, which can form similar unproductive adducts with complexes **2**, would lead to more positive Hammett constant ρ_{obs}. This trend we have indeed observed for the competition experiments using the salt-containing (LiX or MgX) arylzinc solutions of **16a** and **16k** (*cf.* figures 5 and 7).

(eq. 13) $$\rho_{ZnX} = \rho_{obs} + (\rho_4 - \rho_{-4}) \cdot f(K_{\pm4}[\mathbf{2}]_0, [ZnCl_2]_0)$$

To investigate this behavior in more detail, and to test for an associative mechanism, we performed competition experiments of complexes **2** with PhZnCl (**16a**) in the presence of different amounts of $ZnCl_2$ (figure 12). The presence of one equivalent $ZnCl_2$ with respect to **16a** resulted in only a slight change of the Hammett constant ρ_{obs} becoming a bit less negative with $\rho = -1.41$ ($R^2 = 0.97$) compared to the experiment without additional $ZnCl_2$ (*cf.* figure 5), but is essentially the same within the error margin. This is in agreement with the mechanistic proposal of an associative mechanism involving neutral species, because small amounts with respect to complexes **2** should not affect ρ_{obs} since they are in large excess with respect to arylzinc reagent **16a**. Moreover, this lack of influence on the Hammett constant ρ_{obs} further indicates that the dissociative mechanism is not the operating, because the added $ZnCl_2$ is in equal amount to **16a**, which should affect the equilibrium concentration between the zincate [**16a**X(thf)]$^-$ and neutral zinc reagent **16a**. $ZnCl_2$ would certainly preferentially bind free halide ions, resulting in an increase of the concentration of neutral **16a**. As discussed above for the competition experiments with added LiCl, the Hammett constant ρ_{obs} is dependent on the concentration of **16a** in the case of a dissociative mechanism. Addition of 5 equivalents of $ZnCl_2$ with respect to **16a** (0.6 equivalent with respect to **2**) affected the Hammett constant more significantly with $\rho = -1.02$ ($R^2 = 0.96$) (figure 12) becoming more positive as expected for the associative mechanism. Addition of much larger amounts of $ZnCl_2$ gave only poor Hammett correlations with large errors, but the tendency of a more positive Hammett constant ρ_{obs} with increasing amount of $ZnCl_2$ can be still clearly recognized.
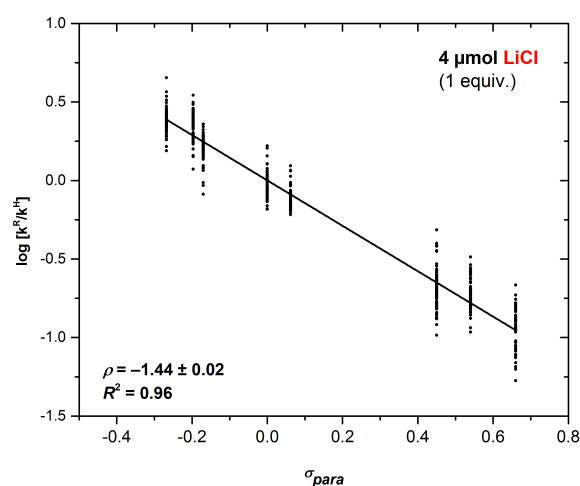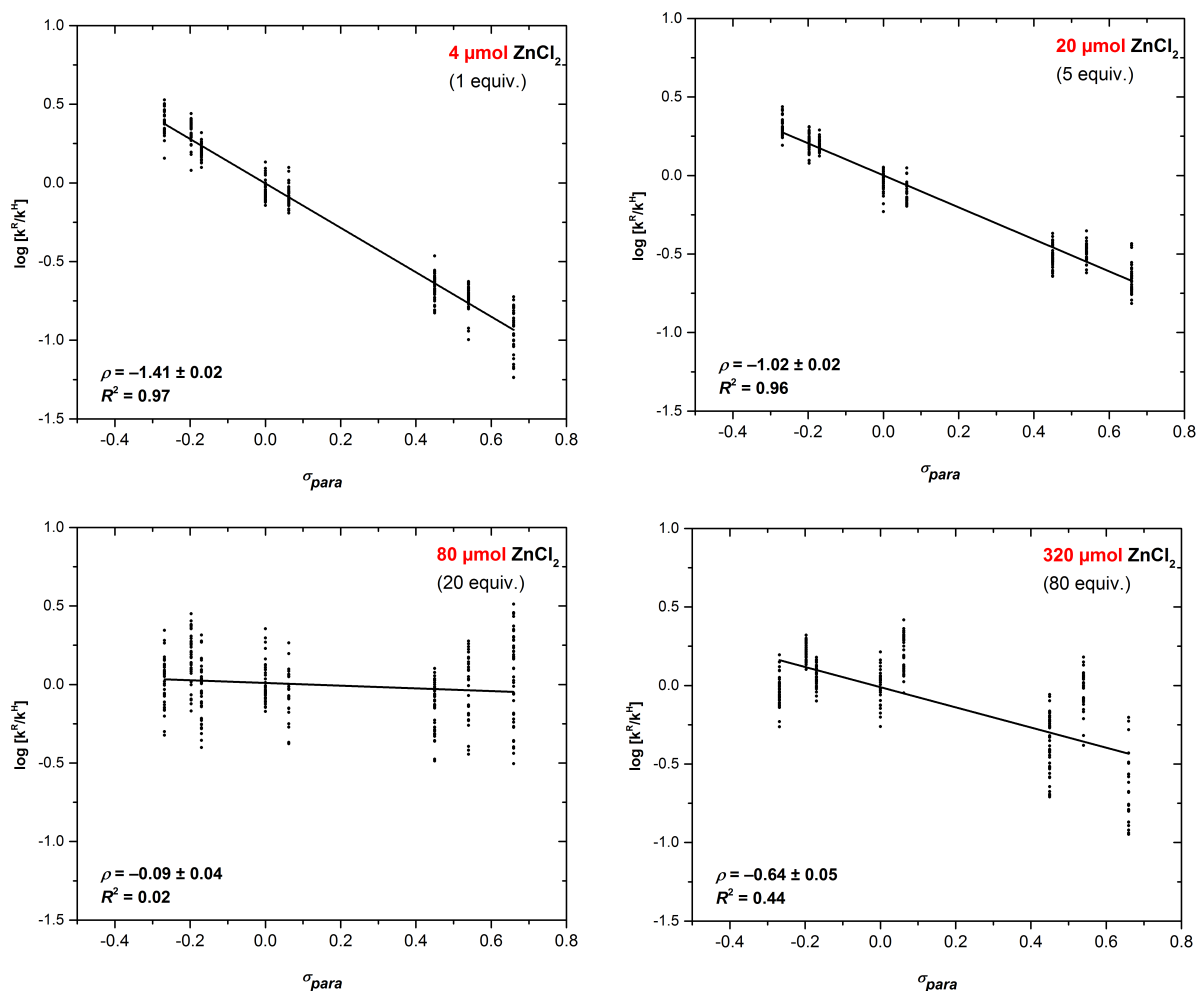
Figure 12. Hammett plots from competition experiments of complexes **2** with PhZnCl (**16a**) in the presence of ZnCl$_2$.

The DFT calculations indicated that the presence of chelating ligands can influence the mechanism. While in the absence of amine (or phosphine) ligands, neutral intermediates are most likely, however in the presence of ligands, cationic intermediates [**2**(L$_2$)]$^+$ might be stabilized. Because ligands are often in excess with respect to the palladium catalyst under typical catalytic conditions, we became curios how the observed Hammett constant ρ_{obs} would change. First we performed the competition experiments with competing complexes **2** in the presence of one equivalent dppe with respect to palladium. Therefore, the dppe ligand was added to the solution of complexes **2**. Notably, the dppe ligand itself is badly soluble in THF, but in solution with the complexes **2**, the dppe ligand fully dissolved, which might indicate formation of cationic complex [**2**(dppe)]$^+$. The formation of similar ligand-stabilized cationic species has been also observed experimentally and computationally by Espinet and co-workers,[46c] as well as, our own DFT calculations with dppe-ligated complexes **2** and tmeda ligand indicate a relatively stable species [**2**(tmeda)]$^+$ (*cf.* figure 8).

In the limiting case that all neutral complexes **2** had converted into the cationic complexes [**2**(dppe)]$^+$, the Hammett constant ρ_{obs} would reflect only the aryl transfer with k_2 between [**16a**X(thf)]$^-$ and

$[\mathbf{2}(dppe)]^+$, if it proceeds via an open transition state such as in the dissociative mechanism B. Because the aryl transfer becomes probably the faster the more electrophilic $[\mathbf{2}(dppe)]^+$ is, as supported by the computational results, the expected observed Hammett constant ρ_{obs} would be positive. However, the experimental Hammett constant ρ_{obs} was even more negative with $\rho = -1.62$ ($R^2 = 0.90$, figure 13) compared to the reference system without any additives ($\rho = -1.47$, figure 5). Therefore, if complexes $\mathbf{2}$ had been fully converted into the cationic species $[\mathbf{2}(dppe)]^+$ before addition of $\mathbf{16a}$, there must still be at least one additional step to observe a negative Hammett constant. Probably, the charged species $[\mathbf{16a}X(thf)]^-$ and $[\mathbf{2}(dppe)]^+$ do not undergo transmetalation directly, but form the neutral Lewis acid-base adduct $[\mathbf{2}–\mathbf{16a}X(dppe)]$ instead, which finally leads to the aryl transfer via an aryl-bridged intermediate, such as $[\mathbf{I}\text{-}\mathbf{2}–ZnX_2(dppe)]$ and corresponding cyclic transition state. However, the DFT calculations showed that the tmeda-coordinated intermediate $[\mathbf{2}–\mathbf{16a}X(tmeda)]$ is much higher in energy, and therefore is unlikely as intermediate at room temperature.
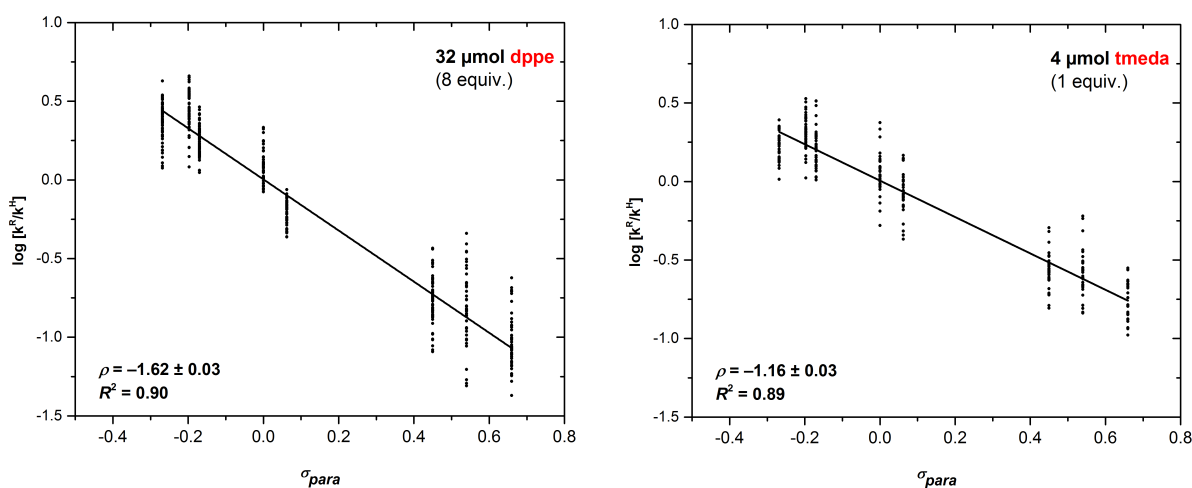
Figure 13. Hammett plots from competition experiments in the presence of dppe and tmeda.

To investigate the influence of the chelating ligand, we also performed the competition experiment with added tmeda ligand to obtain an impression how the Hammett constant ρ_{obs} is actually influenced using arylzinc reagents of type $\mathbf{16a}(L)_2$. Therefore, the arylzinc solution of $\mathbf{16a}$ was treated with an equimolar amount of tmeda, which certainly binds completely to the zinc(II) center replacing the coordinated THF molecules to give $\mathbf{16a}(tmeda)$ (calculated Gibbs free energy difference between $\mathbf{16a}(thf)_2$ and $\mathbf{16a}(tmeda)$ was calculated with $\Delta G^0 = -15.6$ kcal/mol). Because there is no excess tmeda present, additional equilibria involving starting complexes $\mathbf{2}$, such as the formation of cationic species $[\mathbf{2}(tmeda)]^+$ or exchange of the dppe ligand of complexes $\mathbf{2}$, should be negligible. Consequently, a change of the Hammett constant ρ_{obs} reflects most likely only the influence of the tmeda ligand coordinated on arylzinc reagent $\mathbf{16a}(tmeda)$. However, according to the DFT calculations the intermediate adduct $[\mathbf{2}–\mathbf{16a}X(L)]$ is much higher in energy with tmeda-coordinated

arylzinc(II) reagent **16a**(tmeda) than with THF-coordinated **16a**(thf)$_2$. Therefore, there are three conceivable scenarios: 1. Intermediate adduct [**2**–**16a**X(tmeda)] is not passed at room temperature using **16a**(tmeda) resulting in no reaction, or 2. the tmeda ligand has to dissociate to form THF-coordinated species **16a**(thf)$_2$ to pass [**2**–**16a**X(thf)], or 3. the energy barriers to pass [**2**–**16a**X(tmeda)] and [**I-2**–**ZnX**$_2$(tmeda)] are still low enough to be reached at room temperature. While the first scenario would obviously result in no reaction, and no yields of biaryls **17**, respectively, the second scenario would give the same observed Hammett constant ρ_{obs} as observed with THF-coordinated arylzinc reagent **16a**(thf)$_2$, because ρ_{obs} is independent on the concentration of **16a**(thf)$_2$ (*cf.* equation 8). The third scenario would lead to a significant change of the Hammett constant ρ_{obs}, because relatively large changes of the individual Hammett constants $\rho_{\pm n}$, and therefore of the observed Hammett constant ρ_{obs}, are expected.

Indeed, the competition experiments with added tmeda (figure 13) gave a less negative Hammett constants of $\rho = -1.16$ ($R^2 = 0.89$), which finally imply that the energetically higher lying neutral intermediates [**2**–**16a**X(tmeda)] and [**I-2**-ZnX$_2$(tmeda)] of an associative mechanism are passed. It should be mentioned that the outcome of the experiment was strongly dependent on the age of solution of **16a**(tmeda). When the solution was freshly prepared and directly used, reproducible results were obtained. However, in an experiment carried out with the same solution on the next day, the average yields of biaryls **17** were less than 10%, which implies decomposition of **16a** in the presence of tmeda. The solution did not show any obvious degradation indicated by formation of a turbidity or color changes. Unfortunately, no other side products could be detected by GC-FID, which would give information of possible decomposition pathways.

1.3.7   Reactivity of other (phosphine)Pd(Ar)X complexes with phenylzinc chloride

Due to the contradiction between the results of the competition experiments with differently substituted competing arylzinc reagents **16** and *trans*-configured, PPh$_3$-ligated complexes **9** by Mayr and co-workers,[7h] and our experiments with *cis*-configured, dppe-ligated complexes **2** (*cf.* figure 6), we became interested in how other phosphine-ligated complexes with different stereochemical configurations and coordination numbers, which have been typically used in cross-coupling reactions, behave in the transmetalation. Our starting point was initially the competition experiment with competing PPh$_3$-ligated bromide complexes **9**, however we realized that most of the differently substituted complexes **9** are poorly soluble in THF, which would cause large errors for the corresponding Hammett correlation. This might also have been a problem for Mayr and co-workers

for their competition experiments, but unfortunately no experimental details for these particular experiments were reported in the supporting information. Maybe the complexes **9** are sufficiently soluble in higher dilution, which would be the case with competing reagents **16**.

To still investigate the reactivity of PPh₃-ligated complexes nevertheless, we used analogous iodide complexes **8**, which exhibit significant better solubility in THF under the transmetalation conditions than the bromide complexes **9**. The resulting Hammett correlation from the competition experiments with methoxy-substituted arylzinc reagent **16d** resulted in a Hammett constant of $\rho = -0.14$ (figure 14), however with a poor correlation coefficient of only $R^2 = 0.08$, which is the result of the outlying spots for the unsubstituted complex **2a**, as well as the fact that slopes approaching zero result in regression coefficients approaching zero.

Figure 14. Competition experiments of arylpalladium(II) complexes **8** with ArZnCl (**16d**) and the resulting Hammett plot.

Notably, the average yield of the corresponding biaryls **17dx** from the competition experiments with the complexes **8** was 30%, whereas the average yields for the experiments with the dppe-ligated complexes **2** were typically above 90%. Moreover, remarkably high yields were obtained for the symmetrical biaryl **17aa**, which cannot be a product of the transmetalation with arylzinc reagent **16d**. To elucidate the origin of this unexpected biaryl, we performed non-competitive transmetalations with complexes **8** and **9** and detected significant amounts of biaryl **17aa** (table 12), in particular from reactions with complexes bearing electron-donating substituents on the aryl ligand. This effect is more pronounced for the bromide complexes **9** than for the iodide complexes **8**.

Table 12. Non-competitive transmetalation of $(PPh_3)_2Pd(Ar)X$ complexes **8** and **9** with PhZnCl (**16a**).

			X = Br (**9**)			X = I (**8**)		
		x	**17a***x*	**17aa**	recov.**16a**	**17a***x*	**17aa**	recov. **16a**
			[%]	[%]	[%]	[%]	[%]	[%]
1	OMe	**d**	6	50	106	62	23	108
2	^{t}Bu	**e**	36	44	124	55	25	104
3	Me	**f**	–	–	–	53	36	125
4	H	**a**	101	–	–	–	–	–
5	CO_2Et	**i**	106	15	136	89	6	100
6	$CO_2{}^nBu$	**j**	116	16	149	–	–	–
7	CF_3	**k**	87	12	111	88	7	102
8	CN	**l**	87	9	104	94	4	102

Recent work by Lei and co-workers suggested that the aryl transfer is a reversible process, which is finally responsible for the formation of homocoupling products, however only if *ortho*-carbonyl groups, which are able to coordinate to zinc(II), are present in one of the participating aryl groups.[51b] Because only *para*-substituted aryl groups are involved in our competition experiments, back transmetalation from diarylpalladium(II) intermediate *cis*-**I-2** to ZnX_2 is unlikely. We propose that **17aa** is formed by a P-C bond-forming reductive elimination, which gives initially the corresponding phosphonium salt and a highly reactive palladium(0) species (scheme 21). The reductive elimination would be favored for electron-rich aryl ligands, which is in accordance with the observed trend in table 12. Subsequent, oxidative addition of the phosphonium salt to the reactive palladium(0) species gives again a phenylpalladium(II) complex, with a mixed phosphine ligand. The oxidative addition would be faster for the P-C bond with the most electron-deficient aryl group. This reaction has been previously reported,[71] and is consistent with the observation we made for the preparation particularly of the bromide complexes **9** (*cf*. chapter 1.3.1). The following transmetalation with phenylzinc chloride (**16a**) gives then the apparent homocoupling product **17aa**. This would also explain why the data points for the Hammett parameter of hydrogen with $\sigma = 0$ in the Hammett correlation of the competition experiment with PPh$_3$-ligated complex **8** (figure 14) deviates significantly from the linear regression.
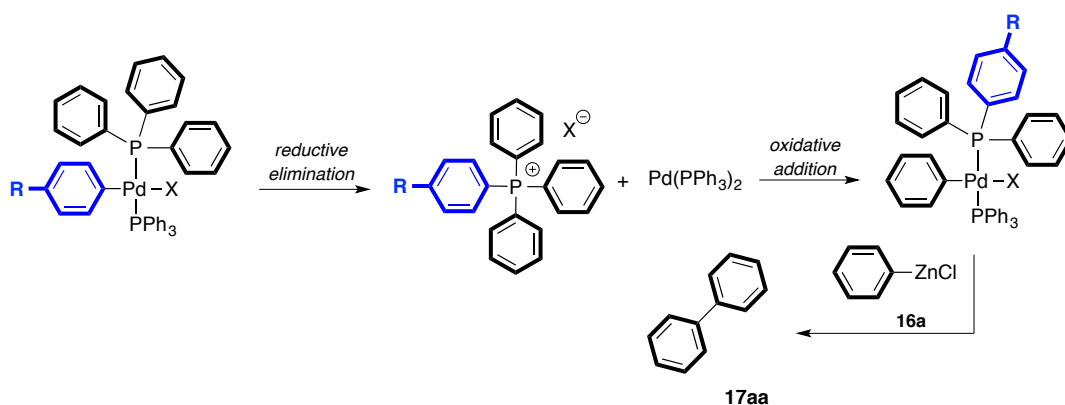
Scheme 21. Mechanism for the formation of **17aa** as side product.

Next, we turned our attention to the investigation of the reactivities for dppf-ligated complexes **3** and **7**. Similar to the PPh$_3$-ligated bromide complexes **9**, we realized that also the corresponding dppf-ligated bromide complexes **7** are also not fully dissolved in the reaction mixture. Nevertheless, we performed the competition experiments with arylzinc reagent **16a** and determined a Hammett constant of $\rho = -0.44$ (figure 15). As expected, the correlation coefficient was only $R^2 = 0.31$, which indicates a poor linear correlation, which might be due to the different solubilites of the bromide complexes **7**. Therefore, we performed the same competition experiments with arylzinc reagents **16d** and **16a**, and the dppf-ligated iodide complexes **3**, which exhibit better solubility in THF. However, the competition experiments provided similarly bad linear correlations with regression coefficients of $R^2 = 0.47$ for **16d** and $R^2 = 0.36$ for **16a**. Notably, correlating the data with the Brown's Hammett parameters σ^- or σ^+ did not provide significantly better correlations, which suggests that there is no charge build up in the transition states and intermediates, respectively, additionally supporting an associative mechanism, where a intermediate Lewis acid-base adduct [complex–**16**(thf)] is formed. The Hammett constant for the experiment with the less Lewis acidic reagent **16d** was determined with $\rho = -0.35$, and for **16a** $\rho = -0.73$, which actually correlates to the previously observed reactivity trend regarding the Lewis acidity of **16**, comparing these results with the Hammett constants for the dppe-ligated complexes **2**, which gave also more negative Hammett constants ρ_{obs} for the more Lewis acidic reagent **16a** ($\rho = -1.47$) than for the methoxy-substituted reagent **16d** ($\rho = -1.26$) (*cf*. figures 5 and 7).
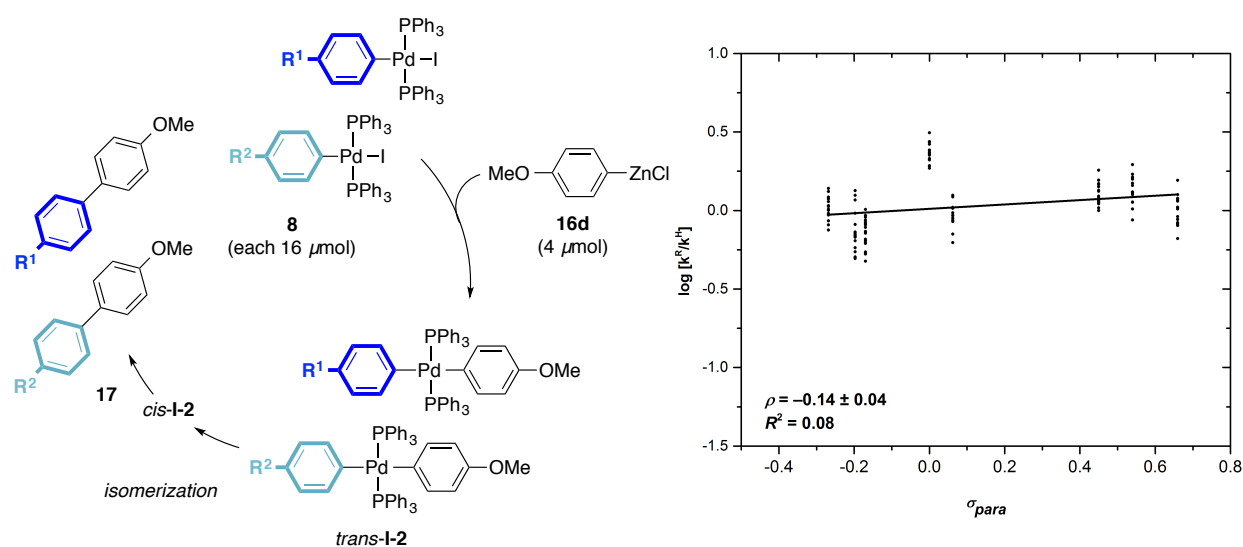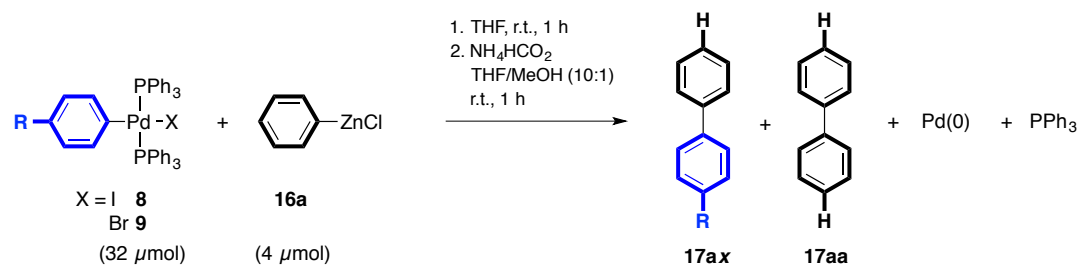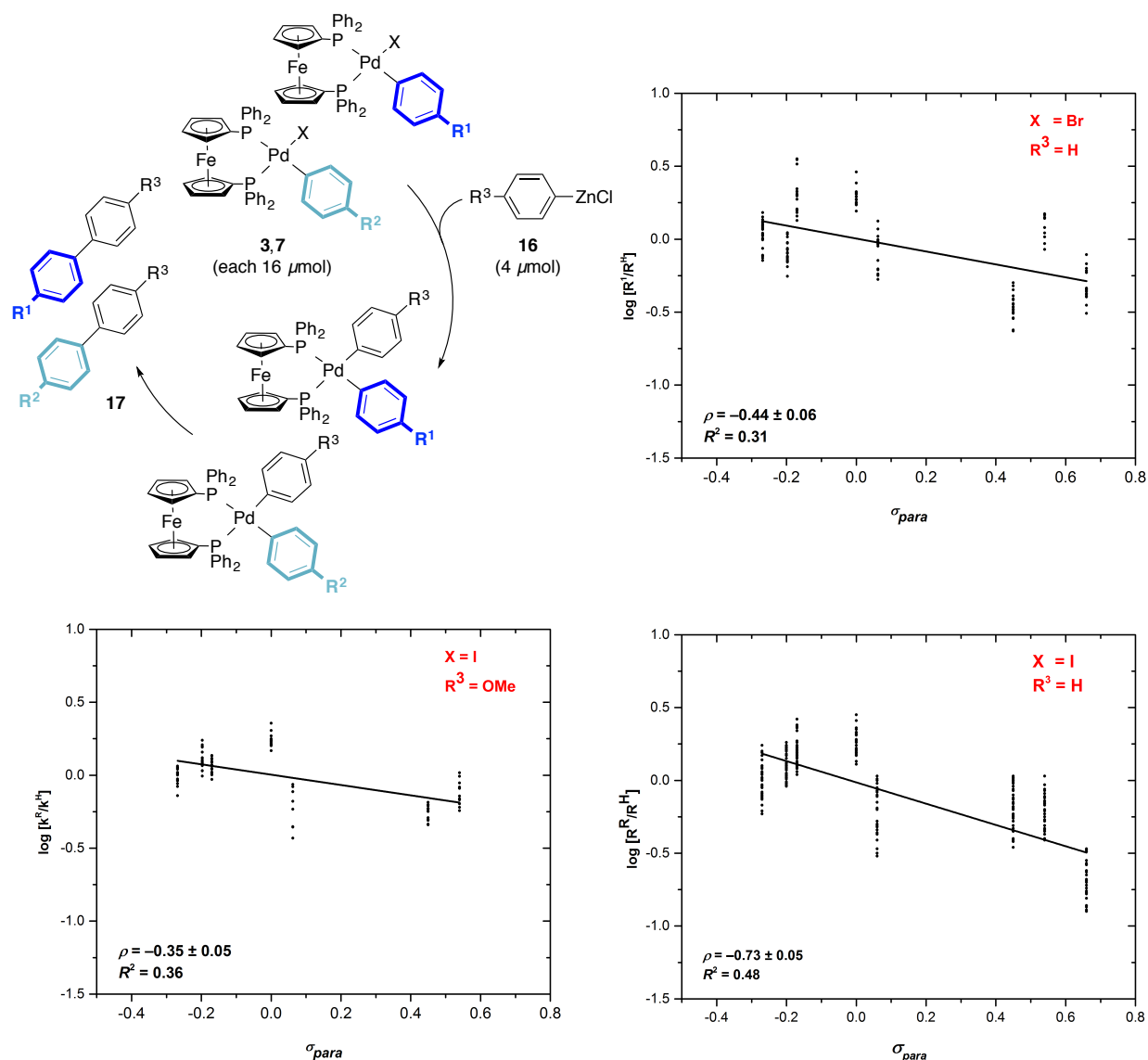
Figure 15. Competition experiments of arylpalladium(II) complexes **3** and **7** with ArZnCl **16** and the resulting Hammett plots.

Although the linear correlations for the PPh$_3$- and dppf-ligated complexes are worse than for the dppe complexes **2**, there is still a clear trend of the Hammett constant ρ_{obs} with respect to the steric properties of the phosphine ligands. The Hammett constants ρ_{obs} become more negative with decreasing steric demand of the ligand (cone angles and bite angles) (table 13). It can be envisaged that a smaller steric demand around the palladium(II) center facilitates the formation of the intermediates [complex–**16**(thf)] and [**I-2**–ZnX$_2$(thf)] leading to a higher reactivity in the first and second step, whereas the formation of diarylpalladium(II) intermediates **I-2** (*cis* and *trans*) is facilitated with bulkier ligands. As previously observed, a higher reactivity of the reactant tends to provide more negative Hammett constants ρ_{obs} from competition experiments. According to this trend, using a bulkier ligand, such as dppf or PPh$_3$, which are probably less reactive in the first and second

step of the associative mechanism, would accordingly lead to less negative Hammett constants ρ_{obs}, as experimentally observed. However, the dppf-ligated bromide complexes **7** seem to be deviating from the general trend. Considering that the bromide ligand is a better bridging ligand than the iodide (harder base than iodide), the complexes **7** would be expected to be more reactive towards the formation of the corresponding intermediate adduct [**7**–**16a**(thf)], which would lead to a more negative Hammett constant ρ_{obs}. However, the opposite trend was observed.

Table 13. Comparison of Hammett constants with steric parameters of arylpalladium(II) complexes.

entry	complex	ligand	X	cone angle[a] [°]	bite angle[b] [°]	ρ (**16a**)	ρ (**16d**)
1	**2**	dppe	I	125	86	–1.47	–1.26
2	**3**	dppf	I	–	101	–0.73	–0.35
3	**7**	dppf	Br	–	101	–0.44	–
4	**8**	PPh$_3$	I	145	–	–	–0.14

[a]Values taken from ref. 91. [b]Values of crystal structures from table 3.

We were also interested to investigate the reactivity trends with coordinatively unsaturated arylpalladium(II) complexes, which are formed with sterically very bulky phosphine ligands, such as P(*o*-tol)$_3$, P^{t}Bu$_3$ or Buchwald ligands. Although we synthesized P(*o*-tol)$_3$-ligated complexes **4** and **5** it unfortunately turned out that they are not suitable for the competition experiments, because they are essentially insoluble in THF. However, the P^{t}Bu$_3$ complexes **14** are excellently soluble in THF, therefore, we performed the competition experiments with complexes **14** and phenylzinc reagent **16a**. The resulting Hammett correlation provided a poor correlation also with a regression coefficient of R^2 = 0.42 (figure 16), which is probably the result of a complicated work-up procedure for the transmetalation samples and the rapid decomposition of the complexes **14** in solution. While the excess of all other complexes could be either quenched with MeOH/NH$_4$HCO$_2$ or removed by filtration upon evaporation of the THF solvent and re-dissolution of the biaryls **17** in pentane or Et$_2$O, the P^{t}Bu$_3$ complexes **14** could not be eliminated from the samples as easily. Moreover, they rapidly decomposed in solution into several unidentified different products, which partially overlapped with the peaks of the analytes in the GC resulting in large errors. Therefore, many of the GC chromatograms had to be excluded for the Hammett correlation analysis.
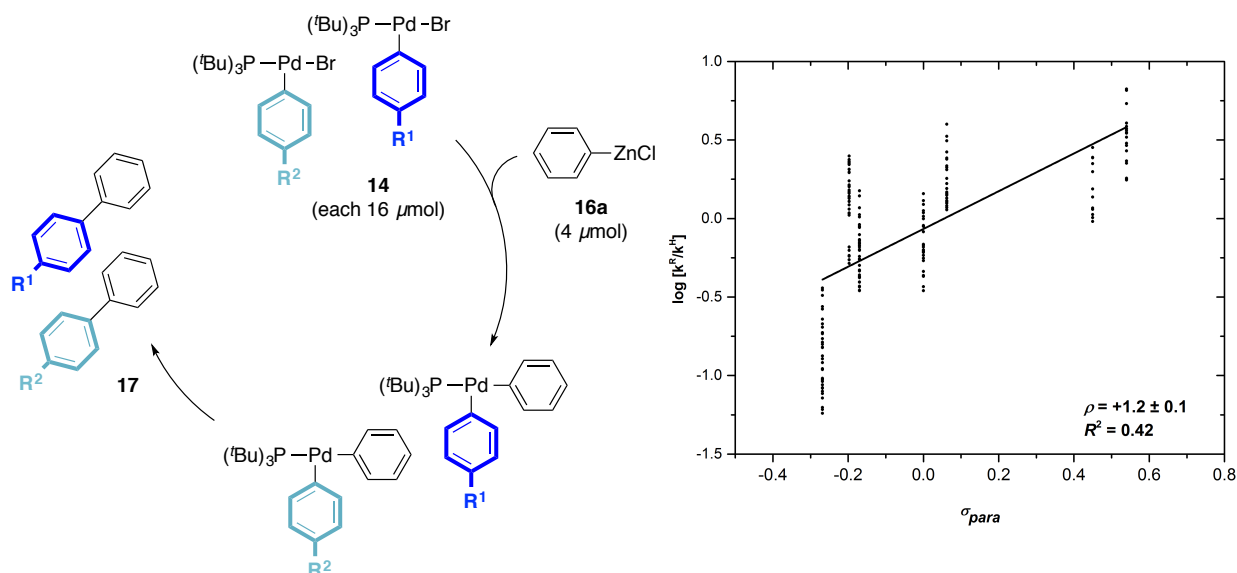
Figure 15. Hammett plots obtained from competition experiments of complexes **14** with PhZnCl (**16a**).

Nevertheless, the included data gave an obviously positive correlation with a Hammett constant of $\rho = +1.2$, which is in sharp contrast to the coordinatively saturated complexes. This result suggests that complexes **14** with electron-withdrawing substituents on the aryl ligand accelerate the transmetalation. Assuming that **16a** coordinates only to the bromide ligand of complex **14** as proposed for transmetalation with dppe-ligated complexes **2**, the intermediate *cis*-[**14**–**16a**], which would lead to *trans*-**I-2** and has to isomerize to *cis*-**I-2** prior reductive elimination, is formed (scheme 22), a negative Hammett constant ρ_{obs} would be expected, because formation of *cis*-[**14**–**16a**] would be most likely favored with more electron-rich complexes **14**, similar to the coordinatively saturated complexes, which is in contrast to the experimental finding. However, regarding the vacant coordination site of the complexes **14**, the pathway via intermediate *cis*-[**14**–**16a**] is certainly unfavored and not the operating pathway.
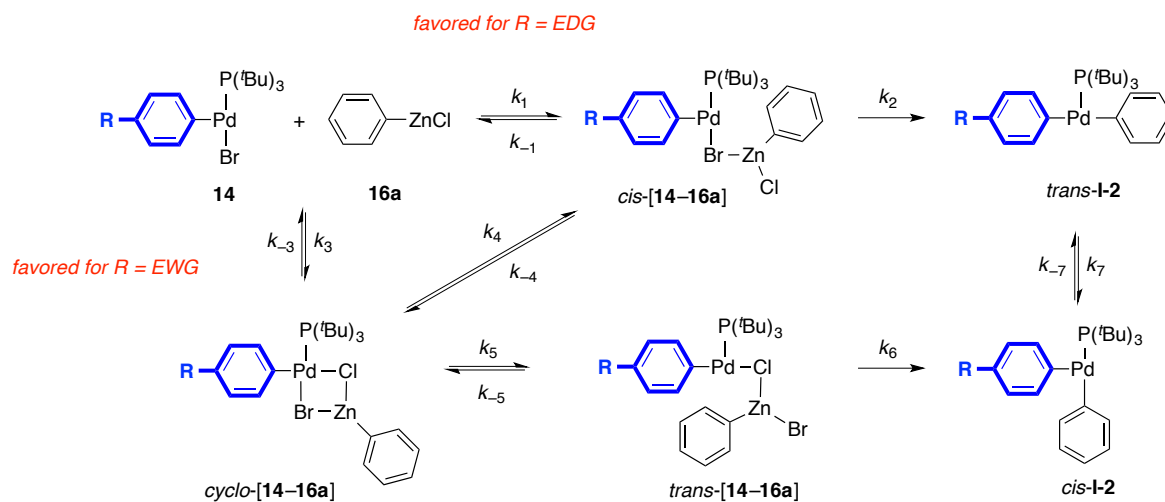
Scheme 22. Possible pathways for the transmetalation with coordinatively unsaturated complexes **14**.

The second most favored pathway with $K_{\pm 3}$, which was previously supported by DFT calculations by Gosmini, Mézailles and co-workers for a similar T-shaped complex,[48] proceeds via probably fast and almost irreversible formation of the halide-bridged cyclic complex *cyclo*-[**14–16a**]. The formation of *cyclo*-[**14–16a**] would be favored over the intermediate *cis*-[**14–16a**], because it is more stabilized since the previously coordinatively unsaturated palladium(II) center becomes saturated by the halide ligand of the arylzinc reagent **16a**. In addition, the intermediate *cyclo*-[**14–16a**] is conceivably too stable to react back into the starting materials, therefore, its formation can be regarded as almost irreversible and product-determining with respect to the competition experiment. Consequently, the Hammett constant ρ_3 is almost equal to the observed Hammett constant ρ_{obs}, which would be positive, as supported by the experimental findings, because the formation of the cyclic intermediate *cyclic*-[**14–16a**] would be favored for the more electrophilic complexes **14**.

The aryl group transfer from zinc(II) to the palladium(II) cannot take place directly from the intermediate *cyclo*-[**14–16a**], because the aryl ligand is to far away from the palladium(II) center constituted by the geometry of *cyclo*-[**14–16a**] (scheme 22). Therefore, one of the palladium-halide bonds must be broken to form either the intermediate *cis*-[**14–16a**], if the chloride ligand would have dissociated with $K_{\pm 4}$, or the intermediate *trans*-[**14–16a**] if the bromide ligand has dissociated with $K_{\pm 5}$. The later case would be presumably more favored, because a Pd-Br is weaker than the Pd-Cl bond. Subsequent aryl transfer, taking place from intermediate *trans*-[**14–16a**], result directly in a *cis*-configured diarylpalladium(II) intermediate *cis*-**I-2**, from which the reductive elimination occurs directly.

1.3.8   Influence of phosphine ligand on the transmetalation with phenylzinc chloride

To elucidate the influence of the phosphine ligands on the transmetalation rate, we performed additional competition experiments where two differently phosphine-ligated bromide complexes with ester-substituted aryl ligands compete with each other for the arylzinc reagent **16a** (scheme 23). The ratio of the two biaryls **17ai** and **17aj** represents the relative rates for the transmetalation with the different phosphine complexes. The σ-values for the ester-substituents are approximately the same, if the alkyl chain at the ester is long enough. Therefore, we chose the ethyl and butyl esters for our study. Although, most of the bromide complexes with essentially all phosphine ligands (except P^{t}Bu$_3$) exhibited poor solubilites in THF, the ester-substituted complexes for all classes of phosphine ligands exhibit sufficiently good solubility in THF, so that they could be used for this study.
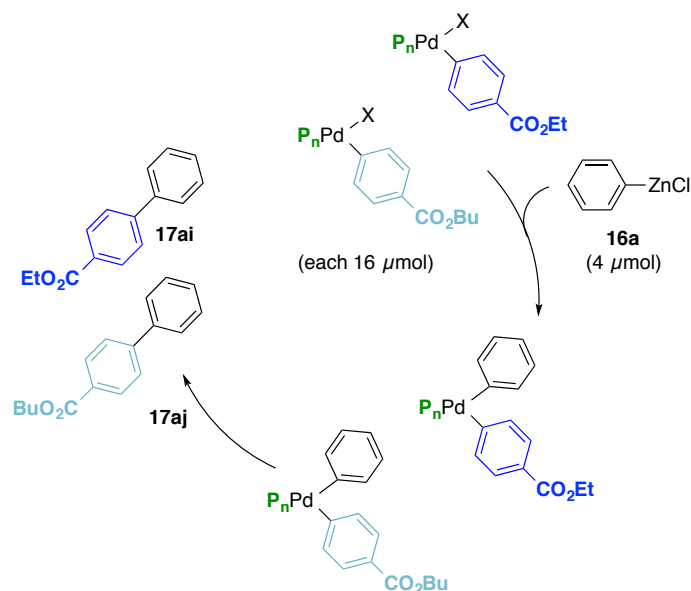
Scheme 23. Competition experiment between two competing complexes with different phosphine ligands.

Table 14. Combinations of the complexes with different phosphine ligands for the competition experiments.

	$R = CO_2Et$					
	dppe	dppf	PPh_3	$P(o\text{-tol})_3$	P^tBu_3	XPhos
	(6i)	**(7i)**	**(9i)**	**(5i)**	**(14i)**	**(13i)**
dppe **(6j)**	A1	A2	A3	A4	A5	A6
dppf **(7j)**	B1	B2	B3	B4	B5	B6
PPh_3 **(9j)**	C1	C2	C3	C4	C5	C6
$P(o\text{-tol})_3$ **(5j)**	D1	D2	D3	D4	D5	D6
XPhos **(13j)**	F1	F2	F3	F4	F5	F6

($R = CO_2Bu$)

According to the results from the competition experiments with the same phosphine-ligated complexes (*cf*. chapter 1.3.7), we would expect that the coordinatively unsaturated complexes would react faster than the coordinatively saturated complexes. Furthermore, the complexes with the least steric demand of the phosphine ligand would also react faster than the ones with sterically more bulky ligands. With the exception of the dimeric $P(o\text{-tol})_3$-ligated complex **5**, which presumably reacts slower than the other complexes, because the formation of the corresponding intermediate adduct [**5**–**16a**] requires that the dimer dissociates into its monomer. However, it was previously shown that the equilibrium lies essentially fully on the site of the dimer.[24b] A potential formation of intermediate adduct [**5**–**16a**] directly from the dimer would be also much slower than with the other complexes, because the bridged bromide ligand is coordinatively saturated und would coordinate to zinc(II) much slower than a non-bridged bromide ligand.

Accordingly the following reactivity order would be expected:
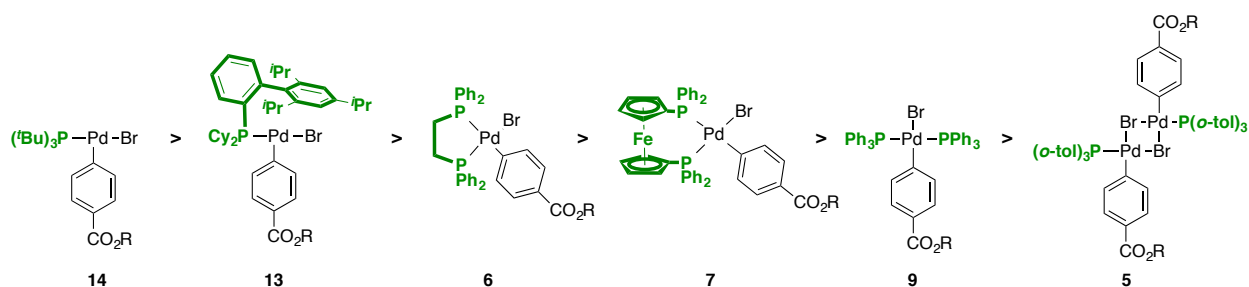
One set-up for the competition experiments was performed analogues to the other competition experiments with same phosphine-ligand but different ester-substituted aryl ligands. The performed combinations are summarized in table 14. The average results of two runs are outlined in table 15 as relative reaction rates $k_{rel} = k^{Et}/k^{Bu}$. As control experiment, we also performed the competition experiment between complexes with the same phosphine ligand, but different ester-substituted aryl ligand to verify that there are no reactivity trends originated by the different alkyl chains of the esters. Within the error range, we could not observe significant reactivity differences between the different esters of complexes **13, 6** and **9**. However with the dppf complexes **7** and P(o-tol)$_3$ complexes **5**, the butyl esters reacted approximately twice as fast than the corresponding ethyl esters. Due to this discrepancy, all relative reaction rates resulting from combinations of dppf complexes **7** and P(o-tol)$_3$ complexes **5** with another phosphine complex (gray values) might be burdened with an large uncertainty.

Nevertheless, the other combination provided apparently more accurate values. The relative reactivity with respect to the dppe-ligated butyl ester complex **6j** (table 15, first row) is almost as expected with the coordinatively unsaturated complex reacting much faster, whereas P^{t}Bu$_3$-ligated complex **14i** was the fastest. The PPh$_3$-ligated complex **9i** reacted slightly faster than the dppe complex **6j**, which is in contrast to the expected reactivity trend. The faster reaction of **9i** is also verified in the cross experiment, where the corresponding butyl ester complex **9j** reacted with the ethyl ester complex **6i** (fourth row). Regarding the reactivity trends with respect to the XPhos-ligated butyl ester complex **13j** (second row), the PPh$_3$-ligated complex **9i** behaved unusual in so far that it reacted even faster than the XPhos complex **13j**, although the other reactivity trends with P^{t}Bu$_3$- and dppe-ligated complexes maintained. Furthermore, competition experiments of butyl ester complexes **9j** with ethyl ester complexes **13i**, **14i** and **6i** showed general higher reactivity of the PPh$_3$-ligated complexes.

Table 15. Relative reaction rates from the competition experiments with complexes ligated by different phosphine ligands.

$$k_{rel} = k^{Et}/k^{Bu}$$

	$P(^tBu)_3$	dppe	XPhos	dppf	PPh_3	$P(o\text{-}tol)_3$
dppe	8.14	**1.01**	5.46	0.08	1.16	0.32
XPhos	5.82	0.26	**1.11**	0.34	3.72	0.32
dppf	3.57	7.68	3.25	**0.48**	1.27	0.33
PPh_3	0.93	0.60	0.48	0.64	**1.04**	0.23
$P(o\text{-}tol)_3$	8.94	0.91	1.48	1.10	1.64	**0.45**

The inconsistent relative reactivity of the PPh_3-ligated complexes **9** with respect to the coordinatively unsaturated complexes **13** and **14**, let us consider ligand scrambling processes between the complexes. Indeed, when we mixed the differently phosphine-ligated complexes bearing different substituents at the aryl ligand in THF, the ^{31}P NMR spectra (see Experimental Section) clearly showed that ligand scrambling occurs with dppf and PPh_3 complexes with all other phosphine complexes except with dppe complexes **6**. The extent of the scrambling seems to follow the trend PPh_3 > dppf > XPhos > P(o-tol)$_3$. Notably, the ^{31}P NMR spectra of the scrambling experiments, as well as the control spectrum recorded of a mixture of differently substituted complexes **14** showed large amounts of cyclometalated complex [Pd(Br)($^tBu_2PCMe_2CH_2$)]$_2$ (dimer **B**), which is a decomposition product of the aryl complex **14**.[92] As mentioned above, P^tBu_3 complexes **14** are inherently unstable in solution, which was already observed when recording NMR spectra for their characterization, as well as during the set-up of the competition experiments.

Nevertheless, because dppe complexes **6** did not show any ligand scrambling with the other phosphine complexes, the results of the corresponding competition experiments provided reliable results for the relative reaction rates (table 15, first row). Accordingly, the reactivity order is:
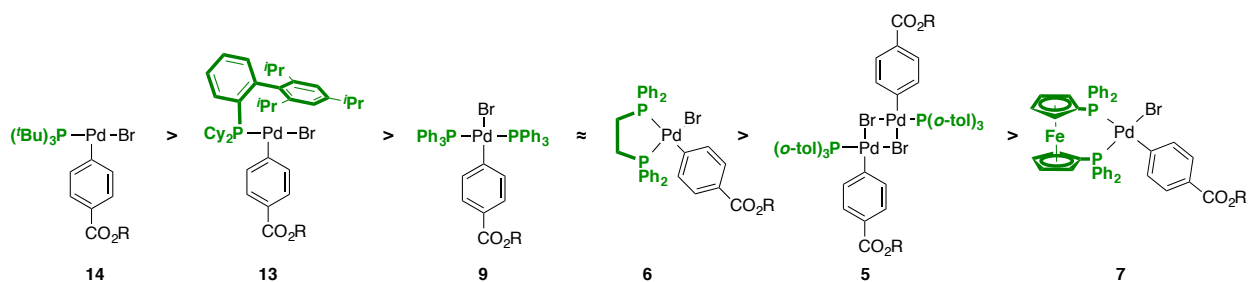
The determined reactivity order with respect to the differently phosphine-coordinated complexes deviates slightly from the expectations based on the steric parameters in so far that the PPh_3 complexes **9** reacted faster and the dppf complexes **7** reacted slower. Possibly, the transmetalation with PPh_3 complex **9** might proceed via a different mechanism, where one phosphine ligand dissociates during the aryl transfer from zinc to palladium as it has been proposed by Espinet and co-workers for the Stille couplings with stannanes.[3] As for the dppf complex **7**, the smaller reactivity might be due to the weaker coordination of the dppf ligand to the palladium(II) metal center, which is supported by the ability of ligand scrambling. The weaker coordination of the ligand would result in a more electrophilic palladium(II) metal center, and therefore making the bromide ligand stronger bound, which finally results in weaker coordination to the zinc(II) center.

1.3.9   Detection of a transmetalation intermediate by cryogenic NMR

Because the computational results suggest that a cyclic intermediate [**I-2**–ZnX_2(thf)] is probably formed as the most stable intermediate along the transmetalation pathway, we became curios if it possible to detect such a species by NMR spectroscopy under cryogenic conditions. Similar to the recent report of Denmark and co-workers, who were able to detect the intermediate adducts of palladium(II) hydroxide complexes and arylboronic acid derivates by NMR spectrsocopy at –30 °C,[28] we performed the corresponding transmetalation experiment with arylpalladium(II) complex **2** and arylzinc reagent **16** under similar conditions. Therefore, the arylpalladium(II) complex **2k** was dissolved in THF in an NMR tube, and a solution of arylzinc reagent **16**, which was prepared by dissolving diarylzinc **15** and $ZnCl_2$ in THF, was added at –78 °C. The NMR tube was sealed and directly transferred into the NMR probe pre-cooled to –40 °C.
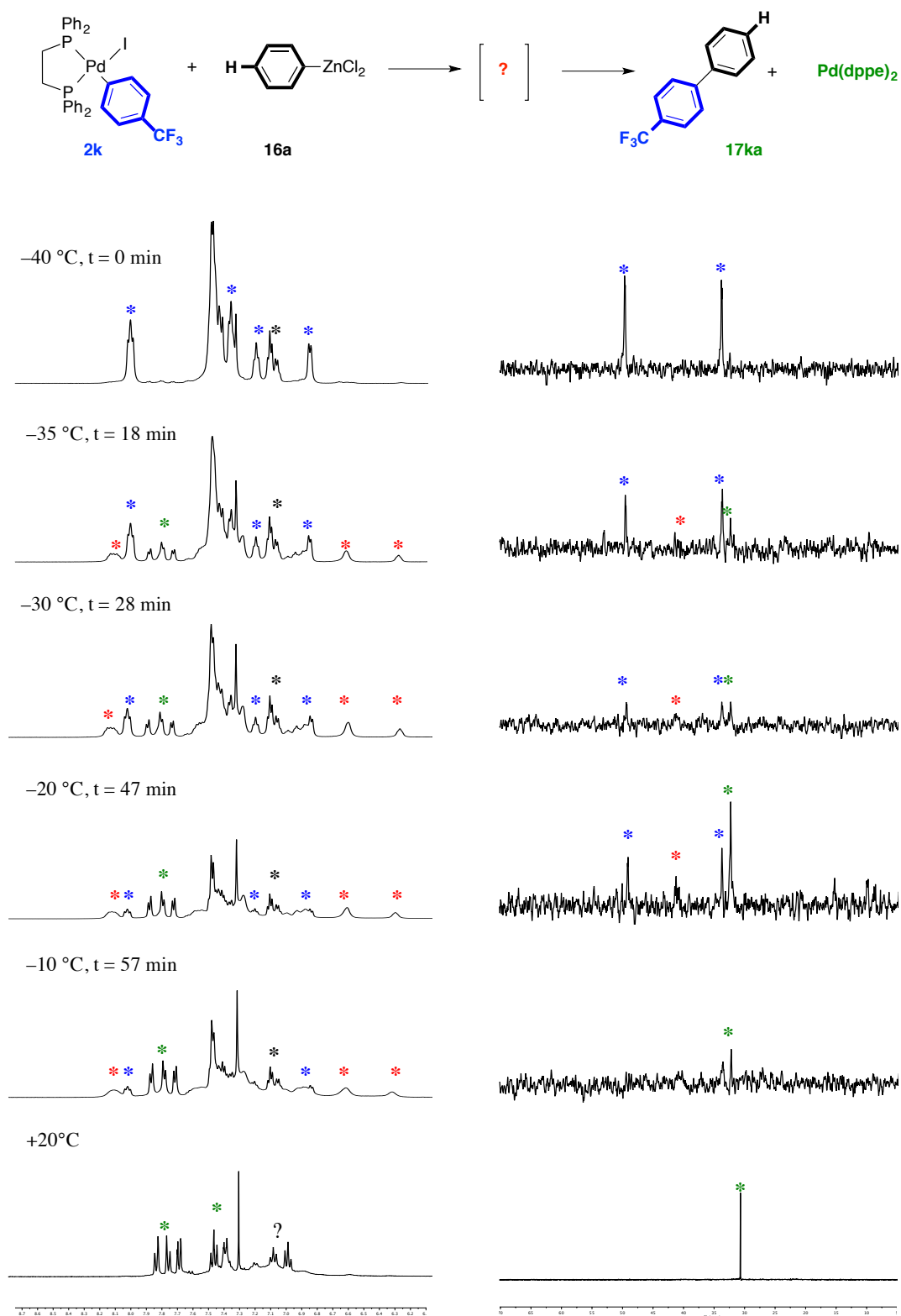
Figure 17. Monitoring of transmetalation between **2k** and **16a** by ^{1}H and ^{31}P NMR in THF-d_8 at different temperatures.

In the first experiment, we mixed arylpalladium(II) complex **2k** and phenylzinc chloride (**16a**) and recorded spectra at increasing temperatures (figure 17) to see at which temperature a reaction becomes observable. The ^{1}H NMR spectrum at –40 °C showed no reaction. At –35 °C product formation was

observed besides an additional set of signals, which might belong to a putative intermediate. The integrals of these signals increased further at –30 °C, however decreased again at –20 °C and –10 °C, while the product signals continuously increased upon warming. The intermediate signals disappeared at room temperature, however, two additional aromatic signals appeared besides the product signals. Unfortunately, the resolutions of the corresponding ^{31}P NMR spectra were low, which makes it difficult to observe an intermediate. Nevertheless, the signal of the dppe-ligated palladium(0) species, which results after reductive elimination of diarylpalladium(II) *cis*-**I-2**, is the only product visible in the ^{31}P NMR at 30.8 ppm (ref. 93: 30.4 ppm in THF-d_8).

To obtain better resolved NMR spectra, we repeated the transmetalation experiment with complex **2k** and anisylzinc chloride (**16d**) with higher concentration of the reactants (figure 18). The signals of the transmetalation product biaryl **17kd** and the additional set of signals, which might belong to an intermediate, appeared already at –40 °C, while with phenylzinc chloride (**16a**) no reaction occurred. This indicates higher reactivity of the more electron-rich arylzinc reagent, which is consistent with our previous findings. Due to the better resolution of the ^{31}P NMR spectra, it becomes more clear that three intermediates are formed. Two sets of doublets (J = 49 Hz and J = 47 Hz) were observed at 41 ppm and 9 ppm, which might belong to two different isomers of an adduct of **2k** and **16d**. The ratio of these signals is always 1:1 at every time point and even at different temperatures. The third set of doublets appeared at 34 ppm and 33 ppm with a coupling constant of 15 Hz and is in an approx. ratio of 1:2 to the other set of doublets.

A second identical sample was prepared and monitored at –25 °C for 50 min. The well separated signal at 8.02 ppm of the complex **2k** (4 protons), at 6.76 ppm of anisylzinc reagent **16d** (2 protons), at 7.69 ppm of biaryl **17kd** (2 protons) and the putative intermediate at 8.16 ppm (presumably 4 protons) were monitored. Integration *vs.* the solvent residual peak for THF-d_8 reveals that in the beginning (approx. 5 min) the complex **2k** and arylzinc **16d** are consumed, while biaryl **17kd** and the intermediate are formed with a high rate, however, after approximately 10 min the concentrations remained constant (figure 19). A similar trend was observed in the corresponding ^{31}P NMR spectra. The integrals of the observed species were plotted as fraction to the total integral of all phosphorous containing species. The starting complex **2k** at 49.7 ppm (1 phosphorous) is consumed very rapidly within the first 5 minutes, while the unknown sets of doublets at 41 ppm (two species in 1:1 ratio each presumably with 1 phosphorous), and at 33 ppm (presumably 1 phosphorous), as well as the palladium(0) complex Pd(dppe)$_n$ at 32.5 ppm (here probably n = 1) are formed. After approximately 10 min, the concentrations did not change anymore.

¹H NMR (500 MHz, THF-d_8)

³¹P NMR (202 MHz, THF-d_8)
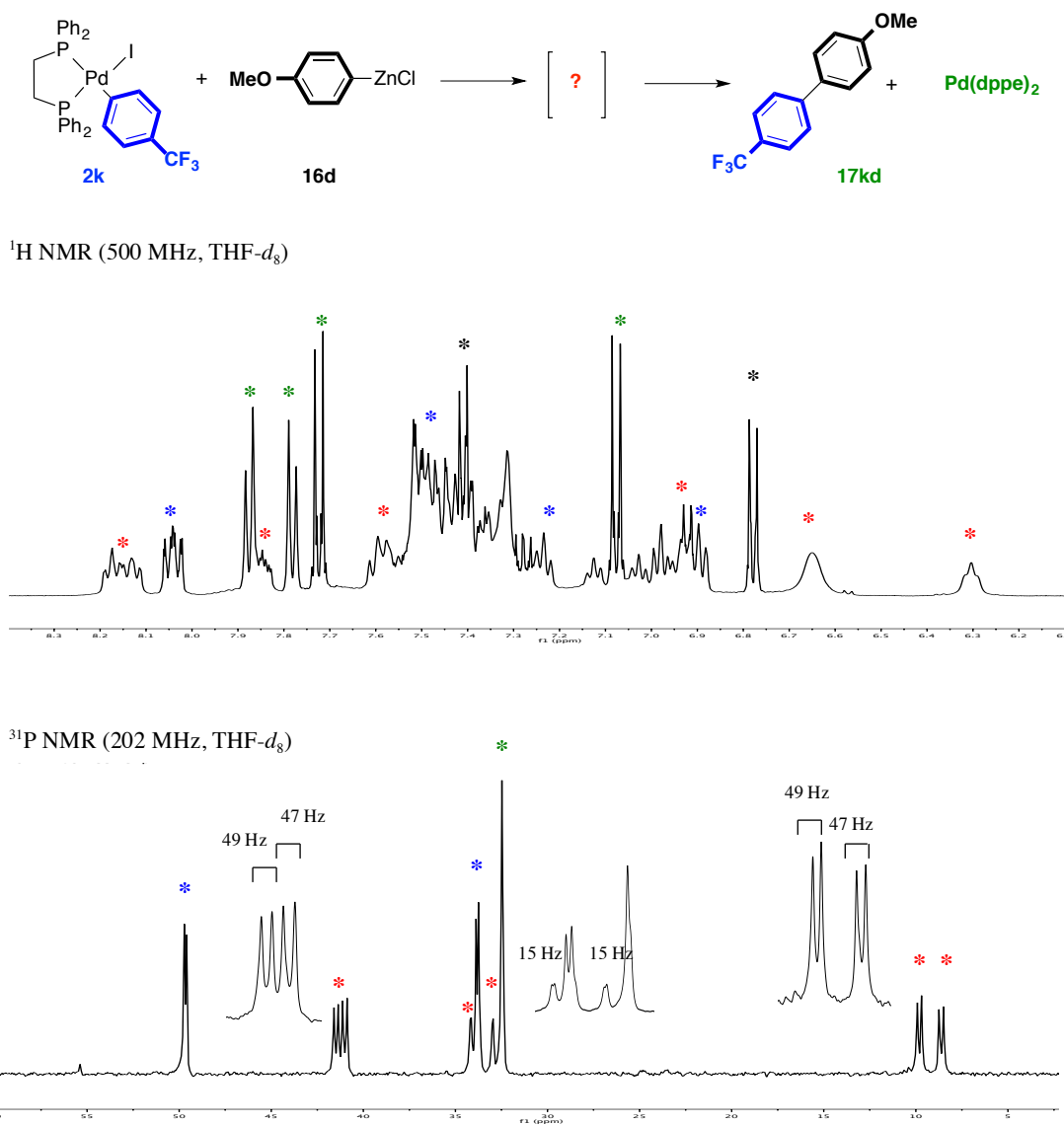
Figure 18. ¹H and ³¹P NMR spectra of transmetalation between **2k** and **16d** at –40 °C.
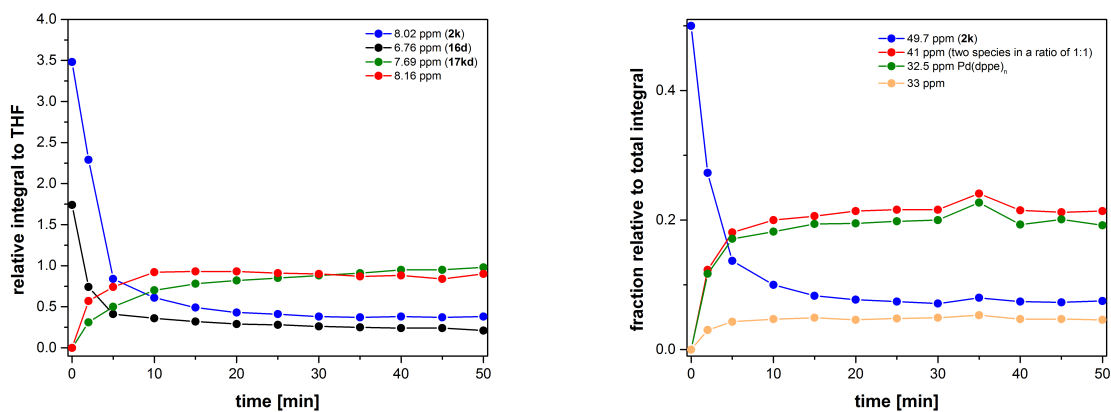
Figure 19. Concentration monitoring of transmetalation between **2k** and **16a** by ¹H and ³¹P NMR in THF-d_8 for 50 min.

The reaction profiles in figure 19 indicate an equilibrium between the starting complex **2k** and another palladium species rather than the occurrence of an productive intermediate, such as [**2k**–**16d**(thf)] or [**I-2**–ZnX$_2$(thf)], because those concentration profiles typically show an initial increase of the concentration of the intermediate, which is than consumed over the reaction time. However, here, the concentrations of the reactants, products and intermediates do not change after the initial reaction time, which suggests that the reaction stopped at some point at a constant temperature. The products, biaryl **17kd** and Pd(dppe)$_n$, apparently participate in this equilibrium, which is unusual considering that the reductive elimination is an irreversible process. One might speculate that the reactants **2k** and **16d** form a short-lived putative productive intermediate, such as aryl-bridged intermediate [**I-2**–ZnX$_2$(thf)]. This intermediate is not observable by NMR spectroscopy, and forms rapidly the products biaryl **17kd** and Pd(dppe)$_2$. At the same time, the unproductive intermediates, such as [**2**–**16′**(thf)] or [**2**–ZnX$_2$(thf)], might be also formed, which are in equilibrium with the starting complex **2k** and anisylzinc reagent **16d**.

Because the signals in the ^{1}H and ^{31}P NMR of the intermediates are not characteristic enough to distinguish between an adduct of **2k** with **17kd** or with the byproduct ZnX$_2$, we performed a titration NMR experiment of complex **2k** with ZnCl$_2$. While the signals in the ^{1}H NMR spectra were not shifted upon addition of 1.25 or 2.40 equivalents of ZnCl$_2$, the doublets in the ^{31}P NMR spectrum shifted slightly from 49.6 and 35.0 ppm to 50.7 and 36.0 ppm with 1.25 equivalents of ZnCl$_2$. More equivalents of ZnCl$_2$ did not lead to further changes of the phosphorous chemical shifts. The changes in the ^{31}P NMR spectrum might be also a result of the change of the dielectricity of the solvent when adding ZnCl$_2$, or due to the formation of cationic complex [**2k**(thf)]$^+$ and zincate [ZnCl$_2$I(thf)]$^-$ rather than formation of an adduct of **2k** an ZnCl$_2$, because the coupling constant of the doublets (26 Hz) remained constant. To investigate the latter case, we prepared the corresponding tosylate complex in CDCl$_3$ using AgOTs *in situ*, which should provide the cationic complex [**2k**(thf)]$^+$. Indeed, the coupling constant did not change significantly (26.6 Hz), and the ^{31}P NMR chemical shifts were shifted to 54.1 ppm and 34.5 ppm, up-field compared to the neutral complex **2k** (49.6 and 35.0 ppm, 26 Hz). Accordingly, the formation of [**2k**(thf)]$^+$ and zincate [ZnCl$_2$I(thf)]$^-$ cannot be excluded in the presence of ZnCl$_2$. Nevertheless, attempted crystallization of a putative salt [**2k**(thf)][ZnCl$_2$I(thf)] or adduct [**2k**–ZnCl$_2$(thf)] failed, providing single crystals only of the starting complex **2k**.
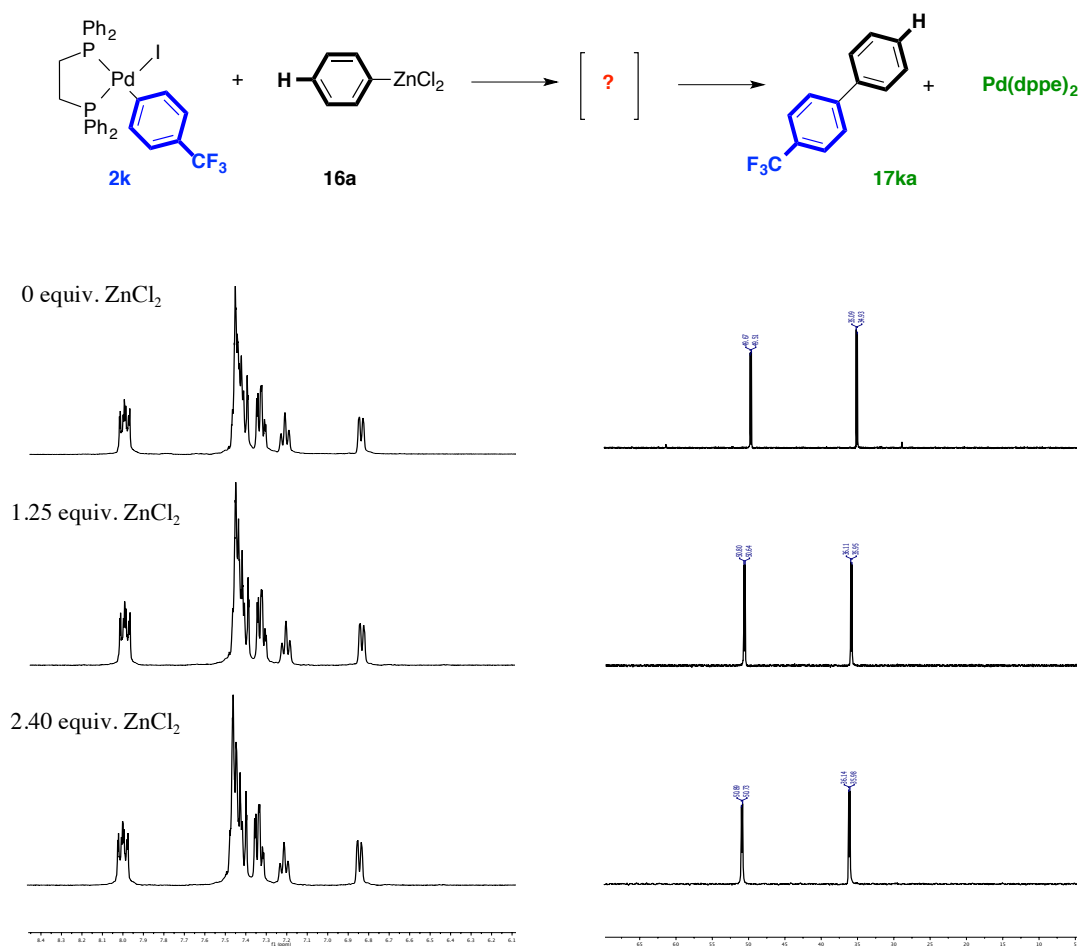
Figure 20. ^{1}H and ^{31}P NMR spectra in THF-d_8 at room temperature of titration experiments of complex **2k** with ZnCl$_2$.

Although the NMR spectra did not unambiguously show the formation of an intermediate of arylpalladium(II) complex **2k** and arylzinc reagents **16a** or **16d**, we are still confident, that the transmetalation proceeds via an intermediate rather than via a concerted mechanism, because we could observe the formation of an unproductive intermediate, probably [**2k**–**16d′**(thf)], which is in equilibrium with the starting materials **2k** and **16d**, because it is consumed upon heating, and probably converts slowly at low temperatures (–40 °C) after longer reaction times. This is supported by the observed decomposition of the reaction solution when attempting crystallization at –30 °C of the unproductive intermediate [**2k**–**16d′**(thf)].

1.4   Conclusion

We prepared different arylpalladium(II) complexes and isolated diarylzinc compounds, which allowed us to study the isolated transmetalation step in Negishi cross-couplings by competition experiments. The transmetalation experiments of competing dppe-ligated complexes **2** with phenylzinc chloride (**16a**) provided a negative Hammett constant, which became even more negative with more Lewis acidic arylzinc reagents. The corresponding experiments with competing arylzinc chlorides **16** in transmetalation with complexes **2** provided also a negative Hammett constant, which is in accordance with previous result by Mayr and co-workers.[7h] However in disagreement with their results, we observed that the Hammett constant became more negative with anisylpalladium(II) complex **2d** compared to the phenyl complex **2a**.

Because negative Hammett constants were obtained from all competition experiments independently whether complexes **2** or arylzinc reagents **16** are the competing reagents, we hypothesized that the transmetalation proceeds via at least one intermediate rather than via a concerted mechanism. DFT calculations support the formation of intermediate adduct [**2**–**16**(thf)] with a bridging iodide ligand (scheme 24). The intermediate adduct [**2**–**16**(thf)] was found to be preferentially formed with nucleophilic complexes **2** and less Lewis acidic arylzinc reagents. This is at first counterintuitive, because a higher Lewis acidity of the arylzinc reagent would be expected to facilitate the coordination of the zinc(II) center to the halide ligand of complex **2**. However, the observed trends can be explained by the HSAB concept. The zinc(II) represents a borderline acid, however, is a hard Lewis acid with respect to the soft iodide ligand. Accordingly, factors, which makes the iodide ligand to a harder Lewis base, such as increased electron-donating properties of the other ligands at the palladium(II) center weakening the Pd-I bond, or factors, which makes the zinc(II) center to a softer Lewis acid, such as electron-donating substituents at the aryl group, lead to more thermodynamically stable intermediate adducts [**2**–**16**(thf)].
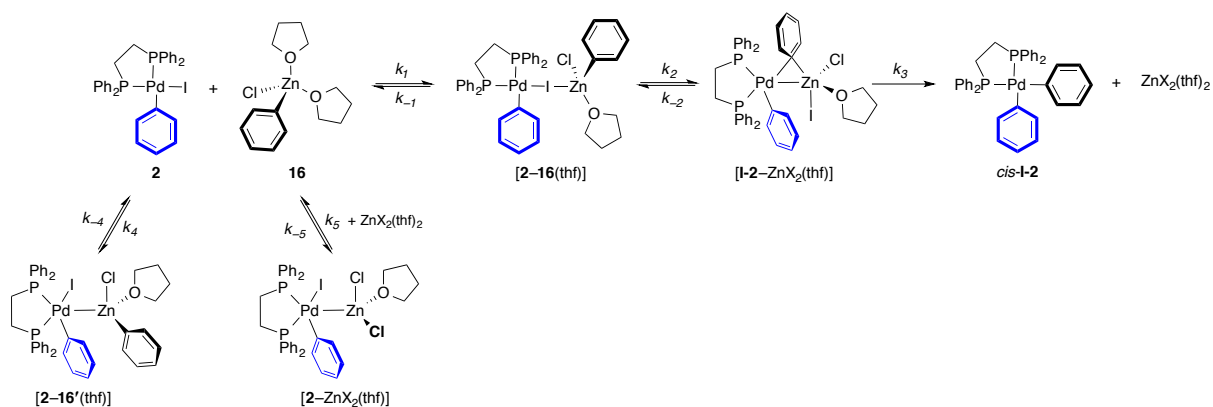
Scheme 24. Modified mechanism of the palladium-catalyzed Negishi cross-coupling reaction.

Furthermore, intermediate adduct [**2–16**(thf)] converts into another cyclic, product-like intermediate [**I-2**–ZnX$_2$(thf)] before finally diarylpalladium(II) complex *cis*-**I-2** is formed. The formation of cationic intermediate [**2**(thf)]$^+$ was calculated to be an unfavored process, which was further supported by additional competition experiments with competing complexes **2** and phenylzinc reagent **16a** using one equivalent of LiCl or ZnCl$_2$ (with respect to **16a**) as additive. If ionic intermediates were passed during the transmetalation, the observed Hammett constant should change, however, no changes were observed. Moreover, competition experiment and computational results with additional ligands (dppe and tmeda) suggest that cationic complexes [**2**(L)$_2$]$^+$ might be formed under these conditions, however, these cationic species do not undergo the actual aryl transfer.

Interestingly, DFT calculations revealed that complexes **2** and arylzinc **16** might form also an unproductive adduct [**2–16′**(thf)], which can be characterized as a conformer of the productive intermediate [**2–16**(thf)]. Presumably, we observed this intermediate during the ^{1}H and ^{31}P NMR monitoring experiments under cryogenic conditions (–40 °C), which showed continuous formation of two or three additional species. Another unproductive intermediate, formed by the complex **2** and the byproduct ZnX$_2$, was found by DFT calculations, and its existence supported by competition experiments. The competition experiments with competing complexes **2** and phenylzinc reagent **16a** in the presence of larger amounts of ZnCl$_2$ (> **16a**) resulted in less negative Hammett constant compared to the one obtained without additive, which suggest that the unproductive intermediate [**2**–ZnX$_2$(thf)] is indeed formed, and is in equilibrium with the complex **2**. Unfortunately, attempted isolation or observation by NMR spectroscopy of [**2**–ZnX$_2$(thf)] failed.

We also performed competition experiments with other competing arylpalladium complexes having different phosphine ligands (dppf, PPh$_3$, P^{t}Bu$_3$ and XPhos) and different coordination numbers. The results revealed that increasing steric bulk of the ligands results in less negative Hammett constants. Whereas the bulkiest ligand (P^{t}Bu$_3$), which forms typically T-shaped coordinatively unsaturated complexes **14**, provided a positive Hammett constant. This unusual reactivity trend can be explained by a fast formation of a much more stable dinuclear intermediate, where both halides bridge the metal centers to fill the vacant coordination site at the palladium(II) center. The reactivity trend with respect to the phosphine ligand was obtained by competition experiments using competing ester-substituted arylpalladium complexes. The relative reaction rates revealed the following reactivity trend: P^{t}Bu$_3$ > XPhos > PPh$_3$ > dppe > P(*o*-tol)$_3$ > dppf.

2 Palladium-Catalyzed Directed Halogenations of Bipyridine *N*-Oxides

2.1 Motivation

C3-Substituted 2,2′-bipyridine is a common structural motif in well-investigated biologically active natural products,[94] such as the cytotoxic Streptonigrinoids, Lavendamycin and Streptonigrin,[95] as well as Camptothecin and the mycotoxin Orellanin (figure 21).[96] Less explored are Caerulomycines, which are natural products from marine-derived bacteria and have shown diverse interesting biological and pharmacological activities in initial studies.[97] Due to their high potential as drug candidate, we are interested in systematically investigating the structure-activity relationships of rationally substituted derivatives, demanding a short synthetic route being flexible in the introduction of functionalities. However, some derivatives are substituted at the synthetically difficulty accessible C3 position.[98]
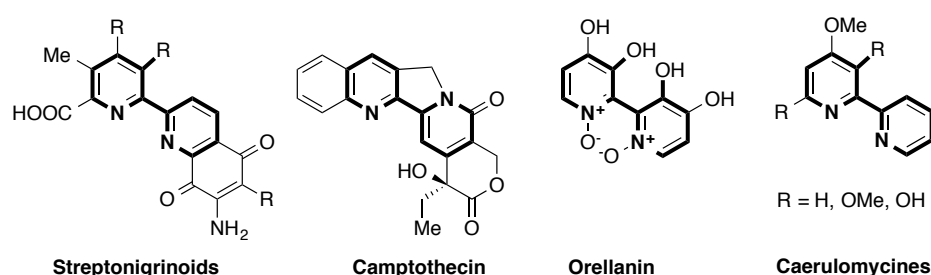
Figure 21. Natural products containing C3-substituted 2,2′-bipyridine motifs.

We thought that introduction of a halogen would provide C3-halogenated bipyridines, which could serve as precursors for nucleophilic aromatic substitutions (S_NAr), halogen-metal exchange followed by quenching with an electrophilic reagent, or for coupling reactions and other transformations. However, a literature search revealed only little precedent for the synthesis of 3-halobipyridines. Some examples have been prepared by cross-coupling procedures (scheme 25A), using 3-halopyridines (or their *N*-oxides) with another pyridyl coupling partner.[99] These procedures are often limited to 3-fluoropyridines and require multi-step preparations of the substrates. Two other reports involve a directed *ortho*-metalation (DoM) (scheme 25B) with strong lithium bases followed by quenching with an electrophilic halogenation reagent,[100] however, these reactions provided only low yields.

A Palladium-catalyzed cross-couplings (Suzuki, Negishi, Stille, Hiyama)
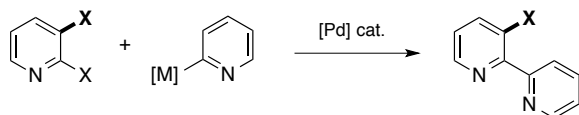
B directed *ortho*-metalation (DoM)
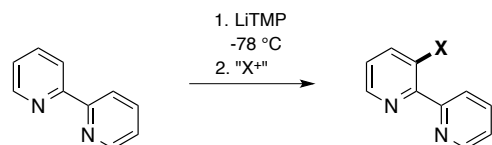
C transition metal-catalyzed chelate-assisted direct functionalizations
(this work)
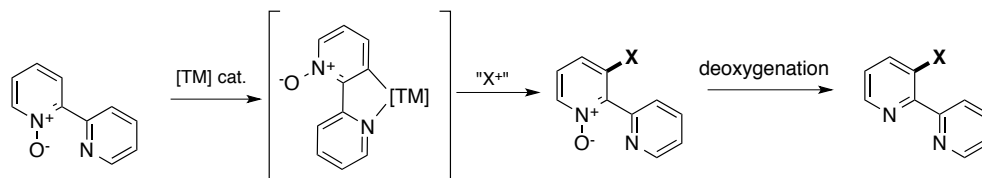
Scheme 25. Strategies for the synthesis of 3-halo-2,2′-bipyridines.

We envisaged transition metal-catalyzed direct functionalization reactions, which have been demonstrated for substrates with numerous directing groups in the *ortho*-position,[101] might be a more efficient for the synthesis of 3-halo-2,2-bipyridines. In particular, pyridyl-directed C-H bond functionalizations have been widely used in the synthesis of *ortho*-substituted 2-arylpyridines, benzo[*h*]quinolines and similar structures.[102] However, structurally related bipyridines are considered to be problematic substrates for the transition metal-catalyzed directed halogenation, because the catalytic process would require intermediate formation of so-called "roll-over" complexes (*C,N*-chelate complex) from a stable bipyridine chelate precursor complex (*N,N*-chelate complex), proceeding via high energy barriers only under certain conditions.[103] Only few examples of roll-over complexes have been reported with iridium,[104] rhodium,[105] platinum,[106] gold,[107] and palladium[108] formed from stoichiometric reactions. Even fewer reports are found for catalytic reactions involving exclusively rhodium-catalyzed C3-alkylations and alkenylations with terminal olefins,[109] and silylacetylenes.[110] Therefore, we assumed that bipyridine *N*-oxides could serve as *N*-protected substrates to circumvent the "roll-over" problem and favor C3 C-H bond activation (scheme 25C).[111] Subsequent deoxygenation of the halogenated bipyridine *N*-oxides would then provide the desired 3-halobipyridines.

2.2   Background

2.2.1   Previous syntheses of 3-halobipyridines

Direct halogenation reactions of bipyridines or structurally related compounds have been rarely described. Simple halogenation of arenes via an electrophilic substitution pathway (S_EAr) with elemental halogens are not suitable, because pyridines (and bipyridines) are general unreactive substrates due to the less stabilized intermediate sigma-complexes. Nevertheless, reaction would takes place under very harsh conditions and would occur at the most electron-rich C5 position of bipyridine.[112] An *ortho*-directed lithiation approach followed by quenching with electrophilic iodine or bromine gave the desired product, however in low yields. Zoltewicz and Dill reported the synthesis of 3-iodo-2,2′-bipyridine by *ortho*-directed lithiation with LiTMP followed by quenching of the bipyridyl anion with elemental iodine (scheme 26).[100a] This protocol provided the desired product only in 11% yield. Similarly, Takahashi *et al.* reported the synthesis of 5,5′-(triethylsilyl)-3-bromo-2,2′-bipyridine using the same lithiation procedure.[100b] Quenching with 1,2-dibromoethane gave the desired product in somewhat higher yields of 52%.
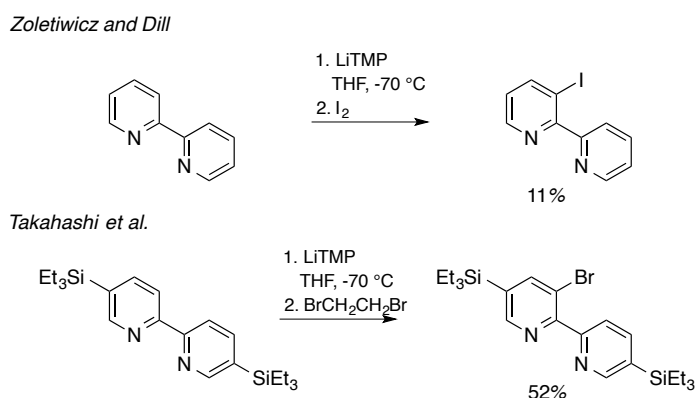
Scheme 26. Synthesis of 3-halobipyridines by directed *ortho*-lithiation.

Deprotonation with strong lithium bases of the corresponding, more reactive bipyridine *N*-oxide **20a** even under kinetic control occurs at the C6 position giving the thermodynamic product due to the highest acidity of the C-H bond next to the electron-withdrawing *N*-oxide. In the context of the total synthesis of Caerulomycines A and E, Trécourt *et al.* obtained 6-iodo-2,2′-bipyridine *N*-oxide in 55% yield by lithiation with LDA and quenching with iodine (scheme 27).[113] Similarly, the brominated product was obtained in 70% using cyanogen bromide as electrophile.

Trécourt et al.
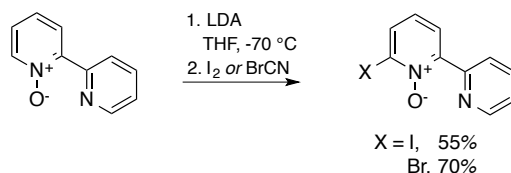
Scheme 27. Synthesis of 6-halobipyridine *N*-oxide by lithiation followed by quenching with electrophilic halogens.

Cross-coupling procedures, such as Suzuki, Stille or Negishi coupling have been applied for the synthesis of various symmetrically and unsymmetrically substituted bipyridines.[114] However, the synthesis of 3-halobipyridines has not been reported to the same extent. Gros and co-workers developed the palladium-catalyzed Hiyama cross-coupling reaction for the preparation of chloro-substituted bipyridines and prepared 3-chlorobipyridine **21a** in 65% by reaction of 2-(trimetylsilyl)-3-chloropyridine with 2-bromopyridine (scheme 28).[99a] In the context of the total synthesis of Lavendamycin, Quéguiner and co-workers synthesized the bipyridine core by a Stille coupling between the 3-fluoropyridyl fragment and 2-quinoline(trimethyl)stannane providing 67% of the coupled product after 60 h in refluxing toluene.[99b]

Gros and co-workers

Quéguiner and co-workers
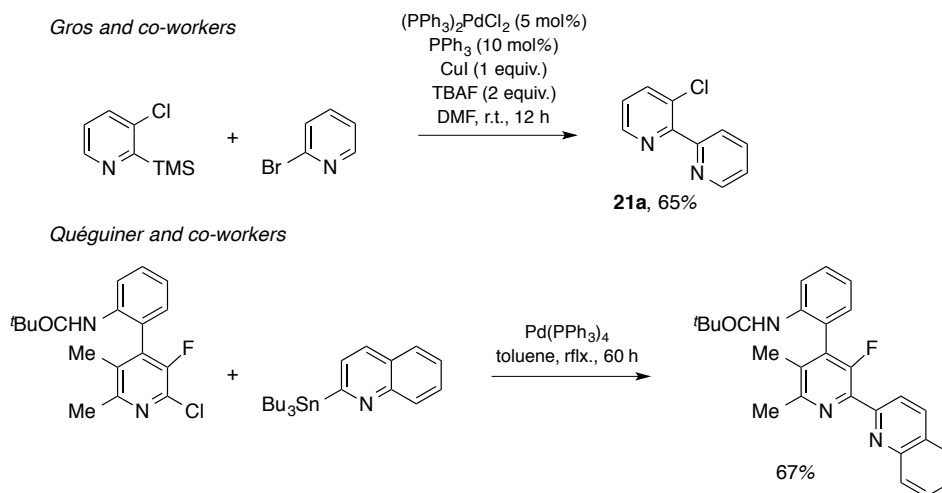
Scheme 28. Synthesis of 3-chloro- (**21a**) and 3-fluorobipyridine by a cross-coupling reaction.

The general challenge of using 2,3-halopyridines (except 2-halo-3-fluoropyridines) as electrophilic coupling partners in cross-coupling reactions is the C2-regioselective oxidative addition (*vs*. C3-oxidative addition) forming a pyridylpalladium(II) intermediate, which then is transmetalated with a pyridyl nucleophile. Nevertheless, we initially attempted the Negishi reaction of 2,3-dibromopyridine with pyridylzinc chloride, because we assumed that the oxidative addition would occur faster/preferentially in the C2 position due to the higher polarization of the C-X bond compared to the one in the C3 position (scheme 29). However, this reaction provided only 14% of the C3-brominated bipyridine **22a** under typical conditions with 2.5 mol% Pd(PPh$_3$)$_4$ as catalyst. Only 37% of the starting

material was recovered indicating decomposition processes, which form volatile side products. These decomposition reactions might be simple dehalogenation of the 2,3-dibromopyridine forming bromopyridines, which are volatile enough to be lost during work-up. An increased catalyst loading (5 mol%) delivered a higher yield of 28% for **22a** but is still unsatisfying low.

22a, 14% (2.5 mol%)
28% (5.0 mol%)
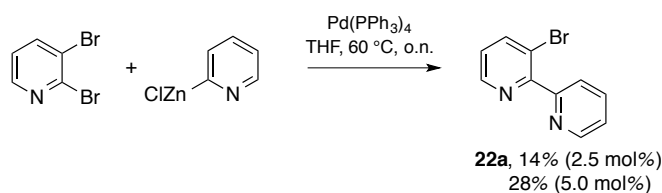
Scheme 29. Attempted synthesis of 3-bromobipyridine **22a** by Negishi cross-coupling.

The coupling reactions are generally complicated by the fact that the bipyridine products themself are strongly chelating ligands for palladium inhibiting the catalytic activity. Therefore, pyridine N-oxides, which are less coordinating to palladium, have been used as starting materials for the synthesis of unsymmetrically substituted bipyridines. The oxygen masks the Lewis-basic nitrogen, and additionally polarizes the adjacent C-H bond, which makes pyridine N-oxides more reactive towards metalation in C2 position by deprotonation with strong non-nucleophilic bases.[99c, 115] This procedure circumvents the use of halopyridine N-oxides making it synthetically more attractive.[116] Gosselin and co-workers demonstrated the synthesis of two 3-fluoro-2,2′-bipyridine N-oxides in yields of 59% and 83%.[99c] Starting from 3-fluoropyridine N-oxide, a zincated species was formed *in situ*, and directly coupled with 2-bromopyridines using (dppf)PdCl$_2$ as catalyst (scheme 30). Encouraged by these reports we also attempted the same procedure for the coupling of analogues 3-bromopyridine N-oxide with 2-bromopyridine, however we recovered mainly unreacted starting material.

R = H   59%
Me 83%
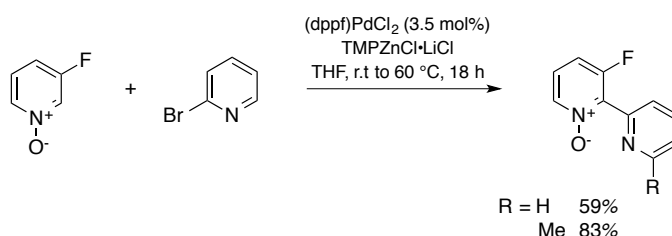
Scheme 30. Synthesis of 3-fluorobipyridine N-oxide by Negishi cross-coupling reported by Gosselin and co-workers.

Our group showed that 3-fluorobipyridine N-oxide can be also synthesized by a palladium-catalyzed direct arylation of 3-fluoropyridine N-oxide with 2-bromopyridine using K$_2$CO$_3$ as base and Pd(OAc)$_2$/P^{t}Bu$_3$ as catalyst system (scheme 31).[117] The product was obtained in 51%, however, this yield might be improved by using K$_3$PO$_4$ as base as shown in the context of the synthesis of unsymmetrical terpyridines using the direct arylation procedure.[118]
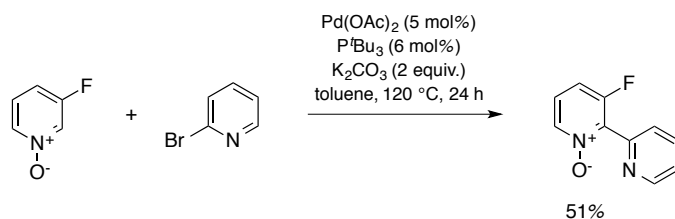
Scheme 31. Synthesis of 3-fluorobipyridine *N*-oxide by direct arylation reported by our group.

The drawback of the direct arylation approach with respect to the synthesis of other 3-halopyridine *N*-oxides is its limitation to 3-fluoropyridine *N*-oxide, since other C3-substituted pyridine *N*-oxides yield C5-substituted bipyridine *N*-oxides, because the C2 position is sterically unfavored.[117-118] The unusual regioselectivity with 3-fluoropyridine *N*-oxides results from the small size of the fluorine atom and the increased acidity and polarity of the adjacent C-H bond, which makes the C2 position more reactive.[92, 119] This would not be expected for other 3-halopyridine *N*-oxides, because of the larger steric bulk of other halogens (compared to fluorine), which would direct the C-H bond activation into the C6 position and provide undesired 5-halobiypridine *N*-oxides. Moreover, potential side reactions are conceivable with other 3-halopyridine *N*-oxides, because other C-X bonds would react with palladium(0) intermediates to give oxidative addition products, which is unlikely for C-F bonds since they are essentially inert towards oxidative addition.

2.2.2   Transition metal-catalyzed pyridyl-assisted direct halogenations

Although bipyridines or bipyridine *N*-oxides have not been reported as substrates in transition metal-catalyzed halogenations so far, we thought that using previously reported protocols would provide the desired 3-halobipyridine *N*-oxides, because the pyridyl ring is a good directing group for *ortho* C-H bond activation.[120] Moreover, this approach would circumvent the use of organometallics, which require additional steps for preparation and limit the functional group scope.

Many procedures for direct halogenation reactions of arenes have been reported for substrates using diverse oxygen- and nitrogen-containing directing groups to occur *ortho* to the specific directing group. Although some examples using rhodium,[102f, 121] cobalt,[122] nickel (stoichiometric),[123] copper,[102g, 102h, 102m, 124] and gold as catalysts have been reported,[125] palladium-catalyzed direct halogenations are more established.[101a, 126] *N*-Halosuccinimides (NXS) have been commonly used as halogen source and as terminal oxidant to functionalize arenes with directing groups, such as benzothiazoles and -quinoxalines,[127] pyrrazolones,[128] triazoles,[129] oximes,[130] carbamates,[131] amides,[132] cyano,[133] diazo compounds[134] and even boronic acid esters.[135] Azine-directed halogenations of 2-arylpyridines,

benzo[*h*]quinolines and related substrates were achieved with NXS,[102a-e] but also with main group metal halides,[102f-h] copper(II) halides,[102i, 102j] acid chlorides,[102k-m] benzyl chloride[102n] or electrochemically with elemental iodine[102o] or HBr.[102p]

Sanford and co-workers developed a general protocol for the palladium-catalyzed directed halogenation of arenes bearing diverse directing groups.[102a, 102b, 126] The substrates are regioselectively halogenated *ortho* to the directing group using simple Pd(OAc)$_2$ as catalyst without any additional ligands (scheme 32). The conditions are applicable for iodinations, brominations and chlorinations and provide the products in good to high yields. 2-Arylpyridines and benzo[*h*]quinolines were halogenated in MeCN or AcOH as solvent at temperatures between 100 °C and 120 °C, whereas the chlorinations and brominations seem to require slightly higher temperatures (120 °C) or larger amounts of NXS (up to 2.5 equiv.) compared to the iodinations. The halogenations of 3-methyl-2-phenylpyridine with different NXS reagents were compared in different solvents. In AcOH, yields of about 60% were obtained independent of the nature of the halide.[102a] However, in MeCN the iodination resulted in 79% isolated yield, while the chlorination and bromination gave slightly lower yields compared to the reactions in AcOH.

X	AcOH	MeCN
Cl	60%(65%)^b	56%
Br	53%(56%)^b	44%
I	64%	87%(79%)^b

^{b} isolated yields

X = Cl 95%
X = Br 93%

X = Br 63%
X = I 41%

catalyzed 68%
uncatalyzed 82%

catalyzed 76%
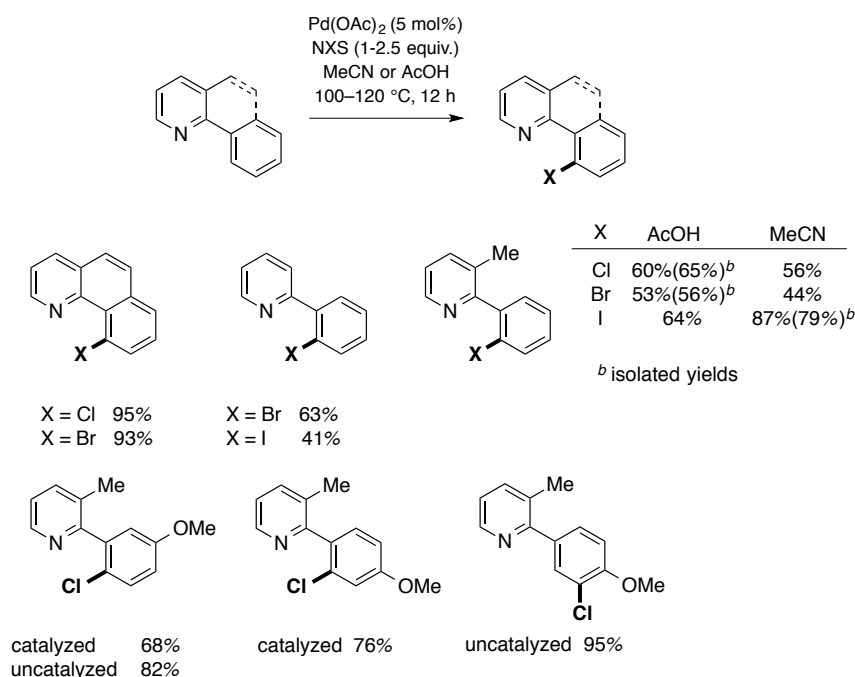
uncatalyzed 95%

Scheme 32. Selected examples of palladium-catalyzed pyridyl-directed direct *ortho*-halogenations developed by Sanford and co-workers.[101b, 102a, 102b]

Noteworthy, the mainly observed side reaction of the NXS halogenation according to Sanford and co-workers is the double halogenation of substrates having chemically and sterically equivalent *ortho* positions at the aryl ring.[102a, 126] Highly mono-selective halogenations are limited to substrates with

steric demand either at the C3 position of the pyridyl ring preventing a second halogenation of the desired monohalogenated product by restricted rotation of the C-C bond between both aryl rings, or *meta*-substituents on the aryl ring complicating C-H bond activation at the sterically more hindered *ortho* position. Control experiments with and without Pd(OAc)₂ catalyst revealed that the uncatalyzed chlorination of electron-rich arylpyridines occurs with selectivities expected for an S_EAr pathway (scheme 32). This implies that the catalyzed halogenation is faster than the uncatalyzed reaction. Nevertheless, in catalyzed reactions, where the uncatalyzed electrophilic substitution would lead to the same regioselectivity, do not result in higher yields for the catalyzed reaction.

Recently, the groups of Greaney and Huang have reported two ruthenium-catalyzed meta-directed brominations of 2-arylpyridines. Tetrabutylammonium tribromide (TBATB) as brominating reagent in combination with K_2CO_3 and substoichiometric amounts of mesitoic acid (MesCO₂H) in dioxane at 110 °C gave *meta*-brominated products in moderate to good yields, which were demonstrated for few examples (scheme 33).[136] Interestingly, the use of NBS instead of TBATB under these reaction conditions provided the product only in traces. In contrast, Huang and co-workers demonstrated that 2-arylpyridines and -pyrimdines are efficiently brominated *meta*-selectively using NBS under even milder conditions (80 °C) in DMA without additional additives.[137] Substrates bearing methoxy, methyl, and halide substituents were shown to be compatible providing high yields. Notably, the bromination occurs *para* with respect to Pd-C bond of the cyclometalated intermediate.
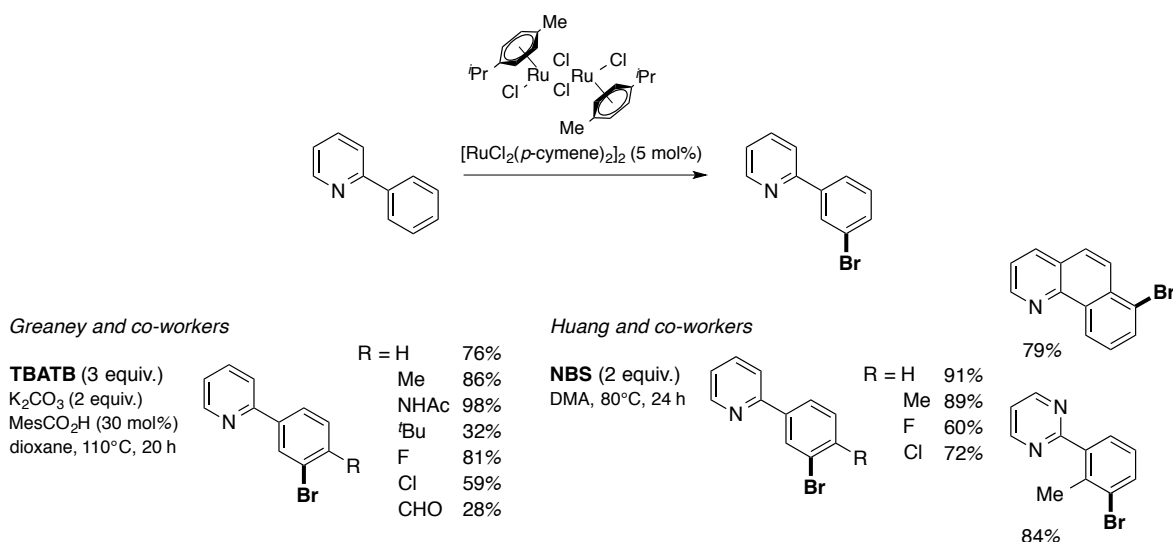
Scheme 33. Examples of *meta*-selective ruthenium-catalyzed direct brominations with TBATB or NBS.[136-137]

Conditions using main group metal halides as halogen source in combination with an oxidant have been reported. For instance, Shen and co-workers demonstrated the copper-catalyzed direct chlorination of 2-arylpyridines and structurally related 2-arylpyrimidines using LiCl and oxygen as terminal and traceless oxidant.[102g, 102h] The dichlorinated products were obtained in good to high yields

with 3 equivalents of LiCl in AcOH at 150 °C (scheme 34). While the selectivities for disubstituted products are high for 2-arylpyridines as substrates, the related arylpyrimidines gave mixtures of mono- and dihalogenated compounds. A more efficient and general method for the mono-selective halogenation with NaX was reported by Hong, Wang and co-workers using a dimeric rhodium-cyclopentadienyl catalyst and PhI(OAc)$_2$ as terminal oxidant.[102f] The reaction proceeds under even milder conditions (50 °C) in acetone with TFA as essential additive. The exclusively mono-halogenated 2-arylpyridines were obtained in overall good to high yields, whereas 2-phenylpicolines and -pyrimidines gave lower yields.
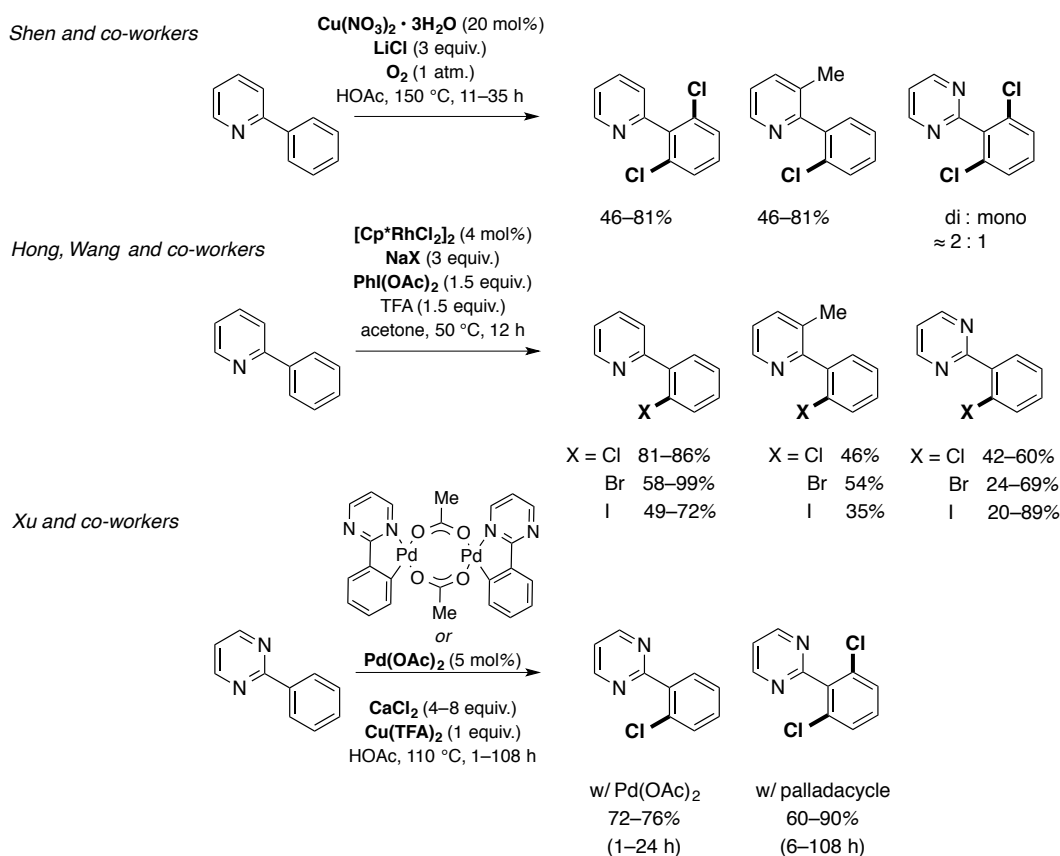
Scheme 34. Examples for direct halogenations using main group halides as halogen source.[102f-h, 138]

Palladium-catalyzed direct chlorinations of arylpyrimidines were reported by Xu and co-workers using CaCl$_2$ as halogen source and Cu(TFA)$_2$ as terminal oxidant (scheme 34).[138] The reaction proceeds at 110 °C in AcOH under air and gave overall high yields for monochlorinated products using Pd(OAc)$_2$ as catalyst, which favors mono-substitution.[138b] While diverse electron-donating and -withdrawing functional groups, as well as multiple substitutions at the phenyl ring were well tolerated, substrates with two sterically easily accessible positions of *para*-substituted arylpyrimidiens gave exclusively dichlorinated products. The problem was solved using Ac$_2$O as co-solvent, which led to the corresponding monochlorinated products. Moreover, targeted dichlorination can be achieved by using

the intermediate palladacycle under otherwise identical conditions, except using much longer reaction times.[138b]

Acid chlorides can be used as chlorinating agents in direct functionalizations. But also benzoxylations and arylsulfonylations can be achieved depending on the reaction conditions.[102k-m] Dong and co-workers reported the palladium-catalyzed *ortho*-selective monochlorination using catalytic amounts of (MeCN)$_2$PdCl$_2$ and CuCl$_2$ in DMF at 120 °C in high yields (scheme 35). Switching to stoichiometric amounts of K$_2$CO$_3$, instead of CuCl$_2$, changing the solvent to dioxane and addition of mole sieve provided the arylsulfones. Similarly, Chen, Cheng and co-workers used benzoyl chlorides in a copper-catalyzed reaction in the presence of Li$_2$CO$_3$ as base in toluene at 145 °C under oxygen atmosphere, to obtain the chlorinated products in similarly high yields.[102m] Using KO^{t}Bu as base, however, arylpyridines were regioselectively benzoxylated in the *ortho* position.
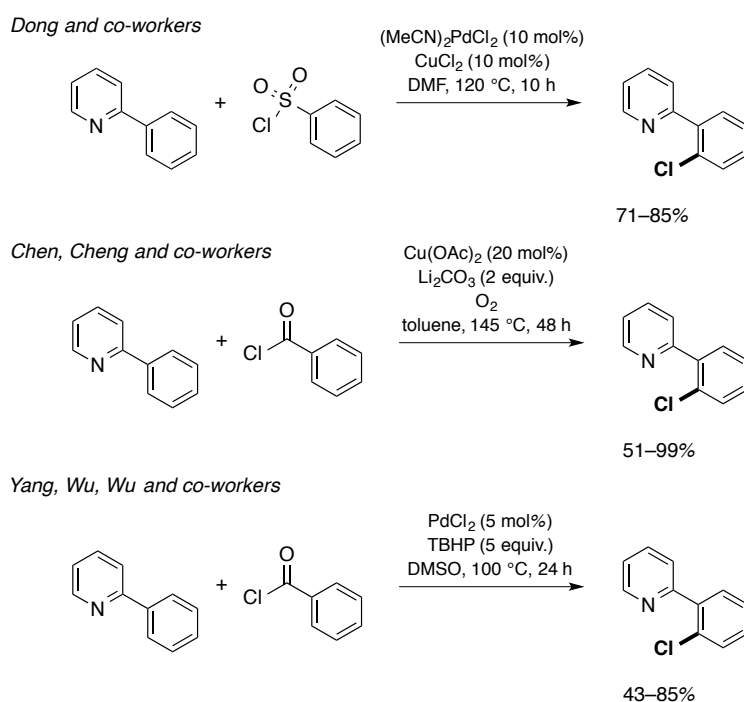
Scheme 35. Direct chlorinations of arylpyridines using acid chlorides.[102k-m]

Another flexible approach for the chlorination and acylation of arylpyridines was reported by Yang, Wu and co-workers using benzyl chloride (scheme 35).[102n] The reaction is catalyzed by PdCl$_2$ and TBHP (*tert*-butyl hydroperoxide)/O$_2$ was used as oxidant in DMSO at 100 °C providing the chlorinated products in good yield regardless of electronic influences. Control experiments with TEMPO as radical scavenger did not afford the product, indicating that radical intermediates are involved in the catalytic cycle.

2.2.3   Mechanistic investigations of palladium-catalyzed direct halogenation reactions

Early mechanistic proposals for palladium-catalyzed chelate-assisted oxidative C-H bond functionalizations of benzo[*h*]quinolines and 2-arylpyridines, in particular C-O and C-X bond-forming reactions,[102a, 102b, 126] involve carboxylate-assisted C-H bond activation at a palladium(II) metal center forming palladacycles,[119a, 139] followed by oxidation with a strong oxidant to a transient mononuclear palladium(IV) intermediate (scheme 36), which has been often proposed for palladium-catalyzed oxidative C-H bond functionalizations.[140] The electrophilic palladium(IV) intermediate releases the product by C-heteroatom bond-forming reductive elimination.[141] The major challenge of mechanistic studies of this cycle are the two last steps of the cycle attributed to the fact that palladium(IV) complexes are usually very reactive and unstable, complicating their investigation as potential intermediates.
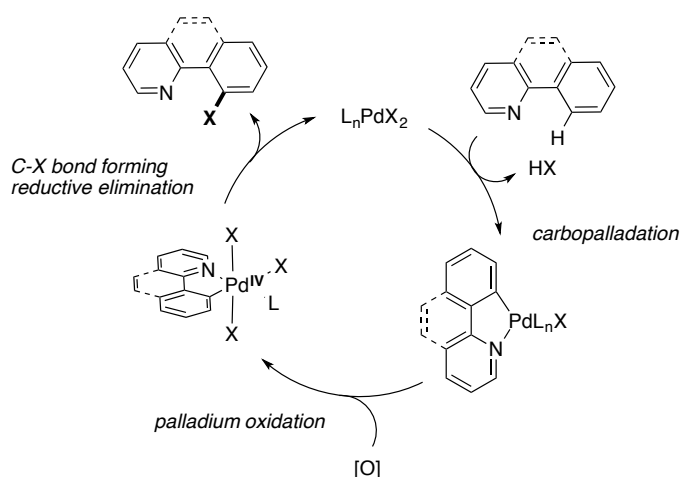
Scheme 36. Early general mechanistic proposal for palladium-catalyzed oxidative C-H bond functionalizations exemplified for benzo[*h*]quinoline.

First double cyclometalated palladium(IV) intermediates, which might be relevant as model complexes to related C-O and C-X bond-forming reductive eliminations, have been reported and studied by Sanford and co-workers.[142] The complexes were readily prepared from the biscyclometalated precursor complex by oxidation with the corresponding oxidant and are unexpectedly stable at ambient temperature. In the context of the study of C-O bond-forming reductive elimination, reaction of the phenylpyridine-cyclometalated complex with PhI(O$_2$CAr) gave octahedral biscarboxylate palladium(IV) species, which smoothly forms the *ortho*-carboxylated phenylpyridine upon thermolysis at 60 °C with first order kinetic (scheme 37). Three probable mechanistic scenarios were investigated and sequentially excluded. Pathway A involves a reversible carboxylate pre-dissociation forming a cationic intermediate followed by either intramolecular or intermolecular nucleophilic attack of the

carboxylate. However, kinetic measurements of C-O bond formation in different solvents with different dielectric constants turned out to be equally fast. This rules out cationic intermediates, which would be stabilized in polar solvents. Further support gave Eyring analysis experiments revealing a positive value and experiments using excess NBu_4OAc did not yield any acetate incorporation, which was expected to result by anion scrambling from cationic palladium complexes. Moreover, Hammett analysis using differently *para*-substituted benzoates resulted in a negative value indicating rate acceleration by electron-donor substituents. This trend would be indicative for pathway B, which involves a direct reductive elimination from the octahedral palladium(IV) complex or pathway C pre-dissociation of one pyridyl arm followed by internal coupling.
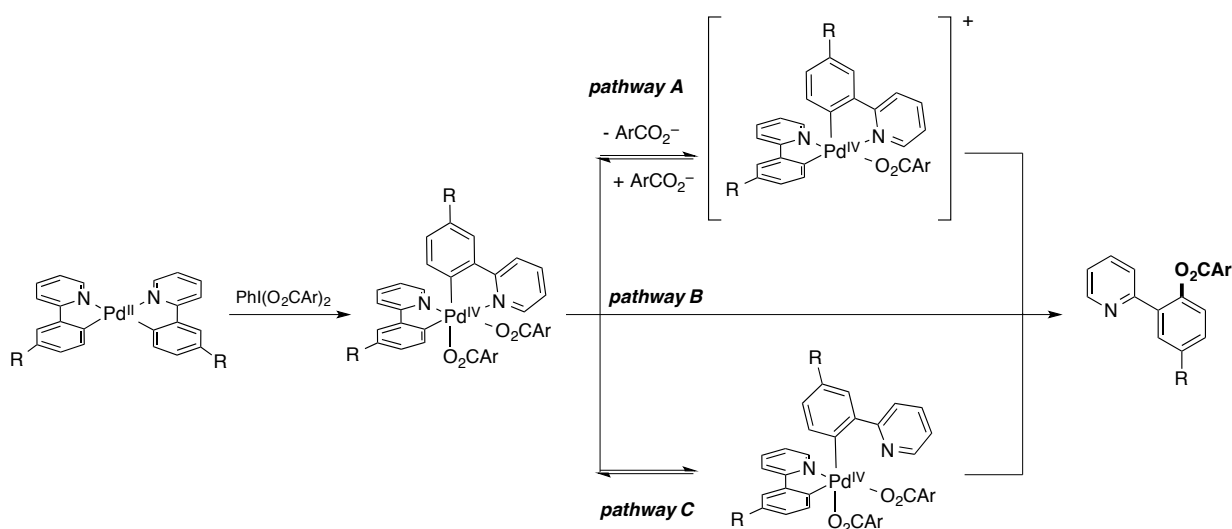
Scheme 37. Preparation of biscyclometalated palladium(IV) complexes and considered reductive elimination pathways.

To distinguish between pathways B and C (scheme 37), which would be kinetically indistinguishable, the authors prepared a benzo[*h*]quinoline-palladium analogue, to introduce higher rigidity keeping similar steric and electronic properties. The measured rate for the reductive elimination was much slower compared to the phenylpyridine-based palladium(IV) complex, which is expected for pathway C, because the rigid nature of the benzanullated ligand is supposed to slow down pre-dissociation of the pyridyl fragment. However, recent results from a comprehensive theoretical study using density functional theory calculations on these three mechanisms by Liu and co-workers revealed that pathway B is more likely.[143] The calculations showed that in all cases the reductive elimination step is rate-limiting and activation barriers were determined to be +31.4, +26.4 and +44.4 kcal/mol for the mechanisms A, B and C, indicating B as the favored pathway. Comparison of the calculated half-lives for bisphenylpyridinyl and bisbenzo[*h*]quinolinyl palladium(IV) complexes showes that the later complex reductively eliminates about 44 times slower, which is in agreement with the experimentally observed value by Sanford and co-workers.

The analogous chloride complexes could be isolated upon oxidation with PhICl$_2$ yielding the palladium(IV) dichloride complex and oxidation with NCS provided a chloride/succinate-mixed complex (scheme 38). Thermolysis initiated reductive elimination, however dependent on solvent. Reaction in pyridine afforded exclusively C-C bond-forming reductive elimination from both complexes to give teraryl in yields of 60% and 81%, respectively. Changing the solvent to benzene, nitrobenzene, acetone, MeCN and AcOH and mixtures thereof resulted in C-Cl and C-C bond-forming reductive elimination, and in case of the succinate complex even C-N bond formation. Reaction in AcOH, which has been shown to be the best solvent for palladium-catalyzed direct halogenations,[102a, 126] gave a product ratio of 5:1 in favor of C-Cl bond formation.
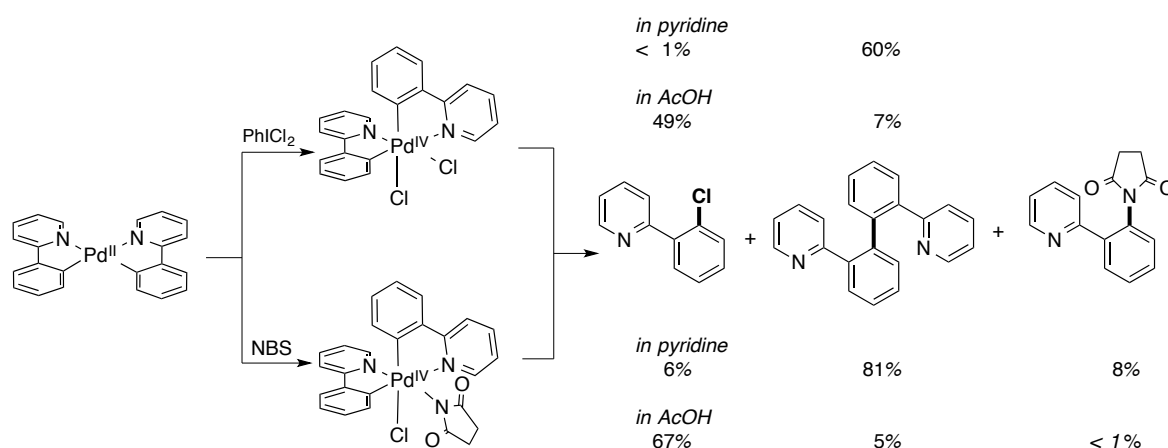
Scheme 38. Observed organic products from reductive elimination of biscyclometalated palladium(IV) complexes.

Although these biscyclometalated palladium(II) complexes were initially sought to be model complexes to investigate the C-heteroatom bond-forming reductive elimination from proposed transient palladium(IV) intermediates, these results were initially interpreted to be strongly indicative for being real in the catalytic reaction. However, up to that point, the biscyclometalated complexes have not been shown to be actual intermediates and to be formed under catalytic conditions. A recent study by Xu *et al*. of the acetoxylation and methoxylation reaction, which proceeds under same reaction conditions but methanol is used as solvent, suggests that biscyclometalated palladium(IV) intermediates might be formed under certain conditions using ESI-MS techniques.[144]

Powers and Ritter have directly investigated the catalytic halogenation and related acetoxylation reaction of 2-phenylpyridine and benzo[*h*]quinoline showing that biscyclometalated palladium(II) complexes (scheme 37) are not kinetically competent catalysts.[145] Moreover, dimeric palladium(III) complexes have been observed under pseudocatalytic conditions, and shown to be kinetically competent (scheme 39).[145-146] Upon treatment of cyclometalated palladium(II) acetate dimer, which has been known to be smoothly formed from reactions generally with chelating substrates and Pd(OAc)$_2$,[147] with strong oxidants PhICl$_2$ and PhI(OAc)$_2$ resulted in formation of thermally unstable

palladium(III) dimers. These were also suggested as intermediates in the context of related Pd(OAc)$_2$-catalyzed arylations of arylpyridines with diaryliodonium salts,[148] and are similar to more stable platinum(III) complexes that have been previously reported as models.[149] These dimeric palladium(III) complexes can also be assigned as a mixed valent palladium(II)/palladium(IV) complex. Crystal structures of related complexes reveal palladium-palladium distances in range of a real metal-metal bond ($\approx$ 2.56 Å), indicating two palladium(III) metal centers.[145-146]
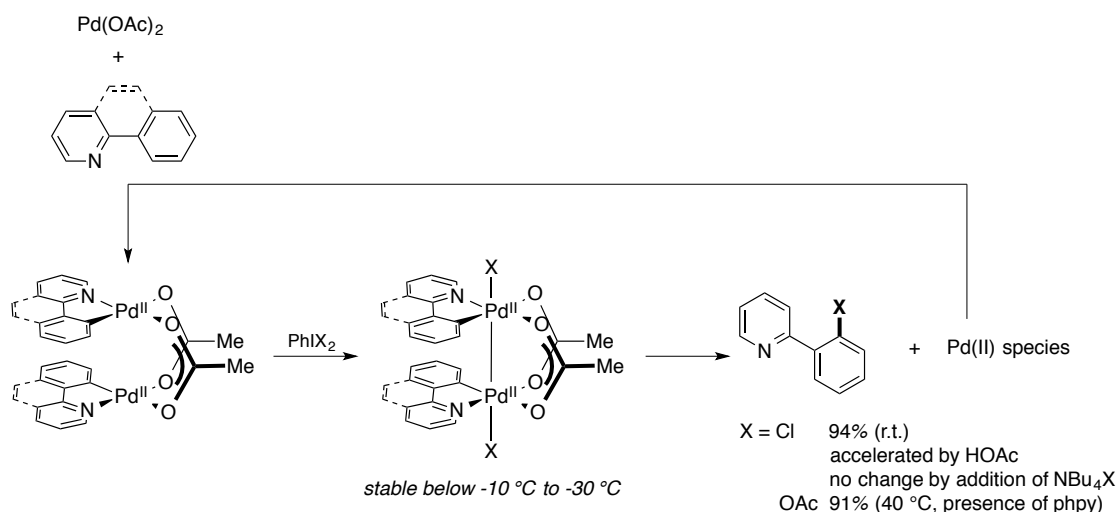
Scheme 39. Reactions of palladium(II) and (III) dimers as proposed intermediates for chelate-assisted C-H bond acetoxylation and chlorination.

Thermolysis at room temperature of the benzo[*h*]quinoline-based palladium(III) chloride dimer gave exclusively C-Cl bond-forming reductive elimination product in 94% besides palladium(II)-containing products consistent with the formula [Pd$_2$(bhq)(OAc)$_2$Cl] (bhq = benzo[*h*]quinoline), which form the well-defined starting palladium(II) acetate dimer after treatment with benzo[*h*]quinoline (scheme 39).[146a] Contrary, phenylpyridine-based palladium(III) acetate dimer does not yield significant amounts of the acetoxylated phenylpyridine (6%) after thermolysis.[145] However in the presence of excess phenylpyridine (phpy) acetoxylation product was obtained in 91%. The reductive elimination of the chloride-analogue was shown to be accelerated in the presence of excess substrate, as well.[146a, 150] Further kinetic studies using added AcOH revealed first order dependence in added acid with non-zero intercept. This indicates, that generated AcOH after reductive elimination and cyclometalation of excess ligand is the origin for the observed rate acceleration and co-catalyzes the reductive elimination. However the results obtained from stoichiometric organometallic reactions do not give evidence to be competent in catalysis, in particular not for reactions using NXS as terminal oxidant and halogenating reagent because NXS or the byproduct succinimide have not been taken into account in these reactions.

Ritter and co-workers found that the Pd(OAc)$_2$-catalyzed direct halogenation with NCS proceeds via a rate-determining oxidation step, judged by first order kinetic behavior of NCS and zeroth order of substrate,[146a] which opens the opportunity for kinetic studies under catalytic conditions on this step to elucidate and valuate the role of the participating reagents and catalyst intermediates. This is in contrast to related acetoxylation reaction, where the carbopalladation was found to be rate determining.[145] Latest results from catalytic reactions revealed that succinate-bridged palladium(II) dimer is the catalyst resting state in direct chlorination of 2-arylpyridines and benzo[h]quinolines with NCS (scheme 40).[146b] This resting state self-assembles after irreversible carbopalladation of the substrate,[151] and ligand exchange with succinimide, which is liberated during catalysis as byproduct. The initial formation is until now unclear, because it is observed although succinimide is not present before the first turnover has taken place, however it is readily formed from the analogous acetate-bridged dimer.

The subsequent oxidation with NCS is proposed to form an acetate/chloride-mixed palladium(III) dimer resulting from a nucleophile/acetate-assisted bimetallic oxidation (scheme 40). The co-catalytic activity of acetate has been shown by first order dependence of acetate.[146b, 150] Moreover, it was shown that purified palladium(II) succinate dimer itself is not a kinetically competent catalyst, but in the presence of added catalytic acetate ions, likewise under conditions using Pd(OAc)$_2$ as catalyst, the reaction rate increased and became comparable. Bimetallic oxidation was further proofed by determination of the equilibrium constant between dimeric benzo[h]quinoline-based palladium(II) complex and pyridine indicating that monomer formation is entropically unfavored (ΔS = −34.3 cal/mol K).[146b]

The mechanism of the product-forming reductive elimination from palladium(III) dimers has been extensively studied, in particular from stoichiometric reactions (*cf.* scheme 39).[146a, 150] Conceivable dissociation of palladium(III) dimers into mononuclear palladium(III) species or disproportionation into mononuclear palladium(II) and palladium(IV) has been experimentally and computationally excluded. Pre-dissociation of either pyridyl-ligand or anionic ligand seem to be unlikely, because addition of anions such as chloride or acetate (NBu$_4$X) do not effect the rate of stoichiometric reductive elimination from palladium(III) dichloride dimer and addition of excess substrate led to rate-enhancement attributed to the catalytic activity of liberated AcOH after newly formed C-Pd bond.[150]
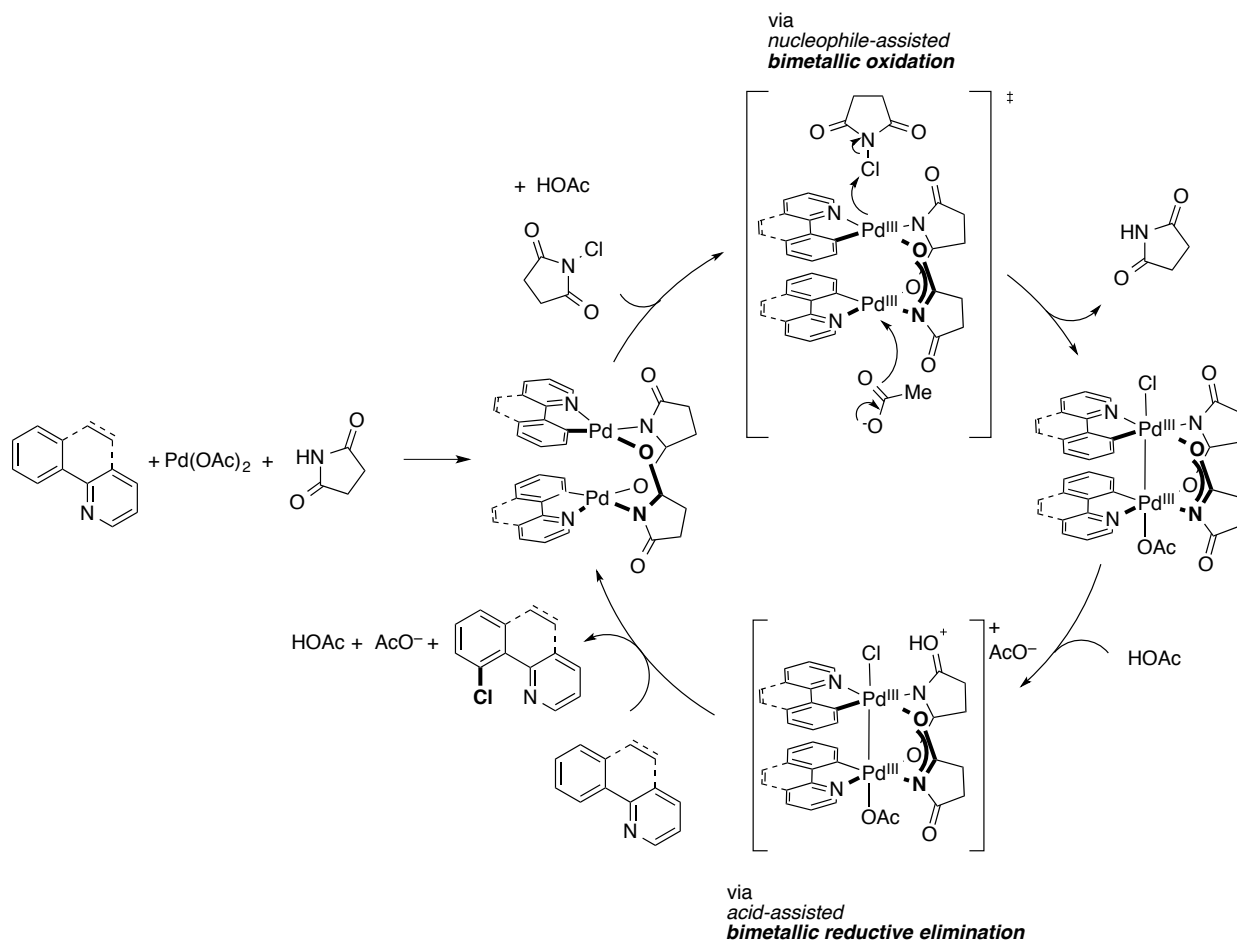
Scheme 40. Detailed mechanism for Pd(OAc)$_2$-catalyzed direct chlorination of 2-arylpyridines and benzo[*h*]quinolines with NCS based on latest mechanistic investigations.

2.3 Results and discussion

2.3.1 Optimization of reaction conditions for direct brominations

Initially, we attempted the synthesis of 3-bromobipyridine *N*-oxide **22a** under conditions previously reported by Sanford and co-workers for direct halogenations of phenylpyridines (scheme 41).[102a, 126] The reaction of bipyridine *N*-oxide **20a** was catalyzed with Pd(OAc)$_2$ and NBS was used as brominating reagent and terminal oxidant. ^{1}H NMR measurement of the crude product showed some conversion and formation of a product in 10% (against TMB as internal standard). However, isolation of this product by column chromatography provided only tiny amounts of pure brominated product **22a** (1% isolated yield), because the starting material and the product exhibit almost the same R$_f$ values making the separation difficult.
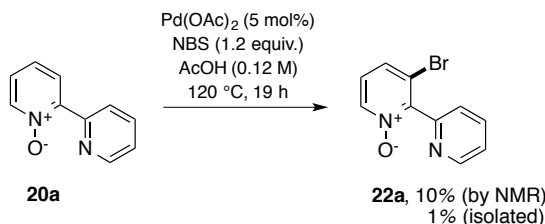
Scheme 41. Initial attempts for direct bromination of **20a**.

NMR characterization, HRESI-MS and X-ray diffraction of single crystals of the pure isolated material confirmed the desired structure of **22a** (figure 21). The average C-C bond distances of the solid state structure within the rings are 1.39 Å and the angles are 120 °, which is expected for aromatic systems and comparable with unsubstituted **20a** (1.37 Å), of which the crystal structure was published by Wheeler and co-workers in a bimolecular complex with *p*-aminobenzoic acid.[152] The Br-C bond has a bond distance of 1.89 Å, and the N-O bond distance is 1.30 Å. Both distances are essentially identical with those measured for 3-bromopyridine *N*-oxide (1.89 Å).[153] Interestingly, the bromobipyridine *N*-oxide **22a** exhibits a large dihedral angle of ≈ 98 °, while for unsubstituted bipyridine *N*-oxide **20a** the dihedral angle was reported with 18 °. The large dihedral angle is certainly a result of the steric hindrance by the C3 substituent, which prevents the co-planar arrangement of the aromatic plains.
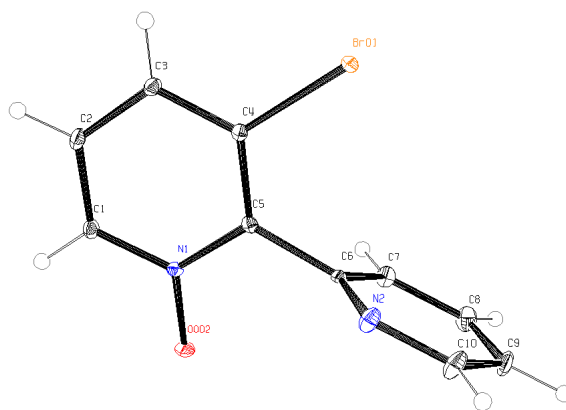
Figure 21. ORTEP 3 diagram of brominated bipyridine *N*-oxide **22a**. Thermal ellipsoids are drawn at 30% probability level. Selected bond distances (Å) and angles (°) for **22a**: N1 - C1 1.36(3), C1 - C2 1.38(4), C2 - C3 1.39(3), C3 - C4 1.38(6), C4 – C5 1.38(6), C5 – N1 1.36(9), N1 – O1 1.30(3), C4 – Br1 1.89(1), C5 – C6 1.48(8), C10 – N2 1.33(3), C6 – N2 1.34(0), N1 – C5 – C6 – N2 98.2

In order to optimize the yield of **22a**, we examined the influence of the solvent on the direct bromination of **20a** (table 16). Reactions were carried out on a 0.25 mmol scale of **20a** in closed reaction vials and were set up in normal atmosphere. Yields were determined by ^{1}H NMR integration against TMB as internal standard. Using CH$_3$CN as solvent and larger amount of NBS, conditions which were previously reported by Sanford and co-workers for direct halogenations of 2-phenylpyridines,[102a, 126] we found a small increase of the yield to 37% of **22a** but still non-converted starting material (entry 1). Because of the difficulties to separate the product **22a** from the starting material, full conversion of the **20a** is required. In addition, we observed 2,2′-bipyridine (**24a**) as side product from deoxygenation of the starting material **20a**. Among other common solvents (for full screening table, see Experimental Section) we first tried solvents that have been used for related reactions. AcOH or AcOH/benzene mixtures, which are often used as solvent for direct functionalizations or oxidative couplings proceeding by a proposed Pd(II)/Pd(IV) mechanism,[140] resulted in product yields up to 42% increasing with higher amounts of benzene (entries 2, 5–7). Reactions with the even stronger acid TFA, or with AcO$_2$ did not provide the desired product **22a** (entries 9–10). However, the reactions with AcO$_2$ resulted in full conversion of the starting material and formation of product **23** in 15–27% yield.

Table 16. Influence of solvent on the direct bromination of **20a**.
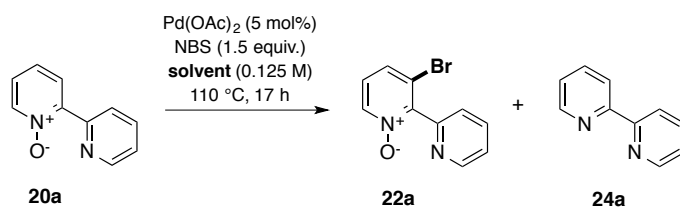
entry	solvent	22a[a] [%]	recov. 20a[a] [%]
1[b]	CH$_3$CN	37	15
2	AcOH	14	34
3[c]	Ac$_2$O	–	–
4[c]	Ac$_2$O/AcOH (1:1)	–	15
5	AcOH/benzene (3:1)	28	34
6	AcOH/benzene (1:1)	42	31
7[d]	AcOH/benzene (1:3)	40	23
8[c]	Ac$_2$O/benzene (1:1)	–	–
9	TFA	–	91
10	TFA/benzene (1:1)	–	84
11	**benzene**	**77**	–
12	benzene[e]	72	–
13[f]	toluene	–	46
14[e]	**chlorobenzene**	**77 (87)[g]**	–
15	benzotrifluoride	56	–

[a]Yields were determined by ^{1}H NMR integration against TMB as internal standard. [b]Formation of **24a**. [c]Formation of coupling product with succinimide **23**. [d]Formation of reduced product **25a**. [e]Sample was extracted with 1 M NaOH/DCM. [f]Formation of benzylated product **26**. [g]Isolated yield from 9 mmol scale reaction set up.
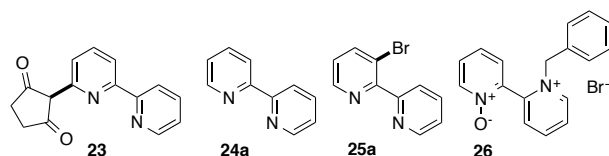
We hypothesized that **23** was formed by a Reissert-Henze-type rearrangement,[154] where **20a** is activated by AcO$_2$ forming an acetylbipyridinium species. Nucleophilic attack of the succinimide anion, which is liberated by decomposition of NBS, at the C6 position would give the observed side product **23** after release of acetate. To test this hypothesis, we carried out the reaction of bipyridine *N*-oxide **20a** with NBS or succinimide in Ac$_2$O at 110 °C (scheme 42). Indeed, **23** was formed and the isolated yields of **23** with succinimide was 62%, and in case with NBS 39%, respectively, showing that the side reaction does not require the palladium catalyst.
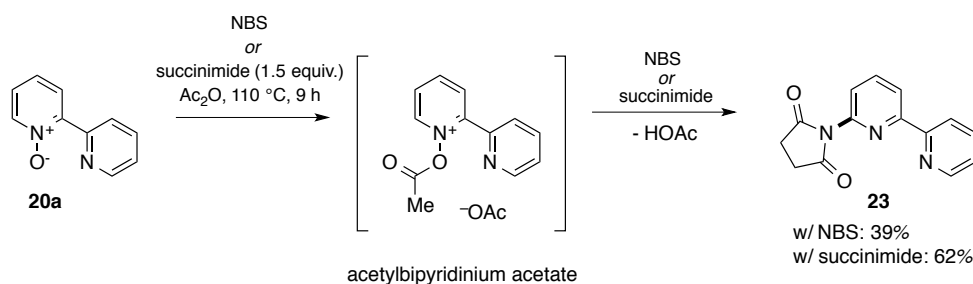
Scheme 42. Formation of succinimide-coupled side product **23** via Reissert-Henze-type rearrangement.

Using benzene alone as the solvent, **22a** was obtained as single product in a satisfactory yield of 77% and full conversion of **20a** was achieved (entry 11). Simple extraction of the reaction mixture with an 1 M NaOH aqueous solution and DCM provided 72% of **20a** as spectroscopically pure product (entry 12). Because of the toxicity of benzene and because its atmospheric boiling point is lower than the reaction temperature, we looked for a substitute. Toluene is often used as good solvent instead of benzene, however benzyl bromide is formed in the presence of NBS, resulting in the consumption of the brominating reagent.[155] Product was not observed from the reaction in toluene, however, we detected conversion of the starting material presumably to a benzylated bipyridine N-oxide **26** in 22% yield (table 16, entry 13). To elucidate its structure, we carried out the reaction under the same conditions at a larger scale (2.00 mmol) and isolated the side product, which appeared as a very polar spot on the TLC, and disappeared after extraction of a sample with 1 M NaOH (scheme 43). The isolated material was investigated by ¹H-, ¹³C NMR, COSY, HMBC and HMQC showing 13 aromatic protons and 2 benzylic protons split into two doublets, which couple to each other. Furthermore, the benzylic carbon showed a cross peak in the HMBC spectrum with the C6′ proton of the pyridyl ring. These observations suggest that the pyridyl ring was benzylated by the *in situ* generated benzyl bromide forming the N′-benzylbipyridium N-oxide **26**. To further support this structural assignment, we carried out the reaction of bipyridine N-oxide **20a** with benzyl bromide in MeCN at 60 °C. After 4 h, the starting material was fully consumed and a product was almost quantitatively formed (94% isolated yield) showing same signals in 1D and 2D NMR spectra supporting the formation of **26** as side product when using toluene as solvent in the catalyzed reaction.

Scheme 43. Benzylation of the pyridyl ring forming bipyridinium N-oxide **26**.

Using chlorobenzene as substitute for benzene on a small scale (0.25 mmol) gave the same high yield of 77% for the desired product **22a** and 22% of the deoxygenated product **25a** (table 16, entry 14). However, repeating the reaction in a larger scale (9.0 mmol) provided exclusively the C3-brominated product **22a** in 87% yield as spectroscopically pure product after simple extraction. When benzotrifluoride was used as less expensive alternative to benzene, only 53% of **22a** were obtained despite complete conversion of **20a** (entry 15).

We performed some control experiments to examine the role of the reagents used for the C3-halogenation of bipyridine *N*-oxide **20a** (table 17). The reaction of **20a** with NBS in benzene at 110 °C under dry and inert conditions surprisingly gave a lower yield of 56% (entry 1) than the reaction set up in ambient atmosphere and using benzene from the bottle without drying and degassing, which gave 77% of **22a** (*cf.* table 16, entry 11). With bipyridine **24a** instead of the *N*-oxide **20a** as substrate, no reaction occurred (entry 2), as expected, since it is known that the formation of so-called roll-over palladium complexes from corresponding bipyridine complexes exhibits high activation barriers, because of the chelating nature of the bipyridine ligand.[103] When the reaction was carried out without Pd(OAc)₂, no reaction was observed as well (entry 3), which demonstrates that the catalyst is necessary not only to achieve the regioselectivity of the bromination but also achieve the functionalization, at all. To figure out if a lower temperature would give the desired product **22a** in acceptable yields, we ran one test reaction at 95 °C, which, however, resulted in only 28% of **22a** besides 72% of unreacted starting material **20a** (entry 4).

Table 17. Control experiments under different conditions.

entry	temp.	remark/conditions	**22a**[a] [%]	recov. **20a**[a] [%]	**24a**[a] [%]	**25a**[a] [%]
1	110 °C	inert conditions	56	–	–	–
2	110 °C	**24a** was used instead of **20a**	–	–	quant.	–
3	110 °C	w/o catalyst	–	quant.	–	–
4	95 °C		28	72	–	–
5	150 °C	in PhCl	6	–	19	52
6	150 °C	in PhCl, w/o catalyst	–	–	53	–
7	150 °C	in PhCl, w/o catalyst and NBS	–	quant.	–	–
8	150 °C	in PhCl, 20 mol% NBS, w/o catalyst	–	80	20	–
9	150 °C	in PhCl, 50 mol% succinimde, w/o catalyst	–	quant.	–	–

[a]Yields were determined by ¹H NMR integration against TMB as internal standard.

Performing the direct bromination of **20a** at a temperature of 150 °C in chlorobenzene provided a low yield of 6% for **22a** but its deoxygenated analogue **25a** in 52% besides bipyridine **24a** in 19% (table 17, entry 5). The deoxygenation of the bipyridine *N*-oxide **20a** results from a stoichiometric side reaction with NBS. Stirring **20a** in chlorobenzene at 150 °C or in the presence of succinimide quantitatively gave starting material (entries 7 and 9). However, addition of 20 mol% of NBS formed bipyridine **24a** in 20% yield corresponding to the NBS loading (entry 10). The mechanism of the deoxygenation with NBS is yet unclear.

Next we investigated if other catalysts, catalyst precursors and ligands are compatible with our substrate (table 18). Almost all tested catalysts gave full conversions of **20a**, except RuCl$_3$ (entry 1). Other arene ruthenium catalysts, which have been shown to be efficient for directed C-H functionalizations,[136-137, 156] gave deoxygenated bipyridine **24a** in approx. 50% yield (entries 2–4). This indicates, that the deoxygenation of bipyridine *N*-oxide **20a** by NBS is facilitated or even catalyzed when using a transition metal catalyst. Similar results have been obtained from reactions using NHC-palladium catalysts (entries 22–23) or Pd(OAc)$_2$ in combination with bidentate phosphine dppf (entry 12) or dinitrogen ligands phenanthroline and bipyridine **24a** (entries 10–11). Related dichloropalladium(II) complexes with bidentate tmeda or dppf ligands resulted in full conversion of the starting material **20a**, however neither bipyridine **24a** nor other products could be detected by ^{1}H NMR (entries 13–14). Surprisingly, cationic (CH$_3$CN)$_4$Pd(BF$_4$)$_2$ gave also approx. 50% yield of bipyridine **24a** (entry 16), but the neutral complex (CH$_3$CN)$_2$PdCl$_2$ gave the desired product **22a** in 60% yield (entry 17). These examples display the crucial role of the anionic ligand bound to the catalyst.

Exclusive formation of the desired product **22a** and full conversions of **20a** was obtained, as well, in reactions using other palladium(II) carboxylates (table 18, entries 5–7), PdCl$_2$, and hexachloropalladate(IV) (entries 8 and 9) resulting in yields between 60–68%, slightly lower than with Pd(OAc)$_2$ (77%). Reactions with cyclometalated palladium dimers (entries 15, 18–21) gave **20a** in moderate to good yields ranging from 35% with the Buchwald's pre-catalyst G1 to 69% with the Herrmann-Beller catalysts. While both versions of the Herrmann-Beller catalyst and the acetate dimer **A** provided full conversion of **20a**, Buchwald's pre-catalyst and the palladium dimer **B** gave only low yields besides bipyridine side product **24a** and unreacted starting material.

Table 18. Catalyst screening for direct brominations of **20a**.

entry	catalyst	22a[a] [%]	recov. 20a[a] [%]	24a[a] [%]
1	RuCl$_3$·H$_2$O	–	quant.	–
2	[(C$_6$H$_6$)RuCl$_2$]$_2$	–	–	54
3	[(p-cymene)RuCl$_2$]$_2$	–	–	52
4	[(p-cymene)Ru(OAc)$_2$]$_2$	–	–	48
5	Pd(OTf)$_2$	65	–	–
6	Pd(O$_2$CPh)$_2$	63	–	–
7	Pd(OPiv)$_2$	68	–	–
8	K$_2$PdCl$_6$	60	–	–
9	PdCl$_2$	62	–	–
10	Pd(OAc)$_2$ + phenanthroline (1:1)	–	–	50
11	(bipy)PdOAc	–	–	46
12	Pd(OAc)$_2$ + dppf (1:1)	–	–	65
13	(tmeda)PdCl$_2$	–	–	–
14	(dppf)PdCl$_2$	–	–	–
15	Buchwald's pre-catalyst G1	35	11	6
16	(CH$_3$CN)$_4$Pd(BF$_4$)$_2$	–	–	48
17	(CH$_3$CN)$_2$PdCl$_2$	60	–	–
18	Dimer **A**	56	–	–
19	Dimer **B**	23	10	16
20	Hermann-Beller (X = OAc)	69	–	–
21	Hermann-Beller (X = Br)	56	–	–
22	(IMes)PdCl$_2$(3-ClPy)	–	–	43
23	(IPr)PdCl$_2$(3-ClPy)	–	–	48

[a]Yields were determined by ^{1}H NMR integration against TMB as internal standard.
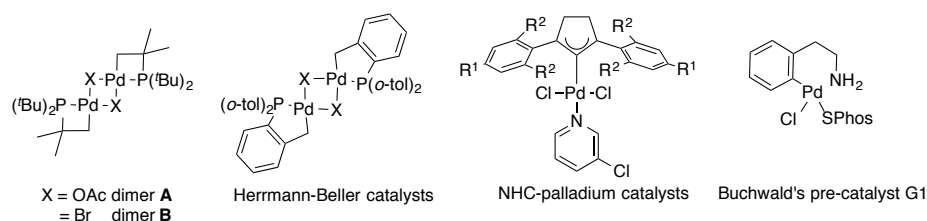
Additionally, we examined catalyst loading, stoichiometry of NBS and substrate concentration for the direct bromination of **20a** (table 19). Decreasing the catalyst loading to 2.5 mol% and 1 mol% resulted in slightly lower yields of 59% and 47%, respectively, but full conversion of **20a** (entries 1 and 2). However, the TLC and ^{1}H NMR spectra of the crude products revealed several minor impurities. In

contrast, decreasing the excess of NBS had a positive effect giving yields up to 90% of **22a** (entries 3 and 4). The same trend was observed for decreasing the substrate concentration (entries 5–9). At the lowest concentration of **20a** (0.13 M), we obtained quantitative yields for the brominated product **22a**. The reaction seems to be very sensitive towards the concentration, because with a slight increase of the substrate concentration to 0.28 M the yields drop to 30% until 21% for the highest concentration of 0.44 M. Notably, the starting material **20a** could not be recovered in the low yielding cases. Bipyridine side product was observed in 30% yield at the higher concentration of 0.3 M.

Table 19. Examination of catalyst loading, amount of NBS and substrate concentration.
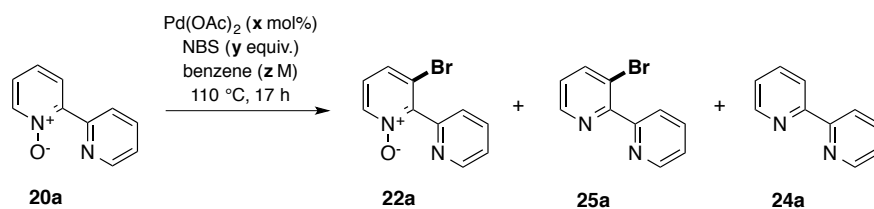
entry	NBS [y equiv.]	Pd(OAc)$_2$ [x mol%]	conc. [z M]	22a[a] [%]	recov. 20a[a] [%]	24a[a] [%]
1	1.5	2.5 mol%	0.125	59	–	–
2	1.5	1 mol%	0.125	47	–	–
3	1.2	5 mol%	0.125	90	–	–
4	1.0	5 mol%	0.125	88	–	–
5	1.5	5 mol%	0.063	quant.	–	–
6	1.5	5 mol%	0.188	30	9	–
7	1.5	5 mol%	0.250	23	–	30
8	1.5	5 mol%	0.312	44	9	–
9	1.5	5 mol%	0.374	21	–	–

[a]Yields were determined by ^{1}H NMR integration against TMB as internal standard.

We initially tested some other bromide sources and terminal oxidants (table 20) but no other reagent gave the brominated product **22a** in more than 2% yield. Moreover, in all test reactions, starting material **20a** was almost fully consumed and could not be recovered. While alkali bromides in combination with Oxone gave 1–2% of **22a** (entries 3–4), elemental bromine with and without an oxidant resulted in bipyridine **24a** in 10–15% yields (entries 1–2). In case of Br$_2$/PhI(OAc)$_2$ the HRESI-MS spectrum revealed the formation of other unidentified products. CuBr was thought to act as brominating reagent and terminal oxidant at the same time, like NBS, however neither the product **22a** (entry 9) nor other side products could be observed (entry 5).

Table 20. Tests of other bromine sources and terminal oxidants for direct brominations of **20a**.

entry	brominating reagent	oxidant	**22a**[a] [%]	recov. **20a**[a] [%]	**24a**[a] [%]
1	Br$_2$	–	–	–	10
2[b]	Br$_2$	PhI(OAc)$_2$	–	–	15
3	LiBr	Oxone	2	6	–
4	KBr	Oxone	1	7	–
5	CuBr	–	–	–	–

[a]Yields were determined by ^{1}H NMR integration against TMB as internal standard. [b]Formation of an unknown products, with a *m/z* ratios of 179.0608, 234.0989, and 249.0044

2.3.2   Synthesis of bipyridine *N*-oxide starting materials

To investigate the substrate scope of the palladium-catalyzed direct bromination reaction, we had to prepare substituted bipyridine *N*-oxides **20**, most of which have not been reported before. However, substituted bipyridine *N*-oxides, in particular unsymmetrically substituted ones, are challenging. Recently, our group developed a palladium-catalyzed direct arylation reaction of pyridine *N*-oxides providing unsymmetrically substituted bipyridine and terpyridine *N*-oxides.[117-118] The pyridine *N*-oxide starting materials **27** were made according to reported procedures by oxidation of the corresponding pyridines with H$_2$O$_2$ in AcOH or with *m*CPBA.[117] Using slightly modified conditions for the direct arylation procedure (K$_3$PO$_4$ instead of K$_2$CO$_3$, and cyclometalated dimer **A** as catalyst instead of Pd(OAc)$_2$/P^{t}Bu$_3$), pyridine *N*-oxides **27** were arylated with bromopyridines **28** in good to moderate yields depending on the substituent (table 21). With the exception of the cyano (**20e**, **20n**) and nitro (**20i**) substituents, electron-poorer pyridine *N*-oxides (**20a**, **20c**, **20d**, **20h**, **20k**, **20l**, **20m**) were arylated in higher yields (41–87%) than more electron-rich pyridine *N*-oxides (**20b**, **20f**, **20g**, **20j**, 15–35%). This reactivity trend has been previously observed and can be explained by the more polarized C-H undergoing faster C-H bond activation via a concerted metalation-deprotonation (CMD) mechanism.[92, 157]

Table 21. Preparation of bipyridine *N*-oxides **20** by palladium-catalyzed direct arylation.
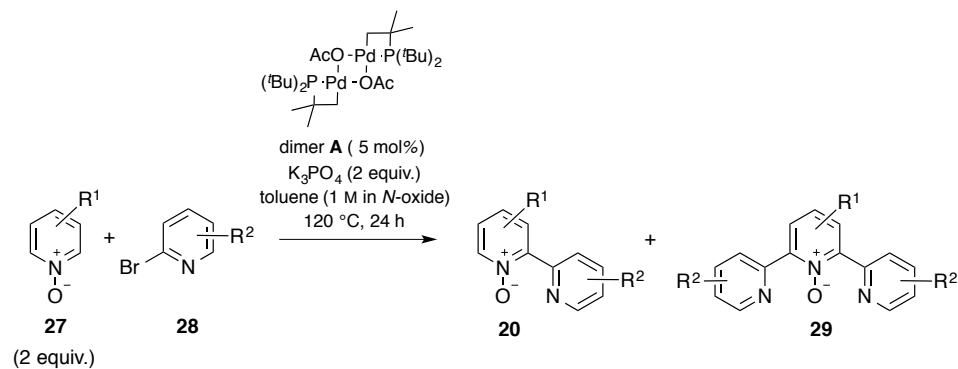
Entry	R^1	R^2		Yield of **20** (%)^a		Yield of **29** (%)^a
1	H	H	**20a**	44 (lit. 23)^b	**29a**	0
2	6-Me	H	**20b**	8, 22^c	**29b**	–
3	6-CO$_2$Et	H	**20c**	59 (lit. 10)^b	**29c**	–
4	6–CF$_3$	H	**20d**	49	**29d**	–
5	6-CN	H	**20e**	8 (lit. 58)^b	**29e**	–
6	5-OMe	H	**20f**	35	**29f**	16
7^c	5-Me	H	**20g**	20	**29g**	0
8	5-CO$_2$Me	H	**20h**	72 (lit. 25)^b	**29h**	0
9	5-NO$_2$	H	**20i**	13	**29i**	3
10^c	4-OMe	H	**20j**	15	**29j**	0
11	4-Cl	H	**20k**	41 (lit. 35)^b	**29k**	12 (lit. 8)^b
12	4-CO$_2$Et	H	**20l**	67 (lit. 67)^b	**29l**	15 (lit. 13)^b
13	4-CF$_3$	H	**20m**	87 (lit. (65)^b	**29m**	10 (lit. 18)^b
14^c	4-CN	H	**20n**	27 (lit. 56)^b	**29n**	5 (lit. 15)^b
15^c	H	6'-OMe	**20p**	64	**29p**	13
16^c	H	6'-Me	**20q**	41	**29q**	5
17	H	6'-CF$_3$	**20r**	65	**29r**	11
18	H	5'-Me	**20s**	13	**29s**	0
19	H	4'-OMe	**20t**	44	**29t**	7
20	H	4'-Me	**20u**	31	**29u**	4
21^d	H	4'-F	**20v**	8	**29v**	0
22	H	4'-CO$_2$Et	**20w**	44	**29w**	11
23^d	H	4'-CF$_3$	**20x**	15	**29x**	0
24	2-quinoline *N*-oxide	H	**20y**	19	**29y**	–
25	2-pyrazine *N*-oxide	H		21		0

^{a}Isolated yields. ^{b}Yields in parenthesis reported in ref. 117 with Pd(OAc)$_2$/P^{t}Bu$_3$ as catalyst and K$_2$CO$_3$ as base. ^{c}Pd(OAc)$_2$ (5 mol %) and P^{t}Bu$_3$ (6 mol %) were used. ^{d}2-Chloropyridine derivative was used.

With respect to the substituent at the bromopyridine, the arylation does not follow an obvious electronic trend. Thus, arylation with the most electron-rich 4-methoxybromopyridine gave the same yield as with the most electron-poor 4-esterbromopyridine (*cf*. Table 21, entry 19 *vs*. 22). However, the position of the substituent apparently has a stronger influence on the yield, since 6-substituted bromopyridines resulted in typically higher yields than the corresponding 4-substituted derivatives (entries 15–17 *vs*. 19–23).

Because the direct arylation of pyridine *N*-oxides **27** provided the bipyridine *N*-oxides **20** particularly with electron-donating substituents, we also used alternative procedures, which have been previously reported to give high yields. The unsubstituted bipyridine *N*-oxide **20a** was prepared by simple oxidation of bipyridine **24a** using H_2O_2 in TFA at room temperature providing a yield of 94% (scheme 44).[158] Similar to this procedure, 2-phenylpyridine was oxidized by using AcOH as solvent and the reaction was heated at 70 °C giving quantitative yields of **27a**.

Y = N,   **22a**, 94%
Y = CH, **32b**, quant.

Scheme 44. Synthesis of unsubstituted bipyridine *N*-oxide **20a** and phenylpyridine *N*-oxide **27a** by *N*-oxidation.

In the context of the synthesis of Caerulomycines **A** and **E**, the preparation of 4-methoxybipyridine *N*-oxide **20j** was reported to proceed smoothly by stepwise nitration of bipyridine *N*-oxide **20a** in H_2SO_4 and subsequent nucleophilic substitution with NaOMe.[113] Nitration was performed according to a procedure reported by Zalas *et al*. applying lower temperatures but longer reaction times.[159] However, the nitrobipyridine *N*-oxide **20i** was obtained only in 28% yield (scheme 45). Subsequent methoxylation using a slightly modified procedure of Wenkert *et al*. gave methoxybipyridine *N*-oxide **20j** in quantitative yield.

20a   **20i**, 28%   **20j**, quant.

Scheme 45. Synthesis of **20i** and **20j** by nitration/methoxylation sequence.

Larger amounts of 6-methylbipyridine *N*-oxide **20b** were obtained by a Negishi cross-coupling reaction between 6-methylpicolin *N*-oxide **27b** and 2-bromopyridine **28a** according to the conditions

developed by Gosselin *et al.*[99c] Thereby, TMPZnCl·LiCl deprotonates the pyridine *N*-oxide *in situ* to give intermediate pyridylzinc reagent, which couples with 2-bromopyridine catalyzed by (dppf)PdCl$_2$·DCM. 86% yield of **20b** was obtained (scheme 46), which is comparable to the reported yield of 88%.
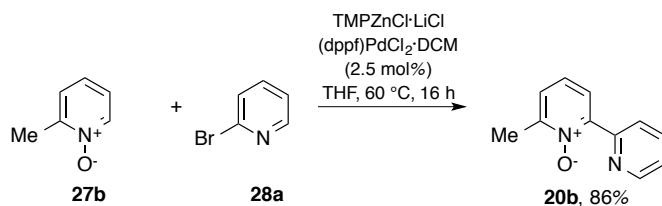
Scheme 46. Synthesis of **20b** by Negishi cross-coupling according to Gosselin *et al.*[99c]

2.3.3 Substrate scope of directed halogenation reactions

With the optimized conditions in hand, we investigated the substrate scope of the direct C-H halogenations. Gratifyingly, the reaction of unsubstituted bipyridine *N*-oxide **20a** with NCS gave the chlorinated product **21a** in even higher yield of 95% than the reaction with NBS (87%, table 22). Examples for direct brominations and chlorinations of bipyridine *N*-oxides **20** with substitutions at the pyridine *N*-oxide ring are shown in table 22. The chlorinated products **21** were obtained in usually higher yields than the brominated products **22**. Substituents at the C6 position resulted in good to excellent yields, except for the nitrile **20e**. While the brominated product **22e** could be obtained in 17% yield, the analogous chlorinated **21e** could not be obtained, instead 85% of the starting material **20e** was recovered. As previously mentioned, the starting materials and the halogenated products tend to have same R$_f$ values making the separation difficult. Therefore, **22e** could not be completely separated from **20e**. The estimated total yield for **22e** was 28% and recovered **20e** 33%. The low yield might be due to the ability of the nitrile to coordinate to the catalyst resulting in catalyst inhibition or deactivation. In contrast, the other electron-withdrawing substituents in C6 position of bipyridine *N*-oxides **20** gave ester-substituted product **22c** and trifluoromethyl-substituted product **22d** 82% and 99% yields. The methyl analogue **20b** gave slightly diminished yields of 60% for the brominated product **22b** and 68% for **21b**, respectively. Noteworthy, if using the bipyridine *N*-oxide **20b** prepared by Negishi cross-coupling (*cf.* scheme 46), the chlorinated product **21b** was obtained containing trace impurities of brominated product **22b**. Both substances elute with identical R$_f$ values during column chromatography making separation difficult. We suppose that NMR silent bromide-containing impurities, such as ZnBr$_2$ from Negishi cross-coupling, might act as bromide source.

Table 22. Direct halogenation of bipyridine *N*-oxides **20** substituted at pyridine *N*-oxide ring.

Pd(OAc)$_2$ (5 mol %)
NXS (1.2 equiv.)
PhCl (0.1 M)
110 °C, 24 h

20

X = Br **22**
Cl **21**

22a, 87%
21a, 95%

22b, 60%
21b, 68%

22c, 82%
21c, 91%

22d, 99%

22e, 17% (**20e**, 14%)
21e, 0% (**20e**, 85%)

22f, 99%
21f, 97%

22g, 40% (**25g**, 35%)
21g, 90%

22h, 3%
21h, 64%

22i, c.m.
21i, 31% (**20i**, 33%)

22n, 37% (**20n**, 32%)
21n, 0% (**20n**, 91%)

R = OMe **22j**, 0% (**20j**, 83%)
    Cl   **22k**, c.m.
    CO$_2$Et **22l**, 0% (**20l**, 99%)
    CF$_3$ **22m**, 0% (**20m**, 53%; **30m**, 36%)
    NO$_2$ **22o**, 0% (**20o**, 72%; **30o**, 12%)[b]

22y, 49% (**25y**, 9%; **30y**, 8%)
21y, 87%

32a, 66% (**33a**, 10%)
       0%[c] (**31a**, 45%)

49% (19%)[d]

0% (78%)[e]
0% (92%)[e]
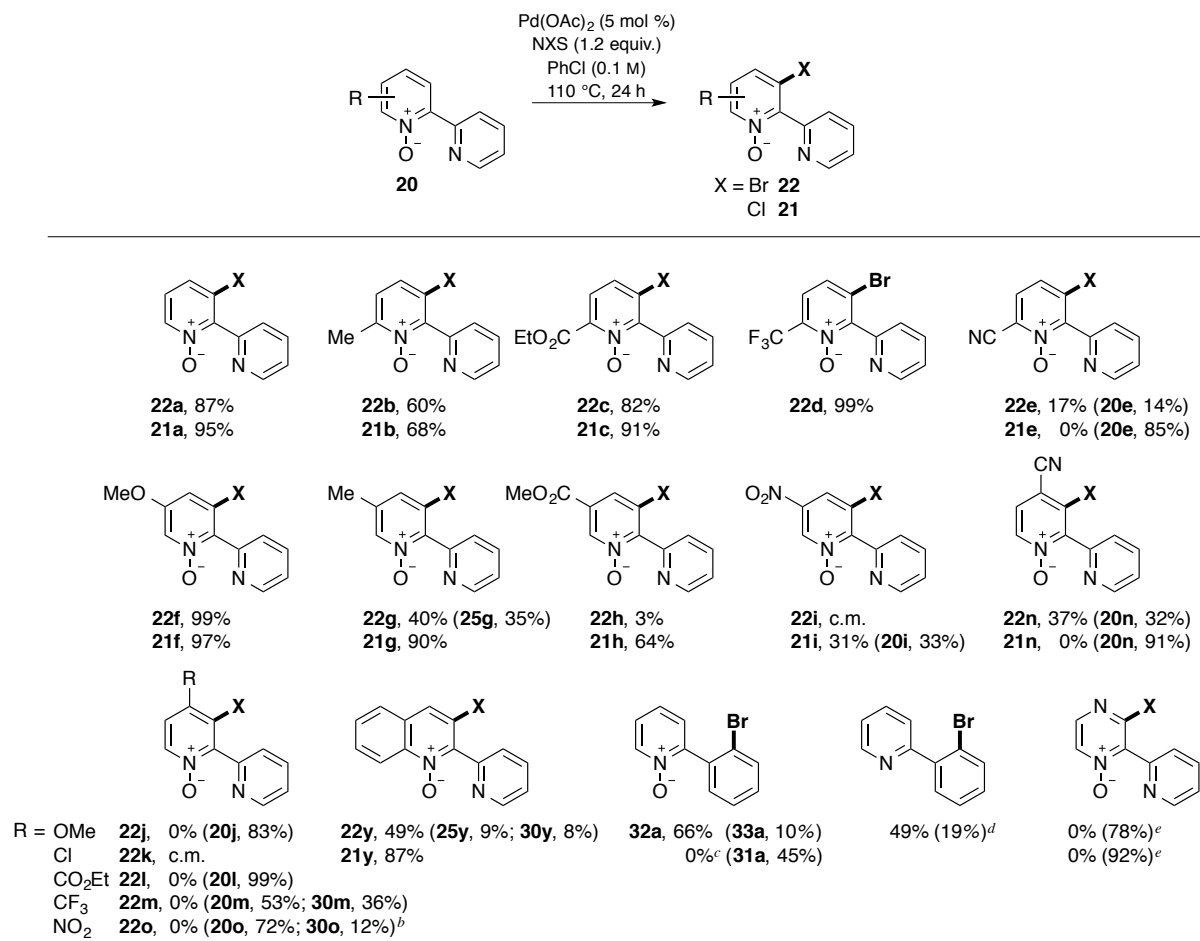
[a]Isolated yields. [b]Obtained as mixture of **20o** and **30o**. [c]Reaction without Pd(OAc)$_2$. [d]Yield of 2-(2,6-dibromophenyl)pyridine. [e]Recovered 2-(pyridin-2-yl)pyrazine *N*-oxide. c.m. = complex product mixture.

R = CF$_3$ **30m**
    NO$_2$ **30o**

30y

33a
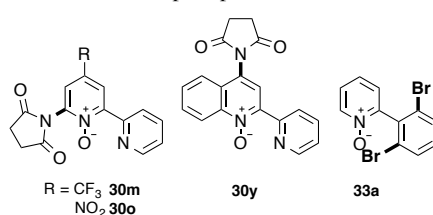
Direct halogenations of C5-substituted bipyridine *N*-oxides **20f–i** apparently follow a clear electronic trend. While the most electron-donating methoxy group gave for both, bromination and chlorination, the products **22f** and **21f**, respectively, in almost quantitative yields (table 22), the electron-withdrawing ester-substituted (**20h**) and nitro-substituted bipyridine *N*-oxide **20i** were chlorinated in lower yields of 64% and 31% (table 6). Similarly, the bromination of more electron-rich methyl-substituted bipyridine *N*-oxide **20g** occurred in an overall yield of 75% (40% of *N*-oxide **22g** and 35% of reduced product **25g**) and ester-substituted bipyridine *N*-oxide **20h** gave only 3% yield of **22h**. It is noteworthy that a loss of mass even after exhaustive extraction with DCM was observed of the crude product from the reaction of **20h** with NBS indicating that either the product itself is very water-soluble, or the ester was hydrolyzed during the reaction or the work-up, which would form a water-

soluble carboxylic acid. Running the reaction on a test scale without subsequent work-up indicate hydrolysis during the halogenation reaction, because quantification of the crude product by ^{1}H NMR using TMB as internal standard revealed a yield for **22h** of 77%, and 16% of unreacted starting material **20h**. The most electron-poor nitro-substituted substrate **20i** could not be brominated. A complex product mixture was obtained instead indicating diverse side reactions probably caused by the very reactive nitro group. In contrast, chlorination of **20i** provided product **21j** in 31% besides 33% of unreacted starting material **20i**.

The palladium-catalyzed direct halogenations of C4-substituted bipyridine *N*-oxides **20** were essentially unsuccessful, as expected due to the steric hindrance. The bromination of 4-chlorobipyridine *N*-oxide **20k** resulted in a complex product mixture (table 22), whereas the chlorination resulted in no conversion. The starting material was completely recovered from the bromination reaction with the ester-substituted **20l**, and in 83% from the reaction of C4-methoxylated bipyridine *N*-oxide **20j**. In cases of the electron-poor trifluoromethyl- and nitro-substituted bipyridine *N*-oxides **20m** and **20o**, the starting materials were recovered along with coupling products with succinimide **30m** and **30o**. The trifluoromethyl-substituted side product **30m** could be isolated in 36% separated from the starting material **20m**, which was recovered in 53%. In case of the nitro-substituted analogue, **30o** was obtained only in a mixture with the starting material **20o** in an estimated yield of 16%. The mechanism for the formation of products **30** is yet unclear and would be only speculative without additional mechanistic experiments. Among the C4-substituted substrates **1j–o**, only nitrile-substituted bipyridine *N*-oxide **20n** gave the desired brominated product **22n** in 37% besides 32% of recovered starting material. The nitrile-substituent is among the others the one with the smallest steric demand,[160] which allows the catalyst to approach the C3 position for the C-H bond activation. However, the chlorination with NCS did not provide any product, instead 91% of starting material **20n** was recovered.

Palladium-catalyzed direct halogenation of pyridylpyrazine *N*-oxide did not provide halogenated products. Only starting material was recovered in 78% and 95% yield instead (table 22). However, the quinoline *N*-oxide **20y** was brominated in 49% yield and chlorinated in 87% yield. In case of the bromination, the reduced brominated product **25y** was found in 9% yield besides 8% of the coupling product of **20y** and succinimide. 1D and 2D NMR revealed that the succinimide was coupled at the C4 position corresponding to the structure of **30y**.

For comparison with the conditions developed by Sanford and co-workers,[102a, 126] we applied our reaction conditions to 2-phenylpyridine, which led to 49% yield of monobrominated product and additional 19% yield of the dibrominated product (table 22). The ratio of mono- and dibrominated products corresponds to the expected statistical mixture if the first functionalization is approximately

2.3 times faster than the second one. Such double C-H bond functionalization has often been observed for palladium- or copper-catalyzed reactions of substrates without steric shielding of the activated C-H bonds.[102h, 102o, 102p, 138] From reaction at 120 °C in CH₃CN under otherwise identical conditions, Sanford and co-workers obtained 63% of monobrominated product,[126] which requires that the first functionalization is at least 4 times faster than the second one.

In case of the brominated bipyridine *N*-oxides **22f** and **22n**, crystals suitable for X-ray diffraction analysis could be grown. The solid state structure of methoxybipyridine *N*-oxide **22f** (figure 22, left) exhibits bond distances similar to the unsubstituted analogue **22a** (*cf*. figure 21), and 3-bromopyridine *N*-oxide,[153] and 4-methoxypyridine *N*-oxide (**27j**) in a 1:1 complex with 2,4-dinitrophenol.[161] The Br-C bond distance is 1.90 Å and is similar to 3-bromopyridine *N*-oxide and brominated bipyridine *N*-oxide **22a** (1.89 Å, *cf*. figure 21). The torsion angle of the two aromatic rings is 72.5 ° and is unexpectedly smaller than for the unsubstituted bipyridine *N*-oxide **22a** (98.2 °), while the C-C bond, connecting both rings, are in the same order of 1.49 Å.
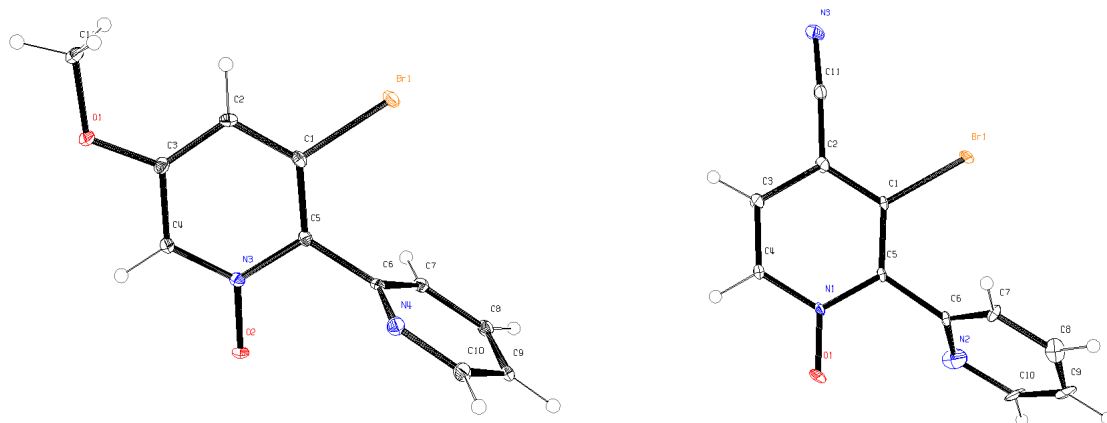
Figure 22. ORTEP 3 diagrams of brominated bipyridine *N*-oxides **22f** (left) and **22n** (right). Thermal ellipsoids are drawn at 30% probability level. Selected bond distances (Å) and angles (°) for **22f**: N3 – C4 1.35(3), C4 – C3 1.38(4), C3 – C2 1.38(6), C2 – C1 1.39(0), C1 - C5 1.37(6), C5 – N3 1.38(1), N3 – O2 1.30(1), C1 – Br1 1.89(5), C3 – O1 1.35(3), C11 – O1 1.43(8), C5 – C6 1.49(0), C6 – N4 1.34(0), C10 – N4 1.34(1), N1 – C5 – C6 – N2 72.5(0). Selected values for **22n**: N1 – C4 1.36(1), C4 – C3 1.34(4), C3 – C2 1.44(7), C2 – C1 1.39(8), C1 - C5 1.38(0), C5 – N1 1.36(9), N1 – O1 1.27(7), C1 – Br1 1.87(3), C2 – C11 1.41(6), C11 – N3 1.16(4), C5 – C6 1.50(2), C6 – N2 1.39(3), C10 – N2 1.409, N1 – C5 – C6 – N2 68.7(7). Only one molecule **22n** of two from the asymmetric unit is shown for clarity.

Although the single crystals of **22n** were only of poor quality, the connectivity of the atoms, in particular the C3 bromine atom is clearly shown. The bond distances between the C(sp^2)-C(sp) and N-C(sp) are about 1.42 Å and 1.16 Å, respectively, which is in the expected range, compared to the values for the solid state structure of 4-cyanopyridine *N*-oxide (1.43 Å and 1.15 Å, respectively).[162] The torsion angle between the two aromatic planes is ≈ 69 °, which is smaller than for **22f** (72.5 °) and

22a (98.2 °, *cf.* figure 21). Notably, the nitrogen atoms of the rings are oriented in a *synclinal* conformation, which is unusual, because antiparallel alignment of the rings's dipole moments typically leads to anticlinal conformations like found for the unsubstituted bipyridine *N*-oxide **20a**.[152] An explanation for the observed orientation might be that for C3-brominated bipyridine *N*-oxides **22** the dipole moments of the *N*-oxide ring are inverted compared to **22a**.

Table 23. Direct halogenation of bipyridine *N*-oxides **20** substituted at the pyridyl ring.

22p, 98%
21p, 96%

22q, 0% (**25b**, 13%)
21q, 0% (**20q**, 99%)

22r, 7% (**25d**, 25%)
21r, 90%

22s, 7% (**20s**, 15%; **25s**, 8%)

22t, 54%

22u, 99%
21u, 98%

21v, 90%

22w, 83%
21w, 90%

21x, 97%
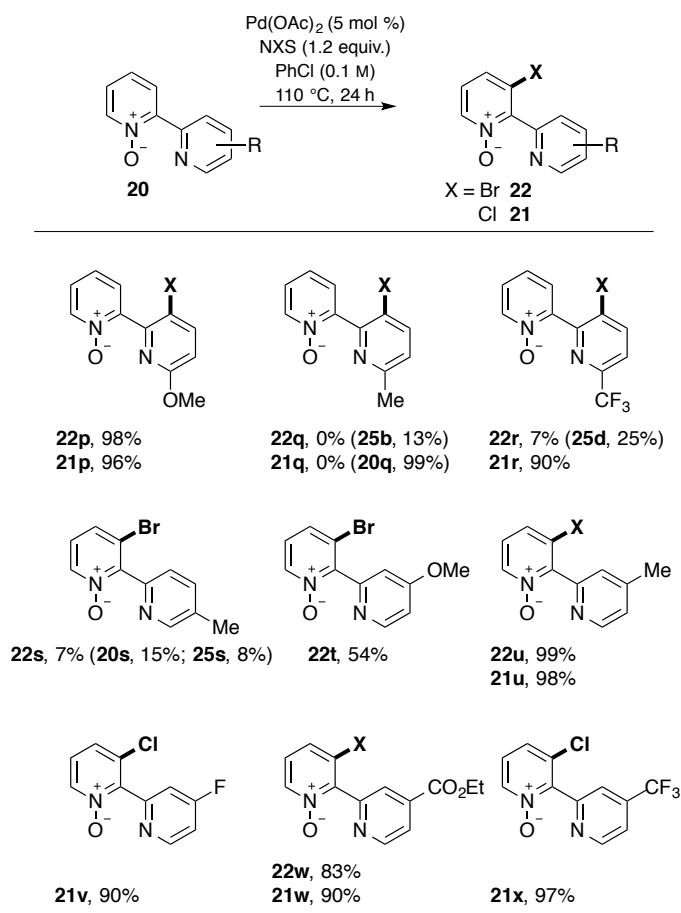
*Isolated yields.

Next, we explored the reactivity of bipyridine *N*-oxides **20** with substituents at the pyridyl ring (table 23). We expected that C-H bond activation of substrates with a substituent at the C6′ position would be more difficult due to hindered coordination of the palladium catalyst to the pyridyl ring. Thus, methoxy-substituted bipyridine *N*-oxide **20p** was halogenated in almost quantitative yields at the unexpected C3′ position. Attempted bromination of methyl-substituted analogue **20q** led only to 13% of deoxygenated product **25q**. Starting material **20q** could not be recovered. A large fraction of several unidentified products was obtained instead. The chlorination of **20q** led to no conversion, and starting material was recovered quantitatively. The trifluoromethyl-substituted bipyridine *N*-oxide **20r** gave only 7% isolated yield of the C3′-brominated *N*-oxide **22r**, besides 25% of the deoxygenated product

25r as the major product. In contrast, the chlorination proceeded smoothly with full conversion of **20r** to **21r** in a high yield of 90%.

The unusual regioselectivity of the direct bromination reaction of C6′-substituted bipyridine *N*-oxides **2p–r** (table 23) cannot be explained by a catalyzed or uncatalyzed S_EAr, because the electron-rich substrate **20p** gave **21p** in similarly high yield (96%) as the electron-poor substrate **20r** for **21r** (90%) in the chlorination reaction. A reasonable explanation might be that the steric bulk of the C6-substituent prevents the catalyst from coordination to the pyridyl nitrogen, however, coordination of the *N*-oxide oxygen to palladium remains possible, which then guides the C-H bond activation to the C3′ position. Palladium complexes with coordinated pyridine *N*-oxide have been previously reported.[163] To probe the directing ability of the *N*-oxide oxygen, we prepared phenylpyridine *N*-oxide **31a** and subjected it to our bromination conditions. For an electrophilic substitution *para*-bromination of the phenyl ring would be expected as major product, however, *ortho*-brominated products were observed. Monobrominated **32a** was obtained in 66% and dibrominated **33a** in 10% yield (table 22). Reaction of **31a** without Pd(OAc)$_2$ under otherwise identical conditions did not provided brominated products. These results support the assumption of *N*-oxide-directed halogenation in cases, where the pyridyl ring of the bipyridine *N*-oxide substrate is sterically too hindered for catalyst binding.

Direct bromination of the C5′-substituted bipyridine *N*-oxide **20s** gave only poor yields of 7% for the *N*-oxide **22s** and the deoxygenated product **25s** in 8% (table 23). Starting material **20s** could only be recovered in 15%. The observation that methyl substituents in certain positions, such as in C6 (**20b**), C5 (**20g**) and C6′ (**20q**) and C5′ (**20s**) give only low to poor yields, in particular from bromination reactions with NBS, possibly results from radical reactions at the benzylic position, induced by thermal decomposition of NBS. Because all reactions were usually carried out under ambient atmosphere without degassed solvents, we hoped to improve the yields by exclusion of air. However, using degassed chlorobenzene and setting up the reaction in an argon-filled glove box did not improve the yields. Contrary to all other methylbipyridine *N*-oxides, the C4′-substituted **20u** was brominated in quantitative yield and chlorinated in 98%.

The other C4′-substituted bipyridine *N*-oxides **20** were halogenated at the expected C3 position of the *N*-oxide ring. While the methoxy-substituted substrate **20t** was brominated in a total yield of 54%, fluoro-, ester- and trifluoromethyl-substituted bipyridine *N*-oxides were brominated and chlorinated in high to almost quantitative yields (83%–97%) independent of the electronic nature of the substituents. These results demonstrate, that changing the donor properties of the pyridyl nitrogen might have an influence on the reaction rate for the C-H bond activation but does not necessarily have an effect on the yield.

2.3.4 Deoxygenations

Deoxygenations of bipyridine *N*-oxides have been reported to proceed catalyzed by palladium on charcoal using either $NH_4(CO_2H)$[157a] or hydrogen gas as reducing reagents.[117] However, halogenated compounds might be dehalogenated under these conditions. Accordingly, an initial attempt to deoxygenate brominated bipyridine *N*-oxide **22a** or the chlorinated analogue **21a** using $NH_4(CO_2H)$ and Pd/C yielded exclusively bipyridine **24a** for **22a** and no conversion for **21a** (scheme 47). An alternative uncatalyzed procedure for deoxygenation employs PCl_3 as reductant.[117, 164] Indeed, deoxygenation of bromobipyridine *N*-oxide **22a** with PCl_3 provided 70% of desired product **25a**.
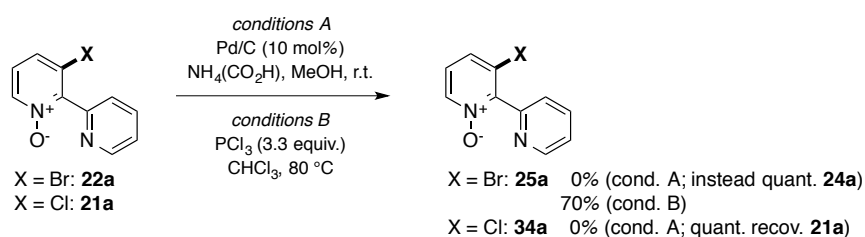
Scheme 47. Initial attempts of deoxygenation of halogenated bipyridine *N*-oxides **21a** and **22a**.

To avoid conceivable halogen exchange side reactions, we explored the substrate scope for the deoxygenations using PCl_3 for the chlorinated products **21** and PBr_3 for the brominated products **22**. Generally, the reductions with PCl_3 gave better yields than the ones with PBr_3 and the latter reactions required usually purification by flash column chromatography, while reductions with PCl_3 often provided pure products after extraction. The halopyridine *N*-oxides were reduced in overall good yields independently of their electronic nature (table 24). High yields were obtained from PCl_3 reductions of halobipyridine *N*-oxides bearing an ester group in yields ranging from 61% to 93%, but also methyl-substituted analogues gave the corresponding bipyridines in good yields of 45–95%. PBr_3 reductions provided high yields for 6-methylbipyridine **7b** and 4′-esterbiypridine **8f** in yields of 79% and 86%, respectively. In all other cases, moderate yields of 37% to 66% were obtained.

While the chlorobipyridine **34p** was obtained in 66% yield, the bromide analogue **25p** was obtained in only 8% yield. A high mass loss was noted after column chromatography for **25p** compared to the mass of the crude product, which contained unconverted starting material **22p** in a 1:1 ratio as judged by ¹H NMR. However, other side products were not found. The reduction of the C5-substituted halobipyridine *N*-oxides **21** and **22** gave high yields of reduced products for **34g** (85%) and **34h** (93%) (table 24). In contrast, the reactions of substrates **21f** and **22f** with the strongly electron-donating methoxy group yielded dihalogenated bipyridines **25f** and **34f**, which result from electrophilic aromatic substitution either with PX_3 or the byproduct $(O)PX_3$.[165] In case of chlorobipyridine **21f**, the deoxygenated product **34f** was obtained in 58% yield in addition to 14% to the dihalogenated product

36f. Whereas, the bromide analogue **35f** could not be isolated, instead 45% of dibrominated bipyridine **35f**. Similarly, deoxygenation of quinoline *N*-oxide **21y** provided 13% of dihalogenated product **36y**, and 57% of the desired product **34z**. In contrast, the reaction of bromoquinoline *N*-oxide **22y** gave exclusively the monobrominated product **25y** in 38% yield.

Table 24. Deoxygenation of halogenated bipyridine *N*-oxides.

aIsolated yields. bYield of **36y**. cYield of 3,6-dihalo-5-methoxybipyridine **35f** or **36f**, repectivetly.

2.3.5   Mechanistic investigations

Recent mechanistic investigations on the direct chlorination of benzo[*h*]quinolines and 2-arylpyridines with NCS by Ritter and co-workers support a catalytic cycle consisting of (i) cyclopalladation, (ii) rate-determining nucleophile-assisted bimetallic oxidation, and (iii) acid-assisted bimetallic reductive elimination. To elucidate how far the reaction with 2,2-bipyridine *N*-oxides **20** as substrates follows the same mechanism, we carried out some initial mechanistic experiments. First, we synthesized potential dimeric palladium(II) intermediates, analogous to the ones proposed for the direct halogenation of phenylpyridines and benzo[*h*]quinolines.[145-146, 150] The phenylpyridine- and benzo[*h*]quinoline-derived acetate-bridged dimers were described to be formed easily from Pd(OAc)$_2$ by cyclometalation in DCM, AcOH or their mixture at room temperatures. However, stirring Pd(OAc)$_2$ with 1 equivalent of bipyridine *N*-oxide **20a** in DCM at room temperature yielded only an insoluble solid, which we assume is the mono-nuclear complex **C1**, where two bipyridine *N*-oxide molecules are coordinated to palladium by the pyridyl nitrogen (scheme 48). A very diluted ^{1}H NMR sample in CDCl$_3$ of the supernatant solution showed 8 protons, indicating that the bipyridine *N*-oxide **20a** was not cyclometalated and the ligands are equivalent. Addition of AcOH and heating at 50 °C formed a solution, which consisted mainly of a mixture of the desired cyclometalated dimer **D** and bipyridine *N*-oxide **20a** in ratio of 1:1.25.
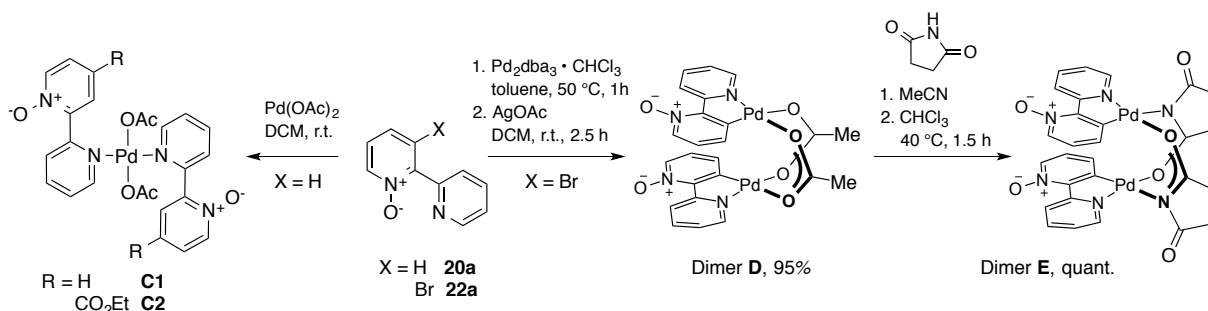
Scheme 48. Synthesis of potential intermediates, palladium(II) dimers **A** and **B**.

Using ester-substituted bipyridine *N*-oxide **20l**, a better soluble sample of the monomer complex **C2** was obtained, of which single crystals could be grown. X-rays diffraction analysis showed that indeed a monomeric complex was formed, which is not cyclometalated and is only coordinated by the nitrogen atoms of two bipyridine *N*-oxide molecules and two acetate ligands (figure 23). The bond distances between the palladium center and pyridyl nitrogens are 2.07 Å and between the acetate oxygen 2.01 Å, which is similar to the solid state structure of a pyridine-coordinated diacetate complex (Pd-N 2.01 Å, and Pd-O 2.01 Å).[166] The torsion between the two aromatic rings is 55.1 °. Interestingly, the distance between the carbonyl oxygen atom of the acetate ligand and the hydrogen

on the C3 carbon of the *N*-oxide ring is 2.35 Å, pointing towards each other, which is the consequence of the torsion of the aromatic rings.
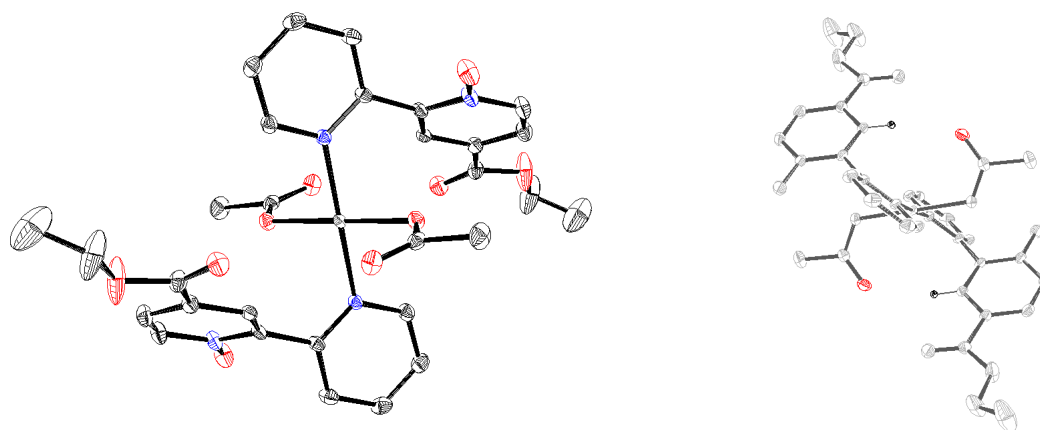

Figure 23. ORTEP 3 diagram of diacetate palladium monomer **C2**. Thermal ellipsoids are drawn at 30% probability level. Hydrogen atoms were omitted for clarity. Left structure of **C2** with highlighted acetate oxygen and C3 hydrogen pointing towards each other. Selected bond distances (Å) and angles (°): Pd–N 2.02(7), Pd–O 2.00(8), O–Pd – O 179.9(7), N–Pd– N 179.97, N–C2′–C2–N(O) 55.1(1). O(=C)–H(C3) 2.34(8).

Because the isolation of the desired well defined palladium(II) acetate dimer **D** by simple carbopalladation, which had been done to prepare related complexes, resulted only in a mixture of different compounds, we followed another strategy for the synthesis of dimer **D**. We were finally able to isolate pure acetate-bridged dimer **D** from an oxidative addition of brominated bipyridine *N*-oxide **22a** to Pd$_2$dba$_3$·CHCl$_3$ in toluene at 50 °C and subsequent stirring of the mixture with AgOAc in DCM (scheme 48). The palladium dimer **D** was isolated in 95% yield as a mixture of two isomers (ratio ≈ 1:6), of which the major isomer is probably the *trans* isomer with respect to the C-N chelating ligand. The dimer **D** could be fully converted into the succinate-bridged dimer **E** by modification of the reported procedure for related succinate palladium(II) complexes.

Single crystals for the dimer **D** suitable for X-ray analysis could be grown by slow diffusion of Et$_2$O into a concentrated DCM solution. Acetate-bridged dimer **D** exhibits two palladium centers, which are held in proximity to each other by two acetate ligands (figure 24), as has been observed for related benzo[*h*]quinoline-derived complexes.[146a, 146b] The Pd-Pd distance is 2.86 Å, which is consistent with a bond of zeroth order.[146a, 167] The bipyridine *N*-oxide ligands show small torsions of the aromatic planes with dihedral angles of 4.8 ° and 3.7 °, respectively, probably induced by the steric demand of the *N*-oxide oxygen.
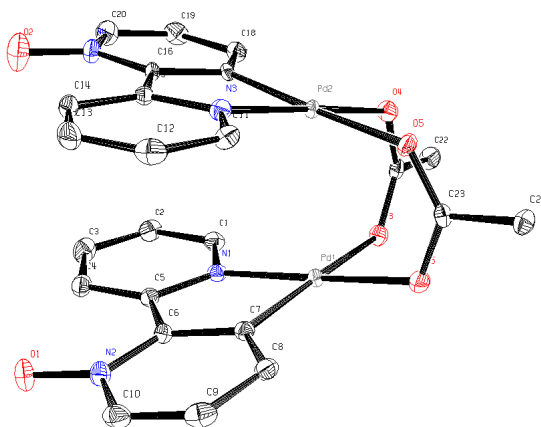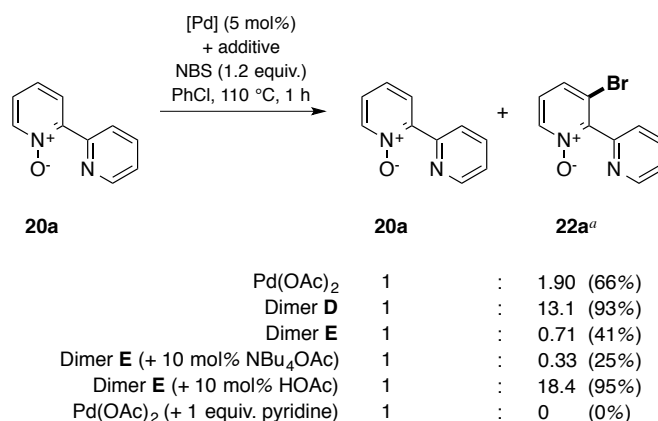
Figure 24. ORTEP 3 diagram of acetate palladium dimer **D**. Thermal ellipsoids are drawn at 30% probability level. Hydrogen atoms were omitted for clarity. Selected bond distances (Å) and angles (°) for **D**: Pd1–N1 2.00(9), Pd2–N3 1.99(3), Pd1–C7 1.95(7), Pd2–C17 1.95(8), Pd1–O(6) 2.06(3), Pd2–O4 2.06(5), Pd1–O3 2.10(8), Pd2–O4 2.09(5), Pd1…Pd2 2.86(3), N1–Pd1–O5 173.9(8), C7–Pd1–O3 172.8(1), N3–Pd2–O4 173.1(4), C1–Pd2–O5 174.63, C1–C16–C15–N3 3.7(1), C7–C6–C5–N1 4.8(2), O5–C23–O6 126.0(9), O4–C21–O3 125.82.

To elucidate, which of these dimers might be catalytically active intermediates, we performed the direct bromination reactions using Pd(OAc)$_2$, as well as dimers **D** and **E** and aborted the reactions after 1 h by cooling to 0 °C. After removal of the volatiles, the residues were dissolved in CDCl$_3$ and the ^{1}H NMR spectra were directly measured. The ratios between unreacted **20a** and brominated product **22a** were determined by integration of isolated, non-overlapping signals. Because no other products were observed in the crude ^{1}H NMRs, an estimated yield for **22a** could be calculated based on the sum of **20a** and **22a**. The reactions were carried out in parallel in reaction vials and heated on a pre-heated aluminum well-plate, on which all vials were arranged in such a way that they were equally heated. This should avoid differences in yields caused by unequal heat distribution or different termination time points.

The reaction under our standard conditions using Pd(OAc)$_2$ provided 66% of **22a** as reference value (scheme 49). The yield was almost quantitative (93%) if the palladium dimer **D** was used as catalyst, indicating kinetic competence. In contrast, analogous succinate dimer **E** gave only 41% of **22a**. The results are in agreement with that obtained by Ritter and co-workers, who found that the succinate dimer of benzo[*h*]quinoline, which was identified as catalyst resting state, is chemically competent, but not a kinetically competent catalyst.[146b] They assumed that this is due the lack of acetate ions, when isolated succinate-dimers are used as catalyst. This led to the conclusion that acetate ions participate during catalysis. Indeed, Ritter and co-workers reported that the reaction rate for the direct halogenation of benzo[*h*]quinoline catalyzed by the succinimide dimer significantly increased when 4 equivalents of AcOH or NBu$_4$OAc (with respect to succinimide dimer) were added. To examine a potential co-catalysis by acetate for the direct bromination of bipyridine *N*-oxides, we performed the

experiments using succinimide dimer **E** in the presence of 10 mol% of AcOH (based on **20a**) or NBu$_4$OAc, respectively. In the presence of AcOH, **20a** was brominated in a much higher yield of 95% compared to the reaction without AcOH, which suggests that the free acid accelerate the rate-determining step. However, the analogous reaction with NBu$_4$OAc gave only 25% of the brominated product **22a**, which indicates that acetate anions inhibit the rate-determining step, and is in contrast to the observations made by Ritter and co-workers.

	[Pd] (5 mol%) + additive NBS (1.2 equiv.) PhCl, 110 °C, 1 h			
20a		**20a**		**22a**^{a}
Pd(OAc)$_2$	1	:	1.90	(66%)
Dimer **D**	1	:	13.1	(93%)
Dimer **E**	1	:	0.71	(41%)
Dimer **E** (+ 10 mol% NBu$_4$OAc)	1	:	0.33	(25%)
Dimer **E** (+ 10 mol% HOAc)	1	:	18.4	(95%)
Pd(OAc)$_2$ (+ 1 equiv. pyridine)	1	:	0	(0%)

Scheme 49. Catalytic reactions of the palladium(II) dimers.

^{a}Yields are based on the ratio **20a**:**22a** in the crude 1H NMR. Conditions: Bipyridine *N*-oxide **20a** (0.25 mmol), NBS (0.30 mmol), palladium source (5 mol% based on [Pd]), chlorobenzene (2.50 mL) and, if applicable, NBu$_4$OAc (0.025 mmol), or AcOH (0.025 mmol as stock solution in chlorobenzene), or pyridine (0.25 mmol) at 110 °C for 1 h.

Based on kinetic investigations, Ritter and co-workers found that the oxidative addition of NCS with the cyclometalated palladium(II) dimers to palladium(III) dimers is the rate-determining step in the direct chlorination of benzo[*h*]quinolines or 2-arylpyridines and is finally the step, which is mediated by acetate (or generally by a nucleophile). Therefore, if the oxidative addition of NBS to the bridged dimer **E** would be rate-determining and co-catalyzed by acetate in the direct bromination of bipyridine *N*-oxides **20**, the addition of both acetate sources (AcOH or NBu$_4$OAc) would accelerate bromination of bipyridine *N*-oxides **20a**. However, we observed that addition of NBu$_4$OAc resulted in lower yields for **22a** than without after 1 h reaction time (scheme 49) indicating inhibition by acetate. This observation suggests that the cyclopalladation of bipyridine *N*-oxide **20a** is the rate-determining step. It is conceivable that excess acetate ions block a free coordination site, which is required for the C-H bond cleavage at the palladium(II) center.[119a, 119c, 139a] In contrast, free AcOH would facilitate de-coordination of acetate ligand by protonation. The requirement for a free coordination site at the palladium(II) center is further supported by the observation that higher substrate concentrations resulted in lower yields of the brominated products (*cf.* table 19), as well as addition of 1 equivalent of pyridine resulted in no conversion (scheme 49).

To investigate the oxidative addition of NBS further, isolated dimeric palladium complexes **D** and **E** were heated with a stoichiometric amount of NBS. In the initial experiments, ^{1}H NMR analysis of the crude products, after heating to 110 °C in chlorobenzene for 15 min, showed exclusively very small amounts of the succinimide dimer **E** irrespective of the starting complex. This indicates succinimide dimer **E** as the resting state, analogues to the direct halogenation of benzo[*h*]quinoline and 2-arylpyridine, for which the corresponding succinimide dimers were found as catalyst resting states.[146b] However, the brominated product **22a** was not detected from these initial experiments, which we thought might be due to coordination of the product to palladium. Indeed, when tmeda as bidentate ligand was added to the crude product to de-coordinate possibly palladium-bound product, signals of **22a** were observed in the ^{1}H NMR spectrum and HRESI-MS.

With the observation that the halogenated product is released by coordination of a strong coordinating ligand, we carried out further stoichiometric experiments with addition of 20 equivalents of pyridine. Although pyridine inhibits the direct halogenation reaction (*cf.* scheme 49), we assumed that it only inhibits the first step of the catalytic cycle, the cyclopalladation, but should not affect the subsequent oxidative addition and reductive elimination. The reactions were carried out in the same manner as the catalytic reactions using Teflon-lined reaction vials, pre-heated aluminum well-plate and setting up all reactions in parallel, as described for the reactions in scheme 49. After 10 min reaction time, the vials were immediately cooled to room temperature and the volatiles removed. A stock solution of TCB (1,3,5-trichlorobenzene) as internal standard in $CDCl_3$ was used to quantify the product **22a** by ^{1}H NMR spectroscopy. The reaction of complex **A** resulted in 66% yield of **22a** (based on [Pd]), while complex **E** led only to 20% of **22a** and 46% of unreacted complex **E** (scheme 50). These results can be explained with the previously proposed acetate-assisted oxidative addition.[146b] In case of complex **D**, acetate is released during the fast formation of succinimide dimer **E**, although the process itself is still unknown.[146b] The acetate then mediates the oxidative addition of NBS to the *in situ* formed dimer **E**. In the reaction of isolated complex **E**, the yield of **22a** is lower, because there is no acetate present in the reaction mixture.

In addition, we performed the stoichiometric reactions of dimers **D** and **E** in the presence of AcOH (4 equivalents based on dimeric complex). In the reaction of acetate complex **D** only a slight increase of the yield from 66% to 71% was observed (scheme 50). In contrast, the reaction with succinimide complex **E** provided a significantly higher yield of 51% for **22a** compared to the reaction without AcOH (20%). Because the C-X bond-forming reductive elimination was proposed to be also mediated by AcOH[146b] and might be slower than the oxidative addition, the positive effect by addition of AcOH might by be due to an enhanced rate of the reductive elimination. Therefore, we performed the stoichiometric reaction of dimer **E** in the presence of 4 equivalents of NBu_4OAc, which resulted in

much higher yield of 81% for **22a**. This supports that the oxidative addition is catalyzed by acetate on the one hand, and on the other hand is slower than the reductive elimination.

(a)	Dimer **D**	66%
(b)	Dimer **E**	20% (46%)[b]
(c)	Dimer **D** (+ HOAc)	71%
(d)	Dimer **E** (+ HOAc)	51%
(e)	Dimer **D** (+ NBu₄OAc)	81%
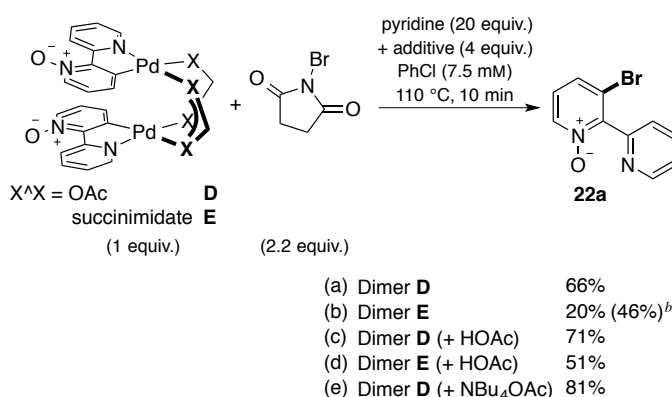
Scheme 50. Stoichiometric reactions of cyclometalated palladium(II) dimers.
[a]Yields were determined by 1H NMR *vs*. TCB (1,3,5-trichlorobenzene) as internal standard. [b]Recovered dimer **E**. Conditions: Dimer **D** or **E** (0.075 mmol), NBS (0.17 mmol), pyridine (1.50 mmol), and, if applicable, NBu₄OAc (0.075 mmol) or AcOH (0.30 mmol, as stock solution in chlorobenzene), at 110 °C for 10 min.

Although additional kinetic investigations are required to fully elucidate the mechanism, our preliminary results, as well as previous studies, indicate a bimetallic mechanism, which was recently proposed by Ritter and co-workers for similar reactions using 2-arylpyridines and benzo[*h*]quinolines as substrates.[146b] The steps can be described as a cyclopalladation, which might be the rate-determining step forming the bimetallic succinimide-bridged palladium(II) dimer **E**, followed by an acetate-assisted bimetallic oxidation to a palladium(III) species, which undergoes rapid C-X bond-forming reductive elimination (scheme 51). Coordination of a new substrate molecule is necessary to release of the C3-brominated product from a palladium(II) succinimide complex to undergo again cyclometalation.
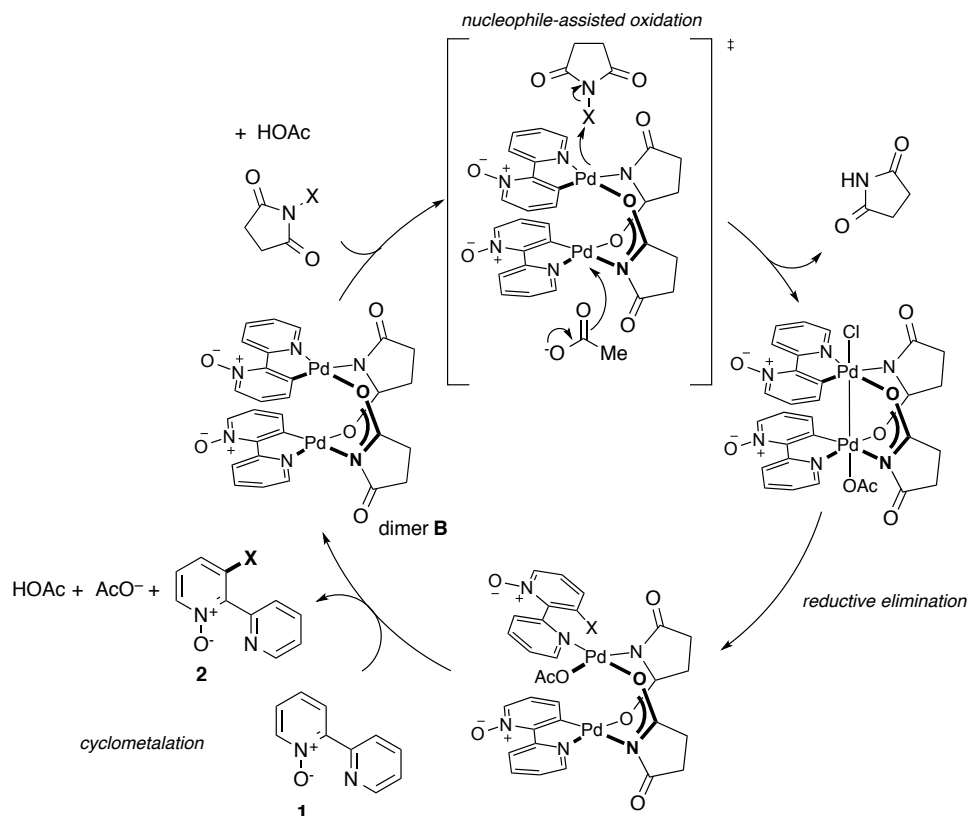
Scheme 51. Proposed mechanism for the palladium-catalyzed direct halogenation of bipyridine *N*-oxides.

2.3.6 Syntheses of C3-substituted Caerulomycins

Caerulomycins are natural products, isolated from marine–derived bacteria *actinoalloteichus cyanogriseus*,[97a, 168] and exhibit a 2,2′-bipyridine core, which can be structurally divided in two classes. Common to all Caerulomycins is a methoxy or hydroxyl group in C4 position, as well as an additional functional group, such as oximes, nitrile, aldehyde, carbamate or hydroxymethyl, in the C6 position (*cf*. 3.1 Motivation, Figure 21). While one class of Caerulomycins is not functionalized in C3 position, the other class bears additionally either a methoxy or hydroxyl group in this synthetically difficulty accessible position (Figure 25).
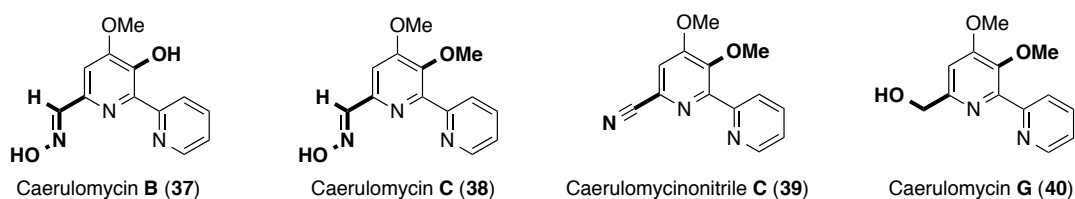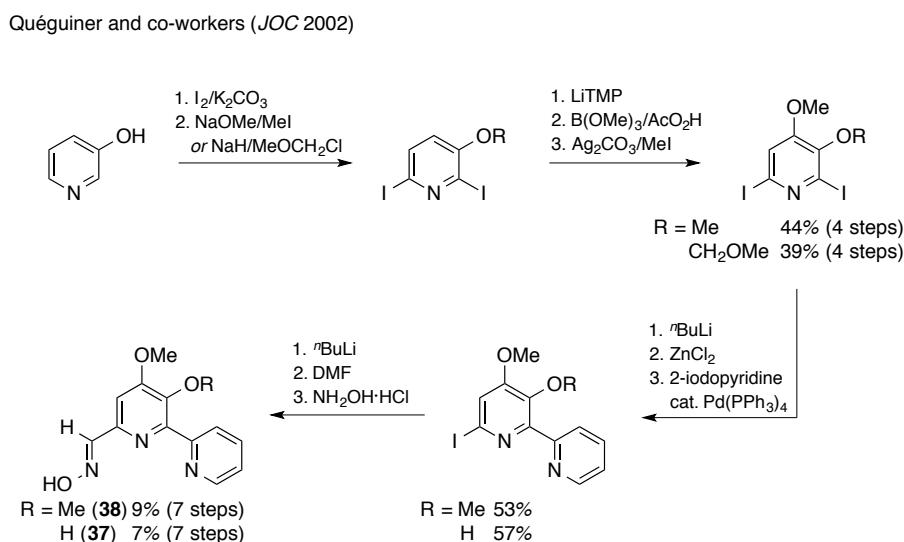

Caerulomycin **B** (37)   Caerulomycin **C** (38)   Caerulomycinonitrile **C** (39)   Caerulomycin **G** (40)

**Figure 25.** Structures of C3-substituted Caerulomycins.

Many synthetic routes have been reported for 4,6-disubstituted Caerulomycins,[113, 114b, 116, 164, 169] but only two routes have been published for the synthesis of Caerulomycins **B** (**37**) and three for Caerulomycin **C** (**38**).[98b-d] To the best of our knowledge, Caerulomycinonitrile **C** (**39**) and Caerulomycin **G** (**40**) have not been synthesized previously. Basically all reported syntheses start with the introduction of functional groups to build up the functionalized pyridyl ring, which is then coupled in Negishi cross-coupling with the second unfunctionalized pyridyl ring. The substituent at the C6 position was subsequently converted into an aldehyde as intermediate, which is then easily transformed into the hydroxyloxime moiety.

Quéguiner and co-workers (*JOC* 2002)

Scheme 52. Previously reported syntheses of Caerulomycins **B** (**37**) and **C** (**38**) by Quéguiner and co-workers.

Quéguiner and co-workers reported the first synthesis of Caerulomycin **C** (**38**) in 1996 starting from commercially available 3-hydroxypicoline to give **38** in 5% yield over seven steps.[98d] In 2002 the same authors reported an improved synthesis, which provided **38** in 9% over seven steps. 3-Hydroxypyridine was iodinated in C2- and C6 position (scheme 52), which introduced the required leaving groups for later Negishi coupling, and for introduction of the aldehyde. Upon alkylation of the hydroxyl group to give the methyl or a methoxymethyl ether (MOM), the C4 methoxy group was introduced by hydroxylation and subsequent methylation. The highly functionalized 2,6-diiodopyridine was then zincated and coupled with 2-iodopyridine in a Negishi reaction, which provided the coupled products only in moderate yields of about 50%, which is because both C-I bonds of the 2,6-diiodopyridine are potentially zincated. In case of the MOM-protected bipyridine, an appropriate acidic work-up provided the unprotected 3-hydroxyl group. Similarly to their previous synthesis, the 6-iodobipyridine was converted into the aldehyde and finally into the oximes, Caerulomycin **B** (**37**) in 9% and Caerulomycin **C** (**38**) in 7% yield, both over seven total steps.

At the same time a similar route was reported by Sammakia and co-workers starting from 2-picolinic acid (scheme 53). Although this synthesis involves three more steps, the Caerulomycin **C** (**38**) was obtained in a higher yield of 12% compared to 9% yield reported by Quéguiner and co-workers. The synthesis starts with the introduction of 4-chloro substituent via oxidation of the *in situ* generated picolinyl chloride, which was converted to a carbamate by subsequent condensation with di-*iso*-propylamine. Upon substitution of the 4-chloro substituent with NaOMe, the second methoxy group was introduced via three additional steps, which involve two lithiation/quenching sequences. The first lithiation/iodine quenching procedure provides first the 3-iodopyridine. The second lithiation/proton quenching procedure shifts the C3-iodide into the C5 position via a so-called halogen-dance reaction. The iodide was then converted into the methoxy group by a copper-mediate methoxylation with NaOMe, which provided 4,5-dimethoxypicolinyl carbamate. Via two additional lithiation/quenching sequences, the C6 bromide was introduced to couple the functionalized pyridine with 2-bromopyridine in a Negishi reaction, which provided the coupled product in 80% yield. Reduction of the carbamate to the aldehyde, and subsequent conversion into the hydroxyloxime provided the final Caerulomycin **C** (**38**).
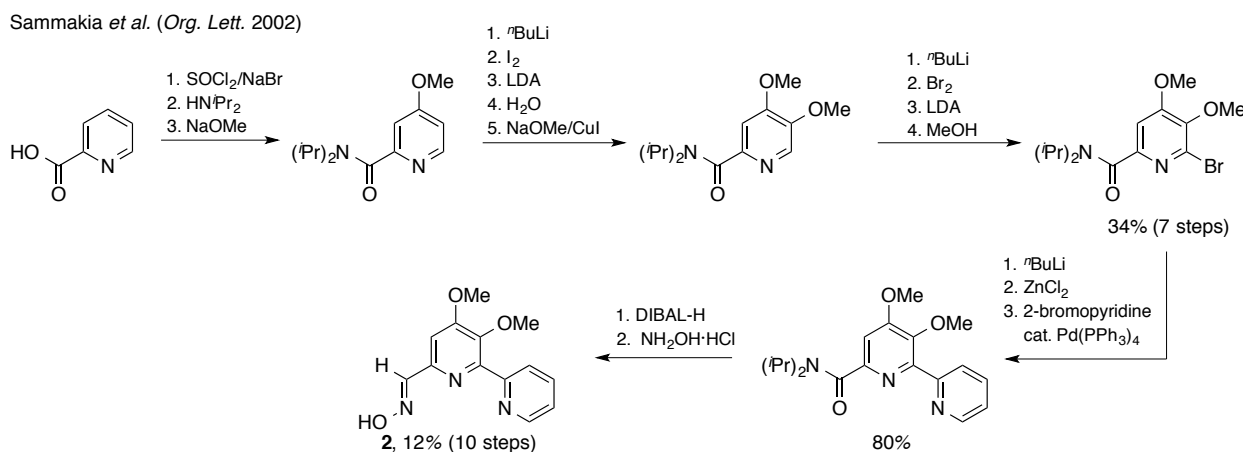
Scheme 53. Synthesis of Caerulomycins **C** (**38**) by Sammakia and co-workers.

The drawback of all previously reported syntheses is that they involve several lithiation/halogenation sequences, which we thought can be avoided by using C3-halogenated bipyridine *N*-oxides as key intermediate. Initially, we attempted the route (scheme 54), which we developed for the synthesis of other Caerulomycins and derivatives,[170] based on previous syntheses,[113, 114b, 116, 164, 169] to obtain structurally varied compounds for the investigation of the structure-activity relationships. Accordingly, methoxylation of the chlorinated bipyridine *N*-oxide **21a**, subsequent nitration and methoxylation should give the 3,4-dimethoxylated intermediate **43a**, which can be converted into **39** by a Reissert-Henze reaction using TMS-CN. However, while the methoxylation of the

chlorobipyridine *N*-oxide gave **41a** in a good yield of 85% (scheme 55), subsequent nitration provided C4- and C6-nitrated products **42a** in 49% yield in an 1:1 ratio besides 12% reduced product **44a**.
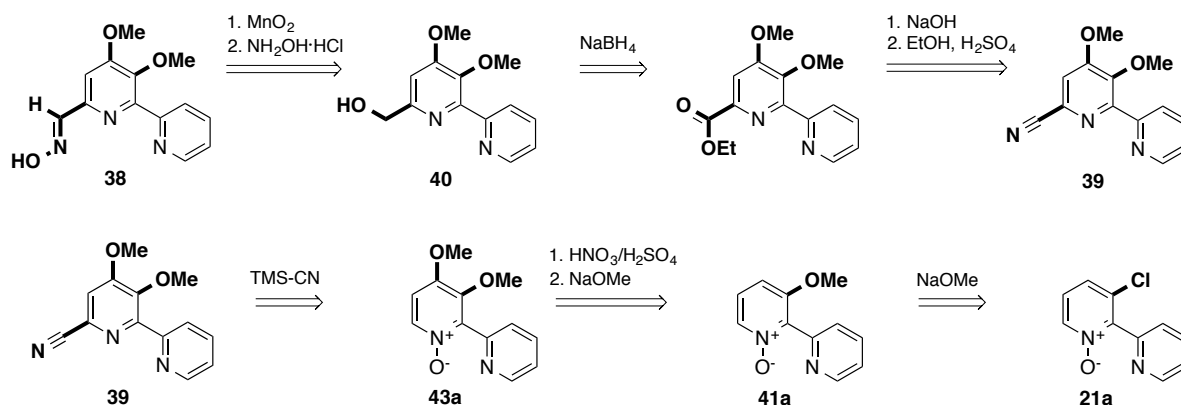
Scheme 54. Retrosynthesis starting form 3-chlorobipyridine *N*-oxide **21a**.

To avoid the undesired C6-nitration, we started from a C6-substituted bipyridine *N*-oxide, which we hoped would lead to a higher yield of the desired C4-nitrated product. Ideally an ester group, which can be converted into the targeted functional groups by reductions to the aldehyde or into the alcohol. The aldehyde would be further converted into the oxime, which leads to the nitrile by dehydration. However already the first step, the methoxylation of the corresponding chlorinated bipyridine *N*-oxide **21c** gave only unsatisfactory 31% yield of the methoxylated product **41c** (scheme 55), which was obtained as the corresponding methyl ester. Additional attempts to convert **21c** into the methoxylated bipyridine *N*-oxide **41c** at higher temperatures or equivalents of NaOMe did not improve the yield.
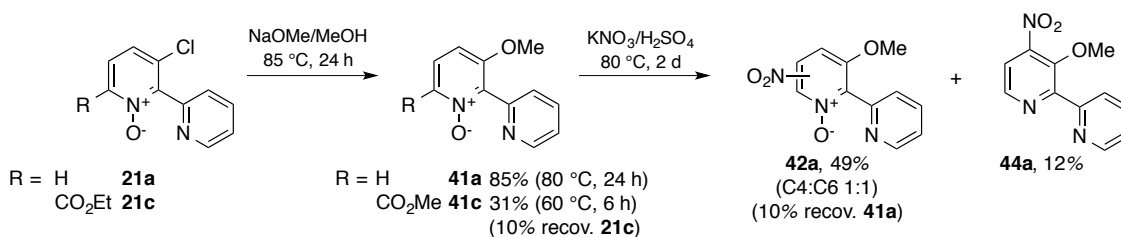
Scheme 55. Initial attempts to synthesize 3,4-dimethoxybipyridine *N*-oxides.

Nevertheless, we finally obtained the C3-methoxylated bipyridine *N*-oxide **41** using 3-bromo-6-methyl-bipyridine *N*-oxide **22b** in a copper-catalyzed reaction in a good yield of 71% on a test scale (0.91 mmol) and 63% on a larger scale (7.73 mmol) (scheme 56). Although the methyl group activates the pyridyl *N*-oxide ring for electrophilic aromatic substitutions, subsequent nitration on a test scale provided the desired 4-nitrobiypridine *N*-oxide **42b** only in 26% yield besides alcohol **45** in 13% yield using KNO$_3$/H$_2$SO$_4$ at 80 °C. Suspecting decomposition of the desired product at long reaction times, we thought that reducing the reaction time from 19 h to 2 h, and using fewer equivalents of the nitrate

might solve this problem. Indeed, at a larger scale the desired product **42b** was obtained in a higher yield of 43% besides 11% of unreacted starting material **22b** using HNO_3 instead of KNO_3 as nitrate source. Subsequent exchange of the nitro group by the methoxy group proceed smoothly in 88% yield of **43b** on the test scale and quantitative on the larger scale.

Following a synthetic route reported by Duan and co-workers for the synthesis of Caerulomycin **E**,[116] the 6-methylbipyridine *N*-oxide **43b** was converted in a Boekelheide rearrangement with AcO_2 into the acidic acid ester of the alcohol, which was subsequently hydrolyzed to give **40** in 77% yield for the test scale (0.13 mmol) and 96% on the larger scale (1.55 mmol). This synthetic route displays the first synthesis of Caerulomycin **G** (**40**), which was obtained in an overall good yield of 15% over 6 steps starting from 2-picoline *N*-oxide.
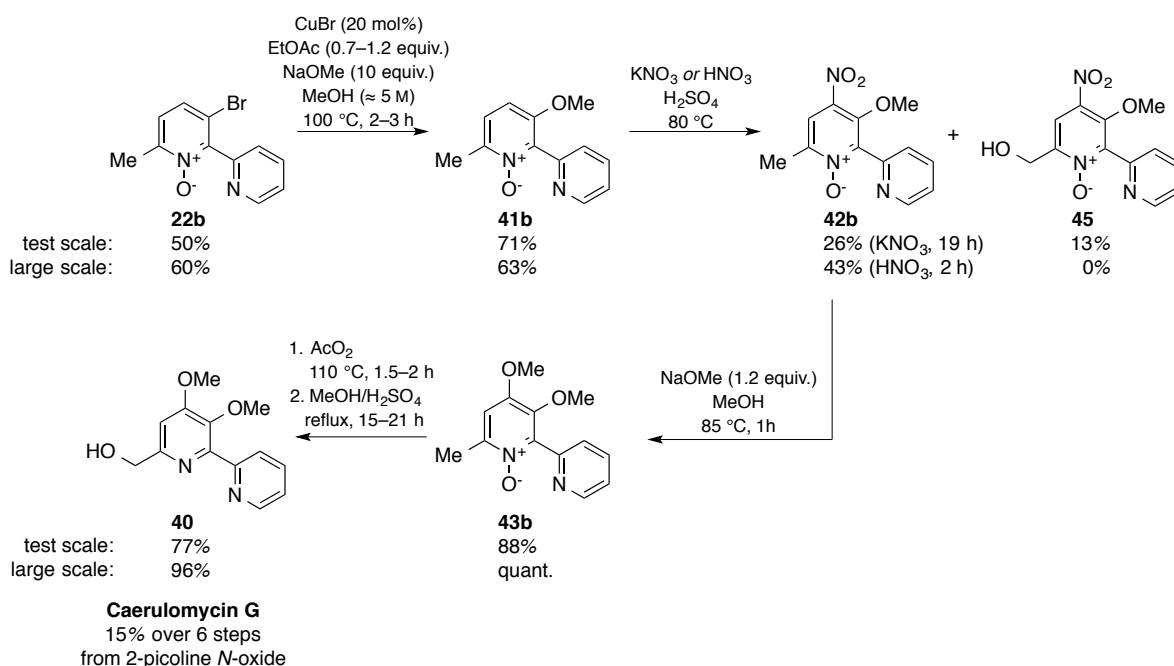
Scheme 56. First synthesis of Caerulomycin **G** (**40**).

The Caerulomycin **G** (**40**) was then oxidized with MnO_2 to give the aldehyde **46** in moderate yields of 51% and 58%, respectively, for the test and larger scale (scheme 57). **46** was then treated with $NH_2OH \cdot HCl$ in the presence of pyridine to give Caerulomycin **C** (**38**) in 89% yield. The overall yield was 7.8% over eight steps, which is lower compared to the previously reported yield of the highest yielding pathway, which gave **38** in 12% yield over 10 steps.[98c] We converted the aldehyde **46** in a TFOH-mediated Schmidt reaction under the conditions reported by Prabhu and co-workers[171] to the desired Caerulomycinonitrile **C** (**39**) in 62% yield. It was reported that three equivalents of TfOH smoothly converted diverse aromatic and heteroaromatic aldehydes into nitriles at room temperature within less than 5 min, however, an initial test reaction with 6-formyl-2,2'-bipyridine as substrate

revealed that under the reported conditions, only little conversion took place, even after stirring for several hours. However, addition of more TfOH resulted in full conversion also within minutes (< 10 min). Probably, the bipyridine nitrogen atoms are initially protonated, which already consumes two equivalents of the acid, while the third equivalent is consumed to liberate HN_3. Therefore, the overall proton concentration is too low to effecinetly catalyze the reaction. Thus, using 10 equivalents of TfOH provided the desired nitrile **39**, which was obtained in a total yield of 5.4% over 8 steps. Alternatively, it was reported by McInnes and Smith, that the natural hydroxyloxime **38** can be dehydrated with AcO_2 to provide the nitrile **39** in 69%.[168]
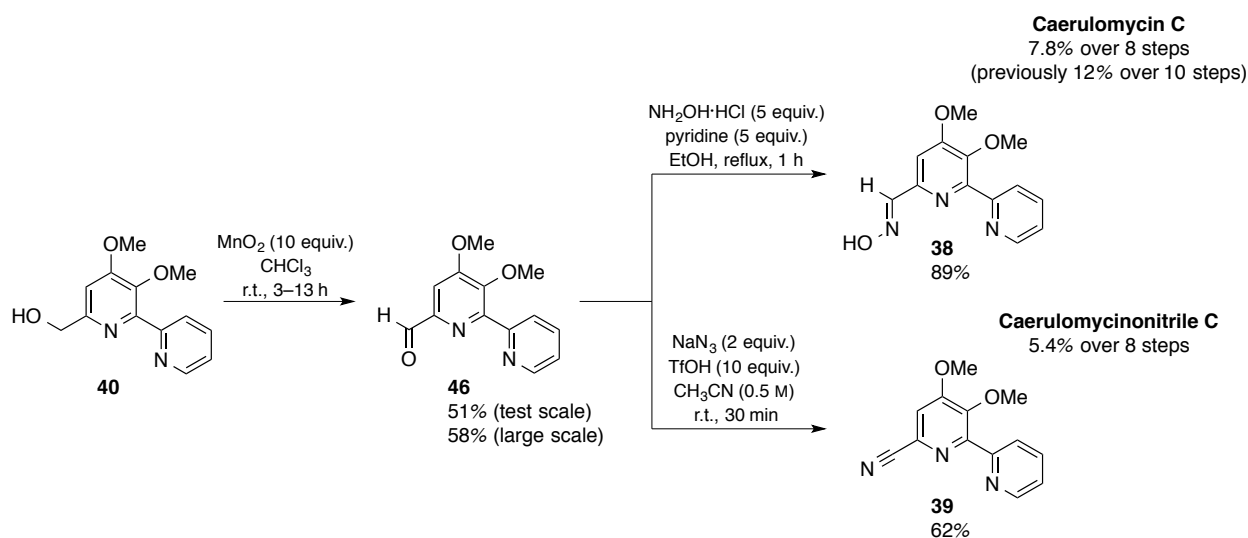
Scheme 57. Syntheses of Caerulomycin **C** (**38**) and Caerulomycinonitrile **C** (**39**).

2.4   Conclusion

In conclusion, we showed that 2,2′-bipyridine *N*-oxides **20** are suitable substrates for the palladium-catalyzed directed halogenations using *N*-halosuccinimides as halogenating reagent. After modification of the previously reported conditions, which have been used for related reactions, we were able to synthesize the C3-brominated (**22**) and -chlorinated (**21**) products in high yields. Moreover, we could show that the 3-halobipyridine *N*-oxides can be easily deoxygenated with PX_3 to the final 3-halobipyridines **25** and **34**, which were obtained in good yields, as well. The halogenated products **21** and **22** are ideal precursors for further transformations, such as lithiation/quenching with an electrophile, cross-coupling reactions or simple S_NAr. For instance, the directed halogenation of bipyridine *N*-oxides **20** as key step allows the synthesis of C3-substituted natural products. This was exemplified for the synthesis of C3-substituted Caerulomycins, of which Caerulomycinonitrile **C** (**39**) and Caerulomycin **G** (**40**) were synthesized for the first time. The nitrile was obtained in an overall yield of 5.8% over 8 steps and Caerulomycin **G** (**40**) in 15% over only 6 steps. In addition, Caerulomycin **C** (**38**) was obtained over 8 steps in 7.8% yield, which is lower than previously reported synthesis (12% over 10 steps), however, the route did not require any lithiation sequences as typical in other synthesis.

The synthesis of this particular class of functionalized bipyridines has been difficult until now mainly due to their strong chelating coordination ability of the two nitrogen atoms to transition metals, which inhibits any catalytic activity. The application of the *N*-protected derivatives, the 2,2′-bipyridine *N*-oxides **20**, as substrates for direct halogenation displays an advantage over the few currently existing procedures for the synthesis of C3-functionalized bipyridines. The *N*-oxide substrates can be efficiently prepared by previously developed methods, such as from pyridine *N*-oxides **27** and 2-bromopyridines **28** by palladium-catalyzed direct arylations or modified Negishi cross-coupling reactions. Moreover, the direct C3-halogenation procedure saves reaction steps and is compatible with diverse functional groups, making it attractive in late stage functionalizations of more complex molecules. Previous syntheses of 3-halo-2,2′-bipyridines suffer from low yields, limited substrates scope, requiring a multi-step synthesis of precursors and are specific to only one particular halogen, mostly fluorine.

In addition, we conducted initial mechanistic investigations with palladium(II) complexes, which are possibly intermediates in the catalytic cycle. The structure of one of these palladium complexes was confirmed by X-ray analysis. The complexes were tested under catalytic, as well as under stoichiometric conditions. The results are in accordance with a mechanism, which was previously

proposed for the palladium-catalyzed NCS chlorination of 2-arylpyridines and benzo[*h*]quinolines. This mechanism consists of (i) rate-determining cyclopalladation forming a dimeric succinate-bridged palladium(II) complex **E**, (ii) rate-determining nucleophile-assisted bimetallic oxidation to a dimeric palladium(III) intermediate, and (iii) bimetallic C-X bond-forming reductive elimination.

Future work regarding this topic will be focused on further transformations of the 3-halobipypyridines, and their *N*-oxides, respectively. On the basis of more detailed investigations for a better understanding of the mechanism and the origin for the formation of side products should help to understand the reasons for the few current limitations, but also advance this methodology to other attractive functionalizations, such as acetoxylations, methoxylations, alkenylations and arylations.

3 Mechanistic Investigations of Direct Arylation of Pyridine *N*-Oxides with Bromoarenes

3.1 Motivation

Transition metal-catalyzed direct functionalization reactions of relatively inert C-H bonds are attractive tools for the construction of multi-functionalized molecules, because they circumvent pre-functionalization of the substrates and save additional preparative steps, and avoid accumulation of byproducts. Large progress has been made in the direct arylation of heteroarenes, in particular with five-membered heteroarenes and their benzanullated derivatives.[172] However, six-membered nitrogen-containing heteroarenes, such as pyridines, (iso)quinolines and pyrimidines, have been challenging substrates for a long time due to their coordinating properties, which result in binding to the transition metal catalyst and its deactivation. Recent developments allow the direct functionalizations of azines giving commonly the C3 functionalized products.[119a, 173] Nevertheless, these reactions require usually harsh temperatures, high catalyst loadings and activating or directing functional groups.

Fagnou and co-workers overcame the difficulties by using inexpensive air- and bench-stable pyridine *N*-oxides **27** as substrates in the direct arylations with bromobenzenes **47** to give regio-selectively the C2 arylated pyridine *N*-oxides **31** in very good yields (scheme 58).[157a] This reaction is catalyzed by Pd(OAc)$_2$/P^{t}Bu$_3$·HBr in the presence of K$_2$CO$_3$ as base and was applied, as well further developed, to other direct functionalizations.[174] The conditions could be also refined towards the direct arylations of diazine *N*-oxides,[175] thiazole-, imidazole,[176] and other (hetero)aryl-annulated pyridine *N*-oxides.[176-177] Interestingly, changing the base to the stronger NaO^{t}Bu, 2-picoline *N*-oxides can be regioselectively arylated at the methyl group providing benzylated pyridine *N*-oxides.[178] Also the use of aryl pseudohalides as electrophilic coupling partner, such as aryl triflates,[179] tosylates and mesylates,[180] has been reported and gives high yields of the *α*-arylated azine *N*-oxides.
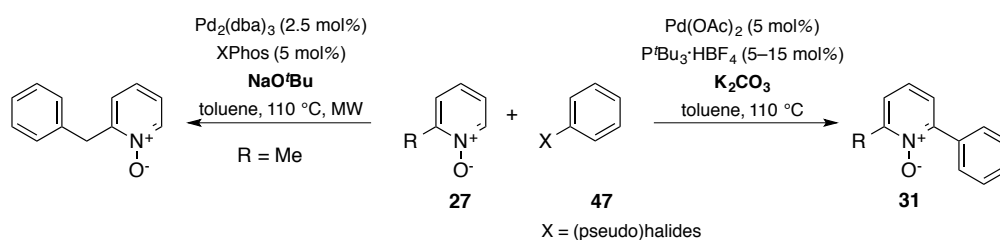
Scheme 58. Regioselective direct arylation of pyridine *N*-oxides.

Besides the high stability, pyridine *N*-oxides **27** are excellent surrogates for pyridines as substrates, because the *N*-oxides induces stronger polarization of the C-H bonds at the C2 and C4 positions, which become therefore more reactive towards transition metal-catalyzed C-H bond activation. In addition, the *N*-oxide oxygen serves as a protection group and prevents substrate inhibition by strong binding to the catalyst.[157a] Substrate or product inhibition is in particular a problem if the coupling partner is an unprotected heteroaryl halide, such as pyridines. Therefore the coupling between pyridine *N*-oxides **27** and bromopyridines **47** were not successful under the previously reported conditions. However, our group was able to modify the reaction conditions to extend the direct arylation of pyridine *N*-oxide **27** with halopyridines **28** to the synthesis of unsymmetrically substituted bi- and terpyridines (scheme 59).[117-118] Nevertheless, the yields of the bi- (**20**) and terpyridine *N*-oxides **29** are lower in comparison to the reactions using bromobenzenes under identical conditions. During our current research, we have synthesized a large number of bipyridine *N*-oxides **20** (*cf.* table 21, chapter 2.3.2) and found bipyridine **24** as a product of homocoupling of the electrophile **28** partially in significant yields. Because biaryl homocoupling products **17** have not been reported in the reactions with bromobenzenes **47**, a connection between the coordinating ability of the unprotected pyridyl nitrogen of **28** and the formation of homocoupling products might exist.
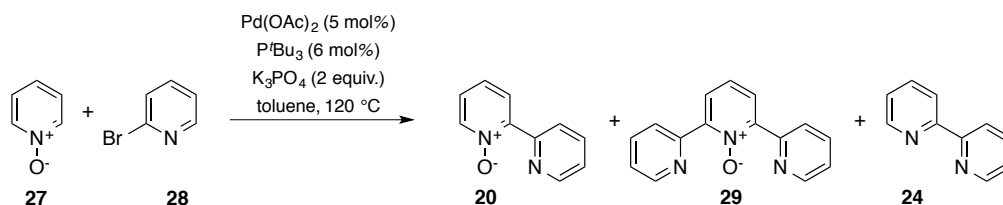
Scheme 59. Direct arylation of pyridine *N*-oxides with bromopyridines.

To improve the yields of bipyridine *N*-oxides **20**, we became interested in understanding the mechanism, particularly with respect to side and decomposition reactions. A previous mechanistic study on the arylations with bromobenzenes by Hartwig and co-workers proposed a cooperative catalytic cycle at two different palladium species.[92] However, this mechanism does not explain the difference in the yields since it is independent on the concentration and nature of the aryl halide. Possible explanations might be inhibition either by the starting material, products or bipyridine side product, or faster degradation of the catalyst. To elucidate this, we conducted mechanistic studies on the direct arylation of pyridine *N*-oxides with bromopyridines and bromoarenes for comparison.

3.2 Previous mechanistic investigations

Fagnou and co-workers undertook first mechanistic investigations by kinetic and computational studies, which were focused on early commonly proposed mechanisms,[157b] that consist of: (i) oxidative addition of the aryl halide **47** to a palladium(0) species, which forms an arylpalladium(II) intermediate and undergoes (ii) C-H bond activation with the pyridine *N*-oxide **27**. In step (iii) the product is released and the palladium(0) species regenerated by C-C bond-forming reductive elimination. Kinetic investigations of the reaction between the electron-deficient pyridine *N*-oxide **27o** and *meta*-bromoxylene (**47**) (scheme 60) revealed zeroth order dependency of bromoarene **47**, which excludes the oxidative addition as the rate-determining step. The dependency of pyridine *N*-oxide **27o** gave first order, which implies participation of **27o** in the rate-determining step. This is additionally supported by the observed primary kinetic isotopic effect (KIE) of $k_H/k_D = 3.3$. Half-order dependency was found for the palladium catalyst suggesting that the catalyst's resting state is a dimer, but the catalytically active species is a monomer. The zeroth order dependency, found for the phosphine ligand, implies that the ligand remains bound at the palladium(II) center during the C-H bond activation.
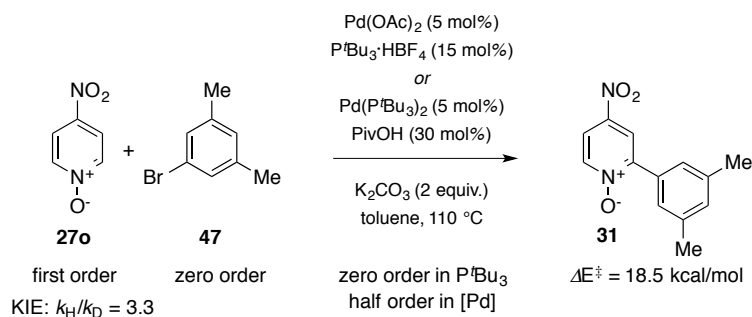
Scheme 60. Results from kinetic investigations of the direct arylation reaction by Fagnou and co-workers.

A computational study was performed of the reaction of pyridine *N*-oxide **27a** and arylpalladium(II) intermediate (PMe₃)Pd(Ph)X (**I-16**, X = bromide or carbonate) with respect to conceivable pathways (scheme 61).[157b] The calculations suggests that a CMD mechanism, which has been commonly proposed for C-H bond activations at palladium(II) centers in the presence of carboxylates,[119c, 181] is the energetically lowest lying pathway for the C-H bond cleaving event. Explicit calculations for the CMD mechanism revealed lowest lying transition states for both, the inner- and outer-sphere mechanism, with the inner-sphere mechanism being a slightly more favored. Comparison between the internal bases (carbonate *vs.* acetate) showed that the most favored transition state was obtained with acetate ($\Delta G^\ddagger = 26.9$ kcal/mol), and the second most favored one with carbonate as base ($\Delta G^\ddagger = 32.4$ kcal/mol). Calculations, regarding the regioselectivity for the C-H bond activation, support the CMD

mechanism, because the highest preference was found for the C2 position, which is consistent with the experimental findings.[157b, 182]
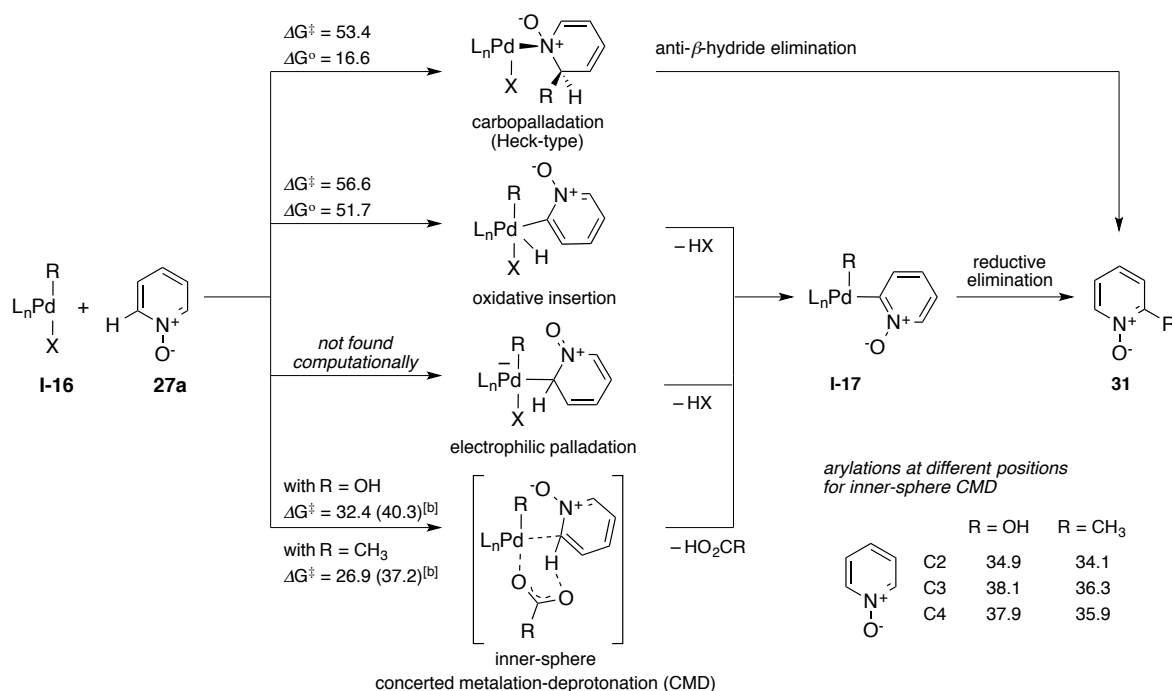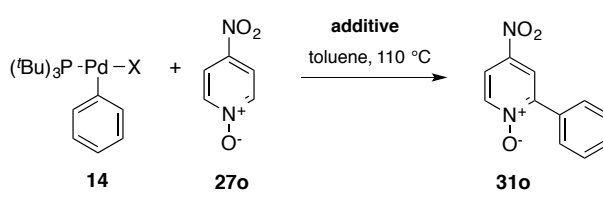
Scheme 61. Conceivable mechanism for C-H bond cleavages at palladium(II) metal centers and calculated Gibbs free energies ΔG given in kcal/mol with R = Ph and L_n = PMe$_3$.[157b] [b] Calculated as an outer-sphere CMD mechanism.

Fagnou and co-workers also investigated the electronic influences of C4 substituents at the pyridine *N*-oxides **27** by measuring relative reaction rates k_{rel} from competition experiments and absolute reaction rates k_{obs} and obtained a Hammett constant of ρ = +1.53 (R^2 = 0.97),[157b] which indicates that electron-withdrawing substituents accelerate the direct arylation reaction supporting the CMD pathway. Moreover, they also investigated the role of the base by stoichiometric reactions of arylpalladium(II) intermediates **14** with pyridine *N*-oxide **27o** (table 25) and found that carboxylates, such as acetate and pivalate, enhance the reactivity of **14** towards the *N*-oxide, while carbonate or bromide are less reactive. Nevertheless, kinetic measurements of the reaction catalyzed by Pd(P^{t}Bu$_3$)$_2$, the reaction was slower if only the base KOPiv or K$_2$CO$_3$ was used. However, addition of substoichiometric amounts of the PivOH (30 mol%) resulted in a 6-fold faster reaction and was comparable to the rate obtained under standard conditions using Pd(OAc)$_2$ (5 mol%), P^{t}Bu$_3$·HBF$_4$ (15 mol%), and K$_2$CO$_3$ (2 equiv.). These results were interpreted as catalyst saturation by excess carbonate or carboxylate at the intermediate **14** if only K$_2$CO$_3$ or KOPiv were used in the absence of an acid. The enhancing effect of substoichiometric amounts of an acid (PivOH or HBF$_4$ liberated from P^{t}Bu$_3$·HBF) was assumed to be due to partially de-coordination of the excess carboxylate or acetate from the metal center by protonation to create space for substrate coordination. Because the acetate complex **14** exhibited higher reactivity in the stoichiometric experiments (table 25) and was shown to be a competent

catalyst, it was concluded that the acetate ligand actually assist in the C-H bond cleaving step. Nevertheless, inconsistent with this proposal is the fact that in the stoichiometric reaction of acetate complex **14** with the *N*-oxide **27o** a lower yield for the coupling product **31** (48%) was obtained compared to the yield obtained from the catalytic reaction.

Table 25. Stoichiometric reactions of arylpalladium(II) intermediates **14** with pyridine *N*-oxide **27o** in the presence or absence of carboxylate additives.

entry	X	additive	yield **31o**
1	Br	none	0%
2	Br	K_2CO_3	5%
3	Br	KOPiv	29%
4	Br	K_2CO_3/KOPiv	31%
5	OAc	none	48%
6	OAc	K_2CO_3	49%

Based on the experimental and computational findings, Fagnou and co-workers proposed a more detailed mechanism for the direct arylation of pyridine *N*-oxides **27** with bromoarenes **47** (scheme 62).[157b] Upon formation of the arylpalladium(II) intermediate **14** by oxidative addition of bromoarene **47** to Pd(P^{t}Bu$_3$)$_2$, the bromide ligand is exchanged by acetate, which finally assists the rate-determining C-H bond cleavage of the pyridine *N*-oxide **27** in an inner-sphere CMD mechanism, which proceeds via a six-membered transition state. The formed acidic acid is deprotonated by the carbonate base to regenerate the required acetate. The resulting diarylpalladium(II) intermediate **I-17** undergoes rapid reductive elimination to form the coupled product **31** and regenerates the palladium(0) catalyst. However, the half-order dependency of the catalyst, which requires a dimeric resting state, remained unclear, because the complexes **14** exist exclusively as monomers.[59] Therefore, the authors suspected the involvement of pyridine *N*-oxide **27** in the formation of dimers with a palladium(II) species.
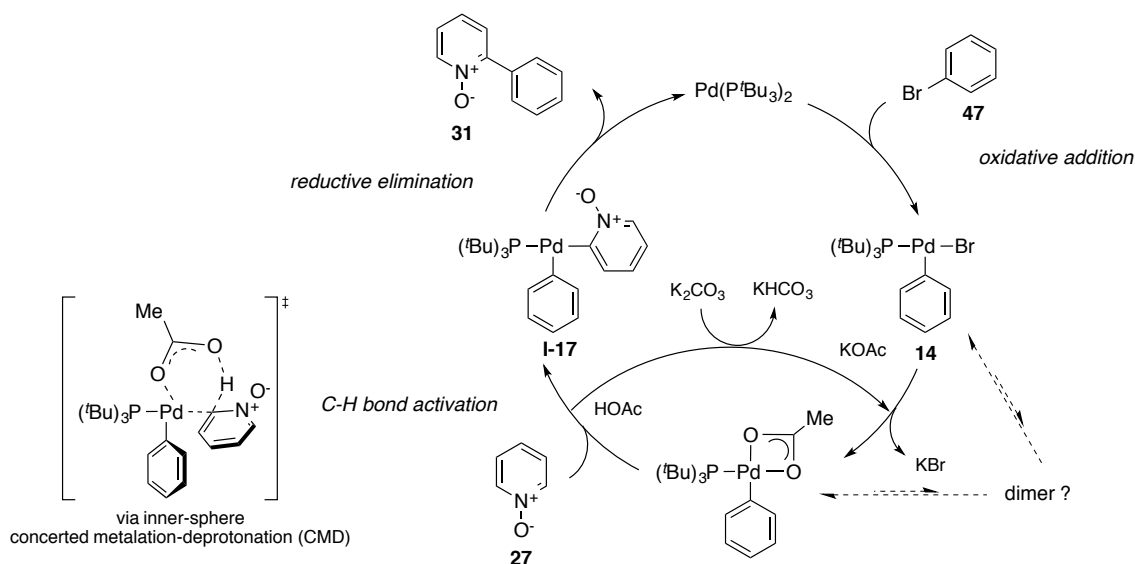
Scheme 62. Proposed mechanism by Fagnou and co-workers.[157b]

Therefore, Hartwig and co-workers re-investigated the reaction, and found in stoichiometric experiments, that the isolated fluoromethyl-substituted complex **14** decays (monitoring by ^{19}F NMR) in the presence of pyridine N-oxide **27a** with an induction period, during which the arylated product **31** was formed in less than 1% yield.[92] Instead, fluoromethylbenzene and the cyclometalated dimer **A** were formed during this period. This observation led to the conclusion that dimer **A** is involved in the reaction between **14** and N-oxide **27a**. Indeed, addition of dimer **A** to the reaction resulted in a much faster reaction of **14** without an induction period providing the coupling product **31** in 84% yield (scheme 63). The decay of **14** was determined to be zeroth order in **14**, first order in N-oxide **27**, and half order in dimer **A**, which suggest that the rate-determining C-H bond cleavage of **27a** occurs without the involvement of **14** and rather with the monomeric form of the dimer **A**. Computational calculations on the transition states for the C-H bond cleavage via CMD mechanism with the dimer **A** and the acetate complex **14** showed that the activation barrier is lower for the monomer of the dimer **A**.

To elucidate whether the acetate or the cyclometalated phosphine ligand is involved in the C-H bond cleavage, the reaction between **14** and **27a** was performed in the presence of dimer **B**, which has bromides instead of acetates as bridging ligands. The arylated product **31** was formed in 37% yield, which is lower than for the reaction without additives.[92] This observation suggests that the acetate ligand is involved in the C-H bond activation rather than the cyclometalated ligand. The participation of the cyclometalated phosphine ligand was further excluded by the reaction of deuterated N-oxide **27a**-d_5 in the presence of dimer **A**, showing no deuterium incorporation into the ligand.
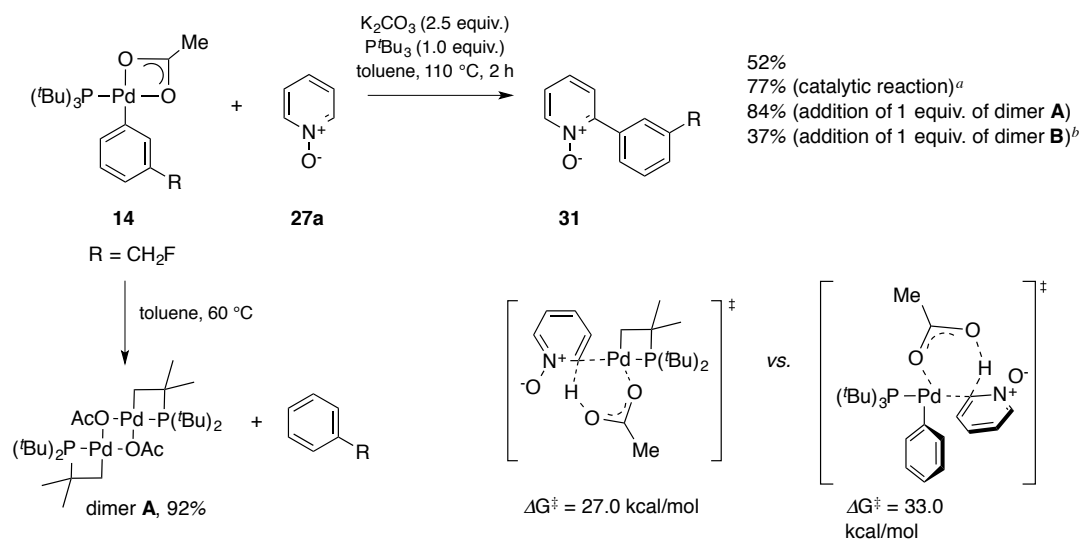
Scheme 63. Stoichiometric reaction of acetate intermediate **14** with pyridine N-oxide **27a**. [a]Yield from the catalytic reaction of 3-(fluoromethyl)phenyl bromide with pyridine N-oxide **27a** catalyzed by Pd(OAc)$_2$/P^{t}Bu$_3$ at 120 °C in toluene. [b]Dimer **B** is equivalent to dimer **A**, but with bromide instead of the acetate.

Based on these experimental findings, Hartwig and co-workers proposed a revised cooperative catalytic cycle for the palladium-catalyzed direct arylation of pyridine *N*-oxides **27** with bromoarenes **47**. Oxidative addition of **47** to palladium(0) gives **14**, which probably undergoes anion metathesis with a carboxylate or carbonate (scheme 64).[92] The second palladium catalyst, dimer **A**, can be either formed by decomposition of intermediate **14**, or by reaction of Pd(OAc)$_2$ and P^{t}Bu$_3$,[183] and dissociates to the catalytically active monomer **A**. A low barrier for the dissociation was computationally found by Gorelsky.[119c] The monomer **A** then mediates the C-H bond cleavage of the pyridine *N*-oxide **27** via a CMD transition state providing the pyridyl-*N*-oxide intermediate **I-18**. This species is proposed to transfer the pyridyl-*N*-oxide ligand to the arylpalladium(II) intermediate **14** by transmetalation forming the diarylpalladium(II) complex **I-17**, which reductively eliminates quickly the arylated product **31** and regenerates the palladium(0) catalyst.
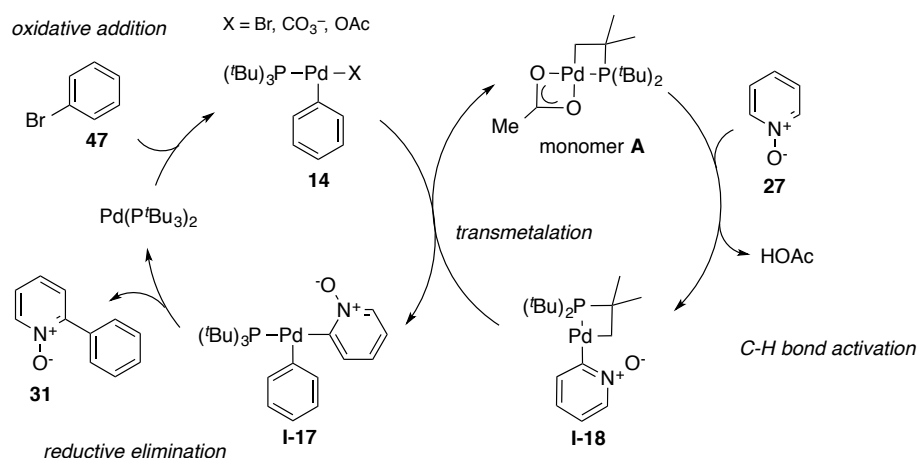
Scheme 64. Proposed mechanism by Hartwig and co-workers.[92]

In support of a possible transmetalation step between intermediates **I-18** and **14**, Hartwig and co-workers performed the transmetalation of the acetate complex **14** and phosphine-cyclometalated 2-benzothienylpalladium(II) complex as model for the intermediate **I-18** (scheme 65), because the corresponding pyridyl-*N*-oxide complex could not be prepared.[92] To verify that the model complex of benzothiophene is relevant for this study, the authors performed the same kinetic experiments as with pyridine *N*-oxide **27a** and found same behaviors, which suggests that the direct arylation of benzothiophene proceed via the same mechanism as for pyridine *N*-oxide **27**. The transmetalation reaction of **14** and 2-benzothienylpalladium(II) complex gave the coupled product in high yield of 74% within five minutes at room temperature, which clearly shows that the intermediate **I-18** is chemically and kinetically competent.
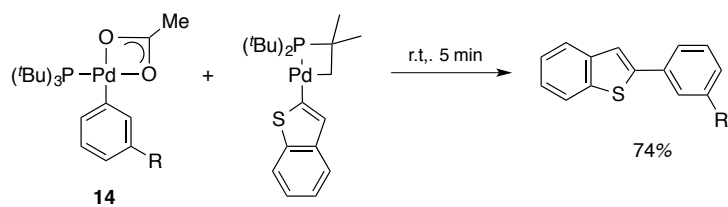
Scheme 65. Transmetalation between acetate complex **14** and 2-benzothienylpalladium(II) complex as surrogate for **I-18**.

3.3   Results and discussion

3.3.1   Kinetic measurements by ReactIR

We found that the direct arylations of pyridine *N*-oxides **27** with bromopyridines **28** provide lower yields compared to the reactions with bromobenzenes **47** under identical conditions.[117-118] The syntheses of diverse bipyridine *N*-oxides **27** gave, besides the desired coupled products **20**, also the homocoupling product of the bromopyridine **28**, the bipyridine **24**, particularly from reactions, which provide low yields for **20** (*cf*. table 21, chapter 2.3.2). Obviously, the consumption of the limiting substrate **28** by the undesired side reaction causes lower yields for the desired product **20**. Because, the formation of homocoupled products **24** have not been reported from related arylations with bromobenzenes **47**, we initially hypothesized there might exist a connection with the coordinating ability of the electrophile **28** or the product **20**. Conceivable coordination of the pyridyl nitrogen to the catalyst might lead to inhibition of the C-H bond activation, which in turn makes undesired side reactions, such as disproportionation of the putative pyridylpalladium(II) intermediate **48** into the homocoupling product **24**, predominant. This assumption is further supported by the observation, that the undesired side product **24** is formed in high yields typically in arylations with electron-rich pyridine *N*-oxides, which react slow in the C-H bond cleaving step.

Based on our previous preliminary investigations,[118] we were confident that the arylations with bromopyridines **28** proceed via the same mechanism as was previously proposed by Hartwig and co-workers for the reactions with bromobenzenes **47**.[184] Accordingly, the reaction rate for the arylation should be independent on the nature of the electrophile, and equal reaction rates would be expected for the coupling with bromobenzene **47** and bromopyridine **28**. However, if bromopyridine **28**, or the corresponding coupling product **20**, inhibited the C-H bond activation, slower reaction rates would be observed.

We performed kinetic *in situ* IR measurements for the direct arylation of differently C4-substituted pyridine *N*-oxides **27** with bromopyridine **28a** and bromobenzene **47a** for comparison. Because biaryl *N*-oxides exhibit characteristic bands in the IR spectra, we thought the *in situ* IR monitoring would also be suitable for our kinetic measurements. The first order reaction rates were calculated from the data obtained between 30 min and 60 min (constant temperatures were usually reached after 30 min). The calculated reaction rates are summarized in table 26. However, a positive slope was obtained for the decay of the substrates for many reactions, which, unfortunately, clearly show that the reactants rates of consumption cannot be reliably determined due to less characteristic IR spectra of the substrates. Nevertheless, most of the reaction rates for the product formations seem to be reliable and

show clear trends. In addition, the reaction mixtures from the kinetic measurements were directly subjected to column chromatography and all products were isolated and the yields determined.

Table 26. Reaction rates for the first arylation of pyridine *N*-oxides **27** measured by ReactIR.
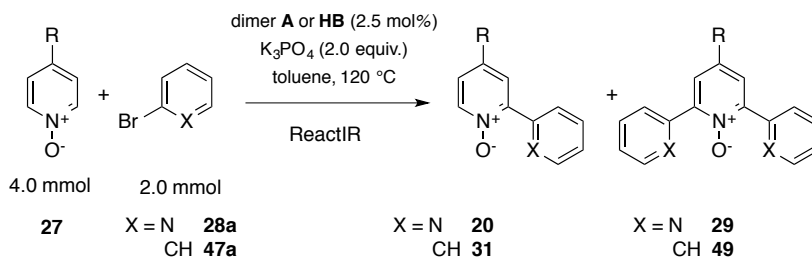
entry	R	*N*-oxide	X	arene	dimer	k_{obs} [mM/min] 27	k_{obs} [mM/min] 28 or 47	k_{obs} [mM/min] 20 or 31	yield[a] [mmol] 20 or 31	yield[a] [mmol] 29 or 49	recov.[b] [mmol]
1	H	**27a**	N	**28a**	**A**	−4.55	−11.5	**+2.81**	0.87 (44%)	–	1.90 (69%)
2	H	**27a**	N	**28a**	**HB**	−1.56	+4.80	−0.13	0.30 (15%)	0.01 (1%)	3.36 (91%)
3	H	**27a**	CH	**47a**	**A**	−1.26	−1.87	−0.00	1.42 (71%)	0.33 (33%)	2.14 (97%)
4	H	**27a**	CH	**47a**	**HB**	+0.24	−0.58	−0.23	n.i.	n.i.	n.i.
5	CO₂Et	**27l**	N	**28a**	**A**	−1.27	−3.50	**+3.34**	1.34 (67%)	0.15 (15%)	2.28 (99%)
6	CO₂Et	**27l**	N	**28a**	**HB**	−3.85	−5.30	**+3.18**	n.i.	n.i.	n.i.
7	CO₂Et	**27l**	CH	**47a**	**A**	−2.26	−3.73	**+2.75**	1.43 (71%)	0.19 (19%)	2.19 (98%)
8	CO₂Et	**27l**	CH	**47a**	**HB**	−1.23	−1.27	**+1.23**	n.i.	n.i.	n.i.
9	*t*Bu	**27z**	N	**28a**	**A**	+2.31	−2.02	**+1.04**	0.57 (29%)	0.05 (5%)	2.95 (89%)
10	*t*Bu	**27z**	CH	**47a**	**A**	+0.78	−1.44	**+0.52**	0.98 (49%)	0.13 (13%)	3.18 (107%)
11	CF₃	**27m**	N	**28a**	**A**	+0.78	−2.36	**+2.10**	1.75 (87%)	0.10 (10%)	3.92 (98%)
12	CF₃	**27m**	CH	**47a**	**A**	+0.25	−1.10	**+1.77**	1.88 (94%)	0.14 (14%)	n.i.

k_{obs} = reaction rates between 30–60 min. HB = Herrmann-Beller catalyst. Reaction rates in gray are not reliable. [a]Yields are based on aryl bromide **28a** or **47a**. [b]Recovery in % are based on the sum of reisolated **27** and all isolated products and side products arising from **27**. n.i. = not isolated.
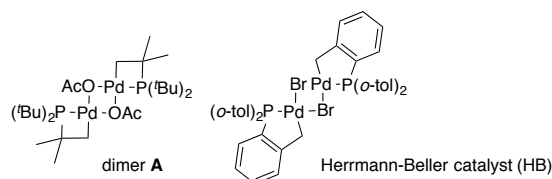
We performed our first measurements for the arylation reaction of the unsubstituted bipyridine *N*-oxide **27a** with bromopyridine **28a** and bromobenzene **47a** catalyzed by the dimer **A**, which is proposed to be the catalyst resting state and its monomer as the active species for the C-H bond

activation at the pyridine *N*-oxide **27**. To compare the results with other cyclometalated palladium(II) catalyst, we performed the same reactions using the analogous cyclometalated Herrmann-Beller catalyst (**HB**), however, these reactions did not provide reliable data, because the product formation rates were not in agreement with isolated yields. Nevertheless, the arylation with bromopyridine **28a**, catalyzed by the dimer **A**, gave apparently reliable product formation rates. The formation rate for the bipyridine *N*-oxide **20a** (table 26, entry 1) was determined with $k = 2.81$ mM/min.

In hope to obtain more reliable reaction rates, we used ester-substituted pyridine *N*-oxide **27l** (table 26, entries 5–8), which exhibit more distinct bands in the IR spectra. Indeed, the formation rates for the corresponding products **20l** and **31l** seemed to be reliable, because the measured final concentrations for the arylated products **20l** and **31l** matched well with the one approximated by the isolated yields. The formation rate for the bipyridine *N*-oxide **20l** was surprisingly faster ($k = 3.34$ mM/min, entry 5) than for the phenylated biaryl *N*-oxide **31l** ($k = 2.75$ mM/min, entry 7) in the reactions catalyzed by the dimer **A**, and is in contrast to what we expected if we presume inhibition of the catalyst. The same trend was also observed in the arylations catalyzed by the Herrmann-Beller catalyst. In addition, comparison of the rates obtained with the dimer **A** reveals that the Herrmann-Beller catalyst reacts only slightly slower with bromopyridine **28a** as electrophile ($k = 3.18$ mM/min, entry 6), but much slower with bromobenzene **48a** ($k = 1.23$ mM/min, entry 8).

To test whether this unexpected trend is also observed for other pyridine *N*-oxides, we performed also kinetic measurements with the electron-rich *tert*-butyl-substituted pyridine *N*-oxide **27z** and with the more electron-poor trifluoromethyl-substituted pyridine *N*-oxide **27m** (table 26, entries 9–12). Indeed, in both cases we obtained faster reaction rates for the reactions with bromopyridine **28a** than with bromobenzene **48a**. The difference in the reaction rates is slightly more pronounced with electron-rich pyridine *N*-oxide **27z** (**28a**: $k = 1.04$ mM/min, **47a**: $k = 0.52$ mM/min) than with the electron-poor pyridine *N*-oxide **27m** (**28a**: $k = 2.10$ mM/min, **47a**: $k = 1.77$ mM/min). These results indicate that the substrate does not inhibit the C-H bond activation. However, comparison of the rates with the isolated yield (table 26, figure 26) reveals that the yields for the coupling products do not follow the same trends. Although, the reaction rates are faster for the arylations with bromopyridine **28a** compared to bromobenzene **47a**, the yields of the bipyridine *N*-oxides **20** are lower than of the phenylpyridine *N*-oxides **31**. This trend was more pronounced for arylations of the more electron-rich pyridine *N*-oxides **20a** and **20z**. An explanation for this observation might be product inhibition rather than substrate inhibition, because during the course of the reaction the concentration of the product increases, which leads to inhibition of the catalyst at later stages, which are not included for the determination of the reaction rates at early stages.
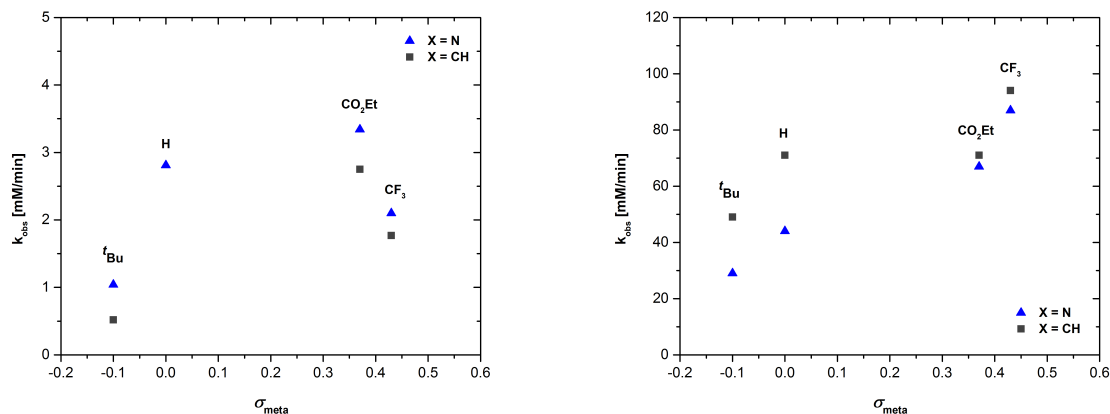
Figure 26. Comparison of reaction rates (left plot) with isolated yields (right plot) for product formations of **20** or **31** from direct arylations measured by ReactIR.

To elucidate potential product inhibition by **20**, we performed kinetic measurements for the second arylation with biaryl *N*-oxides **20l** and **31l**. If there was catalyst inhibition, we would expect that the arylations of bipyridine *N*-oxide **20l** with bromobenzene **47a** is slower than for phenylpyridine *N*-oxide **31l**. Indeed, the measured reaction rate for the bipyridine *N*-oxide **20l** was $k = 0.41$ mM/min (table 27, entry 2), which is slower than for the phenylated analogue **31l** with $k = 0.64$ mM/min (entry 4), however the difference is small. The opposite trend was observed for the corresponding arylations with bromopyridine **28a**. The reaction rate for the arylation of the bipyridine *N*-oxide **20l** was $k = 0.90$ mM/min (entry 1), whereas with phenylpyridine *N*-oxide **31l** the rate was $k = 0.54$ mM/min (entry 3). Probably, the rate-enhancing effect, which was observed for the first arylations of pyridine *N*-oxides **27** with bromopyridine **28a** (*cf.* table 26), overwrites the inhibiting effect of the pyridyl group of the bipyridine *N*-oxide **20**, which turned out to be small. The faster rate for the arylation of **20l** can be simply explained by the additionally electron-withdrawing character of the pyridyl group (2-pyridyl: $\sigma_{meta} = 0.33$, phenyl: $\sigma_{meta} = 0.06$),[9] which polarizes the C-H bond and accelerates the C-H bond cleaving step.

The results from the kinetic measurements led to the conclusion that bromopyridine **28a** does not inhibit the catalyst, but rather unexpectedly enhanced the rate. It is conceivable that the bromopyridine **28a** converts the dimeric catalyst resting state (dimer **A**) faster into its catalytically active monomer, hence accelerating the C-H bond activation, which in turn leads to an overall observed faster reaction rate for the entire reaction. However, during the course of the reaction the concentration of the coupled product **20** increases, which might inhibit the catalyst. Nevertheless, this inhibiting effect was found to be small and does not explain why the yields are lower. Therefore, we assumed that intermediates, which involve the bromopyridine **28**, are inherently less stable than the analogues with bromobenzene **47** and would lead to earlier catalyst decomposition or undergo undesired side reactions.

142

Table 27. Reaction rates for the second arylation of biaryl *N*-oxides **20l** and **31l** measured by ReactIR.
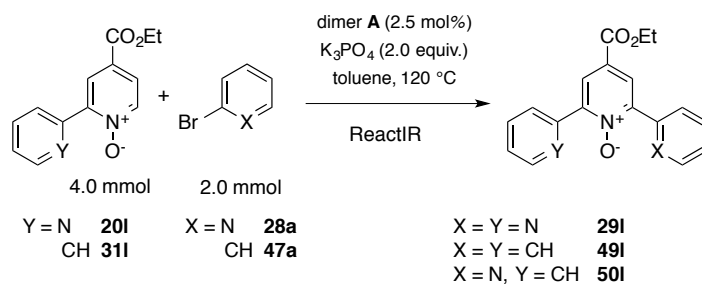
entry	Y	*N*-oxide	X	arene	k_{obs} [mM/min] 20 or 31	k_{obs} [mM/min] 28 or 47	k_{obs} [mM/min] 29, 49 or 50	yield[a] [mmol] 29, 49 or 50	recov.[b] [mmol]
1	N	**20l**	N	**28a**	–0.50	–0.94	**+0.90**	1.84 (92%)	2.21 (96%)
2	N	**20l**	CH	**47a**	–1.04	–1.00	**+0.41**	1.28 (64%)	2.48 (98%)
3	CH	**31l**	N	**28a**	–0.44	–2.68	**+0.54**	1.68 (84%)	2.08 (97%)
4	CH	**31l**	CH	**47a**	–0.85	–0.93	**+0.64**	0.92 (46%)	3.03 (99%)

[a]Yields are based on aryl bromide **28a** or **47a**. [b]Recovery in % are based on the sum of reisolated **20l** or **31l** and all isolated products and side products arising from **20l** or **31l**.

To obtain a hint of possible side reactions, we isolated and identified side products, which are biaryls **24** and **17**, dioxides **51–53** and reduced coupling products **29**, **33–34** (figure 27), and pyridine *N*-oxide starting material **27** from the pervious reaction mixtures, which had been monitored by *in situ* IR. In nearly all cases, the *N*-oxide starting materials **27** could be almost quantitatively accounted (*cf.* table 26), which shows that no other undetected compounds except the isolated products **20**, **29**, **31**, **49** and dioxides **51–53** were formed in significant amounts from **27**. These side products were typically obtained in minor yields, which do not exceed the catalyst loading. However, also larger amounts were obtained from other reactions, which indicate that the homocoupling might be a catalyzed process.[185] The *N,N'*-dioxides **51–53** might result from decomposition of the pyridyl *N*-oxide intermediate **I-18** (*cf.* scheme 64), which is an oxidative process. To obtain larger amounts than the catalyst loading, there must exist an reductive process, which might be either the reduction of the *N*-oxides **27**, **20**, **29** to the corresponding pyridines and bipyridines, or the homocoupling of the bromoarenes **28a** or **47a**.
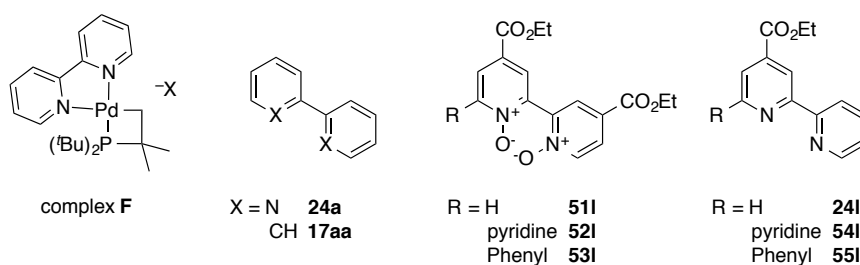
Figure 27. Isolated side products from direct arylations monitored by ReactIR.

Only in case of the reactions with the electron-rich pyridine *N*-oxide **27z** and the unsubstituted *N*-oxide **27a** with bromopyridine **28a** 89% and 69% of the *N*-oxide starting materials were recovered

(table 26). The corresponding *N*,*N*′-dioxide homocoupling products **51a** or **51z** could not be isolated by column chromatography, which might be the results of the very polar nature of the *N*,*N*′-dioxides since already the *N*,*N*′-dioxides with the electron-withdrawing substituents were already very polar and eluted only with very polar solvent mixtures. The more electron-rich *N*,*N*′-dioxides are even more polar and therefore, even bind stronger to the silica gel surface, which makes it difficult to isolate them. Nevertheless, later GC-FID measurements of the deoxygenated (with PCl$_3$) crude reaction mixtures by Emma Svensson revealed that in particular in arylations of electron-rich pyridine *N*-oxides **27**, relatively large amounts of corresponding *N*,*N*′-dioxides are formed exceeding the catalyst loading.[185] With hindsight, this might explain the relatively low mass recovery of the starting *N*-oxides from the reactions with pyridine *N*-oxides **27a** and **27z**.

Besides the homocoupling product of the pyridine *N*-oxides **27**, also the homocoupling products of bromopyridine **28a** and bromobenzene **47a** could be isolated. While the biphenyl **17aa** was found in lower amounts, bipyridine **24a** was isolated in more significant amounts. For instance the arylation of **27z** provided 23% of homocoupling product **24a**, while the arylation with bromobenzene **47a** gave 13% of the corresponding biphenyl **17aa**. Moreover, the biaryl products are generally formed in larger amounts in arylations with electron-rich pyridine *N*-oxides. Interestingly, from the reaction mixture of the arylation reaction of unsubstituted pyridine *N*-oxide **27a** with bromopyridine **28a**, we could isolate a cyclometalated palladium species by column chromatography, which was identified as complex **F** (figure 27) the bipyridine-coordinated monomeric form of the proposed catalyst resting state. The fact that the complex **F** could be isolated by column chromatography indicates high stability, which in turn might point to lower reactivity for the C-H bond activation of the pyridine *N*-oxide substrate, since a free coordination site at the palladium(II) is required. This would mean, that bipyridine side product **24a** inhibits the catalysis. Kinetic measurements by Emma Svensson confirm that added bipyridine result in slower reaction rates.[185]

Unfortunately, we were not able to grow single crystals of complex **F**, however we could isolate and crystalize the cationic complex of the corresponding tetrafluoroborate salt by slow diffusion of Et$_2$O into a DCM solution. The cationic complex of **F** exhibits basically the same structural properties as it was reported previously for the solid state structure of analogous complex with hexafluorophosphate as counter ion.[186] The structure shows a slightly distorted square-planar complex with a strained four-membered metalacycle formed by the cyclometalated phosphine ligand (figure 28). The geometry of the cyclometalated part of the complex resembles similar complexes, of which crystal structures have been reported.[183c, 187]
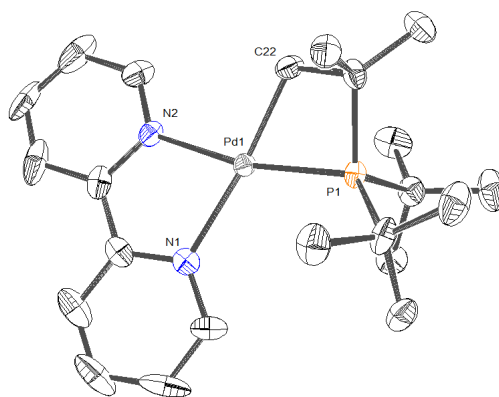
Figure 28. ORTEP 3 diagram of bipyridine-ligated complex **F** (X = BF$_4$). Thermal ellipsoids are drawn at 30% probability level. Hydrogen atoms and tetrafluoroborate counter ion were omitted for clarity. Selected bond distances (Å) and angles (°): Pd1–N1 2.181, Pd1–N2 2.091, Pd1–P1 2.227, Pd1-C22 2.054, N1–Pd1–N2 76.91, P1–Pd–C22 69.30, N1–Pd1–C22 173.32, N2–Pd1–P1 167.42.

3.3.2   Competition experiments

The reaction rates from the *in situ* IR monitoring the Hammett do not correlate linearly with the σ-parameters. The most electron-poor pyridine N-oxide **27m** provided an unexpected slow reaction rate for both arylations with bromopyridine **28a** and bromobenzene **47a** (*cf*. table 26). This observation is in contrast to the results reported by Fagnou and co-workers, who reported a good linear Hammett correlation from observed reaction rates of the arylations of differently C4-substituted pyridine N-oxides **27** and bromo-*m*-xylene ($\rho = 1.53$, $R^2 = 0.97$).[157b] Because the kinetic measurements by *in situ* IR turned out to be less reliable in some cases, we were wondering whether this discrepancy results from inaccurate data. To probe this, we additionally performed competition experiments with the differently C4-substituted pyridine N-oxides **27**. Since the product-determining step and the rate-determining step are the same for the proposed mechanism, the relative rates for the entire reaction should reflect the relative rates for the C-H bond cleaving step.

Initially, we performed the competition experiment between ester-substituted and unsubstituted pyridine N-oxides **27l** and **27a** in the direct arylation with the bromoarenes **28a** and **47a** under the same reaction conditions applied for the *in situ* IR monitoring. However, only arylation products with the electron-poor pyridine N-oxide **27l** could be isolated in both cases, with bromopyridine **28a** and with bromobenzene **47a** (scheme 66). In case of the reaction with bromopyridine **28a** the starting pyridine N-oxides **27a** and **27m** could be quantitatively recovered, besides 12% of the side product **24a**. However, in case of the reaction with bromobenzene **47a**, pyridine N-oxide **27a** could be only recovered in 77% besides 5% of the homocoupling product **17aa**. This indicates, that some of the

pyridine *N*-oxide was converted either into the *N,N'*-dioxide **51a**, which might have been lost on the silica gel, or converted into the deoxygenated product, which is just pyridine and volatile enough to be lost during evaporation of the solvent.
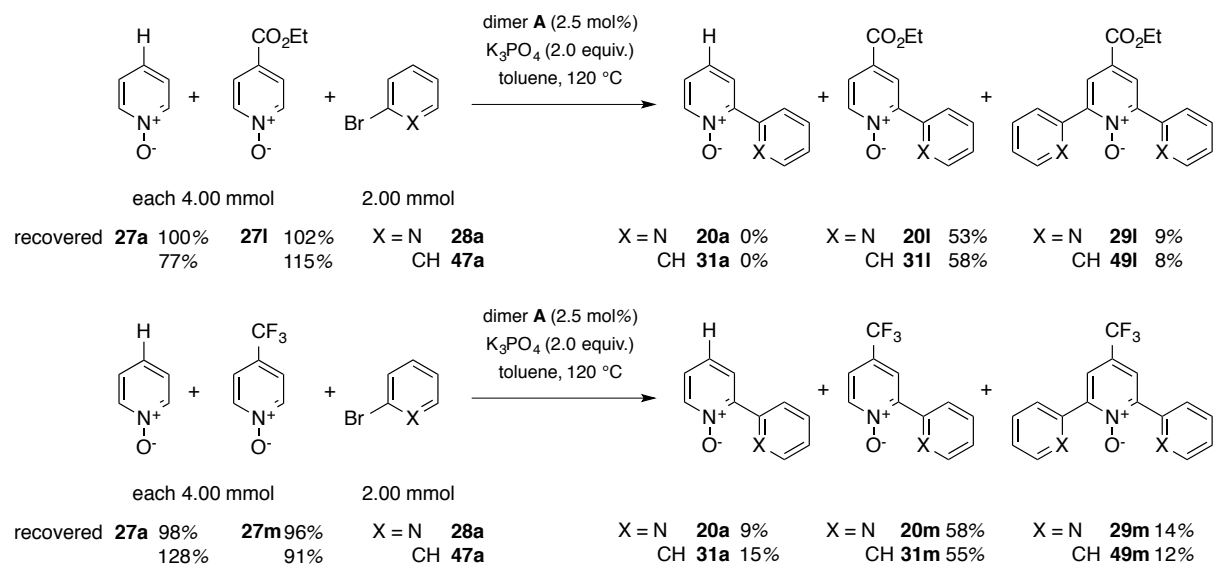
Scheme 66. Isolated yields form competition experiments between differently substituted pyridine *N*-oxides **21**

The results from these initial competition experiments are in stark contrast to what one would expect from the reaction rates measured by *in situ* IR. Accordingly, a product ratio for the biaryl *N*-oxides of approximately 1:1.2 of **20a**:**20l** would be expected in the arylation reaction with bromopyridine **28a**. To exclude that this experiment was a special case, we performed the same competition experiment with the trifluoromethyl-substituted pyridine *N*-oxide **27m** instead of the ester-substituted **27l**, however, we obtained similar results as before. The more electron-poor biaryl *N*-oxides **20m** and **31m** were obtained in yields of 55–58%, besides the corresponding teraryl *N*-oxides **29m** and **49m**, which were isolated in 12–14% yields (scheme 66). In this case, arylated products from the reactions with the unsubstituted pyridine *N*-oxide **27a** could be also obtained. The bipyridine *N*-oxides **20a** was isolated in 9% and the phenylpyridine *N*-oxide **31a** in 15%, besides *N,N'*-dioxide **51m** (4%), reduced terpyridine **54m** (2%) from the reaction with bromopyridine **28a**. The mass recoveries based on **27** were up to 91%.

The relative reaction rates (**28a** 1:6.4 and **47a** 1:3.7) calculated from the competition experiments between unsubstituted (**27a**) and trifluoromethyl-substituted (**20m**) *N*-oxides are also in contrast to results obtained by the *in situ* IR monitoring (*cf*. table 26), because even higher yields for the unsubstituted product **20a** than for the trifluoromethyl-substituted product **20m** would be expected. During isolation of the products, it turned out that the separation of the products is complicated, because the electron-rich *N*-oxides elute slowly from the silica gel, which caused overlapping of

product fractions. To circumvent this problem, we additionally performed the competition experiments in a smaller scale and determined the yield without isolation by ^{1}H NMR using TMB as internal standard. The competition experiment between **27m** and **27a** with bromopyridine **28a** gave a product ratio of 1:3.9 in favor of the electron-poor *N*-oxide **20m** (table 28, entry 5), which corresponds to a corrected relative reaction rate of 4.71 (mathematical derivation for the calculation of corrected product ratios, see Mathematical Section 7.1). This result is still in contrast to the *in situ* IR measurements, however, it is in agreement with the previous data, obtained by Fagnou and co-workers (1:4.55), although a smaller ratio was obtained from the corresponding competition experiment with bromobenzene **47a** (1:2.10, entry 11). However, Fagnou and co-workers used conditions (K_2CO_3, $Pd(OAc)_2$/P^{t}Bu$_3$·HBF$_4$), which are slightly different from ours and may also have an influence on the relative reaction rates.

Table 28. Relative reaction rates calculated from ^{1}H NMR spectra of competition experiments between pyridine *N*-oxides **27**.

entry	R^1	*N*-oxide	R^2	*N*-oxide	X	arene	R^1:R^2	k_{rel} (corrected)
1	^{t}Bu	**27z**	H	**27a**	N	**28a**	0.88	0.83
2	^{t}Bu	**27z**	CO$_2$Et	**27l**	N	**28a**	5.88	7.95
3	^{t}Bu	**27z**	CF$_3$	**27m**	N	**28a**	3.33	3.98
4	H	**27a**	CO$_2$Et	**27l**	N	**28a**	1.86	2.04
5	H	**27a**	CF$_3$	**27m**	N	**28a**	3.85	4.71
6	CO$_2$Et	**27l**	CF$_3$	**27m**	N	**28a**	1.80	1.97
7	^{t}Bu	**27z**	H	**27a**	CH	**47a**	0.82	0.84
8	^{t}Bu	**27z**	CO$_2$Et	**27l**	CH	**47a**	0.76	0.73
9	^{t}Bu	**27z**	CF$_3$	**27m**	CH	**47a**	>10	12.8
10	H	**27a**	CO$_2$Et	**27l**	CH	**47a**	1.02	1.05
11	H	**27a**	CF$_3$	**27m**	CH	**47a**	1.89	2.10
12	CO$_2$Et	**27l**	CF$_3$	**27m**	CH	**47a**	1.71	1.86

Because the initial competition experiments apparently provided more reliable results than the *in situ* IR measurements, we also performed competition experiments for other possible combinations with the four differently substituted pyridine *N*-oxides **27** in reactions with bromopyridine **28a** and **47a** (table 28). However, again no linear correlation between the logarithm of the relative reaction rates and the Hammett parameters σ was observed (figure 29). The data obtained from the *in situ* IR measurements and the competition experiments suggest that the direct arylation of pyridine *N*-oxides **27** with both types of aryl halides, bromopyridine **28a** and bromobenzene **47a**, is faster the more

electron-poor the pyridine *N*-oxide **27** is, which is consistent with rate-determining C-H bond activation via a CMD mechanism. However, for strong electron-poor the *N*-oxides **27l** and **27m** the reactivity trend changes to the opposite. Such behavior has been often interpreted as a change of the rate-determining step.[12] Considering the previous mechanistic proposal by Hartwig and co-workers,[92] the rate-determining step might then be transfer of the pyridyl *N*-oxide ligand from intermediate **I-18** to the arylpalladium(II) complex **14**. As discussed in context of the transmetalation with arylzinc reagents in the previous chapter 1, but also observed in other transmetalations, the transfer of an organic group is faster for nucleophiles with electron-donating substituents. Since it was proposed that the intermediate **I-18** acts as the nucleophilic transmetalating reagent and transfers the pyridyl *N*-oxide to the intermediate complex **14**, the transmetalation in the direct arylation should be faster for intermediates **I-18** with pyridyl *N*-oxides ligands, which bear electron-donating groups.
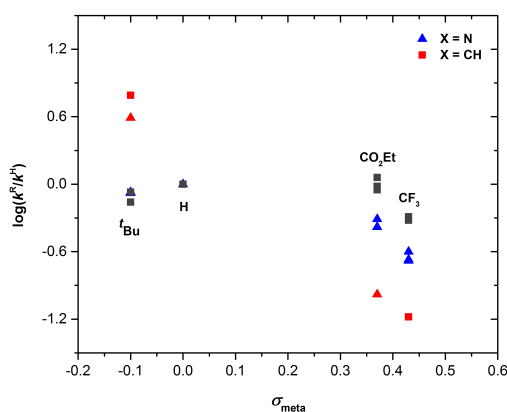

Figure 29. Hammett correlation obtained from competition experiments with differently substituted pyridine *N*-oxides **27**. Corresponding data from table 28. Red data points are apparent outliers.

3.3.3 Electronic influence of aryl halides

Analogous competition experiments with differently substituted bromoarenes would provide only relative reaction rates of the oxidative addition step. To probe the electronic influences of the electrophilic coupling partner on the transmetalation step, we performed individual arylation reactions and determined the yields of the coupled products after a short reaction time to approximate absolute reaction rates from the yields of the coupling products. For comparison, and to identify the coupling products, we additionally conducted the same reactions until full conversion of the aryl halide, and isolated the products by column chromatography.

Table 29. Yields of arylated products from reactions with substituted aryl bromides **28** or **47** after 50 min.

entry	R	X		^{1}H NMR^a 20l or 31l [%]	isolated^b 20l or 31l [%]	isolated^b 29l or 49l [%]	recovered^c [%]
1	OMe	N	**28b**	27	60	12	81
2	Me	N	**28c**	44	54	9	85
3	H	N	**28a**	55	67	15	99
4	CF$_3$	N	**28d**	38	28	0	81
5	NO$_2$	N	**28e**	0	0	0	98
6	OMe	CH	**47b**	32	68	3	87
7	^{t}Bu	CH	**47c**	40	73	3	104
8	H	CH	**47a**	38	71	19	98
9	F	CH	**47d**	35	63	3	86
10	CO$_2$Me	CH	**47e**	36	56	1	84
11	CF$_3$	CH	**47f**	36	53	5	77
12	CN	CH	**47g**	37	53	5	89

^{a} ^{1}H NMR yields. ^{b}Isolated yields from independent syntheses after 16–24 h reaction time. ^{c}Recovery in % are based on the sum of reisolated **27l** and all isolated products and side products arising from **27l**.

With the differently substituted bromobenzenes **47**, yields of 32–40% were obtained after 50 minutes (table 29, entries 6–12), which results in a Hammett constant of zero in the corresponding Hammett correlation (figure 30). This results is expected as the aryl ligand is not involved in the rate-determining C-H bond activation. The Hammett plot obtained from the competition experiments with the differently substituted pyridine *N*-oxides **27** (*cf*. figure 29) suggests that in case of bromobenzenes **47** a change of the rate-determining occurs for substituents with more electron-withdrawing than the ester group. However, for the arylations with bromopyridines **28**, this change of the rate-determining step apparently already occurs with the ester substituent. Indeed, the Hammett constant with respect to the differently substituted bromopyridines **28** show stronger electronic dependencies and provided yields of the corresponding bipyridine *N*-oxides of 27–55% (table 29, entries 1–5). However, the reactions under full conversions with bromopyridines with electron-withdrawing substituents (**28d** and **28e**) provided generally low yields, which might rather be the result of decomposition of the electrophiles **28** than due to a slow arylation reactions. Therefore, the data points corresponding to Hammett parameters $\sigma > 0$ might be not suitable to elucidate electronic trends of the arylation reaction.
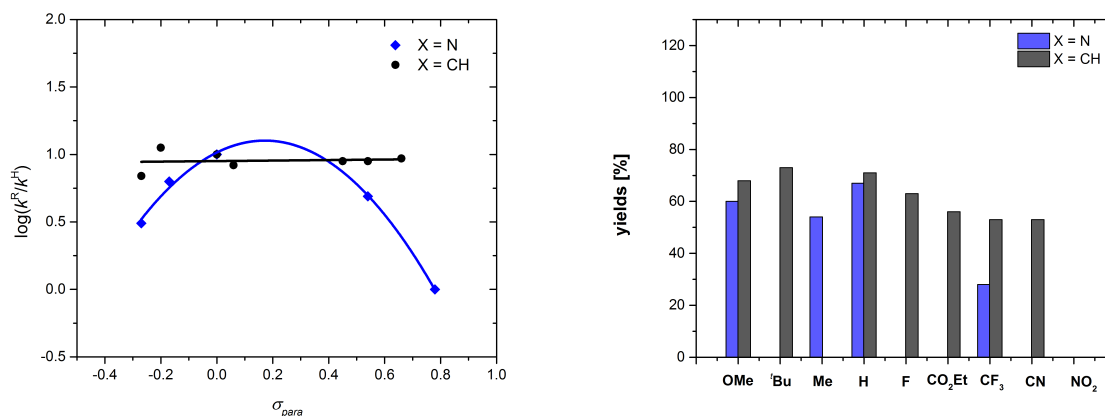
Figure 30. Hammett correlation obtained from termination experiments with differently substituted aryl bromides **28** and **47** (left), and isolated yields of corresponding products **20** and **31** from independent syntheses (right).

Nevertheless, the data points obtained from reactions with electron-donating substituents at the bromopyridine resulted in a positive Hammett constant, which suggests that electron-withdrawing substituents accelerate the overall reaction. This trend would be in accordance with an accelerated transmetalation step as observed from our previous study of the transmetalation of T-shaped P^tBu_3-coordinated arylpalladium(II) complexes **14** with phenylzinc chloride **16a** (*cf.* previous chapter 1).

3.3.4   Monitoring and identification of catalyst species by ^{31}P NMR spectroscopy

The kinetic experiments and the occurrence of homocoupled product **24** suggest, that the low yields obtained for the bipyridine *N*-oxides **27** by the palladium-catalyzed direct arylations are the results of inherent instability of pyridylpalladium(II) intermediate, which is more decisive if the C-H bond activation at **27** is slow. To obtain information about the decomposition pathways, as well as to further elucidate whether both arylations proceed via the same mechanism, we monitored the catalyst and its decomposition products by ^{31}P NMR spectroscopy. We performed the direct arylations of the electron-poor **27l**, and unsubstituted pyridine *N*-oxide **27a** with bromopyridine **28a** and bromobenzene **47a** in sealed NMR tubes using deuterated benzene as solvent. Several reactions for each *N*-oxide **27** were set-up and run at different reaction times by immediately cooling the mixtures in an ice bath and ^{31}P NMR were immediately recorded. The phosphorous shifts were referenced to P(OMe)$_3$ as external capillary standard and the amounts of phosphorous-containing species calculated from integration as percentage of the sum of the total areas.

In the reaction of the electron-poor ester-substituted pyridine *N*-oxide **27l** with bromopyridine **28a**, a dominant species at $\delta = -9.20$ ppm, which corresponds to the bromide-bridged dimer **B**, was observed

as long as bromopyridine **28a** had not been fully consumed (figure 31). This observation is consistent with the previous conclusion that a dimeric species is the catalyst resting state.[157b] However, the phosphor monitoring experiment suggests that the dimer **B** is the catalyst resting state rather than the previously proposed acetate dimer **A**.[92] We also detected the bromide-bridged dimer **B** in the analogues reactions of *N*-oxides **27a** and **27l** with bromobenzene **47a** in an even larger amount and over a longer period than in the reactions with bromopyridine **28a**. These results support that arylations with bromobenzenes **47** and bromopyridines **28** proceed via the same mechanism and the drastic drop in catalytic activity after a few turn overs in the reactions with bromopyridine **28** due to early catalyst decomposition.
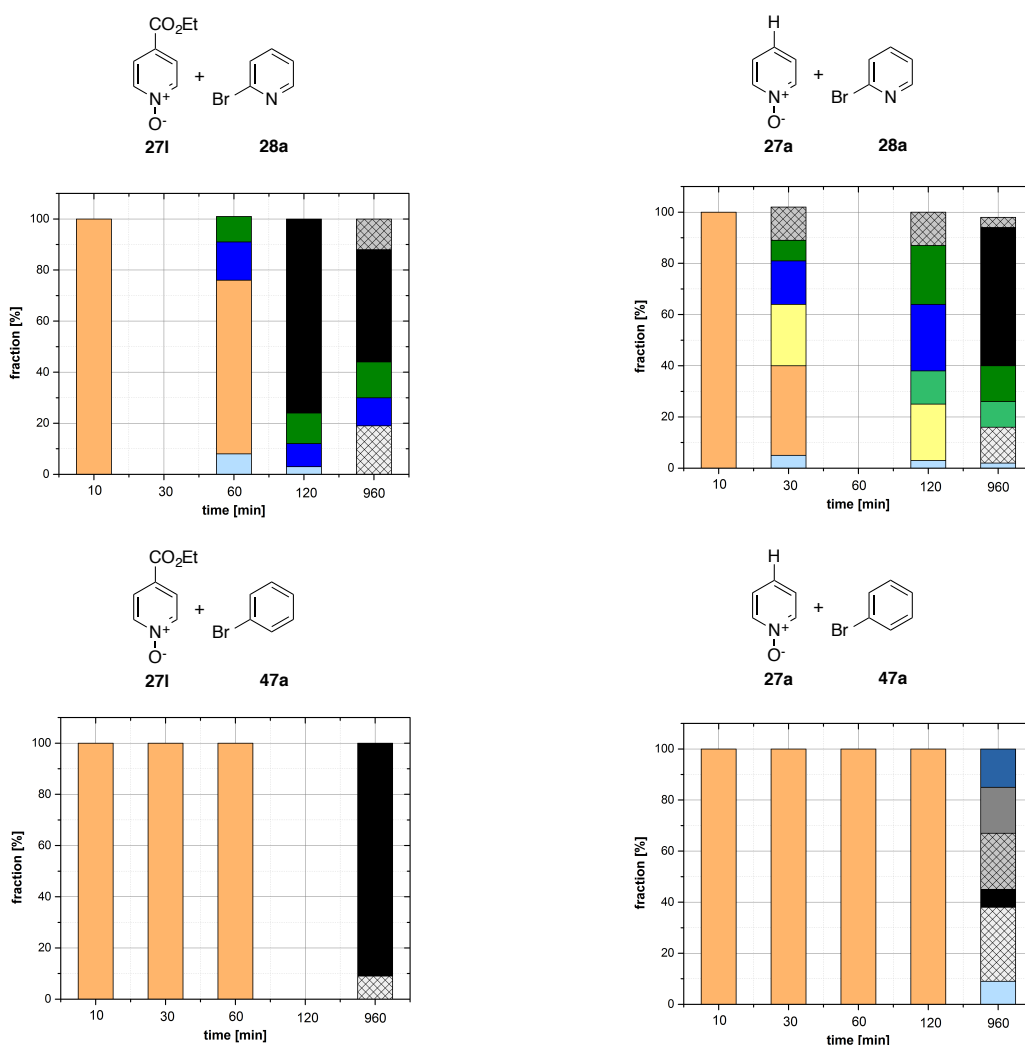

Figure 31. Monitoring of phosphorous species by ^{31}P NMR.

^{31}P NMR chemical shifts of known species:

Pd(P^{r}Bu$_3$)$_2$ +85.0 ppm, O=P^{r}Bu$_3$ +66.0 ppm, P^{r}Bu$_3$ +62.5 ppm, dimer **A** –8.3 ppm, dimer **B** -9.3 ppm

The main catalyst decomposition product in the arylations with ester-substituted pyridine *N*-oxide **27l** was Pd(P^{t}Bu$_3$)$_2$ (+85.0 ppm) and was formed after the aryl halide has been consumed (figure 31). A conceivable pathway would be the disproportionation of an arylpalladium(II) intermediate, presumably the pyridyl *N*-oxide intermediate **I-18**, which would form the bipyridine *N,N'*-dioxide **51l** upon disproportionation. Unfortunately, the resulting *N,N'*-dioxides **51** could not be detected, probably because they are not soluble in benzene or the amounts were just to small to be detected by ^{1}H NMR spectroscopy in the presence of excess **27**. The palladium(0) species was also observed as main decomposition product in the reaction of *N*-oxide **27a** with bromopyridine **28a**, whereas with bromobenzene **47a** only small amounts were detected. Here, many different phosphorous species were detected instead. Also the reactions with bromopyridine **28a** provided additional phosphorous species besides Pd(P^{t}Bu$_3$)$_2$.

Among these additional phosphorous species, in the arylation of the unsubstituted pyridine *N*-oxide **27a** with bromopyridine **28a**, an intermediate (30–120 min) with a chemical shift at $\delta = +8.8$ was observed (figure 31), which had not been observed in any other reactions. Therefore, we hypothesized that this compound might be a cyclometalated complex with the bipyridine *N*-oxide product **20a**, forming a kind of "roll-over" complex, where the C-H bond at the C3 position of **20a** was cleaved with the aid of the directing ability of the unprotected pyridyl ring (for bipyridine *N*-oxide cyclometalated complexes with palladium, see chapter 2). The unsubstituted bipyridine *N*-oxide **20a** does not have any steric hindrance in the C4 position as the ester-substituted *N*-oxide substrates **27l**, and therefore, cyclometalation is possible.

To test this hypothesis, we performed the stoichiometric reaction of bipyridine *N*-oxide **20a** and palladium dimer **A** in the presence of the phosphate base (scheme 67). Stirring the mixture in deuterated benzene at room temperature gave a new species, which exhibited 8 signals in the aromatic region in the ^{1}H NMR spectrum, suggesting that C-H bond activation at **20a** did not occur. However, the chemical shifts of the aromatic signals were significantly shifted compared to the authentic substrate, which implied that **20a** is coordinated to the palladium(II) metal center in a complex like in structure **G**. This complex exhibited a phosphorous chemical shift of $\delta = -8.1$ ppm, which does not significantly deviated from the dimer **A**. Heating complex **G** in the presence of K$_3$PO$_4$ in C$_6$D$_6$ resulted in a new set of 7 aromatic signals in the ^{1}H NMR spectrum, which might belong to the "roll-over" complex **H**. Unfortunately, several attempts to isolate the pure complex **H** failed and provided always mixtures contaminated with complex **G**. ESI-MS spectra are not informative in this case since upon loss of acetate, **G** forms a cation with the same *m/z* ratio as complex **H** plus H$^+$. The phosphorous shift in the ^{31}P NMR spectrum of the mixture showed a new signal at $\delta = +9.5$ ppm in C$_6$D$_6$, which deviates about 0.7 ppm from the species observed in the phosphor monitoring experiment (+8.8 ppm) of the

arylation of pyridine *N*-oxide **20a** with bromopyridine **28a**, which might be due to differences of the solvent's polarity. Noteably, attempted synthesis of complex **H** in the absence of the base failed, indicating the crucial role of the base for the C-H bond activation.
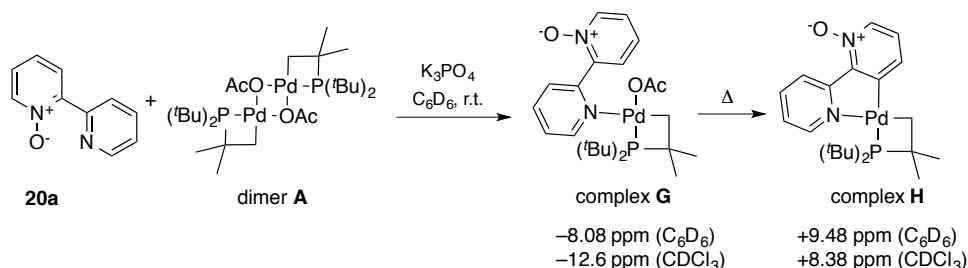
Scheme 67. Formation of roll-over complex **H** with unsubstituted biypridine *N*-oxide **20a**.

Nevertheless, we were able to isolate crystals of the complex **G**, which was independently prepared by simply stirring a solution of bipyridine *N*-oxide **20a** and dimer **A** in CDCl₃ at room temperature. X-ray diffraction analysis of crystals, obtained by slow diffusion of pentane into this solution, confirmed the structure of complex **G** (figure 32), although the acetate ligand was disordered. The phosphine ligand is still cyclometalated to the palladium(II) center and the bipyridine *N*-oxide **20a** coordinates with the pyridyl nitrogen. However, both rings are twisted with a torsion angle of 58 ° probably to avoid steric interactions with the other ligands.
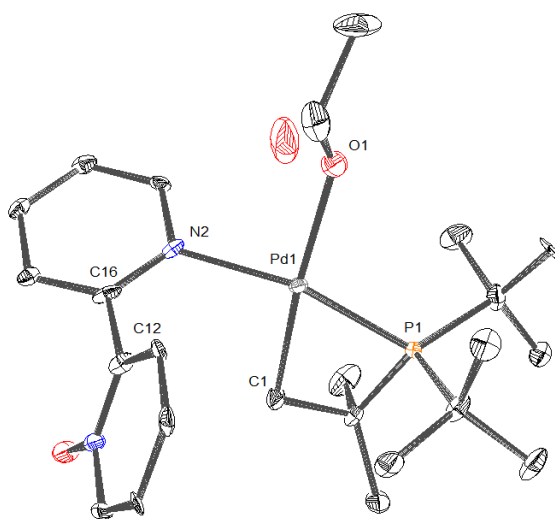

Figure 32. ORTEP 3 diagram of bipyridine *N*-oxide-coordinated palladium(II) complex **G** with disordered acetate ligand. Thermal ellipsoids are drawn at 30% probability level. Hydrogen atoms were omitted for clarity.

Conspicuously, in the arylations with bromopyridine **28a**, two species with a chemical shift at $\delta =$ +66.0 ppm and $\delta =$ +62.5 ppm were observed as the second main decomposition products (figure 31). While, the peak at +62.5 ppm can be clearly assigned to the free phosphine ligand (P^{t}Bu₃), the peak at

δ = +66.0 ppm might belong to the oxidized phosphine ligand (O=P^{t}Bu$_3$). The reported chemical shifts ranges form 66.6 ppm[188] in CD$_2$Cl$_2$ to 60.9 ppm in C$_6$D$_6$.[189] A solution of independently prepared O=P^{t}Bu$_3$ in C$_6$D$_6$ by Emma Svensson gave a chemical shift of δ = 63.1 ppm,[185] however addition of one drop of AcOH shifted the peak to δ = 68.4 ppm, which suggests that the chemical environment has a large impact on the chemical shift and does not allow a clear assignment of the peak at δ = 66.0 ppm. However, the peak at 66.0 ppm was also often observed as phosphine contamination of isolated products from the syntheses of bipyridine N-oxide **20**, as well as when exposing the solutions to air. This observation indicates that the species is very stable towards air and towards acidic silica gel, which excludes any air- or acid-sensitive phosphine-conating species and would support the assumption that the air-stable O=P^{t}Bu$_3$ was formed. Since it is known that phosphines are suitable deoxygenation reagents for pyridine N-oxides, it would be reasonable that the free phosphine ligand deoxygenates the N-oxide substrate under catalytic conditions to give presumably O=P^{t}Bu$_3$, which might be inactive towards catalysis. To test this hypothesis, we performed a control experiment with a catalytic amount of P^{t}Bu$_3$ and without palladium, however, neither conversion of the N-oxide nor of the phosphine was observed.

Furthermore, in all reactions a signal with a chemical shift of δ = +3.2 ppm was detected as decomposition product of the catalyst (figure 31). The largest amount was found in the reaction of **27a** with bromobenzene **47a** after 16 h. To the best of our knowledge, no other P^{t}Bu$_3$-derived compounds have been previously reported with a chemical shift close to +3.2 ppm. In addition, phosphorous species in the range of 60.9–62.3 ppm, as well as at 47.8 ppm, were observed in the arylations of unsubstituted **27a**. The later one might be also an oxidized or protonated phosphine species ([HP^{t}Bu$_3$]$_2$·PdBr$_4$ δ = +44.5 ppm in CD$_2$Cl$_2$, or P^{t}Bu$_3$·HBr δ = +41.0 ppm in C$_6$D$_6$),[78] or a tri-*tert*-butylphenylphosphonium salt with a reported chemical shift of 48.5 ppm in CDCl$_3$.[190]

The phosphorous experiments (figure 31) clearly showed that the active catalyst decomposes much earlier in reactions with bromopyridine **28a** than in reactions with bromobenzene **47a**. To identify the decomposition reactions, we conducted control experiments in the presence of only one of the substrate, the bromoarenes **28a** and **47a** or the pyridine N-oxide **27**, under otherwise identical conditions. We hypothesized that the dimer **A** undergoes the C-H bond activation with **27** forming the transient intermediate **I-18**, which would immediately decompose to give the bipyridine N,N'-dioxide **51**, Pd(P^{t}Bu$_3$)$_2$ and ^{31}P NMR silent Pd(OAc)$_2$. When we heated ester-substituted pyridine N-oxide **27l** in the presence of catalytic amounts of dimer **A**, **A** decomposed almost quantitatively to Pd(P^{t}Bu$_3$)$_2$ (table 30, entry 1) within 10 min at 100 °C. Further heating for 30 min did not significantly change the amount of Pd(P^{t}Bu$_3$)$_2$, which shows that this palladium(0) decomposition product is thermally stable even in the presence of excess pyridine N-oxide **27** and base. This conclusion is further supported by

heating pyridine *N*-oxide **27l** in the presence of catalytic amounts of Pd(P^{t}Bu$_3$)$_2$ for 10 or 30 min (entry 3), which did not cause decomposition of the palladium(0) complex. However, the ^{1}H NMR did not show additional peaks in the region expected for the homocoupling product **51l**.

Table 30. Control experiments under catalytic conditions.
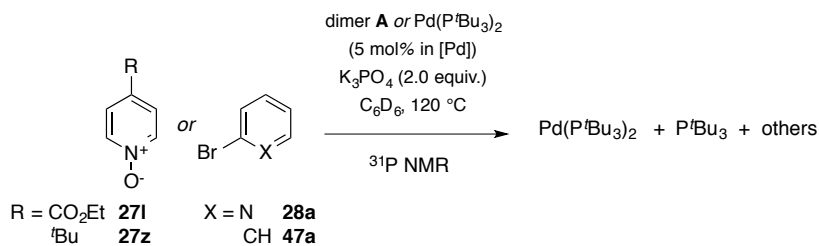
					Fraction in [%] of phosphorous species				
entry	pyridine *N*-oxide	aryl bromide	catalyst	time [min]	dimer **B**	dimer **A**	+3.2	P^{t}Bu$_3$	Pd(P^{t}Bu$_3$)$_2$
1	**27l**	–	dimer **A**	10					95
				30					92
2^a	**27z**	–	dimer **A**	10					65^b
				30					74^b
3	**27l**	–	Pd(P^{t}Bu$_3$)$_2$	10					100
				30					97
4	**27z**	–	Pd(P^{t}Bu$_3$)$_2$	10					98
				30					97
5	–	**28a**	dimer **A**	10	43	41			
				60	81				
6	–	**47a**	dimer **A**	10	96^c				
				60	89				
7^d	–	**28a**	Pd(P^{t}Bu$_3$)$_2$	0					100
				2				52	48
				10				77	21
				30	21		9	61	1
				960	33		11	24	
8	–	**47a**	Pd(P^{t}Bu$_3$)$_2$	0					100
				2				28	72
				10	9		8	47	30
				30	26		3	33	5
				960	15			12	

^{a}Formation of bipyridine *N,N′*-dioxide **51z** and 4-*tert*-buytpyridine confirmed by ^{1}H NMR and GC-MS. ^{b}Formation of several other minor species <10% and one at –0.7 ppm in 18%. ^{c}Appeared as several species at –9.6 ppm. ^{d}Formation of bipyridine **24a** confirmed by ^{1}H NMR with an estimated yield of ≈ 7%.

Since the bipyridine *N,N'*-dioxides **51** are generally poorly soluble in organic solvent particularly in benzene, it might be possible that **51l** precipitated, which would visually not be obvious because of the inhomogeneous mixture with the inorganic phosphate base. We hoped that the analogous experiment with the more lipophilic pyridine *N*-oxide **27z** would result in the corresponding *N,N'*-dioxide **51z**, which might be better soluble in benzene. In the presence of **27z**, the dimer **A** decomposed to 65% of Pd(P^{r}Bu$_3$)$_2$ after 10 min, and 74% after 30 min of heating (table 30, entry 2). The ^{1}H NMR spectra showed that the expected bipyridine *N,N'*-dioxide **51z** was formed. Additionally, deoxygenated starting material **27z** was detected, however, oxidized phosphine ligand was not detected. The formation of **51z** from this control experiment is consistent with the hypothesis that the intermediate **I-18** decomposed to the give homocoupled *N*-oxides **51** and Pd(P^{r}Bu$_3$)$_2$ without the participation the electrophilic aryl halide. Furthermore, we heated the dimer **A** in catalytic concentration and in the presence of excess base (see Experimental Section 4.13.4). Dimer **A** decomposed within few minutes mainly into different species, which have not been observed otherwise. Only 6% of the dimer **A** decomposed to Pd(P^{r}Bu$_3$)$_2$, which shows that the majority of Pd(P^{r}Bu$_3$)$_2$ in the catalytic reaction is formed by decomposition of intermediate **I-18** and not by thermal decomposition of dimer **A**.

When dimer **A** was heated in the presence of the aryl halides, however, the bromide-bridged dimer **B**, which was found to be the catalyst resting state, was formed (table 30). This conversion might be explained by decomposition of dimer **A** into Pd(P^{r}Bu$_3$)$_2$, which subsequently undergoes oxidative addition of the aryl halide forming the arylpalladium(II) complex **14**. Complex **14** might then undergo cyclometalation with the phosphine ligand with concomitant release of benzene or pyridine, respectively. However, pyridine was not detected in this reaction. Furthermore, thermal decomposition of dimer **A** resulted only in small amounts of Pd(P^{r}Bu$_3$)$_2$. Therefore, the exact pathway for the formation of dimer **B** from the reaction between dimer **A** and aryl halide remains unclear.

We also conducted the control experiment with the aryl halide **28a** and **47a** in the presence of catalytic amounts of Pd(P^{r}Bu$_3$)$_2$ and base (table 30), because it was previously proposed that the aryl halide undergoes oxidative addition to form arylpalladium(II) intermediate **14** and free phosphine ligand.[92] Furthermore, it was reported that complex **14a** is formed by oxidative addition of bromobenzene and Pd(P^{r}Bu$_3$)$_2$.[59a] The reported chemical shift of **14a** in C$_6$D$_6$ is $\delta = 63.0$ ppm and the free phosphine ligand appears at $\delta = 62.3$–62.5 ppm. Accordingly, two close peaks would be expected in the control experiment with bromobenzene **47a**. However, exclusively liberation of the phosphine ligand and decay of the Pd(P^{r}Bu$_3$)$_2$ was observed instead in the initial reaction time of 2–10 min (entry 8). Further heating showed a signal for dimer **B** (–9.2 ppm) and another species (–9.7 ppm), which presumably belongs to a cyclometalated species, as well. Additionally, an unassigned minor signal at +3.2 ppm was detected (3–8%). Because, instead of intermediate **14a** only the free phosphine ligand could be

observed, we assume that **14a** rapidly decomposes to a phosphine-free arylpalladium(II) species, which has been previously isolated and proposed as intermediates in the presence of salts, such as bromides and carboxylates.[77a, 184]

The analogous experiment with bromopyridine **28a** resulted in a faster decay of Pd(P^{t}Bu$_3$)$_2$ into free phosphine ligand (table 30, entry 7) compared to the reaction with bromobenzene **47a**, which suggests a faster oxidative addition, as expected since bromopyridine **28a** is a stronger electrophile. Similar to the reaction with bromobenzene **47a**, no signal, which could be assigned to an intermediate **14**, was detected. The formation of an orange precipitate was observed, which decomposed upon further heating into dimer **B** (33%) and also into the species with a chemical shift of +3.2 ppm (11%). The corresponding ^{1}H NMR spectrum of the samples showed conversion into bipyridine **24a** (21% after 16 h). For comparison, the corresponding reaction with bromobenzene **47a** gave only 6% of the homocoupled product biphenyl **17aa**.

To identify the orange precipitate, which was observed at early reaction times, we performed the stoichiometric reaction of bromopyridine **28a** (2 equiv.) and Pd(P^{t}Bu$_3$)$_2$ in the absence of the base (scheme 68). An orange precipitate was also observed and the ^{31}P NMR indicated full conversion of Pd(P^{t}Bu$_3$)$_2$ into free phosphine ligand. Further heating of the mixture resulted in full conversion into bipyridine **24a**, suggesting that the base does not play a role in the formation of the homocoupling product **24a**. The isolated orange precipitate turned out to be essentially insoluble in common solvents and remarkably bench-stable. To obtain a better soluble sample, we repeated the reaction with bromopyridines **28** bearing different lipophilic substituents, however, none of the samples provided soluble material. However, leaving a solution of 2-bromo-3-picoline and Pd(P^{t}Bu$_3$)$_2$ standing at room temperature for two weeks provided single crystals suitable for X-ray analysis. The solid state structure (figure 33) shows a phosphine-free, dimeric pyridylpalladium(II) complex **I**, which is coordinated by unreacted bromopicoline.
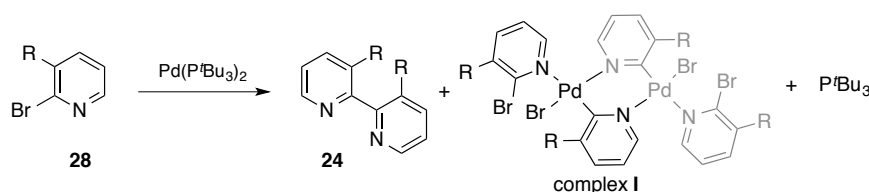
Scheme 68. Formation of biypridine **24a** (R = H) and pyridine-ligated pyridylpalladium(II) complex **I** (R = Me).

In the solid state, complex **I** shows a dimeric structure with square planar coordination of both palladium(II) centers (figure 33). One unreacted bromopicoline coordinates *cis* to the nitrogen of the bridging pyridyl ligand. The bridging pyridyl ligands are *cis* to each other and form a boat-like structure, which resembles the one of a similar 2-pyridiylpalladium(II) complex, which is ligated by

PPh$_3$ instead of another pyridine ligand and was prepared by oxidative addition of a bromopyridine **28** to Pd(PPh$_3$)$_4$.[191]
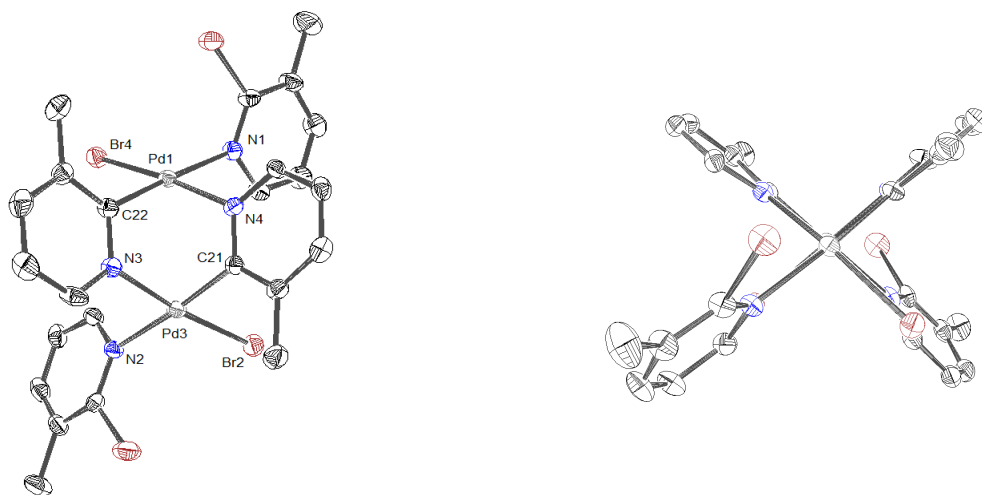

Figure 33. ORTEP 3 diagram of pyridine-ligated pyridylpalladium(II) complex **I** (R = Me) from the side view (left) and front view (right). Thermal ellipsoids are drawn at 30% probability level. Hydrogen atoms were omitted for clarity. Selected bond distances (Å) and angles (°): Pd1–Br4 2.461, Pd1–N1 2.131, Pd1–N4 2.069, Pd1–C22 1.992, Pd3–Br2 2.453, Pd3–N2 2.151, Pd3–N3 2.055, Pd3–C21 1.967, Pd1–Pd3 3.059, Br4–Pd1–C22 92.98, N1–Pd1–N4 87.99, Br4–Pd1–N4 173.08, C22–Pd1–N1 176.31, Br2–Pd3–C21 90.50, N2–Pd3–N3 91.12, Br2–Pd3–N3 172.96 and C21–Pd3–N2 175.64.

The identification of the pyridyl intermediate as the complex **I** might also explain the observed electronic trends with respect to differently substituted bromopyridines (*cf.* figure 30). It is conceivable that the transmetalation with the intermediate **I-18** occurs at the monomeric form of complex **I**. The equilibrium is shifted towards the dimer if electron-donating substituents increase the nucleophilicity and therefore the coordinating ability of the pyridyl nitrogen, which bridges both metal centers. In these cases, the formation of the monomer might become rate-determining, rather than the transmetalation or C-H bond activation, and would provide also a positive Hammett constant ρ. It is also conceivable that the undesired homocoupling product is formed by direct decomposition of the dimer **I**, which would be facilitated with electron-rich pyridyl ligands.

We attempted to synthesize and isolate a palladium(II) bromide complex **14** with a pyridyl ligand, which is sterically blocked in the C6 position by a bulky *tert*-butyl group to prevent dimer formation. Therefore, we generated a highly reactive palladium(0) species *in situ* by treatment of the Buchwald's pre-catalyst G4 with LiHMDS in the presence of P^{r}Bu$_3$ and excess of the substituted bromopyridine.[74, 192] The ^{31}P NMR spectrum of the reaction mixture showed two signals at δ = +91.6 ppm and δ = +70.8 ppm, which can be tendentially assigned to pyridyl complex **14**. The observed species decomposed into the dimer **B** upon standing at room temperature. Attempts to isolate the pyridyl complex **14** failed,

because the carbazole, which is the byproduct of activation of the pre-catalyst, could not be separated. However, later efforts by Emma Svensson using a modified version of the Buchwald's pre-catalyst G4 with lipophilic groups at the carbazole were successful.[185]

3.3.5   Optimization attempts

Our mechanistic studies indicate that the direct arylation of pyridine N-oxides **27** with bromopyridine **28** results in lower yields than the corresponding coupling with bromobenzenes **47**, because of the inherent instability of pyridylpalladium(II) intermediate, which decomposes to exclusively homocoupled product **24**. The undesired decomposition of the pyridylpalladium(II) intermediate is more important if the C-H bond activation of the N-oxide **27** is slow. We presume that in this case the pyridyl complex accumulates, because not enough of **I-18** is generated to consume the pyridyl intermediate (**14** or **I**) directly by transmetalation. The excess of the pyridyl complex then undergoes the homocoupling. We hypothesize that if the concentration of the pyridyl complex could be kept low throughout the reaction, the undesired pathway might be prevented.

To test this hypothesis, we performed the direct arylation of **27a** with slow addition of bromopyridine **28a** by a syringe pump. Initially, we attempted an addition rate of 2.1 mM/min (table 31, entry 3) close to the measured reaction rate for the product formation by the *in situ* IR monitoring (*cf*. table 26, +2.81 mM/min). However, the total yield of arylation, regarding both arylated products bipyridine and terpyridine N-oxide, was comparable to that we previously obtained under standard conditions (entries 1 and 2). Because the competition experiments revealed that the measured reaction rate by the *in situ* IR monitoring might not be reliable and too fast, we tried a slower addition, however, no significant improvements were achieved (entry 4). Similar yields were also obtained by lowering the reaction concentration to the half of the standard concentration (1 M in **27a**).

Failing with the attempts to improve the arylation yields by keeping a low concentration of the electrophile, we then tested if the homocoupling pathways can be suppressed by lowering the reaction temperature and extending the reaction time instead (table 31, entries 6 and 7). While the reaction at 100 °C did not show significant improvements, the reaction run at 80 °C provided indeed increased arylation yields after a reaction time of 2 days. The yield of the bipyridine N-oxide **20a** was 51% and for the terpyridine N-oxide **29a** 11% (total arylation yield: 73%), which demonstrates also that the palladium-catalyzed arylation of pyridine N-oxides with bromopyridines **28** can be efficiently carried out at only 80 °C.

Table 31. Attempts to optimize the direct arylation of pyridine *N*-oxide **27a**.

entry	X	additive (equiv.)	solvent	temp.	catalyst	method	20a [%]	29a [%]	24a [%]
1	Br	–	toluene	120 °C	dimer **A**	isolated	44	0	10
2	Br	–	toluene	120 °C	dimer **A**	^{1}H NMR	45	5	28
3[a]	Br	–	toluene	120 °C	dimer **A**	isolated	33	9	14
4[b]	Br	–	toluene	120 °C	dimer **A**	isolated	34	8	20
5[c]	Br	–	toluene	120 °C	dimer **A**	isolated	38	6	8
6[d]	Br	–	toluene	100 °C	dimer **A**	isolated	44	6	26
7[d]	Br	–	toluene	80 °C	dimer **A**	isolated	51	11	14
6[d]	Br		toluene	80 °C	dimer **A**	^{1}H NMR	53	0	16
8	Br	AgOAc (2.0)	toluene	80 °C	dimer **A**	^{1}H NMR	10	0	0
9	Br	AgOTf (1.0)	toluene	80 °C	dimer **A**	^{1}H NMR	25	0	0
11	Br	Ag$_2$CO$_3$ (2.0)	toluene	80 °C	dimer **A**	isolated	27	8	0
11[d]	Br	Ag$_2$CO$_3$ (2.0)	THF	70 °C	dimer **A**	isolated	3	0	0
12	Br	–	THF	120 °C	dimer **A**	isolated	46	6	–
13[d]	**Br**		**THF**	**80 °C**	**dimer A**	**isolated**	**54**	**13**	**–**
14	Br	–	benzene	120 °C	dimer **A**	isolated	47	7	–
15	Br	–	DME	120 °C	dimer **A**	isolated	44	7	–
16[d]	Br		DME	80 °C	dimer **A**	isolated	53	11	–
17	Br	–	DMF	120 °C	dimer **A**	isolated	42	7	–
18	Br	–	dioxane	120 °C	dimer **A**	isolated	38	4	–
19	Cl	–	toluene	120 °C	dimer **A**	isolated	28	0	–
20	Cl	–	toluene	120 °C	dimer **A**	^{1}H NMR	34	8	38
21	OTf	–	toluene	120 °C	dimer **A**	isolated	16	0	–
22	OTs	–	toluene	120 °C	dimer **A**	isolated	4	0	–
23	Br	–	toluene	120 °C	Herrmann-Beller	isolated	18	0	–

[a]**27a** was added via syringe pump; addition rate 2.1 mM/min. [b]**27a** was added via syringe pump; addition rate 1.1 mM/min. [c]Half-molar reaction solution. [d]Reaction time was 2 days.

We thought we can further improve this result by addition of silver carbonates, which are supposed to facilitate the C-H bond activation via the CMD mechanism on the one hand. On the other hand, silver salts might convert a pyridyl bromide complex into the corresponding acetate or carboxylate complex, which might be less prone to undergo the homocoupling. Chelating acetate or carbonate anionic ligands might prevent formation of dimeric intermediates, at which probably the homocoupling occurs, and increases the concentration of the monomers undergoing transmetalation with **I-18**. However, addition of the different silver salts to the reaction run at 80 °C (table 31, entries 8–11) provided lower yields of the desired coupling products.

We also tested other solvents (table 31, entries 12–18), such as THF, benzene, DME, and dioxane, which resulted in arylation yields comparable to those obtained in toluene, whereas DMF provided slightly lower yields, which demonstrates that the reaction is not limited to toluene as solvent. Using

chloropyridine or corresponding tosylates (entries 19–22) as substrate turned out to decrease the yields. We also tested other catalyst and ligands, however led to lower yields (see Experimental Section). Attempts to bind coordinating pyridyl ligands by addition of weak Lewis acids failed and prevented conversion.

3.4 Conclusion

In conclusion, the results support that the palladium-catalyzed direct arylations of pyridine *N*-oxides **27** with bromopyridines **28** proceed via the same cooperative mechanism (*cf*. scheme 64), which was previously proposed for reactions with bromobenzenes **47**.[92] However, contrary to previous reports,[157b] our kinetic experiments imply that the reactivity of differently substituted pyridine *N*-oxides **27** does not follow a clear electronic trend in terms of a Hammett correlation. Furthermore, the kinetic measurements suggested that the reactions with bromopyridines **28** proceed initially faster than with bromobenzene **47**, although the final yields of the bipyridine *N*-oxides **20** are lower. This observation is more pronounced in reactions with electron-rich pyridine *N*-oxides, which react slower in the C-H bond cleaving step. We assume that the pyridyl palladium(II) intermediate accumulates in the reaction mixture if the C-H bond activation at the dimer **A** is slow. Consequently, the pyridyl intermediate decompose to give bipyridine **24**, which binds to the dimer **A**, or the catalyst resting state dimer **B**, additionally decreasing its catalytic activity towards C-H bond activation. Although the results indicate inhibition by the bipyridine **24**, which is formed by disproportionation of the pyridylpalladium(II) intermediate, substrate or product inhibition could be excluded as reason for the drop in the yields.

The phosphine-free dimeric complex **I** was identified as possible intermediate, which is bridged by the pyridyl ligand. Our results indicate that a similar phosphine-free arylpalladium(II) complex is the actual intermediate in the reactions with bromobenzenes **47**. This intermediate predominantly decompose via reductive elimination with regeneration of the bromobenzene **47**, and only small amounts of the homocoupled product **17aa** are formed. The disproportionation of the pyridyl intermediate is the origin of the lower yields, because this process consumes irreversibly the electrophile, and bipyridine **24**, which inhibits the catalysis, is formed, while the decomposition of analogous phenyl intermediate is only the reversion of the oxidative addition step. The undesired decomposition pathway could be shown to be slowed if the reaction is run at lower temperatures of 80 °C, however longer reaction times are required. Moreover, optimization attempts revealed also that the direct arylation is compatible with various solvents.

4 Experimental Section

4.1 General Procedures and Instrumentation

4.1.1 General procedures

All air and moisture sensitive reactions and experiments were carried out using oven-dried glassware under an argon atmosphere. Reactions were set up either in glove box using glass vials with a Teflon-lined screw cap and heated on an aluminum well plate or by using Schlenk techniques and heated in a pre-heated oil bath using a stirrer and heater with temperature control.

Chemicals were purchased from commercial suppliers and used as received unless otherwise noted. Toluene, THF, pentane, Et$_2$O, dioxane and deuterated solvents (THF, toluene, benzene) were dried and distilled over sodium/benzophenone and degassed using freeze-pump-thaw technique. MeCN was dried and distilled from CaH$_2$. Dry CH$_2$Cl$_2$ was purchased from Sigma-Aldrich and dried via Solvent Purification System *MB-SPS 800* from *MBraun*. Dry DMF, MeOH and EtOH were purchased from Acros in AcroSeal bottles.

Column chromatography was performed on *Merck Silica Gel 60* (230–400 mesh) or *Acros Aluminium Oxide, basic, Brockmann I, 50–200 µm*. Hexane and ethyl acetate were previously distilled using rotary evaporation.

Thin layer chromatography was performed on *Merck TLC Silica gel 60 F$_{254}$*. Compounds were detected using an UV/Vis lamp (254 nm).

4.1.2 Instrumentation

^{1}H, ^{13}C, ^{19}F and ^{31}P NMR spectra were recorded on *Jeol ECX 400* or *Bruker Avance500* or *Joel ECX 400* at room temperature unless otherwise noted. Data were processed by *MestReNova Version: 7.1.2-10008*. Chemical shifts (δ) are reported in parts per million (ppm) and referenced to residual solvent peak (CDCl$_3$: ^{1}H δ = 7.26 ppm, ^{13}C δ = 77.16 ppm; C$_6$D$_6$: ^{1}H δ = 7.16 ppm, ^{13}C δ = 128.06 ppm; ^{31}P and ^{19}F: frequency calibrated log with ± 1 ppm deviation). Multiplicities are given as follows: s = singlet, d = doublet, t = triplet, q = quartet and m = multiplet. Coupling constants (J) are reported in Hertz (Hz).

High resolution ESI-MS spectra were recorded on an Agilent 6210 ESI-TOF, *Agilent Technologies*. The applied charge is reported as positive (+) or negative (–). The spray charge was set to 4 kV. Data are reported in mass to charge (*m/z*).

IR spectra were recorded on a *Jasco FT/IR-4100* FT-IR with a ZnSe optical window. The absorption bands are given in wave numbers (cm^{-1}), intensities are reported as follows: s = strong, m = medium, w = weak. Kinetic measurements by *in situ* IR were performed with *Mettler Toledo ReactIR 15*

Melting points (m.p.) were determined on a BÜCHI 510 melting point apparatus and are uncorrected.

Elemental analyses for contents of carbon, nitrogen, hydrogen, and sulfur were performed on an elemental analyzer VARIO EL, *Elementar*, and results are reported in percentage (%).

Quantitative gas chromatography measurements were performed on a *Varian CP-3800* equipped with a *Varian CP-8400* autosampler, a FID detector and a fused silica capillary column (CP-Sil 8 CB or F&W VF-5ms, 5% phenyl and 95% dimethylsiloxane phase, 30 m x 0.25 mm ID x 0.25 μm film). Quantifications of analytes were done using the internal standard approach from 10 points calibrations. All calibration and sample solutions were measured three times. The injection volume was 1 μmol unless otherwise noted.

Qualitative gas chromatography measurements were performed on a *7820A* gas chromatograph equipped with a fused silica capillary column (F&W VF-5ms, 5% phenyl and 95% dimethylsiloxane phase, 30 m x 0.25 mm ID x 0.25 μm film), *5977E MSD* (single quadrupole) detector from *Agilent Technologies* and *Varian CP-8410* autosampler. Nitrogen was employed as carrier and make-up gas. The data were processed with *Varian Star Chromatography Workstation Version 6.41*.

4.2   Ligands, catalysts and precursors

4.2.1   Ligands

2-Phenyl-*N*-methylaniline

[SZ 1023/1040]
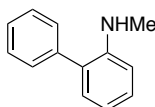
According to the reported procedure,[193] ethyl chloroformate (25.0 mL, 200 mmol) was added dropwise to a mixture of 2-aminobiphenyl (28.5 g, 168 mmol) and pyridine (93.0 mL, 1.15 mol) in DCM (150 mL) under stirring at room temperature. After the solution has been stirred for 18 h at room temperature, an aqueous solution of NaOH (2 M, 115 mL) was added. The aqueous layer was extracted with DCM (3 times), the combined organic layers dried with Na_2SO_4, the desiccant filtered off and the solvent was removed from the filtrate providing 2-ethoxycarbonyl-aminobiphenyl (41.2 g, 171 mmol, 86%) as highly viscous liquid and was used without additional purification in the next step.

Under an argon atmosphere, a solution of crude 2-ethoxycarbonylaminobiphenyl (5.07 g, 21.0 mmol) in dry THF (100 mL) was added dropwise to a suspension of $LiAlH_4$ (4.19 g, 110 mmol) and dry THF (30.0 mL). After the reaction mixture has been stirred at room temperature for 1h, it was further stirred under reflux for 3 h. Upon cooling mixture to 0 °C under ice cooling, distilled water (9.00 mL) and then an aqueous solution of NaOH (2 M, 14.0 mL) were added slowly. The formed precipitate was filtered off, washed with Et_2O and the organic filtrates were dried with Na_2SO_4. After filtration and removal of the volatiles, 2-phenyl-*N*-methylaniline (2.64 g, 14.4 mmol, 69%) was obtained as yellow oil.

^{1}H NMR (400 MHz, CDCl$_3$): δ 7.56–7.53 (m, 4H), 7.49–7.43 (m, 1H), 7.39 (t, J = 7.8 Hz, 1H), 7.22 (dt, J = 7.4, 1.2 Hz, 1H), 6.90 (t, J = 7.4 Hz, 1H), 6.81 (d, J = 8.1 Hz, 1H), 4.07 (s br, 1H), 2.89 (s, 3H) ppm.
The chemical shifts are in agreement with previous reported values.[74]

The 2-phenyl-*N*-methylaniline was re-dissolved in Et_2O (50.0 mL) and MsOH (0.90 mL, 13.9 mmol) was added dropwise to this solution, which resulted in formation of a colorless precipitate. The supernatant liquid was removed and the solid dried in vacuum, providing the title compound (2.27 g, 8.13 mmol, 56%) as colorless solid.

^{1}H NMR (400 MHz, CDCl$_3$): δ 7.70–7.51 (m, 6H), 7.49–7.43 (m, 3H), 4.90 (br s, 3H), 2.96 (s, 3H), 2.69 (s, 3H) ppm.

Dibenzylideneacetone, dba

[SZ 3073]
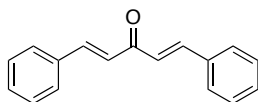
Similar to the reported procedure,[194] a three-necked flask, equipped with a thermometer and a dropping funnel, was charged with NaOH (50.1 g, 1.25 mol), distilled water (0.50 L) and EtOH (0.40 L). The resulting clear solution was cooled to room temperature under stirring using a water bath. The dropping funnel was charged with a mixture of benzaldehyde (50.5 mL, 0.50 mol) and acetone (18.4 mL, 0.25 mol). Approximately one half of this mixture was added to the reaction flask and the resulting solution stirred for 15 min before addition of the other half. While addition the reaction was kept between 20 and 25 °C by cooling the flask with a water/ice bath. After the resulting mixture has been stirred for additional 1.5 h, the formed yellow precipitate was filtered by suction filtration and thoroughly washed with water until the pH of the filtrate was neutral. The solid was then dissolved in EtOAc forming two layers. The aqueous layer was extracted with EtOAc (3 times) and the combined organic layers were dried with Na$_2$SO$_4$, filtered and the solvent was removed from the filtrate. The crude product was recrystallized from boiling EtOAc providing the title compound (49.1 g, 0.21 mol, 84%) as crystalline yellow solid.

^{1}H NMR (400 MHz, CDCl$_3$): δ 7.77 (s, 1H), 7.73 (s, 1H), 7.62 (ddd, J = 6.1, 4.5, 2.8 Hz, 4H), 7.45–7.39 (m, 6H), 7.11 (s, 1H), 7.07 (s, 1H) ppm.

The chemical shifts are in agreement with previous reported values.[194]

Tri-*orto*-tolylphosphine, P(*o*-tol)$_3$

[SZ 4024]
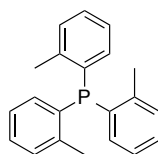
Similar to the reported procedure,[195] an oven-dried 2 L three-necked flask, equipped with a 500 mL dropping funnel and reflux condenser, was set under an atmosphere of argon and charged with magnesium (15.6 g, 0.64 mol), dry THF (100 mL), and some crystals of iodine. The dropping funnel was charged with a solution of 2-bromotoluene (70.0 mL, 0.58 mol) in dry THF (300 mL). Pure 2-

bromotoluene (1.50 mL, 12.0 mmol) were syringed into the reaction flask under vigorous stirring resulting in an immediate exothermic reaction. The 2-bromotoluene solution was added dropwise to maintain boiling of the reaction mixture. After reflux for 2 h, the reaction mixture was cooled to 0 °C and the dropping funnel charged with a solution of PCl_3 (16.0 mL, 0.18 mmol) in THF (150 mL). This solution was slowly dropped to the Grignard solution, which resulted in formation of a precipitate. The reaction mixture was additionally stirred first at room temperature for 30 min and then under reflux for 2 h. Upon cooling to 0 °C, the reaction was opened to air and quenched with an aqueous, saturated NH_4Cl solution. The resulting mixture was stirred at room temperature over night and the THF was removed by rotary evaporation. The white aqueous suspension was extracted with Et_2O (1000 mL), the combined organic extracts dried with Na_2SO_4, filtered and the solvent was removed from the filtrate. The colorless solid residue was recrystallized from boiling hexane, providing the title compound (29.1 g, 0.096 mol, 52%) as a colorless solid.

^{1}H NMR (400 MHz, $CDCl_3$): δ 7.37–7.15 (m, 6H), 7.08 (td, J = 7.3, 1.8 Hz, 3H), 6.73 (ddt, J = 7.5, 4.4, 1.8 Hz, 3H), 2.40 (d, J = 1.4 Hz, 9H) ppm.

^{31}P NMR (162 MHz, $CDCl_3$): δ −28.84 ppm.

The chemical shifts are in agreement with previous reported values.[195]

Tri-*tert*-butylphosphine hydrogen bromide, P*t*Bu$_3$·HBr

[SZ 1059/5044]
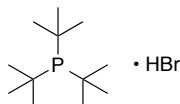
Based on the reported procedure,[78] a reaction flask was charged with P*t*Bu$_3$ (231 mg, 1.14 mmol), pyridinium bromide (163 mg, 1.02 mmol) and dry CH_3CN (4.00 mL) inside the glovebox. The flask was sealed and brought outside the glovebox, where the reaction mixture was stirred at room temperature until the mixture turned into a clear solution. The flask was opened to air and the volatiles removed. The solid residue was washed with Et_2O and dried in vacuum. The title compound (257 mg, 0.91 mmol, 89%) was obtained as colorless solid.

^{1}H NMR (400 MHz, $CDCl_3$): δ 8.69 (d, J = 476 Hz, 1H), 1.69 (d, J = 15 Hz, 27H) ppm.

^{31}P NMR (162 MHz, $CDCl_3$): δ 40.57 ppm.

The chemical shifts are in agreement with previous reported values.[78]

4.2.2 Palladium precursors and catalysts

[(C$_6$H$_6$)RuCl$_2$]$_2$ was prepared by a reported procedure and provided from Ralf Albrecht.[196] NHC-Carbene-based palladium complexes [(IMes)PdCl$_2$(3-ClPy)] and [(IPr)PdCl$_2$(3-ClPy)] were prepared by reported procedures and provided by Stefan Hentschel.[42] (tmeda)PdCl$_2$ was provided by Prof. Dr. C. C. Tzschucke and prepared according to literature procedure.[197] Buchwalds pre-catalyst of first generation G1 was provided from Sasa Duric and prepared according to literature procedure.[73]

Tris(dibenzylideneacetone)dipalladium(0) chloroform adduct, Pd$_2$dba$_3$·CHCl$_3$

[SZ 3144]
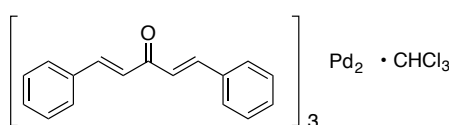
According to the reported procedure,[198] a 500 mL single necked-flask was charged with PdCl$_2$ (2.68 g, 15.1 mmol), dibenzylidineacetone (12.3 g, 52.4 mmol), NaOAc (10.5 g, 128 mmol) and MeOH (300 mL). After the resulting mixture has been stirred at 40 °C for 3 h, the solid was filtered by suction filtration using a glass frit (D3). The solid was first washed with water until the filtrate was neutral, then with MeOH (2 times). The purple solid was dissolved in CDCl$_3$ (1.20 L) and the deep purple solution concentrated ($\approx$ 250 mL). Acetone (800 mL) was added and the resulting mixture was kept at –25 °C over night. The formed solid was again filtered by suction filtration using a glass frit (D3) and dried under vacuum providing the title compound (15.4 g, 99%) as crystalline, dark purple solid, which was used without further purification.

Bis(tri-*tert*-butylphosphine)palladium(0), Pd(P^{t}Bu$_3$)$_2$

[SZ 4023]
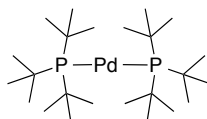
According to the reported procedure,[199] a round bottom Schlenk flask was charged with Pd$_2$dba$_3$ · CHCl$_3$ (7.79 g, 7.52 mmol), P^{t}Bu$_3$ (6.63 g, 32.8 mmol) and dry DMF (100 mL). After stirring at room temperature for 25 h, the mixture was filtered through a reverse frit and the greyish solid thoroughly washed with DMF and MeOH, successively. The crude product was dissolved and washed trough the filter with pentane and collected. Then the solvent was removed by vacuum transfer distillation and the remaining sold dried in vacuum. The title compound (6.12 g, 12.0 mmol, 80%) was isolated as colorless solid.

^{1}H NMR (400 MHz, C$_6$D$_6$): δ 1.46 (t, 54H) ppm.

^{31}P NMR (162 MHz, C$_6$D$_6$): δ 85.42 ppm.

The chemical shifts are in agreement with previous reported values.[199]

[(^{t}Bu$_2$PC(CH$_2$)(CH$_3$)$_2$)Pd(OAc)]$_2$, Dimer A

[SZ 2090]
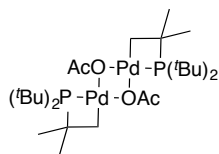
Based on the reported procedure,[118] a round-bottom flask charged with P^{t}Bu$_3$ (2.27 g, 11.2 mmol), Pd(OAc)$_2$ (2.25 g, 10.0 mmol) and toluene (100 mL). The flask was sealad with a glass stopper and brought outside the glovebox, where it was placed in a pre-heated oil bath at 90 °C and stirred for 30 min. After cooling to room temperature, the flask was opened to air and the volatiles removed. Et$_2$O (150 mL) was added and the resulting solution filtered through a pad of Celite. The solvent was removed from the filtrate, the remaining solid washed with pentane and dried in vacuum providing the title compound (2.46 g, 3.35 mmol) as colorless solid. The pentane fractions were collected and stored in the freezer at –20 °C where additional product crystalized. The solid was filtered and dried in vacuum providing additional product (0.90 g, 1.27 mmol, 92% in total).

^{1}H NMR (400 MHz, CDCl$_3$): δ 1.90 (s, 6H), 1.53 (d, J = 13.7 Hz, 36H), 1.48 (d, J = 14.2 Hz, 12H), 1.06 (s, 4H) ppm.

^{31}P NMR (162 MHz, CDCl$_3$): δ –8.85 ppm.

The chemical shifts are in agreement with previous reported values.[92]

[(^{t}Bu$_2$PC(CH$_2$)(CH$_3$)$_2$)Pd(Br)]$_2$, Dimer B

[SZ 2088A]
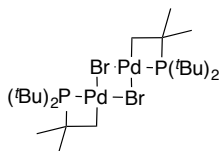
According to the patent procedure,[200] dimer **A** (122 mg, 0.17 mmol) and TBAB (1.08 g, 3.35 mmol) were dissolved in DCM (3.00 mL) and stirred at room temperature for 2 h. The solvent was removed under reduced pressure, the residue taken up in MeOH (2.50 mL) and the mixture stirred at room temperature for 1.5 h. The solids were filtered, washed with MeOH and pentane then dried in vacuum. The title compound (99.6 mg, 0.13 mmol, 76%) was obtained as colorless solid.

^{1}H NMR (400 MHz, CDCl$_3$): δ 1.56 (d, J = 14.0 Hz, 36H), 1.47 (d, J = 14.3 Hz, 12H), 1.18 (s, 4H) ppm.

^{31}P NMR (162 MHz, CDCl$_3$): δ −8.89 ppm.

The chemical shifts are in agreement with previous reported values.[200]

Herrmann-Beller catalyst

[SZ 2005]
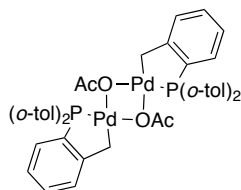
Based on the reported procedure,[201] Pd(OAc)$_2$ 225 mg, 1.00 mmol) and P(o-tol)$_3$ (533 mg, 1.30 mmol) were mixed in toluene (25.0 mL) and stirred at 50 °C for 3 min. The reaction mixture was immediately cooled to room temperature and concentrated to approximately the quarter of the total volume. The hexane (25.0 mL) was added, which resulted in precipitation of a yellow solid, and the mixture was kept in freezer at −20 °C over night. The supernatant liquid was decanted and the solid washed with pentane. The title compound (375 mg, 0.40 mmol, 80%) was obtained as yellow solid and used without further purification.

Palladium(II) triflate, Pd(OTf)$_2$

[FW 1074D]
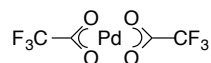
According to the reported procedure,[202] Pd(OAc)$_2$ (256 mg, 1.15 mmol) was heated at 72 °C in TFA (12.0 mL) until a clear solution was formed. The solution was cooled to room temperature and the volatiles removed under vacuum. The remaining solid was redissolved in TFA (6.00 mL) and the volatiles removed again. The title compound (222 mg, 0.67 mmol) was obtained as a grey solid.

IR (v/cm^{-1}): 2357 (w), 2342 (w), 1589 (m), 1499 (m), 1459 (w), 1422 (w), 1189 (s), 1165 (s), 872 (w), 781 (m), 743 (m), 702 (w).

Palladium(II) benzoate, Pd(OBz)$_2$

[FW 1074A]
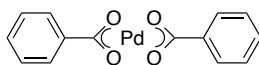
According to the reported procedure,[203] Pd(OAc)$_2$ (159 mg, 0.71 mmol) and benzoic acid (1.30 g, 10.7 mmol) were dissolved in acetone (15.0 mL). The solution was allowed to stand at room temperature over night resulting in the formation of brown crystals, which were filtered and dried in vacuum. The title compound (91.4 mg, 0.26 mmol, 37%) was obtained as brown solid.

^{1}H NMR (400 MHz, CDCl$_3$): δ 7.96–7.92 (m, 4H), 7.42–7.37 (m, 2H), 7.32–7.26 (m, 4H) ppm.

The chemical shifts are in agreement with previous reported values.[203]

Palladium(II) pivalate, Pd(OPiv)$_2$

[FW 1074B]
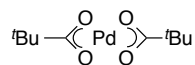
Similar to the preparation of Pd(OPiv)$_2$, Pd(OAc)$_2$ (159 mg, 0.71 mmol) and pivalic acid (1.29 g, 12.6 mmol) were dissolved in acetone (15.0 mL) and the solution allowed to stand at room temperature over night. The formed brown crystals were filtered and dried in vacuum. The title compound (115 mg, 0.37 mmol; 53%) was isolated as brown solid.

^{1}H NMR (400 MHz, CDCl$_3$): δ 0.93 (s, 18H) ppm.

The chemical shifts are in agreement with previous reported values.[204]

Bis(acetonitrile)palladium dichloride, (MeCN)$_2$PdCl$_2$

[SZ 5091]
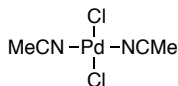
PdCl$_2$ (2.00 g, 11.3 mmol) was added portion-wise to refluxing MeCN (50.0 mL) over 2 h, during which a yellow precipitate was formed. The reaction mixture was additionally stirred under reflux for 2 h before being cooled to room temperature. The supernatant liquid was removed with a pipette and the yellow solid washed with Et$_2$O and dried in vacuum. The liquid layer was concentrated in vacuum resulting in further precipitation of a yellow solid, which was isolated by removing the liquid layer and washed with Et$_2$O. The title compound (2.67 g, 10.3 mmol, 91%) was obtained as yellow solid.

^{1}H NMR (400 MHz, DMSO-d_6): δ 2.07 (s, 3H) ppm.

IR (v/cm^{-1}): 2191.

Elemental analysis (%): C 18.6, H 2.36, N 10.8 calc. C 18.5, H 2.33, N 10.8

Diacetato(p-cymene)ruthenium(II), (p-cymene)Ru(OAc)$_2$

[FW 1074C]

171
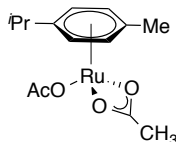
[(p-Cymene)Ru(Cl)$_2$]$_2$ (124 mg, 0.20 mmol) and AgOAc (126mg, 0.76 mmol) were stirred in DCM (10.0 mL) at room temperature for 2 h. The reaction mixture was filtered and the volatiles removed from the filtrate. The title compound (122 mg, 0.17 mmol, 85%) was obtained as orange solid.

^{1}H NMR (400 MHz, CDCl$_3$): δ 5.74 (d, J = 5.7 Hz, 2H), 5.52 (d, J = 5.0 Hz, 2H), 2.83 (p, J = 6.9 Hz, 1H), 2.22 (s, 3H), 1.90 (s, 6H), 1.33 (d, J = 6.9 Hz, 6H) ppm.

The chemical shifts are in agreement with previous reported values.[205]

N-Methyl-2-aminobiphenylpalladium methanesulfonate, Buchwald pre-catalyst G4

[SZ 1027B/1040B]
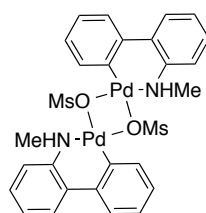
An oven-dried Schlenk flask was set under an atmosphere of argon and charged with 2-phenyl-*N*-methylaniline methanesulfonate (2.24 g, 8.03 mmol), Pd(OAc)$_2$ (1.80 g, 8.02 mmol) and toluene (60.0 mL). The mixture was stirred at 50 °C for 45 min resulting in the formation of a clear solution. After cooling to room temperature, the flask was opened to air and pentane (200 mL) was added. The supernatant liquid was decanted from the precipitate and the solid washed with pentane. The title compound (2.81 g, 3.67 mmol, 91%) was obtained as tan solid. Crystals suitable for X-ray were grown by slow evaporation from a saturated solution in benzene.

^{1}H NMR (400 MHz, CDCl$_3$): δ 7.53 (d, J = 7.6 Hz, 1H), 7.34 (d, J = 7.5 Hz, 1H), 7.22 (t, J = 6.8 Hz, 2H), 7.15 (q, J = 7.4 Hz, 2H), 7.09 (t, J = 7.3 Hz, 1H), 6.98 (t, J = 7.3 Hz, 1H), 6.88 (s br, 1H), 2.81 (s, 3H), 2.61 (d, J = 5.0 Hz, 3H) ppm.

The chemical shifts are in agreement with previous reported values.[74]

4.3 Syntheses of arylpalladium(II) complexes

4.3.1 *cis*-(tmeda)Pd(Ar)X complexes (1)

General procedure:

An oven-dried Schlenk flask was charged with $Pd_2dba_3 \cdot CHCl_3$ (1 equiv.) and aryl iodide (2.5–3.0 equiv.), sealed with rubber septum and set under an atmosphere of argon by cycled evacuation and backfilling with argon. Dry toluene (0.05 M) and TMEDA (2.5 equiv.) were syringed to the reaction flask and the resulting deep purple mixture was stirred at 50 °C for 30–60 min, during which the purple color disappeared. After cooling to room temperature, the mixture was filtered through a pad of celite and the filter washed with DCM. The combined filtrates were concentrated under vacuum, Et_2O (50.0 mL) was added and the resulting solution kept at –25 °C for approximately 3 h. The supernatant liquid was decanted, the solid washed with additional Et_2O until the liquid phase was colorless and the solid dried in vacuum.

cis-(tmeda)Pd(p-Me$_2$NC$_6$H$_4$)I (1b)

[SZ 3066]
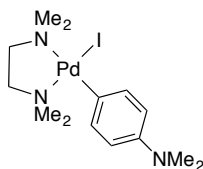
According to the general procedure, the reaction of $Pd_2dba_3 \cdot CHCl_3$ (1.02 g, 0.98 mmol), 4-*N,N*-dimethylaminoiodobenzene (0.70 g, 2.90 mmol) and TMEDA (0.40 mL, 2.50 mmol) in toluene (20.0 mL) the complex **1b** (0.80 g, 1.70 mmol, 87%) was obtained as deep orange, microcrystalline solid.

^{1}H NMR (400 MHz, CDCl$_3$): δ 7.0 (d, J = 8.7 Hz, 2 H), 6.5 (d, J = 8.6 Hz, 2 H), 2.8 (s, 6 H), 2.70–2.66 (m, 2 H), 2.6 (s, 6 H), 2.5 (dd, J = 6.8, 4.2 Hz, 2 H), 2.3 (s, 6 H) ppm.

^{13}C NMR (101 MHz, CDCl$_3$): δ 147.6, 136.0, 127.9, 113.6, 62.1, 58.3, 49.9, 49.7, 41.4 ppm.

IR (v/cm^{-1}): 2972 (w), 2883 (w), 2837 (w), 2790 (w), 1582 (m), 1404 (w), 1490 (m), 1490 (m), 1463 (m), 1344 (m), 1278 (w), 1218 (m), 1192 (m), 1162 (m), 1122 (w), 1066 (w), 1046 (w), 1023 (w), 999 (w), 957 (w), 815 (m), 802 (s), 793 (s), 770 (m).
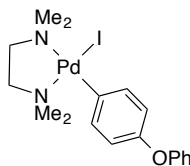
HRESI-MS (MeOH, +, m/z): [(tmeda)Pd(p-Me$_2$NC$_6$H$_4$)I+H]$^+$ 470.0289, calc. 470.0279

Elemental analysis (%): C 36.0, H 5.77, N 8.99 calc. C 35.8, H 5.58, N 8.95

M.p.: 161–165 °C (decomp.)

cis-(tmeda)Pd(*p*-PhOC$_6$H$_4$)I (1c)

[SZ 3065]

According to the general procedure, the reaction of Pd$_2$dba$_3$·CHCl$_3$ (1.03 g, 1.00 mmol), TMEDA (0.38 mL, 2.54 mmol) and 4-phenoxybromobenzene (0.84 g, 2.84 mmol) in toluene (20.0 mL) provided the complex **1c** (0.76 g, 1.47 mmol, 74%) as bright orange solid.

^{1}H NMR (400 MHz, CDCl$_3$): δ 7.28–7.23 (m, 2 H), 7.19 (d, J = 8.6 Hz, 2 H), 6.99 (t, J = 7.4 Hz, 1 H), 6.93 (dd, J = 8.6, 0.9 Hz, 2 H), 6.69 (d, J = 8.6 Hz, 2 H), 2.70 (t, J = 5.5 Hz, 2 H), 2.66 (s, 6 H), 2.54 (dd, J = 6.7, 4.3 Hz, 2 H), 2.31 (d, J = 1.4 Hz, 6 H) ppm.

^{13}C NMR (101 MHz, CDCl$_3$): δ 158.4, 153.2, 137.2, 136.6, 129.5, 122.2, 118.0, 117.9, 62.2, 58.3, 50.0, 49.8 ppm.

IR (v/cm^{-1}): 2974 (w), 2883 (w), 2837 (w), 1588 (w), 1563 (w), 1488 (w), 1467 (s), 1457 (m), 1437 (w), 1289 (w), 1279 (w), 1222 (s), 1206 (m), 1187 (m), 1165 (m), 1124 (w), 1085 (w), 1055 (m), 1046 (m), 1013 (m), 1004 (m), 953 (m), 930 (w), 911 (w), 862 (m), 835 (m), 799 (s), 768 (m), 753 (s), 718 (w), 691 (m).

HRESI-MS (MeOH, +, m/z): [(tmeda)Pd(*p*-PhOC$_6$H$_4$)I+Na]$^+$ 540.9964, calc. 540.9939; [(tmeda)Pd(*p*-PhOC$_6$H$_4$)I+K]$^+$ 556.9695, calc. 556.9678

Elemental analysis (%): C 41.9, H 4.91, N 5.56 calc. C 41.7, H 4.86, N 5.40

M.p.: 141–143 °C (decomp.)

cis-(tmeda)Pd(*p*-MeOC$_6$H$_4$)I[54a] (1d)

[SZ 3061]
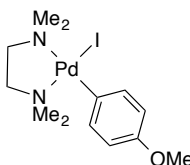
According to the general procedure, the reaction of Pd$_2$dba$_3$·CHCl$_3$ (1.03 g, 0.99 mmol), TMEDA (0.38 mL, 2.54 mmol) and 4-bromoanisole (0.67 g, 2.88 mmol) in toluene (20.0 mL) provided the complex **1d** (0.80 g, 1.76 mmol, 89%) as orange solid.

^{1}H NMR (400 MHz, CDCl$_3$): δ 7.08 (d, J = 8.7 Hz, 2 H), 6.60 (d, J = 8.7 Hz, 2 H), 3.70 (s, 3 H), 2.71–2.67 (m, 2 H), 2.65 (s, 6 H), 2.56–2.51 (m, 2 H), 2.30 (s, 6 H) ppm.

^{13}C NMR (101 MHz, CDCl$_3$): δ 156.5, 136.1, 131.8, 113.0, 62.2, 58.4, 55.2, 49.9, 49.8 ppm.

IR (v/cm^{-1}): 2976 (w), 2885 (w), 2834 (w), 2791 (w), 1576 (w), 1477 (m), 1454 (m), 1405 (w), 1268 (m), 1226 (m), 1170 (m), 1124 (w), 1095 (w), 1065 (w), 1047 (w), 1023 (m), 1003 (m), 957 (m), 825 (m), 802 (s), 772 (m).
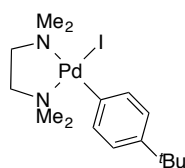
HRESI-MS (MeOH, +, m/z): [(tmeda)Pd(p-MeOC$_6$H$_4$)I+Na]$^+$ 478.9788, calc. 478.9782; [(tmeda)Pd(p-MeOC$_6$H$_4$)I+K]$^+$ 494.9523, calc. 494.9521

Elemental analysis (%): C 33.8, H 5.11, N 5.90 calc. C 34.2, H 5.08, N 6.13

M.p.: 155 °C (decomp.)

cis-(tmeda)Pd(p-^{t}BuC$_6$H$_4$)I (1e)

[SZ 3053 and AC 4050B/4069A/4117A]

According to the general procedure, the reaction of Pd$_2$dba$_3$·CHCl$_3$ (1.56 g, 1.51 mmol), TMEDA (0.56 mL, 3.74 mmol) and 4-*tert*-butyliodobenzene (0.74 mL, 4.18 mmol) in toluene (30.0 mL) provided the complex **1e** (1.11 g, 2.29 mmol, 76%) as pale yellow solid.

^{1}H NMR (400 MHz, CDCl$_3$): δ 7.10 (d, J = 8.4 Hz, 2 H), 6.93 (d, J = 8.4 Hz, 2 H), 2.74–2.70 (m, 2 H), 2.66 (s, 6 H), 2.58–2.53 (m, 2 H), 2.30 (s, 6 H), 1.23 (s, 9 H) ppm.

^{13}C NMR (101 MHz, CDCl$_3$): δ 145.2, 139.6, 135.6, 123.9, 62.2, 58.3, 50.0, 49.8, 33.9, 31.8 ppm.

IR (v/cm^{-1}): 3002 (w), 2957 (m), 2920 (m), 2884 (m), 2863 (m), 2834 (m), 2786 (w), 1575 (w), 1456 (m), 1402 (w), 1390 (w), 1375 (w), 1357 (w), 1285 (w), 1265 (w), 1114 (m), 1064 (m), 1021 (m), 1010 (m), 991 (w), 954 (m), 814 (m), 799 (s), 770 (m), 727 (m)
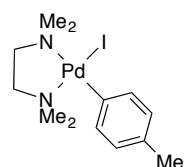
HRESI-MS (MeOH, +, m/z): [(tmeda)Pd(p-^{t}BuC$_6$H$_4$)I+Na]$^+$ 505.0319, calc. 505.0302; [(tmeda)Pd(p-^{t}BuC$_6$H$_4$)I+K]$^+$ 521.0044, calc. 521.0042

Elemental analysis (%): C 39.8, H 6.09, N 5.86 calc. C 39.8, H 6.06, N 5.80

M.p.: 160 °C (decomp.)

cis-(tmeda)Pd(p-MeC$_6$H$_4$)I[54a] (1f)

[SZ 3054 and AC 4047B/4067A/4115A]

According to the general procedure, the reaction of $Pd_2dba_3 \cdot CHCl_3$ (3.01 g, 2.91 mmol), TMEDA (1.13 mL, 7.54 mmol) and 4-iodotoluene (1.83 g, 8.41 mmol) in toluene (40.0 mL) provided the complex **1f** (2.18 g, 4.95 mmol, 85%) as orange solid.

^{1}H NMR (400 MHz, CDCl$_3$): δ 7.09 (d, J = 8.1 Hz, 2 H), 6.75 (d, J = 7.5 Hz, 2 H), 2.73–2.67 (m, 2 H), 2.65 (s, 6 H), 2.56–2.51 (m, 2 H), 2.31 (s, 6 H), 2.21 (s, 3 H) ppm.

^{13}C NMR (101 MHz, CDCl$_3$): δ 139.6, 139.5, 136.1, 131.7, 127.7, 62.2, 58.3, 50.0, 49.8, 20.7 ppm.

IR (v/cm^{-1}): 2991 (w), 2973 (w), 2882 (w), 2838 (w), 2787 (w), 1738 (w), 1476 (m), 1451 (m), 1281 (w), 1206 (w), 1124 (w), 1097 (w), 1056 (m), 1021 (m), 1010 (m), 957 (m), 933 (w), 798 (s), 771 (m).

HRESI-MS (MeOH, +, m/z): [(tmeda)Pd(p-MeC$_6$H$_4$)I+Na]$^+$ 462.9837, calc. 462.9833; [(tmeda)Pd(p-MeC$_6$H$_4$)I+K]$^+$ 478.9569, calc. 478.9572

Elemental analysis (%): C 35.5, H 5.39, N 6.05 calc. C 35.5, H 5.26, N 6.36

M.p.: 165 °C (decomp.)

cis-(tmeda)Pd(C$_6$H$_5$)I[53d] (1a)

[SZ 3044/3048 and AC 4048B/4072A/4118A/4176A]
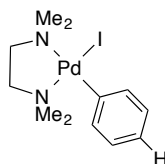
According to the general procedure, the reaction of $Pd_2dba_3 \cdot CHCl_3$ (3.02 g, 2.92 mmol), TMEDA (1.13 mL, 7.54 mmol) and iodobenzene (0.93 mL, 8.40 mmol) in toluene (40.0 mL) provided the complex **1a** (2.23 mg, 5.23 mmol, 90%) as pale orange solid.

^{1}H NMR (400 MHz, CDCl$_3$): δ 7.24 (dd, J = 8.0, 1.2 Hz, 2 H), 6.91 (dd, J = 8.1, 6.9 Hz, 2 H), 6.84–6.74 (m, 1 H), 2.74–2.70 (m, 2 H), 2.67 (s, 6 H), 2.57–2.53 (m, 2 H), 2.32 (s, 6 H) ppm.

^{13}C NMR (101 MHz, CDCl$_3$): δ 144.7, 136.6, 126.7, 122.8, 62.3, 58.4, 50.0, 49.9 ppm.

IR (v/cm^{-1}): 3046 (w), 2992 (w), 2966 (w), 2885 (w), 2837 (w), 2789 (w), 1561 (m), 1456 (m), 1421 (w), 1285 (m), 1192 (w), 1164 (w), 1127 (w), 1101(w), 1061 (m), 1046 (w), 1019 (m), 991 (w), 955 (m), 933 (w), 800 (s), 770 (m), 742 (s), 699 (m), 658 (w).
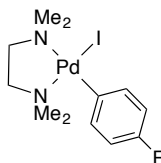
HRESI-MS (MeOH, +, m/z): [(tmeda)Pd(C$_6$H$_5$)I+Na]$^+$ 448.9676, calc. 448.9676; [(tmeda)Pd(C$_6$H$_5$)I+K]$^+$ 464.9499, calc. 464.9416

Elemental analysis (%): C 33.9, H 5.03, N 6.63 calc. C 33.8, H 4.96, N 6.57

M.p.: 173 °C (decomp.)

cis-(tmeda)Pd(_p_-FC$_6$H$_4$)I[55] **(1g)**

[SZ 3063 and AC4073A/4119A]

According to the general procedure, the reaction of Pd$_2$dba$_3$·CHCl$_3$ (1.02 g, 0.99 mmol), TMEDA (0.38 mL, 2.54 mmol) and 4-fluoroiodobenzene (0.33 mL, 2.86 mmol) in toluene (20.0 mL) provided the complex **1g** (0.93 g, 1.97 mmol, 99%) as pale orange solid.

^{1}H NMR (400 MHz, CDCl$_3$): δ 7.15 (dd, J = 8.6, 6.3 Hz, 2 H), 6.71 (dd, J = 9.6, 8.7 Hz, 2 H), 2.72–2.68 (m, 2 H), 2.66 (s, 6 H), 2.57–2.52 (m, 2 H), 2.29 (s, 6 H) ppm.

^{13}C NMR (101 MHz, CDCl$_3$): δ 162.1, 159.8, 136.5, 113.4, 62.2, 58.4, 50.0, 49.9 ppm.

^{19}F NMR (376 MHz, CDCl$_3$): δ −123.83 (dt, J = 14.5, 7.0 Hz) ppm.

IR (ν/cm^{-1}): 2978 (w), 2884 (w), 2836 (w), 2796 (w), 1566 (w), 1473 (m), 1460 (m), 1438 (m), 1406 (w), 1375 (w) , 1248 (w), 1200 (s), 1153 (m), 1128 (w), 1106 (w), 1081 (w), 1068 (w), 1052 (m), 1026 (m), 1007 (m), 959 (m), 937 (w), 815 (s), 805 (s), 775 (m).
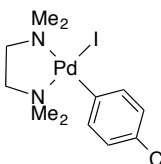
HRESI-MS (MeOH, +, _m/z_): [(tmeda)Pd(_p_-FC$_6$H$_4$)I+Na]$^+$ 466.9590, calc. 466.9582; [(tmeda)Pd(_p_-FC$_6$H$_4$)I+K]$^+$ 482.9318, calc. 482.9322

Elemental analysis (%): C 32.6, H 4.56, N 6.31 calc. C 32.4, H 4.53, N 6.30

M.p.: 145–147 °C (decomp.)

cis-(tmeda)Pd(_p_-ClC$_6$H$_4$)I (1h)

[SZ 3056]

According to the general procedure, the reaction of Pd$_2$dba$_3$·CHCl$_3$ (1.56 g, 1.51 mmol), TMEDA (0.56 mL, 3.74 mmol) and 4-chloroiodobenzene (1.02 g, 4.28 mmol) in toluene (30.0 mL) provided the complex **1h** (1.37 g, 2.96 mmol, 98%) as orange solid.

^{1}H NMR (400 MHz, CDCl$_3$): δ 7.18 (d, J = 8.4 Hz, 2 H), 6.92 (d, J = 8.4 Hz, 2 H), 2.74–2.68 (m, 2 H), 2.67 (s, 6 H), 2.57–2.52 (m, 2H), 2.31 (s, 6 H) ppm.

^{13}C NMR (101 MHz, CDCl$_3$): δ 142.4, 137.4, 129.3, 126.4, 62.3, 58.5, 50.1, 50.0 ppm.

IR (v/cm^{-1}): 2998 (w), 2970 (w), 2884 (w), 2834 (w), 1454 (m), 1431 (w), 1404 (w), 1367 (w), 1279 (w), 1123 (w), 1083 (m), 1063 (w), 1052 (w), 1017 (w), 1004 (m), 955 (m), 932 (w), 908 (w), 800 (s), 768 (m), 731 (w), 719 (w).
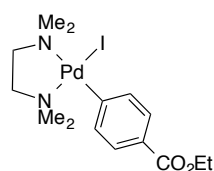
HRESI-MS (MeOH, +, m/z): [(tmeda)Pd(p-ClC$_6$H$_4$)I+Na]$^+$ 484.9294, calc. 484.9291; [(tmeda)Pd(p-ClC$_6$H$_4$)I+K]$^+$ 500.9018, calc. 500.9030

Elemental analysis (%): C 31.2, H 4.36, N 5.78 calc. C 31.3, H 4.37, N 6.08

M.p.: 165 °C (decomp.)

cis-(tmeda)Pd(p-EtO$_2$CC$_6$H$_4$)I[56] (1i)

[SZ 3064 and AC 4074A/4120A/4175A]

According to the general procedure, the reaction of Pd$_2$dba$_3$·CHCl$_3$ (1.02 g, 0.98 mmol), TMEDA (0.38 mL, 2.54 mmol) and ethyl 4-iodobenzoate (0.79 g, 2.87 mmol) in toluene (20.0 mL) provided the complex **1i** (0.87 g, 1.75 mmol, 88%) as pale yellow solid.

^{1}H NMR (400 MHz, CDCl$_3$): δ 7.54 (d, J = 8.4 Hz, 2 H), 7.39 (d, J = 8.4 Hz, 2 H), 4.28 (q, J = 7.1 Hz, 2 H), 2.69–2.66 (m, 2 H), 2.65 (s, 6 H), 2.54–2.50 (m, 2 H), 2.28 (s, 6 H), 1.32 (t, J = 7.1 Hz, 3 H) ppm.

^{13}C NMR (101 MHz, CDCl$_3$): δ 167.8, 156.5, 136.6, 126.6, 125.2, 62.2, 60.4, 58.4, 50.0, 49.9, 14.5 ppm.

IR (v/cm^{-1}): 2989 (w), 2892 (w), 2870 (w), 2838 (w), 1689(m), 1570 (m), 1469 (m), 1385 (w), 1366 (w), 1303 (w), 1277 (s), 1264 (s), 1175 (m), 1104 (m), 1090 (m), 1056 (w), 1014 (m), 956 (m), 932 (w), 834 (w), 799 (s), 761 (s), 698 (w).
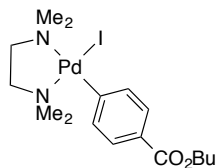
HRESI-MS (MeOH, +, m/z): [(tmeda)Pd(p-EtO$_2$CC$_6$H$_4$)]$^+$ 371.0947, calc. 371.0951; [(tmeda)Pd(p-EtO$_2$CC$_6$H$_4$)I+H]$^+$ 499.0075, calc. 499.0068; [(tmeda)Pd(p-EtO$_2$CC$_6$H$_4$)I+Na]$^+$ 520.9892, calc. 520.9888; [(tmeda)Pd(p-EtO$_2$CC$_6$H$_4$)I+K]$^+$ 536.9628, calc. 536.9627

Elemental analysis (%): C 36.1, H 5.07, N 5.64 calc. C 36.1, H 5.05, N 5.62

M.p.: 180 °C (decomp.)

cis-(tmeda)Pd(*p-^n*BuO$_2$CC$_6$H$_4$)I (1j)

[SZ 3052]

According to the general procedure, the reaction of Pd$_2$dba$_3$·CHCl$_3$ (1.56 g, 1.51 mmol), TMEDA (0.56 mL, 3.74 mmol) and butyl 4-iodobenzoate (1.14 g, 3.74 mmol) in toluene (30.0 mL) provided the complex **1j** (1.19 g, 2.26 mmol, 75%) as pale orange solid.

^{1}H NMR (400 MHz, CDCl$_3$): δ 7.54 (d, J = 8.2 Hz, 2 H), 7.39 (d, J = 8.3 Hz, 2 H), 4.22 (t, J = 6.6 Hz, 2 H), 2.69–2.66 (m, 2 H), 2.65 (s, 6 H), 2.57–2.48 (m, 2 H), 2.28 (s, 6 H), 1.68 (dt, J = 14.5, 6.7 Hz, 2 H), 1.43 (h, J = 7.4 Hz, 2 H), 0.93 (t, J = 7.4 Hz, 3 H) ppm.

^{13}C NMR (101 MHz, CDCl$_3$): δ 167.8, 156.5, 156.4, 136.6, 126.6, 125.3, 64.2, 62.2, 58.4, 50.0, 49.9, 30.9, 19.3, 13.8 ppm.

IR (v/cm^{-1}): 2960 (w), 2889(w), 2873 (w), 2842 (w), 1696 (s), 1574 (m), 1460 (m), 1380 (w), 1277 (s), 1259 (s), 1174 (m), 1116 (m), 1106 (m), 1090 (m), 1050 (w), 1007 (m), 956 (w), 934 (w), 838 (m), 801 (s), 771 (w), 757 (s), 698 (w).
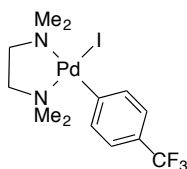
HRESI-MS (MeOH, +, m/z): [(tmeda)Pd(*p-^n*BuO$_2$CC$_6$H$_4$)I+H]$^+$ 527.0406, calc. 527.0381; [(tmeda)Pd(*p-^n*BuO$_2$CC$_6$H$_4$)I+Na]$^+$ 549.0238, calc. 549.0201; [(tmeda)Pd(*p-^n*BuO$_2$CC$_6$H$_4$)I+K]$^+$ 564.9965, calc. 564.9940

Elemental analysis (%): C 38.9, H 5.63, N 5.41 calc. C 38.8, H 5.55, N 5.32

M.p.: 143 °C (decomp.)

cis-(tmeda)Pd(*p-*F$_3$CC$_6$H$_4$)I[54] (1k)

[SZ 3049 and AC 4072A/4118A/4176A]

According to the general procedure, the reaction of Pd$_2$dba$_3$·CHCl$_3$ (3.01 g, 2.90 mmol), TMEDA (1.13 mL, 7.54 mmol) and 4-iodobenzotrifluoride (1.24 mL, 8.41 mmol) in toluene (40.0 mL) provided the complex **1k** (2.34 g, 4.73 mmol, 82%) as yellow solid.

^{1}H NMR (400 MHz, CDCl$_3$): δ 7.42 (d, J = 8.1 Hz, 2 H), 7.15 (d, J = 7.8 Hz, 2 H), 2.76–2.72 (m, 2 H), 2.70 (s, 6 H), 2.60–2.56 (m, 2 H), 2.33 (s, 6 H) ppm.

^{13}C NMR (101 MHz, CDCl$_3$): δ 152.2, 136.7, 125.3 (q, J = 32 Hz), 125.1 (q, J = 271 Hz), 122.5 (q, J = 3.8 Hz), 62.4, 58.5, 50.1, 50.0 ppm.

^{19}F NMR (376 MHz, CDCl$_3$): δ -61.6 ppm.

IR (v/cm^{-1}): 3003 (w), 2978 (w), 2887 (w), 2842 (w), 1584 (m), 1455 (m), 1381 (w), 1318 (m), 1282 (m), 1178 (w), 1153 (m), 1125 (s), 1094 (s), 1069 (s), 1006 (m), 955 (m), 931 (w), 841 (w), 823 (m), 800 (s), 768 (m), 730 (m), 681 (m).
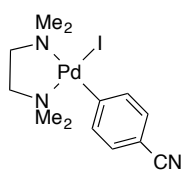
HRESI-MS (MeOH, +, m/z): [(tmeda)Pd(p-F$_3$CC$_6$H$_4$)I+Na]$^+$ 516.9552, calc. 516.9550

Elemental analysis (%): C 31.6, H 4.08, N 5.66 calc. C 31.7, H 4.16, N 5.68

M.p.: 176 °C (decomp.)

cis-(tmeda)Pd(*p*-NCC$_6$H$_4$)I^{54a} (1l)

[SZ 3055 and AC4049B/4066A/4114A]

According to the general procedure, the reaction of Pd$_2$dba$_3$·CHCl$_3$ (1.56 g, 1.51 mmol), TMEDA (0.56 mL, 3.74 mmol) and 4-iodobenzonitrile (0.98 g, 4.30 mmol) in toluene (30.0 mL) provided the complex **1l** (1.17 g, 2.59 mmol, 86%) as tan solid.

^{1}H NMR (400 MHz, CDCl$_3$): δ 7.45 (d, J = 8.3 Hz, 2 H), 7.15 (d, J = 8.3 Hz, 2 H), 2.76–2.71 (m, 2 H), 2.68 (s, 6 H), 2.60–2.55 (m, 2 H), 2.32 (s, 6 H) ppm.

^{13}C NMR (101 MHz, CDCl$_3$): δ 157.1, 137.6, 128.7, 120.2, 106.1, 62.3, 58.5, 50.2, 50.1 ppm.

IR (v/cm^{-1}): 3001 (w), 2973 (w), 2886 (w), 2841 (w), 2218 (m), 1569 (m), 1470 (m), 1453 (m), 1377 (w), 1281 (w), 1171 (w), 1123 (w), 1093 (w), 1064 (w), 1054 (m), 1041 (w), 1011 (m), 955 (m), 929 (w), 818 (s), 802 (s), 268 (m), 713 (w).
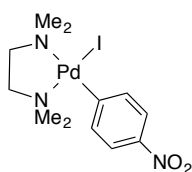
HRESI-MS (MeOH, +, m/z): [(tmeda)Pd(p-NCC$_6$H$_4$)I+Na]$^+$ 473.9633, calc. 473.9629

Elemental analysis (%): C 34.9, H 4.73, N 9.34 calc. C 34.6, H 4.46, N 9.30

M.p.: 169 °C (decomp.)

cis-(tmeda)Pd(*p*-O$_2$NC$_6$H$_4$)I (1m)

[SZ 3062]

According to the general procedure, the reaction of Pd$_2$dba$_3$·CHCl$_3$ (1.03 g, 1.00 mmol), TMEDA (0.38 mL, 2.54 mmol) and 4-iodonitrobenzene (0.70 g, 2.70 mmol) in toluene (20.0 mL) provided the complex **1m** (0.93 g, 1.97 mmol, 99%) as pale orange solid.

^{1}H NMR (400 MHz, CDCl$_3$): δ 7.78 (d, J = 8.8 Hz, 2 H), 7.54 (d, J = 8.8 Hz, 2 H), 2.79–2.74 (m, 2 H), 2.72 (s, 6 H), 2.64–2.58 (m, 2 H), 2.35 (s, 6 H) ppm.

^{13}C NMR (101 MHz, CDCl$_3$): δ 161.7, 145.2, 137.0, 120.1, 62.4, 58.6, 50.3, 50.2 ppm.

IR (v/cm^{-1}): 3005 (w), 2977 (w), 2886 (w), 2840 (w), 1581 (w), 1551 (m), 2499 (m), 1453 (m), 1380 (w), 1337 (s), 1300 (w), 1281 (w), 1170 (w), 1123 (w), 1103 (w), 1087 (w), 1065 (w), 1050 (m), 1015 (w), 1004 (w), 955 (m), 929 (w), 848 (m), 840 (m), 801 (s), 768 (m), 740 (s).

HRESI-MS (MeOH, +, m/z): [(tmeda)Pd(p-O$_2$NC$_6$H$_4$)I+Na]$^+$ 493.9539, calc. 493.9527

Elemental analysis (%): C 30.0, H 4.29, N 8.98 calc. C 30.6, H 4.27, N 8.91

M.p.: 160 °C (decomp.)

4.3.2   *cis*-(dppe)Pd(Ar)X complexes (2,6)

General procedure for the preparation of arylpalladium(II) iodide complexes **2**:

A solution of tmeda-ligated arylpalladium(II) complex **1** (1 equiv.) and dppe (1 equiv.) in DCM was stirred at room temperature for approx. 10 min. Then Et$_2$O (70.0 mL) was added, which resulted in the precipitation of a solid. The supernatant liquid was decanted, the solid washed with Et$_2$O and dried in vacuum.

cis-(dppe)Pd(p-PhOC$_6$H$_4$)I (2c)

[SZ 3068]
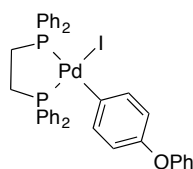
According to the general procedure, the reaction of complex **1c** (518 mg, 1.00 mmol), dppe (412 mg, 1.04 mmol) in DCM (5.00 mL) provided the complex **2c** (810 mg, 1.01 mmol, quant.) as pale orange solid.

^{1}H NMR (400 MHz, CDCl$_3$): δ 7.90 (br t, J = 8.5 Hz, 4 H), 7.50–7.33 (m, 16 H), 7.22 (t, J = 7.9 Hz, 2 H), 7.04 (t, J = 7.8 Hz, 2 H), 6.96 (t, J = 7.3 Hz, 1 H), 6.84 (d, J = 7.6 Hz, 2 H), 6.51 (d, J = 7.8 Hz, 2 H), 2.46–2.32 (m, 2 H), 2.27–2.14 (m, 2 H) ppm.

^{31}P NMR (162 MHz, CDCl$_3$): δ 50.44 (d, J = 27 Hz), 35.63 (d, J = 27.0 Hz) ppm.

IR (ν/cm^{-1}): 3062 (w), 3039 (w), 3013 (w), 2944 (w), 2914 (w), 1588 (w), 1569 (w), 1472 (m), 1434 (m), 1410 (w), 1213 (m), 1196 (m), 1160 (m), 1100 (m), 1068 (w), 1045 (w), 1010 (w), 998 (w), 907 (w), 874 (m), 857 (m), 835 (m), 821 (m), 783 (m), 746 (s), 692 (s), 675 (m).
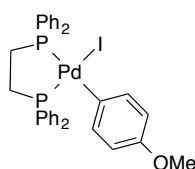
HRESI-MS (DCM/MeOH, +, m/z): [(dppe)Pd(p-PhOC$_6$H$_4$)]$^+$ 673.0999, calc. 673.1041

Elemental analysis (%): C 57.0, H 4.42 calc. C 57.0, H 4.15

M.p.: 165 °C (decomp.)

cis-(dppe)Pd(*p*-MeOC$_6$H$_4$)I[53b] (2d)

[SZ 3069 and AC4121B/4177B]

According to the general procedure, the reaction of complex **1d** (456 mg, 1.00 mmol), dppe (401 mg, 1.01 mmol) in DCM (5.00 mL) provided the complex **2d** (735 mg, 1.00 mmol, quant.) as pale yellow solid.

^{1}H NMR (400 MHz, CDCl$_3$): δ 7.90 (tt, J = 7.6, 2.3 Hz, 4 H), 7.48–7.29 (m, 16 H), 6.92 (td, J = 8.6, 2.2 Hz, 2 H), 6.42 (dd, J = 8.5, 1.9 Hz, 2 H), 3.61 (s, 3 H), 2.36 (dt, J = 27.1, 7.5 Hz, 2 H), 2.29–2.14 (m, 2 H) ppm.

^{31}P NMR (162 MHz, CDCl$_3$): δ 49.91 (d, J = 26 Hz), 35.21 (d, J = 26 Hz) ppm.

IR (ν/cm^{-1}): 3059 (vw), 3004 (vw), 2923 (vw), 2828(vw), 1573 (w), 1477 (m), 1433 (m), 1413 (w), 1306 (w), 1259 (m), 1231 (s), 1173 (m), 1102 (m), 1023 (m), 1002 (m), 931 (w), 876 (m), 849 (w), 820 (m), 803 (m), 782 (w), 749 (s), 739 (m), 704 (s), 689 (s), 675 (s).
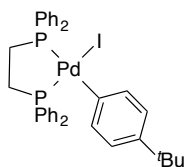
HRESI-MS (DCM/MeOH, +, m/z): [(dppe)Pd(p-MeOC$_6$H$_4$)]$^+$ 611.0868, calc. 611.0885; [(dppe)Pd(I)]$^+$ 630.9407, calc. 630.9433; [(dppe)Pd(p-MeOC$_6$H$_4$)I+Na]$^+$ 760.9791, calc. 760.9822

Elemental analysis (%): C 53.7, H 4.36 calc. C 53.6, H 4.23

M.p.: 144 °C (decomp.)

cis-(dppe)Pd(*p*-^{t}BuC$_6$H$_4$)I (2e)

[SZ 3070 and 4050A/4117B]

According to the general procedure, the reaction of complex **1e** (486 mg, 1.01 mmol), dppe (424 mg, 1.06 mmol) in DCM (5.00 mL) provided the complex **2e** (717 mg, 0.94 mmol, 93%) as tan solid. Crystallization from a solution in DCM by slow diffusion with pentane provided single crystals suitable for X-ray crystallographic analysis.

^{1}H NMR (400 MHz, CD_2Cl_2): δ 7.95–7.88 (m, 4H), 7.54–7.43 (m, 8H), 7.38–7.27 (m, 8H), 6.96 (td, J = 8.1, 2.4 Hz, 2H), 6.81 (dd, J = 8.0, 2.4 Hz, 2H), 2.51–2.34 (m, 2H), 2.31–2.10 (m, 2H), 1.21 (s, 9H) ppm.

^{31}P NMR (162 MHz, CD_2Cl_2): δ 49.20 (d, J = 28 Hz), 33.49 (d, J = 28 Hz) ppm.

IR (v/cm^{-1}): 3053(w), 2955 (w), 2899 (w), 2863 (w), 1481 (m), 1434 (m), 1408 (w), 1360 (w), 1307 (w), 1264 (w), 1183 (w), 1100 (m), 1028 (w), 1007 (m), 875 (m), 824 (m), 810 (m), 746 (m), 723 (w), 712 (s), 690 (s), 656 (w).
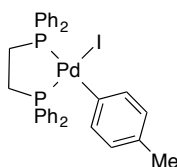
HRESI-MS (DCM/MeOH, +, m/z): [(dppe)Pd(p-^{t}BuC$_6$H$_4$)]$^{+}$ 637.1376, calc. 637.1405; [(dppe)Pd(p-^{t}BuC$_6$H$_4$)I+Na]$^{+}$ 787.0298, calc. 787.0342

Elemental analysis (%): C 56.7, H 4.94 calc. C 56.5, H 4.88

M.p.: 137 °C (decomp.)

cis-(dppe)Pd(p-MeC$_6$H$_4$)I[53b] (2f)

[SZ 3071 and AC 4047A/4115B]

According to the general procedure, the reaction of complex **1f** (446 mg, 1.01 mmol), dppe (420 mg, 1.05 mmol) in DCM (5.00 mL) provided the complex **2f** (736 mg, 1.02 mmol, quant.) as pale yellow solid.

^{1}H NMR (400 MHz, CDCl$_3$): δ 7.95–7.84 (m, 4 H), 7.49–7.41 (m, 8 H), 7.41–7.27 (m, 8 H), 6.93 (t, J = 7.1 Hz, 2 H), 6.58 (d, J = 7.3 Hz, 2 H), 2.43–2.28 (m, 2 H), 2.29–2.13 (m, 2 H), 2.09 (s, 3 H) ppm.

^{31}P NMR (162 MHz, CDCl$_3$): δ 49.32 (d, J = 28 Hz), 34.44 (d, J = 28 Hz) ppm.

IR (v/cm^{-1}): 3048 (w), 3006 (w), 2938 (w), 2912 (w), 1572 (w), 1478 (m), 1434 (s), 1406 (w), 1307 (w), 1234 (w), 1206 (w), 1183 (w), 1160 (w), 1099 (s), 1051 (w), 1027 (w), 1010 (m), 998 (m), 879 (m), 825 (m), 791 (s), 740 (s), 703 (s), 688 (s), 657 (s).

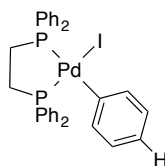HRESI-MS (DCM/MeOH, +, m/z): [(dppe)Pd(p-MeC$_6$H$_4$)]$^{+}$ 595.0910, calc. 595.0936; [(dppe)Pd(p-MeC$_6$H$_4$)I+Na]$^{+}$ 744.9835, calc. 744.9873; [(dppe)Pd(p-MeC$_6$H$_4$)I+K]$^{+}$ 760.9574, calc. 760.9612

Elemental analysis (%): C 54.9, H 4.64 calc. C 54.8, H 4.32

M.p.: 143 °C (decomp.)

cis-(dppe)Pd(C$_6$H$_5$)I[53d, 53e] (2a)

[SZ 3072 and AC 4048A/4116B]

According to the general procedure, the reaction of complex **1a** (283 mg, 0.66 mmol), dppe (270 mg, 0.68 mmol) in DCM (5.00 mL) provided the complex **2a** (469 mg, 0.66 mmol, quant.) as pale yellow solid.

^{1}H NMR (400 MHz, CDCl$_3$): δ 7.90 (ddd, J = 9.9, 5.6, 2.2 Hz, 4 H), 7.50–7.41 (m, 8 H), 7.40–7.28 (m, 8 H), 7.07 (td, J = 6.9, 3.8 Hz, 2 H), 6.73 (td, J = 7.4, 2.6 Hz, 2 H), 6.64 (t, J = 6.7 Hz, 1 H), 2.46–2.28 (m, 2 H), 2.29–2.12 (m, 2 H) ppm.

^{31}P NMR (162 MHz, CDCl$_3$): δ 49.55 (d, J = 28 Hz), 34.54 (d, J = 28 Hz) ppm.

IR (v/cm^{-1}): 3048 (w), 2968 (vw), 2909 (vw), 1562 (w), 1481 (w), 1468 (w), 1434 (m), 1404 (w), 1308 (w), 1185 (w), 1157 (w), 1102 (m), 1056 (w), 1015 (w), 995 (w), 874 (m), 819 (m), 744 (m), 726 (m), 689 (s), 675 (s).
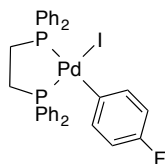
HRESI-MS (DCM/MeOH, +, *m/z*): [(dppe)Pd(C$_6$H$_5$)]$^+$ 581.0738, calc. 581.0779; [(dppe)Pd(C$_6$H$_5$)I+Na]$^+$ 730.9665, calc. 730.9716

Elemental analysis (%): C 54.7, H 4.46 calc. C 54.2, H 4.12

M.p.: 179–181 °C (decomp.)

cis-(dppe)Pd(*p*-FC$_6$H$_4$)I (2g)

[SZ 3074 and AC 4119B]

According to the general procedure, the reaction of complex **1g** (445 mg, 1.00 mmol), dppe (399 mg, 1.00 mmol) in DCM (5.00 mL) provided the complex **2g** (640 mg, 0.88 mmol, 88%) as pale yellow solid. Crystallization from a solution in DCM by slow diffusion with pentane provided single crystals suitable for X-ray crystallographic analysis.

¹H NMR (400 MHz, CD$_2$Cl$_2$): δ 7.89 (ddt, J = 10.7, 7.6, 1.5 Hz, 4 H), 7.56–7.45 (m, 8 H), 7.45–7.33 (m, 8 H), 6.97 (qt, J = 8.3, 1.8 Hz, 2 H), 6.52 (ddd, J = 10.4, 8.6, 2.0 Hz, 2 H), 2.43 (dtd, J = 27.6, 8.4, 8.0, 5.2 Hz, 2 H), 2.25 (dtd, J = 28.0, 8.8, 8.1, 5.5 Hz, 2 H) ppm.

³¹P NMR (162 MHz, CD$_2$Cl$_2$): δ 51.46 (d, J = 26 Hz), 37.03 (d, J = 26 Hz) ppm.

¹⁹F NMR (376 MHz, CD$_2$Cl$_2$): δ –124.28 ppm.

IR (v/cm⁻¹): 3046 (w), 3017 (w), 2954 (w), 2915 (w), 1569 (w), 1476 (m), 1435 (m), 1402 (w), 1310 (w), 1214 (m), 1155 (m), 1106 (m), 1079 (w), 1058 (w), 1044 (w), 1027 (w), 1014 (w), 998 (w), 874 (m), 818 (m), 801 (m), 743 (s), 706 (s), 687 (s).
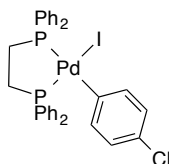
HRESI-MS (DCM/MeOH, +, m/z): [(dppe)Pd(p-FC$_6$H$_4$)]⁺ 599.0659, calc. 599.0685; [(dppe)Pd(p-FC$_6$H$_5$)I+Na]⁺ 748.9586, calc. 748.9622

Elemental analysis (%): C 52.9, H 4.02 calc. C 52.9, H 3.88

M.p.: 168 °C (decomp.)

cis-(dppe)Pd(p-ClC$_6$H$_4$)I⁵³ᵇ (2h)

[SZ 3075]

According to the general procedure, the reaction of complex **1h** (462 mg, 1.00 mmol), dppe (400 mg, 1.00 mmol) in DCM (5.00 mL) provided the complex **2h** (312 mg, 0.42 mmol, 42%) as pale yellow solid.

¹H NMR (400 MHz, CDCl$_3$): δ 7.88 (ddd, J = 10.2, 7.3, 2.1 Hz, 4H), 7.50–7.42 (m, 8H), 7.41–7.30 (m, 8H), 6.98 (td, J = 8.1, 2.1 Hz, 2H), 6.72 (dd, J = 8.3, 2.2 Hz, 2H), 2.46–2.31 (m, 2H), 2.31–2.14 (m, 2H) ppm.

³¹P NMR (162 MHz, CDCl$_3$): δ 50.82 (d, J = 27 Hz), 36.47 (d, J = 27 Hz) ppm.

IR (v/cm⁻¹): 3050 (w), 1483 (w), 1466 (w), 1435 (m), 1409 (w), 1309 (w), 1186 (w), 1160 (w), 1102 (m), 1084 (m), 1026 (w), 1004 (m), 877 (w), 800 (m), 743 (m), 691 (s).

HRESI-MS (DCM/MeOH, +, m/z): [(dppe)Pd(p-ClC$_6$H$_4$)]⁺ 617.0439, calc. 617.0394; [(dppe)$_2$Pd(p-ClC$_6$H$_5$)]⁺ 1015.1790, calc. 1015.1747; [(dppe)$_2$Pd$_2$(p-ClC$_6$H$_5$)$_2$I]⁺ 1358.9844, calc. 1358.9828

Elemental analysis (%): C 52.0, H 4.07 calc. C 51.7, H 3.80

M.p.: 124–126 °C (decomp.)

cis-(dppe)Pd(p-EtO₂CC₆H₄)I (2i)

cis-(dppe)Pd(*p*-EtO$_2$CC$_6$H$_4$)I (2i)

[SZ 3077 and AC 4120B/4175B]
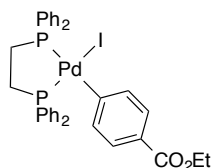
According to the general procedure, the reaction of complex **1i** (500 mg, 1.00 mmol), dppe (400 mg, 1.00 mmol) in DCM (5.00 mL) provided the complex **2i** (769 mg, 0.98 mmol, 98%) as pale yellow solid.

^{1}H NMR (400 MHz, CD$_2$Cl$_2$): δ 7.94–7.85 (m, 4 H), 7.57–7.45 (m, 8 H), 7.45–7.32 (m, 10 H), 7.21 (tt, J = 8.1, 1.9 Hz, 2 H), 4.24 (q, J = 7.1 Hz, 2 H), 2.45 (dtd, J = 28.2, 8.8, 5.4 Hz, 2 H), 2.27 (dtd, J = 28.2, 8.7, 8.2, 5.5 Hz, 2 H), 1.30 (t, J = 7.1 Hz, 3 H) ppm.

^{31}P NMR (162 MHz, CD$_2$Cl$_2$): δ 50.96 (dd, J = 26 Hz), 36.96 (d, J = 26 Hz) ppm.

IR (v/cm^{-1}): 3053 (w), 2984 (w), 2943 (w), 1699 (s), 1577 (m), 1482 (w), 1433 (m), 1388 (w), 1366 (w), 1305 (w), 1282 (s), 1173 (m), 1112 (s), 1100 (s), 1050 (w), 1013 (m), 998 (w), 869 (m), 838 (m), 819 (m), 783 (w), 747 (s), 739 (s), 690 (s), 674 (s).

HRESI-MS (DCM/MeOH, +, *m/z*): [(dppe)Pd(*p*-Et$_2$OCC$_6$H$_4$)]$^+$ 653.1025, calc. 653.0991; [(dppe)Pd(*p*-Et$_2$OCC$_6$H$_5$)I+Na]$^+$ 802.9970, calc. 802.9928; [(dppe)$_2$Pd$_2$(*p*-Et$_2$OCC$_6$H$_5$)$_2$I]$^+$ 1435.1088, calc. 1435.1030

Elemental analysis (%): C 53.9, H 4.54 calc. C 53.8, H 4.26

M.p.: 166–168 °C (decomp.)

cis-(dppe)Pd(*p*-^{n}BuO$_2$CC$_6$H$_4$)I (2j)

[SZ 3076]
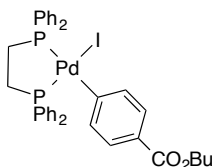
According to the general procedure, the reaction of complex **1j** (528 mg, 1.00 mmol), dppe (400 mg, 1.00 mmol) in DCM (5.00 mL) provided the complex **2j** (793 mg, 0.98 mmol, 98%) as pale yellow solid.

^{1}H NMR (400 MHz, CD$_2$Cl$_2$): δ 7.91 (t, J = 8.9 Hz, 4 H), 7.58–7.46 (m, 8 H), 7.45–7.32 (m, 10 H), 7.23 (t, J = 7.9 Hz, 2 H), 4.20 (t, J = 6.5 Hz, 2 H), 2.55–2.35 (m, 2 H), 2.35–2.19 (m, 2 H), 1.69 (p, J = 6.8 Hz, 2 H), 1.45 (h, J = 7.4 Hz, 2 H), 0.96 (t, J = 7.4 Hz, 3 H) ppm.

^{31}P NMR (162 MHz, CD$_2$Cl$_2$): δ 51.06 (d, J = 26 Hz), 36.93 (d, J = 26 Hz) ppm.

IR (v/cm^{-1}): 3051 (w), 2958 (w), 2929 (w), 2868 (w), 1697 (s), 1574 (m), 1484 (w), 1434 (m), 1410 (w), 1383 (w), 1285 (s), 1261 (m), 1178 (m), 1133 (w), 1103 (s), 1066 (w), 1028 (w), 1012 (m), 999 (w), 971 (w), 875 (m), 845 (m), 835 (m), 820 (m), 808 (m), 753 (s), 740 (s), 690 (s), 676 (s).

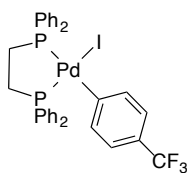HRESI-MS (DCM/MeOH, +, m/z): [(dppe)Pd(p-^{n}Bu$_2$OCC$_6$H$_4$)]$^+$ 831.0276, calc. 831.0241; [(dppe)$_2$Pd$_2$(p- ^{n}Bu$_2$OCC$_6$H$_5$)$_2$I]$^+$ 1491.1696, calc. 1491.1656; [(dppe)$_2$Pd$_2$(p- ^{n}Bu$_2$OCC$_6$H$_5$)$_2$I$_2$+Na]$^+$ 1641.0612, calc. 1641.0593

Elemental analysis (%): C 55.0, H 5.00 calc. C 54.9, H 4.61

M.p.: 158–160 °C (decomp.)

cis-(dppe)Pd(p-F$_3$CC$_6$H$_4$)I (2k)

[SZ 3050 and AC 4118B/4176B]

According to the general procedure, the reaction of complex **1k** (107 mg, 0.22 mmol), dppe (86.7 mg, 0.22 mmol) in DCM (3.00 mL) provided the complex **2k** (140 mg, 0.18 mmol, 83%) as pale yellow solid.

^{1}H NMR (400 MHz, CDCl$_3$): δ 7.94–7.85 (m, 4 H), 7.53–7.43 (m, 8 H), 7.39–7.29 (m, 8 H), 7.21 (t, J = 7.5 Hz, 2 H), 6.93 (d, J = 7.7 Hz, 2 H), 2.40 (dq, J = 26.1, 7.7, 7.0 Hz, 2 H), 2.23 (dtd, J = 28.0, 8.8, 8.0, 5.3 Hz, 2 H) ppm.

^{31}P NMR (162 MHz, CDCl$_3$): δ 50.97 (d, J = 27 Hz), 36.24 (d, J = 27 Hz) ppm.

^{19}F NMR (376 MHz, CDCl$_3$): δ –61.69 ppm.

IR (v/cm^{-1}): 3063 (w), 3043 (w), 3013 (w), 2949 (w), 2913 (w), 1586 (m), 1482 (w), 1433 (m), 1412 (w),1385 (w), 1325 (s), 1269 (w), 1159 (m), 1099 (s), 1091 (s), 1065 (s), 1041 (w), 1027 (w), 1007 (m), 875 (m), 848 (w), 823 (s), 813 (s), 750 (s), 742 (m), 725 (w), 703 (s), 690 (s), 677 (s).

HRESI-MS (DCM/MeOH, +, m/z): [(dppe)Pd(p-F$_3$CC$_6$H$_4$)]$^+$ 649.0680, calc. 649.0653; [(dppe)Pd(p-F$_3$CC$_6$H$_5$)I+Na]$^+$ 798.9618, calc. 798.9590; [(dppe)$_2$Pd$_2$(p- F$_3$CC$_6$H$_5$)$_2$I]$^+$ 1427.0393, calc. 1427.0355; [(dppe)$_2$Pd$_2$(p- F$_3$CC$_6$H$_5$)$_2$I$_2$+Na]$^+$ 1576.9309, calc. 1576.9292

Elemental analysis (%): C 51.1, H 3.97 calc. C 51.0, H 3.63

M.p.: 163–164 °C (decomp.)

cis-(dppe)Pd(*p*-NCC₆H₄)I (2l)

cis-(dppe)Pd(p-NCC$_6$H$_4$)I (2l)

[SZ 3078 and AC 4049A/4114B]
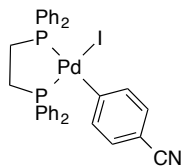
According to the general procedure, the reaction of complex **1l** (453 mg, 1.00 mmol), dppe (400 mg, 1.00 mmol) in DCM (5.00 mL) provided the complex **2l** (665 mg, 0.91 mmol, 91%) as pale yellow solid.

^{1}H NMR (400 MHz, CD$_2$Cl$_2$): δ 7.88 (ddd, J = 10.2, 7.5, 1.8 Hz, 4 H), 7.59–7.47 (m, 8 H), 7.46–7.35 (m, 8 H), 7.25 (td, J = 7.9, 1.8 Hz, 2 H), 6.94 (dd, J = 8.0, 2.2 Hz, 2 H), 2.46 (dtd, J = 27.8, 8.5, 8.0, 5.2 Hz, 2 H), 2.35–2.19 (m, 2 H) ppm.

^{31}P NMR (162 MHz, CD$_2$Cl$_2$): δ 52.00 (d, J = 26 Hz), 38.11 (d, J = 26 Hz) ppm.

IR (v/cm^{-1}): 3049 (w), 2954 (w), 2913 (w), 2221 (m), 1574 (m), 1483 (w), 1473 (w), 1434 (m), 1404 (w), 1310 (w), 1233 (w), 1181 (w), 1159 (w), 1104 (m), 1059 (w), 1047 (w), 1026 (w), 1013 (w), 998 (w), 873 (m), 820 (m), 808 (s), 743 (s), 705 (s), 687 (s), 675 (s).

HRESI-MS (DCM/MeOH, +, m/z): [(dppe)Pd(p-NCC$_6$H$_4$)]$^+$ 606.0750, calc. 606.0732; [(dppe)Pd(p-NCC$_6$H$_5$)I+Na]$^+$ 755.9680, calc. 755.9669; [(dppe)$_2$Pd$_2$(p-NCC$_6$H$_5$)$_2$I]$^+$ 1341.0502, calc. 1341.0512; [(dppe)$_2$Pd$_2$(p-NCC$_6$H$_5$)$_2$I$_2$+Na]$^+$ 1490.9432, calc. 1490.9449

Elemental analysis (%): C 54.3, H 4.38, N 1.93 calc. C 54.0, H 3.85, N 1.91

M.p.: 167–168 °C (decomp.)

cis-(dppe)Pd(p-O$_2$NC$_6$H$_4$)I (2m)

[SZ 3079]
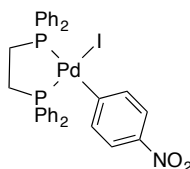
According to the general procedure, the reaction of complex **1m** (472 mg, 1.00 mmol), dppe (399 mg, 1.00 mmol) in DCM (5.00 mL) provided the complex **2m** (694 mg, 0.92 mmol, 92%) as pale yellow solid.

^{1}H NMR (400 MHz, CD$_2$Cl$_2$): δ 7.89 (ddt, J = 10.9, 6.3, 1.8 Hz, 4 H), 7.58–7.47 (m, 8 H), 7.46–7.35 (m, 10 H), 7.32 (ddd, J = 8.8, 7.2, 1.7 Hz, 2 H), 2.55–2.38 (m, 2 H), 2.37–2.20 (m, 2 H) ppm.

^{31}P NMR (162 MHz, CD$_2$Cl$_2$): δ 52.22 (d, J = 25 Hz), 38.72 (d, J = 25 Hz) ppm.

IR (v/cm^{-1}): 3053 (w), 3024 (w), 2959 (w), 2902 (w), 1584 (w), 1555 (w), 1498 (m), 1435 (m), 1399 (w), 1332 (s), 1180 (w), 1101 (m), 1044 (w), 1010 (w), 998 (w), 872 (m), 848 (m), 833 (m), 816 (m), 754 (m), 737 (s), 711 (m), 690 (s), 676 (s).
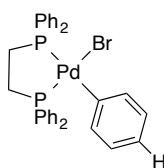
HRESI-MS (DCM/MeOH, +, m/z): [(dppe)Pd(p-O$_2$NC$_6$H$_4$)]$^+$ 626.0662, calc. 626.0630; [(dppe)Pd(p-O$_2$NC$_6$H$_5$)I+Na]$^+$ 775.9597, calc. 775.9569; [(dppe)$_2$Pd$_2$(p-O$_2$NC$_6$H$_5$)$_2$I]$^+$ 1381.0334, calc. 1381.0309; [(dppe)$_2$Pd$_2$(p-O$_2$NC$_6$H$_5$)$_2$I$_2$+Na]$^+$ 1530.9251, calc. 1530.9246

Elemental analysis (%): C 51.0, H 3.94, N 1.88 calc. C 51.0, H 3.74, N 1.86

M.p.: 161–163 °C (decomp.)

cis-(dppe)Pd(C$_6$H$_5$)Br (6a)

[SZ 4016.a]

[(Po-tol$_3$)Pd(Ph)Br]$_2$ (**5a**) (56.9 mg, 0.050 mmol) and dppe (40.8 mg, 0.102 mmol) were dissolved in DCM (ca. 2.00 mL) and stirred at room temperature for 20 min. Then a mixture of Et$_2$O (20.0 mL) and pentane (20.0 mL) was added, which resulted in the formation of a precipitation. The supernatant liquid was decanted and the solid washed with additional Et$_2$O. After drying into vacuum, complex **6a** (60.2 mg, 0.091 mmol, 91%) was isolated as a colorless solid.

^{1}H NMR (400 MHz, CD$_2$Cl$_2$): δ 7.99–7.88 (m, 4 H), 7.54–7.31 (m, 16 H), 7.03 (tdq, J = 7.6, 2.7, 1.5 Hz, 2 H), 6.80–6.67 (m, 2 H), 2.57–2.37 (m, 2 H), 2.30–2.11 (m, 2 H) ppm.

^{31}P NMR (162 MHz, CD$_2$Cl$_2$): δ 52.15 (d, J = 27 Hz), 33.60 (d, J = 27 Hz) ppm.

IR (v/cm^{-1}): 3052 (w), 1563 (w), 1470 (w), 1434 (m), 1403 (w), 1308 (w), 1185 (w), 1102 (m), 1056 (w), 1016 (w), 995 (w), 878 (w), 820 (m), 762 (w), 748 (m), 728 (s), 692 (s), 677 (m).
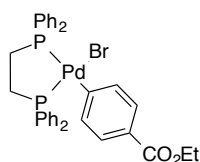
HRESI-MS (MeOH, +, m/z): [(dppe)Pd(C$_6$H$_5$)]$^+$ 581.0828, calc. 581.0774;

Elemental analysis (%): C 58.1, H 4.53, calc. C 58.1, H 4.42

M.p.: 170 °C (decomp.)

cis-(dppe)Pd(p-EtO$_2$CC$_6$H$_4$)Br (6i)

[SZ 4158, SZ 4124]

[(Po-tol$_3$)Pd(p-EtO$_2$CC$_6$H$_4$)Br]$_2$ (**5i**) (163 mg, 0.13 mmol) and dppe (105 mg, 0.27 mmol) were dissolved in DCM (ca. 2.00 mL) and stirred at room temperature for 10 min. Then a mixture of Et$_2$O (20.0 mL) and pentane (20.0 mL) were added, which resulted in the formation of a precipitate. The supernatant liquid was decanted and the solid washed with additional Et$_2$O. After drying into vacuum, complex **6i** (160 mg, 0.21 mmol, 82%) was isolated as a colorless solid.

^{1}H NMR (400 MHz, CDCl$_3$): δ 8.20–7.80 (m, 4H), 7.50–7.29 (m, 18H), 7.19 (td, J = 8.2, 2.3 Hz, 2H), 4.24 (q, J = 7.1 Hz, 2H), 2.47 (ddd, J = 27.8, 14.0, 8.7 Hz, 2H), 2.22 (dq, J = 27.5, 7.7 Hz, 2H), 1.30 (t, J = 7.1 Hz, 3H) ppm.

^{31}P NMR (162 MHz, CDCl$_3$): δ 52.50 (d, J = 27.2 Hz), 34.09 (d, J = 27.2 Hz) ppm.

IR (v/cm^{-1}): 3060 (w), 979 (w), 2943 (w), 2909 (w), 1693 (s), 1574 (m), 1475 (w), 1435 (m), 1414 (w), 1382 (w), 1365 (w), 1279 (s), 1176 (m), 1102 (s), 1011 (m), 875 (w), 836 (w), 819 (w), 746 (s), 691 (s).

HRESI-MS (MeOH, +, m/z): [(dppe)Pd(p-EtO$_2$CC$_6$H$_4$)]$^+$ 653.1017, calc. 653.0991; [(dppe)$_2$Pd$_2$(p-EtO$_2$CC$_6$H$_4$)$_2$Br]$^+$ 1387.1197, calc. 1387.1169

Elemental analysis (%): C 57.5, H 4.93, calc. C 57.3, H 4.53

M.p.: 160 °C (decomp.)

cis-(dppe)Pd(p-BuO$_2$CC$_6$H$_4$)Br (6j)

[SZ 4128A]
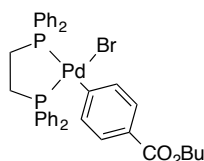
A solution of *trans*-[(Py)$_2$Pd(p-BuO$_2$CC$_6$H$_4$)Br] (**11j**) (208 mg, 0.40 mmol) and dppe (163 mg, 0.41 mmol) in DCM (2.50 mL) was stirred at room temperature for 10 min, the reaction solution was concentrated and Et$_2$O (40.0 mL) was added, which resulted in precipitation of a colorless solid. The solid was washed with Et$_2$O and dried in vacuum. The complex **6j** (303 mg, 0.40 mmol, quant.) was obtained as colorless solid.

^{1}H NMR (400 MHz, CDCl$_3$): δ 7.94 (d, J = 8.0 Hz, 4H), 7.51–7.28 (m, 14H), 7.19 (t, J = 6.8 Hz, 2H), 4.19 (t, J = 6.6 Hz, 2H), 2.59–2.37 (m, 2H), 2.30–2.14 (m, 2H), 1.66 (dt, J = 14.7, 6.7 Hz, 2H), 1.41 (dq, J = 14.7, 7.4 Hz, 2H), 0.93 (t, J = 7.4 Hz, 3H) ppm.

^{31}P NMR (162 MHz, CDCl$_3$): δ 52.52 (d, J = 26.9 Hz), 34.06 (d, J = 26.8 Hz) ppm.

IR (v/cm^{-1}): 3053 (w), 2949 (w), 1690 (m), 1574 (m), 1484 (w), 1435 (m), 1382 (w), 1306 (w), 1282 (s), 1176 (m), 1102 (s), 1012 (m), 940 (w), 873 (w), 844 (w), 818 (m), 749 (s), 691 (s).
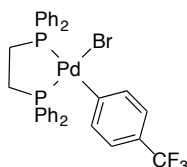
HRESI-MS (MeOH, +, m/z): [(dppe)Pd(p-BuO$_2$CC$_6$H$_4$)]$^+$ 681.1308, calc. 681.1304

Elemental analysis (%): C 58.4, H 4.99, calc. C 58.3, H 4.89

M.p.: 135–140 °C (decomp.)

cis-(dppe)Pd(p-F$_3$CC$_6$H$_4$)Br[53b] (6k)

[SZ 4016.b]

Trans-(PPh$_3$)$_2$Pd(p-F$_3$CC$_6$H$_4$)Br (**9k**) (86.0 mg, 0.10 mmol) and dppe (41.0 mg, 0.103 mmol) were dissolved in DCM (ca. 2.00 mL) and the solution stirred at room temperature for 20 min. Then a mixture of Et$_2$O (20.0 mL) and pentane (20.0 mL) were added, which resulted in the formation of a precipitate. The supernatant liquid was decanted and the solid washed with additional Et$_2$O. After drying into vacuum, complex **6k** (52.7 mg, 0.072 mmol, 72%) was isolated as a colorless solid.

^{1}H NMR (400 MHz, CD$_2$Cl$_2$): δ 7.97–7.88 (m, 4 H), 7.58–7.45 (m, 8 H), 7.45–7.32 (m, 8 H), 7.20 (dddd, J = 8.5, 7.6, 2.1, 0.9 Hz, 2 H), 6.96 (ddq, J = 7.4, 2.4, 0.9 Hz, 2 H), 2.59–2.43 (m, 2 H), 2.31–2.16 (m, 2 H) ppm.

^{31}P NMR (162 MHz, CD$_2$Cl$_2$): δ 53.56 (d, J = 26 Hz), 35.47 (d, J = 26 Hz) ppm.

^{19}F NMR (376 MHz, CD$_2$Cl$_2$): δ –62.07 ppm.

IR (v/cm^{-1}): 3049 (w), 2966 (w), 1582 (m), 1481 (w), 1434 (m), 1405 (w), 1383 (w), 1317 (s), 1186 (w), 1156 (m), 1104 (s), 1068 (s), 1010 (m), 876 (m), 818 (s), 743 (m), 715 (m), 689 (s), 656 (w).

HRESI-MS (MeOH, +, m/z): [(dppe)Pd(p-FC$_3$C$_6$H$_4$)]$^+$ 649.0683, calc. 649.0648;

Elemental analysis (%): C 54.4, H 3.97, calc. C 54.3, H 3.87

M.p.: 175 °C (decomp.)

4.3.3   *cis*-(dppf)Pd(Ar)X complexes (3,7)

General procedure A for the preparation of arylpalladium(II) iodide complexes **3**:

A solution of tmeda-ligated arylpalladium(II) complex **1** (1 equiv.) and dppf (1 equiv.) in DCM was stirred at room temperature for approx. 10 min. Then Et$_2$O (70.0 mL) was added, which resulted in precipitation of a solid. The supernatant liquid was decanted, the solid washed with Et$_2$O and dried in vacuum.

General procedure B for the preparation of arylpalladium(II) bromide complexes **7**:

A solution of P(*o*-tol)$_3$-ligated arylpalladium(II) complex **5** (1 equiv.) and dppf (2 equiv.) in DCM was stirred at room temperature for approx. 20 min. Then Et$_2$O (70.0 mL) was added, which resulted in precipitation of a solid. After the mixture has been stirring for 2 h at room temperature, the supernatant liquid was decanted, the solid washed with Et$_2$O and dried in vacuum.

cis-(dppf)Pd(*p*-MeOC$_6$H$_4$)I[57] (3d)

[SZ 4025/5011]
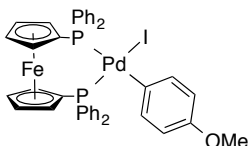
According to the general procedure A, the reaction of complex **1d** (230 mg, 0.50 mmol) and dppf (284 mg, 0.51 mmol) in DCM (ca. 10.0 mL) provided complex **3d** (366 mg, 0.41 mmol, 81%) as yellow, microcrystalline solid.

^{1}H NMR (400 MHz, CD$_2$Cl$_2$): δ 8.03 (ddd, *J* = 9.8, 6.5, 3.1 Hz, 4 H), 7.56–7.47 (m, 6 H), 7.37 (dq, *J* = 15.1, 7.5 Hz, 6 H), 7.18 (dt, *J* = 7.6, 3.9 Hz, 4 H), 6.75–6.69 (m, 2 H), 6.22 (d, *J* = 6.9 Hz, 2 H), 4.66–4.60 (m, 2 H), 4.47 (s, 2 H), 4.15 (s, 2 H), 3.76–3.69 (m, 2 H), 3.55 (s, 3 H) ppm.

^{31}P NMR (162 MHz, CD$_2$Cl$_2$): δ 26.88 (d, *J* = 33 Hz), 8.70 (d, *J* = 33 Hz) ppm.

IR (v/cm^{-1}): 3075 (w), 2989 (w), 2828 (w), 1478 (m), 1434 (m), 1385 (w), 1306 (w), 1267 (w), 1230 (m), 1176 (m), 1166 (m), 1094 (m), 1032 (m), 1006 (w), 846 (w), 822 (w), 801 (m), 751 (m), 738 (m), 690 (s).

HRESI-MS (CH$_3$CN, +, *m/z*): [(dppf)Pd(*p*-MeOC$_6$H$_4$)]$^+$ 767.0579, calc. 767.0542

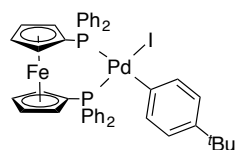Elemental analysis (%): C 53.8, H 4.29 calc. C 55.0, H 3.94

A better elemental analysis could not be obtained.

M.p.: 164–169 °C (decomp.)

cis-(dppf)Pd(*p*-^{t}BuC$_6$H$_4$)I (3e)

[SZ 4152A]

According to the general procedure A, the reaction of complex **1e** (483 mg, 1.03 mmol) and dppf (554 mg, 1.02 mmol) in DCM (ca. 10.0 mL) provided complex **3e** (912 mg, 0.99 mmol, 98%) as orange solid.

^{1}H NMR (400 MHz, CDCl$_3$): δ 8.09–7.98 (m, 4H), 7.51–7.43 (m, 6H), 7.39–7.32 (m, 4H), 7.32–7.26 (m, 2H), 7.10 (td, J = 8.0, 2.3 Hz, 4H), 6.84 (td, J = 8.3, 2.4 Hz, 2H), 6.59 (ddd, J = 8.5, 2.5, 0.9 Hz, 2H), 4.65 (q, J = 2.1 Hz, 2H), 4.50–4.43 (m, 2H), 4.13–4.10 (m, 2H), 3.66 (q, J = 1.8 Hz, 2H), 1.10 (s, 9H) ppm.

^{31}P NMR (162 MHz, CDCl$_3$): δ 27.21 (d, J = 34.9 Hz), 8.17 (d, J = 34.9 Hz) ppm.

IR (ν/cm^{-1}): 3052 (w), 2954 (w), 2863 (w), 1480 (m), 1434 (m), 1385 (w), 1360 (w), 1307 (w), 1267 (w), 1193 (w), 1165 (m), 1095 (m), 1027 (w), 1005 (m), 837 (w), 804 (m), 743 (m), 722 (w), 691 (s).

HRESI-MS (MeOH, +, m/z): [(dppf)Pd(p-^{t}BuC$_6$H$_4$)]$^+$ 793.1115, calc. 793.1068

Elemental analysis (%): C 56.4, H 4.65 calc. C 57.4, H 4.49

A better elemental analysis could not be obtained.

M.p.: 136–138 °C (decomp.)

cis-(dppf)Pd(p-MeC$_6$H$_4$)I[53b, 57] (3f)

[SZ 4027/5013]
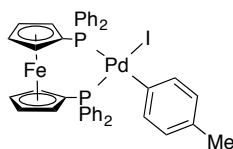
According to the general procedure A, the reaction of complex **1f** (363 mg, 0.82 mmol), dppf (281 mg, 0.51 mmol) in DCM (5.00 mL) provided the complex **3f** (414 mg, 0.47 mmol, 93%) as yellow solid.

^{1}H NMR (400 MHz, CDCl$_3$): δ 8.08–7.99 (m, 4 H), 7.47 (dt, J = 5.0, 1.9 Hz, 6 H), 7.42–7.27 (m, 6 H), 7.12 (td, J = 8.1, 2.3 Hz, 4 H), 6.77 (td, J = 7.9, 2.3 Hz, 2 H), 6.39 (d, J = 5.7 Hz, 2 H), 4.62 (q, J = 2.1 Hz, 2 H), 4.49–4.41 (m, 2 H), 4.16–4.09 (m, 2 H), 3.72 (q, J = 1.8 Hz, 2 H), 2.01 (s, 3 H) ppm.

^{31}P NMR (162 MHz, CDCl$_3$): δ 26.49 (d, J = 35 Hz), 8.45 (d, J = 35 Hz) ppm.

IR (ν/cm^{-1}): 3054 (w), 2996 (w), 2913 (w), 2859 (w), 1478 (m), 1433 (m), 1383 (w), 1300 (w), 1187 (w), 1160 (m), 1096 (m), 1052 (m), 1038 (w), 1025 (w), 1009 (w), 998 (w), 843 (w), 824 (m), 787 (s), 745 (s), 693 (s).

HRESI-MS (CH$_3$CN, +, m/z): [(dppf)Pd(p-MeC$_6$H$_4$)]$^+$ 751.0587, calc. 751.0593; [(dppf)$_2$Pd$_2$(p-MeC$_6$H$_4$)$_2$I]$^+$ 1631.0162, calc. 1631.0240

Elemental analysis (%): C 56.3, H 4.03 calc. C 56.0, H 4.01

M.p.: 165–168 °C (decomp.)

cis-(dppf)Pd(C$_6$H$_5$)I[57] (3a)

[SZ 4152B]
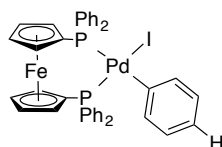
According to the general procedure A, the reaction of complex **1a** (427 mg, 1.00 mmol), dppf (554 mg, 1.01 mmol) in DCM (5.00 mL) provided the complex **3a** (843 mg, 0.97 mmol, 97%) as yellow solid.

^{1}H NMR (400 MHz, CDCl$_3$): δ 8.05 (br s, 4H), 7.47 (br s, 6H), 7.41–7.28 (m, 6H), 7.12 (t, J = 6.8 Hz, 4H), 6.95 (t, J = 7.2 Hz, 2H), 6.54 (t, J = 6.2 Hz, 2H), 6.43 (t, J = 7.0 Hz, 3H), 4.64 (s, 2H), 4.47 (s, 2H), 4.13 (s, 2H), 3.69 (s, 2H) ppm.

^{31}P NMR (162 MHz, CDCl$_3$): δ 27.13 (d, J = 34.6 Hz), 8.58 (d, J = 34.3 Hz) ppm.

IR (v/cm^{-1}): 3049 (w), 1558 (w), 1479 (w), 1467 (w), 1434 (m), 1188 (w), 1160 (w) 1096 (m), 1054 (w), 1037 (w), 1024 (w), 1014 (w), 993 (w), 887 (w), 823 (m), 747 (m), 721 (m), 690 (s).

HRESI-MS (MeOH, +, m/z): [(dppf)Pd(C$_6$H$_5$)]$^+$ 737.0493, calc. 737.0436

Elemental analysis (%): C 55.3, H 4.02 calc. C 55.6, H 3.85

M.p.: 139–141 °C (decomp.)

cis-(dppf)Pd(*p*-FC$_6$H$_4$)I (3g)

[SZ 4028/5014]
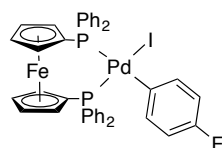
According to the general procedure A, the reaction of complex **1g** (364 mg, 0.82 mmol), dppe (280 mg, 0.51 mmol) in DCM (5.00 mL) provided the complex **3g** (427 mg, 0.48 mmol, 97%) as yellow powder. Crystallization from a solution in DCM by slow diffusion with pentane provided single crystals suitable for X-ray crystallographic analysis.

^{1}H NMR (400 MHz, CDCl$_3$): δ 8.03 (ddd, J = 9.7, 6.5, 2.9 Hz, 4 H), 7.53–7.44 (m, 6 H), 7.42–7.30 (m, 6 H), 7.20–7.11 (m, 4 H), 6.84 (q, J = 6.7 Hz, 2 H), 6.35 (t, J = 8.4 Hz, 2 H), 4.67–4.63 (m, 2 H), 4.48 (s, 2 H), 4.14 (s, 2 H), 3.72–3.67 (m, 2 H), 3.48 (q, J = 7.0 Hz, 2 H) ppm.

^{31}P NMR (162 MHz, CDCl$_3$): δ 27.07 (d, J = 33 Hz), 9.09 (d, J = 33 Hz) ppm.

^{19}F NMR (376 MHz, CDCl$_3$): δ –125.21 ppm

IR (v/cm^{-1}): 3060 (w), 1473 (m), 1434 (m), 1384 (w), 1301 (w), 1206 (m), 1152 (m), 1096 (m), 1038 (w), 1025 (w), 998 (w), 889 (w), 824 (m), 803 (s), 745 (s), 694 (s).

HRESI-MS (CH$_3$CN, +, m/z): [(dppf)Pd(p-FC$_6$H$_4$)]$^+$ 755.0355, calc. 755.0342; [(dppf)$_2$Pd$_2$(p-FC$_6$H$_4$)$_2$I]$^+$ 1638.9706, calc. 1638.9738

Elemental analysis (%): C 54.6, H 3.68 calc. C 54.4, H 3.65

M.p.: 175–180 °C (decomp.)

cis-(dppf)Pd(p-EtO$_2$CC$_6$H$_4$)I (3i)

[SZ 4026]
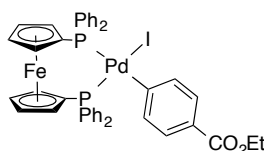
According to the general procedure A, the reaction of complex **1i** (250 mg, 0.50 mmol), dppe (278 mg, 0.50 mmol) in DCM (5.00 mL) provided the complex **3i** (446 mg, 0.48 mmol, 95%) as yellow powder.

^{1}H NMR (400 MHz, CDCl$_3$): δ 8.03 (ddd, J = 9.9, 5.8, 2.9 Hz, 4 H), 7.50–7.47 (m, 6 H), 7.39–7.28 (m, 6 H), 7.19 (dd, J = 8.2, 2.4 Hz, 2 H), 7.15–7.05 (m, 6 H), 4.66 (q, J = 2.1 Hz, 2 H), 4.48 (s, 2 H), 4.23 (q, J = 7.1 Hz, 2 H), 4.17–4.12 (m, 2 H), 3.72–3.68 (m, 2 H), 1.28 (t, J = 7.1 Hz, 3 H) ppm.

^{31}P NMR (162 MHz, CDCl$_3$): δ 26.56 (d, J = 33 Hz), 9.14 (d, J = 33 Hz) ppm.

IR (v/cm^{-1}): 3076 (w), 1698 (s), 1576 (m), 1478 (w), 1434 (m), 1385 (w), 1365 (w), 1279 (m), 1177 (m), 1012 (m), 921 (w), 824 (w), 749 (s), 691 (s).

HRESI-MS (CH$_3$CN, +, m/z): [(dppf)Pd(p-EtO$_2$CC$_6$H$_4$)]$^+$ 809.0650, calc. 809.0648

Elemental analysis (%): C 55.2, H 4.01 calc. C 55.1, H 3.98

M.p.: 201–204 °C (decomp.)

cis-(dppf)Pd(p-F$_3$CC$_6$H$_4$)I[54b] (3k)

[SZ 4029]
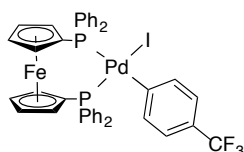
According to the general procedure A, the reaction of complex **1k** (393 mg, 0.79 mmol), dppe (286 mg, 0.52 mmol) in DCM (5.00 mL) provided the complex **3k** (435 mg, 0.47 mmol, 90%) as yellow powder.

^{1}H NMR (400 MHz, CDCl$_3$): δ 8.03 (ddd, J = 9.9, 6.6, 3.1 Hz, 4 H), 7.49 (dt, J = 3.9, 2.2 Hz, 6 H), 7.39–7.30 (m, 6 H), 7.12 (qd, J = 8.7, 8.3, 4.7 Hz, 6 H), 6.75 (d, J = 7.5 Hz, 2 H), 4.67 (q, J = 2.1 Hz, 2 H), 4.50 (t, J = 1.8 Hz, 2 H), 4.15 (t, J = 1.9 Hz, 2 H), 3.68 (q, J = 1.9 Hz, 2 H) ppm.

^{31}P NMR (162 MHz, CDCl$_3$): δ 27.13 (d, J = 34 Hz), 9.23 (d, J = 34 Hz) ppm.

^{19}F NMR (376 MHz, CDCl$_3$): δ –61.69 ppm

IR (v/cm^{-1}): 3076 (w), 1587 (m), 1480 (w), 1437 (m), 1387 (w), 1324 (s), 1191 (w), 1149 (m), 1110 (s), 1095 (m), 1070 (s), 1038 (w), 1025 (w), 1009 (m), 845 (w), 809 (m), 750 (m), 738 (m), 722 (w), 692 (s).

HRESI-MS (CH$_3$CN, +, m/z): [(dppf)Pd(p-F$_3$CC$_6$H$_4$)]$^+$ 805.0318, calc. 805.0310

Elemental analysis (%): C 52.9, H 3.56 calc. C 52.8, H 3.46

M.p.: 203–207 °C (decomp.)

cis-(dppf)Pd(p-NCC$_6$H$_4$)I (3l)

[SZ 4030]
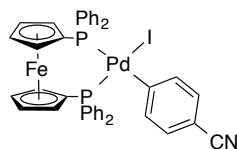
According to the general procedure A, the reaction of complex **1l** (369 mg, 0.82 mmol), dppe (280 mg, 0.51 mmol) in DCM (5.00 mL) provided the complex **3l** (452 mg, 0.51 mmol, quant.) as yellow powder.

^{1}H NMR (400 MHz, CDCl$_3$): δ 8.01 (ddd, J = 9.8, 6.5, 3.0 Hz, 4 H), 7.49 (dq, J = 4.5, 2.6, 2.1 Hz, 6 H), 7.40–7.31 (m, 6 H), 7.14 (tdd, J = 7.1, 4.2, 2.1 Hz, 6 H), 6.76 (dd, J = 8.1, 2.4 Hz, 2 H), 4.68 (q, J = 2.1 Hz, 2 H), 4.51 (t, J = 1.9 Hz, 2 H), 4.16 (t, J = 2.0 Hz, 2 H), 3.66 (q, J = 1.9 Hz, 2 H) ppm.

^{31}P NMR (162 MHz, CDCl$_3$): δ 27.01 (d, J = 32 Hz), 9.63 (d, J = 32 Hz) ppm.

IR (v/cm^{-1}): 3078 (w), 2974 (w), 2217 (m), 1574 (m), 1471 (m) 1435 (m), 1386 (w), 1308 (w), 1197 (w), 1181 (w), 1166 (m), 1095 (m), 1037 (w), 1014 (m), 998 (w), 845 (w), 821 (m), 801 (s), 749 (s), 691 (s).

HRESI-MS (CH$_3$CN, +, m/z): [(dppf)Pd(p-NCC$_6$H$_4$)]$^+$ 762.0407, calc. 762.0389; [(dppf)$_2$Pd$_2$(p-CNC$_6$H$_4$)$_2$I]$^+$ 1652.9832, calc. 1652.9835

Elemental analysis (%): C 55.5, H 3.81, N 1.63 calc. C 55.3, H 3.62, N 1.57

M.p.: 208–211 °C (decomp.)

cis-(dppf)Pd(p-MeOC₆H₄)Br⁶⁴ (7d) → *cis*-(dppf)Pd(*p*-MeOC$_6$H$_4$)Br[64] **(7d)**

[SZ 4031]
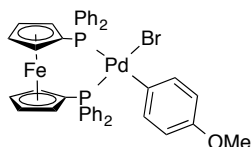
According to the general procedure B, the reaction of complex **5d** (423 mg, 0.35 mmol) and dppf (277 mg, 0.50 mmol) in DCM (10.0 mL) provided complex **7d** (373 mg, 0.44 mmol, 88%) was isolated as an orange solid.

^{1}H NMR (400 MHz, CDCl$_3$): δ 8.06 (ddd, *J* = 9.8, 6.6, 3.0 Hz, 4H), 7.46 (dt, *J* = 3.9, 2.1 Hz, 6H), 7.41–7.29 (m, 6H), 7.13 (td, *J* = 7.7, 2.4 Hz, 4H), 6.79 (ddd, *J* = 7.6, 6.3, 2.6 Hz, 2H), 6.26 (dd, *J* = 8.6, 2.2 Hz, 2H), 4.66 (q, *J* = 2.1 Hz, 2H), 4.47 (t, *J* = 1.8 Hz, 2H), 4.14 (t, *J* = 1.9 Hz, 2H), 3.65 (q, *J* = 1.8 Hz, 2H), 3.56 (s, 3H) ppm.

^{31}P NMR (162 MHz, CDCl$_3$): δ 30.71 (d, *J* = 33 Hz), 9.50 (d, *J* = 33 Hz) ppm.

IR (v/cm^{-1}): 3053 (w), 2830 (w), 1567 (w), 1478 (m), 1434 (m) 1385 (w), 1305 (w), 1269 (w), 1229 (m), 1176 (m), 1166 (m), 1094 (m) 1030 (m), 1006 (w), 847 (w), 803 (m), 751 (m), 690 (s).

HRESI-MS (CH$_3$CN, +, *m/z*): [(dppf)Pd(*p*-MeOC$_6$H$_4$)]$^+$ 767.0564, calc. 767.0542

Elemental analysis (%): C 58.1, H 4.23 calc. C 58.1, H 4.16

M.p.: 168–170 °C (decomp.)

cis-(dppf)Pd(p-ᵗBuC₆H₄)Br (7e) → *cis*-(dppf)Pd(*p*-^{t}BuC$_6$H$_4$)Br **(7e)**

[SZ 4163]
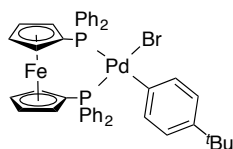
According to the general procedure B, the reaction of complex **11e** (240 mg, 0.50 mmol) and dppf (283 mg, 0.51 mmol) in DCM (10.0 mL) provided complex **7e** (445 mg, 0.51 mmol, quant.) was isolated as a red solid.

^{1}H NMR (400 MHz, CDCl$_3$): δ 8.08 (ddd, *J* = 9.9, 6.6, 3.0 Hz, 4H), 7.48–7.45 (m, 6H), 7.42–7.32 (m, 6H), 7.10 (td, *J* = 8.0, 2.3 Hz, 4H), 6.85 (td, *J* = 8.2, 3.1 Hz, 2H), 6.61 (dd, *J* = 8.0, 2.2 Hz, 2H), 4.68 (q, *J* = 1.9 Hz, 2H), 4.54–4.33 (m, 2H), 4.19–4.05 (m, 2H), 3.60 (q, *J* = 1.7 Hz, 2H), 1.10 (s, 9H) ppm.

^{31}P NMR (162 MHz, CDCl$_3$): δ 50.9 (d, *J* = 34 Hz), 9.00 (d, *J* = 34 Hz) ppm.

The complex **7e** decomposes rapidly in solution.

IR (v/cm^{-1}): 3051 (w), 2952 (w), 2863 (w), 1480 (w), 1434 (m), 1385 (w), 1360 (w), 1306 (w), 1266 (w), 1193 (w), 1165 (m), 1096 (m) 1027 (m), 1006 (m), 805 (m), 742 (m), 722 (m), 691 (s).

HRESI-MS (CH$_3$CN, +, m/z): [(dppf)Pd(p-MeOC$_6$H$_4$)]$^+$ 793.1095, calc. 793.1068

Elemental analysis (%): C 60.7, H 4.73 calc. C 60.5, H 4.73

M.p.: 110 °C (decomp.)

cis-(dppf)Pd(*p*-MeC$_6$H$_4$)Br (7f)

[SZ 4043]
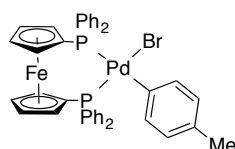
According to the general procedure B, the reaction of complex **5f** (293 mg, 0.25 mmol) and dppf (282 mg, 0.51 mmol) in DCM (5.00 mL) provided the complex **7f** (374 mg, 0.45 mmol, 89%) as yellow powder.

^{1}H NMR (400 MHz, CDCl$_3$): δ 8.06 (ddt, J = 9.8, 6.5, 3.0 Hz, 4 H), 7.46 (dp, J = 6.0, 2.1 Hz, 6 H), 7.40–7.27 (m, 6 H), 7.11 (td, J = 7.6, 2.4 Hz, 4 H), 6.80 (td, J = 7.9, 2.9 Hz, 2 H), 6.41 (dd, J = 7.9, 2.6 Hz, 2 H), 4.65 (q, J = 2.1 Hz, 2 H), 4.47 (t, J = 1.9 Hz, 2 H), 4.14 (t, J = 1.9 Hz, 2 H), 3.65 (q, J = 1.8 Hz, 2 H), 2.00 (s, 3 H) ppm.

^{31}P NMR (162 MHz, CDCl$_3$): δ 30.36 (d, J = 34 Hz), 9.24 (d, J = 34 Hz) ppm.

IR (v/cm^{-1}): 3049 (w), 1583 (w), 1478 (m), 1435 (m), 1385 (w), 1306 (m), 1193 (w), 1179 (w), 1165 (m), 1054 (w), 1033 (m), 1009 (m), 890 (w), 833 (w), 819 (m), 783 (m), 743 (s), 691 (s).

HRESI-MS (CH$_3$CN, +, m/z): [(dppf)Pd(p-MeC$_6$H$_4$)]$^+$ 751.0625, calc. 751.0593; [(dppf)$_2$Pd$_2$(p-MeC$_6$H$_4$)$_2$Br]$^+$ 1583.0391, calc. 1583.0378

Elemental analysis (%): C 59.4, H 4.21 calc. C 59.2, H 4.24

M.p.: 186–190 °C (decomp.)

cis-(dppf)Pd(C$_6$H$_5$)Br[64] (7a)

[SZ 3047/4018/4153]
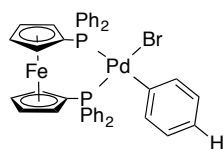
According to the general procedure B, the reaction of complex **5a** (57.4 mg, 0.051 mmol) and dppf (57.6 mg, 0.104 mmol) in DCM (2.00 mL) provided the complex **7a** (70.7 mg, 0.086 mmol, 86%) as yellow powder.

^{1}H NMR (400 MHz, CDCl$_3$): δ 8.07 (ddd, J = 9.7, 6.6, 3.0 Hz, 4 H), 7.46 (dq, J = 6.5, 2.8, 2.3 Hz, 6 H), 7.40–7.33 (m, 4 H), 7.30 (td, J = 7.3, 1.7 Hz, 2 H), 7.12 (dt, J = 7.7, 3.9 Hz, 4 H), 6.99–6.92 (m, 2 H), 6.57 (td, J = 7.5, 2.6 Hz, 2 H), 6.52–6.46 (m, 1 H), 4.67 (q, J = 2.1 Hz, 2 H), 4.48 (t, J = 1.8 Hz, 2 H), 4.14 (t, J = 1.9 Hz, 2 H), 3.63 (q, J = 1.9 Hz, 2 H) ppm.

^{31}P NMR (162 MHz, CDCl$_3$): δ 30.78 (d, J = 34 Hz), 9.35 (d, J = 34 Hz) ppm.

IR (v/cm^{-1}): 3049 (w), 1558 (w), 1481 (w), 1467 (w), 1433 (m), 1386 (w), 1301 (w), 1265 (w), 1193 (w), 1164 (m), 1098 (m), 1056 (w), 1038 (w), 1027 (w), 1015 (w), 993 (w), 823 (m), 741 (m), 723 (m), 689 (s).

HRESI-MS (CH$_3$CN, +, m/z): [(dppf)Pd(C$_6$H$_5$)]$^+$ 737.0446, calc. 737.0436; [(dppf)$_2$Pd$_2$(C$_6$H$_5$)$_2$Br]$^+$ 1555.0020, calc. 1555.0065

Elemental analysis (%): C 58.9, H 2.76 calc. C 58.8, H 4.07

A better elemental analysis could not be obtained.

M.p.: 179–181 °C (decomp.)

***cis*-(dppf)Pd(*p*-FC$_6$H$_4$)Br**[64] **(7g)**

[SZ 4032]
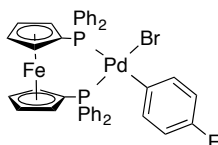
According to the general procedure B, the reaction of complex **5g** (310 mg, 0.26 mmol) and dppf (298 mg, 0.54 mmol) in DCM (5.00 mL) provided the complex **7g** (396 mg, 0.47 mmol, 89%) as yellow powder. Crystallization from a solution in DCM by slow diffusion with pentane provided single crystals suitable for X-ray crystallographic analysis.

^{1}H NMR (400 MHz, CDCl$_3$): δ 8.08–8.02 (m, 4 H), 7.47 (dt, J = 4.3, 2.1 Hz, 6 H), 7.40–7.29 (m, 6 H), 7.15 (td, J = 8.0, 2.4 Hz, 4 H), 6.87 (tdd, J = 8.7, 6.5, 2.3 Hz, 2 H), 6.40–6.33 (m, 2 H), 4.68 (q, J = 2.1 Hz, 2 H), 4.49 (t, J = 1.9 Hz, 2 H), 4.15 (t, J = 1.9 Hz, 2 H), 3.63 (q, J = 1.8 Hz, 2 H) ppm.

^{31}P NMR (162 MHz, CDCl$_3$): δ 30.97 (d, J = 32 Hz), 10.00 (d, J = 32 Hz) ppm.

^{19}F NMR (376 MHz, CDCl$_3$): δ –124.45 ppm

IR (v/cm^{-1}): 3062 (w), 1563 (w), 1473 (m), 1433 (m), 1384 (w), 1300 (w), 1206 (m), 1162 (m), 1151 (m), 1097 (m), 1047 (w), 1037 (w), 1025 (w), 998 (w), 888 (w), 845 (w), 823 (m), 803 (m), 745 (s), 693 (s).

HRESI-MS (CH$_3$CN, +, m/z): [(dppf)Pd(p-FC$_6$H$_4$)]$^+$ 755.0414, calc. 755.0342; [(dppf)$_2$Pd$_2$(p-FC$_6$H$_4$)$_2$Br]$^+$ 1588.9993, calc. 1588.9873

Elemental analysis (%): C 57.6, H 3.98 calc. C 57.5, H 3.86

M.p.: 181–184 °C (decomp.)

cis-(dppf)Pd(p-EtO$_2$CC$_6$H$_4$)Br (7i)

[SZ 4040/5030]
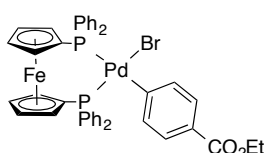
According to the general procedure B, the reaction of complex **5i** (320 mg, 0.25 mmol) and dppf (278 mg, 0.50 mmol) in DCM (5.00 mL) provided the complex **7i** (408 mg, 0.46 mmol, 92%) as yellow solid.

Alternatively, a solution of *trans*-[(Py)$_2$Pd(p-EtO$_2$CC$_6$H$_4$)Br] (**11i**) (123 mg, 0.25 mmol) and dppf (139 mg, 0.0.25 mmol) in DCM (2.50 mL) was stirred at room temperature for 10 min, the reaction solution was concentrated and Et$_2$O (20.0 mL) was added, which resulted in precipitation of yellow solid. The solid was washed with Et$_2$O and dried in vacuum. The complex **7i** (210 mg, 0.24 mmol, 94%) was obtained as colorless solid.

^{1}H NMR (400 MHz, CDCl$_3$): δ 8.05 (ddd, J = 9.9, 6.6, 3.0 Hz, 4 H), 7.48 (dq, J = 4.2, 1.9 Hz, 6 H), 7.40–7.28 (m, 6 H), 7.25–7.21 (m, 2 H), 7.10 (dddd, J = 10.4, 7.6, 4.5, 2.4 Hz, 6 H), 4.68 (q, J = 2.0 Hz, 2 H), 4.50 (t, J = 1.8 Hz, 2 H), 4.23 (q, J = 7.1 Hz, 2 H), 4.16 (t, J = 1.9 Hz, 2 H), 3.64 (q, J = 1.8 Hz, 2 H), 1.28 (t, J = 7.1 Hz, 3 H) ppm.

^{31}P NMR (162 MHz, CDCl$_3$): δ 30.52 (d, J = 33 Hz), 10.09 (d, J = 33 Hz) ppm.

IR (v/cm^{-1}): 3054 (w), 1697 (m), 1571 (m), 1480 (w), 1434 (w), 1362 (w), 1279 (s), 1169 (m), 1099 (s), 1039 (w), 1028 (w), 1009 (w), 997 (w), 847 (w), 824 (w), 744 (s), 690 (s).

HRESI-MS (CH$_3$CN, +, m/z): [(dppf)Pd(p-EtO$_2$CC$_6$H$_4$)]$^+$ 809.0681, calc. 809.0648

Elemental analysis (%): C 58.1 H 4.24 calc. C 58.0, H 4.19

M.p.: 195–200 °C (decomp.)

cis-(dppf)Pd(p-BUO₂CC₆H₄)Br (7j)

[SZ 4128B]
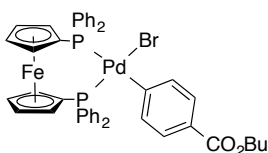
A solution of *trans*-[(Py)₂Pd(*p*-BuO₂CC₆H₄)Br] (**10j**) (214 mg, 0.41 mmol) and dppf (224 mg, 0.40 mmol) in DCM (5.00 mL) was stirred at room temperature for 10 min, the reaction solution was concentrated and Et₂O (40.0 mL) was added, which resulted in precipitation of an orange solid. The solid was washed with Et₂O and dried in vacuum. The complex **7j** (376 mg, 0.41 mmol, quant.) was obtained as orange solid.

^{1}H NMR (400 MHz, CDCl₃): δ 8.05 (ddd, J = 9.9, 6.6, 3.0 Hz, 4H), 7.57–7.44 (m, 6H), 7.40–7.27 (m, 6H), 7.22 (dd, J = 8.3, 1.7 Hz, 2H), 7.14–7.05 (m, 6H), 4.69 (q, J = 2.1 Hz, 2H), 4.50 (s, 2H), 4.24–4.11 (m, 4H), 3.64 (d, J = 1.8 Hz, 2H), 1.70–1.60 (m, 2H), 1.40 (dq, J = 14.5, 7.4 Hz, 2H), 0.93 (t, J = 7.4 Hz, 3H) ppm.

^{31}P NMR (162 MHz, CDCl₃): δ 30.54 (d, J = 33 Hz), 10.05 (d, J = 33 Hz) ppm.

IR (v/cm^{-1}): 3056 (w), 2985 (w), 1698 (m), 1572 (m), 1481 (w), 1434 (m) 1363 (w), 1280 (s), 1172 (m), 1100 (s), 1011 (w), 825 (w), 747 (s), 690 (s).

HRESI-MS (CH₃CN, +, *m/z*): [(dppf)Pd(*p*-BuO₂CC₆H₄)]$^+$ 837.0988, calc. 837.0966

Elemental analysis (%): C 60.7, H 4.77 calc. C 58.9, H 4.50

A better elemental analysis could not be obtained.

M.p.: 158–160 °C (decomp.)

cis-(dppf)Pd(p-F₃CC₆H₄)Br[53f, 64] **(7k)**

[SZ 4039]
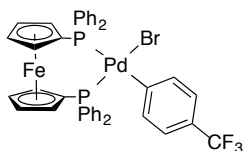
According to the general procedure B, the reaction of complex **5k** (320 mg, 0.25 mmol) and dppf (284 mg, 0.51 mmol) in DCM (5.00 mL) provided the complex **7k** (336 mg, 0.38 mmol, 75%) as yellow powder.

^{1}H NMR (400 MHz, CDCl₃): δ 8.06 (ddd, J = 9.8, 6.6, 3.0 Hz, 4 H), 7.48 (dt, J = 4.4, 2.1 Hz, 6 H), 7.39–7.29 (m, 6 H), 7.12 (dq, J = 8.4, 2.9 Hz, 6 H), 6.78 (dd, J = 8.2, 2.2 Hz, 2 H), 4.70 (q, J = 2.0 Hz, 2 H), 4.51 (t, J = 1.8 Hz, 2 H), 4.16 (t, J = 1.9 Hz, 2 H), 3.63 (q, J = 1.8 Hz, 2 H) ppm.

^{31}P NMR (162 MHz, CDCl$_3$): δ 30.99 (d, J = 33 Hz), 10.24 (d, J = 33 Hz) ppm.

^{19}F NMR (376 MHz, CDCl$_3$): δ –61.80 ppm

IR (v/cm^{-1}): 3050 (w), 1583 (m), 1482 (w), 1435 (m), 1384 (w), 1322 (s), 1153 (m) 1108 (s), 1094 (s), 1066 (s), 1034 (m), 1007 (m), 821 (m), 806 (m), 743 (s), 723 (w), 692 (s).

HRESI-MS (CH$_3$CN, +, m/z): [(dppf)Pd(p-F$_3$CC$_6$H$_4$)]$^+$ 805.0352, calc. 805.0310; [(dppf)$_2$Pd$_2$(p-F$_3$CC$_6$H$_4$)$_2$Br]$^+$ 1690.9842, calc. 1690.9813

Elemental analysis (%): C 55.8, H 3.71 calc. C 55.6, H 3.64

M.p.: 203–205 °C (decomp.)

cis-(dppf)Pd(p-NCC$_6$H$_4$)Br[64] (7l)

[SZ 4041]
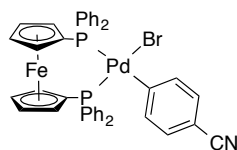
According to the general procedure B, the reaction of complex **5l** (299 mg, 0.25 mmol) and dppf (283 mg, 0.51 mmol) in DCM (5.00 mL) provided the complex **7l** (409 mg, 0.49 mmol, 96%) as yellow powder.

^{1}H NMR (400 MHz, CDCl$_3$): δ 8.07–7.99 (m, 4 H), 7.48 (dt, J = 5.1, 2.0 Hz, 6 H), 7.39–7.31 (m, 6 H), 7.18–7.10 (m, 6 H), 6.82–6.77 (m, 2 H), 4.70 (q, J = 2.0 Hz, 2 H), 4.53 (t, J = 1.8 Hz, 2 H), 4.19–4.14 (m, 2 H), 3.61 (p, J = 1.6 Hz, 2 H) ppm.

^{31}P NMR (162 MHz, CDCl$_3$): δ 30.96 (d, J = 32 Hz), 10.69 (d, J = 32 Hz) ppm.

IR (v/cm^{-1}): 3078 (w), 2973 (w), 2218 (m), 1575 (m), 1479 (m), 1436 (m), 1386 (w), 1307 (w), 1195 (w), 1167 (m), 1095 (s), 1037 (w), 1015 (w), 997 (w), 847 (w), 822 (w), 801 (s), 750 (s), 692 (s).

HRESI-MS (CH$_3$CN, +, m/z): [(dppf)Pd(p-NCC$_6$H$_4$)]$^+$ 762.0387, calc. 762.0389; [(dppf)$_2$Pd$_2$(p-NCC$_6$H$_4$)$_2$Br]$^+$ 1604.9923, calc. 1604.9970

Elemental analysis (%): C 58.4, H 3.94 calc. C 58.4, H 3.83

M.p.: 205–210 °C (decomp.)

4.3.4   dimeric [P(o-tol)₃]Pd(Ar)X]₂ complexes (4,5)

General procedure:

Similar to the previous reported procedure,[62] a 100 mL Schlenk flask was charged with $Pd_2dba_3 \cdot CHCl_3$ (1 equiv.) and P(*o*-tol)₃ (4 equiv.). The flask was sealed with a rubber septum and set under an atmosphere of argon by cycled evacuation and backfilling with argon. Dry toluene (60.0 mL) and 4-bromoanisole (15–20 equiv.) were syringed into the flask. The deep purple reaction mixture was stirred at room temperature until the color remarkably changed indicating consumption of the $Pd_2dba_3 \cdot CHCl_3$ (approx. 3 h). The reaction solution was diluted with DCM and filtered through a pad of celite, the filter was rinsed with DCM and the combined filtrates were concentrated in vacuum. Upon addition of Et₂O and additional stirring at room temperature for 4 h, the supernatant liquid was decanted from the formed solid and the solid washed with Et₂O.

[(P*o*-tol₃)Pd(C₆H₅)I]₂ (4a)

[SZ 3155]
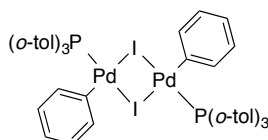
Similar to the general procedure, the reaction of $Pd_2dba_3 \cdot CHCl_3$ (521 mg, 0.50 mmol), P(*o*-tol)₃ (510 mg, 1.68 mmol) and iodobenzene (0.60 mL, 5.38 mmol) in toluene at room temperature for 2 h provided **4a** (527 mg, 0.86 mmol, 86%) as orange insoluble solid.

IR (v/cm^{-1}): 2359 (w), 1589 (w), 1561 (m), 1466 (m), 1445 (m), 1381 (w), 1272 (w), 1200 (w), 1164 (w), 1131 (w), 1056 (w), 1033 (w), 1016 (m), 890 (w), 804 (m), 752 (m), 728 (s), 715 (m), 692 (m), 675 (w).

HRESI-MS (CH₃CN, +, m/z): [P(*o*-tol)₃Pd(C₆H₅)]⁺ 487.0844, calc. 487.0807;

[P(*o*-tol)₃Pd(C₆H₅)(MeCN)]⁺ 528.1100, calc. 528.1072

Elemental analysis (%): C 52.8, H 4.27 calc. C 52.8, H 4.27

M.p.: 191–195 °C (decomp.)

[(P*o*-tol₃)Pd(*p*-MeOC₆H₄)Br]₂[62, 65] (5d)

[SZ 4021]
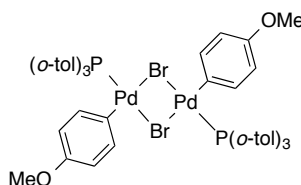
According to the general procedure, the reaction of Pd$_2$dba$_3$·CHCl$_3$ (1.57 g, 1.52 mmol), P(o-tol)$_3$ (1.84 g, 6.05 mmol) and 4-bromoanisole (3.59 mL, 30.0 mmol) in toluene (60.0 mL) provided the complex **5d** (1.32 g, 1.11 mmol, 73%) as an orange solid.

IR (v/cm^{-1}): 3058 (w), 2923 (w), 590 (w), 1577 (w), 1562 (w), 1479 (m), 1440 (m), 1380 (w), 1270 (s), 1234 (s), 1200 (w), 1175 (m), 1132 (w), 1067 (w), 1028 (m), 1002 (m), 955 (w), 821 (m), 806 (m), 752 (s), 716 (m), 678 (w).

HRESI-MS (CH$_3$CN, +, m/z): [(Po-tol$_3$)Pd(p-MeOC$_6$H$_4$)]$^+$ 517.0917, calc. 517.0913

Elemental analysis (%): C 56.8, H 4.69 calc. C 56.3, H 4.72

M.p.: 173 °C (decomp.)

[(Po-tol$_3$)Pd(p-MeC$_6$H$_4$)Br]$_2$[58, 62] (5f)

[SZ 4042]
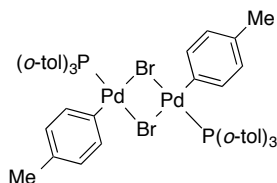
According to the general procedure, the reaction of Pd$_2$dba$_3$·CHCl$_3$ (1.03 g, 1.00 mmol), P(o-tol)$_3$ (1.36 g, 4.47 mmol) and 4-bromotoluene (2.50 mL, 20.3 mmol) in toluene (30.0 mL) provided complex **5f** (0.73 g, 0.63 mmol, 63%) as pale yellow insoluble powder.

IR (v/cm^{-1}): 3055 (w), 2963 (w), 2919 (w), 1589 (w), 1566 (w), 1469 (m), 1446 (m), 1380 (w), 1281 (w), 1200 (w), 1163 (w), 1129 (w), 1117 (w), 1068 (w), 1048 (w), 1031 (w), 1010 (m), 795 (s), 756 (s), 716 (m), 678 (w).

HRESI-MS (CH$_3$CN, +, m/z): [(Po-tol$_3$)Pd(p-MeC$_6$H$_4$)]$^+$ 501.0993, calc. 501.0963

Elemental analysis (%): C 58.5, H 4.95 calc. C 57.8, H 4.85

A better elemental analysis could not be obtained.

M.p.: 167 °C (decomp.)

[(Po-tol$_3$)Pd(C$_6$H$_5$)Br]$_2$[66] (5a)

[SZ 3038/3036]
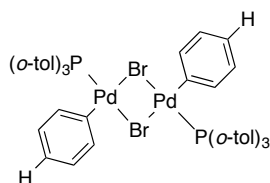
According to the general procedure, the reaction of Pd$_2$dba$_3$ (222 mg, 0.24 mmol), P(o-tol)$_3$ (316 mg, 1.04 mmol) and bromobenzene (723 mg, 4.60 mmol) in toluene (12.0 mL) provided complex **5a** (199 mg, 0.18 mmol, 72%) as pale yellow insoluble powder.

IR (v/cm^{-1}): 3052 (w), 1561 (m), 1468 (m), 1444 (m), 1281 (w), 1273 (w), 1200 (w), 1164 (w), 1131 (w), 1056 (w), 1032 (w), 1016 (m), 994 (w), 803 (m), 751 (m), 728 (s), 690 (m), 676 (w).

HRESI-MS (CH$_3$CN, +, m/z): [(Po-tol$_3$)Pd(C$_6$H$_5$)]$^+$ 487.0781, calc. 487.0801

Elemental analysis (%): C 57.4, H 4.63 calc. C 57.1, H 4.62

M.p.: 164–166 °C (decomp.)

[(Po-tol$_3$)Pd(p-FC$_6$H$_4$)Br]$_2$[63] (5g)

[SZ 4022]
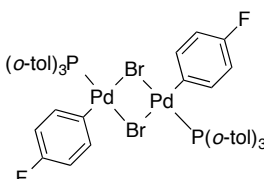
According to the general procedure, the reaction of Pd$_2$dba$_3$·CHCl$_3$ (1.57 g, 1.53 mmol), P(o-tol)$_3$ (1.80 g, 5.91 mmol) and 4-fluorobromobenzene (3.27 mL, 30.0 mmol) in toluene (60.0 mL) provided complex **5g** (1.72 g, 2.94 mmol, 96%) as pale yellow insoluble powder.

IR (v/cm^{-1}): 3059 (w), 2973 (w), 1590 (w), 1568 (w), 1477 M), 1448 (m), 1383 (w), 1275 (w), 1215 (m), 1156 (w), 1119 (w), 1069 (w), 1041 (w), 1008 (w), 819 (s), 804 (m), 756 (s), 716 (m), 697 (w), 679 (w).

HRESI-MS (CH$_3$CN, +, m/z): [(Po-tol$_3$)Pd(p-FC$_6$H$_4$)]$^+$ 505.0733, calc. 505.0713

Elemental analysis (%): C 57.3, H 4.49 calc. C 55.4, H 4.30

A better elemental analysis could not be obtained.

M.p.: 185–187 °C (decomp.)

[(Po-tol$_3$)Pd(p-EtO$_2$CC$_6$H$_4$)Br]$_2$ (5i)

[SZ 4037]
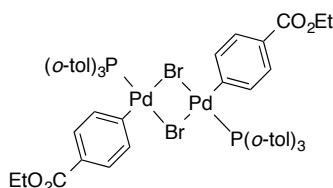
According to the general procedure, the reaction of Pd$_2$dba$_3$·CHCl$_3$ (1.06 g, 1.02 mmol), P(o-tol)$_3$ (1.27 g, 4.17 mmol) and ethyl 4-bromobenzoate (1.63 mL, 10.0 mmol) in toluene (50.0 mL) provided complex **5i** (1.10 g, 1.71 mmol, 84%) as pale yellow less soluble powder.

IR (v/cm^{-1}): 3056 (w), 2975 (w), 1700 (m), 1574 (m), 1445 (m), 1383 (w), 1367 (w), 1281 (s), 1200 (w), 1176 (m), 1107 (s), 1009 (m), 843 (w), 803 (w), 753 (s), 716 (m), 678 (w).

HRESI-MS (CH$_3$CN, +, *m/z*): [(Po-tol$_3$)Pd(p-EtO$_2$CC$_6$H$_4$)]$^+$ 559.0936, calc. 559.1013

Elemental analysis (%): C 56.2, H 4.62 calc. C 56.3, H 4.73

M.p.: 208–210 °C (decomp.)

[(P*o*-tol$_3$)Pd(*p*-BuO$_2$CC$_6$H$_4$)Br]$_2$ (5j)

[SZ 4115]
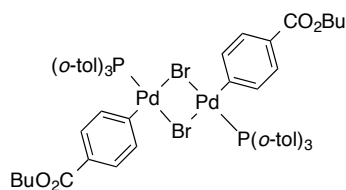
According to the general procedure, the reaction of Pd$_2$dba$_3$·CHCl$_3$ (1.05 g, 1.01 mmol), P(o-tol)$_3$ (1.30 g, 4.29 mmol) and butyl 4-bromobenzoate (1.84 g, 7.14 mmol) in toluene (24.0 mL) provided complex **5j** (245 mg, 0.37 mmol, 18%) as orange yellow moderate soluble powder.

IR (v/cm^{-1}): 3057 (w), 2957 (w), 1713 (m), 1575 (m), 1470 (m), 1446 (m), 1383 (w), 1277 (m), 1261 (m), 1200 (w), 1175 (w), 1102 (m), 1011 (m), 837 (w), 804 (w), 751 (s), 716 (w) 677 (w).

HRESI-MS (MeOH, +, *m/z*): [(Po-tol$_3$)Pd(p-BuO$_2$CC$_6$H$_4$)]$^+$ 587.1352, calc. 587.1331

Elemental analysis (%): C 57.6, H 5.17 calc. C 57.5, H 5.13

M.p.: 141–145 °C (decomp.)

[(P*o*-tol$_3$)Pd(*p*-F$_3$CC$_6$H$_4$)Br]$_2$ (5k)

[SZ 4036]
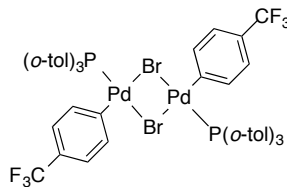
According to the general procedure, the reaction of Pd$_2$dba$_3$ • CHCl$_3$ (1.04 g, 1.01 mmol), P(o-tol)$_3$ (1.25 g, 4.12 mmol) and 4-bromobenzotrifluoride (1.40 mL, 10.0 mmol) in toluene (50.0 mL) provided complex **5k** (1.05 g, 1.65 mmol, 82%) as pale yellow powder.

IR (v/cm^{-1}): 3056 (w), 1561 (w), 1687 (m), 1469 (w), 1446 (m), 1384 (w), 1323 (s), 1281 (w), 1200 (w), 1154 (m), 1115 (m), 1069 (s), 1009 (m), 983 (w), 814 (m9, 749 (s), 716 (m), 694 (w), 678 (w).

HRESI-MS (CH$_3$CN, +, m/z): [(Po-tol$_3$)Pd(p-F$_3$CC$_6$H$_4$)]$^+$ 555.0705, calc. 555.0681

Elemental analysis (%): C 53.0, H 3.95 calc. C 52.9, H 3.96

M.p.: 170–175 °C (decomp.)

[(Po-tol$_3$)Pd(p-NCC$_6$H$_4$)Br]$_2$ (5l)

[SZ 4035]
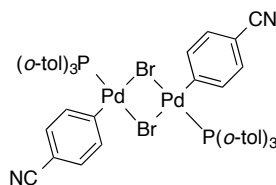
According to the general procedure, the reaction of Pd$_2$dba$_3$·CHCl$_3$ (1.06 g, 1.03 mmol), P(o-tol)$_3$ (1.23 g, 4.03 mmol) and 4-bromobenzonitrile (1.84 g, 10.0 mmol) in toluene (50.0 mL) provided complex **5l** (1.11 g, 1.87 mmol, 91%) as pale yellow powder.

IR (v/cm^{-1}): 3049 (w), 2220 (m), 1561 (w), 1576 (m), 1473 (m), 1446 (m), 1385 (w), 1340 (w), 1278 (w), 1198 (w), 1130 (w), 1067 (w), 1050 (w), 1032 (w), 1011 (m), 983 (w), 811 (s), 755 (s), 716 (m), 696 (m), 675 (w).

HRESI-MS (CH$_3$CN, +, m/z): [(Po-tol$_3$)Pd(p-NCC$_6$H$_4$)]$^+$ 512.0782, calc. 512.0759

Elemental analysis (%): C 56.8, H 4.15, N 2.43 calc. C 56.7, H 4.25, N 2.36

M.p.: 198 °C (decomp.)

4.3.5 *trans*-(PPh$_3$)$_2$Pd(Ar)X complexes (8,9)

General procedure A for the preparation of arylpalladium(II) iodide complexes **8**:

An 100 mL round-bottom Schlenk flask was charged with Pd(PPh$_3$)$_4$ (1 equiv.) and 4-iodoanisole (2 equiv.), sealed with a rubber septum and set under an atmosphere of argon by cycled evacuation and backfilling with argon. Upon addition of THF the mixture was stirred for 3 h at room temperature. Then the flask was opened to air and the resulting mixture was filtered through a pad of Celite. The filtrate was concentrated under vacuum and Et$_2$O was added resulting in the formation of a precipitate. After the mixture has been additionally stirred for 1 h, the supernatant liquid was decanted and the remaining solid washed with Et$_2$O and dried in vacuum.

General procedure B for the preparation of arylpalladium(II) bromide complexes **9**:

Similar to general procedure A, the reaction was carried out in toluene at 50 °C.

trans-(PPh₃)₂Pd(*p*-MeOC₅H₄)I[53c, 70b] (8d)

[SZ 3126]
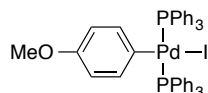
According to general procedure A, the reaction of Pd(PPh₃)₄ (1.15 g, 1.00 mmol) and 4-iodoanisole (0.45 g, 1.94 mmol) in THF (6.00 mL) provided complex **8d** (0.74 g, 0.86 mmol, 86%) was isolated as very pale solid.

^{1}H NMR (400 MHz, CDCl₃): δ 7.55–7.49 (m, 12 H), 7.32 (t, J = 7.3 Hz, 6 H), 7.25 (ddt, J = 8.5, 6.9, 1.3 Hz, 12 H), 6.42 (dt, J = 8.7, 1.9 Hz, 2 H), 5.94 (d, J = 8.6 Hz, 2 H), 3.50 (s, 3 H) ppm.

^{13}C NMR (101 MHz, CDCl₃): δ 156.1, 135.7 (t, J = 5.4 Hz), 135.0 (t, J = 6.2 Hz), 132.3 (t, J = 23.0 Hz), 129.8, 127.8 (t, J = 5.1 Hz), 114.6, 55.6 ppm.

^{31}P NMR (162 MHz, CDCl₃): δ 23.48 ppm.

IR (v/cm^{-1}): 3040 (w), 1478 (m), 1433 (m), 1270 (w), 1232 (m), 1180 (w), 1166 (w), 1092 (m), 1026 (w), 1000 (w), 797 (m), 740 (m), 689 (s).

HRESI-MS (CH₃CN, +, m/z): [(PPh₃)₂Pd(*p*-MeOC₆H₄)]$^+$ 737.138, calc. 737.1349

Elemental analysis (%): C 60.0, H 4.05, calc. C 59.7, H 4.31

M.p.: 140–141 °C (decomp.)

trans-(PPh₃)₂Pd(*p*-^{t}BuC₅H₄)I (8e)

[SZ 3141]
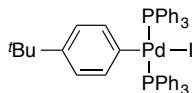
According to general procedure A, the reaction of Pd(PPh₃)₄ (1.15 g, 1.00 mmol) and 4-*tert*-butyliodobenzene (0.27 mL, 1.51 mmol) in THF (6.00 mL) provided complex **8e** (0.64 g, 0.72 mmol, 72%) as a colorless solid.

^{1}H NMR (400 MHz, CDCl₃): δ 7.54–7.47 (m, 12 H), 7.33–7.28 (m, 6 H), 7.23 (ddt, J = 8.4, 7.0, 1.2 Hz, 12 H), 6.49 (dt, J = 8.5, 2.1 Hz, 2 H), 6.27 (d, J = 8.4 Hz, 2 H), 1.05 (s, 9 H) ppm.

^{13}C NMR (101 MHz, CDCl₃): δ 135.1 (t, J = 6.2 Hz), 132.4 (t, J = 23.0 Hz), 129.8, 127.9 (t, J = 5.2 Hz), 125.2, 33.8, 31.8 ppm.

^{31}P NMR (162 MHz, CDCl₃): δ 23.48 ppm.

IR (v/cm^{-1}): 3045 (w), 2952 (w), 1711 (m), 1573 (m), 1479 (w), 1433 (m), 1383 (w), 1272 (m), 1173 (w), 1097 (m), 1011 (w), 834 (w), 742 (s), 690 (s).

HRESI-MS (CH$_3$CN, +, m/z): [(PPh$_3$)$_2$Pd(p-^{t}BuC$_5$H$_4$)]$^+$ 763.1985, calc. 763.1869

Elemental analysis (%): C 62.3, H 4.96, calc. C 62.0, H 4.86

M.p.: 140–141 °C (decomp.)

trans-(PPh$_3$)$_2$Pd(p-MeC$_5$H$_4$)I[53c, 70c] (8f)

[SZ 3133]
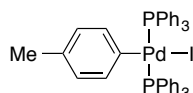
According to general procedure A, the reaction of Pd(PPh$_3$)$_4$ (1.81 g, 1.56 mmol) and 4-iodotoluene (0.66 g, 3.01 mmol) in toluene (9.00 mL) provided complex **8f** (0.45 g, 0.53 mmol, 34%) as a yellow solid.

^{1}H NMR (400 MHz, CDCl$_3$): δ 7.53–7.46 (m, 12 H), 7.32 (t, J = 7.3 Hz, 6 H), 7.23 (t, J = 7.3 Hz, 12 H), 6.41 (dt, J = 8.1, 2.1 Hz, 2 H), 6.07 (d, J = 7.6 Hz, 2 H), 1.91 (s, 3 H) ppm.

^{13}C NMR (101 MHz, CDCl$_3$): δ 152.9, 135.6 (t, J = 5.1 Hz), 135.1 (t, J = 6.2 Hz), 132.4 (t, J = 22.9 Hz), 131.1, 129.8, 129.1, 127.8 (t, J = 5.1 Hz), 20.3 ppm.

^{31}P NMR (162 MHz, CDCl$_3$): δ 23.17 ppm.

IR (v/cm^{-1}): 3048 (w), 1477 (m), 1433 (m), 1373 (w), 1183 (w), 1093 (m), 1012 (w), 843 (w), 782 (m), 740 (m) 689 (s).

HRESI-MS (CH$_3$CN, +, m/z): [(PPh$_3$)$_2$Pd(p-MeC$_5$H$_4$)]$^+$ 721.1409, calc. 721.1400

Elemental analysis (%): C 60.5, H 4.69, calc. C 60.8, H 4.39

M.p.: 153–156 °C (decomp.)

trans-(PPh$_3$)$_2$Pd(C$_5$H$_5$)I[69, 70c] (8a)

[SZ 5001]
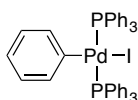
According to general procedure A, the reaction of Pd(PPh$_3$)$_4$ (1.15 g, 0.99 mmol) and iodobenzene (0.25 mL, 2.24 mmol) in THF (6.00 mL) provided complex **8f** (0.45 g, 0.78 mmol, 78%) as a tan solid.

^{1}H NMR (400 MHz, CDCl$_3$): δ 7.52 (dtd, J = 6.8, 5.4, 1.4 Hz, 12H), 7.33 (t, J = 7.3 Hz, 6H), 7.29 ? 7.18 (m, 12H), 6.63 (d, J = 6.8 Hz, 2H), 6.35 (t, J = 7.2 Hz, 1H), 6.24 (t, J = 7.3 Hz, 2H) ppm.

^{13}C NMR (101 MHz, CDCl$_3$): δ 159.2 (t, J = 2.4 Hz), 136.1 (t, J = 5.0 Hz), 134.9 (t, J = 6.2 Hz), 132.2 (t, J = 23.1 Hz), 129.8, 127.9 (t, J = 5.1 Hz), 121.9 ppm.

^{31}P NMR (162 MHz, CDCl$_3$): δ 23.58 ppm.

IR (v/cm^{-1}): 3048 (w), 1559 (w), 1480 (w), 1434 (m), 1185 (w), 1094 (m), 1016 (w), 993 (w), 741 (m), 726 (m), 689 (s).

HRESI-MS (CH$_3$CN, +, m/z): [(PPh$_3$)$_2$Pd(C$_5$H$_5$)]$^+$ 707.1265, calc. 707.1249

Elemental analysis (%): C 60.5, H 4.47, calc. C 60.4, H 4.23

M.p.: 148–150 °C (decomp.)

trans-(PPh$_3$)$_2$Pd(*p*-FC$_5$H$_4$)I (8g)

[SZ 5002]
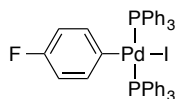
According to general procedure A, the reaction of Pd(PPh$_3$)$_4$ (1.18 g, 1.02 mmol) and 4-fluoro-iodobenzene (0.25 mL, 2.17 mmol) in THF (6.00 mL) provided complex **8g** (0.75 g, 0.88 mmol, 86%) as a tan solid.

^{1}H NMR (400 MHz, CDCl$_3$): δ 7.58–7.47 (m, 12H), 7.34 (t, J = 7.3 Hz, 6H), 7.30–7.22 (m, 12H), 6.50 (td, J = 6.5, 1.8 Hz, 2H), 6.04 (t, J = 9.2 Hz, 2H) ppm.

^{13}C NMR (101 MHz, CDCl$_3$): δ 151.76 (q, J = 2.9 Hz), 135.89 (q, J = 5.3 Hz), 134.96 (t, J = 6.2 Hz), 132.07 (t, J = 23.3 Hz), 129.98, 127.93 (t, J = 5.1 Hz), 114.60 (d, J = 19.1 Hz) ppm.

^{31}P NMR (162 MHz, CDCl$_3$): δ 23.52 ppm.

^{19}F NMR (376 MHz, CDCl$_3$): δ –124.92 ppm.

IR (v/cm^{-1}): 3050 (w), 1473 (m), 1434 (m), 1287 (w), 1211 (m), 1152 (w), 1094 (m), 1000 (w), 843 (w), 803 (m), 740 (m), 689 (s).

HRESI-MS (CH$_3$CN, +, m/z): [(PPh$_3$)$_2$Pd(*p*-FC$_5$H$_4$)]$^+$ 725.1177, calc. 725.1155

Elemental analysis (%): C 59.3, H 4.32, calc. C 59.1, H 4.02

M.p.: 145–150 °C (decomp.)

trans-(PPh$_3$)$_2$Pd(*p*-EtO$_2$CC$_5$H$_4$)I (8i)

[SZ 3135]
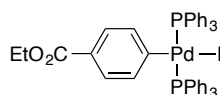
According to general procedure A, the reaction of Pd(PPh$_3$)$_4$ (1.74 g, 1.50 mmol) and ethyl 4-iodobenzoate (0.60 g, 2.17 mmol) in THF (9.00 mL) provided complex **8i** (1.08 g, 1.19 mmol, 79%) as a tan solid.

^{1}H NMR (400 MHz, CDCl$_3$): δ 7.54–7.48 (m, *12* H), 7.32 (t, *J* = 7.4 Hz, 6 H), 7.26–7.20 (m, 12 H), 6.84 (d, *J* = 8.3 Hz, 2 H), 6.71 (dt, *J* = 8.4, 2.0 Hz, 2 H), 4.22 (q, *J* = 7.1 Hz, 2 H), 1.29 (t, *J* = 7.1 Hz, 3 H) ppm.

^{13}C NMR (101 MHz, CDCl$_3$): δ 170.9, 167.7, 135.8 (t, *J* = 4.8 Hz), 134.9 (t, *J* = 6.2 Hz), 131.8 (t, *J* = 23.4 Hz), 130.1, 128.0 (t, *J* = 5.3 Hz), 124.2, 60.2, 14.5 ppm.

^{31}P NMR (162 MHz, CDCl$_3$): δ 23.30 ppm.

IR (*v*/cm^{-1}): 3052 (w), 2978 (w), 1704 (m), 1575 (w), 1480 (w), 1433 (m), 1381 (w), 1367 (w), 1276 (m), 1169 (m), 1111 (m), 1095 (m), 1011 (w), 835 (w), 746 (s), 690 (s).

HRESI-MS (CH$_3$CN, +, *m/z*): [(PPh$_3$)$_2$Pd(*p*-EtO$_2$CC$_5$H$_4$)]$^+$ 779.1492, calc. 779.1455

Elemental analysis (%): C 59.6, H 4.82, calc. C 59.6, H 4.33

M.p.: 137 °C (decomp.)

trans-(PPh$_3$)$_2$Pd(*p*-^{n}BuO$_2$CC$_5$H$_4$)I (8j)

[SZ 3142]
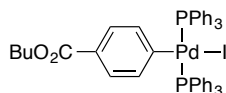
According to general procedure A, the reaction of Pd(PPh$_3$)$_4$ (1.15 g, 1.00 mmol) and Butyl 4-iodo-benzoate (0.53 g, 1.74 mmol) in THF (6.00 mL) provided complex **8j** (0.73 g, 0.78 mmol, 78%) as a tan solid.

^{1}H NMR (400 MHz, CDCl$_3$): δ 7.55–7.48 (m, 12 H), 7.31 (t, *J* = 7.3 Hz, 6 H), 7.23 (ddt, *J* = 8.3, 7.0, 1.4 Hz, 12 H), 6.84 (d, *J* = 8.4 Hz, 2 H), 6.72 (dt, *J* = 8.4, 1.9 Hz, 2 H), 4.18 (t, *J* = 6.5 Hz, 2 H), 1.65 (dq, *J* = 8.4, 6.6 Hz, 2 H), 1.41 (dq, *J* = 14.6, 7.4 Hz, 2 H), 0.95 (t, *J* = 7.4 Hz, 3 H) ppm.

^{13}C NMR (101 MHz, CDCl$_3$): δ 171.0, 167.8, 135.8 (t, *J* = 5.0 Hz), 135.0 (t, *J* = 6.2 Hz), 131.8 (t, *J* = 23.5 Hz), 130.1, 128.0 (t, *J* = 5.4 Hz), 124.2, 64.1, 31.0, 19.4, 13.9 ppm.

^{31}P NMR (162 MHz, CDCl$_3$): δ 23.34 ppm.

IR (*v*/cm^{-1}): 3056 (w), 2949 (w), 1479 (w), 1434 (m), 1376 (w), 1266 (w), 1186 (w), 1114 (w), 1095 (m), 1028 (w), 1008 (w), 811 (m), 743 (s), 690 (s).

HRESI-MS (CH$_3$CN, +, *m/z*): [(PPh$_3$)$_2$Pd(*p*-^{n}BuO$_2$CC$_5$H$_4$)]$^+$ 807.1870, calc. 807.1768

Elemental analysis (%): C 60.8, H 5.29, calc. C 60.4, H 4.64

M.p.: 140 °C (decomp.)

trans-(PPh₃)₂Pd(p-F₃CC₅H₄)I[53c] (**8k**)

[SZ 3134]
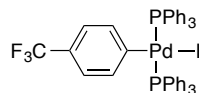
According to general procedure A, the reaction of Pd(PPh₃)₄ (1.81 g, 1.57 mmol) and 4-iodobenzotriflouride (0.29 g, 1.97 mmol) in THF (9.00 mL) provided complex **8k** (1.19 g, 1.32 mmol, 84%) as a tan solid.

^{1}H NMR (400 MHz, CDCl₃): δ 7.56–7.48 (m, 12 H), 7.33 (t, J = 7.3 Hz, 6 H), 7.25 (tt, J = 7.0, 1.2 Hz, 12 H), 6.72 (d, J = 7.8 Hz, 2 H), 6.41 (d, J = 7.9 Hz, 2 H) ppm.

^{13}C NMR (101 MHz, CDCl₃): δ 168.2, 135.8 (t, J = 5.1 Hz), 134.9 (t, J = 6.2 Hz), 131.7 (t, J = 23.5 Hz), 130.1, 128.0 (t, J = 5.2 Hz), 123.5 (q, J = 3.7, 2.8 Hz) ppm.

^{31}P NMR (162 MHz, CDCl₃): δ 23.61 ppm.

^{19}F NMR (376 MHz, CDCl₃): δ −61.98 ppm.

IR (v/cm^{-1}): 3047 (w), 1588 (m), 1478 (w), 1432 (m), 1387 (w), 1324 (m), 1157 (m), 1119 (m), 1092 (m), 1069 (m), 1014 (w), 811 (m), 741 (m), 689 (s).

HRESI-MS (CH₃CN, +, m/z): [(PPh₃)₂Pd(p-F₃CC₅H₄)]⁺ 775.1101, calc. 775.1117

Elemental analysis (%): C 57.7, H 4.19, calc. C 57.2, H 3.80

M.p.: 169–171 °C (decomp.)

trans-(PPh₃)₂Pd(p-NCC₅H₄)I (**8l**)

[SZ 3136]
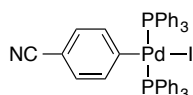
According to general procedure A, the reaction of Pd(PPh₃)₄ (1.74 g, 1.50 mmol) and 4-iodobenzo-nitrile (0.51 g, 2.24 mmol) in THF (9.00 mL) provided complex **8l** (1.11 g, 1.29 mmol, 86%) as a colorless solid.

^{1}H NMR (400 MHz, CDCl₃): δ 7.55–7.48 (m, 12 H), 7.35 (t, J = 7.4 Hz, 6 H), 7.29–7.23 (m, 12 H), 6.78 (dt, J = 8.2, 1.7 Hz, 2 H), 6.41 (d, J = 8.2 Hz, 2 H) ppm.

^{13}C NMR (101 MHz, CDCl₃): δ 136.6 (t, J = 4.7 Hz), 134.9 (t, J = 6.2 Hz), 131.6 (t, J = 23.6 Hz), 130.3, 129.7, 128.1 (t, J = 5.2 Hz), 120.1, 104.9 ppm.

^{31}P NMR (162 MHz, CDCl₃): δ 23.37 ppm.

IR (v/cm^{-1}): 3051 (w), 2216 (m), 1572 (m), 1471 (m), 1434 (m), 1184 (w), 1094 (), 1070 (w), 1048 (w), 1026 (w), 1011 (w), 805 (m), 739 (m), 689 (s).

HRESI-MS (CH$_3$CN, +, m/z): [(PPh$_3$)$_2$Pd(p-NCC$_5$H$_4$)]$^+$ 732.1225, calc. 732.1196

Elemental analysis (%): C 60.3, H 4.01, N 1.64, calc. C 60.1, H 3.99, N 1.63

M.p.: 173–176 °C (decomp.)

trans-(PPh$_3$)$_2$Pd(p-MeOC$_6$H$_4$)Br (9d)

[SZ 3018/4116]
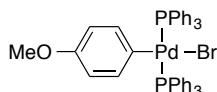
A solution of P(o-tol)$_3$-ligated arylpalladium(II) complex **5d** (117 mg, 0.10 mmol) and PPh$_3$ (136 mg, 0.52) in DCM (2.00 mL) was stirred at room temperature for approx. 20 min. Then Et$_2$O (20.0 mL) was added, which resulted in precipitation of a solid. After the mixture has been stirring for 2 h at room temperature, the supernatant liquid was decanted, the solid washed with Et$_2$O and dried in vacuum. The complex **9d** (158 mg, 0.19 mmol, 98%) was obtained as pale yellow solid.

^{1}H NMR (400 MHz, CDCl$_3$): δ 7.56–7.48 (m, 12H), 7.36–7.30 (m, 6H), 7.29–7.22 (m, 12H), 6.43 (dt, J = 8.7, 1.9 Hz, 2H), 5.94 (d, J = 8.6 Hz, 2H), 3.50 (s, 3H) ppm.

^{13}C NMR (101 MHz, CDCl$_3$): δ 156.11, 143.77 (t, J = 3.6 Hz), 135.99 (t, J = 5.2 Hz), 134.87 (t, J = 6.3 Hz), 131.67 (t, J = 22.7 Hz), 129.82, 127.93 (t, J = 5.1 Hz), 114.51, 55.57 ppm.

^{31}P NMR (162 MHz, CDCl$_3$): δ 24.08 ppm.

IR (v/cm^{-1}): 3049 (w), 2841 (w), 1591 (m), 1563 (w), 1501 (w), 1479 (w), 1435 (m), 1413 (w), 1298 (w), 1264 (m), 1228 (w), 1184 (m), 1107 (s), 1015 (m9, 997 (m), 833 (m), 804 (m), 752 (m), 724 (m), 689 (s).

HRESI-MS (MeOH, +, m/z): [(PPh$_3$)$_2$Pd(p-MeOC$_5$H$_4$)]$^+$ 737.1375 , calc. 737.1354

Elemental analysis (%): C 62.9, H 4.75, calc. C 63.1, H 4.56

M.p.: 134–136 °C (decomp.)

trans-(PPh$_3$)$_2$Pd(p-^{t}BuC$_6$H$_4$)Br[70d] (9e)

[SZ 3019/3143]
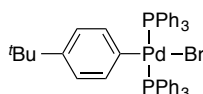
According to the general procedure B, the reaction of Pd(PPh$_3$)$_4$ (1.23 g, 1.07 mmol) and 4-_tert_-butyl-bromobenzene (0.28 mL, 1.61 mmol) in toluene (6.00 mL) provided complex **9e** (177 mg, 0.21 mmol, 13%) as a dark tan solid, which contained minor unknown impurities.

^{1}H NMR (400 MHz, CDCl$_3$): δ 7.53–7.47 (m, 12H), 7.31 (t, J = 7.2 Hz, 6H), 7.28–7.17 (m, 12H), 6.49 (dt, J = 8.5, 2.1 Hz, 2H), 6.26 (d, J = 8.0 Hz, 2H), 1.06 (s, 9H) ppm.

^{13}C NMR (101 MHz, CDCl$_3$): δ 151.42 (t, J = 3.3 Hz), 144.53, 135.45 (t, J = 5.0 Hz), 135.26 (t, J = 6.1 Hz), 134.88 (t, J = 6.4 Hz), 131.75 (t, J = 22.6 Hz), 129.76, 127.91 (t, J = 5.1 Hz), 125.05, 33.80, 31.73 ppm.

^{31}P NMR (162 MHz, CDCl$_3$): δ 24.07 ppm.

IR (v/cm^{-1}): 3054 (w), 2950 (w), 1478 (m), 1433 (m), 1387 (w), 1267 (w), 1183 (w), 1157 (w), 1094 (m), 1028 (w), 1008 (w), 807 (w), 737 (s), 689 (s).

HRESI-MS (MeOH, +, m/z): [(PPh$_3$)$_2$Pd(p-^{t}BuC$_5$H$_4$)]$^+$ 763.1858, calc. 763.1875

Elemental analysis (%): C 65.5, H 5.25, calc. C 65.5, H 5.13

M.p.: 160 °C (decomp.)

trans-(PPh$_3$)$_2$Pd(p-MeC$_6$H$_4$)Br[70b] (9f)

[SZ 3020/5151]
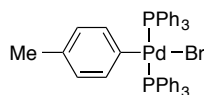
A solution of P(o-tol)$_3$-ligated arylpalladium(II) complex **5f** (116 mg, 0.10 mmol) and PPh$_3$ (151 mg, 0.58) in DCM (0.50 mL) was stirred at room temperature for approx. 10 min. Then Et$_2$O (20.0 mL) was added, which resulted in the precipitation of a solid. After the mixture has been stirring for 2 h at room temperature, the supernatant liquid was decanted, the solid washed with Et$_2$O and dried in vacuum. The complex **9f** (113 mg, 0.14 mmol, 70%) was obtained as pale yellow solid. Single crystals suitable for X-ray diffraction analysis were grown by slow diffusion of Et$_2$O into a saturated solution of **9f** in DCM at –25 °C.

^{1}H NMR (400 MHz, CDCl$_3$): δ 7.52 (q, J = 5.9 Hz, 12H), 7.32 (t, J = 7.3 Hz, 6H), 7.24 (t, J = 7.5 Hz, 12H), 6.45 (dd, J = 7.9, 2.3 Hz, 2H), 6.10 (d, J = 7.7 Hz, 2H), 1.94 (s, 3H) ppm.

^{13}C NMR (101 MHz, CDCl$_3$): δ 149.9 (t, J = 3.4 Hz), 135.8 (t, J = 4.9 Hz), 134.9 (t, J = 6.3 Hz), 131.7 (t, J = 22.6 Hz), 131.0, 129.7, 128.9, 127.9 (t, J = 5.1 Hz), 20.3 ppm.

^{31}P NMR (162 MHz, CDCl$_3$): δ 23.79 ppm.

IR (v/cm^{-1}): 3051 (w), 1478 (m), 1433 (m), 1185 (w), 1093 (m), 1053 (w), 1025 8w), 1012 (w), 999 (w), 844 (w), 782 (m), 751 (m), 740 (m), 725 (m), 688 (s).

HRESI-MS (MeOH, +, m/z): [(PPh$_3$)$_2$Pd(p-MeC$_5$H$_4$)]$^+$ 721.1458, calc. 721.1405

Elemental analysis (%): C 64.6, H 5.04, calc. C 64.4, H 4.65

M.p.: 158–161 °C (decomp.)

***trans*-(PPh₃)₂Pd(C₆H₅)Br**[69, 70b, 70c, 70e] **(9a)**

[SZ 3002]
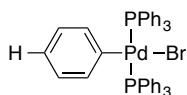
According to the general procedure B, the reaction of $Pd(PPh_3)_4$ (1.16 g, 1.00 mmol) and bromobenzene (1.05 mL, 10.0 mmol) in toluene (5.00 mL) provided the complex **9a** (0.552 g, 0.70 mmol, 70%) as crystalline, colorless after recrystallization from DCM and Et_2O.

^{1}H NMR (400 MHz, CDCl₃): δ 7.50 (dtd, J = 8.5, 5.4, 1.4 Hz, 12H), 7.32 (t, J = 7.3 Hz, 6H), 7.27–7.21 (m, 12H), 6.62 (dtd, J = 7.9, 2.2, 1.2 Hz, 2H), 6.36 (t, J = 7.3 Hz, 1H), 6.22 (t, J = 7.5 Hz, 2H) ppm.

^{13}C NMR (101 MHz, CDCl₃): δ 156.2 (t, J = 3.3 Hz), 136.4 (t, J = 5.0 Hz), 134.9 (t, J = 6.3 Hz), 131.6 (t, J = 22.7 Hz), 129.8 (d, J = 1.3 Hz), 128.0 (t, J = 5.2 Hz), 127.8, 121.9 ppm.

^{31}P NMR (162 MHz, CDCl₃): δ = 24.24 ppm.

IR (ν/cm^{-1}): 3049 (w), 1561 (w), 1482 (w), 1466 (w), 1434 (m), 1331 (w), 1309 (w), 1187 (w), 1158 (w), 1096 (m), 1071 (w), 1057 (w), 1027 (w), 1017 (w), 995 (w), 892 (w), 743 (m), 729 (m), 690 (s).

HRESI-MS (CH₃CN , +, *m/z*): [(PPh₃)₂Pd(Ph)]$^+$ 707.1288, calc. 707.1249

Elemental analysis (%): C 64.0, H 4.87, calc. C 64.0, H 4.48

M.p.: 200–204 °C (decomp.)

***trans*-(PPh₃)₂Pd(*p*-FC₆H₄)Br (9g)**

[SZ 3021]
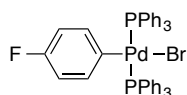
According to the general procedure B, the reaction of $Pd(PPh_3)_4$ (345 mg, 0.30 mmol) and 4-fluorobromobenzene (82.5 mg, 0.45 mmol) in toluene (1.50 mL) provided the complex **9g** (177 mg, 0.22 mmol, 74%) as crystalline, colorless solid after recrystallization from DCM and Et_2O. Crystallization by slow diffusion of pentane into a saturated solution of **9g** in DCM delivered single crystals suitable for X-ray crystallographic analysis.

^{1}H NMR (400 MHz, CDCl₃): δ 7.55–7.48 (m, 12H), 7.34 (t, J = 7.3 Hz, 6H), 7.29–7.23 (m, 12H), 6.50 (ddt, J = 8.4, 6.3, 1.8 Hz, 2H), 6.03 (d, J = 9.2 Hz, 2H) ppm.

^{13}C NMR (101 MHz, CDCl₃): δ 148.8 , 136.2 (q, J = 5.6 Hz), 134.9 (t, J = 6.3 Hz), 131.5 (t, J = 23.0 Hz), 130.0 , 128.0 (t, J = 5.1 Hz), 114.7, 114.5 ppm.

^{31}P NMR (162 MHz, CDCl$_3$): δ 24.21 ppm.

^{19}F NMR (376 MHz, CDCl$_3$): δ −125.02 ppm.

IR (v/cm^{-1}): 3070 (w), 3056 (w), 1588 (w), 1572 (w), 1474 (m), 1310 (w), 1289 (w), 1208 (m), 1182 (w), 1155 (w), 1096 (m), 1048 (w), 1028 (w), 999 (w), 845 (w), 803 (m), 753 (m), 741 (m), 704 (m), 688 (s).

HRESI-MS (CH$_3$CN , +, m/z): [(PPh$_3$)$_2$Pd(p-FC$_6$H$_4$)]$^+$ 725.1242, calc. 725.1155

Elemental analysis (%): C 62.7, H 4.51, calc. C 62.6, H 4.25

M.p.: 180–183 °C (decomp.)

trans-(PPh$_3$)$_2$Pd(p-EtO$_2$CC$_6$H$_4$)Br (9i)

[SZ 3022/3138]
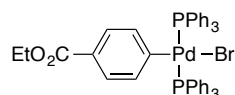
According to the general procedure B, the reaction of Pd(PPh$_3$)$_4$ (0.85 g, 0.73 mmol) and ethyl 4-bromobenzoate (0.24 g, 1.04 mmol) in THF (4.50 mL) provided complex **9i** (0.53 g, 0.61 mmol, 83%) as colorless solid.

^{1}H NMR (400 MHz, CDCl$_3$): δ 7.56–7.47 (m, 12 H), 7.33 (t, J = 7.3 Hz, 6 H), 7.29–7.19 (m, 12 H), 6.84 (dt, J = 8.5, 0.9 Hz, 2 H), 6.74 (dq, J = 8.4, 1.9 Hz, 2 H), 4.23 (q, J = 7.1 Hz, 2 H), 1.30 (t, J = 7.1 Hz, 3 H) ppm.

^{13}C NMR (101 MHz, CDCl$_3$): δ 168.1, 167.8, 136.0 (t, J = 5.1 Hz), 134.8 (t, J = 6.2 Hz), 131.2 (t, J = 23.1 Hz), 130.1, 128.1 (t, J = 5.1 Hz), 127.9, 124.1, 60.2, 14.5 ppm.

^{31}P NMR (162 MHz, CDCl$_3$): δ 24.12 ppm.

IR (v/cm^{-1}): 3075 (w), 3051 (w), 1702 (m), 1573 (m), 1480 (w), 1435 (m), 1383 (w), 1368 (w), 1275 (m), 1260 (m), 1187 (w), 1167 (w), 1111 (m), 1095 (m), 1028 (w), 1012 (w), 1000 (w), 849 (w), 755 (m), 741 (m), 691 (s).

HRESI-MS (CH$_3$CN, +, m/z): [(PPh$_3$)$_2$Pd(p-EtO$_2$CC$_6$H$_4$)]$^+$ 779.1506, calc. 779.1460

Elemental analysis (%): C 62.9, H 4.98, calc. C 62.8, H 4.57

M.p.: 162–163 °C (decomp.)

trans-(PPh$_3$)$_2$Pd(p-^{n}BuO$_2$CC$_6$H$_4$)Br (9j)

[SZ 3023/3139]
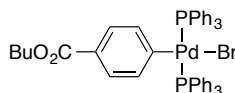
According to the general procedure B, the reaction of Pd(PPh$_3$)$_4$ (0.85 g, 0.73 mmol) and butyl 4-bromobenzoate (0.25 g, 0.99 mmol) in THF (4.50 mL) provided complex **9j** (0.65 g, 0.733 mmol, 99%) as pale tan solid.

^{1}H NMR (400 MHz, CDCl$_3$): δ 7.56–7.49 (m, 12 H), 7.33 (t, J = 7.3 Hz, 6 H), 7.27–7.21 (m, 12 H), 6.86 (d, J = 8.0 Hz, 2 H), 6.75 (dt, J = 8.4, 1.9 Hz, 2 H), 4.20 (t, J = 6.5 Hz, 2 H), 1.67 (dq, J = 8.5, 6.6 Hz, 2 H), 1.47–1.37 (m, 2 H), 0.97 (t, J = 7.4 Hz, 3 H) ppm.

^{13}C NMR (101 MHz, CDCl$_3$): δ 168.2 (t, J = 3.8 Hz), 167.8, 136.0 (t, J = 4.9 Hz), 134.8 (t, J = 6.3 Hz), 131.1 (t, J = 23.1 Hz), 130.1, 128.0 (t, J = 5.1 Hz), 127.8, 124.1, 64.0, 30.9, 19.3, 13.9 ppm.

^{31}P NMR (162 MHz, CDCl$_3$): δ 24.17 ppm.

IR (v/cm^{-1}): 3076 (w), 3054 (w), 2949 (w), 1711 (m), 1574 (m), 1480 (w), 1433 (m), 1384 (w), 1293 (m), 1263 (m), 1174 (w), 1115 (w), 1097 (m), 1014 (w), 998 (w), 836 (w), 756 (m), 742 (m), 692 (s).

HRESI-MS (CH$_3$CN, +, m/z): [(PPh$_3$)$_2$Pd(p-^{n}BuO$_2$CC$_6$H$_4$)]$^+$ 807.1763, calc. 807.1773

Elemental analysis (%): C 63.6, H 4.90, calc. C 63.6, H 4.80

M.p.: 175–178 °C (decomp.)

trans-(PPh$_3$)$_2$Pd(p- F$_3$CC$_6$H$_4$)Br[53f, 70b, 72] **(9k)**

[SZ 3011/3137]
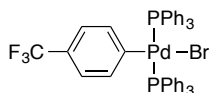
Analogues to the general procedure B, the reaction of Pd(PPh$_3$)$_4$ (349 mg, 0.30 mmol) and 4-bromobenztrifluoride (68.8 mg, 0.31 mmol) in toluene (1.50 mL) provided the complex **9k** (141 mg, 0.16 mmol, 54%) as colorless, crystalline solid after recrystallization from DCM and pentane. According to the general procedure B, the reaction of Pd(PPh$_3$)$_4$ (1.72 g, 1.49 mmol) and 4-bromobenzotrifluoride (0.28 mL, 2.00 mmol) in THF (9.00 mL) provided complex **9k** (0.61 g, 0.71 mmol, 48%) as colorless solid.

^{1}H NMR (400 MHz, CDCl$_3$): δ 7.56–7.47 (m, 12 H), 7.34 (t, J = 7.4 Hz, 6 H), 7.25 (tt, J = 7.0, 1.1 Hz, 12 H), 6.73 (d, J = 7.7 Hz, 2 H), 6.40 (d, J = 8.0 Hz, 2 H) ppm.

^{13}C NMR (101 MHz, CDCl$_3$): δ 136.0 (t, J = 4.9 Hz), 134.8 (t, J = 6.3 Hz), 131.1 (t, J = 23.1 Hz), 130.2, 129.2, 128.4, 128.1 (t, J = 5.1 Hz), 123.4 (t, J = 3.3 Hz) ppm.

^{31}P NMR (162 MHz, CDCl$_3$): δ 24.38 ppm.

^{19}F NMR (376 MHz, CDCl$_3$): δ –61.97 ppm.

IR (v/cm^{-1}): 3056 (w), 1585 (w), 1481 (w), 1435 (w), 1384 (w), 1320 (m), 1156 (w), 1110 (m), 1095 (m), 1068 (m), 1009 (w), 1001 (w), 816 (m), 744 (s), 727 (w), 691 (s).

HRESI-MS (CH$_3$CN, +, *m/z*): [(PPh$_3$)$_2$Pd(*p*-F$_3$CC$_6$H$_4$)]$^+$ 775.1082, calc. 775.1123

Elemental analysis (*%*): C 60.6, H 4.03, calc. C 60.3, H 4.00

M.p.: 159 °C (decomp.)

trans-(PPh$_3$)$_2$Pd(_p_-NCC$_6$H$_4$)Br[70b, 70c, 70f] **(9m)**

[SZ 3004/3140]
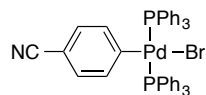
Analogues to the general procedure B, the reaction of Pd(PPh$_3$)$_4$ (116 mg, 0.10 mmol) and 4-bromobenzonitrile (18.6 mg, 0.10 mmol) in toluene (0.50 mL) provided the complex **9m** (70.5 mg, 0.09 mmol, 86%) as colorless, crystalline solid after recrystallization from DCM and pentane. According to the general procedure B, the reaction of Pd(PPh$_3$)$_4$ (0.87 g, 0.76 mmol) and 4-bromobenzonitrile (0.23 g, 1.27 mmol) in THF (4.50 mL) provided complex **9m** (0.50 g, 0.61 mmol, 84%) as pale tan solid.

^{1}H NMR (400 MHz, CDCl$_3$): δ 7.56–7.48 (m, 12 H), 7.36 (t, *J* = 7.4 Hz, 6 H), 7.30–7.22 (m, 12 H), 6.80 (dt, *J* = 8.3, 1.7 Hz, 2 H), 6.41 (d, *J* = 7.9 Hz, 2 H) ppm.

^{13}C NMR (101 MHz, CDCl$_3$): δ 136.9 (t, *J* = 4.9 Hz), 134.8 (t, *J* = 6.3 Hz), 130.9 (t, *J* = 23.4 Hz), 130.3, 129.6, 128.2 (t, *J* = 5.2 Hz), 120.2, 104.8 ppm.

^{31}P NMR (162 MHz, CDCl$_3$): δ 24.29 ppm.

IR (*v*/cm^{-1}): 3077 (w), 3050 (w), 2221 (w), 1589 (w), 1573 (w), 1481 (w), 1472 (w), 1436 (w), 1267 (w), 1230 (w), 1184 (w), 1111 (w), 1095 (w), 1049 (w), 1028 (w), 1013 (w), 1000 (w), 805 (m), 755 (m), 743 (m), 706 (m), 690 (s).

HRESI-MS (CH$_3$CN, +, *m/z*): [(PPh$_3$)$_2$Pd(*p*-NCC$_6$H$_4$)]$^+$ 732.1216, calc. 732.1201

Elemental analysis (*%*): C 63.5, H 4.36, N 1.69 calc. C 63.5, H 4.22, N 1.72

M.p.: 205–208 °C (decomp.)

4.3.6 *trans*-(Py)$_2$Pd(Ar)X complexes (10,11)

General procedure:

A Schlenk flask was charged with Pd$_2$dba$_3$·CHCl$_3$ (1.0 equiv.) and P(*o*-tol)$_3$ (1.0 equiv.) and set under an argon atmosphere before toluene (0.25 M), the aryl bromide (15 equiv.) and pyridine (15 equiv.) were syringed into the flask, successively. The reaction mixture was stirred at 50 °C for 30–45 min,

while the deep purple color of Pd$_2$dba$_3$·CHCl$_3$ disappeared. The flask was opened to air, the reaction solution diluted with DCM, filtered through a pad of Celite and the filtrate concentrated in vacuum. After addition of Et$_2$O (200 mL) and stirring for 1 h, a precipitate was formed. The solids were allowed to settle, the supernatant liquid was decanted and the solid washed with Et$_2$O.

trans-(Py)$_2$Pd(Ph)I (10a)

[SZ 3153A2]
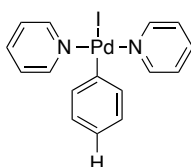
A Schlenk flask was charged with of Pd$_2$dba$_3$·CHCl$_3$ (1.02 g, 1.00 mmol) and set under an argon atmosphere before iodobenzene (0.50 mL, 4.49 mmol) and pyridine (10.0 mL) were syringed into the flask, successively. The resulting deep purple mixture was stirred at room temperature for 2 h turning into a greenish-grey mixture. The flask was opened to air, Et$_2$O (30.0 mL) was added and the mixture stirred at room temperature for 30 min. The solids were allowed to settle and the supernatant liquid was decanted, the remaining solid washed with Et$_2$O and dried in vacuum. The complex **10a** (832 mg, 1.77 mmol, 89%) was obtained as an insoluble greyish solid.

IR (v/cm^{-1}): 3051 (w), 1598 (w), 1560 (w), 1483 (w), 1442 (m), 1212 (w), 1064 w), 1018 (w), 756 (m), 732 (m), 695 (s).

HRESI-MS (MeOH, +, *m/z*): [(py)$_2$Pd(C$_6$H$_5$)]$^+$ 341.0273, calc. 341.0265

Elemental analysis (%): C 41.2, H 3.22, N 6.02 calc. C 41.0, H 3.23, N 5.98

M.p.: 159–162 °C (decomp.)

trans-(Py)$_2$Pd(^{t}BuC$_6$H$_4$)Br (11e)

[SZ 4154]
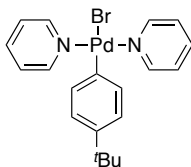
According to the general procedure, reaction of of Pd$_2$dba$_3$·CHCl$_3$ (2.09 g, 2.02 mmol), P(*o*-tol)$_3$ (670 mg, 2.20 mmol), 4-*tert*-butylbromobenzene (2.50 mL, 14.4 mmol) and pyridine (1.60 mL, 20.1 mmol) in toluene (10.0 mL) at 50 °C for 30 min gave complex **11e** (830 mg, 1.74 mmol, 43%) as orange solid.

^{1}H NMR (400 MHz, CDCl$_3$): δ 8.80 (d, J = 5.0 Hz, 4H), 7.63 (td, J = 7.7, 1.2 Hz, 2H), 7.18 (ddd, J = 7.6, 6.4, 1.1 Hz, 4H), 6.93 (d, J = 8.3 Hz, 2H), 6.86 (d, J = 8.4 Hz, 2H), 1.17 (s, 9H) ppm.

^{13}C NMR (101 MHz, CDCl$_3$): δ 153.6, 148.8, 146.4, 137.5, 132.8, 124.7, 124.7, 124.3, 31.5 ppm.

IR (ν/cm^{-1}): 2949 (w), 1603 (w), 1482 (w), 1448 (m), 1380 (w), 1359 (w), 1266 (w), 1211 (w), 1148 (w), 1114 (w), 1070 (w), 1009 (w), 856 (w), 813 (m), 764 (m), 691 (s).

HRESI-MS (MeOH, +, m/z): [(Py)$_2$Pd(p-^{t}BuC$_6$H$_4$)]$^+$ 397.0914, calc. 397.0896

Elemental analysis (%): C 49.4, H 4.57, N 5.16 calc. C 50.3, H 4.85, N 5.86

A better elemental analysis could not be obtained.

M.p.: 111 °C (decomp.)

trans-(Py)$_2$Pd(C$_6$H$_5$)Br (11a)

[SZ 4157]
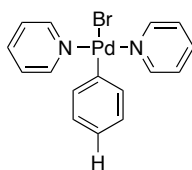
According to the general procedure, reaction of Pd$_2$dba$_3$·CHCl$_3$ (2.10 g, 2.03 mmol), P(o-tol)$_3$ (636 mg, 2.09 mmol), bromobenzene (2.50 mL, 14.4 mmol) and pyridine (1.60 mL, 20.1 mmol) in toluene (10.0 mL) at 50 °C for 30 min gave complex **11a** (925 mg, 2.19 mmol, 54%) as pale yellow solid.

^{1}H NMR (400 MHz, CDCl$_3$): δ 8.80 (d, J = 5.0 Hz, 4H), 7.65 (tt, J = 7.6, 1.5 Hz, 2H), 7.19 (ddd, J = 7.5, 5.1, 1.4 Hz, 4H), 7.07 (dd, J = 6.8, 2.4 Hz, 2H), 6.85 (dd, J = 4.9, 1.9 Hz, 3H) ppm.

^{13}C NMR (101 MHz, CDCl$_3$): δ 153.5, 137.6, 133.6, 127.3, 124.8, 123.9 ppm.

IR (ν/cm^{-1}): 3053 (w), 1602 (w), 1561 (w), 1444 (m9, 1213 (w), 1154 (w), 1065 (w), 1020 (w), 759 (m), 734 (m), 694 (s).

HRESI-MS (MeOH, +, m/z): [(Py)$_2$Pd(C$_6$H$_5$)]$^+$ 341.0285, calc. 341.0270

Elemental analysis (%): C 45.6, H 3.65, N 6.70 calc. C 45.6, H 3.59, N 6.64

M.p.: 141–145 °C (decomp.)

trans-(Py)$_2$Pd(p-EtO$_2$CC$_6$H$_4$)Br (11i)

[SZ 4123/4127]
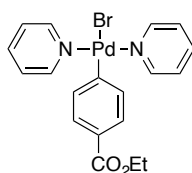
According to the general procedure, reaction of Pd$_2$dba$_3$·CHCl$_3$ (3.12 g, 3.01 mmol) and P(o-tol)$_3$ (0.93 g, 3.07 mmol), ethyl 4-bromobenzoate (4.90 mL, 30.0 mmol) and pyridine (2.42 mL,

30.0 mmol) in toluene (12.0 mL) provided complex **11i** (1.63 g, 3.31 mmol, 55%) was obtained as a pale yellow solid.

^{1}H NMR (400 MHz, CDCl$_3$): δ 8.77 (d, J = 5.2 Hz, 4H), 7.68 (t, J = 7.7 Hz, 2H), 7.52 (d, J = 7.8 Hz, 2H), 7.25–7.17 (m, 6H), 4.26 (q, J = 7.1 Hz, 2H), 1.29 (t, J = 7.1 Hz, 3H) ppm.

^{13}C NMR (101 MHz, CDCl$_3$): δ 167.3, 162.9, 153.5, 137.9, 133.7, 127.7, 126.5, 125.0, 60.6, 14.4 ppm.

IR (v/cm^{-1}): 3053 (w), 2983 (w), 1693 (m), 1602 (w), 1570 (m), 1474 (w), 1450 (m), 1362 (w), 1279 (s), 1261 (m), 1236 (m) 1208 (w), 1173 (m), 1146 (w), 1106 (m), 1068 (m), 1009 (m), 858 (w), 843 (w), 761 (s), 694 (s).

HRESI-MS (MeOH, +, m/z): [(Py)$_2$Pd(p-EtO$_2$CC$_6$H$_4$)]$^+$ 413.0494, calc. 413.0481

Elemental analysis (%): C 46.7, H 4.03, N 5.73 calc. C 46.2, H 3.88, N 5.67

M.p.: 136–140 °C (decomp.)

trans-(Py)$_2$Pd(p-^{n}BuO$_2$CC$_6$H$_4$)Br (11j)

[SZ 4126]
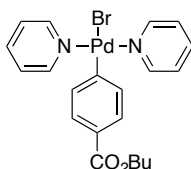
According to the general procedure, reaction of Pd$_2$dba$_3$·CHCl$_3$ (3.10 g, 3.00 mmol), P(o-tol)$_3$ (0.93 g, 3.07 mmol), butyl 4-bromobenzoate (7.69 g, 29.9 mmol) and pyridine (2.42 mL, 30.0 mmol) in toluene (12.0 mL) at 50 °C for 30 min gave complex **11j** (1.69 g, 3.20 mmol, 53%) as a colorless solid.

^{1}H NMR (400 MHz, CDCl$_3$): δ 8.78 (dd, J = 6.5, 1.5 Hz, 4H), 7.69 (tt, J = 7.7, 1.6 Hz, 2H), 7.52 (d, J = 8.4 Hz, 2H), 7.23 (ddt, J = 6.5, 3.8, 1.6 Hz, 6H), 4.21 (t, J = 6.6 Hz, 2H), 1.66 (dt, J = 14.4, 6.7 Hz, 2H), 1.41 (dq, J = 14.6, 7.4 Hz, 2H), 0.92 (t, J = 7.4 Hz, 3H) ppm.

^{13}C NMR (101 MHz, CDCl$_3$): δ 167.4, 162.9, 153.5, 137.9, 133.8, 127.7, 126.6, 125.0, 64.5, 30.9, 19.4, 13.9 ppm.

IR (v/cm^{-1}): 3055 (w), 2960 (w), 2933 (w), 2874 (w), 1695 (s), 1603 (w), 1570 (m), 1480 (w), 1454 (m9, 1379 (w), 1324 (w), 1276 (s), 1263 (m), 1238 (w), 1208 (w), 1173 (w), 1146 (w), 1105 (m), 1068 (w), 1010 (m), 9945 (w), 861 (w), 842 (w), 766 (s), 695 (s).

HRESI-MS (MeOH, +, m/z): [(Py)$_2$Pd(p-BuO$_2$CC$_6$H$_4$)]$^+$ 441.0826, calc. 441.0794

Elemental analysis (%): C 48.7, H 4.68, N 5.32 calc. C 48.3, H 4.44, N 5.32

M.p.: 130–133 °C (decomp.)

4.3.7 T-shaped (XPhos)Pd(Ar)X complexes (12,13)

(XPhos)Pd(C$_6$H$_5$)I (12a)

[SZ 3153A4/4117A]
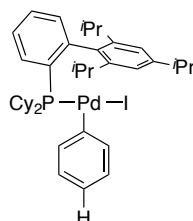
Pyridine-ligated complex **10a** (118 mg, 0.25 mmol) and XPhos (142 mg, 0.30 mmol) in a mixture of DCM/MeCN (9.00 mL, 1:2) were stirred at room temperature for 30 min, during which the mixture turned into a solution, which was filtered through a short plug of Celite. Then Et$_2$O (50.0 mL) was added to the filtrate, which resulted in of a colorless solid. The supernatant liquid was removed, the solid washed with Et$_2$O and dried in vacuum. The complex **12a** (139 mg, 0.18 mmol, 70%) was isolated as an insoluble colorless solid.

IR (v/cm^{-1}): 3052 (w), 2958 (m), 2932 (m), 2850 (w), 1558 (m), 1461 (m), 1421 (w), 1382 (w), 1361 (w), 1199 (w), 1055 (w), 1015 (w), 993 (w), 876 (w), 851 (w), 818 (w), 783 (w), 768 (m), 733 (s), 715 (w), 699 (w).

HRESI-MS (MeOH, +, *m/z*): [(XPhos)Pd(C$_6$H$_5$)]$^+$ 659.3027, calc. 659.2998

Elemental analysis (%): C 59.2, H 6.87 calc. C 59.5, H 6.91

M.p.: 170–173 °C (decomp.)

(XPhos)Pd(C$_6$H$_5$)Br (13a)

[SZ 1077/5143]
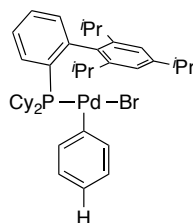
In an argon-filled glovebox, a flask was charged with Buchwald pre-catalyst G4 (99.9 mg, 0.13 mmol), XPhos (128 mg, 0.27 mmol) and THF. The mixture was stirred at room temperature until it turned into a clear solution (approx. 20 min). The solvent was removed under vacuum and the residue redissolved in toluene (5.00 mL). Then bromobenzene (1.00 mL, 9.55 mmol) was added and a solution of LiHMDS (0.50 M, 0.45 mL, 0.23 mmol) was syringed dropwise to the solution. After stirring at room temperature for 5 min, the volatiles were removed in vacuum and the residue suspended in Et$_2$O. The solid was allowed to settle and the supernatant liquid was removed. The solid

was washed with pentane and dried in vacuum. The complex **13a** (147 mg, 0.20 mmol, 87%) was isolated as a colorless solid.

Alternatively, under argon atmosphere pyridine-ligated complex **11a** (86.0 mg, 0.20 mmol) and XPhos (113 mg, 0.24 mmol) were dissolved in dry THF (2.00 mL) for 13 h at room temperature. The flask was opened to air and the volatiles removed in vacuum. The residue was dissolved in pentane (25.0 mL) and the solution stirred at room temperature (approx. 1 h) resulting in slow formation of a colorless precipitate. The supernatant liquid was decanted, the solid washed with Et$_2$O and dried in vacuum to give the complex **13a** (132 mg, 0.18 mmol, 90%) as colorless solid.

^{1}H NMR (400 MHz, CDCl$_3$): δ 7.70–7.63 (m, 1H), 7.43–7.38 (m, 2H), 7.13 (s, 2H), 7.04 (d, J = 7.6 Hz, 2H), 6.89 (dt, J = 8.7, 5.4 Hz, 3H), 6.80 (t, J = 7.2 Hz, 1H), 3.12 (hept, J = 7.1 Hz, 1H), 2.45 (p, J = 6.7 Hz, 2H), 2.22 (dtt, J = 13, 5.3, 2.8 Hz, 2H), 1.95 (br s, 2H), 1.79 (d, J = 10.2 Hz, 2H), 1.72–1.63 (m, 5H), 1.60 (d, J = 6.7 Hz, 6H), 1.39 (d, J = 6.9 Hz, 6H), 1.32–1.05 (m, 9H), 0.90 (d, J = 6.6 Hz, 6H), 0.61 (tdt, J = 13, 8.8, 3.7 Hz, 2H) ppm.

^{13}C NMR (101 MHz, CDCl$_3$): δ 156.04, 149.30, 147.75, 147.59, 137.00, 134.64, 134.55, 133.67, 133.58, 131.95, 130.46, 127.32, 126.90, 125.90, 124.79, 123.46, 35.33, 35.12, 34.30, 31.60, 28.27, 27.79, 27.72, 27.70, 27.43, 27.34, 25.96, 25.65, 24.80, 24.56 ppm.

^{31}P NMR (162 MHz, CDCl$_3$): δ 26.8 ppm.

IR (v/cm^{-1}): 3052 (w), 2959 (m), 2924 (m), 2849 (w), 1559 (m), 1459 (m), 1417 (w), 1382 (w), 1358 (w), 1054 (w), 1014 (w), 990 (w), 875 (w), 851 (w), 765 (m), 735 (s), 700 (m).

HRESI-MS (MeOH, +, m/z): [(XPhos)Pd(C$_6$H$_5$)]$^+$ 659.2954, calc. 659.2998

Elemental analysis (%): C 66.8, H 8.14 calc. C 71.2, H 8.51

A better elemental analysis could not be obtained.

M.p.: 170–173 °C (decomp.)

(XPhos)Pd(*p*-EtO$_2$CC$_6$H$_4$)Br (13i)

[SZ 4140]
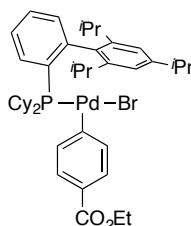
An oven-dried Schlenk flask was charged with pyridine-ligated complex **11i** (300 mg, 0.61 mmol), XPhos (292 mg, 0.61 mmol) and degassed toluene (9.00 mL). While the reaction mixture was stirred at room temperature for 16 h, it turned into a clear yellow solution. The flask was opened to air and the solution concentrated in vacuum. Then cyclohexan was added, which resulted in the formation of a

colorless solid. The mixture was filtered and the solvent removed from the filtrate. The remaining solid was dried in vacuum providing the complex **13i** (446 mg, 0.55 mmol, 90%) as yellow solid, which is soluble in all common solvents and contained some unlnown trace impurities.

^{1}H NMR (400 MHz, CDCl$_3$): δ 7.68–7.63 (m, 1H), 7.45–7.39 (m, 2H), 7.19 (dd, J = 8.5, 1.9 Hz, 2H), 7.14 (s, 2H), 7.06–6.96 (m, 2H), 6.87 (dt, J = 6.0, 3.4 Hz, 1H), 3.12 (p, J = 6.9 Hz, 1H), 2.98–2.85 (m, 1H), 2.44 (hept, J = 7.5 Hz, 2H), 2.21 (dd, J = 23.3, 12.1 Hz, 2H), 1.94 (br s, 2H), 1.79 (br d, J = 8.5 Hz, 2H), 1.72–1.66 (m, 5H), 1.60 (d, J = 6.8 Hz, 6H), 1.39 (d, J = 6.9 Hz, 6H), 1.34 (t, J = 7.1 Hz, 3H), 1.31–1.12 (m, 9H), 0.90 (d, J = 6.6 Hz, 6H), 0.75–0.59 (m, 2H) ppm.

A reliable ^{13}C NMR spectrum could not be obtained.

^{31}P NMR (162 MHz, CDCl$_3$): δ 27.1 ppm.

IR (v/cm^{-1}): 3052 (w), 2958 (m), 2925 (m), 2851 (m), 1712 (m), 1604 (w), 1575 (m), 1462 (m), 1445 (m9, 1419 (w), 1382 (w), 1361 (w), 1272 (s), 1173 (m), 1103 (s), 1053 (w), 1011 (m), 876 (w), 849 (m9, 756 (s), 735 (m), 693 (w).

HRESI-MS (MeOH, +, m/z): [(XPhos)Pd(p-EtO$_2$CC$_6$H$_4$)]$^+$ 731.3208, calc. 731.3209

Elemental analysis (%): C 66.2, H 7.83 calc. C 62.1, H 7.20

A better elemental analysis could not be obtained.

M.p.: 120–122 °C (decomp.)

(XPhos)Pd(p-BuO$_2$CC$_6$H$_4$)Br (13j)

[SZ 4130B/4139/5020]
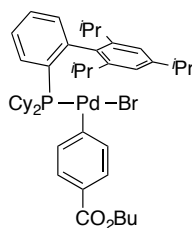
Similar to the preparation of **13i**, the reaction of pyridine-ligated complex **11j** (183 mg, 0.35 mmol), XPhos (167 mg, 0.35 mmol) in toluene (5.00 mL) at room temperature for 21 h provided complex **13j** 8305 mg, 0.36 mmol, quant.) as a yellow solid, which is soluble in all common solvents and contained some unknown trace impurities.

^{1}H NMR (400 MHz, CDCl$_3$): δ 7.67–7.63 (m, 1H), 7.57 (d, J = 8.0 Hz, 2H), 7.44–7.40 (m, 2H), 7.21–7.16 (m, 2H), 7.14 (s, 2H), 6.88–6.85 (m, 1H), 4.25 (t, J = 6.6 Hz, 2H), 3.12 (p, J = 6.9 Hz, 1H), 2.44 (p, J = 6.7 Hz, 2H), 2.20 (q, J = 12 Hz, 2H), 1.95 (br s, 2H), 1.94 (br d, J = 14 Hz, 7H), 1.60 (d, J = 6.8 Hz, 6H), 1.39 (d, J = 6.9 Hz, 6H), 1.23–1.09 (m, 11H), 0.95 (t, J = 7.4 Hz, 3H), 0.90 (d, J = 6.7 Hz, 6H), 0.73–0.58 (m, 2H) ppm.

A reliable ^{13}C NMR spectrum could not be obtained.

^{31}P NMR (162 MHz, CDCl$_3$): δ 27.1 ppm.

IR (v/cm[-1]): 3053 (w), 2957 (m), 2925 (m), 2851 (m), 1712 (s), 1604 (w), 1574 (m9, 1462 (m), 1445 (m), 1419 (w), 1382 (w), 1361 (w), 1272 (s), 1173 (m), 1101 (s), 1052 (w), 1011 (m), 939 (w), 877 (w), 838 (w), 755 (s), 692 (w).

HRESI-MS (MeOH, +, m/z): [(XPhos)Pd(p-BuO$_2$CC$_6$H$_4$)][+] 759.3484, calc. 759.3522

Elemental analysis (%): C 64.2, H 7.75 calc. C 62.9, H 7.44

A better elemental analysis could not be obtained.

M.p.: 107–109 °C (decomp.)

4.3.8   T-shaped (P^{t}Bu$_3$)Pd(Ar)Br complexes (14)

General procedure:

Inside a glovebox, an oven-dried Schlenk flask was charged with Pd(P^{t}Bu$_3$)$_2$ (1 equiv.) and P^{t}Bu$_3$·HBr (3 mol%). The sealed flask was brought outside the glovebox and degassed MEK and the bromoarene were syringed into the flask. After stirring the reaction solution at 70 °C for 1–4 h, degassed pentane was added (approx. 70.0 mL) resulting in the formation of a precipitate. The mixture was cooled to 0 °C and the solid allowed to settle. The supernatant liquid was removed via syringe, washed with degassed pentane and dried in vacuum. The complexes **14** were transferred into vials and stored in an argon-filled glovebox.

(P^{t}Bu$_3$)Pd(p-MeOC$_6$H$_4$)Br[65] (14d)
[SZ 5038]
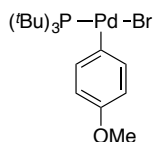
Similar to the general procedure, Pd(P^{t}Bu$_3$)$_2$ (511 mg, 1.00 mmol), and 4-bromoanisole (5.00 mL, 39.9 mmol) in MEK (10.0 mL) provided complex **14d** (102 mg, 0.21 mmol, 21%) as orange solid.

^{1}H NMR (400 MHz, C$_6$D$_6$): δ 7.40 (dd, J = 8.8, 2.1 Hz, 2H), 6.71 (d, J = 8.9 Hz, 2H), 3.40 (s, 3H), 1.13 (d, J = 27 Hz, 27H) ppm.

^{31}P NMR (162 MHz, C$_6$D$_6$): δ 63.3 ppm.

(P^{t}Bu$_3$)Pd(p-^{t}BuC$_6$H$_4$)Br (14e)

[SZ 5005]
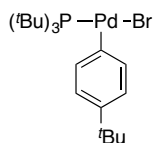
According to the general procedure, the reaction of Pd(P^{t}Bu$_3$)$_2$ (514 mg, 1.01 mmol), P^{t}Bu$_3$·HBr (9.5 mg, 0.03 mmol), 4-*tert*-butyl-bromobenzene (6.00 mL, 34.6 mmol) in MEK (20.0 mL) provided complex **14e** (319 mg, 0.61 mmol, 61%) as yellow solid.

^{1}H NMR (400 MHz, CD$_3$CN): δ 7.15 (dd, J = 8.7, 3.1 Hz, 2H), 6.95 (dd, J = 8.8, 0.9 Hz, 2H), 1.44 (d, J = 12.7 Hz, 27H), 1.23 (s, 9H) ppm.

^{13}C NMR (101 MHz, CD$_3$CN): δ 136.4 (d, J = 3.5 Hz), 125.1 (d, J = 2.2 Hz), 41.4 (d, J = 11 Hz), 32.3 (d, J = 3.0 Hz), 31.7 ppm.

The aromatic *ipso* carbon atoms were not visible.

^{31}P NMR (162 MHz, CD$_3$CN): δ 64.7 ppm.

(P^{t}Bu$_3$)Pd(p-MeC$_6$H$_4$)Br (14f)

[SZ 4049/5045]
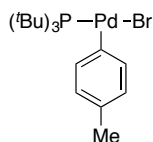
According to the general procedure, the reaction of Pd(P^{t}Bu$_3$)$_2$ (511 mg, 1.00 mmol), P^{t}Bu$_3$·HBr (8.8 mg, 0.03 mmol), 4-bromotoluene (4.85 mL, 40.0 mmol) in MEK (20.0 mL) provided complex **14f** (289 mg, 0.60 mmol, 60%) as yellow solid.

^{1}H NMR (400 MHz, CD$_3$CN): δ 7.11 (dd, J = 8.2, 3.0 Hz, 2H), 6.74 (d, J = 8.3 Hz, 2H), 2.20 (s, 3H), 1.45 (d, J = 12.7 Hz, 27H) ppm.

^{31}P NMR (162 MHz, CD$_3$CN): δ 64.8 ppm.

Because complex **14f** decomposes rapidly in solution, reliable ^{13}C NMR spectrum could not be obtained.

(P^{t}Bu$_3$)Pd(C$_6$H$_5$)Br[59a] (14a)

[SZ 5004]
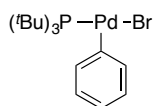
According to the general procedure, the reaction of Pd(P^{t}Bu$_3$)$_2$ (514 mg, 1.01 mmol), P^{t}Bu$_3$·HBr (8.6 mg, 0.03 mmol), bromobenzene (6.00 mL, 57.1 mmol) in MEK (20.0 mL) provided complex **14a** (377 mg, 0.81 mmol, 80%) as yellow solid.

^{1}H NMR (400 MHz, CD$_3$CN): δ 7.26 (ddd, J = 8.4, 3.1, 1.1 Hz, 2H), 6.89 (t, J = 7.3 Hz, 2H), 6.83 (t, J = 7.0 Hz, 1H), 1.45 (d, J = 12.7 Hz, 27H) ppm.

^{13}C NMR (101 MHz, CD$_3$CN): δ 137.3, 127.9, 124.6, 41.4 (d, J = 10.4 Hz), 32.2 (d, J = 3.0 Hz) ppm.

^{31}P NMR (162 MHz, CD$_3$CN): δ 64.6 ppm.

(P^{t}Bu$_3$)Pd(p-FC$_6$H$_5$)Br[77a] (14g)

[SZ 4048/5037]
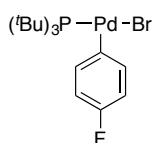
Similar to the general procedure, the reaction of Pd(P^{t}Bu$_3$)$_2$ (512 mg, 1.00 mmol) and 4-fluorobromobenzene (4.40 mL, 40.3 mmol) in MEK (10.0 mL) provided complex **14g** (375 mg, 0.77 mmol, 77%) as yellow solid.

^{1}H NMR (400 MHz, CD$_3$CN): δ 7.23 (ddd, J = 8.9, 5.8, 2.4 Hz, 2H), 6.75 (t, J = 9.2 Hz, 2H), 1.44 (d, J = 12.7 Hz, 27H) ppm.

^{13}C NMR (101 MHz, CD$_3$CN): δ 162.7, 160.3, 137.8 (d, J = 4.0 Hz), 114.2 (d, J = 20.4 Hz), 41.5 (d, J = 10.1 Hz), 32.4 (d, J = 2.9 Hz) ppm.

^{31}P NMR (162 MHz, CD$_3$CN): δ 64.9 ppm.

^{19}F NMR (376 MHz, CDCl$_3$): δ −123.9 (p, J = 8.9) ppm.

(P^{t}Bu$_3$)Pd(p-EtO$_2$CC$_6$H$_5$)Br (14i)

[SZ 4038]
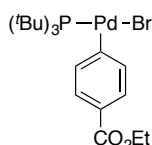
According to the general procedure, the reaction of Pd(P^{t}Bu$_3$)$_2$ (513 mg, 1.00 mmol), P^{t}Bu$_3$·HBr (9.5 mg, 0.03 mmol), ethyl 4-bromobenzoate (6.50 mL, 39.8 mmol) in MEK (20.0 mL) provided complex **14i** (322 mg, 0.60 mmol, 60%) as yellow solid.

¹H NMR (400 MHz, CD₃CN): δ 7.50–7.43 (m, 4H), 4.26 (q, J = 7.1 Hz, 2H), 1.44 (d, J = 12.7 Hz, 27H), 1.31 (t, J = 7.1 Hz, 3H) ppm.

³¹P NMR (162 MHz, CD₃CN): δ 66.5 ppm.

(P^{t}Bu₃)Pd(p-F₃CC₆H₅)Br[7e, 77b] (14k)

[SZ 4020]
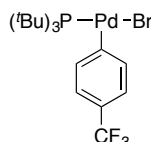
According to the general procedure, the reaction of Pd(P^{t}Bu₃)₂ (510 mg, 1.00 mmol), P^{t}Bu₃·HBr (8.6 mg, 0.03 mmol), 4-bromobenzotrifluoride (6.00 mL, 42.9 mmol) in MEK (20.0 mL) provided complex **14k** (305 mg, 0.57 mmol, 57%) as yellow solid.

¹H NMR (400 MHz, CD₃CN): δ 7.50 (ddq, J = 7.8, 2.6, 0.9 Hz, 2H), 7.16 (ddt, J = 7.6, 1.5, 0.7 Hz, 2H), 1.44 (d, J = 12.7 Hz, 27H) ppm.

¹³C NMR (101 MHz, CD₃CN): δ 138.6, 123.21, 41.7 (d, J = 10 Hz), 32.5 (d, J = 3.0 Hz) ppm.

The aromatic *ipso* carbon atoms were not visible.

³¹P NMR (162 MHz, CD₃CN): δ 66.87 ppm.

¹⁹F NMR (376 MHz, CDCl₃): δ −62.27 ppm.

4.4 Arylzinc compounds

Bis-(4-methoxyphenyl)zinc[41] (15d)

[SZ 4101]
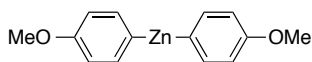
A hot Schlenk tube was charged with magnesium (271 mg, 11.1 mmol) and allowed to cool to room temperature under vacuum and vigorous stirring. After the flask was set under argon, THF (1.00 mL) and 4-bromoanisole (1.30 mL, 10.4 mL) were added resulting in immediate ignition of the Grignard formation. Additional THF (9.00 mL) was added and the reaction mixture stirred at ambient temperature for 3.5 h, then 1.5 h at 50 °C. The concentration of the Grignard solution was c = 0.84 M determined by titration.[206] Inside a glovebox, ZnCl₂ (422 mg, 3.10 mmol) was weighted in a Schlenk tube and dissolved in THF (6.00 mL). Outside the glovebox, the Grignard solution (7.37 mL, 6.19 mmol) was syringed to the ZnCl₂ solution and the resulting mixture was stirred at room

temperature until the Gilman test was negative (over night).[207] The mixture was cooled to –78 °C without stirring and the supernatant liquid was transferred into another Schlenk tube by syringe. The volatiles were removed by vacuum transfer distillation and the remaining solids dried in vacuum. The crude product was washed with dry pentane and the Schlenk tube sealed with a cold finger. The solid was dried in vacuum, before being heated for sublimation. Then the Schlenk tube was placed in a pre-heated oil bath and the product sublimized at 150 °C under continues vacuum (18 h). Inside a glovebox, the product **15d** (380 mg, 1.36 mmol, 44%) was collected as colorless crystals. The purity was determined by ^{1}H NMR against TMB as internal standard and was found to be 103%.

^{1}H NMR (400 MHz, THF-d_8): δ 7.47 (d, J = 8.3 Hz, 4H), 6.74 (d, J = 8.3 Hz, 4H), 3.70 (s, 6H) ppm.

^{13}C NMR (101 MHz, THF-d_8): δ 54.7, 113.3, 140.2, 146.7, 159.4 ppm.

Bis-(4-methylphenyl)zinc (15f)

[SZ 4105]

Me —⟨⟩— Zn —⟨⟩— Me
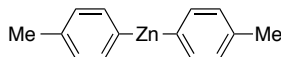
Similar to the preparation of **15d**, the reaction of magnesium (742 mg, 30.5 mmol) and 4-bromo-toluene (3.1 mL, 25.0 mL) in Et$_2$O (40.0 mL) was initiated by gentle heating with the heat gun and stirred at ambient temperature for 4 h. The concentration of the Grignard was c = 0.5 M determined by titration.[206] The reaction of the Grignard (30.0 mL, 15.0 mmol) with ZnCl$_2$ (1.0 g, 7.5 mmol) in Et$_2$O (10.0 mL) was stirred at room temperature for 17 h until the Gilman test was negative.[207] After removal of the volatiles by vacuum transfer distillation, washing the remaining solid with pentane, the product was sublimized at 160 °C under continuous vacuum over night. The product **15f** (582 mg, 2.4 mmol, 31%) was collected as pure colorless solid (purity of 111% as determined by ^{1}H NMR using TMB as internal standard).

^{1}H NMR (400 MHz, THF-d_8): δ 7.4 (d, J = 7.8 Hz, 4H), 6.9 (dd, J = 7.8, 0.7 Hz, 4H), 2.2 (s, 6H) ppm.

^{13}C NMR (101 MHz, THF-d_8): δ 21.7, 128.15, 134.8, 139.6, 152.7 ppm.

General procedure for the preparation of solutions of arylzinc chlorides **16·LiCl·MgICl** solutions:

In a glovebox an oven-dried Schlenk flask was charged with magnesium (2.7 g, 109 mmol), LiCl (4.2 g, 99.0 mmol), one crystal of iodine, sealed with a rubber septum and brought outside the glovebox, where THF (45.0 mL) and *iso*-propyl chloride (9.0 mL, 99.0 mmol) were syringed to the flask. The reaction mixture has been stirred at ambient temperature for 4.5 h when the Grignard formation started resulting in a very exothermic reaction. The reaction mixture was additionally stirred

for 14 h. Titration of the Grignard solution gave a concentration of $c = 1.6$ M and was directly used for the preparation of arylzinc solutions.[206]

An oven-dried Schlenk tube was set under argon and the aryl iodides (2.0 mmol) and THF (4.0 mL). The solution was cooled to –30 °C (acetone/dry ice) before syringing the ^{i}PrMgCl solution (2.0 mmol) to the flask. After stirring at –30 °C for 45 min, a solution of ZnCl$_2$ in THF (0.5 M, 2.0 mmol) was added and the reaction stirred at –30 °C for additional 45 min. The reaction was allowed to reach room temperature and the volatiles were removed by vacuum transfer distillation. The residue was dried in high vacuum, before being redissolved in THF (10.0 mL). Two aliquots (0.20 mL) were withdrawn and quenched with excess iodine. Additional two aliquots (0.20 mL) were quenched with MeOH. A stock solution of TMB (20 mM, 0.20 mL) was added to each aliquot and the concentration of aryl iodide was quantified by GC-GID measurements.

4-(Ethoxycarbonyl)phenylzinc chloride lithium chloride adduct (16k)

[SZ 5021]
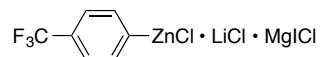
According to the general procedure, the reaction of 4-iodobenzotrifluoride (554 mg, 2.0 mmol), ^{i}PrMgCl (1.3 mL, 2.0 mmol), and ZnCl$_2$ (4.1 mL, 2.0 mmol) gave arylzinc reagent **16k** with a concentration of $c = 0.3$ M (redissolved in 7.00 mL, yield ≈ 105%) containing no unreacted aryl iodide.

4-(Ethoxycarbonyl)phenylzinc chloride lithium chloride adduct (16i)

[SZ 5019]
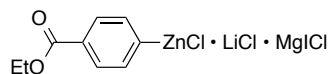
According to the general procedure, the reaction of ethyl 4-iodobenzoate (577 mg, 2.1 mmol), ^{i}PrMgCl (1.3 mL, 2.1 mmol), and ZnCl$_2$ (4.2 mL, 2.1 mmol) gave arylzinc reagent **16i** with a concentration of $c = 0.2$ M (yield ≈ 95%) containing no unreacted aryl iodide.

Phenylzinc chloride lithium chloride adduct (16a)

[SZ 5022]
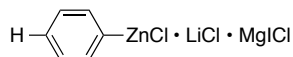
According to the general procedure, the reaction of iodobenzene (421 mg, 2.1 mmol), ^{i}PrMgCl (1.3 mL, 2.1 mmol), and ZnCl$_2$ (4.1 mL, 2.1 mmol) gave arylzinc reagent **16a** with a concentration of $c = 0.2$ M containing unreacted aryl iodide $c = 0.02$ M. The solvent was removed again by vacuum transfer distillation, the residue washed with dry pentane and redissolved with THF (8.0 mL).

Quantification by GC-FID gave a concentration of $c = 0.1$ M (yield $\approx 38\%$) containing no unreacted aryl iodide.

4-Methylphenylzinc chloride lithium chloride adduct (16f)

[SZ 5028]

$$\text{Me} - \langle\rangle - \text{ZnCl} \cdot \text{LiCl} \cdot \text{MgICl}$$
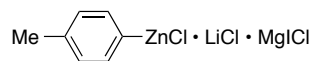
According to the general procedure, the reaction of 4-iodotoluene (419 mg, 1.9 mmol), ^{i}PrMgCl (1.2 mL, 1.9 mmol), and ZnCl$_2$ (3.8 mL, 1.9 mmol) gave arylzinc reagent **16f** with a concentration of $c = 0.2$ M containing unreacted aryl iodide $c = 0.02$ M. The solvent was removed again by vacuum transfer distillation, the residue washed with dry pentane and redissolved with THF (8.0 mL). Quantification by GC-FID gave a concentration of $c = 0.2$ M (yield $\approx 84\%$) containing no unreacted aryl iodide.

4-Methoxyphenylzinc chloride lithium chloride adduct (16d)

[SZ 5029]

$$\text{MeO} - \langle\rangle - \text{ZnCl} \cdot \text{LiCl} \cdot \text{MgICl}$$
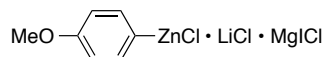
According to the general procedure, the reaction of 4-iodotoluene (465 mg, 2.0 mmol), ^{i}PrMgCl (1.3 mL, 2.0 mmol), and ZnCl$_2$ (4.0 mL, 2.0 mmol) gave arylzinc reagent **16d** with a concentration of $c = 0.2$ M containing unreacted aryl iodide $c = 0.0$ M. The solvent was removed again by vacuum transfer distillation, the residue washed with dry pentane and redissolved with THF (8.0 mL). Quantification by GC-FID gave a concentration of $c = 0.2$ M (yield $\approx 80\%$) containing no unreacted aryl iodide.

4.5 Syntheses of biaryls and GC reference compounds

All reagents, 4-biphenylcarboxylic acid, benzoic acid, 4-bromo- and 4-iodoarenes were purchased from commercial suppliers and used as received. Anhydrous ZnCl$_2$ was immediately stored in an argon-filled glovebox directly after receiving.

4.5.1   Starting materials

Ethyl 4-bromobenzoate

[SZ 3016]
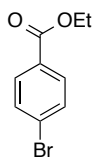
Via a general esterfication procedure, 4-bromobenzoic acid (2.21 g, 11.0 mmol) was dissolved in the ethanol (30.0 mL) and conc. H_2SO_4 (3.00 mL) was added. After the reaction solution has been stirred over night under reflux the volatiles were removed. The residue was diluted in DCM and neutralized with sat. aqueous Na_2CO_3. The water phase was extracted with DCM (3 times), the combined organic layers dried over Na_2SO_4, filtered and the solvent was removed. Analytically pure ethyl 4-bromobenzoate (2.38 g, 10.4 mmol, 95%) was obtained as colorless liquid.

^{1}H NMR (400 MHz, CDCl$_3$): δ 7.90 (d, J = 8.4 Hz, 2H), 7.57 (d, J = 8.3 Hz, 2H), 4.37 (q, J = 7.1 Hz, 2H), 1.39 (t, J = 7.1 Hz, 3 H) ppm.

The chemical shifts are in agreement with previous reported values.[208]

Ethyl 4-iodobenzoate

[SZ 3028]
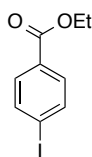
Analogous to the preparation of ethyl 4-bromobenzoate, the reaction of 4-iodobenzoic acid (1.12 g, 4.51 mmol), conc. H_2SO_4 (1.00 mL) in ethanol (10.0 mL) provided the title compound (1.17 g, 4.22 mmol, 94%) as colorless viscous liquid.

^{1}H NMR (400 MHz, CDCl$_3$): δ 7.82–7.72 (m, 4H), 4.37 (q, J = 7.1 Hz, 2H), 1.39 (t, J = 7.1 Hz, 3H) ppm.

The chemical shifts are in agreement with previous reported values.[209]

n-Butyl 4-bromobenzoate

[SZ 3015]
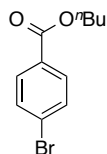
Reaction of 4-bromobenzoic acid (2.21 g, 11.0 mmol), conc. H_2SO_4 (3.00 mL) in *n*-butanol (30.0 mL) provided the title compound (2.38 g, 95%) as colorless viscous liquid.

^{1}H NMR (400 MHz, CDCl$_3$): δ 7.90 (d, J = 8.4 Hz, 2H), 7.57 (d, J = 8.4 Hz, 2H), 4.32 (t, J = 6.6 Hz, 2H), 1.75 (p, J = 6.8 Hz, 2H), 1.47 (h, J = 7.4 Hz, 2H), 0.98 (t, J = 7.4 Hz, 3H) ppm.

The chemical shifts are in agreement with previous reported values.[210]

n-Butyl 4-iodobenzoate

[SZ 3029]
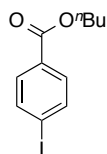
Reaction of 4-iodobenzoic acid (1.15 g, 4.65 mmol), conc. H_2SO_4 (1.00 mL) and *n*-butanol (10.0 mL) provided the title compound (1.37 g, 4.49 mmol, 96%) as colorless viscous liquid.

^{1}H NMR (400 MHz, CDCl$_3$): δ 7.82–7.72 (m, 4H), 4.31 (t, J = 6.6 Hz, 2H), 1.79–1.69 (m, 2H), 1.46 (dq, J = 14.7, 7.4 Hz, 2H), 0.98 (t, J = 7.4 Hz, 3H) ppm.

The chemical shifts are in agreement with previous reported values.[211]

4-Phenoxyiodobenzene

[SZ 3058]
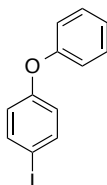
According to a reported procedure for a copper-catalyzed aromatic Finkelstein reaction,[212] an oven-dried Schlenk flask was charged with 4-phenoxybromobenzene (1.75 mL, 10.0 mmol), copper(I) iodide (95.4 mg, 0.50 mmol), NaI (3.03 g, 20.2 mmol) and sealed with a rubber septum. The flask was set under argon by repeated evacuation and backfill with argon. Dry dioxane (10.0 mL) and *N,N'*-dimethylethylenediamine (108 μL, 1.00 mmol) were syringed to the flask and the mixture heated at

110 °C for 24 h. The reaction mixture was poured into am aqueous ammonia solution (w = 25%, 25.0 mL), diluted with water (150 mL) and extracted with DCM. The combined organic layers were dried with Na_2SO_4, the desiccant was filtered and the solvent removed from the filtrate. The title compound (3.02 g, 10.2 mmol, quant.) was obtained as colorless solid.

^{1}H NMR (400 MHz, CDCl$_3$): δ 7.61 (d, J = 8.9 Hz, 2H), 7.35 (dd, J = 8.6, 7.4 Hz, 2H), 7.13 (ddt, J = 8.5, 7.2, 1.2 Hz, 1H), 7.00 (dd, J = 8.7, 1.1 Hz, 2H), 6.77 (d, J = 8.8 Hz, 2H) ppm.

The chemical shifts are in agreement with previous reported values.[213]

4-Iodo-*N*,*N*-dimethylaniline

[SZ 3059]
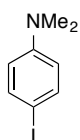
Similar to 4-phenoxyiodobenzene via aromatic Finkelstein reaction, the reaction of 4-bromo-*N*,*N*-dimethylaniline (1.79 g, 8.95 mmol), copper(I) iodide (92.2 mg, 0.48 mmol), NaI (2.68 g, 17.9 mmol), and *N*,*N'*-dimethylethylenediamine (108 μL, 1.00 mmol) in dioxane (10.0 mL) gave the title compound (2.22 g, 8.98 mmol, quant.) as colorless solid.

^{1}H NMR (400 MHz, CDCl$_3$): δ 7.43 (d, J = 9.1 Hz, 2H), 6.45 (d, J = 9.0 Hz, 2H), 3.32 (q, J = 7.1 Hz, 2H), 1.14 (t, J = 7.1 Hz, 6H) ppm.

The chemical shifts are in agreement with previous reported values.[214]

4-Methylphenylboronic acid

[AC 4020/4022]
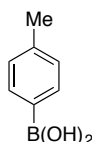
An oven-dried 1-L-Schlenk-flask, equipped with a dropping funnel, was set under argon and charged with magnesium turnings (8.06 g, 0.33 mol), few crystals of iodine, and THF (70.0 mL). Then a solution of 4-bromotoluene (37.0 mL, 0.30 mol) in THF (375 mL) was added and the reaction mixture was stirred for additional 2 h at ambient temperatures. After the reaction solution has been cooled to 0 °C, a solution of trimethylborate (85.0 mL, 0.76 mol) in THF (317 mL) was slowly added. The resulting mixture was warmed to room temperature and stirred over night. The reaction was quenched with sat. aqueous solution of NH_4Cl (260 mL) and the volatiles were removed by rotary evaporation. The precipitate was filtered, washed with cold water and diethyl ether. The solid was dissolved in

acetone, the unsoluble solids filtered, and the solvent removed from the filtrate. The crude yellow solid was recrystallized from a boiling mixture of acetone and ethyl acetate. The title compound (7.87 g, 57.9 mmol, 31%) was obtained as a colorless solid.

^{1}H NMR (400 MHz, CDCl$_3$): δ 8.13 (d, J = 7.9 Hz, 2H), 7.32 (d, J = 7.9 Hz, 2H, 2.45 (s, 3H) ppm. The chemical shifts are in agreement with previous reported values.[215]

4-(Trifluormethyl)phenylboronic acid

[AC 4037/4040]
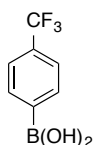
An oven-dried 1-L-Schlenk flask, equipped with a magnetic stir bar and a rubber septum, was set under an atmosphere of argon and charged with magnesium turnings (8.81 g, 0.36 mol), and a solution of LiCl (7.68 g, 0.18 mol) in THF (362 mL). Then, DIBAL-H (1.00 M in hexane, 1.45 mL, 2.90 mmol) was added and the mixture stirred for 10 min. 1-Bromo-4-(trifluoromethyl)benzene (20.3 mL, 0.14 mol) was syrringed to flask (under ice bath cooling) and the reaction mixture stirred at 0 °C for 30 min. Trimethylborate (32.0 mL, 0.29 mol) was slowly added and the mixture stirred for additional 2 h. After quenching with an aqueous HCl (0.1 M, 250 mL) and extraction with EtOAc, the combined organic layers were dried with Na$_2$SO$_4$, filtered, and the solvent removed from the filtrate. The product (19.4 g, 102 mmol, 71%) was obtained as a yellow solid.

^{1}H NMR (400 MHz, DMSO-d_6): δ 8.38 (s, 2H), 7.99 (d, J = 7.6 Hz, 2H), 7.69 (d, J = 8.2 Hz, 2H) ppm.

^{19}F NMR (376 MHz, DMSO-d_6): δ −61.2 ppm.

The chemical shifts are in agreement with previous reported values.[216]

4.5.2 Reference compounds for GC quantification

4.5.2.1 *Via esterfication*

n-Butyl benzoate

[SZ 3026]
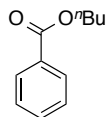
Via esterfication, the reaction of benzoic acid (2.49 g, 20.4 mmol), conc. H_2SO_4 (3.00 mL) and *n*-butanol (30.0 mL) provided the title compound (3.59 g, 20.1 mmol, 99%) as colorless liquid.

^{1}H NMR (400 MHz, CDCl$_3$): δ 8.10–7.99 (m, 2H), 7.61–7.49 (m, 1H), 7.49–7.37 (2, 1H), 4.33 (t, J = 6.6 Hz, 2H), 1.80–1.71 (m, 2H), 1.48 (dq, J = 14.7, 7.4 Hz, 2H), 0.98 (t, J = 7.4 Hz, 3H) ppm.
The chemical shifts are in agreement with previous reported values.[217]

Ethyl biphenyl-4-carboxylate (17ai)

[SZ 1037]
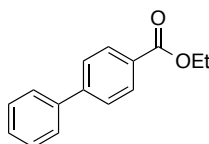
Via esterfication, the reaction of biphenyl-4-carboxylic acid (1.05 g, 5.30 mmol), conc. H_2SO_4 (0.50 mL) in ethanol (15.0 mL) provided the title compound (1.20 g, 5.30 mmol, quant.) as pale yellow solid.

^{1}H NMR (400 MHz, CDCl$_3$): δ 8.13 (d, J = 8.2 Hz, 2H), 7.71–7.60 (m, 4H), 7.48 (t, J = 7.4 Hz, 2H), 7.40 (t, J = 7.3 Hz, 1H), 4.42 (q, J = 7.1 Hz, 2H), 1.43 (t, J = 7.1 Hz, 3H) ppm.
The chemical shifts are in agreement with previous reported values.[218]

n-Butyl biphenyl-4-carboxylate (17aj)

[SZ 3017]
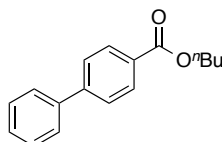
Via esterfication, the reaction of biphenyl-4-carboxylic acid (1.22 g, 6.15 mmol), conc. H_2SO_4 (1.50 mL) in *n*-butanol (15.0 mL) provided the title compound (1.22 g, 78%) as pale brown oil.

^{1}H NMR (400 MHz, CDCl$_3$): δ 8.11 (d, J = 8.7 Hz, 2H), 7.66 (d, J = 8.7 Hz, 2H), 7.63 (d, J = 7.0 Hz, 2H), 7.47 (t, J = 7.4 Hz, 2H), 7.42–7.36 (m, 1H), 4.35 (t, J = 6.6 Hz, 2H), 1.80 (d, J = 6.6 Hz, 2H), 1.51 (dt, J = 14.9, 7.4 Hz, 2H), 1.00 (t, J = 7.4 Hz, 3H) ppm.

The chemical shifts are in agreement with previous reported values.[219]

4.5.2.2   *Via palladium-catalyzed Negishi cross-coupling*

Synthesis of phenylzinc chloride solution:

An oven-dried Schlenk flask was charged with magnesium (1.22 g, 50.0 mol), one crystal of iodine and THF (5.00 mL). Pure bromobenzene (0.20 mL) was added to the mixture resulting in an immediate initiation of the Grignard reaction. Then a solution of bromobenzene (5.23 mL, 50.2 mmol) in THF (45.0 mL) was added dropwise within 20 min. The reaction was stirred for additional 2 h at ambient temperature before a solution of ZnCl$_2$ (6.84 g, 50.2 mmol) in THF (50.0 mL) was added. After stirring at room temperature for 1 h, the concentration was determined to be c = 0.41 M by titration.[220]

General procedure for the Negishi cross-coupling:

Based on the reported procedure for Negishi couplings with the Buchwald pre-catalysts,[221] an oven-dried Schlenk flask was charged with the aryl halide, XPhos (2 mol%), Buchwald's pre-catalyst G4 (0.5 mol%), sealed with a rubber septum and set under argon by evacuation and backfill with argon. The phenylzinc chloride solution was syringed into the flask resulting in an immediate exothermic reaction. After stirring room temperature 18 h, the reaction mixture was poured into beaker with crushed ice. Then DCM and aqueous HCl (w = 1.0 M) was added and the mixture extracted several times with DCM. The combined organic layers were dries with Na$_2$SO$_4$, filtered and the solvent removed from the filtrate.

4-Phenyl-*N*,*N*-dimethylaniline (17ab)

[SZ 3081b]
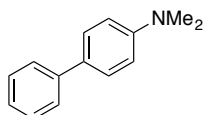
According to the general procedure, the reaction of 4-bromo-*N*,*N*-dimethylaniline (2.00 g, 10.0 mmol), XPhos (97.8 mg, 0.21 mmol), pre-catalyst G4 (38.4 mg, 0.05 mmol) and phenylzinc reagent solution (0.41 M, 30.0 mL, 12.3 mmol) gave **17ab** (1.80 g, 9.14 mmol, 91%) as yellow solid after column chromatography (SiO$_2$, EtOAc in hexane 5%) as colorless solid.

^{1}H NMR (400 MHz, CDCl$_3$): δ 7.62–7.53 (m, 4H), 7.43 (td, J = 7.8, 1.8 Hz, 2H), 7.29 (td, J = 7.3, 1.6 Hz, 1H), 6.84 (dd, J = 8.8, 1.6 Hz, 2H), 3.02 (d, J = 1.3 Hz, 6H) ppm.

The chemical shifts are in agreement with previous reported values.[222]

4-Phenylphenoxybenzene (17ac)

[SZ 3081a]
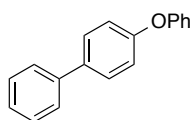
According to the general procedure, the reaction of 4-phenoxyiodobenzene (1.50 g, 5.07 mmol), XPhos (47.2mg, 0.10 mmol), pre-catalyst G4 (19.5 mg, 0.025 mmol) and phenylzinc reagent solution (0.41 M, 15.0 mL, 6.15 mmol) gave **17ac** (1.13 g, 4.61 mmol, 91%) as colorless solid after column chromatography (SiO$_2$, hexane) as tan solid.

^{1}H NMR (400 MHz, CDCl$_3$): δ 7.66–7.56 (m, 4H), 7.47 (t, J = 7.8 Hz, 2H), 7.43–7.33 (m, 3H), 7.16 (ddt, J = 7.9, 7.2, 1.1 Hz, 1H), 7.13–7.09 (m, 4H) ppm.

The chemical shifts are in agreement with previous reported values.[223]

4-Phenylchlorobenzene (17ah)

[SZ 3081a]
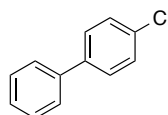
According to the general procedure, the reaction of 4-chlorobromobenzene (1.91 g, 10.0 mmol), XPhos (97.3 mg, 0.20 mmol), pre-catalyst G4 (38.4 mg, 0.05 mmol) and phenylzinc reagent solution (0.41 M, 30.0 mL, 12.3 mmol) gave **17ah** (1.13 g, 6.00 mmol, 60%) as colorless solid after column chromatography (SiO$_2$, hexane) as colorless solid.

^{1}H NMR (400 MHz, CDCl$_3$): δ 7.58–7.50 (m, 4H), 7.48–7.34 (m, 5H) ppm.

The chemical shifts are in agreement with previous reported values.[224]

4.5.2.3 *Via palladium-catalyzed Suzuki cross-coupling*

General procedure:

Based on the reported procedure for Suzuki couplings with the Buchwald's pre-catalysts G4,[74] a Schlenk flask was charged with aryl bromide, arylboronic acid (1.5 equiv.), XPhos and pre-catalyst G4 and set under argon by repeated evacuation and backfill with argon. Then a degassed mixture of THF and aqueous K_3PO_4 (0.50 M, 1:2) was syringed to the flask. The reaction mixture was stirred either at room temperature or at 40 °C until the starting material was consumed as judged by TLC. The reaction mixture was extracted with Et_2O and the combined organic layers dried with Na_2SO_4, filtered and the solvent removed from the filtrate. The crude product was purified by column chromatography (SiO_2, EtOAc/hexane mixtures).

4-Phenyl-*N*,*N*-dimethylaniline (17ab)

[SZ 3007]
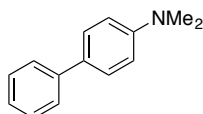
According to the general procedure, reaction of 4-bromo-*N*,*N*-dimethylaniline (401 mg, 2.00 mmol), phenylboronic acid (368 mg, 3.02 mmol), pre-catalyst G4 (19.2 mg, 0.025 mmol), XPhos (18.9 mg, 0.04 mmol) in a mixture of THF (4.00 mL) and aq. K_3PO_4 (8.00 mL) at room temperature over night provided biaryl **17ab** (342 mg, 1.73 mmol, 87%) as yellow solid after column chromatography (EOAc in hexane 0–3%, 1% increments).

^{1}H NMR (400 MHz, $CDCl_3$): see above

The chemical shifts are in agreement with previous reported values.[222]

4-Methoxybiphenyl (17ad)

[AC 4059]
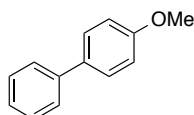
According to the general procedure, reaction of bromobenzene (1.57 g, 10.0 mmol), 4-methoxy-phenylboronic acid (2.28 g, 23.0 mmol), pre-catalyst G4 (38.4 mg, 0.05 mmol), XPhos (47.7 mg, 0.10 mmol) in a mixture of THF (20.0 mL) and aq. K_3PO_4 (40.0 mL) at 40 °C over night provided biaryl **17ad** (1.59 g, 8.63 mmol, 86%) as colorless solid after column chromatography (EOAc in hexane 2%).

^{1}H NMR (400 MHz, CDCl$_3$): δ 7.61–7.50 (m, 4H), 7.42 (t, J = 7.1 Hz, 2H), 7.30 (t, J = 8.1 Hz, 1H), 6.98 (d, J = 8.9 Hz, 2H), 3.86 (s, 3H) ppm.

The chemical shifts are in agreement with previous reported values.[222]

4-*tert*-Butylbiphenyl (17ae)

[SZ 1070c]
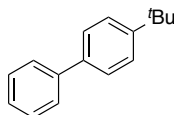
According to the general procedure, reaction of 4-*tert*-butylbromobenzene (0.35 mL, 2.02 mmol), phenylboronic acid (382 g, 3.13 mmol), pre-catalyst G4 (15.2 mg, 0.04 mmol), XPhos (23.9 mg, 0.05 mmol) in a mixture of THF (4.00 mL) and aq. K$_3$PO$_4$ (8.00 mL) at room temperature for 1.5 h provided biaryl **17ae** (308 mg, 1.46 mmol, 72%) as colorless solid after column chromatography (hexane).

^{1}H NMR (400 MHz, CDCl$_3$): δ 7.61 (dd, J = 8.3, 1.2 Hz, 2H), 7.57–7.52 (m, 2H), 7.51–7.41 (m, 4H), 7.38–7.30 (m, 1H), 1.38 (s, 9H) ppm.

The chemical shifts are in agreement with previous reported values.[225]

4-Methylbiphenyl (17af)

[AC 4057]
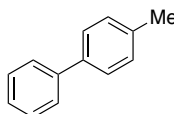
According to the general procedure, reaction of 4-bromotoluene (1.71 g, 10.0 mmol), phenylboronic acid (1.82 g, 14.9 mmol), pre-catalyst G4 (38.4 mg, 0.05 mmol), XPhos (47.7 mg, 0.10 mmol) in a mixture of THF (20.0 mL) and aq. K$_3$PO$_4$ (40.0 mL) at 40 °C over night provided biaryl **17af** (1.64 g, 9.59 mmol, 96%) as colorless solid after column chromatography (hexane).

^{1}H NMR (400 MHz, CDCl$_3$): δ 7.60–7.56 (m, 2H), 7.50 (d, J = 8.2 Hz, 2H), 7.43 (t, J = 7.6 Hz, 1H), 7.36–7.29 (m, 1H), 7.26 (d, J = 1.7 Hz, 2H), 2.40 (s, 3H) ppm.

The chemical shifts are in agreement with previous reported values.[222]

4-Fluorobiphenyl (17ag)

[SZ 1070b]
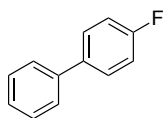
According to the general procedure, reaction of 4-fluorobromobenzene (0.22 mL, 2.00 mmol), phenylboronic acid (384 mg, 3.15 mmol), pre-catalyst G4 (16.7 mg, 0.04 mmol), XPhos (27.5 mg, 0.06 mmol) in a mixture of THF (4.00 mL) and aq. K_3PO_4 (8.00 mL) at room temperature for 1.5 h provided biaryl **17ag** (2.92 mg, 1.70 mmol, 85%) as colorless solid after column chromatography (hexane).

^{1}H NMR (400 MHz, CDCl$_3$): δ 7.58–7.52 (m, 4H), 7.47–7.40 (m, 2H), 7.38–7.32 (m, 1H), 7.17–7.09 (m, 2H) ppm.

^{19}F NMR (376 MHz, CDCl$_3$): δ -115.8 ppm.

The chemical shifts are in agreement with previous reported values.[222]

4-Phenylchlorobenzene (17ah)

[SZ 3008]

According to the general procedure, reaction of 4-chlorobromobenzene (392 m g, 2.05 mmol), phenylbronic acid (392 mg, 3.22 mmol), pre-catalyst G4 (38.4 mg, 0.026 mmol), XPhos (18.6 mg, 0.04 mmol) in a mixture of THF (4.00 mL) and aq. K_3PO_4 (8.00 mL) at room temperature over night provided biaryl **17ah** (243 mg, 1.29 mmol, 63%) as colorless solid after column chromatography (EOAc in hexane 0–3%, 1% increments).

^{1}H NMR (400 MHz, CDCl$_3$): see above

The chemical shifts are in agreement with previous reported values.[224]

4-(Trifluoromethyl)biphenyl (17ak)

[SZ 1070a]
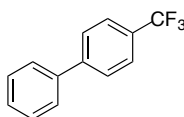
According to the general procedure, reaction of 4-(trifluoromethyl)bromobenzene (0.28 mL, 2.00 mmol), phenylboronic acid (383g, 3.14 mmol), pre-catalyst G4 (18.6 mg, 0.05 mmol), XPhos

(25.8 mg, 0.05 mmol) in a mixture of THF (4.00 mL) and aq. K_3PO_4 (8.00 mL) at room temperature for 1.5 h provided biaryl **17ak** (382, 1.72 mmol, 86%) as colorless solid after column chromatography (hexane).

^{1}H NMR (400 MHz, CDCl$_3$): δ 7.70 (d, J = 0.4 Hz, 4H), 7.63–7.59 (m, 2H), 7.51–7.46 (m, 2H), 7.44–7.38 (m, 1H) ppm.

^{19}F NMR (376 MHz, CDCl$_3$): δ −115.8 ppm.

The chemical shifts are in agreement with previous reported values.[222]

4-Cyanobiphenyl (17al)

[AC 4021]
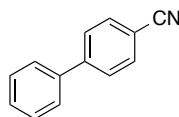
According to the general procedure, reaction of 4-bromobenzonitrile (1.82 g, 10.0 mmol), phenylboronic acid (1.83 g, 15.0 mmol), pre-catalyst G4 (38.4 mg, 0.05 mmol), XPhos (47.7 mg, 0.10 mmol) in a mixture of THF (20.0 mL) and aq. K_3PO_4 (40.0 mL) at room temperature over night provided biaryl **17al** (1.21 g, 6.75 mmol, 68%) as colorless solid after column chromatography (EtOAc in hexane 0–5%, 1% increments).

^{1}H NMR (400 MHz, CDCl$_3$): δ 7.73 (d, J = 8.5 Hz, 2H), 7.69 (d, J = 8.3 Hz, 2H), 7.59 (d, J = 7.0 Hz, 2H), 7.53–7.46 (m, 2H), 7.43 (t, J = 7.2 Hz, 1H) ppm.

The chemical shifts are in agreement with previous reported values.[224]

4-Nitrobiphenyl (17am)

[SZ 3009]

According to the general procedure, reaction of 4-nitrobromobenzene (400 mg, 2.00 mmol), phenylboronic acid (380 mg, 3.11 mmol), pre-catalyst G4 (19.4 mg, 0.025 mmol), XPhos (18.3 mg, 0.04 mmol) in a mixture of THF (4.00 mL) and aq. K_3PO_4 (8.00 mL) at room temperature over night provided biaryl **17am** (384 mg, 1.93 mmol, 96%) as yellow solid after column chromatography (EtOAc in hexane 0–4%, 1% increments).

^{1}H NMR (400 MHz, CDCl$_3$): δ 8.30 (d, J = 9.0 Hz, 2H), 7.74 (d, J = 9.0 Hz, 2H), 7.63 (dd, J = 8.3, 1.4 Hz, 2H), 7.53–7.43 (m, 3H) ppm.

The chemical shifts are in agreement with previous reported values.[224]

4,4′-Dimethoxybiphenyl (17dd)

[AC 4035]
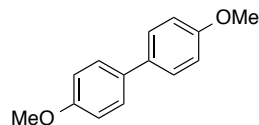
According to the general procedure, reaction of 4-bromoanisole (1.25 mL, 9.99 mmol), 4-methoxy-phenylboronic acid (2.28 g, 15.0 mmol), pre-catalyst G4 (38.4 mg, 0.05 mmol), XPhos (47.7 mg, 0.10 mmol) in a mixture of THF (20.0 mL) and aq. K_3PO_4 (40.0 mL) at room temperature over night provided biaryl **17dd** (0.98 g, 4.57 mmol, 46%) as colorless solid after column chromatography (EtOAc in hexane 0–2%, 1% increments).

^{1}H NMR (400 MHz, CDCl$_3$): δ 7.48 (d, J = 8.9 Hz, 4H), 6.96 (d, J = 8.9 Hz, 4H), 3.85 (s, 6H) ppm.
The chemical shifts are in agreement with previous reported values.[226]

4-(*tert*-Butyl)-4′-methoxybiphenyl (17de)

[AC 4029]
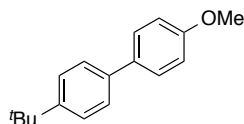
According to the general procedure, reaction of 4-(*tert*-butyl)bromobenzene (1.73 mL, 9.98 mmol), 4-methoxyphenylboronic acid (2.28 g, 15.0 mmol), pre-catalyst G4 (38.4 mg, 0.05 mmol), XPhos (47.7 mg, 0.10 mmol) in a mixture of THF (20.0 mL) and aq. K_3PO_4 (40.0 mL) at room temperature over night provided biaryl **17de** (1.40 g, 5.83 mmol, 58%) as colorless solid after column chromatography (EtOAc in hexane 1%).

^{1}H NMR (400 MHz, CDCl$_3$): δ 7.55–7.41 (m, 6H), 6.97 (d, J = 8.8 Hz, 2H), 3.85 (s, 3H), 1.36 (s, 9H) ppm.
The chemical shifts are in agreement with previous reported values.[227]

4-Methyl-4′methoxybiphenyl (17df)

[AC 4026]
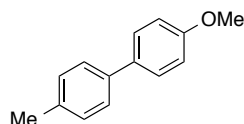
According to the general procedure, reaction of 4-bromotoluene (1.22 mL, 9.92 mmol), 4-methoxy-phenylboronic acid (2.28 g, 15.0 mmol), pre-catalyst G4 (38.4 mg, 0.05 mmol), XPhos (47.7 mg, 0.10 mmol) in a mixture of THF (20.0 mL) and aq. K_3PO_4 (40.0 mL) at room temperature over night provided biaryl **17df** (1.07 g, 5.40 mmol, 54%) as colorless solid after column chromatography (EtOAc in hexane 1%).

^{1}H NMR (400 MHz, CDCl$_3$): δ 7.51 (d, J = 8.7 Hz, 2H), 7.45 (d, J = 8.2 Hz, 2H), 7.23 (d, J = 8.4 Hz, 2H), 6.97 (d, J = 8.8 Hz, 2H), 3.85 (s, 3H), 2.38 (s, 3H) ppm.

The chemical shifts are in agreement with previous reported values.[227]

4-Fluoro-4′-methoxybiphenyl (17dg)

[AC 4025]
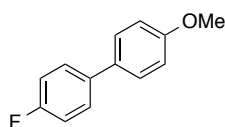
According to the general procedure, reaction of 4-fluorobromobenzene (1.01 mL, 9.19 mmol), 4-methoxyphenylboronic acid (2.28 g, 15.0 mmol), pre-catalyst G4 (38.4 mg, 0.05 mmol), XPhos (47.8 mg, 0.10 mmol) in a mixture of THF (20.0 mL) and aq. K_3PO_4 (40.0 mL) at room temperature over night provided biaryl **17dg** (0.94 g, 4.65 mmol, 51%) as colorless solid after column chromatography (EtOAc in hexane 0–2%, 1% increments).

^{1}H NMR (400 MHz, CDCl$_3$): δ 7.54–7.44 (m, 4H), 7.10 (t, J = 8.8 Hz, 2H), 6.97 (d, J = 8.8 Hz, 2H), 3.85 (s, 3H) ppm.

^{19}F NMR (376 MHz, CDCl$_3$): δ −116.6 ppm.

The chemical shifts are in agreement with previous reported values.[227]

Ethyl 4′-methoxy-4-biphenylcarboxylate (17di)

[AC 4030]
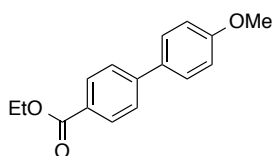
According to the general procedure, reaction of ethyl 4-bromobenzoate (1.63 mL, 9.98 mmol), 4-methoxyphenylboronic acid (2.28 g, 15.0 mmol), pre-catalyst G4 (38.5 mg, 0.05 mmol), XPhos (47.8 mg, 0.10 mmol) in a mixture of THF (20.0 mL) and aq. K_3PO_4 (40.0 mL) at room temperature over night provided biaryl **17di** (1.40 g, 5.46 mmol, 55%) as colorless solid after column chromatography (EtOAc in hexane 1%).

^{1}H NMR (400 MHz, CDCl$_3$): δ 8.09 (d, J = 8.6 Hz, 2H), 7.62 (d, J = 8.6 Hz, 2H), 7.58 (d, J = 8.8 Hz, 2H), 7.00 (d, J = 8.9 Hz, 2H), 4.40 (q, J = 7.1 Hz, 2H), 3.86 (s, 3H), 1.41 (t, J = 7.1 Hz, 3H) ppm.

The chemical shifts are in agreement with previous reported values.[218]

4-(Trifluoromethyl)-4′-methoxybiphenyl (17dk)

[AC 4028]
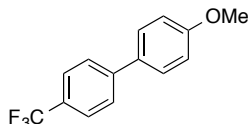
According to the general procedure, reaction of 4-bromobenzotrifluoride (1.40 mL, 10.0 mmol), 4-methoxyphenylboronic acid (2.28 g, 15.0 mmol), pre-catalyst G4 (38.5 mg, 0.05 mmol), XPhos (47.8 mg, 0.10 mmol) in a mixture of THF (20.0 mL) and aq. K$_3$PO$_4$ (40.0 mL) at room temperature over night provided biaryl **17dk** (1.45 g, 5.75 mmol, 58%) as colorless solid after column chromatography (EtOAc in hexane 1%).

^{1}H NMR (400 MHz, CDCl$_3$): δ 7.69–7.63 (m, 4H), 7.55 (d, J = 8.8 Hz, 2H), 7.01 (d, J = 8.8 Hz, 2H), 3.87 (s, 3H) ppm.

^{19}F NMR (376 MHz, CDCl$_3$): δ –62.2 ppm.

The chemical shifts are in agreement with previous reported values.[227]

4-Cyano-4′-methoxybiphenyl (17dl)

[AC 4027]
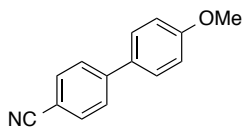
According to the general procedure, reaction of 4-bromobenzonitrile (1.82 g, 10.0 mmol), 4-methoxy-phenylboronic acid (2.28 g, 15.0 mmol), pre-catalyst G4 (38.5 mg, 0.05 mmol), XPhos (47.8 mg, 0.10 mmol) in a mixture of THF (20.0 mL) and aq. K$_3$PO$_4$ (40.0 mL) at room temperature over night provided biaryl **17dl** (1.34 g, 6.40 mmol, 64%) as colorless solid after column chromatography (EtOAc in hexane 0–3%, 1% increments).

^{1}H NMR (400 MHz, CDCl$_3$): δ 7.75–7-59 (m, 4H), 7.54 (d, J = 8.8 Hz, 2H), 7.01 (d, J = 8.8 Hz, 2H), 3.87 (s, 3H) ppm.

The chemical shifts are in agreement with previous reported values.[218]

4-(*tert*-Butyl)-4′-(trifluoromethyl)biphenyl (17ke)

[AC 4041]
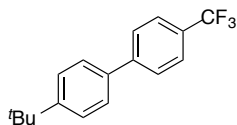
According to the general procedure, reaction of 4-(*tert*-butyl)bromobenzene (1.73 mL, 9.98 mmol), 4-(trifluoromethyl)phenylboronic acid (2.85 g, 15.0 mmol), pre-catalyst G4 (38.4 mg, 0.05 mmol), XPhos (47.6 mg, 0.10 mmol) in a mixture of THF (20.0 mL) and aq. K_3PO_4 (40.0 mL) at room temperature for 3 h provided biaryl **17ke** (2.25 g, 8.08 mmol, 81%) as colorless solid after column chromatography (hexane).

^{1}H NMR (400 MHz, CDCl$_3$): δ 7.68 (s, 4H), 7.57–7.48 (m, 4H), 1.37 (s, 9H) ppm.

^{19}F NMR (376 MHz, CDCl$_3$): δ −62.3 ppm.

The chemical shifts are in agreement with previous reported values.[225]

4-Methyl-4′-(trifluoromethyl)biphenyl (17kf)

[AC 4042]
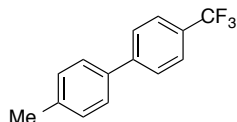
According to the general procedure, reaction of 4-bromotoluene (1.22 mL, 9.92 mmol), 4-(trifluoromethyl)phenylboronic acid (2.85 g, 15.0 mmol), pre-catalyst G4 (38.1 mg, 0.05 mmol), XPhos (47.7 mg, 0.10 mmol) in a mixture of THF (20.0 mL) and aq. K_3PO_4 (40.0 mL) at room temperature for 3 h provided biaryl **19kf** (2.01 g, 8.51 mmol, 86%) as colorless solid after column chromatography (hexane).

^{1}H NMR (400 MHz, CDCl$_3$): δ 7.68 (s, 4H), 7.50 (d, J = 8.2 Hz, 2H), 7.32–7.26 (m, 4H), 1.37 (s, 9H) ppm.

^{19}F NMR (376 MHz, CDCl$_3$): δ −62.2 ppm.

The chemical shifts are in agreement with previous reported values.[225]

4-Fluoro-4′-(trifluoromethyl)biphenyl (17kg)

[AC 4043]
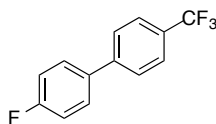
According to the general procedure, reaction of 4-bromofluorobenzene (1.01 mL, 9.19 mmol), 4-(trifluoromethyl)phenylboronic acid (2.85 g, 15.0 mmol), pre-catalyst G4 (38.3 mg, 0.05 mmol), XPhos (47.8 mg, 0.10 mmol) in a mixture of THF (20.0 mL) and aq. K_3PO_4 (40.0 mL) at room temperature for 3 h provided biaryl **17kg** (1.73 g, 7.20 mmol, 78%) as colorless solid after column chromatography (hexane).

^{1}H NMR (400 MHz, CDCl$_3$): δ 7.72–7.62 (m, 4H), 7.59–7.53 (m, 2H), 7.16 (t, J = 8.7 Hz, 2H) ppm.

^{19}F NMR (376 MHz, CDCl$_3$): δ −62.3, −114.0 ppm.

The chemical shifts are in agreement with previous reported values.[228]

Ethyl 4′-(trifluoromethyl)-4-biphenylcarboxylate (17ki)

[AC 4044]
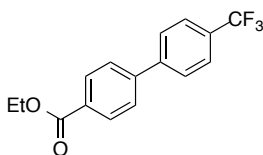
According to the general procedure, reaction of ethyl 4-bromobenzoate (1.63 mL, 9.98 mmol), 4-(trifluoromethyl)phenylboronic acid (2.83 g, 14.9 mmol), pre-catalyst G4 (38.3 mg, 0.05 mmol), XPhos (47.7 mg, 0.10 mmol) in a mixture of THF (20.0 mL) and aq. K_3PO_4 (40.0 mL) at room temperature for 3 h provided biaryl **17ki** (2.36 g, 8.02 mmol, 80%) as colorless solid after column chromatography (EtOAc in hexane 0–3%, 1% increments).

^{1}H NMR (400 MHz, CDCl$_3$): δ 8.15 (d, J = 8.3 Hz, 2H), 7.72 (s, 4H), 7.67 (d, J = 8.6 Hz, 2H), 4.42 (q, J = 7.1 Hz, 2H), 1.42 (t, J = 7.1 Hz, 3H) ppm.

^{19}F NMR (376 MHz, CDCl$_3$): δ −62.4 ppm.

The chemical shifts are in agreement with previous reported values.[218]

4,4′-Bis(trifluoromethyl)biphenyl (17kk)

[AC 4046]
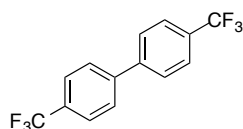
According to the general procedure, reaction of 4-bromobenzotrifluoride (1.40 mL, 10.0 mmol), 4-(trifluoromethyl)phenylboronic acid (2.85 g, 15.0 mmol), pre-catalyst G4 (38.3 mg, 0.05 mmol), XPhos (47.8 mg, 0.10 mmol) in a mixture of THF (20.0 mL) and aq. K_3PO_4 (40.0 mL) at room temperature for 7 h provided biaryl **17kk** (2.43 g, 8.37 mmol, 84%) as colorless solid after column chromatography (hexane).

^{1}H NMR (400 MHz, CDCl$_3$): δ 7.77–7.63 (m, 8H) ppm.

^{19}F NMR (376 MHz, CDCl$_3$): δ −62.5 ppm.

The chemical shifts are in agreement with previous reported values.[226]

4-Cyano-4′-(trifuoromethyl)biphenyl (17kl)

[AC 4045]
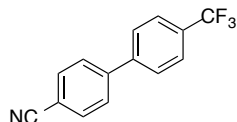
According to the general procedure, reaction of 4-bromobenzonitrile (1.82 g, 10.0 mmol), 4-(trifluoromethyl)phenylboronic acid (2.85 g, 15.0 mmol), pre-catalyst G4 (38.3 mg, 0.05 mmol), XPhos (47.7 mg, 0.10 mmol) in a mixture of THF (20.0 mL) and aq. K$_3$PO$_4$ (40.0 mL) at room temperature for 7 h provided biaryl **17kl** (2.01 g, 8.13 mmol, 81%) as colorless solid after column chromatography (EtOAc in hexane 0–3%, 1% increments).

^{1}H NMR (400 MHz, CDCl$_3$): δ 7.80–7.73 (m, 4H), 7.72–7.67 (m, 4H) ppm.

^{19}F NMR (376 MHz, CDCl$_3$): δ −62.5 ppm.

The chemical shifts are in agreement with previous reported values.[229]

4-(*tert*-Butyl)-4′-methylbiphenyl (17fe)

[AC 4056]
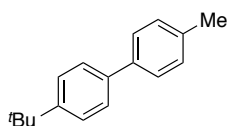
According to the general procedure, reaction of 4-(*tert*-butyl)bromobenzene (2.13 g, 10.0 mmol), 4-methylphenylboronic acid (2.04 g, 15.0 mmol), pre-catalyst G4 (38.3 mg, 0.05 mmol), XPhos (47.8 mg, 0.10 mmol) in a mixture of THF (20.0 mL) and aq. K$_3$PO$_4$ (40.0 mL) at 40 °C over night provided biaryl **17fe** (2.10 g, 9.36 mmol, 94%) as colorless solid after column chromatography (hexane).

^{1}H NMR (400 MHz, CDCl$_3$): δ 7.55–7.43 (m, 6H), 7.24 (d, J = 8.4 Hz, 2H), 2.39 (s, 3H), 1.36 (s, 9H) ppm.

The chemical shifts are in agreement with previous reported values.[225]

4,4′-Dimethylbiphenyl (17ff)

[AC 4052]
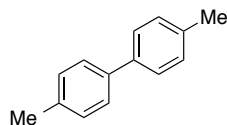
According to the general procedure, reaction of 4-bromotoluene (1.22 g, 7.13 mmol), 4-methylphenylboronic acid (2.04 g, 15.0 mmol), pre-catalyst G4 (38.3 mg, 0.05 mmol), XPhos (47.8 mg, 0.10 mmol) in a mixture of THF (20.0 mL) and aq. K_3PO_4 (40.0 mL) at room temperature over night provided biaryl **17ff** (1.02 g, 5.60 mmol, 79%) as colorless solid after column chromatography (hexane).
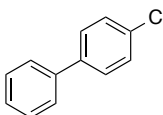
^{1}H NMR (400 MHz, CDCl$_3$): δ 7.48 (d, J = 8.1 Hz, 2H), 7.24 (d, J = 8.2 Hz, 4H), 2.39 (s, 6H) ppm.

The chemical shifts are in agreement with previous reported values.[226]

4-Fluoro-4′-methylbiphenyl (17fg)

[AC 4038]
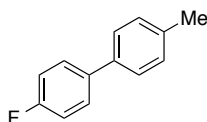
According to the general procedure, reaction of 4-fluorobromobenzene (1.10 mL, 10.0 mmol), 4-methylphenylboronic acid (2.04 g, 15.0 mmol), pre-catalyst G4 (38.3 mg, 0.05 mmol), XPhos (47.8 mg, 0.10 mmol) in a mixture of THF (20.0 mL) and aq. K_3PO_4 (40.0 mL) at room temperature over night provided biaryl **17fg** (0.76 g, 4.08 mmol, 41%) as colorless solid after column chromatography (hexane).

^{1}H NMR (400 MHz, CDCl$_3$): δ 7.55–7.51 (m, 2H), 7.46–7.42 (m, 2H), 7.26–7.23 (m, 2H), 7.14–7.07 (m, 2H), 2.40 (s, 3H) ppm.

^{19}F NMR (376 MHz, CDCl$_3$): δ –116.2 ppm.

The chemical shifts are in agreement with previous reported values.[228]

4-Cyano-4′-methylbiphenyl (17fl)

[AC 4053]
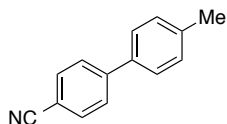
According to the general procedure, reaction of 4-bromobenzonitrile (1.82 g, 10.0 mmol), 4-methyl-phenylboronic acid (2.04 g, 15.0 mmol), pre-catalyst G4 (38.3 mg, 0.05 mmol), XPhos (47.8 mg,

0.10 mmol) in a mixture of THF (20.0 mL) and aq. K_3PO_4 (40.0 mL) at room temperature over night provided biaryl **17fl** (0.90 g, 4.66 mmol, 47%) as colorless solid after column chromatography (EtOAc in hexane 1%).
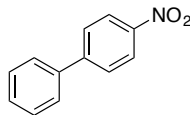
^{1}H NMR (400 MHz, CDCl$_3$): δ 7.75–7.64 (m, 4H), 7.49 (d, J 0 8.2 Hz, 2H), 7.29 (d, J = 7.8 Hz, 2H), 2.42 (s, 3H) ppm.

The chemical shifts are in agreement with previous reported values.[230]

Ethyl 4′-(*tert*-butyl)-4-biphenylcarboxylate (17ie)

[AC 4055]
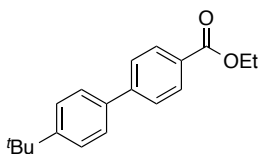
According to the general procedure, reaction of 4-(*tert*-butyl)bromobenzene (2.13 g, 10.0 mmol), 4-(ethoxycarbonyl)phenylboronic acid (2.91 g, 15.0 mmol), pre-catalyst G4 (38.3 mg, 0.05 mmol), XPhos (47.8 mg, 0.10 mmol) in a mixture of THF (20.0 mL) and aq. K_3PO_4 (40.0 mL) at room temperature over night provided biaryl **17ie** (2.53 g, 8.96 mmol, 90%) as pale yellow solid after column chromatography (EtOAc in hexane 0–20%, 5% increments).

^{1}H NMR (400 MHz, CDCl$_3$): δ 8.10 (d, J = 8.4 Hz 2H), 7.70–7.44 (m, 6H), 4.40 (q, J = 7.1 Hz, 2H), 1.41 (t, J = 7.1 Hz, 3H), 1.37 (s, 9H) ppm.

^{13}C NMR (101 MHz, CDCl$_3$): δ 14.5, 31.6, 34.3, 61.1, 126.0, 126.9, 127.1, 129.1, 130.2, 137.4, 138.2, 145.5, 166.7 ppm.

HRESI-MS (MeOH, +, m/z): [C$_{19}$H$_{22}$O$_2$Na]$^+$ 305.1533, calc. 305.1512

M.p.: 70–72 °C

Ethyl 4′-methyl-4-biphenylcarboxylate (17if)

[AC 4054]
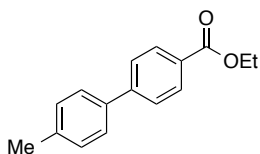
According to the general procedure, reaction of 4-bromotoluene (1.22 mL, 9.92 mmol), 4-(ethoxycarbonyl)phenylboronic acid (2.91 g, 15.0 mmol), pre-catalyst G4 (38.3 mg, 0.05 mmol), XPhos (47.8 mg, 0.10 mmol) in a mixture of THF (20.0 mL) and aq. K_3PO_4 (40.0 mL) at room

temperature over night provided biaryl **17if** (2.19 g, 9.11 mmol, 92%) as colorless solid after column chromatography (EtOAc in hexane 0–15%, 5% increments).

^{1}H NMR (400 MHz, CDCl$_3$): δ 8.10 (d, J = 8.5 Hz 2H), 7.64 (d, J = 8.5 Hz 2H), 7.53 (d, J = 8.2 Hz 2H), 7.28 (d, J = 7.8 Hz 2H), 4.40 (q, J = 7.1 Hz, 2H), 2.41 (s, 3H), 1.41 (t, J = 7.1 Hz, 3H) ppm. The chemical shifts are in agreement with previous reported values.[231]

Ethyl 4′-fluoro-4-biphenylcarboxylate (17ig)

[AC 4058]
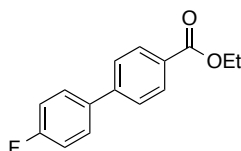
According to the general procedure, reaction of 4-fluorobromobenzene (1.10 mL, 10.0 mmol), 4-(ethoxycarbonyl)phenylboronic acid (2.91 g, 15.0 mmol), pre-catalyst G4 (38.3 mg, 0.05 mmol), XPhos (47.8 mg, 0.10 mmol) in a mixture of THF (20.0 mL) and aq. K$_3$PO$_4$ (40.0 mL) at 40 °C over night provided biaryl **17ig** (2.27 g, 9.29 mmol, 93%) as colorless solid after column chromatography (EtOAc in hexane 0–20%, 5% increments).

^{1}H NMR (400 MHz, CDCl$_3$): δ 8.10 (d, J = 8.7 Hz 2H), 7.64–7.53 (m, 4H), 7.15 (t, J = 8.7 Hz 2H), 4.40 (q, J = 7.1 Hz, 2H), 1.41 (t, J = 7.1 Hz, 3H) ppm.
^{19}F NMR (376 MHz, CDCl$_3$): δ −114.2 ppm.
The chemical shifts are in agreement with previous reported values.[218]

## Diethyl 4,4′-biphenyldicarboxylate (17ii)

[AC 4061]
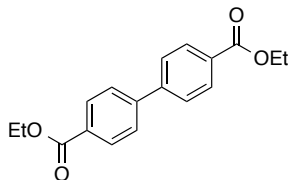
According to the general procedure, reaction of ethyl 4-bromobenzoate (1.60 mL, 9.80 mmol), 4-(ethoxycarbonyl)phenylboronic acid (2.91 g, 15.0 mmol), pre-catalyst G4 (38.3 mg, 0.05 mmol), XPhos (47.8 mg, 0.10 mmol) in a mixture of THF (20.0 mL) and aq. K$_3$PO$_4$ (40.0 mL) at 40 °C over night provided biaryl **17ii** (2.18 g, 7.30 mmol, 74%) as colorless solid after column chromatography (EtOAc in hexane 0–20%, 5% increments).

^{1}H NMR (400 MHz, CDCl$_3$): δ 8.14 (d, J = 8.7 Hz 4H), 7.69 (d, J = 8.0 Hz 4H), 4.41 (q, J = 7.1 Hz, 4H), 1.42 (t, J = 7.5 Hz, 6H) ppm.

The chemical shifts are in agreement with previous reported values.[232]

Ethyl 4′-cyano-4-biphenylcarboxylate (17il)

[AC 4060]
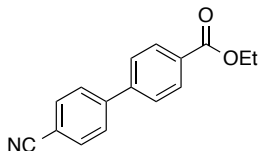
According to the general procedure, reaction of ethyl 4-bromobenzonitrile (1.82 mL, 10.0 mmol), 4-(ethoxycarbonyl)phenylboronic acid (2.91 g, 15.0 mmol), pre-catalyst G4 (38.3 mg, 0.05 mmol), XPhos (47.8 mg, 0.10 mmol) in a mixture of THF (20.0 mL) and aq. K$_3$PO$_4$ (40.0 mL) at 40 °C over night provided biaryl **17il** (1.96 g, 7.80 mmol, 78%) as colorless solid after column chromatography (EtOAc in hexane 0–20%, 5% increments).


^{1}H NMR (400 MHz, CDCl$_3$): δ 8.20–8.11 (m, 2H), 7.80–7.69 (m, 4H), 7.68–7.63 (m, 2H), 4.42 (q, J = 7.1 Hz, 2H), 1.42 (t, J = 7.1 Hz, 3H) ppm.

The chemical shifts are in agreement with previous reported values.[218]

4.6 Optimization of Transmetalation experiments
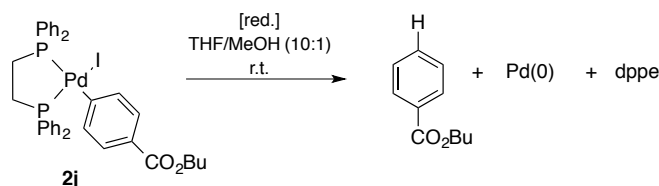
[SZ 3094]

A solution of complex **2j**, prepared from a stock solution of **2j** in THF (c = 10.0 mM, 0.50 mL, 5.0 μmol) and a stock solution of TMB (internal standard) in MeOH (c = 5.0 mM, 0.40 mL, 2.0 μmol), was treated with a spatula tip or drop of the reducing reagent. The resulting mixture was stirred at room temperature for 20 min, then directly transferred into a GC vial and analyzed by GC-FID.

entry	[red.]	yield [%] of butyl benzoate after		
		1 h	3 h	5 h
1^a	Et_3SiH, Na_2CO_3	44	10	5
2^a	Na_2CO_3	21	3	2
3	$NaBH_4$	46	56	49
4	NH_4HCO_2	85	107	102
5	AcOH	11	65	83
6	none	21	60	61

^{a}Transfer esterfication was observed.
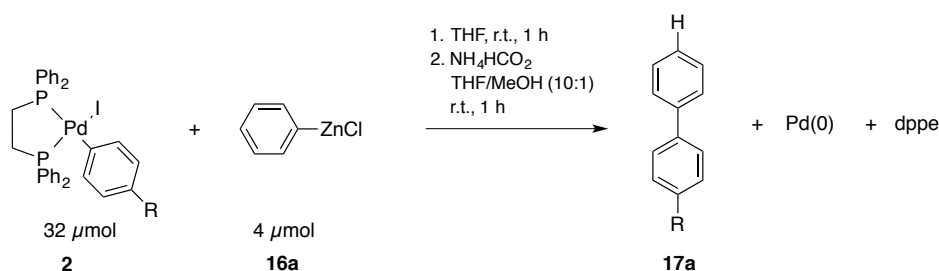
[SZ 4097]

Teflon-lined screw cap reaction vials were charged with complexes **2** (each 32 μmol), and transferred into a glovebox. The complexes were dissolved in THF (2.00 mL), and a stock solution of ZnPh$_2$ (21.9 mg, 0.10 mmol) and ZnCl$_2$ (14.1 mg, 0.10 mmol) in THF (10.0 mL, c[PhZnCl] = 19.9 mM, 0.20 mL, 4.0 μmol) was syringed to the complex solutions. The vials were sealed and stirred at room temperature for 1 h outside the glovebox before a stock solution of TMB (84.3 mg, 0.50 mmol) in MeOH (50.0 mL, c = 10.0 mM, 0.40 mL, 4.0 μmol) and a spatula of NH$_4$HCO$_2$ were added. The reaction mixtures were stirred at room temperature for 1 h and transferred into GC vials.

R	2	m [mg]	n [μmol]	yield 17a [%]	σ [%]	σ(x) [%]
OPh	c	25.6	32.0	16	2	8
OMe	d	23.7	32.1	97	2	1
^{t}Bu	e	24.8	32.4	98	0	0
Me	f	23.4	32.4	95	1	0
H	a	22.9	32.3	114	1	1
F	g	23.4	32.2	115	1	0
Cl	h	24.1	32.4	75	1	1
CO$_2$Et	i	26.2	32.4	63	1	1
CO$_2$Bu	j	25.4	32.5	95	3	2
CF$_3$	k	24.9	32.1	93	1	1
CN	l	23.5	32.0	92	0	0
NO$_2$	m	24.2	32.1	18	2	5
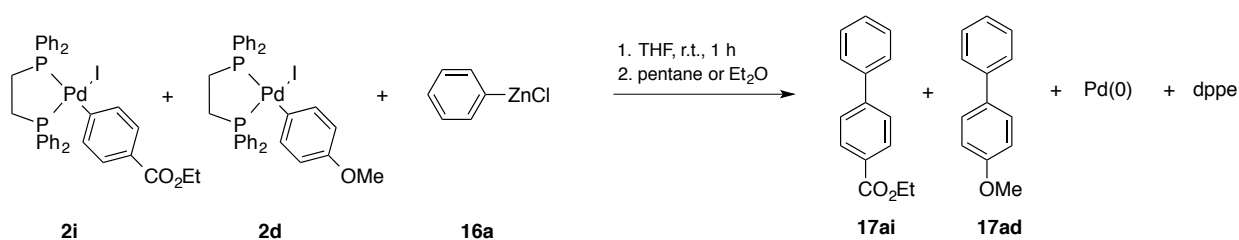
[SZ 4107]

Samples A and B: Complexes **2i** and **2d** (each 16 μmol) were weighted out in 8 mL reaction vials equipped with a stir bar and transferred into a glovebox, where the complexes were dissolved in THF (2.00 mL) under stirring. The resulting solution was treated with a stock solution of ZnPh$_2$ (21.9 mg, 0.10 mmol) and ZnCl$_2$ (14.6 mg, 0.11 mmol) in THF (10.0 mL) and stirred for approximately 1 h at room temperature outside the glovebox. A methanolic stock solution of TMB (c = 20 mM, 0.20 mL, 4 μmol) was added and the solution concentrated in vacuum almost until dryness. The residue was treated with either pentane or Et$_2$O (1.50 mL), and the resulting mixture additionally stirred at room temperature for approximately 15 min. The mixtures were filtered through Celite (pipette) and the filtrate collected in a GC vial and analyzed by GC-FID.

Sample C: 0.48 mL of the biaryl calibration stock solution (c = 5 mM, 2.4 μmol of **17a**) was diluted with THF (1.5 mL), and the solution concentrated in vacuum almost until dryness. The residue was redissolved in Et$_2$O (1.50 mL), and the resulting solution analyzed by GC-FID.

Sample D: Complexes **2i** and **2d** (each 16 μmol) were weighted out in 8 mL reaction vials equipped with a stir bar and transferred into a glovebox, where the complexes were dissolved in THF (2.00 mL)

under stirring. The resulting solution was treated with a stock solution of $ZnPh_2$ (21.9 mg, 0.10 mmol) and $ZnCl_2$ (14.6 mg, 0.11 mmol) in THF (10.0 mL) and stirred for approximately 1 h at room temperature outside the glovebox. A methanolic stock solution of TMB (c = 20 mM, 0.20 mL, 4 μmol) and a spatula tip of NH_4CO_2H were added. The resulting mixture was additionally stirred for 1 h at room temperature, and the mixtures were filtered through Celite (pipette) and the filtrate collected in a GC vial and analyzed by GC-FID.

| measurement | Sample A | | Sample B | | Sample C | | Sample D | |
| | w/ pentane yields [%] | | w/ Et$_2$O yields [%] | | Cal. std. 5 w/ Et$_2$O recov. **17** [%] | | reduction w/ NH$_4$HCO$_2$ yields [%] | |
No.	**17ad**	**17ai**	**17ad**	**17ai**	**17ad**	**17ai**	**17ad**	**17ai**
1	75	4	58	0	102	112	87	4
2	81	6	77	11	100	107	71	0
3	79	5	71	9	98	104	76	2
4	80	5	70	8	99	108	95	3
5	75	4	72	8	109	130	93	4
6	81	5	71	8	94	96	66	0
7	79	4	65	0	96	97	76	0
8	84	5	82	12	91	89	98	0
9	77	4	70	7	100	101	72	0
Avg. [%]	**79**	**5**	**71**	**7**	**99**	**105**	**81**	**1**
Std. dev.	3	1	7	4	5	12	12	2
Error [%]	1	0	2	1	2	4	4	1

4.7 Transmetalation competition experiments

4.7.1 Competition in (dppe)Pd(Ar)I with PhZnX

General procedure:

Reaction vials were charged with complexes **2** (each 16 μmol) and a stir bar outside the glovebox. Inside the glovebox, the complexes were dissolved in THF (2.00 mL) under stirring and a solution of ZnAr$_2$ and ZnX$_2$ in THF (c[ArZnX] = 20 mM, 0.20 mL, 4.0 μmol) was syringed to the complex solutions. The vials were sealed and stirred at room temperature for 1 h outside the glovebox before a stock solution of TMB in MeOH (4.0 μmol) and a spatula tip of NH_4HCO_2 were added. The reaction mixtures were stirred at room temperature for 1 h, if necessary, filtrated through a short pad of Celite (pipette), and transferred into GC vials. Alternatively, a stock solution of internal standard (TMB or BBP) in THF (4.0 μmol) was added and the samples concentrated in vacuum. Pentane or Et_2O (1.50 mL) was added, the mixtures stirred for 10 min, filtered through a short pad of Celite and the filtrate directly transferred into GC vials.

[SZ 3099]

According to the general procedure, complexes **2x** and **2y** (each 16 μmol) were treated with a solution of ZnPh$_2$ (21.9 mg, 0.10 mmol) and ZnCl$_2$ (14.1 mg, 0.10 mmol) in THF (10.0 mL, c[PhZnCl] = 19.9 mM, 0.20 mL, 4.0 μmol). A stock solution of TMB (84.1 mg, 0.50 mmol) in MeOH (50.0 mL, c = 10.0 mM, 0.40 mL, 4.0 μmol) was added for biaryl quantifications by GC-FID.

sample	R^1	2x	m [mg]	n [μmol]	R^2	2y	m [mg]	n [μmol]	17ax/17ay	σ	yield 17 [%]	σ [%]
A1	OMe	d	12.7	17.2	H	a	12.1	17.1	**3.37**	0.13	113	6
A2	^{t}Bu	e	12.5	16.3	H	a	11.6	16.4	**2.81**	0.08	115	9
A3	Me	f	11.9	16.5	H	a	11.6	16.4	**2.03**	0.03	106	1

A4	CO$_2$Et	**i**	12.5	16.0	H	**a**	11.6	16.3	**0.31**	0.03	109	2
A5	CF$_3$	**k**	12.6	16.2	H	**a**	11.6	16.3	**0.23**	0.01	106	2
A6	CN	**l**	11.7	16.0	H	**a**	11.6	16.4	**0.15**	0.02	93	3
B1	^{t}Bu	**e**	12.1	15.6	OMe	**d**	11.7	15.9	**0.82**	0.03	100	3
B2	Me	**f**	11.6	16.0	OMe	**d**	11.8	16.0	**0.71**	0.03	101	5
B3	F	**g**	11.6	15.9	OMe	**d**	11.8	16.0	**0.27**	0.01	103	0
B4	CO$_2$Et	**i**	12.8	16.4	OMe	**d**	11.9	16.1	**0.11**	0.03	108	5
B5	CF$_3$	**k**	12.4	15.9	OMe	**d**	11.9	16.1	**0.07**	0.00	109	0
B6	CN	**l**	11.7	16.0	OMe	**d**	11.8	16.0	**0.06**	0.00	100	3
C1	Me	**f**	11.7	16.2	^{t}Bu	**e**	12.3	16.0	**0.65**	0.02	99	3
C2	F	**g**	11.7	16.1	^{t}Bu	**e**	12.2	16.0	**0.29**	0.01	110	0
C3	CO$_2$Et	**i**	12.5	16.1	^{t}Bu	**e**	12.5	16.3	**0.10**	0.01	113	2
C4	CF$_3$	**k**	12.7	16.4	^{t}Bu	**e**	12.5	16.3	**0.07**	0.00	116	8
C5	CN	**l**	11.7	16.0	^{t}Bu	**e**	12.3	16.0	**0.00**	0.00	112	6
D1	F	**g**	11.9	16.3	Me	**f**	11.9	16.4	**0.43**	0.00	110	6
D2	CO$_2$Et	**i**	12.6	16.1	Me	**f**	11.9	16.5	**0.15**	0.01	105	3
D3	CF$_3$	**k**	9.43	12.1	Me	**f**	9.08	12.6	**0.09**	0.00	107	4
D4	CN	**l**	11.7	16.0	Me	**f**	11.7	16.2	**0.00**	0.00	91	4
E1	CO$_2$Et	**i**	12.5	16.0	F	**g**	11.6	15.9	**0.37**	0.02	101	1
E2	CN	**l**	11.7	15.9	F	**g**	11.6	15.9	**0.14**	0.02	94	6
F1	CN	**l**	11.8	16.1	CO$_2$Et	**i**	12.6	16.1	**0.59**	0.08	111	5

[SZ 3102]

According to the general procedure, complexes **2x** and **2y** (each 16 μmol) were treated with a solution of ZnPh$_2$ (54.8 mg, 0.25 mmol) and ZnCl$_2$ (31.1 mg, 0.25 mmol) in THF (25.0 mL, c[PhZnCl] = 20.0 mM, 0.20 mL, 4.0 μmol). A stock solution of TMB (85.2 mg, 0.51 mmol) in MeOH (50.0 mL, c = 10.1 mM, 0.40 mL, 4.1 μmol) was added for biaryl quantifications by GC-FID.

sample	R^1 **2x**		m [mg]	n [μmol]	R^2 **2y**		m [mg]	n [μmol]	**17ax/17ay**	σ	yield 17 [%]	σ [%]
A1	OMe	**d**	11.9	16.2	H	**a**	11.4	16.1	**3.50**	0.14	101	5
A2	^{t}Bu	**e**	12.9	16.9	H	**a**	11.8	16.7	**3.02**	0.15	100	3
A3	Me	**f**	11.5	16.0	H	**a**	11.3	16.0	**1.89**	0.10	96	4
A4	CO$_2$Et	**i**	12.5	16.0	H	**a**	11.3	16.0	**0.26**	0.05	94	5
A5	CF$_3$	**k**	12.8	16.4	H	**a**	11.6	16.4	**0.25**	0.01	92	1
A6	CN	**l**	11.9	16.2	H	**a**	11.6	16.3	**0.16**	0.03	91	5
B1	^{t}Bu	**e**	13.1	17.1	OMe	**d**	12.6	17.0	**0.80**	0.04	100	1
B2	Me	**f**	11.6	16.0	OMe	**d**	11.8	16.0	**0.57**	0.03	104	1
B3	F	**g**	11.7	16.1	OMe	**d**	11.8	16.0	**0.29**	0.01	103	2
B4	CO$_2$Et	**i**	12.8	16.4	OMe	**d**	12.1	16.4	**0.10**	0.01	103	5
B5	CF$_3$	**k**	12.6	16.2	OMe	**d**	11.9	16.1	**0.07**	0.00	110	1

B6	CN	l	11.7	16.0	OMe	d	11.8	16.0	**0.03**	0.05	93	4
C1	Me	f	11.8	16.3	^{t}Bu	e	12.3	16.1	**0.60**	0.02	102	4
C2	F	g	11.7	16.1	^{t}Bu	e	12.2	16.0	**0.29**	0.01	106	3
C3	CO$_2$Et	i	12.8	16.4	^{t}Bu	e	12.6	16.4	**0.08**	0.01	109	3
C4	CF$_3$	k	12.4	16.0	^{t}Bu	e	12.2	16.0	**0.06**	0.00	114	1
C5	CN	l	11.8	16.1	^{t}Bu	e	12.3	16.1	**0.03**	0.05	103	11
D1	F	g	11.6	16.0	Me	f	11.6	16.1	**0.47**	0.02	50	2
D2	CO$_2$Et	i	12.7	16.3	Me	f	11.7	16.2	**0.12**	0.00	96	2
D3	CF$_3$	k	12.4	16.0	Me	f	11.5	15.9	**0.09**	0.01	103	5
D4	CN	l	11.9	16.2	Me	f	11.7	16.2	**0.00**	0.00	87	2
E1	CO$_2$Et	i	12.5	16.0	F	g	11.5	15.9	**0.31**	0.02	110	1
E2	CF$_3$	k	12.5	16.1	F	g	11.7	16.0	**0.22**	0.00	107	2
E3	CN	l	11.7	16.0	F	i	11.7	16.0	**0.10**	0.04	96	4
F1	CF$_3$	k	12.4	16.0	CO$_2$Et	i	12.5	16.0	**0.66**	0.05	109	2
F2	CN	l	11.7	16.0	CO$_2$Et	i	12.5	16.0	**0.58**	0.04	116	9
G1	CN	l	14.0	16.0	CF$_3$	k	14.5	18.7	**0.94**	0.02	87	1

[SZ 4162]

According to the general procedure, complexes **2x** and **2y** (each 16 μmol) were treated with a solution of ZnPh$_2$ (11.0 mg, 0.05 mmol) and ZnCl$_2$ (8.4 mg, 0.06 mmol) in THF (5.00 mL, c[PhZnCl] = 20.0 mM, 0.20 mL, 4.0 μmol). A stock solution of TMB (87.8 mg, 0.51 mmol) in THF (25.0 mL, c = 20.1 mM, 0.20 mL, 4.2 μmol) was added for biaryl quantifications by GC-FID.

sample	R^1 **2x**		m [mg]	n [μmol]	R^2 **2y**		m [mg]	n [μmol]	**17ax/17ay**	σ	yield 17 [%]	σ [%]
A1	OMe	d	11.8	16.0	H	a	11.8	16.6	**1.97**	0.12	72	3
A2	^{t}Bu	e	12.7	16.6	H	a	12.7	17.9	**1.82**	0.17	84	3
A3	Me	f	12.4	17.2	H	a	13.7	19.3	**1.45**	0.02	75	0
A4	CO$_2$Et	i	14.5	18.6	H	a	11.2	15.8	**0.23**	0.11	84	8
A6	CN	l	15.5	21.1	H	a	11.8	16.6	**0.35**	0.01	80	18
B1	^{t}Bu	e	14.2	18.6	OMe	d	12.8	17.3	**0.90**	0.03	62	4
B2	Me	f	12.2	16.9	OMe	d	12.0	16.2	**0.65**	0.04	62	3
B3	F	g	12.3	16.9	OMe	d	14.1	19.1	**0.43**	0.04	63	2
B4	CO$_2$Et	i	27.5	35.2	OMe	d	15.1	20.4	**0.13**	0.01	58	2
B5	CF$_3$	k	18.1	23.3	OMe	d	14.1	19.1	**0.13**	0.01	63	5
B6	CN	l	15.3	20.8	OMe	d	11.7	15.8	**0.06**	0.05	50	7
C1	Me	f	11.4	15.8	^{t}Bu	e	13.5	17.6	**0.61**	0.02	67	2
C2	F	g	12.4	17.1	^{t}Bu	e	14.4	18.8	**0.49**	0.06	79	5
C3	CO$_2$Et	i	17.1	21.9	^{t}Bu	e	12.2	15.9	**0.08**	0.00	62	7
C4	CF$_3$	k	13.7	17.6	^{t}Bu	e	13.8	18.0	**0.13**	0.00	73	2
D1	F	g	12.0	16.5	Me	f	13.2	18.3	**0.49**	0.02	72	2

D2	CO$_2$Et	i	12.5	16.0	Me	f	13.8	19.1	**0.08**	0.01	65	2
D3	CF$_3$	k	14.6	18.8	Me	f	11.5	15.9	**0.15**	0.01	62	1
D4	CN	l	13.8	18.8	Me	f	13.6	18.8	**0.46**	0.00	64	18
E1	CO$_2$Et	i	14.2	18.2	F	g	12.0	16.5	**0.23**	0.05	70	5
E3	CN	l	12.5	17.0	F	i	11.7	16.1	**0.14**	0.00	59	7
F1	CF$_3$	k	14.1	18.2	CO$_2$Et	i	14.0	17.9	**3.32**	0.70	123	15
F2	CN	l	14.3	19.5	CO$_2$Et	i	12.0	15.4	**0.55**	0.09	37	7
G1	CN	l	16.9	19.5	CF$_3$	k	13.8	17.8	**0.78**	0.30	58	9

(SZ 3099)

(SZ 3102)

(SZ 4162)

(SZ 3099+3102+4162)
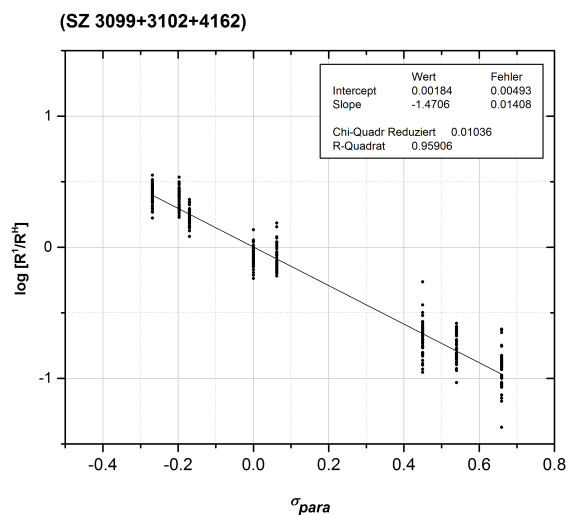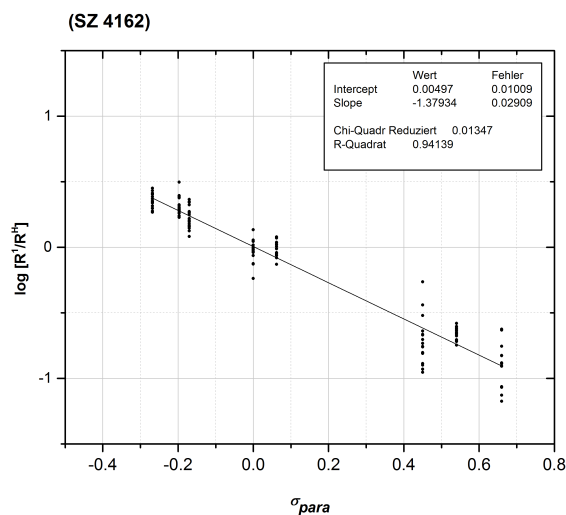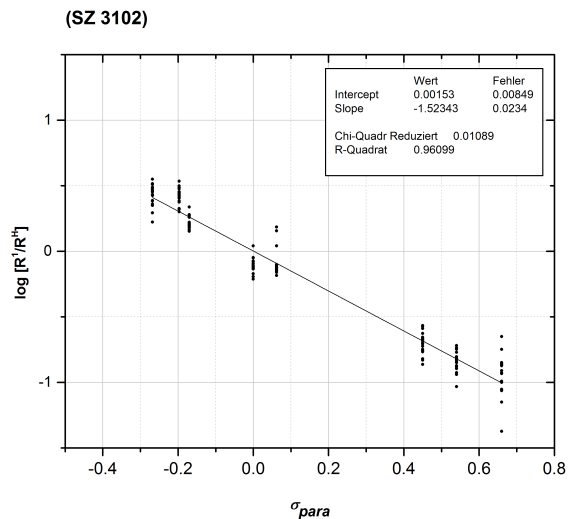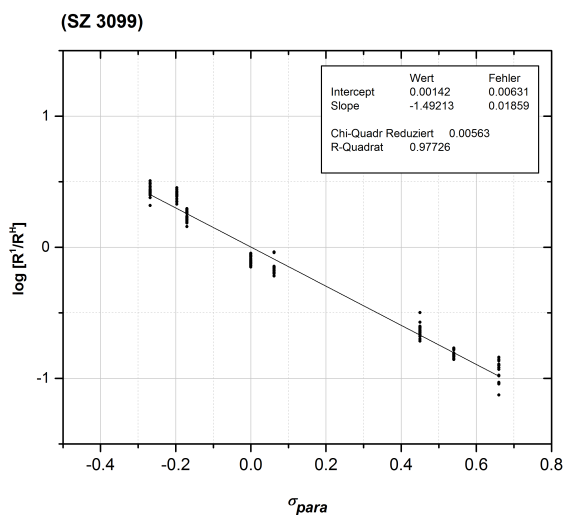
Exp. No.	slope	R^2
SZ 3099	-1.49±0.02	0.977
SZ 3102	-1.52±0.03	0.961
SZ 4162	-1.38±0.03	0.941
total	-1.47±0.02	0.959
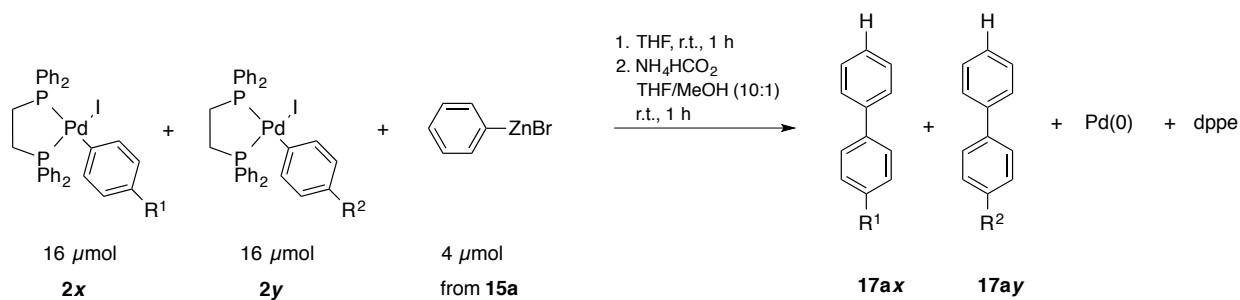
[SZ 3105]

According to the general procedure, complexes **2x** and **2y** (each 16 μmol) were treated with a solution of ZnPh$_2$ (43.9 mg, 0.20 mmol) and ZnBr$_2$ (46.7 mg, 0.21 mmol) in THF (20.0 mL, c[PhZnBr] = 20.0 mM, 0.20 mL, 4.0 μmol). A stock solution of TMB (85.0 mg, 0.51 mmol) in MeOH (50.0 mL, c = 10.1 mM, 0.40 mL, 4.0 μmol) was added for biaryl quantifications by GC-FID.

sample	R^1	2x	m [mg]	n [μmol]	R^2	2y	m [mg]	n [μmol]	17ax/17ay	σ	yield 17 [%]	σ [%]
A1	OMe	d	12.0	16.2	H	a	11.5	16.2	**2.95**	0.11	93	1
A2	^{t}Bu	e	12.4	16.1	H	a	11.5	16.2	**2.92**	0.12	90	2
A3	Me	f	11.6	16.0	H	a	11.4	16.1	**1.87**	0.12	100	2
A4	CO$_2$Et	i	12.4	15.9	H	a	11.3	15.9	**0.19**	0.02	85	3
A5	CF$_3$	k	12.6	16.2	H	a	11.5	16.2	**0.19**	0.00	84	1
A6	CN	l	11.8	16.1	H	a	11.5	16.2	**0.03**	0.05	80	7
B1	^{t}Bu	e	12.5	16.4	OMe	d	12.1	16.4	**0.81**	0.01	92	2
B2	Me	f	11.8	16.3	OMe	d	12.1	16.3	**0.54**	0.01	90	1
B3	F	g	11.6	15.9	OMe	d	11.8	15.9	**0.28**	0.01	101	4
B4	CO$_2$Et	i	12.9	16.5	OMe	d	11.3	15.3	**0.05**	0.00	96	2
B5	CF$_3$	k	13.1	16.8	OMe	d	12.4	16.7	**0.06**	0.00	100	1
B6	CN	l	12.5	17.0	OMe	d	12.6	17.1	**0.00**	0.00	86	3
C1	Me	f	11.6	16.0	^{t}Bu	e	12.3	16.1	**0.62**	0.00	89	1
C2	F	g	11.8	16.2	^{t}Bu	e	12.5	16.3	**0.31**	0.02	100	2
C3	CO$_2$Et	i	12.6	16.1	^{t}Bu	e	12.2	15.9	**0.05**	0.04	98	3
C4	CF$_3$	k	13.4	17.2	^{t}Bu	e	13.2	17.2	**0.06**	0.00	100	4
C5	CN	l	12.0	16.4	^{t}Bu	e	12.6	16.4	**0.00**	0.00	85	3
D1	F	g	11.5	15.9	Me	f	11.5	16.0	**0.45**	0.01	95	1
D2	CO$_2$Et	i	12.6	16.1	Me	f	11.5	15.9	**0.09**	0.01	94	3
D3	CF$_3$	k	12.5	16.1	Me	f	11.6	16.0	**0.08**	0.00	91	4
D4	CN	l	11.7	15.9	Me	f	11.5	15.9	**0.00**	0.00	82	1
E1	CO$_2$Et	i	12.6	16.1	F	g	11.6	15.9	**0.24**	0.01	102	2
E2	CF$_3$	k	12.4	15.9	F	g	11.6	16.0	**0.20**	0.01	103	2
E3	CN	l	11.9	16.2	F	i	11.8	16.2	**0.02**	0.04	87	2
F1	CF$_3$	k	12.5	16.1	CO$_2$Et	i	12.6	16.1	**0.84**	0.03	89	5

F2	CN	l	12.0	16.4	CO$_2$Et	i	12.8	16.4	**0.60**	0.04	95	1
G1	CN	l	11.7	16.4	CF$_3$	k	12.5	16.1	**0.71**	0.06	82	3

[SZ 3107]

According to the general procedure, complexes **2x** and **2y** (each 16 μmol) were treated with a solution of ZnPh$_2$ (43.9 mg, 0.20 mmol) and ZnBr$_2$ (46.7 mg, 0.21 mmol) in THF (20.0 mL, c[PhZnBr] = 20.0 mM, 0.20 mL, 4.0 μmol). A stock solution of TMB (89.4 mg, 0.53 mmol) in MeOH (50.0 mL, c = 10.6 mM, 0.40 mL, 4.3 μmol) was added for biaryl quantifications by GC-FID.

sample	R^1	**2x**	m [mg]	n [μmol]	R^2	**2y**	m [mg]	n [μmol]	σ **17ax/17ay**	yield 17 [%]	σ [%]
A1	OMe	d	12.3	16.6	H	a	11.9	16.8	**2.61**	0.53	90	1
A2	^{t}Bu	e	12.2	15.9	H	a	11.2	15.8	**2.84**	0.43	87	5
A3	Me	f	11.6	16.0	H	a	11.2	15.8	**1.88**	0.08	90	3
A4	CO$_2$Et	i	12.5	16.0	H	a	11.4	16.1	**0.19**	0.01	88	4
A5	CF$_3$	k	12.8	16.5	H	a	11.3	15.9	**0.18**	0.01	89	2
A6	CN	l	11.8	16.1	H	a	11.5	16.2	**0.00**	0.00	87	1
B1	^{t}Bu	e	12.6	16.5	OMe	d	12.1	16.4	**0.86**	0.04	92	2
B2	Me	f	12.7	17.6	OMe	d	12.6	17.1	**0.62**	0.03	85	2
B3	F	g	11.8	16.2	OMe	d	11.8	16.0	**0.30**	0.02	100	2
B4	CO$_2$Et	i	13.1	16.8	OMe	d	11.8	16.0	**0.06**	0.00	146	2
B5	CF$_3$	k	12.8	16.5	OMe	d	12.0	16.2	**0.05**	0.04	96	2
B6	CN	l	11.8	16.1	OMe	d	11.8	16.0	**0.00**	0.00	39	3
C1	Me	f	11.8	16.3	^{t}Bu	e	12.5	16.3	**0.66**	0.02	89	2
C2	F	g	11.8	16.2	^{t}Bu	e	12.4	16.2	**0.33**	0.00	105	3
C3	CO$_2$Et	i	12.4	15.9	^{t}Bu	e	12.2	15.9	**0.00**	0.00	88	2
C4	CF$_3$	k	12.5	16.1	^{t}Bu	e	12.4	16.2	**0.00**	0.00	98	4
C5	CN	l	11.7	15.9	^{t}Bu	e	12.4	16.2	**0.00**	0.00	90	4
D1	F	g	11.4	15.7	Me	f	11.5	15.9	**0.48**	0.01	94	1
D2	CO$_2$Et	i	13.1	16.8	Me	f	11.9	16.5	**0.06**	0.05	87	3
D3	CF$_3$	k	12.9	16.6	Me	f	12.5	17.3	**0.08**	0.00	96	0
D4	CN	l	11.7	15.9	Me	f	11.7	16.2	**0.00**	0.00	86	0
E1	CO$_2$Et	i	12.7	16.3	F	g	11.7	16.1	**0.24**	0.01	105	2
E2	CF$_3$	k	12.2	15.7	F	g	11.5	15.8	**0.00**	0.00	88	1
E3	CN	l	11.3	15.4	F	i	11.6	16.0	**0.00**	0.00	89	1
F1	CF$_3$	k	12.2	15.7	CO$_2$Et	i	12.3	15.8	**0.84**	0.04	92	5
F2	CN	l	7.5	10.2	CO$_2$Et	i	11.4	14.6	**0.33**	0.03	89	3

(SZ 3105)

	Wert	Fehler
Intercept	0.00204	0.00789
Slope	-1.67524	0.0225

Chi-Quadr Reduziert   0.00872
R-Quadrat   0.97264

(SZ 3107)

	Wert	Fehler
Intercept	0.00368	0.00579
Slope	-1.69828	0.01789

Chi-Quadr Reduziert   0.00405
R-Quadrat   0.9862

(SZ 3105+3107)

	Wert	Fehler
Intercept	0.00295	0.00502
Slope	-1.68495	0.01483

Chi-Quadr Reduziert   0.0066
R-Quadrat   0.97847

Exp. No.	slope	R^2
SZ 3105	-1.67 ± 0.03	0.973
SZ 3107	-1.70 ± 0.02	0.986
total	-1.70 ± 0.02	0.990

[SZ 3106]

According to the general procedure, complexes **2x** and **2y** (each 16 μmol) were treated with a solution of ZnPh$_2$ (22.2 mg, 0.10 mmol) and ZnI$_2$ (34.0 mg, 0.11 mmol) in THF (10.0 mL, c[PhZnI] = 20.2 mM, 0.20 mL, 4.0 μmol). A stock solution of TMB (88.0 mg, 0.52 mmol) in MeOH (50.0 mL, c = 10.5 mM, 0.40 mL, 4.2 μmol) was added for biaryl quantifications by GC-FID.

sample	R¹	2x	m [mg]	n [μmol]	R²	2y	m [mg]	n [μmol]	17ax/17ay	σ	yield 17 [%]	σ [%]
A1	OMe	**d**	12.1	16.3	H	**a**	11.4	16.1	**3.63**	0.35	83	1
A2	^{t}Bu	**e**	12.2	15.9	H	**a**	11.2	15.8	**3.05**	0.20	85	1
A3	Me	**f**	11.5	15.8	H	**a**	11.2	15.8	**2.00**	0.05	85	1
A4	CO$_2$Et	**i**	12.6	16.2	H	**a**	11.5	16.2	**0.15**	0.02	93	1
A5	CF$_3$	**k**	12.3	15.9	H	**a**	11.2	15.8	**0.16**	0.00	104	2
A6	CN	**l**	11.8	16.1	H	**a**	11.4	16.0	**0.09**	0.15	85	16
B1	^{t}Bu	**e**	12.2	15.9	OMe	**d**	11.9	16.1	**0.83**	0.01	89	1
B2	Me	**f**	11.7	16.1	OMe	**d**	12.0	16.2	**0.50**	0.01	84	1
B3	F	**g**	11.9	16.4	OMe	**d**	12.0	16.3	**0.26**	0.01	98	3
B4	CO$_2$Et	**i**	12.5	16.0	OMe	**d**	11.7	15.9	**0.23**	0.01	104	5
B5	CF$_3$	**k**	12.4	16.0	OMe	**d**	11.8	15.9	**0.00**	0.00	95	3
B6	CN	**l**	11.6	15.9	OMe	**d**	11.8	16.0	**0.00**	0.00	80	2
C1	Me	**f**	11.9	16.5	^{t}Bu	**e**	12.5	16.4	**0.63**	0.00	87	1
C2	F	**g**	11.9	16.3	^{t}Bu	**e**	12.4	16.2	**0.31**	0.02	101	3
C3	CO$_2$Et	**i**	13.2	16.9	^{t}Bu	**e**	12.9	16.9	**0.00**	0.00	96	2
C4	CF$_3$	**k**	12.4	16.0	^{t}Bu	**e**	12.2	15.9	**0.00**	0.00	97	2
C5	CN	**l**	11.7	16.0	^{t}Bu	**e**	12.1	15.8	**0.00**	0.00	92	2
D1	F	**g**	11.5	15.9	Me	**f**	11.4	15.7	**0.46**	0.00	99	1
D2	CO$_2$Et	**i**	12.7	16.3	Me	**f**	11.8	16.3	**0.02**	0.04	85	3
D3	CF$_3$	**k**	11.2	14.4	Me	**f**	11.3	15.6	**0.02**	0.04	93	2
D4	CN	**l**	11.6	15.7	Me	**f**	11.4	15.7	**0.00**	0.00	85	1
E1	CO$_2$Et	**i**	12.8	16.3	F	**g**	11.9	16.4	**0.18**	0.01	114	2
E2	CF$_3$	**k**	12.6	16.3	F	**g**	11.8	16.3	**0.15**	0.01	108	3
E3	CN	**l**	11.7	16.0	F	**i**	11.6	15.9	**0.00**	0.00	93	1
F1	CF$_3$	**k**	12.8	16.4	CO$_2$Et	**i**	12.8	16.4	**0.83**	0.07	97	6
F2	CN	**l**	11.7	15.9	CO$_2$Et	**i**	12.5	16.0	**0.56**	0.06	79	4
G1	CN	**l**	14.9	15.9	CF$_3$	**k**	15.9	20.5	**0.60**	0.08	81	3

[SZ 3114]

According to the general procedure, complexes **2x** and **2y** (each 16 μmol) were treated with a solution of ZnPh$_2$ (22.0 mg, 0.10 mmol) and ZnI$_2$ (32.6 mg, 0.10 mmol) in THF (10.0 mL, c[PhZnI] = 20.2 mM, 0.20 mL, 4.0 μmol). A stock solution of TMB (84.8 mg, 0.50 mmol) in MeOH (50.0 mL, c = 10.1 mM, 0.40 mL, 4.0 μmol) was added for biaryl quantifications by GC-FID.

sample	R¹	2x	m [mg]	n [μmol]	R²	2y	m [mg]	n [μmol]	17ax/17ay	σ	yield 17 [%]	σ [%]
A1	OMe	**d**	11.6	15.7	H	**a**	11.5	16.2	**2.69**	0.47	96	8
A2	^{t}Bu	**e**	12.5	16.3	H	**a**	11.6	16.4	**2.24**	0.25	100	9

4 Experimental Section

A3	Me	f	11.9	16.5	H	a	11.2	15.8	**1.78**	0.17	101	2
A4	CO$_2$Et	i	12.6	16.1	H	a	11.5	16.2	**0.13**	0.02	93	2
A5	CF$_3$	k	12.7	16.3	H	a	11.3	15.9	**0.18**	0.00	108	3
A6	CN	l	11.6	15.8	H	a	11.7	16.5	**0.12**	0.04	84	7
B1	^{t}Bu	e	12.3	16.1	OMe	d	12.0	16.2	**0.78**	0.04	88	3
B2	Me	f	11.7	16.2	OMe	d	11.8	16.0	**0.55**	0.02	84	2
B3	F	g	11.3	15.5	OMe	d	11.6	15.7	**0.24**	0.04	92	1
B4	CO$_2$Et	i	12.2	15.6	OMe	d	11.5	15.6	**0.20**	0.06	99	5
B5	CF$_3$	k	12.7	16.3	OMe	d	11.5	15.6	**0.00**	0.00	85	2
B6	CN	l	11.9	16.2	OMe	d	12.1	16.4	**0.00**	0.00	0	0
C1	Me	f	12.6	17.4	^{t}Bu	e	13.2	17.3	**0.60**	0.03	92	4
C2	F	g	11.7	16.1	^{t}Bu	e	12.6	16.5	**0.27**	0.23	87	16
C3	CO$_2$Et	i	12.7	16.3	^{t}Bu	e	11.9	15.6	**0.04**	0.03	91	4
C4	CF$_3$	k	12.4	16.0	^{t}Bu	e	12.7	16.6	**0.00**	0.00	89	5
C5	CN	l	11.5	15.7	^{t}Bu	e	12.5	16.3	**0.09**	0.02	101	1
D1	F	g	11.7	16.1	Me	f	11.8	16.3	**0.43**	0.03	99	2
D2	CO$_2$Et	i	13.5	17.3	Me	f	12.4	17.2	**0.04**	0.03	84	3
D3	CF$_3$	k	13.3	17.1	Me	f	12.9	17.8	**0.00**	0.00	91	2
D4	CN	l	13.0	17.7	Me	f	12.5	17.3	**0.03**	0.06	84	5
E1	CO$_2$Et	i	12.1	15.5	F	g	11.7	16.1	**0.16**	0.01	101	5
E2	CF$_3$	k	12.2	15.7	F	g	11.5	15.8	**0.17**	0.01	112	10
E3	CN	l	12.0	16.4	F	i	11.8	16.2	**0.09**	0.03	98	6
F1	CF$_3$	k	12.1	15.6	CO$_2$Et	i	12.3	15.8	**0.79**	0.05	89	3
F2	CN	l	12.0	16.4	CO$_2$Et	i	12.8	16.4	**0.54**	0.03	83	3
G1	CN	l	12.0	16.4	CF$_3$	k	13.0	16.7	**0.75**	0.04	82	7

(SZ 3106)

	Wert	Fehler
Intercept	0.02153	0.01199
Slope	-1.66624	0.03643
Chi-Quadr Reduziert	0.01598	
R-Quadrat	0.94619	

y-axis: log [R^1/R^{II}], *x*-axis: σ_{para}

(SZ 3114)

	Wert	Fehler
Intercept	0.01169	0.01172
Slope	-1.65529	0.03336
Chi-Quadr Reduziert	0.01685	
R-Quadrat	0.94693	

y-axis: log [R^1/R^{II}], *x*-axis: σ_{para}

(SZ 3106+3114)

	Wert	Fehler
Intercept	0.01638	0.00836
Slope	-1.66075	0.02449
Chi-Quadr Reduziert	0.01634	
R-Quadrat	0.94667	

Exp. No.	slope	R^2
SZ 3106	-1.67 ± 0.04	0.946
SZ 3114	-1.65 ± 0.04	0.947
total	-1.66 ± 0.03	0.947

4.7.2 Competition in (dppe)Pd(Ar)I with PhZnCl in presence of salt additives
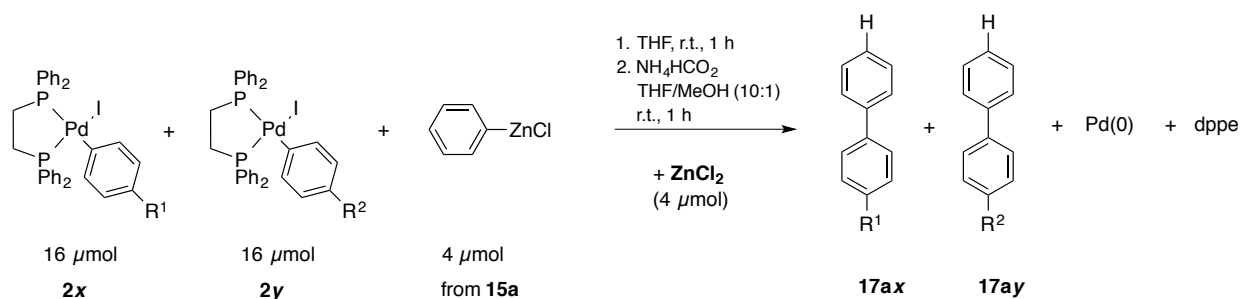
[SZ 3103]

Similar to the general procedure, complexes **2x** and **2y** (each 16 μmol) were treated with a solution of ZnPh$_2$ (54.8 mg, 0.25 mmol) and ZnCl$_2$ (70.6 mg, 0.52 mmol) in THF (25.0 mL, c[PhZnCl] = 20.0 mM, 0.20 mL, 4.0 μmol). A stock solution of TMB (84.8 mg, 0.50 mmol) in MeOH (50.0 mL, c = 10.1 mM, 0.40 mL, 4.0 μmol) was added for biaryl quantifications by GC-FID.
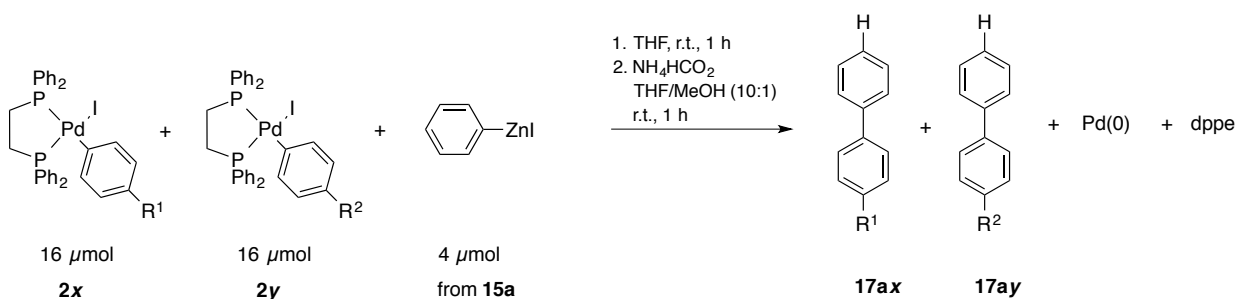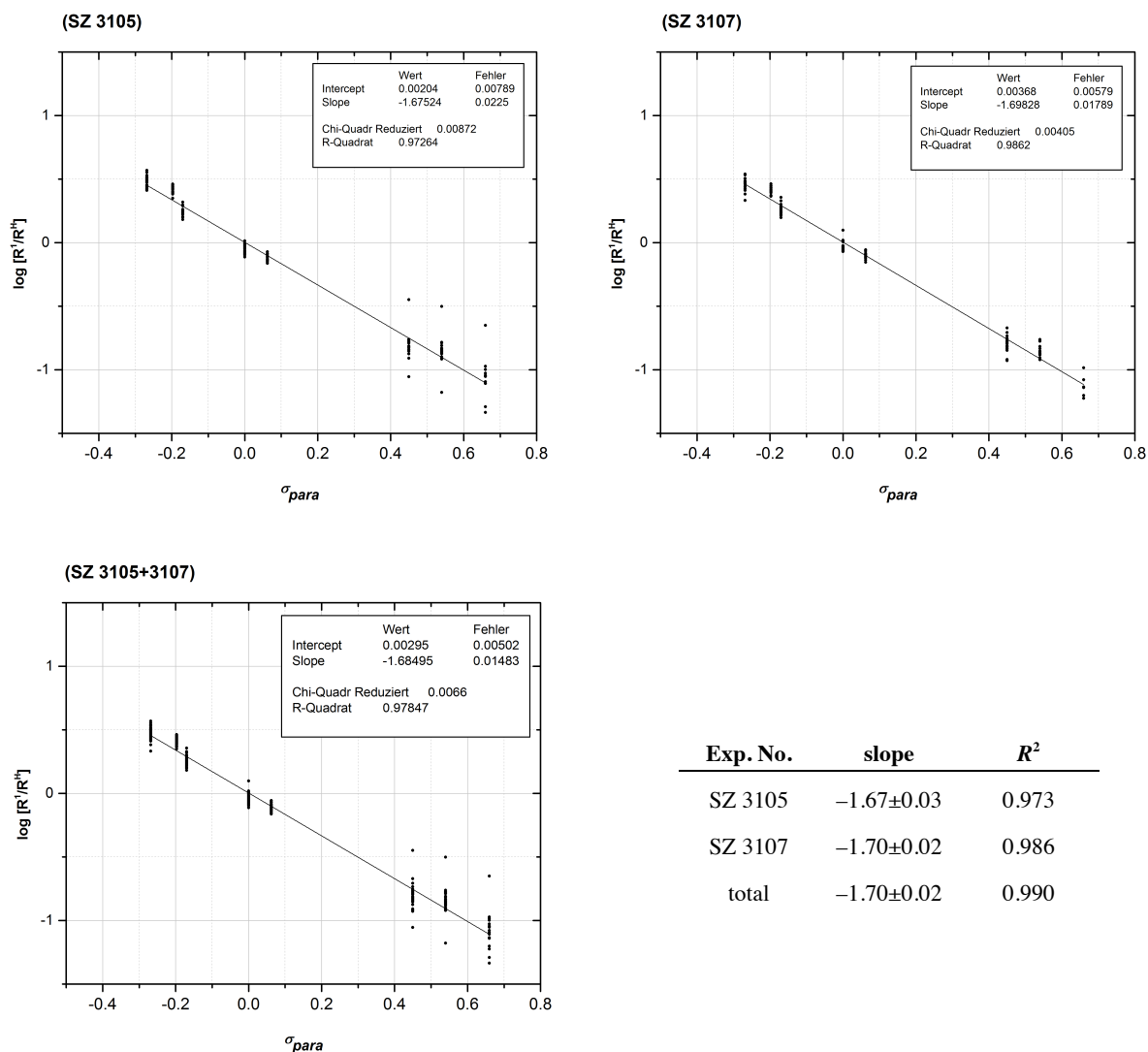
sample	R^1 **2x**		m [mg]	n [μmol]	R^2 **2y**		m [mg]	n [μmol]	**17ax/17ay**	σ	yield 17 [%]	σ [%]
A1	OMe	**d**	11.8	16.0	H	**a**	11.3	16.0	**2.83**	0.11	78	1
A2	^{t}Bu	**e**	12.4	16.2	H	**a**	11.4	16.1	**2.92**	0.20	79	2
A3	Me	**f**	11.6	16.1	H	**a**	11.4	16.1	**1.92**	0.07	88	1
A4	CO$_2$Et	**i**	12.7	16.2	H	**a**	11.5	16.3	**0.31**	0.03	80	1
A5	CF$_3$	**k**	12.8	16.4	H	**a**	11.6	16.4	**0.25**	0.00	82	1

265

sample	R¹		m	n	R²		m	n	17a*x*/17a*y*	σ	yield	σ
A6	CN	l	11.7	16.0	H	a	11.3	15.9	**0.12**	0.06	74	3
B1	^{t}Bu	e	12.8	16.8	OMe	d	12.4	16.8	**0.81**	0.03	91	2
B2	Me	f	11.6	16.0	OMe	d	11.9	16.1	**0.63**	0.01	86	1
B3	F	g	11.5	15.9	OMe	d	11.8	15.9	**0.38**	0.00	94	2
B4	CO$_2$Et	i	15.5	19.9	OMe	d	14.6	19.8	**0.13**	0.02	100	3
B5	CF$_3$	k	12.7	16.4	OMe	d	12.2	16.5	**0.09**	0.01	96	4
B6	CN	l	13.3	18.1	OMe	d	13.3	18.0	**0.00**	0.00	80	3
C1	Me	f	11.9	16.4	^{t}Bu	e	12.6	16.5	**0.69**	0.01	89	1
C2	F	g	11.6	15.9	^{t}Bu	e	12.3	16.0	**0.34**	0.02	100	2
C3	CO$_2$Et	i	12.6	16.1	^{t}Bu	e	12.4	16.1	**0.12**	0.00	105	2
C4	CF$_3$	k	12.7	16.3	^{t}Bu	e	12.4	16.3	**0.09**	0.00	98	1
C5	CN	l	12.0	16.4	^{t}Bu	e	12.6	16.4	**0.00**	0.00	87	2
D1	F	g	11.6	16.0	Me	f	11.6	16.0	**0.52**	0.01	100	3
D2	CO$_2$Et	i	14.5	18.6	Me	f	13.4	18.6	**0.15**	0.03	81	1
D3	CF$_3$	k	12.2	15.7	Me	f	11.4	15.7	**0.12**	0.01	88	2
D4	CN	l	11.7	15.9	Me	f	11.6	16.0	**0.05**	0.04	80	3
E1	CO$_2$Et	i	13.0	16.6	F	g	12.1	16.7	**0.35**	0.03	101	2
E2	CF$_3$	k	12.4	16.0	F	g	11.6	16.0	**0.29**	0.03	95	2
E3	CN	l	11.7	15.9	F	i	11.6	16.0	**0.13**	0.05	87	3
F1	CF$_3$	k	13.2	17.0	CO$_2$Et	i	13.3	17.1	**0.71**	0.02	97	3
F2	CN	l	12.6	17.2	CO$_2$Et	i	13.4	17.2	**0.66**	0.03	94	5
G1	CN	l	11.7	17.2	CF$_3$	k	12.4	16.0	**0.85**	0.04	79	2

[SZ 3117]

Similar to the general procedure, complexes **2x** and **2y** (each 16 μmol) were treated with a solution of ZnPh$_2$ (22.1 mg, 0.10 mmol) and ZnCl$_2$ (29.4 mg, 0.12 mmol) in THF (10.0 mL, c[PhZnCl] = 20.1 mM, 0.20 mL, 4.0 μmol). A stock solution of TMB (84.5 mg, 0.50 mmol) in MeOH (50.0 mL, c = 10.1 mM, 0.40 mL, 4.0 μmol) was added for biaryl quantifications by GC-FID.

sample	R¹	**2x**	m [mg]	n [μmol]	R²	**2y**	m [mg]	n [μmol]	17a*x*/17a*y*	σ	yield 17 [%]	σ [%]
A1	OMe	d	12.7	17.2	H	a	12.6	17.8	**2.35**	0.22	81	9
A2	^{t}Bu	e	12.5	16.3	H	a	11.5	16.2	**2.20**	0.04	81	3
A3	Me	f	11.9	16.5	H	a	11.9	16.8	**1.78**	0.13	83	3
A4	CO$_2$Et	i	13.6	17.4	H	a	12.8	18.1	**0.20**	0.01	86	2
A5	CF$_3$	k	12.1	15.6	H	a	11.9	16.8	**0.24**	0.01	89	2
A6	CN	l	11.7	15.9	H	a	11.9	16.8	**0.08**	0.07	77	7
B1	^{t}Bu	e	12.1	15.8	OMe	d	12.1	16.4	**0.92**	0.07	85	3
B2	Me	f	11.3	15.6	OMe	d	11.8	16.0	**0.51**	0.01	76	2
B3	F	g	11.3	15.5	OMe	d	12.1	16.4	**0.27**	0.03	87	2
B4	CO$_2$Et	i	12.8	16.4	OMe	d	11.8	16.0	**0.08**	0.01	77	5

B5	CF$_3$	k	12.7	16.3	OMe	d	11.7	15.8	**0.03**	0.06	81	7
B6	CN	l	12.1	16.5	OMe	d	12.1	16.4	**0.18**	0.04	81	5
C1	Me	f	11.4	15.8	^{t}Bu	e	12.5	16.3	**0.73**	0.05	95	5
C2	F	g	12.1	16.6	^{t}Bu	e	12.9	16.9	**0.50**	0.02	102	2
C3	CO$_2$Et	i	12.8	16.4	^{t}Bu	e	12.5	16.3	**0.12**	0.01	97	6
C4	CF$_3$	k	12.5	16.1	^{t}Bu	e	12.4	16.2	**0.11**	0.01	94	1
C5	CN	l	13.0	17.7	^{t}Bu	e	13.4	17.5	**0.15**	0.06	95	6
D1	F	g	11.5	15.8	Me	f	11.7	16.2	**0.58**	0.06	83	20
D2	CO$_2$Et	i	12.4	15.9	Me	f	11.8	16.3	**0.14**	0.01	83	3
D3	CF$_3$	k	12.8	16.5	Me	f	12.0	16.6	**0.12**	0.01	87	5
D4	CN	l	12.0	16.4	Me	f	11.6	16.0	**0.00**	0.00	72	2
E1	CO$_2$Et	i	12.8	16.4	F	g	12.0	16.5	**0.28**	0.01	102	2
E2	CF$_3$	k	12.3	15.8	F	g	11.6	16.0	**0.29**	0.01	86	2
E3	CN	l	11.7	15.9	F	i	12.0	16.5	**0.13**	0.07	91	8
F1	CF$_3$	k	12.4	16.0	CO$_2$Et	i	12.7	16.3	**0.82**	0.04	83	1
F2	CN	l	11.6	15.8	CO$_2$Et	i	12.6	16.1	**0.49**	0.26	66	9
G1	CN	l	11.7	15.8	CF$_3$	k	12.5	16.1	**0.60**	0.09	73	1

(SZ 3103)

	Wert	Fehler
Intercept	-0.00163	0.00686
Slope	-1.40144	0.01903
Chi-Quadr Reduziert	0.00701	
R-Quadrat	0.96961	

(SZ 3117)

	Wert	Fehler
Intercept	5.86946E-5	0.00908
Slope	-1.38225	0.02514
Chi-Quadr Reduziert	0.01174	
R-Quadrat	0.94915	

(SZ 3103+3117)

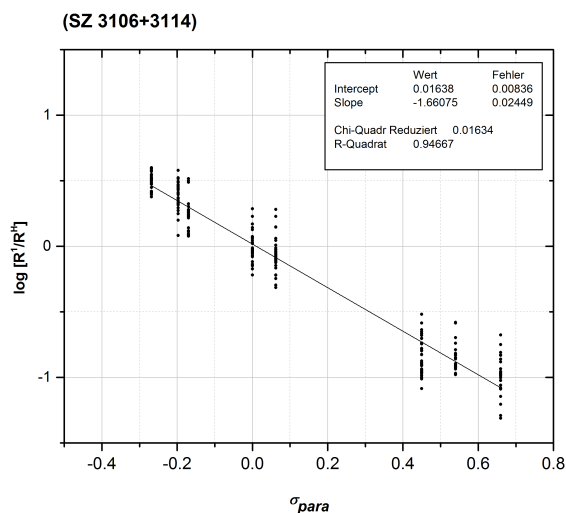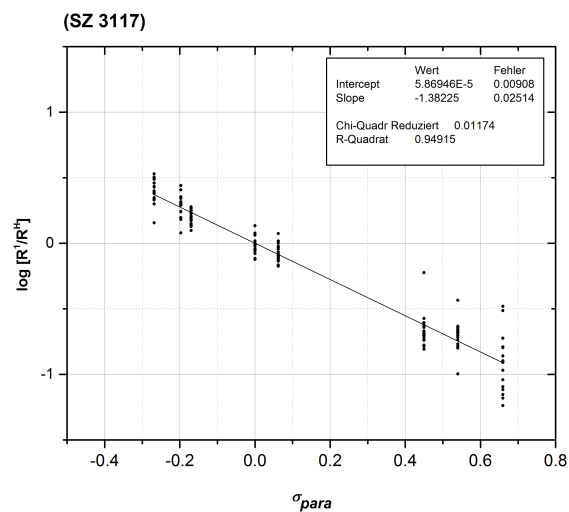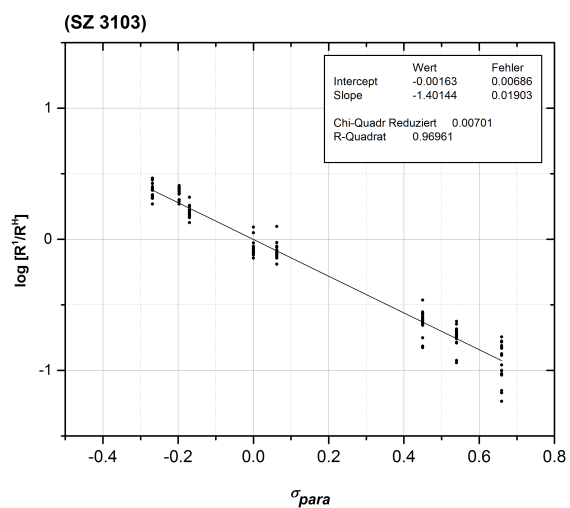| Exp. No.	slope	R^2
SZ 3103	-1.40 ± 0.02	0.970
SZ 3117	-1.38 ± 0.03	0.949
total	-1.41 ± 0.02	0.969

[SZ 3123]

Similar to the general procedure, complexes **2x** and **2y** (each 16 μmol) were treated with a solution of ZnPh$_2$ (54.9 mg, 0.25 mmol) and ZnCl$_2$ (376 mg, 2.76 mmol) in THF (25.0 mL, c[PhZnCl] = 20.0 mM, 0.20 mL, 4.0 μmol). A stock solution of TMB (86.4 mg, 0.51 mmol) in MeOH (50.0 mL, c = 10.3 mM, 0.40 mL, 4.1 μmol) was added for biaryl quantifications by GC-FID.

sample	R^1	2x	m [mg]	n [μmol]	R^2	2y	m [mg]	n [μmol]	17ax/17ay	σ	yield 17 [%]	σ [%]
A1	OMe	d	11.6	15.7	H	a	11.6	16.4	**1.81**	0.08	66	2
A2	^{t}Bu	e	12.1	15.8	H	a	11.6	16.4	**1.54**	0.14	92	3
A3	Me	f	11.6	16.0	H	a	11.8	16.6	**1.51**	0.05	90	1
A4	CO$_2$Et	i	12.6	16.1	H	a	11.2	15.8	**0.36**	0.00	86	2
A5	CF$_3$	k	12.3	15.8	H	a	11.3	15.9	**0.41**	0.03	94	8
A6	CN	l	12.1	16.5	H	a	11.4	16.1	**0.37**	0.10	84	9
B1	^{t}Bu	e	12.5	16.3	OMe	d	11.8	16.0	**0.92**	0.04	62	3
B2	Me	f	12.0	16.6	OMe	d	11.8	16.0	**0.83**	0.04	55	2
B3	F	g	1.7	2.3	OMe	d	11.5	15.6	**0.44**	0.01	57	0

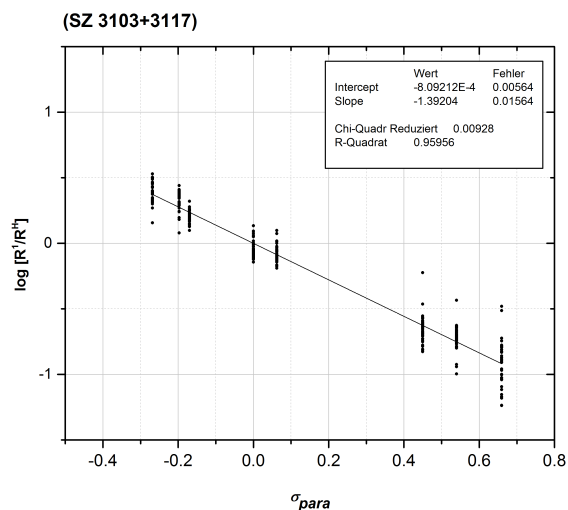| sample	R^1	2x	m [mg]	n [μmol]	R^2	2y	m [mg]	n [μmol]	17ax/17ay	σ	yield 17 [%]	σ [%]
B4	CO_2Et	i	12.3	15.8	OMe	d	11.7	15.8	**0.13**	0.01	55	3
B5	CF_3	k	12.4	16.0	OMe	d	11.5	15.6	**0.17**	0.01	58	2
B6	CN	l	12.1	16.5	OMe	d	12.1	16.4	**0.03**	0.06	47	1
C1	Me	f	11.6	16.0	^tBu	e	12.4	16.2	**0.96**	0.08	70	3
C2	F	g	11.8	16.2	^tBu	e	12.2	15.9	**0.53**	0.06	69	4
C3	CO_2Et	i	12.8	16.4	^tBu	e	12.1	15.8	**0.28**	0.00	72	6
C4	CF_3	k	12.2	15.7	^tBu	e	12.5	16.3	**0.19**	0.03	76	11
C5	CN	l	11.5	15.7	^tBu	e	12.0	15.7	**0.08**	0.07	61	6
D1	F	g	11.6	16.0	Me	f	11.7	16.2	**0.58**	0.01	64	0
D2	CO_2Et	i	12.7	16.3	Me	f	11.6	16.0	**0.23**	0.02	70	1
D3	CF_3	k	12.4	16.0	Me	f	11.9	16.5	**0.20**	0.01	74	2
D4	CN	l	12.2	16.6	Me	f	11.4	15.8	**0.05**	0.08	57	4
E1	CO_2Et	i	12.7	16.3	F	g	11.6	16.0	**0.18**	0.25	42	22
E2	CF_3	k	12.7	16.3	F	g	11.6	16.0	**0.47**	0.03	56	12
E3	CN	l	11.6	15.8	F	i	11.8	16.2	**0.30**	0.02	55	11
F1	CF_3	k	12.6	16.2	CO_2Et	i	12.8	16.4	**1.09**	0.02	58	-
F2	CN	l	11.6	15.8	CO_2Et	i	12.3	15.8	**0.60**	0.52	55	23
G1	CN	l	12.0	15.8	CF_3	k	12.5	16.1	**0.60**	0.09	111	74

[SZ 3124]

Similar to the general procedure, complexes **2x** and **2y** (each 16 μmol) were treated with a solution of $ZnPh_2$ (54.9 mg, 0.25 mmol) and $ZnCl_2$ (376 mg, 2.76 mmol) in THF (25.0 mL, $c[PhZnCl] =$ 20.0 mM, 0.20 mL, 4.0 μmol). A stock solution of TMB (86.4 mg, 0.51 mmol) in MeOH (50.0 mL, $c =$ 10.3 mM, 0.40 mL, 4.1 μmol) was added for biaryl quantifications by GC-FID.

sample	R^1	2x	m [mg]	n [μmol]	R^2	2y	m [mg]	n [μmol]	17ax/17ay	σ	yield 17 [%]	σ [%]
A1	OMe	d	11.4	15.4	H	a	11.3	15.9	**2.06**	0.14	72	1
A2	^tBu	e	12.8	16.7	H	a	11.4	16.1	**1.50**	0.08	89	4
A3	Me	f	11.1	15.4	H	a	11.8	16.6	**1.38**	0.05	96	2
A4	CO_2Et	i	12.5	16.0	H	a	11.5	16.2	**0.41**	0.03	90	2
A5	CF_3	k	12.8	16.5	H	a	11.4	16.1	**0.42**	0.01	88	0
A6	CN	l	11.9	16.2	H	a	11.2	15.8	**0.25**	0.02	84	3
B1	^tBu	e	12.3	16.1	OMe	d	11.8	16.0	**0.91**	0.03	60	6
B2	Me	f	11.7	16.2	OMe	d	11.7	15.8	**0.86**	0.05	57	2
B3	F	g	11.4	15.7	OMe	d	11.7	15.8	**0.21**	0.30	45	6
B4	CO_2Et	i	12.3	15.8	OMe	d	11.9	16.1	**0.11**	0.03	55	3
B5	CF_3	k	12.1	15.6	OMe	d	11.5	15.6	**0.15**	0.01	56	3
B6	CN	l	12.3	16.8	OMe	d	11.7	15.8	**0.03**	0.06	52	1
C1	Me	f	11.9	16.5	^tBu	e	12.4	16.2	**0.97**	0.11	76	5
C2	F	g	11.6	16.0	^tBu	e	12.0	15.7	**0.44**	-	61	-

C3	CO$_2$Et	**i**	12.2	15.6	^{t}Bu	**e**	12.0	15.7	**0.20**	0.01	75	6
C4	CF$_3$	**k**	12.8	16.5	^{t}Bu	**e**	12.4	16.2	**0.18**	0.01	74	5
C5	CN	**l**	11.6	15.8	^{t}Bu	**e**	12.2	15.9	**0.12**	0.01	67	6
D1	F	**g**	11.5	15.8	Me	**f**	11.4	15.8	**0.44**	0.02	61	1
D2	CO$_2$Et	**i**	12.7	16.3	Me	**f**	11.8	16.3	**0.21**	0.01	72	1
D3	CF$_3$	**k**	12.6	16.2	Me	**f**	11.6	16.0	**0.23**	0.02	78	3
D4	CN	**l**	12.2	16.6	Me	**f**	11.5	15.9	**0.17**	0.03	66	6
E1	CO$_2$Et	**i**	12.9	16.5	F	**g**	11.4	15.7	**0.39**	0.07	58	1
E2	CF$_3$	**k**	12.4	16.0	F	**g**	11.4	15.7	**0.48**	0.01	60	1
E3	CN	**l**	11.4	15.5	F	**i**	11.4	15.7	**0.31**	0.08	56	8
F1	CF$_3$	**k**	12.3	15.8	CO$_2$Et	**i**	12.9	16.5	**0.98**	0.16	66	4
F2	CN	**l**	11.9	16.2	CO$_2$Et	**i**	12.3	15.8	**0.72**	0.10	67	4
G1	CN	**l**	11.5	16.2	CF$_3$	**k**	12.6	16.2	**0.63**	0.07	64	3

(SZ 3123)

	Wert	Fehler
Intercept	0.00363	0.00628
Slope	-0.99077	0.01765
Chi-Quadr Reduziert	0.0054	
R-Quadrat	0.95456	

(SZ 3124)

	Wert	Fehler
Intercept	-6.54175E-4	0.00575
Slope	-1.044	0.01572
Chi-Quadr Reduziert	0.0047	
R-Quadrat	0.96457	

(SZ 3123+3124)

	Wert	Fehler
Intercept	0.00122	0.00428
Slope	-1.01911	0.01186
Chi-Quadr Reduziert	0.00512	
R-Quadrat	0.95923	
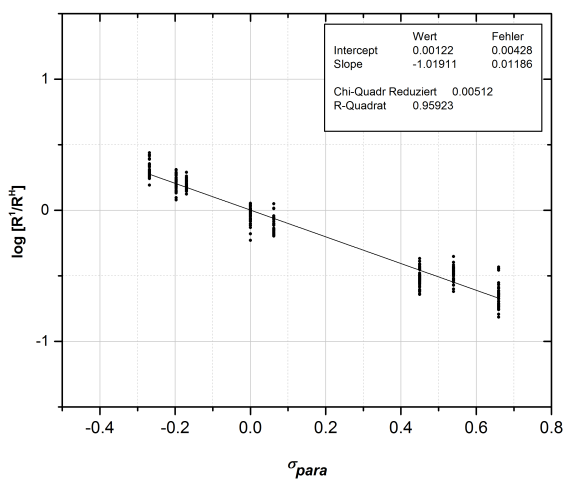
Exp. No.	slope	R^2
SZ 3123	−0.99±0.02	0.955
SZ 3124	−1.04±0.02	0.965
total	−1.02±0.02	0.959

[SZ 3118]

Similar to the general procedure, complexes **2x** and **2y** (each 16 μmol) were treated with a solution of ZnPh$_2$ (54.7 mg, 0.25 mmol) and ZnCl$_2$ (717 mg, 5.26 mmol) in THF (25.0 mL, c[PhZnCl] = 20.0 mM, 0.20 mL, 4.0 μmol). A stock solution of TMB (84.5 mg, 0.50 mmol) in MeOH (50.0 mL, c = 10.1 mM, 0.40 mL, 4.0 μmol) was added for biaryl quantifications by GC-FID.
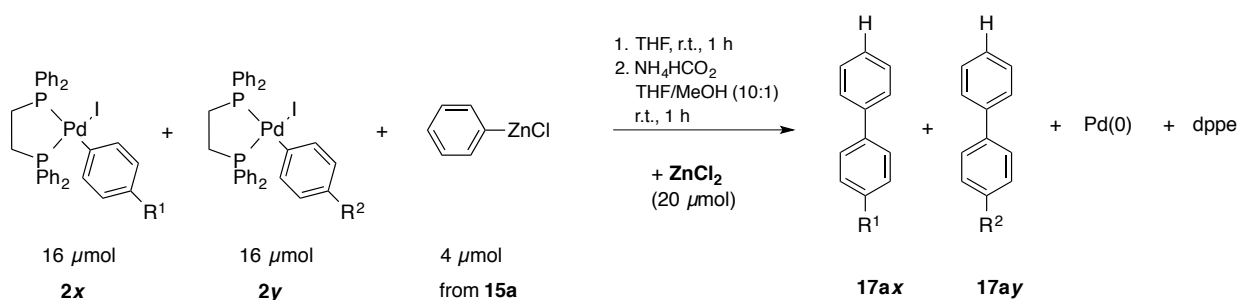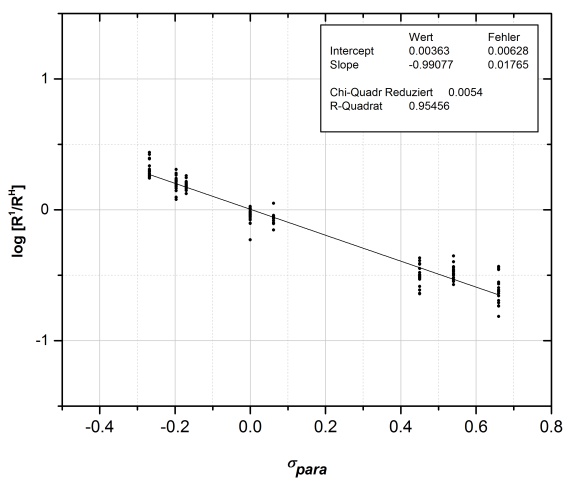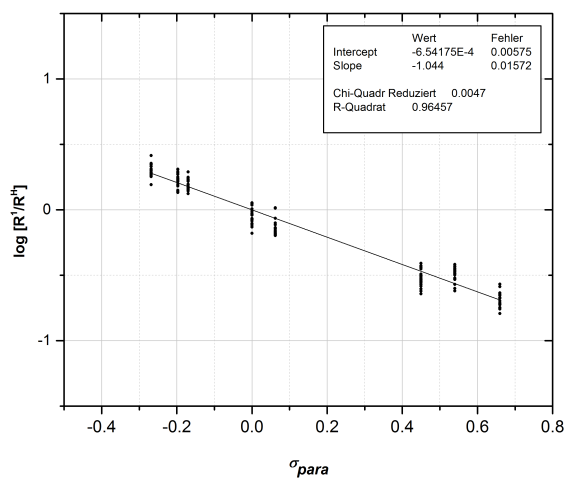
sample	R^1	2x	m [mg]	n [μmol]	R^2	2y	m [mg]	n [μmol]	17ax/17ay	σ	yield 17 [%]	σ [%]
A1	OMe	d	12.4	16.8	H	a	12.2	17.2	1.10	-	13	6
A2	^{t}Bu	e	12.2	15.9	H	a	11.3	15.9	1.25	1.08	43	34
A3	Me	f	11.6	16.0	H	a	11.5	16.2	0.78	0.50	37	32
A4	CO$_2$Et	i	13	16.6	H	a	11.6	16.4	0.72	0.41	78	55
A5	CF$_3$	k	13	16.7	H	a	11.8	16.6	1.28	0.31	181	75
A6	CN	l	11.8	16.1	H	a	11.6	16.4	1.49	0.15	98	53
B1	^{t}Bu	e	11.9	15.6	OMe	d	11.5	15.6	1.12	0.13	17	2
B2	Me	f	11.3	15.6	OMe	d	11.2	15.2	0.98	0.12	9	8
B3	F	g	11.9	16.4	OMe	d	13.3	18.0	0.00	0.00	10	1
B4	CO$_2$Et	i	12.4	15.9	OMe	d	11.7	15.8	0.87	0.34	21	7
B5	CF$_3$	k	12.2	15.7	OMe	d	11.4	15.4	0.36	0.62	17	7
B6	CN	l	13.8	18.8	OMe	d	13.4	18.1	1.89	1.03	33	13
C1	Me	f	11.7	16.2	^{t}Bu	e	12.4	16.2	0.58	0.13	23	3
C2	F	g	12.6	17.3	^{t}Bu	e	13.1	17.1	0.76	1.31	34	30
C3	CO$_2$Et	i	12.7	16.3	^{t}Bu	e	12.3	16.1	0.56	0.44	31	10
C4	CF$_3$	k	12.3	15.8	^{t}Bu	e	12.4	16.2	0.24	0.42	30	6
C5	CN	l	12	16.4	^{t}Bu	e	11.8	15.4	0.88	0.69	41	14
D1	F	g	11.4	15.7	Me	f	11.2	15.5	1.03	1.08	21	14
D2	CO$_2$Et	i	13.1	16.8	Me	f	12.0	16.6	1.00	0.66	29	12
D3	CF$_3$	k	12.9	16.6	Me	f	12.2	16.9	1.22	1.58	29	21
D4	CN	l	11.8	16.1	Me	f	11.6	16.0	2.23	1.80	45	27
E1	CO$_2$Et	i	14.3	18.3	F	g	13.8	19.0	1.65	1.49	75	64
E2	CF$_3$	k	12.1	15.6	F	g	11.2	15.4	1.60	0.89	48	40
E3	CN	l	12.1	16.5	F	i	12.3	16.9	1.89	1.32	50	31
F1	CF$_3$	k	15.1	19.4	CO$_2$Et	i	15.6	20.0	1.23	0.49	63	49

sample	R^1	2x	m [mg]	n [µmol]	R^2	2y	m [mg]	n [µmol]	17ax/17ay	σ	yield 17 [%]	σ [%]
F2	CN	**l**	11.8	16.1	CO$_2$Et	**i**	12.8	16.4	**1.59**	0.26	65	33
G1	CN	**l**	11.7	16.1	CF$_3$	**k**	12.9	16.6	**0.64**	0.36	130	125

[SZ 3121]

Similar to the general procedure, complexes **2x** and **2y** (each 16 μmol) were treated with a solution of ZnPh$_2$ (54.7 mg, 0.25 mmol) and ZnCl$_2$ (717 mg, 5.26 mmol) in THF (25.0 mL, c[PhZnCl] = 20.0 mM, 0.20 mL, 4.0 μmol). A stock solution of TMB (84.5 mg, 0.50 mmol) in MeOH (50.0 mL, c = 10.1 mM, 0.40 mL, 4.0 μmol) was added for biaryl quantifications by GC-FID.

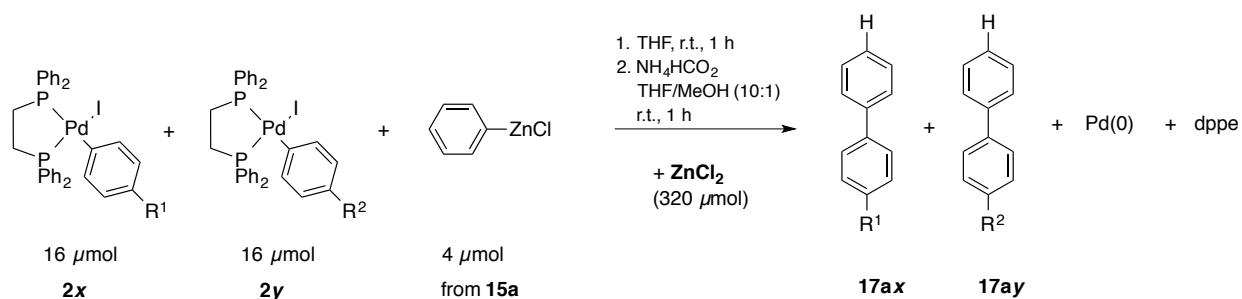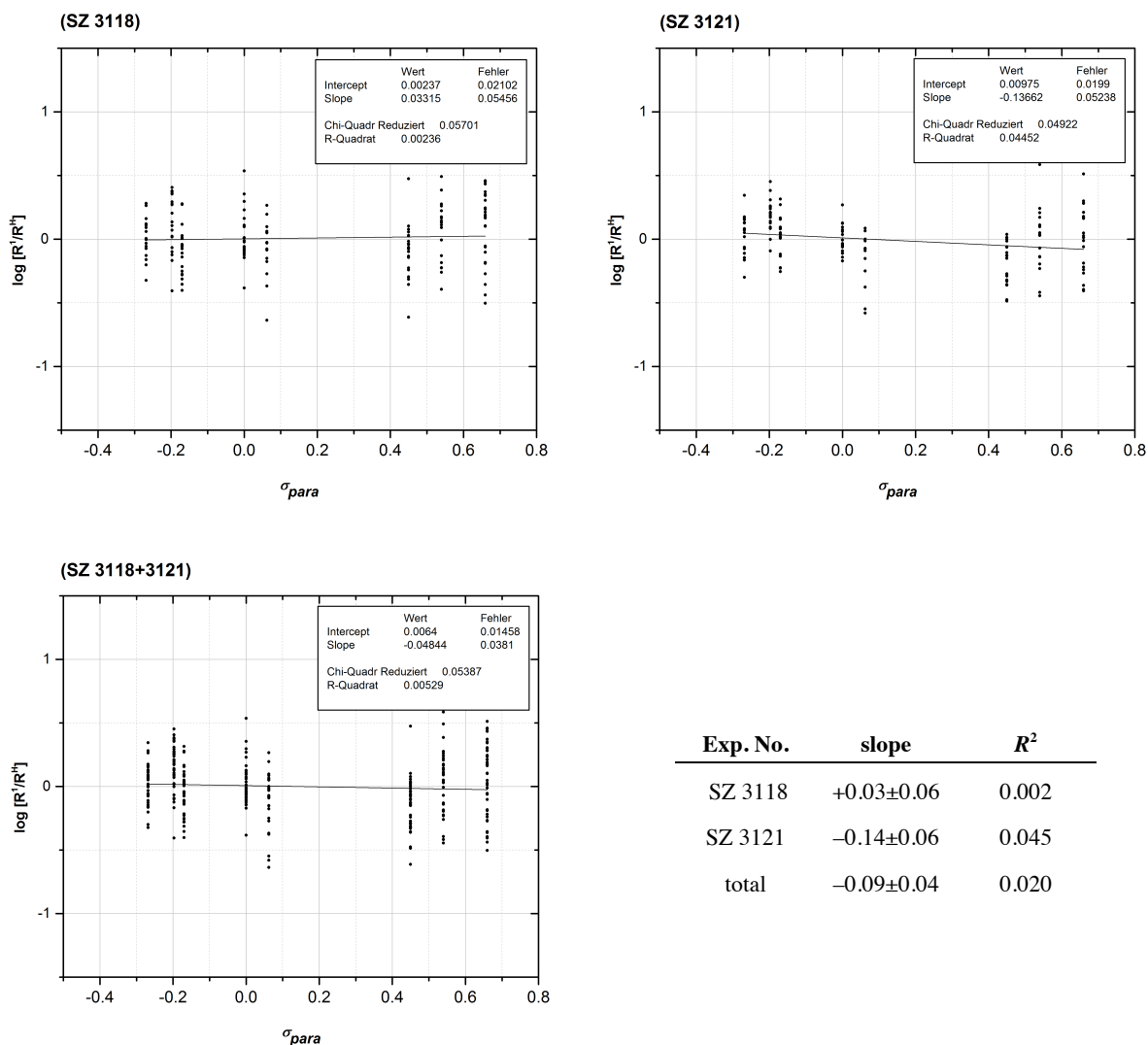| sample	R^1	2x	m [mg]	n [µmol]	R^2	2y	m [mg]	n [µmol]	17ax/17ay	σ	yield 17 [%]	σ [%]
A1	OMe	**d**	11.2	15.2	H	**a**	11.0	15.5	**1.47**	0.36	16	2
A2	^{t}Bu	**e**	12.4	16.2	H	**a**	11.2	15.8	**1.47**	0.76	22	5
A3	Me	**f**	11.6	16.0	H	**a**	11.7	16.5	**1.02**	0.42	20	8
A4	CO$_2$Et	**i**	12.9	16.5	H	**a**	11.5	16.2	**0.69**	0.32	48	46
A5	CF$_3$	**k**	12.3	15.8	H	**a**	11.4	16.1	**0.82**	0.77	50	48
A6	CN	**l**	11.6	15.8	H	**a**	11.5	16.2	**1.08**	0.62	55	44
B1	^{t}Bu	**e**	12.1	15.8	OMe	**d**	11.4	15.4	**1.55**	0.36	17	3
B2	Me	**f**	13	18.0	OMe	**d**	12.7	17.2	**0.74**	-	15	-
B3	F	**g**	11.2	15.4	OMe	**d**	11.7	15.8	**0.00**	0.00	8	1
B4	CO$_2$Et	**i**	12.2	15.6	OMe	**d**	11.4	15.4	**0.67**	0.49	21	7
B5	CF$_3$	**k**	12.5	16.1	OMe	**d**	11.4	15.4	**0.83**	1.02	23	13
B6	CN	**l**	12.5	17.0	OMe	**d**	12.2	16.5	**1.63**	0.66	31	8
C1	Me	**f**	11.8	16.3	^{t}Bu	**e**	12.1	15.8	**0.71**	0.25	20	6
C2	F	**g**	11.5	15.8	^{t}Bu	**e**	12.2	15.9	**0.28**	0.48	21	13
C3	CO$_2$Et	**i**	12.6	16.1	^{t}Bu	**e**	12.3	16.1	**0.38**	0.28	28	8
C4	CF$_3$	**k**	13.2	17.0	^{t}Bu	**e**	12.2	15.9	**0.19**	0.33	29	11
C5	CN	**l**	12.5	17.0	^{t}Bu	**e**	12.1	15.8	**0.48**	0.61	30	15
D1	F	**g**	11.5	15.8	Me	**f**	10.8	14.9	**0.39**	0.67	13	9
D2	CO$_2$Et	**i**	13.9	17.8	Me	**f**	11.2	15.5	**0.60**	0.20	20	3
D3	CF$_3$	**k**	13.9	17.9	Me	**f**	11.4	15.8	**0.55**	0.95	19	11
D4	CN	**l**	12.5	17.0	Me	**f**	11.1	15.4	**0.79**	0.39	23	5
E1	CO$_2$Et	**i**	15.1	19.3	F	**g**	12.2	16.8	**0.98**	0.18	36	28
E2	CF$_3$	**k**	13.6	17.5	F	**g**	12.3	16.9	**3.20**	2.34	104	100
E3	CN	**l**	12.0	16.4	F	**i**	11.3	15.5	**1.60**	2.04	29	25
F1	CF$_3$	**k**	13.1	16.9	CO$_2$Et	**i**	13.2	16.9	**1.21**	0.40	44	30
F2	CN	**l**	12.5	17.0	CO$_2$Et	**i**	13.0	16.6	**1.56**	0.51	52	36
G1	CN	**l**	12.1	17.0	CF$_3$	**k**	12.3	15.8	**1.35**	0.37	47	31

(SZ 3118)

	Wert	Fehler
Intercept	0.00237	0.02102
Slope	0.03315	0.05456
Chi-Quadr Reduziert	0.05701	
R-Quadrat	0.00236	

(SZ 3121)

	Wert	Fehler
Intercept	0.00975	0.0199
Slope	-0.13662	0.05238
Chi-Quadr Reduziert	0.04922	
R-Quadrat	0.04452	

(SZ 3118+3121)

	Wert	Fehler
Intercept	0.0064	0.01458
Slope	-0.04844	0.0381
Chi-Quadr Reduziert	0.05387	
R-Quadrat	0.00529	

Exp. No.	slope	R^2
SZ 3118	+0.03±0.06	0.002
SZ 3121	−0.14±0.06	0.045
total	−0.09±0.04	0.020

[SZ 4131]

Similar to the general procedure, complexes **2x** and **2y** (each 16 μmol) were dissolved in a solution of ZnCl$_2$ (2.18 g, 16.0 mmol) in THF (100 mL, c = 0.16 M) and treated with a solution, prepared from ZnPh$_2$ (22.4 mg, 0.10 mmol) and the ZnCl$_2$ reaction solution (0.63 mL, 0.10 mmol) in THF (10.0 mL,

c[PhZnCl] = 20.4 mM, 0.20 mL, 4.0 μmol). A stock solution of TMB (86.0 mg, 0.51 mmol) in THF (25.0 mL, c = 20.5 mM, 0.20 mL, 4.1 μmol) was added for biaryl quantifications by GC-FID.

sample	R^1	2x	m [mg]	n [μmol]	R^2	2y	m [mg]	n [μmol]	17ax/17ay	σ	yield 17 [%]	σ [%]
A1	OMe	d	11.7	15.8	H	a	11.7	16.5	**1.09**	0.09	323	17
A2	^{t}Bu	e	12.6	16.5	H	a	11.4	16.1	**1.53**	0.32	346	35
A3	Me	f	11.7	16.2	H	a	11.7	16.5	**1.12**	0.06	346	21
A4	CO$_2$Et	i	12.6	16.1	H	a	11.5	16.2	**0.76**	0.21	358	25
A6	CN	l	19.6	26.7	H	a	11.6	16.4	**0.28**	0.05	289	16
B1	^{t}Bu	e	12.6	16.5	OMe	d	12.1	16.4	**1.74**	0.01	193	3
B2	Me	f	11.7	16.2	OMe	d	12.1	16.4	**1.42**	0.11	175	15
B3	F	g	11.8	16.2	OMe	d	12.1	16.4	**1.44**	0.03	190	7
B4	CO$_2$Et	i	12.2	15.6	OMe	d	12.0	16.2	**0.70**	0.01	155	14
B5	CF$_3$	k	12.4	16.0	OMe	d	11.9	16.1	**1.22**	0.19	227	19
B6	CN	l	11.7	15.9	OMe	d	11.7	15.8	**0.27**	0.24	133	17
C1	Me	f	12.0	16.6	^{t}Bu	e	12.2	15.9	**0.73**	0.04	196	13
C2	F	g	11.5	15.8	^{t}Bu	e	12.1	15.8	**0.72**	0.06	210	9
C3	CO$_2$Et	i	12.2	15.6	^{t}Bu	e	12.5	16.3	**0.34**	0.02	211	31
C4	CF$_3$	k	12.8	16.5	^{t}Bu	e	12.1	15.8	**0.75**	-	229	-
D1	F	g	11.8	16.2	Me	f	11.9	16.5	**1.04**	0.06	199	5
D2	CO$_2$Et	i	12.4	15.9	Me	f	11.6	16.0	**0.61**	0.01	192	9
D3	CF$_3$	k	12.2	15.7	Me	f	11.8	16.3	**0.70**	0.00	216	10
D4	CN	l	11.8	16.1	Me	f	11.8	16.3	**0.09**	0.15	132	27
E1	CO$_2$Et	i	12.2	15.6	F	g	11.3	15.5	**0.40**	0.04	216	13
E3	CN	l	12.1	16.5	F	i	11.5	15.8	**0.14**	0.01	208	0
F1	CF$_3$	k	12.8	16.5	CO$_2$Et	i	12.3	15.8	**1.43**	0.41	225	15
F2	CN	l	11.8	16.1	CO$_2$Et	i	12.4	15.9	**0.22**	0.19	118	26
G1	CN	l	11.9	16.1	CF$_3$	k	12.3	15.8	**0.52**	0.46	228	68

[SZ 4134]

Similar to the general procedure, complexes **2x** and **2y** (each 16 μmol) were dissolved in a solution of ZnCl$_2$ (2.18 g, 16.0 mmol) in THF (100 mL, c = 0.16 M) and treated with a solution, prepared from ZnPh$_2$ (22.4 mg, 0.10 mmol) and the ZnCl$_2$ reaction solution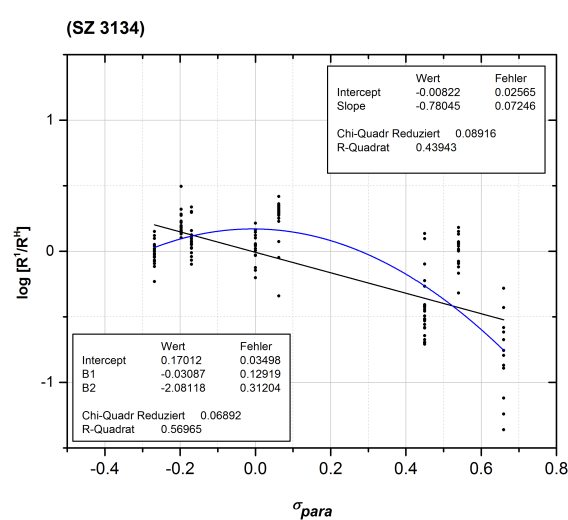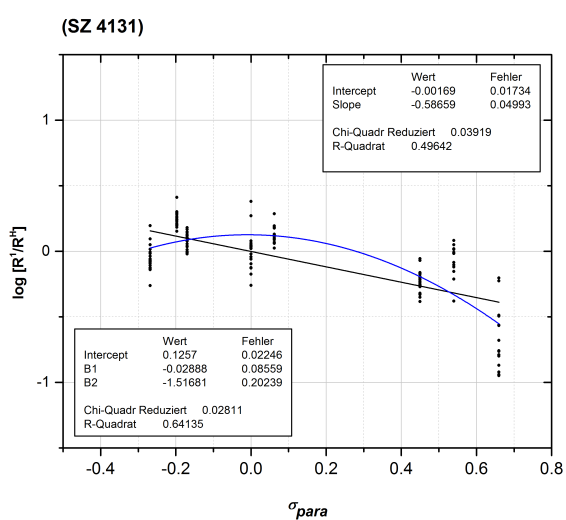 (0.63 mL, 0.10 mmol) in THF (10.0 mL, c[PhZnCl] = 20.4 mM, 0.20 mL, 4.0 μmol). A stock solution of TMB (86.0 mg, 0.51 mmol) in THF (25.0 mL, c = 20.5 mM, 0.20 mL, 4.1 μmol) was added for biaryl quantifications by GC-FID.

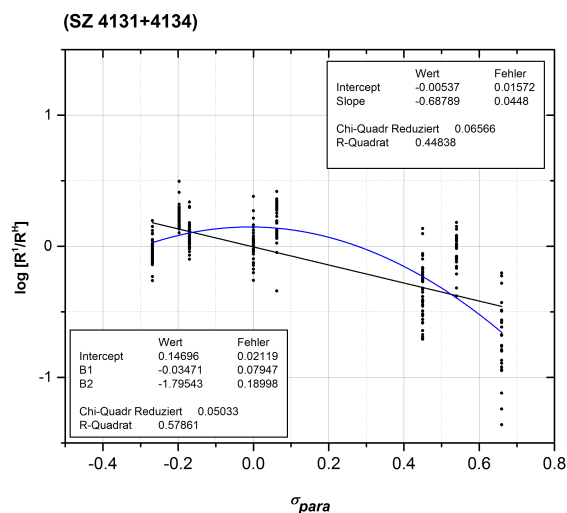| sample	R^1 2x	m [mg]	n [μmol]	R^2 2y	m [mg]	n [μmol]	17ax/17ay	σ	yield 17 [%]	σ [%]
A1	OMe **d**	13.0	17.6	H **a**	13.6	19.2	**0.87**	0.04	330	142
A2	^{t}Bu **e**	12.8	16.7	H **a**	14.6	20.6	**1.31**	0.27	364	132
A3	Me **f**	12.0	16.6	H **a**	13.9	19.6	**1.12**	0.03	417	104
A4	CO$_2$Et **i**	21.4	27.4	H **a**	11.3	15.9	**0.60**	0.20	349	8
A6	CN **l**	14.4	19.6	H **a**	12.0	16.9	**0.18**	0.11	314	27
B1	^{t}Bu **e**	12.0	15.7	OMe **d**	12.0	16.2	**1.40**	0.01	207	24
B2	Me **f**	11.8	16.3	OMe **d**	12.1	16.4	**1.19**	0.17	270	64
B3	F **g**	11.4	15.7	OMe **d**	14.0	18.9	**1.58**	0.08	312	24
B4	CO$_2$Et **i**	14.1	18.1	OMe **d**	12.9	17.5	**0.37**	0.12	188	47
B5	CF$_3$ **k**	13.8	17.8	OMe **d**	11.3	15.3	**1.03**	0.09	235	16
B6	CN **l**	16.1	21.9	OMe **d**	11.5	15.6	**0.29**	0.31	138	37
C1	Me **f**	11.9	16.5	^{t}Bu **e**	13.1	17.1	**0.74**	0.08	240	38
C2	F **g**	13.4	18.4	^{t}Bu **e**	12.3	16.1	**1.37**	0.10	339	38
C3	CO$_2$Et **i**	16.6	21.3	^{t}Bu **e**	13.0	17.0	**0.27**	0.06	197	25
C4	CF$_3$ **k**	13.8	17.8	^{t}Bu **e**	13.0	17.0	**0.77**	0.12	293	28
D1	F **g**	12.0	16.5	Me **f**	14.4	19.9	**1.39**	0.03	233	15
D2	CO$_2$Et **i**	15.2	19.5	Me **f**	13.1	18.1	**0.31**	0.09	216	20
D3	CF$_3$ **k**	14.5	18.7	Me **f**	14.5	20.1	**1.10**	0.11	303	7
D4	CN **l**	13.4	18.3	Me **f**	12.3	17.0	**0.05**	0.09	165	5
E1	CO$_2$Et **i**	13.1	16.8	F **g**	12.1	16.6	**0.22**	0.07	293	29
E3	CN **l**	14.5	19.8	F **i**	11.8	16.2	**0.27**	0.15	306	39
F1	CF$_3$ **k**	12.7	16.3	CO$_2$Et **i**	16.5	21.1	**1.80**	0.92	235	28
F2	CN **l**	16.1	21.9	CO$_2$Et **i**	16.7	21.4	**0.13**	0.08	102	33
G1	CN **l**	13.3	21.9	CF$_3$ **k**	15.1	19.4	**0.00**	0.00	217	14

(SZ 4131)

	Wert	Fehler
Intercept	-0.00169	0.01734
Slope	-0.58659	0.04993

Chi-Quadr Reduziert 0.03919
R-Quadrat 0.49642

	Wert	Fehler
Intercept	0.1257	0.02246
B1	-0.02888	0.08559
B2	-1.51681	0.20239

Chi-Quadr Reduziert 0.02811
R-Quadrat 0.64135

(SZ 3134)

	Wert	Fehler
Intercept	-0.00822	0.02565
Slope	-0.78045	0.07246

Chi-Quadr Reduziert 0.08916
R-Quadrat 0.43943

	Wert	Fehler
Intercept	0.17012	0.03498
B1	-0.03087	0.12919
B2	-2.08118	0.31204

Chi-Quadr Reduziert 0.06892
R-Quadrat 0.56965

(SZ 4131+4134)

Exp. No.	slope	R^2
SZ 4131	–0.59±0.05	0.496
SZ 4134	–0.78±0.08	0.439
total	–0.64±0.05	0.444

16 μmol	16 μmol	4 μmol		17ax	17ay
2x	2y	from 15a			
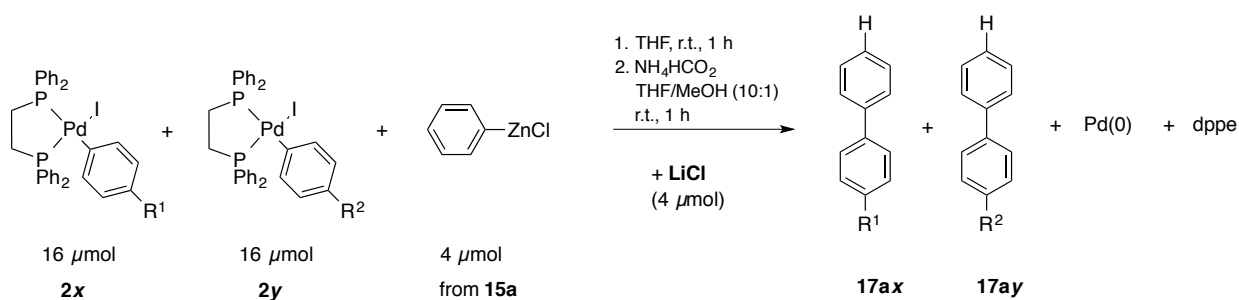
[SZ 3104]

Similar to the general procedure, complexes **2x** and **2y** (each 16 μmol) were treated with a solution of ZnPh$_2$ (54.9 mg, 0.25 mmol), ZnCl$_2$ (38.2 mg, 0.28 mmol) and LiCl (10.8 mg, 0.26 mmol) in THF (25.0 mL, c[PhZnCl] = 20.0 m$_M$, 0.20 mL, 4.0 μmol). A stock solution of TMB (85.7 mg, 0.51 mmol) in MeOH (50.0 mL, c = 10.2 m$_M$, 0.40 mL, 4.1 μmol) was added for biaryl quantifications by GC-FID.

sample	R^1	2x	m [mg]	n [μmol]	R^2	2y	m [mg]	n [μmol]	17ax/17ay	σ	yield 17 [%]	σ [%]
A1	OMe	d	11.8	16.0	H	a	11.3	16.0	**3.03**	0.17	86	0
A2	^{t}Bu	e	12.3	16.1	H	a	11.4	16.0	**3.11**	0.19	91	3
A3	Me	f	11.6	16.1	H	a	11.3	15.9	**2.02**	0.15	79	3
A4	CO$_2$Et	i	12.5	16.0	H	a	11.3	16.0	**0.22**	0.04	81	2
A5	CF$_3$	k	12.5	16.1	H	a	11.4	16.1	**0.20**	0.01	81	1
A6	CN	l	11.7	15.9	H	a	11.3	15.9	**0.03**	0.06	70	3
B1	^{t}Bu	e	12.4	16.2	OMe	d	11.8	15.9	**0.96**	0.01	88	1
B2	Me	f	12.5	17.3	OMe	d	12.8	17.3	**0.59**	0.04	89	4

sample	R¹	2x	m [mg]	n [μmol]	R²	2y	m [mg]	n [μmol]	17a*x*/17a*y*	σ	yield 17 [%]	σ [%]
B3	F	g	12.0	16.5	OMe	d	12.3	16.7	**0.29**	0.01	93	3
B4	CO₂Et	i	13.3	17.0	OMe	d	12.6	17.0	**0.09**	0.01	93	4
B5	CF₃	k	12.4	15.9	OMe	d	11.9	16.1	**0.08**	0.00	98	3
B6	CN	l	11.7	15.9	OMe	d	11.9	16.1	**0.00**	0.00	82	4
C1	Me	f	11.9	16.4	ᵗBu	e	11.5	15.1	**0.72**	0.02	154	3
C2	F	g	11.8	16.2	ᵗBu	e	12.5	16.3	**0.28**	0.02	97	1
C3	CO₂Et	i	13.3	17.0	ᵗBu	e	13.1	17.1	**0.09**	0.01	96	3
C4	CF₃	k	12.4	15.9	ᵗBu	e	12.2	15.9	**0.07**	0.00	97	2
C5	CN	l	12.0	16.4	ᵗBu	e	12.6	16.4	**0.00**	0.00	89	3
D1	F	g	11.7	16.0	Me	f	11.6	16.1	**0.41**	0.00	91	3
D2	CO₂Et	i	12.1	15.4	Me	f	11.9	16.5	**0.08**	0.07	84	5
D3	CF₃	k	12.4	15.9	Me	f	11.6	16.0	**0.10**	0.00	84	0
D4	CN	l	11.9	16.2	Me	f	11.6	16.0	**0.00**	0.00	79	1
E1	CO₂Et	i	12.4	15.9	F	g	11.6	16.0	**0.31**	0.05	109	2
E2	CF₃	k	12.6	16.2	F	g	11.6	16.0	**0.26**	0.03	96	2
E3	CN	l	11.8	16.1	F	i	11.7	16.0	**0.11**	0.02	86	1
F1	CF₃	k	12.5	16.1	CO₂Et	i	12.3	15.8	**0.74**	0.03	96	3
F2	CN	l	11.6	15.8	CO₂Et	i	12.4	15.8	**0.58**	0.06	86	7
G1	CN	l	11.8	15.8	CF₃	k	12.4	16.0	**0.78**	0.10	83	3

[SZ 3113]

Similar to the general procedure, complexes **2x** and **2y** (each 16 μmol) were treated with a solution of ZnPh₂ (54.9 mg, 0.25 mmol), ZnCl₂ (38.2 mg, 0.28 mmol) and LiCl (10.8 mg, 0.26 mmol) in THF (25.0 mL, c[PhZnCl] = 20.0 mM, 0.20 mL, 4.0 μmol). A stock solution of TMB (84.7 mg, 0.50 mmol) in MeOH (50.0 mL, c = 10.1 mM, 0.40 mL, 4.0 μmol) was added for biaryl quantifications by GC-FID.

sample	R¹ 2x		m [mg]	n [μmol]	R² 2y		m [mg]	n [μmol]	17a*x*/17a*y*	σ	yield 17 [%]	σ [%]
A1	OMe	d	11.6	15.7	H	a	11.0	15.5	**2.90**	0.19	66	4
A2	ᵗBu	e	12.1	15.8	H	a	11.1	15.7	**2.57**	0.37	76	5
A3	Me	f	11.3	15.6	H	a	11.3	15.9	**1.81**	0.20	74	3
A4	CO₂Et	i	12.2	15.6	H	a	11.3	15.9	**0.19**	0.03	71	4
A5	CF₃	k	13.4	17.2	H	a	12.5	17.6	**0.31**	0.01	82	4
A6	CN	l	12.1	16.5	H	a	11.8	16.6	**0.08**	0.13	70	11
B1	ᵗBu	e	12.2	15.9	OMe	d	11.5	15.6	**1.05**	0.06	74	3
B2	Me	f	11.7	16.2	OMe	d	11.7	15.8	**0.74**	0.07	69	3
B3	F	g	11.7	16.1	OMe	d	11.6	15.7	**0.32**	0.02	74	2
B4	CO₂Et	i	12.2	15.6	OMe	d	11.7	15.8	**0.07**	0.06	75	5
B5	CF₃	k	12.2	15.7	OMe	d	12.0	16.2	**0.00**	0.00	69	1
B6	CN	l	11.5	15.7	OMe	d	11.8	16.0	**0.00**	0.00	61	2

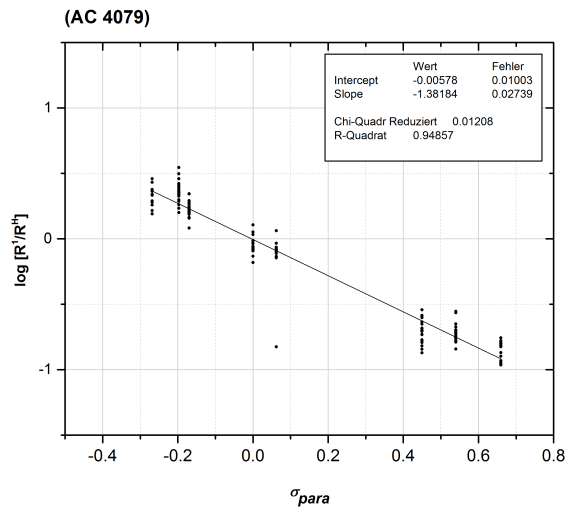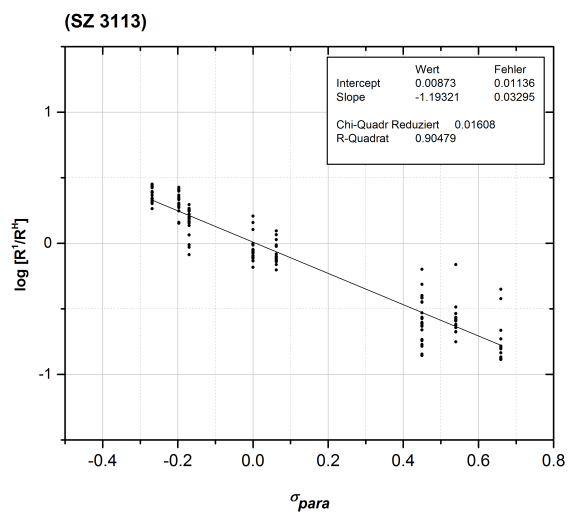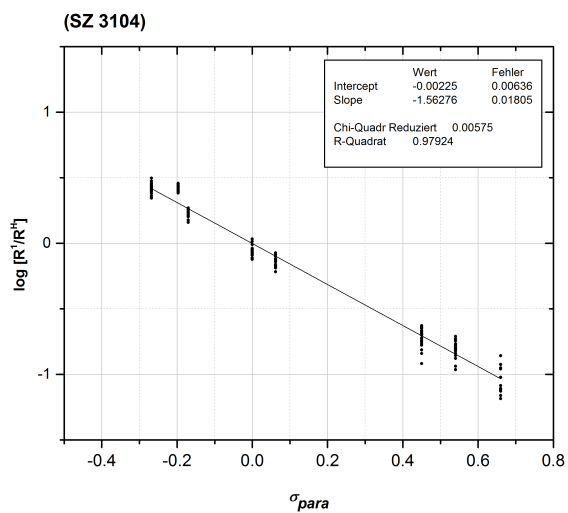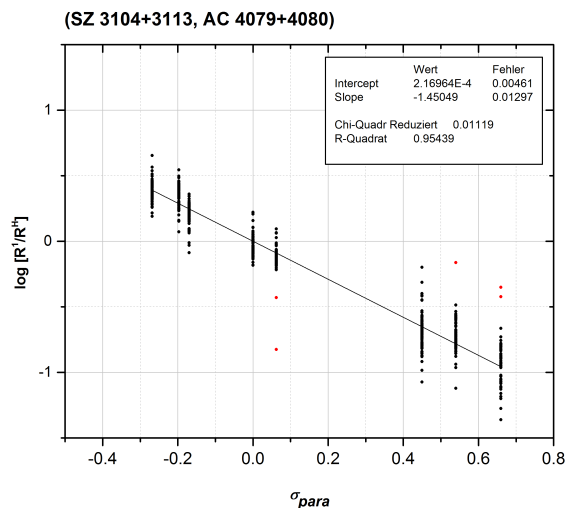| sample	R¹		m [mg]	n [μmol]	R²		m [mg]	n [μmol]	17ax/17ay	σ	yield 17 [%]	σ [%]
C1	Me	f	11.8	16.3	ᵗBu	e	12.1	15.8	**0.78**	0.03	79	0
C2	F	g	11.4	15.7	ᵗBu	e	12.2	15.9	**0.24**	0.21	74	20
C3	CO₂Et	i	13.3	17.0	ᵗBu	e	13.6	17.8	**0.17**	0.04	79	4
C4	CF₃	k	12.2	15.7	ᵗBu	e	12.6	16.5	**0.00**	0.00	75	4
C5	CN	l	11.6	15.8	ᵗBu	e	12.3	16.1	**0.00**	0.00	71	3
D1	F	g	11.3	15.5	Me	f	11.6	16.0	**0.47**	0.06	79	3
D2	CO₂Et	i	13.6	17.4	Me	f	12.9	17.8	**0.30**	0.04	82	1
D3	CF₃	k	12.5	16.1	Me	f	11.8	16.3	**0.04**	0.07	71	4
D4	CN	l	12.6	17.1	Me	f	12.7	17.6	**0.37**	0.05	87	5
E1	CO₂Et	i	12.6	16.1	F	g	11.4	15.7	**0.25**	0.01	81	2
E2	CF₃	k	12.2	15.7	F	g	11.5	15.8	**0.30**	0.01	88	1
E3	CN	l	11.6	15.8	F	i	11.9	16.4	**0.00**	0.00	67	2
F1	CF₃	k	12.7	16.3	CO₂Et	i	12.2	15.6	**1.11**	0.06	70	4
F2	CN	l	11.6	15.8	CO₂Et	i	12.6	16.1	**0.59**	0.03	62	4
G1	CN	l	11.9	15.8	CF₃	k	12.5	16.1	**0.59**	0.08	64	3

[AC 4079]

Similar to the general procedure, complexes **2x** and **2y** (each 16 μmol) were treated with a solution of ZnPh₂ (45.1 mg, 0.21 mmol), ZnCl₂ (28.2 mg, 0.21 mmol) and LiCl (17.4 mg, 0.41 mmol) in THF (20.0 mL, c[PhZnCl] = 20.5 mM, 0.20 mL, 4.1 μmol). A stock solution of TMB (84.1 mg, 0.50 mmol) in MeOH (50.0 mL, c = 10.0 mM, 0.40 mL, 4.0 μmol) was added for biaryl quantifications by GC-FID.

sample	R¹	**2x**	m [mg]	n [μmol]	R²	**2y**	m [mg]	n [μmol]	**17ax/17ay**	σ	yield 17 [%]	σ [%]
A1	OMe	d	13.0	17.6	H	a	12.5	17.6	**2.47**	0.75	81	2
A2	ᵗBu	e	12.0	15.7	H	a	11.5	16.2	**2.16**	0.60	91	4
A3	Me	f	11.5	15.9	H	a	11.4	16.1	**1.70**	0.07	96	4
A4	CO₂Et	i	12.1	15.5	H	a	11.2	15.8	**0.21**	0.03	80	1
A5	CF₃	k	12.3	15.8	H	a	11.5	16.2	**0.23**	0.03	86	8
A6	CN	l	11.7	15.9	H	a	11.5	16.2	**0.17**	0.03	77	4
B1	ᵗBu	e	12.1	15.8	OMe	d	11.6	15.7	**1.17**	0.05	94	29
B2	Me	f	11.6	16.0	OMe	d	11.6	15.7	**0.74**	0.10	80	10
B3	F	g	11.6	16.0	OMe	d	11.9	16.1	**0.50**	0.14	72	2
B4	CO₂Et	i	12.5	16.0	OMe	d	11.6	15.7	**0.09**	0.02	73	7
B5	CF₃	k	12.6	16.2	OMe	d	12.0	16.2	**0.11**	0.02	75	14
B6	CN	l	11.8	16.1	OMe	d	11.8	16.0	**0.51**	0.19	103	11
C1	Me	f	11.6	16.0	ᵗBu	e	12.3	16.1	**0.70**	0.04	80	3
C2	F	g	11.7	16.1	ᵗBu	e	12.2	15.9	**0.37**	0.08	82	3
C3	CO₂Et	i	12.6	16.1	ᵗBu	e	12.1	15.8	**0.12**	0.02	74	11
C4	CF₃	k	12.4	16.0	ᵗBu	e	12.3	16.1	**0.11**	0.03	71	3

sample	R¹	2x	m [mg]	n [µmol]	R²	2y	m [mg]	n [µmol]	17ax/17ay	σ	yield 17 [%]	σ [%]
C5	CN	l	12.0	16.4	ᵗBu	e	12.3	16.1	**0.07**	0.03	69	22
D1	F	g	11.6	16.0	Me	f	11.7	16.2	**0.47**	0.04	99	3
D2	CO₂Et	i	12.3	15.8	Me	f	11.7	16.2	**0.11**	0.01	71	1
D3	CF₃	k	12.4	16.0	Me	f	11.4	15.8	**0.11**	0.01	77	1
D4	CN	l	11.9	16.2	Me	f	11.7	16.2	**0.09**	0.01	74	1
E1	CO₂Et	i	12.6	16.1	F	g	11.7	16.1	**0.27**	0.03	86	9
E2	CF₃	k	12.6	16.2	F	g	11.8	16.2	**0.27**	0.03	80	5
E3	CN	l	11.7	15.9	F	i	11.6	16.0	**0.17**	0.03	79	1
F1	CF₃	k	12.7	16.3	CO₂Et	i	12.3	15.8	**1.01**	0.38	67	7
F2	CN	l	11.9	16.2	CO₂Et	i	12.6	16.1	**0.62**	0.04	86	25
G1	CN	l	11.9	16.2	CF₃	k	12.2	15.7	**0.81**	0.09	69	5

[AC 4080]

Similar to the general procedure, complexes **2x** and **2y** (each 16 µmol) were treated with a solution of ZnPh₂ (45.1 mg, 0.21 mmol), ZnCl₂ (28.2 mg, 0.21 mmol) and LiCl (17.4 mg, 0.41 mmol) in THF (20.0 mL, c[PhZnCl] = 20.5 mM, 0.20 mL, 4.1 µmol). A stock solution of TMB (84.1 mg, 0.50 mmol) in MeOH (50.0 mL, c = 10.0 mM, 0.40 mL, 4.0 µmol) was added for biaryl quantifications by GC-FID.

sample	R¹	2x	m [mg]	n [µmol]	R²	2y	m [mg]	n [µmol]	σ 17ax/17ay	σ	yield 17 [%]	σ [%]
A1	OMe	d	11.9	16.1	H	a	11.6	16.4	**2.62**	0.04	70	4
A2	ᵗBu	e	12.3	16.1	H	a	11.2	15.8	**2.44**	0.21	80	4
A3	Me	f	12.6	17.4	H	a	11.3	15.9	**1.82**	0.06	83	2
A4	CO₂Et	i	12.2	15.6	H	a	11.4	16.1	**0.20**	0.04	70	1
A5	CF₃	k	12.6	16.2	H	a	11.2	15.8	**0.23**	0.01	79	2
A6	CN	l	11.8	16.1	H	a	11.3	15.9	**0.06**	0.07	64	3
B1	ᵗBu	e	12.0	15.7	OMe	d	11.8	16.0	**1.02**	0.01	68	4
B2	Me	f	11.6	16.0	OMe	d	11.9	16.1	**0.81**	0.02	64	1
B3	F	g	11.5	15.8	OMe	d	11.7	15.8	**0.30**	0.02	67	6
B4	CO₂Et	i	12.5	16.0	OMe	d	11.6	15.7	**0.05**	0.01	64	2
B5	CF₃	k	12.6	16.2	OMe	d	11.9	16.1	**0.08**	0.01	68	3
B6	CN	l	11.7	15.9	OMe	d	11.8	16.0	**0.02**	0.02	62	4
C1	Me	f	11.8	16.3	ᵗBu	e	12.0	15.7	**0.81**	0.02	70	2
C2	F	g	11.6	16.0	ᵗBu	e	12.3	16.1	**0.32**	0.01	69	0
C3	CO₂Et	i	12.6	16.1	ᵗBu	e	12.5	16.3	**0.11**	0.01	73	10
C4	CF₃	k	12.6	16.2	ᵗBu	e	12.3	16.1	**0.06**	0.05	61	2
C5	CN	l	11.6	15.8	ᵗBu	e	12.2	15.9	**0.03**	0.02	66	7
D1	F	g	11.8	16.2	Me	f	11.7	16.2	**0.40**	0.01	77	2
D2	CO₂Et	i	12.2	15.6	Me	f	11.7	16.2	**0.13**	0.03	72	3
D3	CF₃	k	12.6	16.2	Me	f	11.6	16.0	**0.08**	0.11	70	7

D4	CN	l	12.0	16.4	Me	f	11.6	16.0	**0.04**	0.04	68	3
E1	CO_2Et	i	12.2	15.6	F	g	11.7	16.1	**0.22**	0.02	72	1
E2	CF_3	k	12.3	15.8	F	g	11.6	16.0	**0.27**	0.01	76	2
E3	CN	l	11.8	16.1	F	i	12.0	16.5	**0.08**	0.07	64	5
F1	CF_3	k	12.6	16.2	CO_2Et	i	12.4	15.9	**0.94**	0.04	68	1
F2	CN	l	12.0	16.4	CO_2Et	i	12.4	15.9	**0.53**	0.03	60	2
G1	CN	l	11.8	16.4	CF_3	k	12.2	15.7	**0.55**	0.07	59	2

(SZ 3104)

	Wert	Fehler
Intercept	-0.00225	0.00636
Slope	-1.56276	0.01805
Chi-Quadr Reduziert	0.00575	
R-Quadrat	0.97924	

(SZ 3113)

	Wert	Fehler
Intercept	0.00873	0.01136
Slope	-1.19321	0.03295
Chi-Quadr Reduziert	0.01608	
R-Quadrat	0.90479	

(AC 4079)

	Wert	Fehler
Intercept	-0.00578	0.01003
Slope	-1.38184	0.02739
Chi-Quadr Reduziert	0.01208	
R-Quadrat	0.94857	

(AC 4080)

	Wert	Fehler
Intercept	-0.00153	0.00888
Slope	-1.55458	0.02451
Chi-Quadr Reduziert	0.01122	
R-Quadrat	0.9613	

(SZ 3104+3113, AC 4079+4080)

Exp. No.	slope	R^2
SZ 3104	−1.56±0.02	0.979
SZ 3113	−1.19±0.04	0.905
AC 4079	−1.38±0.03	0.949
AC 4080	−1.55±0.03	0.961
total	−1.44±0.02	0.956

4.7.3   Competition in (dppe)Pd(Ar)I with PhZnCl in presence of ligands

[AC 4170]

Similar to the general procedure, complexes **2x** and **2y** (each 16 μmol) and dppe (32 μmol) were dissolved in THF (2.00 mL) and treated with a solution of ZnPh$_2$ (49.4 mg, 0.225 mmol) and ZnCl$_2$ (28.0 mg, 0.21 mmol) in THF (20.0 mL, c[PhZnCl] = 22.5 mM, 0.20 mL, 4.5 μmol). A stock solution of TMB (84.9 mg, 0.51 mmol) in MeOH (50.0 mL, c = 10.1 mM, 0.40 mL, 4.0 μmol) was added for biaryl quantifications by GC-FID.

sample	dppe [mg]	dppe [mmol]	R^1	**2x**	m [mg]	n [μmol]	R^2	**2y**	m [mg]	n [μmol]	**17ax/17ay**	σ	yield **17** [%]	σ [%]
A1	12.8	32.1	OMe	d	11.8	16.0	H	a	11.2	15.8	**3.43**	0.55	28	1
A2	13.1	32.9	^{t}Bu	e	12.1	15.8	H	a	11.5	16.2	**4.48**	1.06	41	10
A3	13.0	32.6	Me	f	11.3	15.6	H	a	11.4	16.1	**1.68**	0.25	28	3
A4	13.1	32.9	CO$_2$Et	i	12.5	16.0	H	a	11.6	16.4	**0.32**	0.09	19	2
A6	13.1	32.9	CN	l	11.5	15.7	H	a	11.5	16.2	**0.40**	0.26	30	12

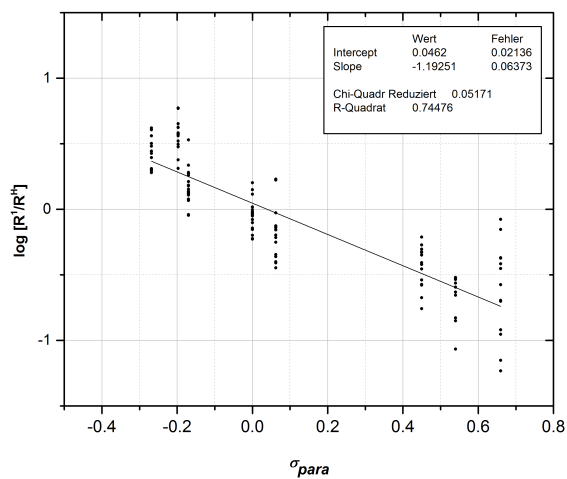| sample	dppe [mg]	dppe [mmol]	R¹	2x	m [mg]	n [μmol]	R²	2y	m [mg]	n [μmol]	17ax/17ay	σ	yield 17 [%]	σ [%]
B1	13.1	32.9	^{t}Bu	e	12.0	15.7	OMe	d	12.1	16.4	**1.40**	0.13	31	4
B2	13.1	32.9	Me	f	11.7	16.2	OMe	d	11.7	15.8	**0.62**	0.08	28	5
B3	12.9	32.4	F	g	11.3	15.5	OMe	d	11.8	16.0	**0.22**	0.01	28	2
B4	12.8	32.1	CO_2Et	i	12.3	15.8	OMe	d	11.6	15.7	**3.76**	2.08	109	49
B5	12.8	32.1	CF_3	k	12.1	15.6	OMe	d	11.8	16.0	**0.00**	0.00	20	1
B6	13.0	32.6	CN	l	11.8	16.1	OMe	d	12.0	16.2	**0.99**	0.24	46	6
C1	13.0	32.6	Me	f	11.8	16.3	^{t}Bu	e	12.4	16.2	**0.44**	0.13	42	8
C2	13.0	32.6	F	g	11.5	15.8	^{t}Bu	e	12.2	15.9	**0.07**	0.06	76	70
C3	13.0	32.6	CO_2Et	i	12.8	16.4	^{t}Bu	e	12.5	16.3	**2.00**	1.36	113	47
C4	13.1	32.9	CF_3	k	12.1	15.6	^{t}Bu	e	12.0	15.7	**0.04**	0.05	20	17
D1	12.9	32.4	F	g	11.4	15.7	Me	f	11.9	16.5	**1.38**	1.90	24	1
D2	12.9	32.4	CO_2Et	i	12.7	16.3	Me	f	11.8	16.3	**0.36**	0.06	26	1
D3	12.8	32.1	CF_3	k	12.7	16.3	Me	f	11.8	16.3	**0.15**	0.13	59	13
D4	12.9	32.4	CN	l	11.3	15.4	Me	f	11.8	16.3	**0.74**	0.81	41	19
E1	13.0	32.6	CO_2Et	i	12.2	15.6	F	g	11.6	16.0	**0.65**	0.18	23	2
E3	13.1	32.9	CN	l	11.6	15.8	F	i	11.6	16.0	**0.21**	0.05	21	1
F1	13.1	32.9	CF_3	k	12.9	16.6	CO_2Et	i	12.6	16.1	**0.39**	0.36	19	6
F2	13.0	32.6	CN	l	11.6	15.8	CO_2Et	i	12.2	15.6	**0.04**	0.07	12	4
G1	13.1	32.9	CN	l	11.7	15.8	CF_3	k	12.2	15.7	**1.78**	1.46	17	15

[AC 4171]

Similar to the general procedure, complexes **2x** and **2y** (each 16 μmol) and dppe (32 μmol) were dissolved in THF (2.00 mL) and treated with a solution of ZnPh₂ (49.4 mg, 0.225 mmol) and ZnCl₂ (28.0 mg, 0.21 mmol) in THF (20.0 mL, c[PhZnCl] = 22.5 mM, 0.20 mL, 4.5 μmol). A stock solution of TMB (84.9 mg, 0.51 mmol) in MeOH (50.0 mL, c = 10.1 mM, 0.40 mL, 4.0 μmol) was added for biaryl quantifications by GC-FID.
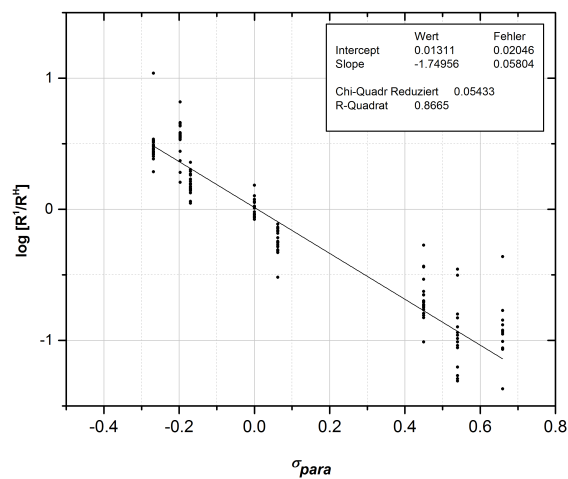
sample	dppe [mg]	dppe [mmol]	R¹	2x	m [mg]	n [μmol]	R²	2y	m [mg]	n [μmol]	17ax/17ay	σ	yield 17 [%]	σ [%]
A1	13.1	32.9	OMe	d	11.7	15.8	H	a	11.4	16.1	**2.86**	0.47	90	4
A2	12.9	36.6	^{t}Bu	e	12.5	16.3	H	a	11.5	16.2	**3.46**	0.67	104	4
A3	13.1	35.1	Me	f	11.3	15.6	H	a	11.6	16.4	**1.47**	0.29	84	8
A4	12.9	32.9	CO_2Et	i	12.1	15.5	H	a	11.5	16.2	**0.30**	0.19	91	11
A6	13.0	32.6	CN	l	11.9	16.2	H	a	11.2	15.8	**0.04**	0.05	84	15
B1	13.0	32.6	^{t}Bu	e	12.1	15.8	OMe	d	11.6	15.7	**1.23**	0.05	94	7
B2	13.0	33.9	Me	f	11.4	15.8	OMe	d	12.0	16.2	**0.51**	0.03	85	5
B3	13.0	34.6	F	g	11.5	15.8	OMe	d	11.7	15.8	**0.22**	0.03	92	6
B4	13.1	33.6	CO_2Et	i	12.6	16.1	OMe	d	12.1	16.4	**0.11**	0.06	94	18
B5	12.0	34.1	CF_3	k	12.9	16.6	OMe	d	11.6	15.7	**0.02**	0.02	103	33
B6	12.9	33.6	CN	l	11.6	15.8	OMe	d	11.9	16.1	**0.56**	0.04	166	16
C1	13.0	32.9	Me	f	11.4	15.8	^{t}Bu	e	12.4	16.2	**0.35**	0.08	99	17
C2	13.0	31.6	F	g	12.0	16.5	^{t}Bu	e	12.5	16.3	**0.16**	0.02	104	5

sample	dppe [mg]	dppe [mmol]	R1	2x	m [mg]	n [µmol]	R2	2y	m [mg]	n [µmol]	17ax/17ay	σ	yield 17 [%]	σ [%]
C3	13.1	34.4	CO$_2$Et	i	12.9	16.5	^{t}Bu	e	12.3	16.1	**0.06**	0.01	136	51
C4	12.9	32.1	CF$_3$	k	12.1	15.6	^{t}Bu	e	12.4	16.2	**0.05**	0.04	116	5
D1	12.8	33.6	F	g	11.5	15.8	Me	f	11.4	15.8	**0.41**	0.06	79	3
D2	13.0	32.6	CO$_2$Et	i	12.5	16.0	Me	f	11.3	15.6	**0.43**	0.24	99	17
D3	12.9	48.2	CF$_3$	k	12.3	15.8	Me	f	11.8	16.3	**0.05**	0.02	125	89
D4	13.1	35.4	CN	l	11.9	16.2	Me	f	11.6	16.0	**0.17**	0.13	89	12
E1	13.2	33.6	CO$_2$Et	i	12.9	16.5	F	g	11.4	15.7	**0.54**	0.30	103	19
E3	13.1	33.6	CN	l	11.6	15.8	F	i	11.4	15.7	**0.23**	0.05	94	2
F1	13.2	36.9	CF$_3$	k	12.1	15.6	CO$_2$Et	i	12.5	16.0	**0.43**	0.38	73	41
F2	12.9	34.9	CN	l	12.0	16.4	CO$_2$Et	i	12.3	15.8	**0.55**	0.02	121	39
G1	13.2	36.4	CN	l	11.5	16.4	CF$_3$	k	12.2	15.7	**1.20**	0.98	121	41

[SZ 4132]

Similar to the general procedure, complexes **2x** and **2y** (each 16 µmol) and dppe (32 µmol) were dissolved in THF (2.00 mL) and treated with a solution, prepared from ZnPh$_2$ (22.4 mg, 0.10 mmol) and a solution of ZnCl$_2$ (2.18 g, 16.0 mmol) in THF (100 mL, c = 0.16 M, 0.63 mL, 0.10 mmol) diluted with THF (10.0 mL, c[PhZnCl] = 20.4 mM, 0.20 mL, 4.1 µmol). A stock solution of TMB (86.0 mg, 0.51 mmol) in THF (25.0 mL, c = 20.5 mM, 0.20 mL, 4.1 µmol) was added for biaryl quantifications by GC-FID.

sample	dppe [mg]	dppe [mmol]	R1	2x	m [mg]	n [µmol]	R2	2y	m [mg]	n [µmol]	17ax/17ay	σ	yield 17 [%]	σ [%]
A1	12.9	32.4	OMe	d	11.2	15.2	H	a	11.1	15.7	**1.60**	0.13	74	3
A2	14.1	35.4	^{t}Bu	e	12.4	16.2	H	a	11.2	15.8	**2.39**	0.25	89	7
A3	12.8	32.1	Me	f	11.4	15.8	H	a	11.6	16.4	**1.77**	0.00	84	0
A4	12.7	31.9	CO$_2$Et	i	12.5	16.0	H	a	11.3	15.9	**0.11**	0.03	75	2
A6	13.5	33.9	CN	l	12.0	16.4	H	a	11.6	16.4	**0.07**	0.01	79	2
B1	13.6	34.1	^{t}Bu	e	12.0	15.7	OMe	d	12.0	16.2	**1.91**	0.00	79	8
B2	14.2	35.6	Me	f	11.8	16.3	OMe	d	11.6	15.7	**1.15**	0.05	72	3
B3	13.6	34.1	F	g	11.3	15.5	OMe	d	11.7	15.8	**0.44**	0.07	81	15
B4	14.1	35.4	CO$_2$Et	i	12.6	16.1	OMe	d	11.6	15.7	**0.08**	0.02	63	6
B5	13.3	33.4	CF$_3$	k	12.5	16.1	OMe	d	11.9	16.1	**0.18**	0.00	72	2

sample	dppe [mg]	dppe [mmol]	R¹	2x	m [mg]	n [µmol]	R²	2y	m [mg]	n [µmol]	17ax/17ay	σ	yield 17 [%]	σ [%]
B6	16.7	41.9	CN	l	12.0	16.4	OMe	d	11.8	16.0	**0.02**	0.03	65	8
C1	13.4	33.6	Me	f	11.5	15.9	^{t}Bu	e	12.6	16.5	**0.59**	0.08	84	16
C2	13.0	32.6	F	g	11.4	15.7	^{t}Bu	e	12.6	16.5	**0.25**	0.02	73	2
C3	16.0	40.2	CO$_2$Et	i	12.3	15.8	^{t}Bu	e	12.4	16.2	**0.10**	0.03	90	9
C4	14.4	36.1	CF$_3$	k	12.3	15.8	^{t}Bu	e	12.3	16.1	**0.32**	0.09	88	10
D1	13.2	33.1	F	g	11.5	15.8	Me	f	11.6	16.0	**0.33**	0.01	86	1
D2	13.6	34.1	CO$_2$Et	i	12.6	16.1	Me	f	11.4	15.8	**0.09**	0.02	77	2
D3	12.9	32.4	CF$_3$	k	12.2	15.7	Me	f	11.6	16.0	**0.23**	0.22	28	5
D4	13.2	33.1	CN	l	11.7	15.9	Me	f	11.4	15.8	**0.03**	0.02	77	2
E1	14.1	35.4	CO$_2$Et	i	12.2	15.6	F	g	11.4	15.7	**0.30**	0.08	72	4
E3	13.2	33.1	CN	l	11.9	16.2	F	i	12.0	16.5	**0.33**	0.04	85	1
F1	16.6	41.7	CF$_3$	k	12.8	16.5	CO$_2$Et	i	12.8	16.4	**1.27**	0.04	43	3
F2	12.8	32.1	CN	l	12.1	16.5	CO$_2$Et	i	12.8	16.4	**0.55**	0.00	60	5
G1	12.8	32.1	CN	l	11.9	16.5	CF$_3$	k	12.8	16.5	**0.55**	0.02	80	0

[SZ 4135]

Similar to the general procedure, complexes **2x** and **2y** (each 16 μmol) and dppe (32 μmol) were dissolved in THF (2.00 mL) and treated with a solution, prepared from ZnPh$_2$ (22.4 mg, 0.10 mmol) and a solution of ZnCl$_2$ (2.18 g, 16.0 mmol) in THF (100 mL, c = 0.16 M, 0.63 mL, 0.10 mmol) diluted with THF (10.0 mL, c[PhZnCl] = 20.4 mM, 0.20 mL, 4.1 μmol). A stock solution of TMB (86.0 mg, 0.51 mmol) in THF (25.0 mL, c = 20.5 mM, 0.20 mL, 4.1 μmol) was added for biaryl quantifications by GC-FID.

sample	dppe [mg]	dppe [mmol]	R¹	2x	m [mg]	n [µmol]	R²	2y	m [mg]	n [µmol]	17ax/17ay	σ	yield 17 [%]	σ [%]
A1	13.1	32.9	OMe	d	11.8	16.0	H	a	12.1	17.1	**2.11**	0.74	96	18
A2	14.6	36.6	^{t}Bu	e	12.5	16.3	H	a	12.5	17.6	**1.54**	0.09	83	3
A3	14.0	35.1	Me	f	11.6	16.0	H	a	11.1	15.7	**1.86**	0.05	108	2
A4	13.1	32.9	CO$_2$Et	i	13.0	16.6	H	a	11.7	16.5	**0.06**	0.05	119	8
A6	13.0	32.6	CN	l	13.0	17.7	H	a	11.5	16.2	**0.03**	0.03	68	3
B1	13.0	32.6	^{t}Bu	e	12.2	15.9	OMe	d	11.5	15.6	**1.02**	0.01	78	9
B2	13.5	33.9	Me	f	12.5	17.3	OMe	d	11.7	15.8	**0.75**	0.07	69	5
B3	13.8	34.6	F	g	12.1	16.6	OMe	d	11.6	15.7	**0.34**	0.03	102	7
B4	13.4	33.6	CO$_2$Et	i	12.7	16.3	OMe	d	11.8	16.0	**0.03**	0.02	88	6
B5	13.6	34.1	CF$_3$	k	12.9	16.6	OMe	d	12.2	16.5	**0.13**	0.04	73	6
B6	13.4	33.6	CN	l	11.9	16.2	OMe	d	11.3	15.3	**0.00**	0.00	99	4
C1	13.1	32.9	Me	f	11.5	15.9	^{t}Bu	e	12.2	15.9	**0.87**	0.06	83	4
C2	12.6	31.6	F	g	11.6	16.0	^{t}Bu	e	12.8	16.7	**0.23**	0.01	90	5
C3	13.7	34.4	CO$_2$Et	i	15.4	19.7	^{t}Bu	e	14.2	18.6	**0.00**	0.00	66	2
C4	12.8	32.1	CF$_3$	k	14.0	18.0	^{t}Bu	e	12.8	16.7	**0.08**	0.01	63	2
D1	13.4	33.6	F	g	11.5	15.8	Me	f	12.6	17.4	**0.37**	0.01	50	0
D2	13.0	32.6	CO$_2$Et	i	14.6	18.7	Me	f	12.7	17.6	**0.10**	0.01	76	1

D3	19.2	48.2	CF$_3$	**k**	13.1	16.9	Me	**f**	11.7	16.2	**0.09**	0.00	90	1
D4	14.1	35.4	CN	**l**	12.6	17.2	Me	**f**	11.2	15.5	**0.06**	0.01	73	0
E1	13.4	33.6	CO$_2$Et	**i**	15.8	20.2	F	**g**	11.7	16.1	**0.31**	0.05	85	2
E3	13.4	33.6	CN	**l**	15.8	21.5	F	**i**	11.9	16.4	**0.14**	0.03	75	1
F1	14.7	36.9	CF$_3$	**k**	14.8	19.1	CO$_2$Et	**i**	14.3	18.3	**0.83**	0.08	72	2
F2	13.9	34.9	CN	**l**	12.2	16.6	CO$_2$Et	**i**	14.1	18.1	**0.44**	0.03	63	15
G1	14.5	36.4	CN	**l**	16.1	16.6	CF$_3$	**k**	12.5	16.1	**0.74**	0.10	68	4

(AC 4170)

	Wert	Fehler
Intercept	0.0462	0.02136
Slope	-1.19251	0.06373
Chi-Quadr Reduziert	0.05171	
R-Quadrat	0.74476	

(AC 4171)

	Wert	Fehler
Intercept	0.01311	0.02046
Slope	-1.74956	0.05804
Chi-Quadr Reduziert	0.05433	
R-Quadrat	0.8665	

(SZ 4132)

	Wert	Fehler
Intercept	0.00117	0.0157
Slope	-1.40951	0.04501
Chi-Quadr Reduziert	0.0332	
R-Quadrat	0.87195	

(SZ 4135)

	Wert	Fehler
Intercept	-0.00111	0.01094
Slope	-1.66744	0.03041
Chi-Quadr Reduziert	0.01603	
R-Quadrat	0.95307	

(SZ 4132+4135, AC 4171)

Exp. No.	slope	R^2
AC 4170	-1.19 ± 0.07	0.745
AC 4171	-1.75 ± 0.06	0.867
SZ 4132	-1.41 ± 0.05	0.872
SZ 4135	-1.67 ± 0.03	0.953
total (AC 4171+SZ 4132+SZ 4135)	-1.62 ± 0.03	0.899

[SZ 4143]

Similar to the general procedure, complexes **2x** and **2y** (each 16 μmol) were treated with a solution of ZnPh$_2$ (22.0 mg, 0.10 mmol), ZnCl$_2$ (14.1 mg, 0.10 mmol) and tmeda (30.0 μL, 0.20 mmol) in THF (10.0 mL, c[PhZnCl] = 20.0 m$_M$, 0.20 mL, 4.0 μmol). A stock solution of TMB (86.0 mg, 0.51 mmol) in THF (25.0 mL, c = 20.5 m$_M$, 0.20 mL, 4.1 μmol) was added for biaryl quantifications by GC-FID.
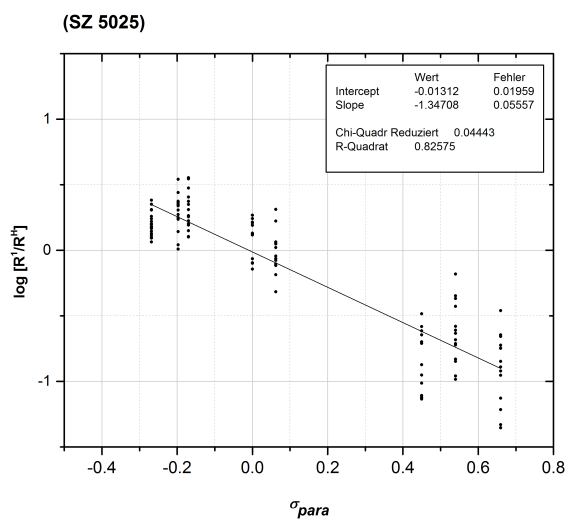
sample	R^1	2x	m [mg]	n [μmol]	R^2	2y	m [mg]	n [μmol]	17ax/17ay	σ	yield 17 [%]	σ [%]
A1	OMe	d	13.3	18.0	H	a	12.5	17.6	**1.50**	0.08	85	3
A2	^{t}Bu	e	12.5	16.3	H	a	11.6	16.4	**1.96**	0.06	96	3
A3	Me	f	12.5	17.3	H	a	11.6	16.4	**1.80**	0.05	70	1
A4	CO$_2$Et	i	13.0	16.6	H	a	11.6	16.4	**0.20**	0.06	60	3
A6	CN	l	12.7	17.3	H	a	12.4	17.5	**0.20**	0.10	61	3
B1	^{t}Bu	e	13.1	17.1	OMe	d	11.7	15.8	**1.33**	0.01	66	3
B2	Me	f	14.4	19.9	OMe	d	12.7	17.2	**0.84**	0.04	72	3
B3	F	g	12.7	17.5	OMe	d	12.0	16.2	**0.55**	0.07	76	7
B4	CO$_2$Et	i	14.1	18.1	OMe	d	12.2	16.5	**0.20**	0.01	70	4

sample	R¹	2x	m [mg]	n [µmol]	R²	2y	m [mg]	n [µmol]	17ax/17ay	σ	yield 17 [%]	σ [%]
B5	CF$_3$	k	15.3	19.7	OMe	d	11.9	16.1	**0.18**	0.01	80	3
B6	CN	l	15.6	21.3	OMe	d	12.4	16.8	**0.11**	0.10	66	7
C1	Me	f	13.8	19.1	^{t}Bu	e	13.1	17.1	**0.67**	0.04	78	4
C2	F	g	14.7	20.2	^{t}Bu	e	15.2	19.9	**0.47**	0.06	84	3
C3	CO$_2$Et	i	15.6	20.0	^{t}Bu	e	13.0	17.0	**0.17**	0.01	72	3
C4	CF$_3$	k	13.4	17.2	^{t}Bu	e	12.4	16.2	**0.19**	0.02	72	3
D1	F	g	12.4	17.1	Me	f	12.2	16.9	**0.44**	0.01	72	1
D2	CO$_2$Et	i	20.4	26.1	Me	f	15.4	21.3	**0.03**	0.05	62	3
D3	CF$_3$	k	14.1	18.2	Me	f	11.4	15.8	**0.21**	0.01	75	1
D4	CN	l	15.9	21.7	Me	f	12.2	16.9	**0.04**	0.04	57	3
E1	CO$_2$Et	i	17.8	22.8	F	g	13.0	17.9	**0.44**	0.01	72	1
E3	CN	l	14.1	19.2	F	i	12.9	17.7	**0.23**	0.05	55	1
F1	CF$_3$	k	18.8	24.2	CO$_2$Et	i	14.8	19.0	**1.38**	0.31	59	7
F2	CN	l	16.6	22.6	CO$_2$Et	i	16.5	21.1	**0.60**	0.10	40	3
G1	CN	l	17.6	22.6	CF$_3$	k	21.6	27.8	**0.44**	0.19	57	8

[SZ 4161]

Similar to the general procedure, complexes **2x** and **2y** (each 16 µmol) were treated with a solution of ZnPh$_2$ (22.0 mg, 0.10 mmol), ZnCl$_2$ (14.1 mg, 0.10 mmol) and tmeda (30.0 µL, 0.20 mmol) in THF (10.0 mL, c[PhZnCl] = 20.0 mM, 0.20 mL, 4.0 µmol). A stock solution of TMB (86.0 mg, 0.51 mmol) in THF (25.0 mL, c = 20.5 mM, 0.20 mL, 4.1 µmol) was added for biaryl quantifications by GC-FID.

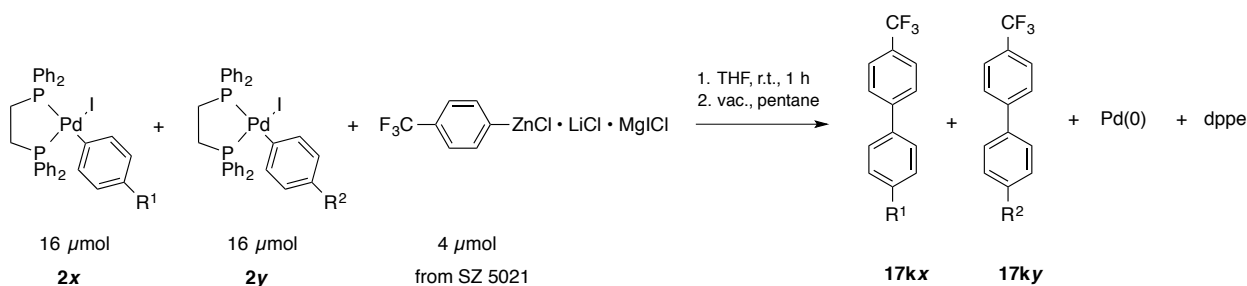| sample	R¹	2x	m [mg]	n [µmol]	R²	2y	m [mg]	n [µmol]	σ 17ax/17ay	σ	yield 17 [%]	σ [%]
A1	OMe	d	13.6	18.4	H	a	12.7	17.9	**1.22**	0.03	133	6
A2	^{t}Bu	e	12.5	16.3	H	a	12.8	18.1	**0.96**	0.15	220	35
A3	Me	f	12.5	17.3	H	a	12.3	17.4	**1.16**	0.02	154	6
A4	CO$_2$Et	i	12.1	15.5	H	a	11.3	15.9	**0.29**	0.00	77	6
A6	CN	l	13.3	18.1	H	a	12.4	17.5	**0.46**	0.02	165	11
B1	^{t}Bu	e	12.8	16.7	OMe	d	13.0	17.6	**1.93**	0.35	131	16
B2	Me	f	12.6	17.4	OMe	d	12.1	16.4	**0.87**	0.07	104	3
B3	F	g	13.7	18.8	OMe	d	13.4	18.1	**0.91**	0.08	142	2
B4	CO$_2$Et	i	14.4	18.4	OMe	d	12.2	16.5	**0.23**	0.02	109	12
B5	CF$_3$	k	14.4	18.5	OMe	d	13.0	17.6	**0.36**	0.20	110	11
B6	CN	l	14.0	19.1	OMe	d	13.2	17.9	**0.05**	0.08	76	22
C1	Me	f	14.7	20.3	^{t}Bu	e	12.6	16.5	**0.77**	0.07	156	17
C2	F	g	14.9	20.5	^{t}Bu	e	14.0	18.3	**0.38**	0.26	139	21
C3	CO$_2$Et	i	14.1	18.1	^{t}Bu	e	12.0	15.7	**0.09**	0.09	97	8
C4	CF$_3$	k	18.2	23.4	^{t}Bu	e	14.7	19.2	**1.91**	0.45	314	64
D1	F	g	11.0	15.1	Me	f	12.6	17.4	**0.40**	0.14	130	20
D2	CO$_2$Et	i	14.3	18.3	Me	f	15.3	21.2	**0.03**	0.05	112	11

287

D3	CF$_3$	**k**	17.8	22.9	Me	**f**	13.9	19.2	**0.12**	0.00	113	3
D4	CN	**l**	31.4	42.8	Me	**f**	12.7	17.6	**0.00**	0.00	79	2
E1	CO$_2$Et	**i**	13.2	16.9	F	**g**	11.0	15.1	**0.16**	0.14	158	9
E3	CN	**l**	20.0	27.3	F	**i**	11.6	16.0	**0.19**	0.18	80	12
F1	CF$_3$	**k**	13.0	16.7	CO$_2$Et	**i**	13.1	16.8	**2.91**	0.14	91	10
F2	CN	**l**	15.3	20.8	CO$_2$Et	**i**	13.2	16.9	**0.66**	0.66	38	16
G1	CN	**l**	12.5	20.8	CF$_3$	**k**	12.0	15.4	**1.06**	0.11	318	111

(SZ 4143)

(SZ 4161)

(SZ 4143+4161)
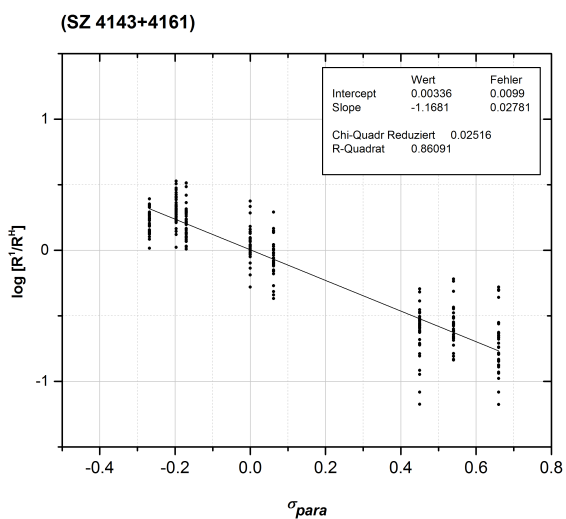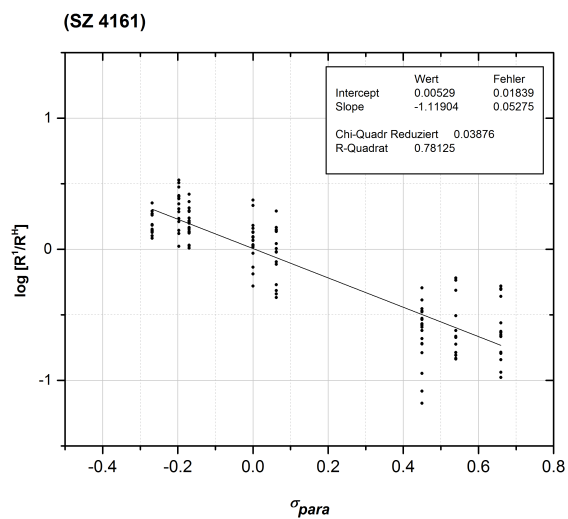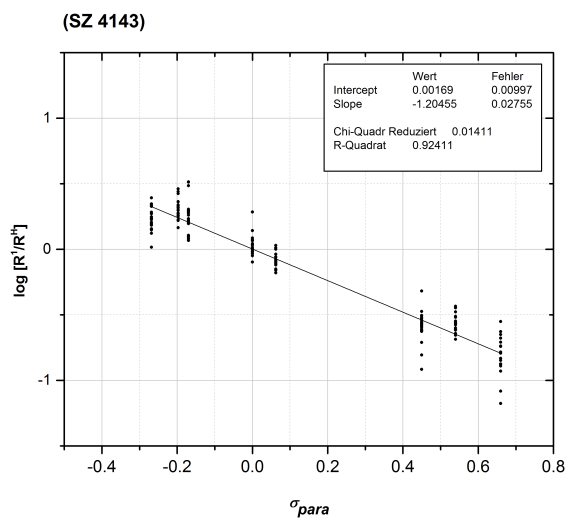
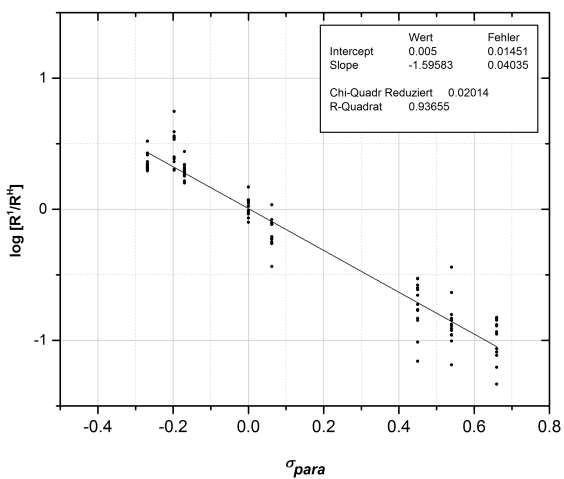| Exp. No.	slope	R^2
SZ 4143	−1.20±0.03	0.924
SZ 4161	−1.12±0.06	0.781
total	−1.16±0.03	0.890

4.7.4 Competition in (dppe)Pd(Ar)I with other arylzinc reagents

[SZ 4136]

According to the general procedure, complexes **2x** and **2y** (each 16 μmol) were treated with a solution of ZnAr$_2$ **15d** (32.5 mg, 0.12 mmol) and ZnCl$_2$ (19.3 mg, 0.14 mmol) in THF (10.0 mL, c[ArZnCl] = 23.2 mM, 0.20 mL, 4.6 μmol). A stock solution of TMB (84.6 mg, 0.50 mmol) in THF (25.0 mL, c = 20.1 mM, 0.20 mL, 4.0 μmol) was added for biaryl quantifications by GC-FID.
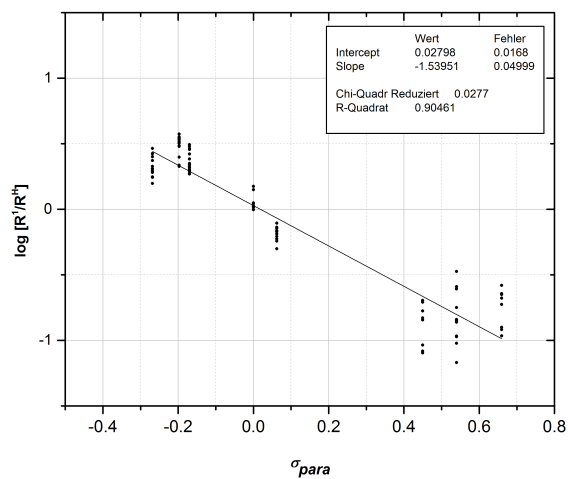
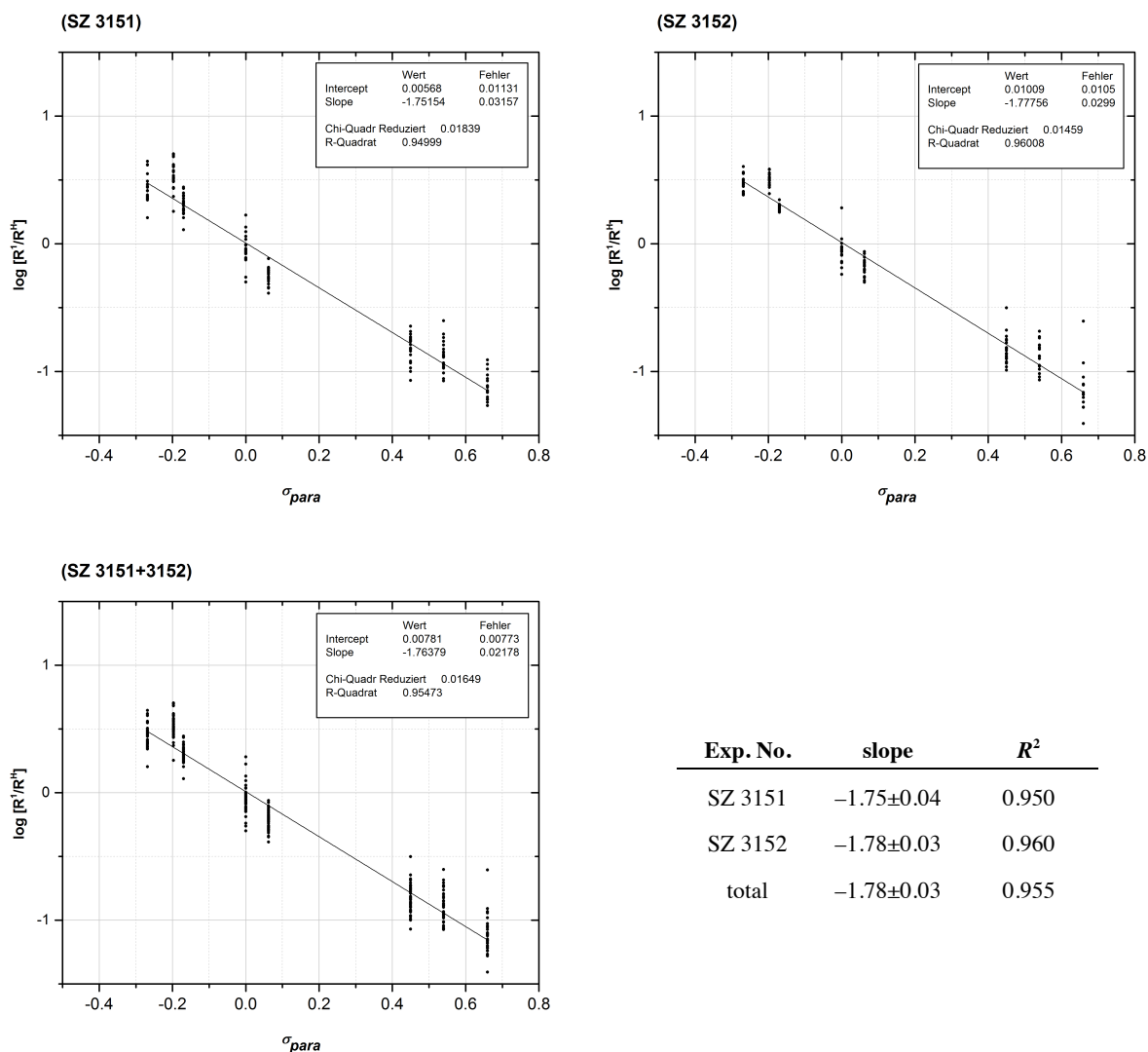| sample	R^1 **2x**		m [mg]	n [μmol]	R^2 **2y**		m [mg]	n [μmol]	**17dx/17dy**	σ	yield 17 [%]	σ [%]
A1	OMe	d	12.5	16.9	H	a	11.8	16.6	**1.15**	0.14	102	13
A2	^{t}Bu	e	13.2	17.3	H	a	12.0	16.9	**2.34**	0.18	62	4
A3	Me	f	11.5	15.9	H	a	11.3	15.9	**1.35**	0.19	59	3
A4	CO$_2$Et	i	15.0	19.2	H	a	11.2	15.8	**0.26**	0.10	69	13
A6	CN	l	11.9	16.2	H	a	11.4	16.1	**0.00**	0.00	54	2
B1	^{t}Bu	e	12.8	16.7	OMe	d	12.7	17.2	**1.00**	0.03	78	7
B2	Me	f	11.8	16.3	OMe	d	12.1	16.4	**0.85**	0.07	62	11
B3	F	g	11.7	16.1	OMe	d	11.8	16.0	**0.36**	0.04	68	15
B4	CO$_2$Et	i	13.2	16.9	OMe	d	12.0	16.2	**0.08**	0.07	64	18
B5	CF$_3$	k	18.0	23.2	OMe	d	13.3	18.0	**0.22**	0.01	75	12
B6	CN	l	16.9	23.0	OMe	d	14.3	19.4	**0.00**	0.00	62	5
C1	Me	f	11.5	15.9	^{t}Bu	e	13.4	17.5	**0.48**	0.06	59	5
C2	F	g	11.4	15.7	^{t}Bu	e	14.0	18.3	**0.25**	0.02	59	4
C3	CO$_2$Et	i	13.9	17.8	^{t}Bu	e	13.3	17.4	**0.05**	0.05	61	11
C4	CF$_3$	k	12.9	16.6	^{t}Bu	e	13.0	17.0	**0.08**	0.01	81	24
D1	F	g	11.8	16.2	Me	f	12.0	16.6	**0.53**	0.01	56	8
D2	CO$_2$Et	i	17.7	22.7	Me	f	12.3	17.0	**0.22**	0.01	63	1
D3	CF$_3$	k	17.7	22.8	Me	f	14.3	19.8	**0.17**	0.01	56	3
D4	CN	l	14.3	19.5	Me	f	11.2	15.5	**0.05**	0.09	54	16
E1	CO$_2$Et	i	16.3	20.9	F	g	12.3	16.9	**0.19**	0.16	52	8
E3	CN	l	12.5	17.0	F	i	11.1	15.3	**0.18**	0.03	53	1
F1	CF$_3$	k	13.2	17.0	CO$_2$Et	i	14.5	18.6	**0.92**	0.09	47	2

F2	CN	l	13.3	18.1	CO$_2$Et	i	14.2	18.2	**0.52**	0.06	44	6
G1	CN	l	16.6	18.1	CF$_3$	k	14.4	18.5	**0.81**	0.33	53	14

[SZ 4137]

According to the general procedure, complexes **2x** and **2y** (each 16 μmol) were treated with a solution of ZnAr$_2$ **15d** (32.5 mg, 0.12 mmol) and ZnCl$_2$ (19.3 mg, 0.14 mmol) in THF (10.0 mL, c[ArZnCl] = 23.2 mM, 0.20 mL, 4.6 μmol). A stock solution of TMB (84.6 mg, 0.50 mmol) in THF (25.0 mL, c = 20.1 mM, 0.20 mL, 4.0 μmol) was added for biaryl quantifications by GC-FID.

sample	R^1	**2x**	m [mg]	n [μmol]	R^2	**2y**	m [mg]	n [μmol]	**17dx/17dy**	σ	yield **17** [%]	σ [%]
A1	OMe	d	11.9	16.1	H	a	11.4	16.1	**1.40**	0.01	112	6
A2	^{t}Bu	e	12.8	16.7	H	a	11.6	16.4	**2.22**	0.28	82	13
A3	Me	f	11.6	16.0	H	a	12.3	17.4	**1.24**	0.03	73	8
A4	CO$_2$Et	i	15.9	20.4	H	a	11.7	16.5	**0.23**	0.01	77	13
A6	CN	l	12.1	16.5	H	a	11.4	16.1	**0.18**	0.03	72	8
B1	^{t}Bu	e	14.7	19.2	OMe	d	12.2	16.5	**1.25**	0.07	94	15
B2	Me	f	11.7	16.2	OMe	d	11.8	16.0	**0.73**	0.01	76	4
B3	F	g	11.5	15.8	OMe	d	12.9	17.5	**0.39**	0.04	76	27
B4	CO$_2$Et	i	12.9	16.5	OMe	d	12.4	16.8	**0.16**	0.01	87	13
B5	CF$_3$	k	13.3	17.1	OMe	d	12.8	17.3	**0.15**	0.01	81	5
B6	CN	l	12.2	16.6	OMe	d	11.9	16.1	**0.17**	0.01	93	15
C1	Me	f	11.9	16.5	^{t}Bu	e	12.4	16.2	**0.64**	0.03	71	11
C2	F	g	11.6	16.0	^{t}Bu	e	12.5	16.3	**0.34**	0.02	64	2
C3	CO$_2$Et	i	13.1	16.8	^{t}Bu	e	12.4	16.2	**0.12**	0.02	73	13
C4	CF$_3$	k	13.2	17.0	^{t}Bu	e	13.0	17.0	**0.10**	0.00	50	4
D1	F	g	11.5	15.8	Me	f	11.7	16.2	**0.48**	0.01	80	15
D2	CO$_2$Et	i	15.0	19.2	Me	f	12.0	16.6	**0.17**	0.01	30	2
D3	CF$_3$	k	13.0	16.7	Me	f	12.6	17.4	**0.14**	0.01	60	7
D4	CN	l	17.3	23.6	Me	f	12.0	16.6	**0.19**	0.03	72	14
E1	CO$_2$Et	i	14.6	18.7	F	g	11.8	16.2	**0.33**	0.08	65	5
E3	CN	l	12.1	16.5	F	i	12.7	17.5	**0.18**	0.02	60	1
F1	CF$_3$	k	12.6	16.2	CO$_2$Et	i	14.5	18.6	**0.80**	0.04	63	6
F2	CN	l	11.8	16.1	CO$_2$Et	i	14.0	17.9	**0.61**	0.02	82	16
G1	CN	l	12.2	16.1	CF$_3$	k	13.2	17.0	**0.81**	0.07	61	2

(SZ 4136)

	Wert	Fehler
Intercept	1.61336E-4	0.01049
Slope	-1.34149	0.02997
Chi-Quadr Reduziert	0.01443	
R-Quadrat	0.93382	

(SZ 4137)

	Wert	Fehler
Intercept	0.00283	0.00774
Slope	-1.20203	0.02114
Chi-Quadr Reduziert	0.0088	
R-Quadrat	0.95172	

(SZ 4136+4137)

	Wert	Fehler
Intercept	0.00192	0.00656
Slope	-1.26393	0.0183
Chi-Quadr Reduziert	0.01198	
R-Quadrat	0.93936	
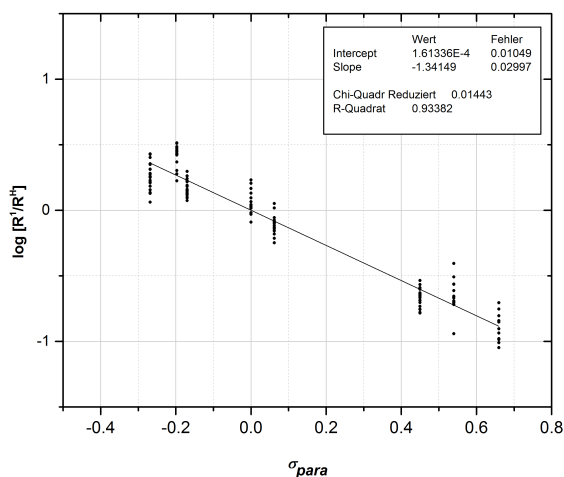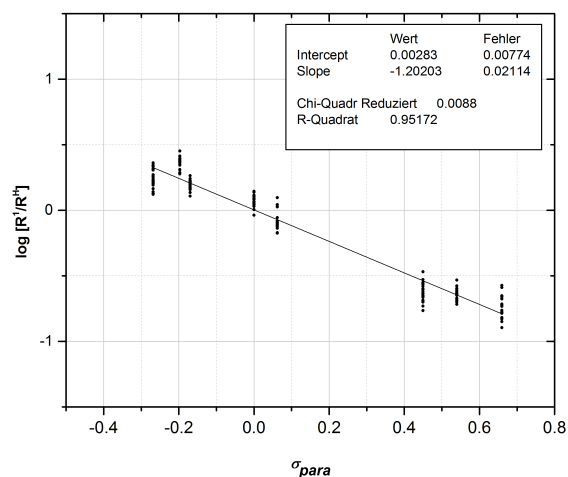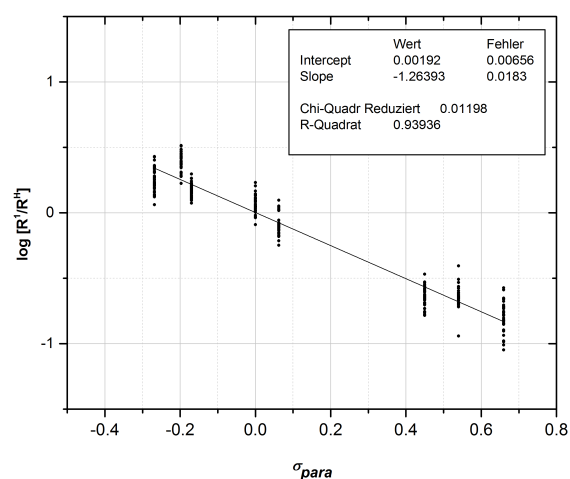
Exp. No.	slope	R^2
SZ 4136	-1.34 ± 0.03	0.934
SZ 4137	-1.20 ± 0.03	0.952
total	-1.26 ± 0.02	0.939

[SZ 5025]

According to the general procedure, complexes **2x** and **2y** (each 16 μmol) were treated with a solution of PhZnCl·LiCl·MgICl (SZ 5022, c = 20 mM, 4.0 μmol) in THF. A stock solution of TMB (84.6 mg, 0.50 mmol) in THF (25.0 mL, c = 20.1 mM, 0.20 mL, 4.0 μmol) was added for biaryl quantifications by GC-FID.

291

sample	R¹	2x	m [mg]	n [μmol]	R²	2y	m [mg]	n [μmol]	17ax/17ay	σ	yield 17 [%]	σ [%]
A1	OMe	d	12.1	16.4	H	a	12.1	17.1	**0.82**	0.06	50	3
A2	ᵗBu	e	12.3	16.1	H	a	11.8	16.6	**0.66**	0.15	84	7
A3	Me	f	11.7	16.2	H	a	11.4	16.1	**1.20**	0.05	43	3
A4	CO₂Et	i	12.6	16.1	H	a	11.4	16.1	**0.16**	0.02	62	3
A6	CN	l	12.0	16.4	H	a	11.3	15.9	**0.29**	0.05	88	3
B1	ᵗBu	e	12.4	16.2	OMe	d	11.7	15.8	**1.53**	0.02	29	5
B2	Me	f	12.5	17.3	OMe	d	12.3	16.6	**1.09**	–	43	–
B3	F	g	11.9	16.4	OMe	d	12.3	16.6	**0.66**	0.13	32	6
B4	CO₂Et	i	18.7	23.9	OMe	d	11.9	16.1	**0.12**	0.06	26	5
B5	CF₃	k	14.1	18.2	OMe	d	11.9	16.1	**0.15**	0.01	27	4
B6	CN	l	14.0	19.1	OMe	d	13.7	18.5	**0.12**	0.02	19	17
C1	Me	f	11.8	16.3	ᵗBu	e	12.1	15.8	**0.72**	0.02	34	3
C2	F	g	11.7	16.1	ᵗBu	e	12.2	15.9	**0.42**	0.08	39	6
C3	CO₂Et	i	13.8	17.7	ᵗBu	e	11.9	15.6	**0.03**	0.03	35	6
C4	CF₃	k	12.7	16.3	ᵗBu	e	12.1	15.8	**0.50**	0.45	38	2
D1	F	g	13.4	18.4	Me	f	13.1	18.1	**0.53**	0.03	36	1
D2	CO₂Et	i	12.7	16.3	Me	f	12.5	17.3	**0.00**	0.00	29	2
D3	CF₃	k	12.9	16.6	Me	f	11.6	16.0	**0.08**	0.01	31	2
D4	CN	l	12.6	17.2	Me	f	12.3	17.0	**0.01**	0.02	29	1
E1	CO₂Et	i	12.5	16.0	F	g	12.0	16.5	**0.04**	0.04	18	0
E3	CN	l	12.2	16.6	F	i	11.8	16.2	**0.18**	0.08	37	7
F1	CF₃	k	12.7	16.3	CO₂Et	i	12.9	16.5	**4.47**	1.29	16	1
F2	CN	l	12.8	17.4	CO₂Et	i	13.6	17.4	**0.29**	0.28	6	1
G1	CN	l	12.5	17.4	CF₃	k	13.7	17.6	**0.38**	0.20	37	5

[SZ 5026]

According to the general procedure, complexes **2x** and **2y** (each 16 μmol) were treated with a solution of PhZnCl·LiCl·MgICl (SZ 5022, c = 20 mM, 4.0 μmol) in THF. A stock solution of TMB (84.6 mg, 0.50 mmol) in THF (25.0 mL, c = 20.1 mM, 0.20 mL, 4.0 μmol) was added for biaryl quantifications by GC-FID.

sample	R¹	2x	m [mg]	n [μmol]	R²	2y	m [mg]	n [μmol]	17ax/17ay	σ	yield 17 [%]	σ [%]
A1	OMe	d	12.4	16.8	H	a	11.6	16.4	**0.78**	0.13	52	3
A2	ᵗBu	e	12.7	16.6	H	a	12.2	17.2	**0.63**	0.24	94	6
A3	Me	f	11.6	16.0	H	a	11.7	16.5	**1.10**	0.06	43	1
A4	CO₂Et	i	12.7	16.3	H	a	12.4	17.5	**0.17**	0.01	63	1
A6	CN	l	11.9	16.2	H	a	11.5	16.2	**0.30**	0.07	76	4

B1	ᵗBu	e	12.7	16.6	OMe	d	12.1	16.4	**1.82**	0.12	30	3
B2	Me	f	12.2	16.9	OMe	d	12.2	16.5	**1.96**	0.20	28	1
B3	F	g	12.4	17.1	OMe	d	12.7	17.2	**0.87**	0.24	27	0
B4	CO$_2$Et	i	13.9	17.8	OMe	d	12.7	17.2	**0.14**	0.07	23	2
B5	CF$_3$	k	12.8	16.5	OMe	d	11.9	16.1	**0.46**	0.18	39	4
B6	CN	l	12.3	16.8	OMe	d	11.8	16.0	**0.04**	0.06	22	4
C1	Me	f	12.7	17.6	ᵗBu	e	12.3	16.1	**0.79**	0.06	33	2
C2	F	g	11.9	16.4	ᵗBu	e	12.3	16.1	**0.36**	0.01	35	0
C3	CO$_2$Et	i	12.7	16.3	ᵗBu	e	12.7	16.6	**0.05**	–	42	–
C4	CF$_3$	k	12.7	16.3	ᵗBu	e	12.4	16.2	**0.06**	–	45	–
D1	F	g	11.8	16.2	Me	f	12.4	17.2	**0.41**	0.09	33	2
D2	CO$_2$Et	i	12.9	16.5	Me	f	12.2	16.9	**0.00**	0.00	30	1
D3	CF$_3$	k	12.6	16.2	Me	f	12.3	17.0	**0.10**	0.03	30	2
D4	CN	l	14.4	19.6	Me	f	12.2	16.9	**0.01**	0.02	29	2
E1	CO$_2$Et	i	13.6	17.4	F	g	12.5	17.2	**0.00**	0.00	20	1
E3	CN	l	12.6	17.2	F	i	11.4	15.7	**0.18**	0.17	30	7
F1	CF$_3$	k	13.4	17.2	CO$_2$Et	i	12.3	15.8	**2.16**	0.20	86	14
F2	CN	l	14.2	19.3	CO$_2$Et	i	15.3	19.6	**8.71**	14.7	6	1
G1	CN	l	12.0	19.3	CF$_3$	k	12.4	16.0	**0.89**	0.30	37	5

(SZ 5025)

	Wert	Fehler
Intercept	-0.01312	0.01959
Slope	-1.34708	0.05557
Chi-Quadr Reduziert	0.04443	
R-Quadrat	0.82575	

(SZ 5026)

	Wert	Fehler
Intercept	-0.00362	0.01993
Slope	-1.24515	0.05717
Chi-Quadr Reduziert	0.04533	
R-Quadrat	0.79541	

(SZ 5025+5026)

	Wert	Fehler
Intercept	-0.00841	0.01398
Slope	-1.29715	0.03987
Chi-Quadr Reduziert	0.04491	
R-Quadrat	0.81021	
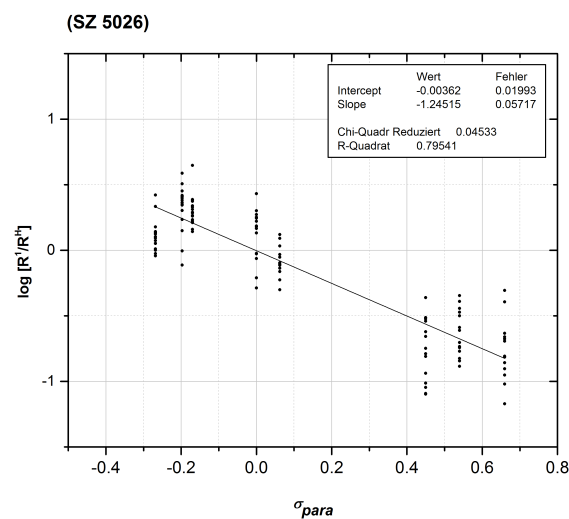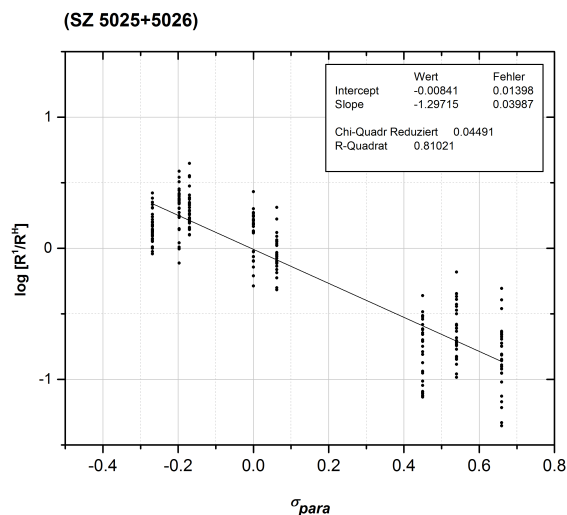
Exp. No.	slope	R^2
SZ 5025	−1.35±0.06	0.826
SZ 5026	−1.25±0.06	0.795
total	−1.30±0.04	0.810

16 μmol	16 μmol	4 μmol
2x	**2y**	from SZ 5021

17kx	**17ky**

[SZ 5023]

According to the general procedure, complexes **2x** and **2y** (each 16 μmol) were treated with a solution of ArZnCl·LiCl·MgICl (from SZ 5021, c = 20 mM, 4.0 μmol) in THF. A stock solution of TMB (84.6 mg, 0.50 mmol) in THF (25.0 mL, c = 20.1 mM, 0.20 mL, 4.0 μmol) was added for biaryl quantifications by GC-FID.

sample	R^1	**2x**	m [mg]	n [μmol]	R^2	**2y**	m [mg]	n [μmol]	17kx/17ky	σ	yield 17 [%]	σ [%]
A1	OMe	d	12.3	16.6	H	a	13.1	18.5	**2.08**	0.20	39	1
A2	^{t}Bu	e	12.8	16.7	H	a	11.8	16.6	**2.34**	1.66	52	17
A3	Me	f	12.0	16.6	H	a	12.9	18.2	**1.62**	0.07	37	1
A4	CO$_2$Et	i	12.7	16.3	H	a	11.7	16.5	**0.18**	–	23	1
A6	CN	l	12.6	17.2	H	a	12.4	17.5	**0.84**	0.34	70	24
B1	^{t}Bu	e	14.1	18.4	OMe	d	12.0	16.2	**1.16**	0.08	38	5
B2	Me	f	11.7	16.2	OMe	d	12.0	16.2	**0.95**	0.01	32	2
B3	F	g	12.0	16.5	OMe	d	11.7	15.8	**0.13**	0.23	40	7
B4	CO$_2$Et	i	13.8	17.7	OMe	d	13.1	17.7	**0.00**	0.00	30	4

| sample	R^1	2x	m [mg]	n [μmol]	R^2	2y	m [mg]	n [μmol]	17kx/17ky	σ	yield 17 [%]	σ [%]
B5	CF$_3$	k	12.6	16.2	OMe	d	12.3	16.6	**0.92**	0.10	139	12
B6	CN	l	17.8	24.3	OMe	d	11.9	16.1	**0.07**	0.06	27	5
C1	Me	f	11.6	16.0	^{t}Bu	e	12.6	16.5	**0.58**	0.04	44	3
C2	F	g	11.4	15.7	^{t}Bu	e	12.3	16.1	**0.38**	0.49	48	15
C3	CO$_2$Et	i	12.9	16.5	^{t}Bu	e	12.4	16.2	**0.00**	0.00	38	2
C4	CF$_3$	k	13.6	17.5	^{t}Bu	e	12.5	16.3	**0.19**	0.24	44	9
D1	F	g	11.9	16.4	Me	f	12.1	16.7	**0.30**	0.01	41	2
D2	CO$_2$Et	i	14.3	18.3	Me	f	12.5	17.3	**0.00**	0.00	31	2
D3	CF$_3$	k	12.5	16.1	Me	f	12.1	16.7	**0.04**	0.04	31	1
D4	CN	l	12.0	16.4	Me	f	12.0	16.6	**0.00**	0.00	35	0
E1	CO$_2$Et	i	13.9	17.8	F	g	12.5	17.2	**0.30**	0.20	34	3
E3	CN	l	14.4	19.6	F	i	11.6	16.0	**0.44**	0.25	32	7
F1	CF$_3$	k	12.6	16.2	CO$_2$Et	i	12.4	15.9	**0.68**	0.11	19	2
F2	CN	l	15.0	20.4	CO$_2$Et	i	13.4	17.2	**0.60**	0.07	13	1
G1	CN	l	11.9	20.4	CF$_3$	k	14.1	18.2	**0.70**	0.17	62	1

[SZ 5024]

According to the general procedure, complexes **2x** and **2y** (each 16 μmol) were treated with a solution of ArZnCl·LiCl·MgICl (from SZ 5021, c = 20 mM, 4.0 μmol) in THF. A stock solution of TMB (84.6 mg, 0.50 mmol) in THF (25.0 mL, c = 20.1 mM, 0.20 mL, 4.0 μmol) was added for biaryl quantifications by GC-FID.

sample	R^1	2x	m [mg]	n [μmol]	R^2	2y	m [mg]	n [μmol]	17kx/17ky	σ	yield 17 [%]	σ [%]
A1	OMe	d	11.7	15.8	H	a	11.4	16.1	**1.22**	0.05	24	0
A2	^{t}Bu	e	12.7	16.6	H	a	11.6	16.4	**3.16**	0.09	23	2
A3	Me	f	11.8	16.3	H	a	11.6	16.4	**1.92**	0.05	24	0
A4	CO$_2$Et	i	13.0	16.6	H	a	11.3	15.9	**0.03**	0.05	20	1
A6	CN	l	12.0	16.4	H	a	11.6	16.4	**0.27**	0.23	22	4
B1	^{t}Bu	e	12.8	16.7	OMe	d	11.7	15.8	**1.27**	0.09	18	2
B2	Me	f	11.6	16.0	OMe	d	11.7	15.8	**1.10**	0.03	20	0
B3	F	g	12.4	17.1	OMe	d	12.5	16.9	**0.34**	0.01	18	1
B4	CO$_2$Et	i	14.1	18.1	OMe	d	11.6	15.7	**0.03**	0.05	16	2
B5	CF$_3$	k	13.2	17.0	OMe	d	12.2	16.5	**0.09**	0.01	19	1
B6	CN	l	14.3	19.5	OMe	d	13.3	18.0	**0.08**	0.07	19	2
C1	Me	f	11.8	16.3	^{t}Bu	e	12.2	15.9	**0.62**	0.03	23	1
C2	F	g	12.5	17.2	^{t}Bu	e	12.1	15.8	**0.25**	0.00	17	0
C3	CO$_2$Et	i	17.7	22.7	^{t}Bu	e	17.4	22.7	**0.00**	0.00	20	0
C4	CF$_3$	k	12.6	16.2	^{t}Bu	e	12.6	16.5	**0.33**	0.01	27	1
D1	F	g	11.6	16.0	Me	f	12.5	17.3	**0.25**	0.02	19	0
D2	CO$_2$Et	i	14.0	17.9	Me	f	13.1	18.1	**0.00**	0.00	19	1

D3	CF$_3$	k	12.4	16.0	Me	f	11.9	16.5	**0.05**	0.00	19	0
D4	CN	l	13.4	18.3	Me	f	12.3	17.0	**0.00**	0.00	18	0
E1	CO$_2$Et	i	13.6	17.4	F	g	12.5	17.2	**0.04**	0.07	8	1
E3	CN	l	14.4	19.6	F	i	12.3	16.9	**0.00**	0.00	7	0
F1	CF$_3$	k	12.6	16.2	CO$_2$Et	i	12.1	15.5	**0.87**	0.11	8	1
F2	CN	l	13.4	18.3	CO$_2$Et	i	14.0	17.9	**0.17**	0.30	5	2
G1	CN	l	11.6	18.3	CF$_3$	k	13.3	17.1	**0.77**	0.04	18	0

(SZ 5023)

	Wert	Fehler
Intercept	0.005	0.01451
Slope	-1.59583	0.04035
Chi-Quadr Reduziert	0.02014	
R-Quadrat	0.93655	

(SZ 5024)

	Wert	Fehler
Intercept	0.02798	0.0168
Slope	-1.53951	0.04999
Chi-Quadr Reduziert	0.0277	
R-Quadrat	0.90461	

(SZ 5023+5024)

	Wert	Fehler
Intercept	0.01578	0.01108
Slope	-1.57269	0.03179
Chi-Quadr Reduziert	0.02387	
R-Quadrat	0.92167	
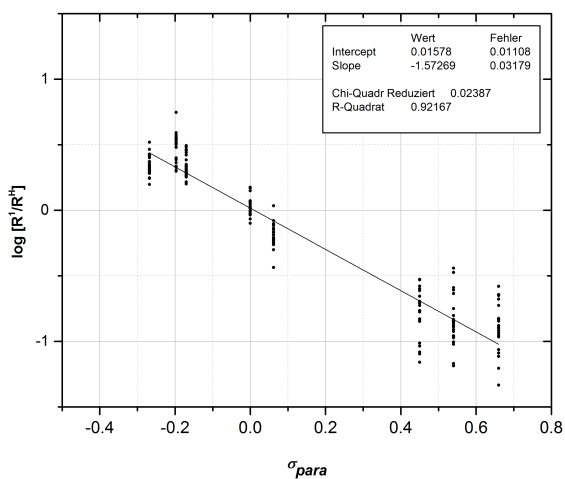
Exp. No.	slope	R^2
SZ 5023	-1.60 ± 0.04	0.937
SZ 5024	-1.53 ± 0.05	0.905
total	-1.57 ± 0.04	0.922

[SZ 3151]

Similar to the general procedure, complexes **2x** and **2y** (each 16 μmol) were treated with a solution of ZnPh$_2$ (**15a**, 44.2 mg, 0.20 mmol) in THF (20.0 mL, c[Ph$_2$Zn] = 10.1 mM, 0.20 mL, 4.0 μmol). A stock solution of TMB (86.4 mg, 0.51 mmol) in MeOH (50.0 mL, c = 20.5 mM, 0.40 mL, 4.1 μmol) was added for biaryl quantifications by GC-FID.

| sample	R^1 **2x**	m [mg]	n [μmol]	R^2 **2y**	m [mg]	n [μmol]	σ **17ax/17ay**		yield **17** [%]	σ [%]
A1	OMe **d**	11.8	16.0	H **a**	11.5	16.2	**2.40**	0.63	82	16
A2	^{t}Bu **e**	12.2	15.9	H **a**	11.5	16.2	**2.95**	1.06	132	3
A3	Me **f**	11.7	16.2	H **a**	11.4	16.1	**2.03**	0.21	121	12
A4	CO$_2$Et **i**	12.7	16.3	H **a**	11.6	16.4	**0.20**	0.05	111	3
A5	CF$_3$ **k**	12.7	16.3	H **a**	11.6	16.4	**0.25**	0.04	132	36
A6	CN **l**	11.9	16.2	H **a**	11.6	16.4	**0.10**	0.03	107	9
B1	^{t}Bu **e**	12.5	16.3	OMe **d**	11.5	15.6	**1.39**	0.03	94	5
B2	Me **f**	11.4	15.8	OMe **d**	11.6	15.7	**0.75**	0.06	88	1
B3	F **g**	11.9	16.4	OMe **d**	11.8	16.0	**0.22**	0.08	76	8
B4	CO$_2$Et **i**	12.4	15.9	OMe **d**	11.7	15.8	**0.05**	0.02	87	3
B5	CF$_3$ **k**	12.6	16.2	OMe **d**	11.6	15.7	**0.04**	0.03	88	4
B6	CN **l**	11.5	15.7	OMe **d**	11.9	16.1	**0.00**	0.00	80	2
C1	Me **f**	11.3	15.6	^{t}Bu **e**	12.6	16.5	**0.64**	0.06	113	1
C2	F **g**	12.0	16.5	^{t}Bu **e**	12.3	16.1	**0.16**	0.01	97	1
C3	CO$_2$Et **i**	12.6	16.1	^{t}Bu **e**	12.3	16.1	**0.04**	0.04	118	9
C4	CF$_3$ **k**	12.7	16.3	^{t}Bu **e**	12.0	15.7	**0.02**	0.02	129	6
C5	CN **l**	11.4	15.5	^{t}Bu **e**	12.3	16.1	**0.01**	0.02	120	7
D1	F **g**	11.3	15.5	Me **f**	11.7	16.2	**0.35**	0.03	88	5
D2	CO$_2$Et **i**	12.9	16.5	Me **f**	12.0	16.6	**0.08**	0.03	49	1
D3	CF$_3$ **k**	12.5	16.1	Me **f**	11.2	15.5	**0.07**	0.01	104	7
D4	CN **l**	12.0	16.4	Me **f**	12.1	16.7	**0.03**	0.03	88	6
E1	CO$_2$Et **i**	12.6	16.1	F **g**	11.8	16.2	**0.22**	0.19	92	9
E2	CF$_3$ **k**	12.6	16.2	F **g**	11.4	15.7	**0.28**	0.03	91	7
E3	CN **l**	11.4	15.5	F **i**	11.7	16.1	**0.14**	0.03	87	6
F1	CF$_3$ **k**	12.8	16.5	CO$_2$Et **i**	12.5	16.0	**0.81**	0.03	95	1

F2	CN	**l**	11.6	15.8	CO₂Et	**i**	12.7	16.3	**0.51**	0.01	101	11
G1	CN	**l**	12.0	15.8	CF₃	**k**	12.2	15.7	**0.56**	0.08	88	1

[SZ 3152]

Similar to the general procedure, complexes **2x** and **2y** (each 16 μmol) were treated with a solution of ZnPh$_2$ (**15a**, 44.2 mg, 0.20 mmol) in THF (20.0 mL, c[Ph$_2$Zn] = 10.1 mM, 0.20 mL, 4.0 μmol). A stock solution of TMB (86.4 mg, 0.51 mmol) in MeOH (50.0 mL, c = 20.5 mM, 0.40 mL, 4.1 μmol) was added for biaryl quantifications by GC-FID.

sample	R^1	**2x**	m [mg]	n [μmol]	R^2	**2y**	m [mg]	n [μmol]	**17ax/17ay**	σ	yield 17 [%]	σ [%]
A1	OMe	**d**	12.1	16.4	H	**a**	11.8	16.6	**2.81**	0.35	98	6
A2	^{t}Bu	**e**	12.1	15.8	H	**a**	11.6	16.4	**3.41**	0.47	135	3
A3	Me	**f**	12.0	16.6	H	**a**	11.6	16.4	**2.08**	0.09	119	4
A4	CO₂Et	**i**	12.0	15.4	H	**a**	11.2	15.8	**0.18**	0.05	112	6
A5	CF₃	**k**	12.3	15.8	H	**a**	11.5	16.2	**0.23**	0.02	112	12
A6	CN	**l**	11.9	16.2	H	**a**	11.8	16.6	**0.02**	0.03	104	7
B1	^{t}Bu	**e**	11.9	15.6	OMe	**d**	12.1	16.4	**1.09**	0.03	97	2
B2	Me	**f**	11.8	16.3	OMe	**d**	11.6	15.7	**0.67**	0.02	86	4
B3	F	**g**	11.7	16.1	OMe	**d**	12.0	16.2	**0.26**	0.03	83	3
B4	CO₂Et	**i**	12.0	15.4	OMe	**d**	11.8	16.0	**0.04**	0.01	89	3
B5	CF₃	**k**	13.0	16.7	OMe	**d**	12.0	16.2	**0.01**	0.02	84	7
B6	CN	**l**	11.7	15.9	OMe	**d**	12.0	16.2	**0.01**	0.01	85	3
C1	Me	**f**	11.9	16.5	^{t}Bu	**e**	12.2	15.9	**0.68**	0.02	105	4
C2	F	**g**	11.9	16.4	^{t}Bu	**e**	12.5	16.3	**0.24**	0.04	99	5
C3	CO₂Et	**i**	12.7	16.3	^{t}Bu	**e**	12.3	16.1	**0.03**	0.03	105	15
C4	CF₃	**k**	12.3	15.8	^{t}Bu	**e**	12.4	16.2	**0.03**	0.02	140	9
C5	CN	**l**	11.9	16.2	^{t}Bu	**e**	12.1	15.8	**0.04**	0.05	125	9
D1	F	**g**	11.2	15.4	Me	**f**	11.3	15.6	**0.36**	0.01	86	3
D2	CO₂Et	**i**	12.9	16.5	Me	**f**	11.2	15.5	**0.09**	0.02	100	5
D3	CF₃	**k**	12.4	16.0	Me	**f**	11.9	16.5	**0.03**	0.05	100	7
D4	CN	**l**	12.0	16.4	Me	**f**	11.7	16.2	**0.00**	0.00	89	4
E1	CO₂Et	**i**	13.0	16.6	F	**g**	11.7	16.1	**0.24**	0.04	91	2
E2	CF₃	**k**	12.7	16.3	F	**g**	11.5	15.8	**0.27**	0.01	92	8
E3	CN	**l**	11.6	15.8	F	**i**	11.3	15.5	**0.04**	0.07	89	11
F1	CF₃	**k**	12.2	15.7	CO₂Et	**i**	12.9	16.5	**0.65**	0.05	102	4
F2	CN	**l**	12.1	16.5	CO₂Et	**i**	12.6	16.1	**0.56**	0.08	96	9
G1	CN	**l**	11.9	16.5	CF₃	**k**	12.8	16.5	**0.54**	0.04	86	4

(SZ 3151)

	Wert	Fehler
Intercept	0.00568	0.01131
Slope	-1.75154	0.03157
Chi-Quadr Reduziert	0.01839	
R-Quadrat	0.94999	

(SZ 3152)

	Wert	Fehler
Intercept	0.01009	0.0105
Slope	-1.77756	0.0299
Chi-Quadr Reduziert	0.01459	
R-Quadrat	0.96008	

(SZ 3151+3152)

	Wert	Fehler
Intercept	0.00781	0.00773
Slope	-1.76379	0.02178
Chi-Quadr Reduziert	0.01649	
R-Quadrat	0.95473	

Exp. No.	slope	R^2
SZ 3151	-1.75 ± 0.04	0.950
SZ 3152	-1.78 ± 0.03	0.960
total	-1.78 ± 0.03	0.955

4.7.5   Competition in ArZnCl with (dppe)Pd(Ar)I

Competition experiments were carried out with arylzinc chloride solutions in THF prepared from iodoarenes and ^{i}PrMgCl·LiCl (*cf.* chapter 4.4). The concentrations were determined by GC-FID. The volumes and corresponding amounts of each arylzinc species, added to the transmetalation samples, are listed below.

Exp. No.	*p*-R	*c* [M]	V [mL]	n [μmol]
SZ 5029	OMe	0.17 ± 0.01	0.23	39
SZ 5028	Me	0.18 ± 0.01	0.21	38
SZ 5022	H	0.13 ± 0.01	0.27	41
SZ 5021	CO_2Et	0.23 ± 0.01	0.18	41
SZ 5019	CF_3	0.25 ± 0.26	0.16	37

299

General procedure:

Inside the glovebox, oven-dried reaction vials were charged with arylzinc chloride solutions (40 μmol each) and diluted with THF to 0.50 mL. A stock solution of (dppe)Pd(Ar)I **2** (0.10 mmol) in THF (5.00 mL, c = 20.0 mM, 0.20 mL, 4.0 μmol) was added to each reaction vial under vigorous stirring. Outside the glovebox, the reactions were quenched with a stock solution of TMB (169 mg, 1.00 mmol) in MeOH (25.0 mL, c = 40.0 mM, 0.10 mL, 4.0 μmol) and concentrated in vacuum. The residue were extracted with pentane (1.00 mL) and the pentane solutions transferred into GC vials for biaryl quantifications.
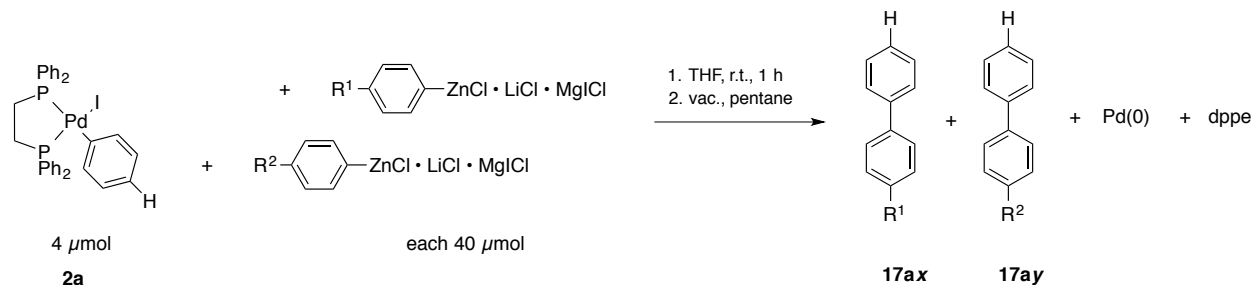
[SZ 5033+5034]

According to the general procedure using (dppe)Pd(Ph)I **2a** (71.0 mg, 0.10 mmol).

sample	R^1	R^2	**17ax/17ay** 1st run	σ	**17ax/17ay** 2nd run	σ
A1	OMe	OMe	**1.08**	0.01	**1.00**	0.10
A2	Me	OMe	**0.73**	0.09	**0.65**	0.07
A3	H	OMe	**0.30**	0.01	**0.11**	0.02
A4	CO$_2$Et	OMe	**0.73**	0.05	**0.46**	0.08
B1	CF$_3$	Me	**0.49**	0.01	**0.52**	0.01
B2	H	Me	**0.10**	0.01	**0.12**	0.02
B3	CO$_2$Et	Me	**0.61**	0.02	**0.47**	0.02
C1	CO$_2$Et	H	**0.32**	0.03	**0.48**	0.18
D1	CF$_3$	CO$_2$Et	**3.33**	0.17	**0.99**	0.22

(SZ 5033 + 5034)

	Wert	Fehler
Intercept	-0.06033	0.01294
Slope	-1.13443	0.04756
Chi-Quadr Reduziert	0.01859	
R-Quadrat	0.83992	
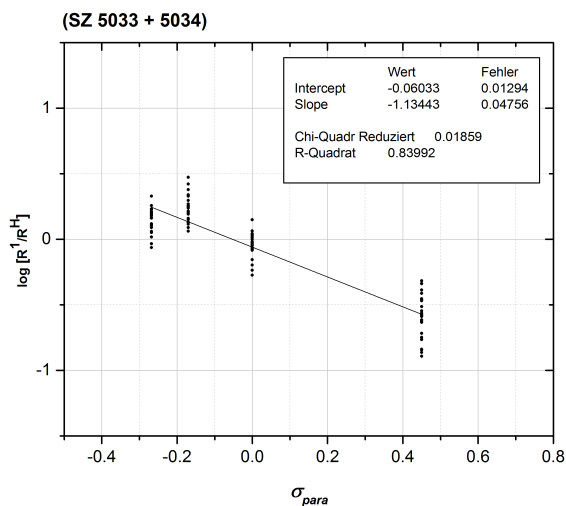
Exp. No.	slope	R^2
SZ 5033+5034	-1.13 ± 0.05	0.840
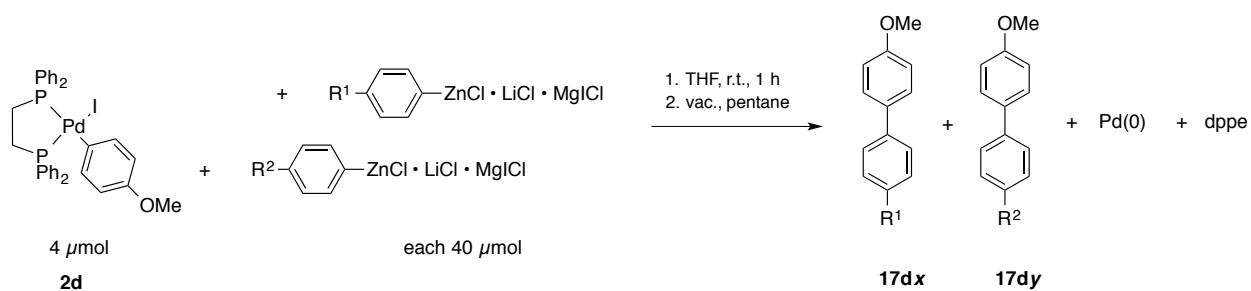
[SZ 5035+5036]

According to the general procedure using $(dppe)Pd(p\text{-}MeOC_6H_4)I$ **2d** (72.2 mg, 0.10 mmol).

sample	R^1	R^2	17dx/17dy 1st run	σ	17dx/17dy 2nd run	σ
A1	OMe	OMe	**1.69**	0.40	**1.84**	0.32
A2	Me	OMe	**1.29**	0.35	**2.13**	0.49
A3	H	OMe	**0.37**	0.11	**0.50**	0.10
A4	CO_2Et	OMe	**0.86**	0.18	**0.77**	0.20
B1	CF_3	Me	**0.49**	0.11	**0.47**	0.12
B2	H	Me	**0.11**	0.03	**0.11**	0.03
B3	CO_2Et	Me	**0.06**	0.00	**0.08**	0.02
C1	CO_2Et	H	**0.22**	0.15	**0.24**	0.09
D1	CF_3	CO_2Et	**0.98**	0.32	**0.82**	0.29

301

(SZ 5035 + 5036)

	Wert	Fehler
Intercept	0.18654	0.02368
Slope	-1.49868	0.06709
Chi-Quadr Reduziert	0.04204	
R-Quadrat	0.83029	
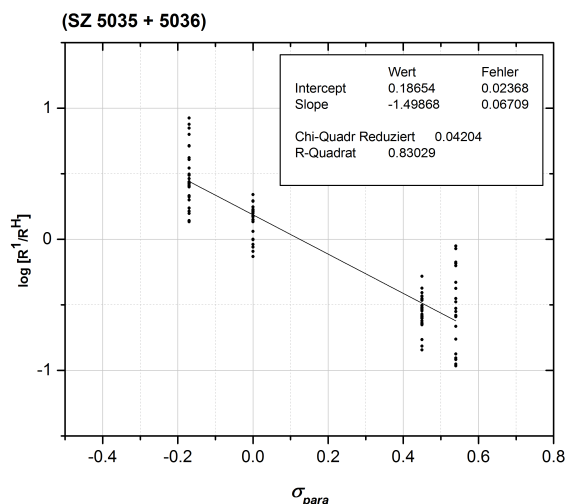
Exp. No.	slope	R^2
SZ 5035+5036	−1.50±0.07	0.830

4.7.6 Competition in (dppf)Pd(Ar)X with ArZnCl

16 μmol	16 μmol	4 μmol		17ax	17ay
3x	3y	from 15a			

1. THF, r.t., 1 h
2. vac., pentane

[SZ 4164]

According to the general procedure, complexes 3x and 3y (each 16 μmol) were treated with a solution of ZnPh$_2$ (22.5 mg, 0.10 mmol) and ZnCl$_2$ (14.4 mg, 0.11 mmol) in THF (10.0 mL, c[PhZnCl] = 20.6 mM, 0.20 mL, 4.1 μmol). A stock solution of TMB (83.9 mg, 0.50 mmol) in THF (25.0 mL, c = 20.0 mM, 0.20 mL, 4.0 μmol) was added for biaryl quantifications by GC-FID.

sample	R^1 3x		m [mg]	n [μmol]	R^2 3y		m [mg]	n [μmol]	17ax/17ay	σ	yield 17 [%]	σ [%]
A1	OMe	d	14.1	15.8	H	a	14.4	16.7	**0.47**	0.09	66	3
A2	ᵗBu	e	14.6	15.9	H	a	15.2	17.6	**0.49**	0.04	88	1
A3	Me	f	14.8	16.8	H	a	14.0	16.2	**0.89**	0.03	70	1
A4	CO$_2$Et	i	15.4	16.4	H	a	13.8	16.0	**0.40**	0.05	72	5
A5	CF$_3$	k	14.8	16.6	H	a	14.4	16.7	**0.08**	0.02	64	3
A6	CN	l	15.9	17.3	H	a	15.6	17.4	**1.48**	0.09	41	4

sample	R¹		m [mg]	n [µmol]	R²		m [mg]	n [µmol]	17a*x*/17a*y*	σ	yield 17 [%]	σ [%]
B1	ᵗBu	e	15.6	17.8	OMe	d	14.2	15.9	**1.75**	0.23	42	3
B2	Me	f	14.4	16.3	OMe	d	14.2	15.9	**0.75**	0.13	40	4
B3	F	g	15.0	16.0	OMe	d	15.0	16.8	**1.06**	0.06	37	6
B4	CO₂Et	i	15.4	16.5	OMe	d	15.2	17.0	**1.50**	0.22	47	2
B5	CF₃	k	15.5	17.4	OMe	d	14.1	15.8	**0.23**	0.02	28	4
B6	CN	l	14.7	16.7	OMe	d	15.5	16.8	**1.38**	0.13	68	4
C1	Me	f	15.8	17.9	ᵗBu	e	14.8	16.1	**0.94**	0.04	62	2
C2	F	g	14.9	15.9	ᵗBu	e	14.3	15.5	**0.45**	0.01	47	1
C3	CO₂Et	i	15.2	16.3	ᵗBu	e	15.1	16.4	**0.54**	0.06	59	3
C4	CF₃	k	15.4	17.4	ᵗBu	e	14.3	16.3	**0.12**	0.00	50	5
C5	CN	l	15.1	16.1	ᵗBu	e	14.1	16.0	**0.58**	0.00	27	0
D1	F	g	16.1	17.3	Me	f	15.8	18.0	**0.48**	0.01	59	0
D2	CO₂Et	i	14.0	15.7	Me	f	14.4	16.4	**0.00**	0.00	52	1
D3	CF₃	k	15.2	16.2	Me	f	15.7	17.8	**0.60**	0.18	18	2
D4	CN	l	14.1	15.8	Me	f	13.8	15.6	**0.30**	0.04	25	1
E1	CO₂Et	i	14.8	15.9	F	g	15.1	16.1	**0.84**	0.29	45	8
E2	CF₃	k	14.7	16.5	F	g	15.6	16.7	**0.19**	0.02	27	5
E3	CN	l	14.5	16.5	F	i	15.2	16.3	**0.34**	0.01	44	0
F1	CF₃	k	14.1	15.8	CO₂Et	i	14.4	16.7	**0.47**	0.09	66	3
F2	CN	l	14.6	15.9	CO₂Et	i	15.2	17.6	**0.49**	0.04	88	1
G1	CN	l	14.8	16.8	CF₃	k	14.0	16.2	**0.89**	0.03	70	1

[SZ 5009]

According to the general procedure, complexes **3x** and **3y** (each 16 μmol) were treated with a solution of ZnPh₂ (22.3 mg, 0.10 mmol) and ZnCl₂ (14.9 mg, 0.11 mmol) in THF (10.0 mL, c[PhZnCl] = 20.4 mM, 0.20 mL, 4.1 μmol). A stock solution of TMB (171 mg, 1.01 mmol) in THF (50.0 mL, c = 20.3 mM, 0.20 mL, 4.1 μmol) was added for biaryl quantifications by GC-FID.

sample	R¹	3x	m [mg]	n [µmol]	R²	3y	m [mg]	n [µmol]	17a*x*/17a*y*	σ	yield 17 [%]	σ [%]
A1	OMe	d	13.9	15.5	H	a	14.2	16.4	**0.52**	0.09	58	1
A2	ᵗBu	e	16.3	17.7	H	a	13.6	15.7	**0.77**	0.09	72	0
A3	Me	f	14.0	15.9	H	a	13.7	15.8	**1.20**	0.20	60	6
A4	CO₂Et	i	16.6	17.7	H	a	13.7	15.8	**0.40**	0.02	68	1
A5	CF₃	k	15.8	17.8	H	a	14.8	17.1	**0.13**	0.03	65	1
A6	CN	l	14.4	15.6	H	a	14.4	16.1	**1.25**	0.12	47	3
B1	ᵗBu	e	14.1	16.0	OMe	d	15.1	16.9	**1.12**	0.07	48	2
B2	Me	f	14.1	16.0	OMe	d	14.7	16.4	**0.17**	0.02	33	3
B3	F	g	15.6	16.7	OMe	d	15.9	17.8	**0.69**	0.13	28	3
B4	CO₂Et	i	14.6	15.7	OMe	d	14.5	16.2	**0.62**	0.13	36	2
B5	CF₃	k	14.3	16.1	OMe	d	14.3	16.0	**0.19**	0.03	36	4

B6	CN	l	13.8	15.7	OMe	d	15.0	16.3	**1.04**	0.09	59	2
C1	Me	f	14.4	16.3	^{t}Bu	e	15.0	16.3	**0.40**	0.12	51	1
C2	F	g	15.1	16.1	^{t}Bu	e	14.6	15.9	**0.48**	0.07	44	5
C3	CO$_2$Et	i	15.0	16.1	^{t}Bu	e	15.0	16.3	**0.63**	0.28	70	19
C4	CF$_3$	k	13.5	15.3	^{t}Bu	e	13.3	15.1	**0.20**	0.01	51	2
C5	CN	l	15.2	16.2	^{t}Bu	e	13.4	15.2	**0.64**	0.08	54	2
D1	F	g	15.3	16.4	Me	f	14.3	16.3	**0.43**	0.01	49	4
D2	CO$_2$Et	i	14.4	16.2	Me	f	14.5	16.5	**0.14**	0.01	37	2
D3	CF$_3$	k	15.1	16.1	Me	f	13.6	15.4	**0.90**	0.14	22	2
D4	CN	l	14.4	16.2	Me	f	15.7	17.8	**0.38**	0.04	24	2
E1	CO$_2$Et	i	15.6	16.7	F	g	15.7	16.8	**0.66**	0.15	48	2
E2	CF$_3$	k	14.4	16.2	F	g	15.9	17.0	**0.20**	0.01	24	2
E3	CN	l	14.4	16.2	F	i	17.0	18.2	**0.34**	0.08	46	3
F1	CF$_3$	k	13.9	15.5	CO$_2$Et	i	14.2	16.4	**0.52**	0.09	58	1
F2	CN	l	16.3	17.7	CO$_2$Et	i	13.6	15.7	**0.77**	0.09	72	0
G1	CN	l	14.0	15.9	CF$_3$	k	13.7	15.8	**1.20**	0.20	60	6
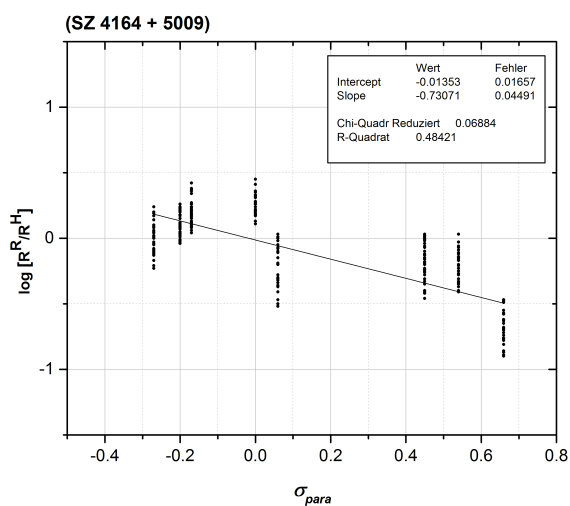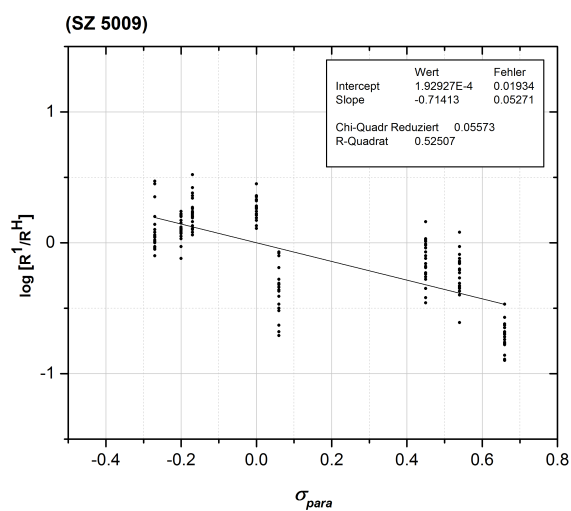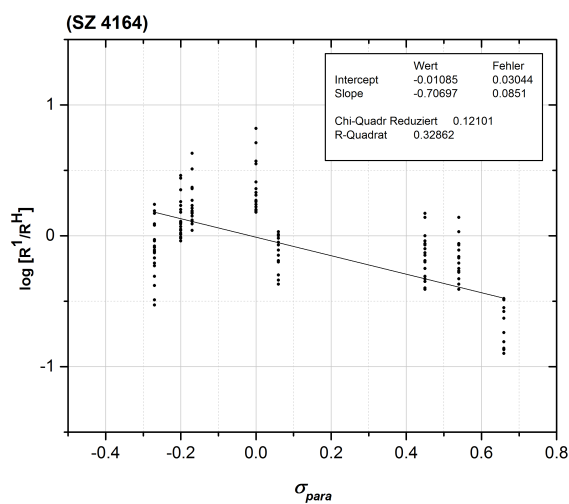
Exp. No.	slope	R^2
SZ 4164	-0.71 ± 0.09	0.329
SZ 5009	-0.71 ± 0.06	0.525
total	-0.73 ± 0.05	0.484
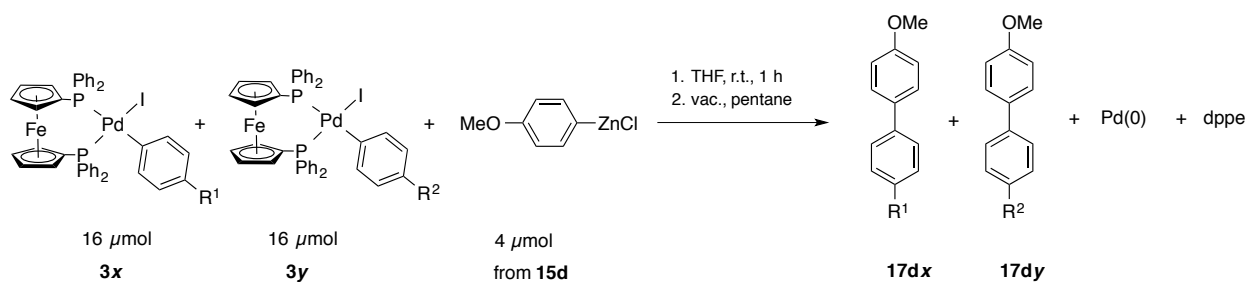
[SZ 5008]

According to the general procedure, complexes **3x** and **3y** (each 16 μmol) were treated with a solution of ZnAr$_2$ **15d** (28.3 mg, 0.10 mmol) and ZnCl$_2$ (13.8 mg, 0.10 mmol) in THF (10.0 mL, c[ArZnCl] = 20.2 mM, 0.20 mL, 4.0 μmol). A stock solution of TMB (85.2 mg, 0.51 mmol) in THF (25.0 mL, c = 20.3 mM, 0.20 mL, 4.1 μmol) was added for biaryl quantifications by GC-FID.

sample	R^1	3x	m [mg]	n [μmol]	R^2	3y	m [mg]	n [μmol]	17dx/17dy	σ	yield 17 [%]	σ [%]
A1	OMe	d	14.1	15.8	H	a	14.1	15.8	0.62	0.10	36	1
A2	^{t}Bu	e	16.2	17.6	H	a	16.2	17.6	0.74	0.03	39	2
A3	Me	f	14.0	15.9	H	a	14.0	15.9	0.71	0.01	43	4
A4	CO$_2$Et	i	14.9	15.9	H	a	14.9	15.9	0.29	0.01	32	4
A5	CF$_3$	k	14.6	16.4	H	a	14.6	16.4	0.00	0.00	34	0
A6	CN	l	14.9	16.2	H	a	14.9	16.2	1.16	0.03	25	2
B1	^{t}Bu	e	14.0	15.9	OMe	d	14.0	15.9	1.10	0.01	27	2
B2	Me	f	15.0	17.0	OMe	d	15.0	17.0	0.26	0.22	22	2
B3	F	g	14.7	15.7	OMe	d	14.7	15.7	0.57	0.04	19	5
B4	CO$_2$Et	i	15.8	16.9	OMe	d	15.8	16.9	0.94	0.19	28	4
B5	CF$_3$	k	14.2	16.0	OMe	d	14.2	16.0	0.00	0.00	20	1
B6	CN	l	14.3	16.3	OMe	d	14.3	16.3	1.03	0.07	33	5
C1	Me	f	15.1	17.1	^{t}Bu	e	15.1	17.1	0.52	0.08	23	1
C2	F	g	15.3	16.3	^{t}Bu	e	15.3	16.3	0.00	0.00	15	2
C3	CO$_2$Et	i	17.4	18.7	^{t}Bu	e	17.4	18.7	0.58	0.03	33	1
C4	CF$_3$	k	14.9	16.9	^{t}Bu	e	14.9	16.9	0.00	0.00	27	1
C5	CN	l	15.9	17.0	^{t}Bu	e	15.9	17.0	0.50	0.09	28	4
D1	F	g	14.9	16.0	Me	f	14.9	16.0	0.63	0.02	34	3
D2	CO$_2$Et	i	14.1	15.8	Me	f	14.1	15.8	0.00	0.00	27	2
D3	CF$_3$	k	15.6	16.7	Me	f	15.6	16.7	–	–	2	3
D4	CN	l	14.7	16.5	Me	f	14.7	16.5	–	–	0	0
E1	CO$_2$Et	i	14.8	15.9	F	g	14.8	15.9	1.20	0.48	21	7
E2	CF$_3$	k	14.6	16.4	F	g	14.6	16.4	0.00	0.00	8	1
E3	CN	l	14.5	16.4	F	i	14.5	16.4	0.00	0.00	20	3
F1	CF$_3$	k	14.1	15.8	CO$_2$Et	i	14.1	15.8	0.62	0.10	36	1

F2	CN	**l**	16.2	17.6	CO$_2$Et	**i**	16.2	17.6	**0.74**	0.03	39	2
G1	CN	**l**	14.0	15.9	CF$_3$	**k**	14.0	15.9	**0.71**	0.01	43	4
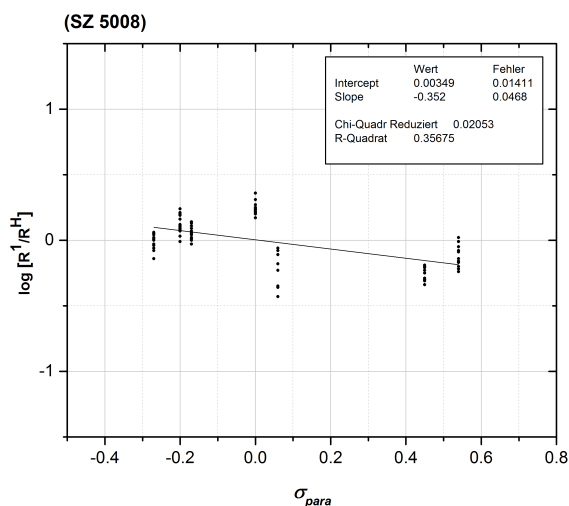
Exp. No.	slope	R^2
SZ 5008	−0.35±0.05	0.357

16 μmol	16 μmol	4 μmol
7x	**7y**	from **15a**
	17ax	**17ay**
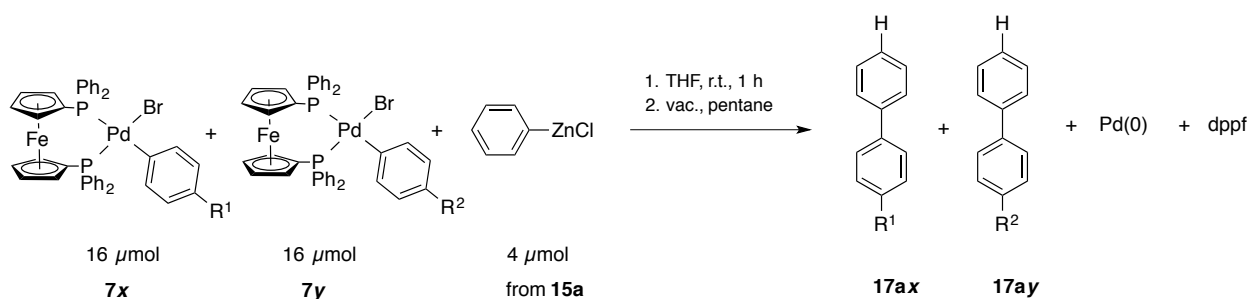
[SZ 4165]

According to the general procedure, complexes **7x** and **7y** (each 16 μmol) were treated with a solution of ZnPh$_2$ (22.5 mg, 0.10 mmol) and ZnCl$_2$ (14.4 mg, 0.11 mmol) in THF (10.0 mL, c[PhZnCl] = 20.6 mM, 0.20 mL, 4.1 μmol). A stock solution of TMB (83.9 mg, 0.50 mmol) in THF (25.0 mL, c = 20.0 mM, 0.20 mL, 4.0 μmol) was added for biaryl quantifications by GC-FID.

sample	R^1	**7x**	m [mg]	n [μmol]	R^2	**7y**	m [mg]	n [μmol]	**17ax/17ay**	σ	yield 17 [%]	σ [%]
A1	OMe	**d**	13.8	16.3	H	**a**	13.8	16.3	**0.59**	0.03	61	1
A2	^{t}Bu	**e**	14.8	16.9	H	**a**	14.8	16.9	**0.46**	0.02	55	3
A3	Me	**f**	14.2	17.1	H	**a**	14.2	17.1	**1.04**	0.11	36	1
A4	CO$_2$Et	**i**	14.9	16.7	H	**a**	14.9	16.7	**0.15**	0.03	71	5
A5	CF$_3$	**k**	13.4	15.9	H	**a**	13.4	15.9	**0.19**	0.02	64	2
A6	CN	**l**	15.0	17.2	H	**a**	15.0	17.2	**0.96**	0.09	35	8

B1	^tBu	**e**	13.2	15.9	OMe	**d**	13.2	15.9	**1.68**	0.07	27	1
B2	Me	**f**	13.9	16.6	OMe	**d**	13.9	16.6	**0.63**	0.05	56	3
B3	F	**g**	15.7	17.6	OMe	**d**	15.7	17.6	**0.33**	0.00	46	3
B4	CO_2Et	**i**	15.7	17.7	OMe	**d**	15.7	17.7	**1.14**	0.08	59	2
B5	CF_3	**k**	14.1	16.7	OMe	**d**	14.1	16.7	**0.60**	0.02	46	2
B6	CN	**l**	14.7	17.7	OMe	**d**	14.7	17.7	**2.16**	0.13	42	1
C1	Me	**f**	15.0	17.9	^tBu	**e**	15.0	17.9	**1.36**	0.22	42	0
C2	F	**g**	14.5	16.3	^tBu	**e**	14.5	16.3	**0.49**	0.05	35	3
C3	CO_2Et	**i**	15.1	17.0	^tBu	**e**	15.1	17.0	**1.91**	0.14	51	1
C4	CF_3	**k**	13.6	16.3	^tBu	**e**	13.6	16.3	**0.29**	0.01	66	1
C5	CN	**l**	14.9	16.7	^tBu	**e**	14.9	16.7	**0.24**	0.02	66	2
D1	F	**g**	14.5	16.4	Me	**f**	14.5	16.4	**0.00**	0.00	51	0
D2	CO_2Et	**i**	13.9	16.5	Me	**f**	13.9	16.5	**0.00**	0.00	50	0
D3	CF_3	**k**	15.6	17.5	Me	**f**	15.6	17.5	**0.36**	0.00	52	9
D4	CN	**l**	14.1	16.7	Me	**f**	14.1	16.7	**0.45**	0.08	58	1
E1	CO_2Et	**i**	14.9	16.8	F	**g**	14.9	16.8	**1.58**	0.00	26	7
E2	CF_3	**k**	14.7	17.4	F	**g**	14.7	17.4	**1.51**	0.46	52	10
E3	CN	**l**	13.8	17.4	F	**i**	13.8	17.4	**0.46**	0.05	52	3
F1	CF_3	**k**	13.8	16.3	CO_2Et	**i**	13.8	16.3	**0.59**	0.03	61	1
F2	CN	**l**	14.8	16.9	CO_2Et	**i**	14.8	16.9	**0.46**	0.02	55	3
G1	CN	**l**	14.2	17.1	CF_3	**k**	14.2	17.1	**1.04**	0.11	36	1
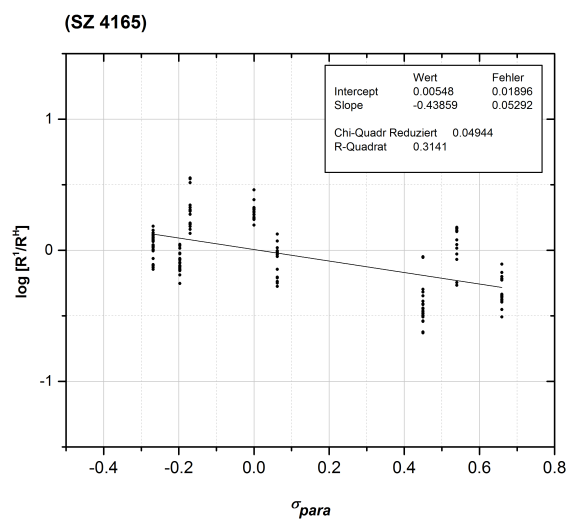
(SZ 4165)

Exp. No.	slope	R^2
SZ 4165	-0.44 ± 0.06	0.314

4.7.7 Competition in (PPh₃)₂Pd(Ar)I with *p*-MeOPhZnCl
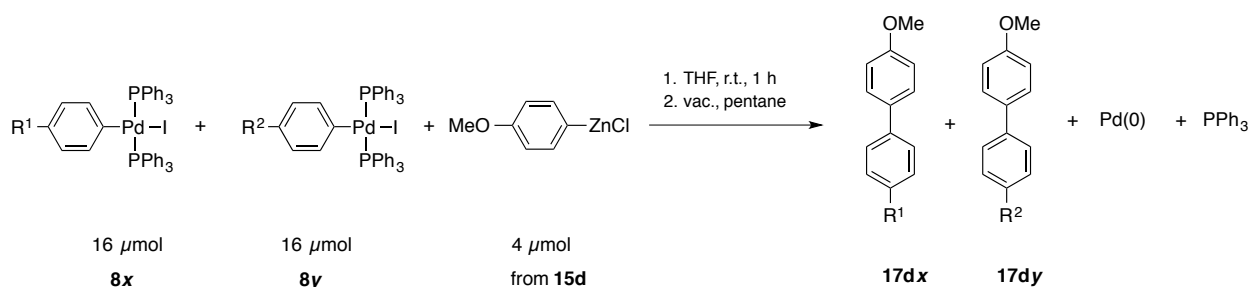
[5006]

According to the general procedure, complexes **8x** and **8y** (each 16 μmol) were treated with a solution of ZnAr₂ **15d** (28.2 mg, 0.10 mmol) and ZnCl₂ (15.7 mg, 0.12 mmol) in THF (10.0 mL, c[ArZnCl] = 20.2 mM, 0.20 mL, 4.0 μmol). A stock solution of TMB (83.9 mg, 0.50 mmol) in THF (25.0 mL, c = 20.0 mM, 0.20 mL, 4.0 μmol) was added for biaryl quantifications by GC-FID.

sample	R^1	8x	m [mg]	n [μmol]	R^2	8y	m [mg]	n [μmol]	17d*x*/17d*y*	σ	yield 17 [%]	σ [%]
A1	OMe	d	14.1	16.3	H	a	14.1	16.3	**0.42**	0.01	44	2
A2	ᵗBu	e	13.9	15.6	H	a	13.9	15.6	**0.29**	0.00	40	1
A3	Me	f	13.4	15.8	H	a	13.4	15.8	**0.27**	0.00	45	1
A4	CO₂Et	i	14.1	15.5	H	a	14.1	15.5	**0.56**	0.06	38	3
A5	CF₃	k	14.1	16.4	H	a	14.1	16.4	**0.42**	0.04	38	4
A6	CN	l	14.2	15.9	H	a	14.2	15.9	**0.68**	0.03	23	1
B1	ᵗBu	e	15.4	18.1	OMe	d	15.4	18.1	**0.66**	0.12	30	6
B2	Me	f	14.5	17.0	OMe	d	14.5	17.0	**1.17**	0.19	23	1
B3	F	g	15.3	16.9	OMe	d	15.3	16.9	**1.00**	0.31	32	7
B4	CO₂Et	i	14.4	15.9	OMe	d	14.4	15.9	**1.35**	0.23	36	3
B5	CF₃	k	14.2	16.5	OMe	d	14.2	16.5	**0.92**	0.09	42	2
B6	CN	l	13.7	16.1	OMe	d	13.7	16.1	**1.40**	0.08	23	1
C1	Me	f	14.0	16.4	ᵗBu	e	14.0	16.4	**0.77**	0.07	21	1
C2	F	g	14.7	16.2	ᵗBu	e	14.7	16.2	**2.57**	0.40	22	6
C3	CO₂Et	i	14.7	16.3	ᵗBu	e	14.7	16.3	**1.79**	0.27	32	3
C4	CF₃	k	14.2	16.6	ᵗBu	e	14.2	16.6	**1.25**	0.07	21	1
C5	CN	l	14.4	15.9	ᵗBu	e	14.4	15.9	**1.52**	0.15	22	3
D1	F	g	14.3	15.8	Me	f	14.3	15.8	**1.69**	0.04	39	2
D2	CO₂Et	i	13.8	16.0	Me	f	13.8	16.0	**1.73**	0.18	27	2
D3	CF₃	k	14.7	16.2	Me	f	14.7	16.2	**1.45**	0.13	26	3
D4	CN	l	13.7	15.9	Me	f	13.7	15.9	**1.19**	0.48	23	5
E1	CO₂Et	i	14.8	16.4	F	g	14.8	16.4	**1.22**	0.16	35	4
E2	CF₃	k	13.8	16.0	F	g	13.8	16.0	**0.70**	0.02	30	5

E3	CN	l	13.8	16.0	F	i	13.8	16.0	**0.63**	0.14	32	4
F1	CF$_3$	k	14.1	16.3	CO$_2$Et	i	14.1	16.3	**0.42**	0.01	44	2
F2	CN	l	13.9	15.6	CO$_2$Et	i	13.9	15.6	**0.29**	0.00	40	1
G1	CN	l	13.4	15.8	CF$_3$	k	13.4	15.8	**0.27**	0.00	45	1

(SZ 5006)

	Wert	Fehler
Intercept	0.0022	0.01484
Slope	0.13836	0.04034
Chi-Quadr Reduziert	0.03148	
R-Quadrat	0.06848	
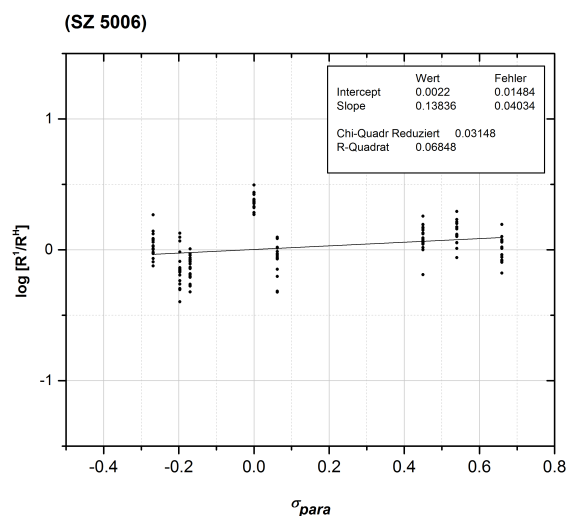
Exp. No.	slope	R^2
SZ 5006	-0.14 ± 0.04	0.068

4.7.8 Competition in (P^{t}Bu$_3$)Pd(Ar)Br complexes with PhZnCl
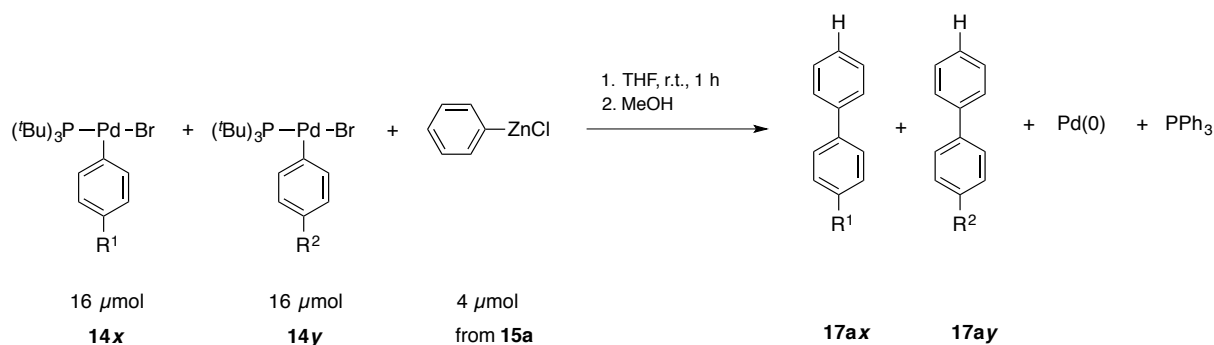
[SZ 5042]

According to the general procedure with the exception that the complexes **14x** and **14y** (each 20 μmol) were weighted out inside the glovebox, dissolved in THF (1.00 mL) and being treated with a solution of ZnPh$_2$ (22.3 mg, 0.10 mmol) and ZnCl$_2$ (14.1 mg, 0.10 mmol) in THF (10.0 mL, c[PhZnCl] = 20.3 mM, 0.20 mL, 4.1 μmol). A stock solution of TMB (169 mg, 1.00 mmol) in MeOH (25.0 mL, c = 40.1 mM, 0.10 mL, 4.1 μmol) was added, and the reaction solutions directly transferred into GC vials for biaryl quantifications by GC-FID.

sample	R¹	14x	m [mg]	n [μmol]	R²	14y	m [mg]	n [μmol]	17ax/17ay	σ	yield 17 [%]	σ [%]
A1	OMe	d	9.7	19.6	H	a	10.8	23.2	**0.14**	0.02	294	12
A2	ᵗBu	e	9.9	19.0	H	a	9.5	20.4	**2.01**	0.18	394	21
A3	Me	f	9.6	20.0	H	a	9.9	21.3	**0.73**	0.26	150	22
A4	CO₂Et	i	11.0	20.5	H	a	9.4	20.2	**2.08**	0.04	397	5
B1	ᵗBu	e	11.4	21.8	OMe	d	9.5	19.2	**7.97**	1.53	83	9
B2	Me	f	9.3	19.4	OMe	d	9.9	20.0	**4.78**	1.77	52	6
B3	F	g	12.3	25.4	OMe	d	11.1	22.4	**10.7**	3.31	207	2
B4	CO₂Et	i	10.6	19.7	OMe	d	9.3	18.8	**2.94**	0.27	75	12
B5	CF₃	k	10.2	19.1	OMe	d	9.5	19.2	**15.6**	3.71	207	7
C1	Me	f	9.5	19.8	ᵗBu	e	10.5	20.1	**0.22**	0.05	101	17
C2	F	g	8.3	17.2	ᵗBu	e	9.4	18.0	**1.95**	0.14	144	5
C3	CO₂Et	i	10.6	19.7	ᵗBu	e	10.1	19.4	**0.63**	0.17	90	16
C4	CF₃	k	9.6	18.0	ᵗBu	e	8.7	16.7	**1.66**	0.50	172	10
D1	F	g	9.8	20.3	Me	f	9.5	19.8	**3.37**	0.08	136	11
D2	CO₂Et	i	10.1	18.8	Me	f	8.8	18.3	**0.90**	0.08	66	1
D3	CF₃	k	9.1	17.0	Me	f	8.8	18.3	**1.69**	0.13	125	14
E1	CO₂Et	i	10.5	19.5	F	g	9.7	20.1	**0.42**	0.03	155	11
F1	CF₃	k	12.1	22.7	CO₂Et	i	11.2	20.8	**4.74**	0.40	211	2

[SZ 5043]

According to the general procedure with the exception that the complexes **14x** and **14y** (each 20 μmol) were weighted out inside the glovebox being treated with a solution of ZnPh₂ (22.3 mg, 0.10 mmol) and ZnCl₂ (14.1 mg, 0.10 mmol) in THF (10.0 mL, c[PhZnCl] = 20.3 mM, 0.20 mL, 4.1 μmol). A stock solution of TMB (169 mg, 1.00 mmol) in MeOH (25.0 mL, c = 40.1 mM, 0.10 mL, 4.1 μmol) was added, and the reaction solutions directly transferred into GC vials for biaryl quantifications by GC-FID.

sample	R¹	14x	m [mg]	n [μmol]	R²	14y	m [mg]	n [μmol]	17ax/17ay	σ	yield 17 [%]	σ [%]
A1	OMe	d	10.5	21.2	H	a	9.5	20.4	**0.27**	0.04	250	5
A2	ᵗBu	e	9.6	18.4	H	a	9.3	20.0	**1.77**	0.16	370	28
A3	Me	f	8.6	17.9	H	a	9.9	21.3	**0.71**	0.08	239	10
A4	CO₂Et	i	10.7	19.9	H	a	9.5	20.4	**1.94**	0.17	413	11
B1	ᵗBu	e	9.7	18.6	OMe	d	9.5	19.2	**18.3**		82	30
B2	Me	f	8.8	18.3	OMe	d	9.6	19.4	**7.13**	3.85	50	5
B3	F	g	8.5	17.6	OMe	d	8.5	17.1	**10.7**	2.51	207	28
B4	CO₂Et	i	9.6	17.9	OMe	d	8.5	17.1	**3.35**	0.31	99	15

B5	CF$_3$	**k**	10.8	20.2	OMe	**d**	3.2	6.5	**9.31**	4.05	258	21
C1	Me	**f**	8.0	16.7	^{t}Bu	**e**	8.6	16.5	**0.31**	0.09	88	17
C2	F	**g**	9.8	20.3	^{t}Bu	**e**	8.7	16.7	**2.31**	0.20	147	35
C3	CO$_2$Et	**i**	9.8	18.2	^{t}Bu	**e**	8.4	16.1	**0.86**	0.05	101	6
C4	CF$_3$	**k**	7.3	13.7	^{t}Bu	**e**	5.2	10.0	**1.99**	0.36	144	7
D1	F	**g**	9.0	18.6	Me	**f**	9.1	19.0	**2.57**	0.20	136	12
D2	CO$_2$Et	**i**	10.3	19.2	Me	**f**	9.4	19.6	**0.98**	0.16	72	8
D3	CF$_3$	**k**	10.4	19.5	Me	**f**	9.3	19.4	**2.51**	0.46	144	26
E1	CO$_2$Et	**i**	11.3	21.0	F	**g**	11.1	22.9	**0.52**	0.13	181	11
F1	CF$_3$	**k**	11.1	20.8	CO$_2$Et	**i**	10.7	19.9	**10.9**	0.19	208	23

(SZ 5042)

(SZ 5043)

(SZ 5042+5043)
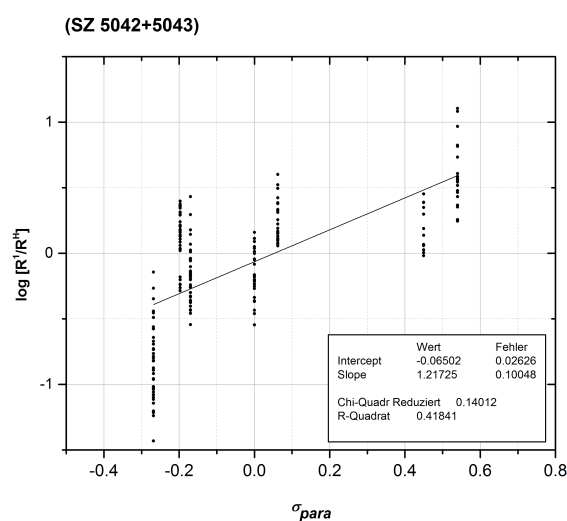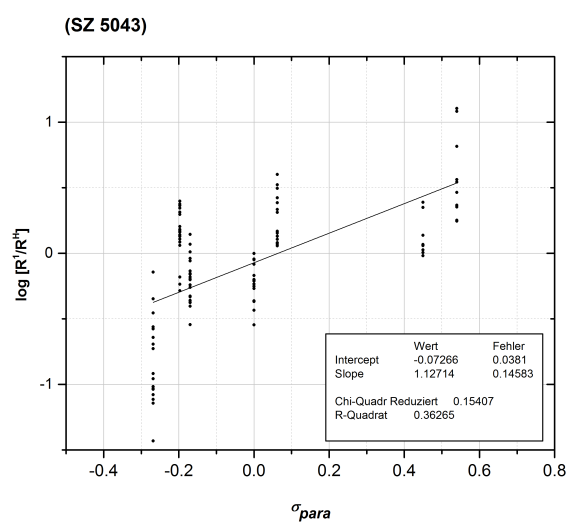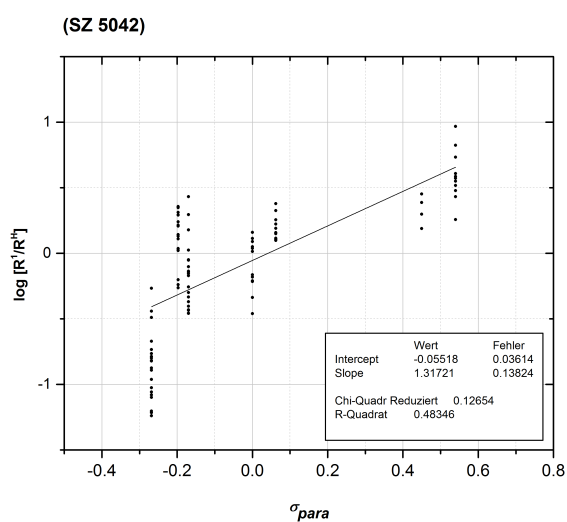
Exp. No.	slope	R^2
SZ 5042	1.3±0.2	0.483
SZ 5043	1.1±0.2	0.363
total	1.2±0.2	0.418

4.7.9   Competition in (phosphine)Pd(Ar)Br with PhZnCl
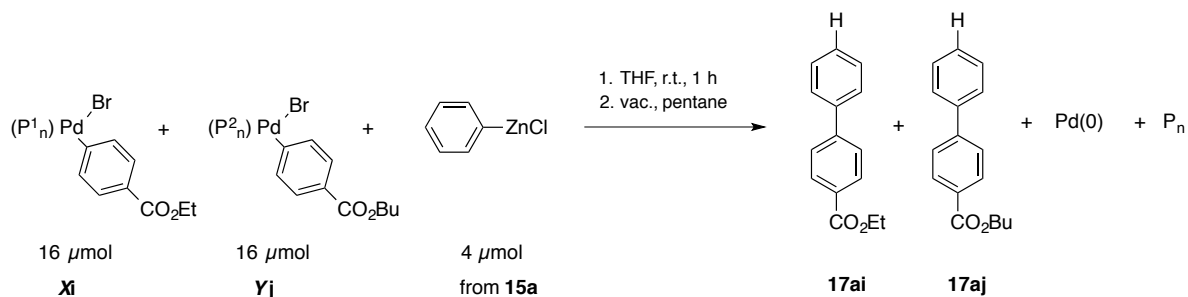
[SZ 4150+5027]

According to the general procedure, complexes Xi and Yj (each 16 μmol) were treated with a solution of ZnPh$_2$ **15a** (21.9 mg, 0.10 mmol) and ZnCl$_2$ (14.2 mg, 0.10 mmol) in THF (10.0 mL, c[PhZnCl] = 20.0 mM, 0.20 mL, 4.0 μmol). A stock solution of BBP (158 mg, 0.51 mmol) in THF (25.0 mL, c = 20.2 mM, 0.20 mL, 4.0 μmol) was added for biaryl quantifications by GC-FID.

sample	P^1	X	m	n	P^2	Y	m	n	17ai/17aj	σ	yield **17**	σ
			[mg]	[μmol]			[mg]	[μmol]			[%]	[%]
A1	dppe	**6i**	11.0	15.0	dppe	**6j**	12.0	15.7	**1.03**	0.02	80	2
A2	dppf	**7i**	14.3	16.1	dppe	**6j**	12.6	16.5	**0.06**	0.05	74	4
A3	PPh$_3$	**9i**	13.9	16.2	dppe	**6j**	12.5	16.4	**1.16**	0.02	77	1
A4	P(o-tol)$_3$	**5i**	10.8	16.9	dppe	**6j**	12.1	15.9	**0.28**	0.02	90	4
A5	P^{t}Bu$_3$	**14i**	9.0	16.7	dppe	**6j**	12.5	16.4	**6.99**	0.12	79	1
A6	XPhos	**13i**	12.9	15.9	dppe	**6j**	12.1	15.9	**5.86**	0.36	85	5
B1	dppe	**6i**	9.9	13.5	dppf	**7j**	14.7	16.0	**8.12**	0.20	73	2
B2	dppf	**7i**	16.0	18.0	dppf	**7j**	14.1	15.4	**0.52**	0.01	60	0
B3	PPh$_3$	**9i**	13.8	16.0	dppf	**7j**	14.9	16.2	**1.17**	0.04	98	7
B4	P(o-tol)$_3$	**5i**	10.3	16.1	dppf	**7j**	14.7	16.0	**0.24**	0.00	79	4
B5	P^{t}Bu$_3$	**14i**	9.3	17.3	dppf	**7j**	14.9	16.2	**2.72**	0.01	76	1
B6	XPhos	**13i**	14.5	17.9	dppf	**7j**	15.1	16.5	**3.63**	0.04	95	10
C1	dppe	**6i**	11.7	15.9	PPh$_3$	**9j**	15.9	17.9	**0.58**	0.02	114	3
C2	dppf	**7i**	15.6	17.5	PPh$_3$	**9j**	15.4	17.3	**0.60**	0.00	110	2
C3	PPh$_3$	**9i**	14.3	16.6	PPh$_3$	**9j**	14.5	16.3	**0.97**	0.03	76	1
C4	P(o-tol)$_3$	**5i**	10.6	16.6	PPh$_3$	**9j**	14.8	16.7	**0.10**	0.01	73	2
C5	P^{t}Bu$_3$	**14i**	9.4	17.5	PPh$_3$	**9j**	14.1	15.9	**0.94**	0.03	66	3
C6	XPhos	**13i**	12.8	15.8	PPh$_3$	**9j**	13.8	15.5	**0.46**	0.09	107	11
D1	dppe	**6i**	11.7	15.9	P(o-tol)$_3$	**5j**	10.8	16.2	**0.87**	0.03	90	3
D2	dppf	**7i**	14.3	16.1	P(o-tol)$_3$	**5j**	11.5	17.2	**0.92**	0.04	93	3
D3	PPh$_3$	**9i**	13.7	15.9	P(o-tol)$_3$	**5j**	10.6	15.9	**1.48**	0.08	66	10
D4	P(o-tol)$_3$	**5i**	10.5	16.4	P(o-tol)$_3$	**5j**	10.7	16.0	**0.43**	0.01	56	0
D5	P^{t}Bu$_3$	**14i**			P(o-tol)$_3$	**5j**						

sample	P¹	X	m [mg]	n [µmol]	P²	Y	m [mg]	n [µmol]	17ai/17aj	σ	yield 17 [%]	σ [%]
D6	XPhos	**13i**	13.4	16.5	P(*o*-tol)$_3$	**5j**	10.5	15.7	**1.44**	0.03	84	2
F1	dppe	**6i**	11.7	15.9	XPhos	**13j**	13.8	16.4	**0.29**	0.00	94	3
F2	dppf	**7i**	15.4	17.3	XPhos	**13j**	14.0	16.7	**0.45**	0.05	99	6
F3	PPh$_3$	**9i**	15.3	17.8	XPhos	**13j**	13.5	16.1	**1.59**	0.08	117	13
F4	P(*o*-tol)$_3$	**5i**	10.3	16.1	XPhos	**13j**	13.5	16.1	**0.22**	0.03	85	8
F5	P^{t}Bu$_3$	**14i**	10.6	19.7	XPhos	**13j**	13.7	16.3	**11.6**	1.38	82	8
F6	XPhos	**13i**	15.5	19.1	XPhos	**13j**	15.8	18.8	**1.31**	0.52	95	30

[SZ 5017+5027]

According to the general procedure, complexes *X*i and *Y*j (each 16 µmol) were treated with a solution of ZnPh$_2$ **15a** (22.3 mg, 0.10 mmol) and ZnCl$_2$ (13.9 mg, 0.10 mmol) in THF (10.0 mL, c[PhZnCl] = 20.3 mM, 0.20 mL, 4.1 µmol). A stock solution of BBP (158 mg, 0.51 mmol) in THF (25.0 mL, c = 20.2 mM, 0.20 mL, 4.0 µmol) was added for biaryl quantifications by GC-FID.

sample	P¹	X	m [mg]	n [µmol]	P²	Y	m [mg]	n [µmol]	17ai/17aj	σ	yield 17 [%]	σ [%]
A1	dppe	**6i**	12.5	17.0	dppe	**6j**	12.9	16.9	**0.98**	0.28	98	4
A2	dppf	**7i**	14.7	16.5	dppe	**6j**	12.9	16.9	**0.09**	0.00	84	2
A3	PPh$_3$	**9i**	13.8	16.0	dppe	**6j**	12.3	16.1	**1.16**	0.14	94	6
A4	P(*o*-tol)$_3$	**5i**	12.8	20.0	dppe	**6j**	12.3	16.1	**0.35**	0.02	100	2
A5	P^{t}Bu$_3$	**14i**	8.6	16.0	dppe	**6j**	12.2	16.0	**9.29**	0.30	93	4
A6	XPhos	**13i**	13.4	16.5	dppe	**6j**	12.6	16.5	**5.06**	0.10	105	2
B1	dppe	**6i**	12.2	16.6	dppf	**7j**	14.6	15.9	**7.23**	0.27	94	6
B2	dppf	**7i**	14.5	16.3	dppf	**7j**	15.0	16.4	**0.43**	0.03	72	3
B3	PPh$_3$	**9i**	13.8	16.0	dppf	**7j**	14.8	16.1	**1.37**	0.06	102	7
B4	P(*o*-tol)$_3$	**5i**	10.4	16.3	dppf	**7j**	15.1	16.5	**0.42**	0.01	101	4
B5	P^{t}Bu$_3$	**14i**	9.1	16.9	dppf	**7j**	14.7	16.0	**4.41**	0.15	92	4
B6	XPhos	**13i**	13.0	16.0	dppf	**7j**	15.4	16.8	**2.87**	0.13	108	4
C1	dppe	**6i**	11.7	15.9	PPh$_3$	**9j**	14.7	16.6	**0.62**	0.03	118	1
C2	dppf	**7i**	12.7	14.3	PPh$_3$	**9j**	14.1	15.9	**0.68**	0.05	112	18
C3	PPh$_3$	**9i**	13.7	15.9	PPh$_3$	**9j**	14.1	15.9	**1.10**	0.03	112	10
C4	P(*o*-tol)$_3$	**5i**	10.6	16.6	PPh$_3$	**9j**	14.2	16.0	**0.35**	0.01	94	2
C5	P^{t}Bu$_3$	**14i**	9.3	17.3	PPh$_3$	**9j**	14.5	16.3	**0.91**	0.06	73	4
C6	XPhos	**13i**	13.6	16.7	PPh$_3$	**9j**	14.1	15.9	**0.50**	0.02	131	10
D1	dppe	**6i**	12.0	16.4	P(*o*-tol)$_3$	**5j**	11.0	16.5	**0.94**	0.05	98	8
D2	dppf	**7i**	14.1	15.8	P(*o*-tol)$_3$	**5j**	10.7	16.0	**1.28**	0.00	98	2
D3	PPh$_3$	**9i**	14.0	16.3	P(*o*-tol)$_3$	**5j**	10.5	15.7	**1.79**	0.05	84	5
D4	P(*o*-tol)$_3$	**5i**	10.9	17.0	P(*o*-tol)$_3$	**5j**	10.9	16.3	**0.47**	0.00	76	2
D5	P^{t}Bu$_3$	**14i**	8.8	16.4	P(*o*-tol)$_3$	**5j**	10.9	16.3	**8.94**	0.26	96	6
D6	XPhos	**13i**	14.0	17.2	P(*o*-tol)$_3$	**5j**	11.0	16.5	**1.51**	0.06	99	4
F1	dppe	**6i**	12.2	16.6	XPhos	**13j**	14.3	17.0	**0.23**	0.01	107	5

F2	dppf	**7i**	14.3	16.1	XPhos	**13j**	13.4	15.9	**0.22**	0.02	92	8
F3	PPh$_3$	**9i**	14.1	16.4	XPhos	**13j**	13.2	15.7	**5.84**	0.42	94	2
F4	P(o-tol)$_3$	**5i**	11.0	17.2	XPhos	**13j**	14.3	17.0	**0.42**	0.01	104	2
F5	P^{t}Bu$_3$	**14i**	8.7	16.2	XPhos	**13j**	13.6	16.2	**0.04**	0.04	92	6
F6	XPhos	**13i**	13.7	16.9	XPhos	**13j**	13.8	16.4	**0.91**	0.01	115	5

4.8 Ligand scrambling experiments
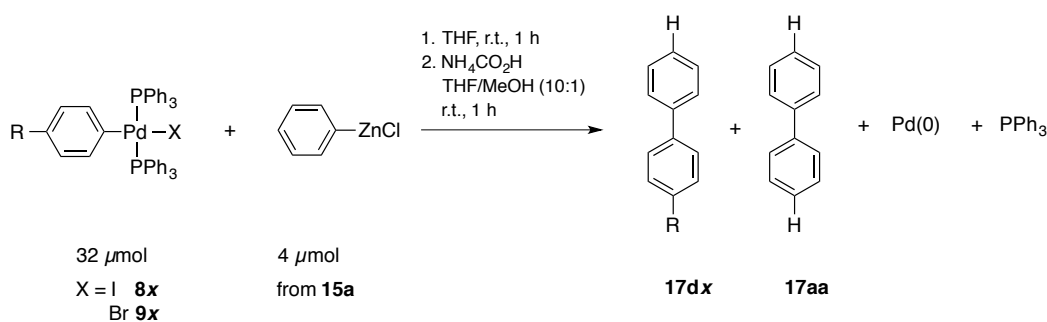
[SZ 3147 and SZ 3148]

Similar to the general procedure for the competition experiments (*cf.* chapter 4.7), the solutions of complexes **8x** or **9x** (32 μmol) in THF (1.00 mL) were treated with a solution of ZnPh$_2$ (55.5 mg, 0.25 mmol) and ZnCl$_2$ (36.5 mg, 0.27 mmol) in THF (20.0 mL, c[PhZnCl] = 25.0 mM, 0.20 mL, 5.0 μmol). A stock solution of TMB (86.5 mg, 0.51 mmol) in MeOH (50.0 mL, c = 10.3 mM, 0.40 mL, 4.1 μmol) was added, and the reaction solutions directly transferred into GC vials for biaryl quantifications by GC-FID.

			X = Br (**9**)			X = I (**8**)		
			17ax	**17aa**	recov.**16a**	**17ax**	**17aa**	recov. **16a**
			[%]	[%]	[%]	[%]	[%]	[%]
1	OMe	**d**	6	50	106	62	23	108
2	^{t}Bu	**e**	36	44	124	55	25	104
3	Me	**f**	–	–	–	53	36	125
4	H	**a**	101	–	–	–	–	–
5	CO$_2$Et	**i**	106	15	136	89	6	100
6	CO$_2$^{n}Bu	**j**	116	16	149	–	–	–
7	CF$_3$	**k**	87	12	111	88	7	102
8	CN	**l**	87	9	104	94	4	102

[SZ 5133/5159]

An NMR tube was charged with a spatula tip of complexes **X***x* and **Y***y* and dissolved in THF. The NMR tube was shaken and the resulting solutions analyzed by ^{31}P NMR spectroscopy with 10–15 min.
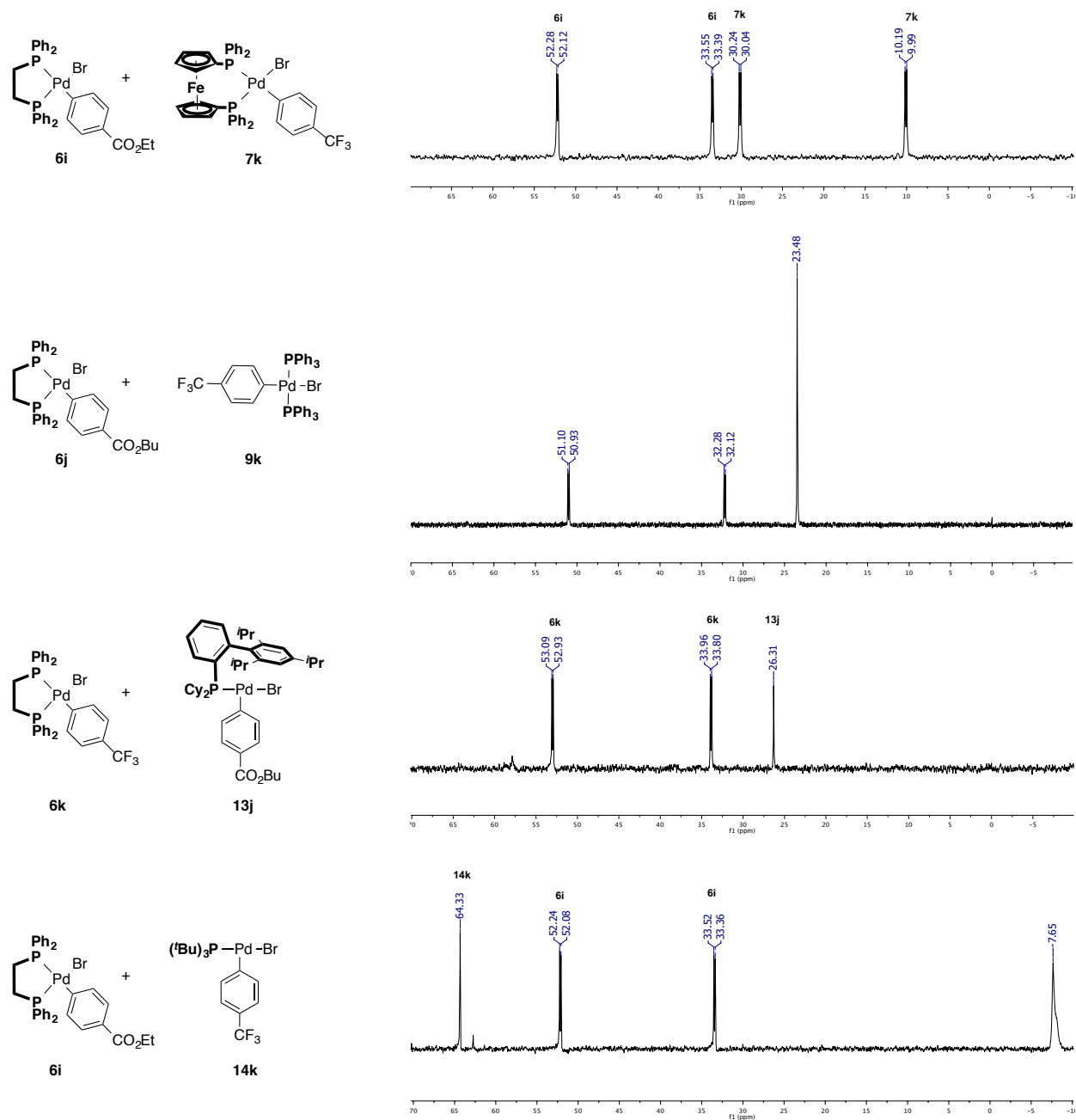
Remark: The signal at $\delta = -7.65$ ppm corresponds to the cyclometalated dimer

B.
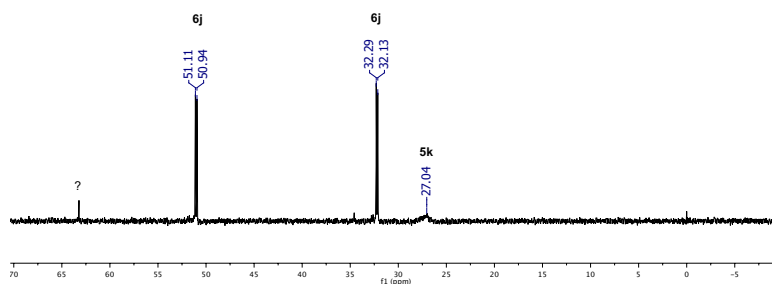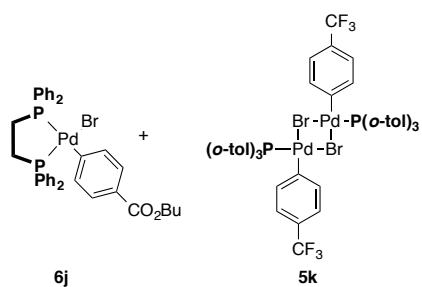
Remark: NMR spectra of P(o-tol)$_3$-ligated complexes **5** are generally badly resolved and typically show broad signals of low intensity.

Remark: The signal at $\delta = -7.65$ ppm corresponds to the cyclometalated dimer **B**.

9k **5i**

9k + 9i

24.66
24.42

31.77
?

9k **13j**

9k + 9j

24.65
24.44

49.91 ?
47.41 ?
42.35 ?
31.76 ?
31.41

9k **14i**

9k

24.67
23.06
22.33
19.72

31.78 ?
31.60

7.67

14.79 ?
17.39 ?

Remark: The signal at $\delta = -7.67$ ppm corresponds to the cyclometalated dimer **B**.

5k **13j**

5 13j

57.46 ?

28.11
26.33

317
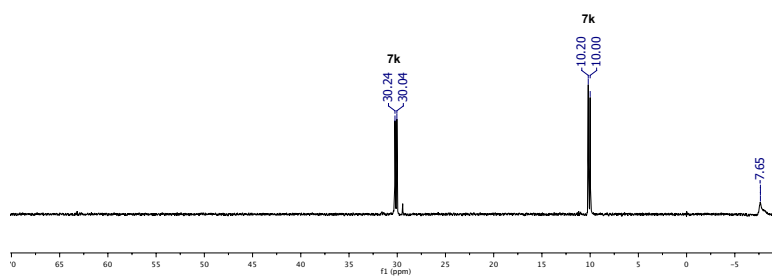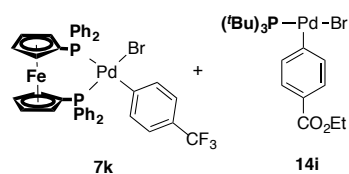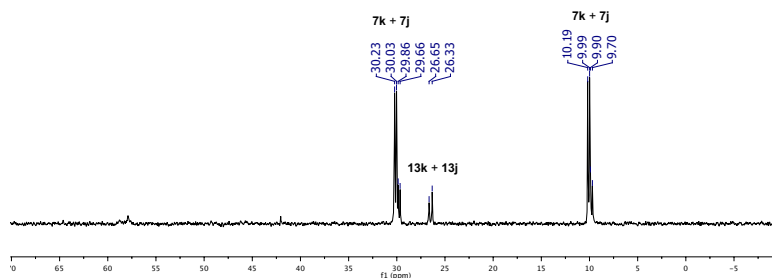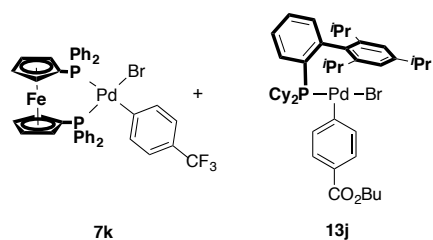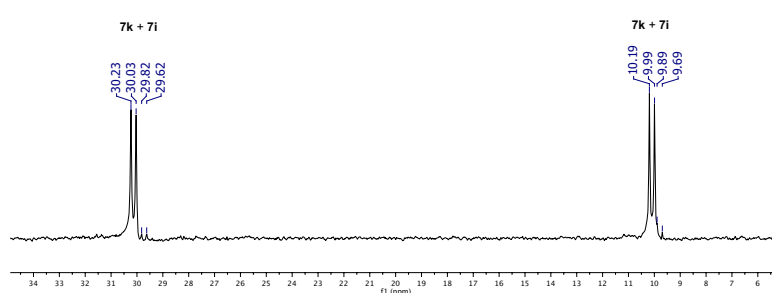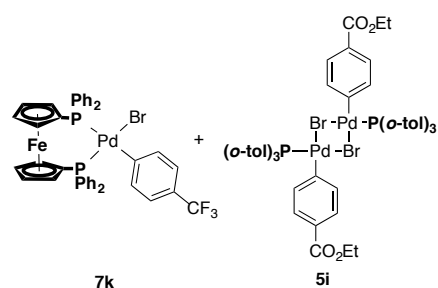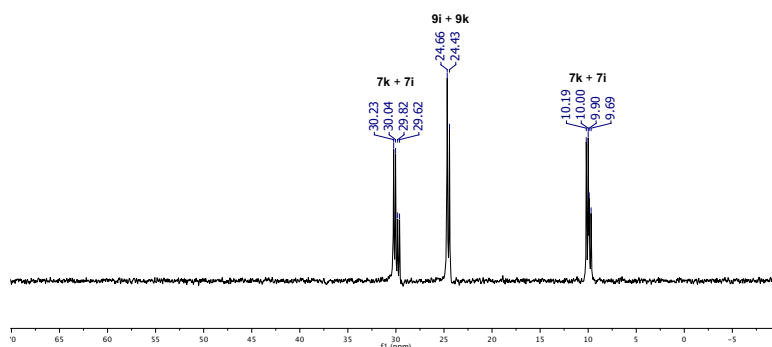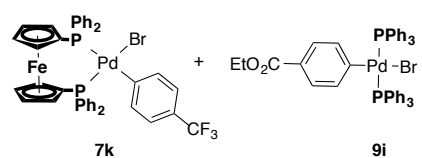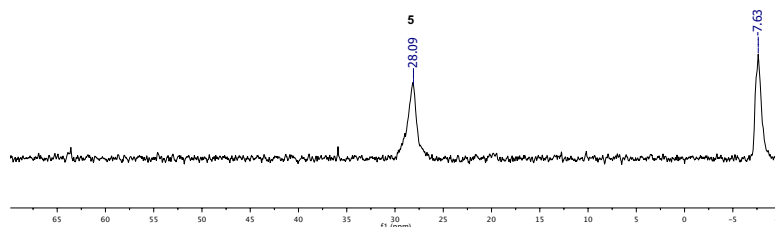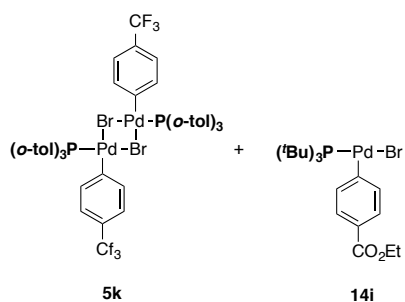
Remark: The signal at $\delta = -7.63$ ppm corresponds to the cyclometalated dimer **B**.
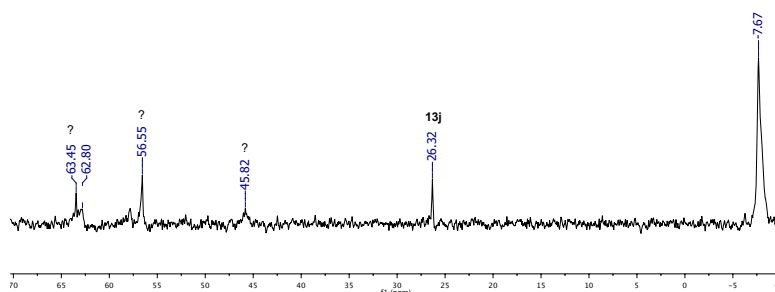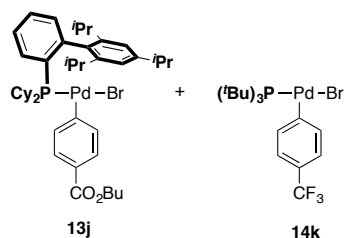
Remark: The signal at $\delta = -7.67$ ppm corresponds to the cyclometalated dimer **B**.

4.9 Detection of transmetalation intermediate by NMR
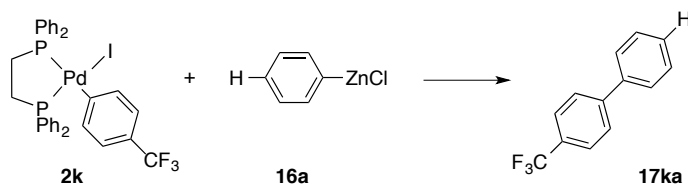
[SZ 5131]

In side the glovebox, an oven-dried NMR tube was charged with complex **2k** (31.5 mg, 0.04 mmol), which was dissolved in THF-d_8 (0.40 mL), and connected to a melting adapter. In addition, ZnPh$_2$ (**15a**, 26.3 mg, 0.12 mmol) and ZnCl$_2$ (20.4 mg, 0.15 mmol) were dissolved in THF-d_8 (1.20 mL) in an oven-dried Schlenk flask. The NMR tube and the Schlenk flask were brought outside the glovebox and cooled to -78 °C (acetone/dry ice). The phenylzinc solution (0.20 mL, 0.04 mmol) was syringed into the NMR tube, which was then immediately cooled to -196 °C with liquid nitrogen. The NMR tube was sealed by ablating, and then carefully thawed in the acetone/dry ice cooling bath just before being transferred into the pre-cooled (-40 °C) NMR spectroscope to monitor the reaction at different temperatures. For representative spectra, see chapter 1.3.9.
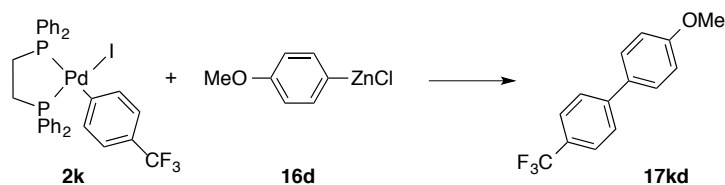
[SZ 5158.A]

Following the same procedure as for [SZ 5131], the reaction of complex **2k** (38.8 mg, 0.05 mmol) in THF-d_8 (0.50 mL) and a solution (0.10 mL, 0.05 mmol [Zn]) of **15d** (34.9 mg, 0.125 mmol) and ZnCl$_2$ (17.2 mg, 0.126 mmol) in THF-d_8 (0.50 mL) was monitored by ^{1}H and ^{31}P NMR spectroscopy at different temperatures. For representative spectra, see chapter 1.3.9.

[SZ 5158.B]

Following the same procedure as for [SZ 5131], the reaction of complex **2k** (38.9 mg, 0.05 mmol) in THF-d_8 (0.50 mL) and a solution (0.10 mL, 0.05 mmol [Zn]) of **15d** (34.9 mg, 0.125 mmol) and ZnCl$_2$ (17.2 mg, 0.126 mmol) in THF-d_8 (0.50 mL) was monitored by ^{1}H and ^{31}P NMR spectroscopy at –25 °C for 50 min.

time [min]	δ = 8.02 ppm (**2k**)[a]	δ = 6.76 ppm (**16d**)[a]	δ = 7.69 ppm (**17kd**)[a]	δ = 8.16 ppm (**intermediate**)[a]
0	3.48	1.74	0	0
2	2.29	0.74	0.31	0.57
5	0.84	0.41	0.5	0.74
10	0.61	0.36	0.7	0.92
15	0.49	0.32	0.78	0.93
20	0.43	0.29	0.82	0.93
25	0.41	0.28	0.85	0.91
30	0.38	0.26	0.88	0.9
35	0.37	0.25	0.91	0.87
40	0.38	0.24	0.95	0.88
45	0.37	0.24	0.95	0.84
50	0.38	0.21	0.98	0.9

[a]Integrals relative to THF-d_8 solvent residual peak of the ^{1}H NMR spectra.

time [min]	$\delta = 49.7$ ppm (2k)^{a,b}	$\delta = 41$ ppm (intermediate)^{a,c}	$\delta = 33$ ppm (intermediate)^{a,d}	$\delta = 32.5$ ppm (Pd(dppe)$_n$)^{a,e}	total integral
0	1	0	0	0	1
2	3.66	0.45	0.22	0.43	3.66
5	7.29	1.32	0.62	1.25	7.29
10	10.02	2	0.95	1.82	10.02
15	11.99	2.47	1.18	2.33	11.99
20	12.97	2.77	1.2	2.53	12.97
25	13.46	2.91	1.28	2.67	13.46
30	14.1	3.05	1.39	2.82	14.1
35	12.53	3.02	1.32	2.85	12.53
40	13.58	2.92	1.28	2.62	13.58
45	13.7	2.91	1.3	2.76	13.7
50	13.27	2.84	1.23	2.55	13.27

^{a}Integrals of the corresponding species in the ^{31}H NMR spectra.
^{b}One phosphor atom.
^{c}Integral of two species observed as doublets in a 1:1 ratio. Probably two phosphor atoms.
^{e}Presumably n = 1, which corresponds to two phosphor atoms.

[SZ 5132]

Complex **2k** (30.3 mg, 0.039 mmol) and ZnCl$_2$ (Sample A: 6.5 mg, 0.048 mmol, Sample B: 13.6 mg, 0.100 mmol) were dissolved in THF-d_8 (0.55 mL) in an NMR tube. The resulting sultions were measured at room temperature within 10–15 min upon preparation.

^{1}H NMR (400 MHz, THF-d_8)

0 equiv. ZnCl$_2$

^{1}H NMR (400 MHz, THF-d_8)

1.25 equiv. ZnCl$_2$

^{1}H NMR (400 MHz, THF-d_8)

2.40 equiv. ZnCl$_2$

^{31}P NMR (162 MHz, THF-d_8)

0 equiv. ZnCl$_2$

^{31}P NMR (162 MHz, THF-d_8)

1.25 equiv. ZnCl$_2$

³¹P NMR (162 MHz, THF-d_8)

2.40 equiv. ZnCl$_2$

[SZ 4052]

Complex **2k** (389 mg, 0.50 mmol) and AgOTs (141 mg, 0.51 mmol) were dissolved in CDCl$_3$ (5.00 mL) and stirred for 1 h at room temperature. The resulting mixture was filtered through Celite and the filtrate analyzed by NMR spectroscopy. Attempts to isolate cationic complex [**2k**]$^+$ failed and resulted in decomposition into palladium black.

¹H NMR (400 MHz, CDCl$_3$): δ 8.01–7.91 (m, 4H), 7.51–7.39 (m, 12H), 7.33 (td, J = 7.8, 2.6 Hz, 4H), 7.17–7.08 (m, 4H), 6.81 (d, J = 7.1 Hz, 2H), 6.77 (d, J = 8.1 Hz, 2H), 2.45 (ddd, J = 28.2, 14.0, 8.9 Hz, 2H), 2.22–2.08 (m, 5H) ppm.

³¹P NMR (162 MHz, CDCl$_3$): δ 54.1 (d, J = 27 Hz), 34.5 (d, J = 27 Hz) ppm.

¹⁹F NMR (376 MHz, CDCl$_3$): δ –61.9 ppm.

4.10 Synthesis of pyridines and pyridine *N*-oxides

Commercial and non-commercial pyridine *N*-oxides were dried by azeotropic distillation of water content with toluene in a Dean-Sark-apparatus, dried under high vacuum, and stored and weighted out in an argon-filled glovebox prior further conversion. K_3PO_4 was dried by repeated heating with a heat gun under high vacuum and stored and weighted out in a glovebox. 4-*tert*-Butylpyridine *N*-oxide (**27z**) was provided by Sasa Duric.[117]

4.10.1 Esterfications

General procedure:

The substrate was dissolved in the corresponding alcoholic solvent and catalytic amounts of H_2SO_4 were added. The resulting mixture was stirred under reflux for several hours. The solvent was removed, the residue dissolved in DCM, neutralized with sat. aqueous N_2CO_3 and the mixture extracted with DCM. The combined organic layers were dried with Na_2SO_4, filtered and the solvent was removed from the filtrate. The esterified products were obtained in an spectroscopically pure grade without further purification.

2-Bromo-(4-ethoxycarbonyl)pyridine

[FW 2008]
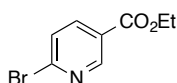
According to the general procedure, reaction of 2-bromoisonicotinic acid (1.21 g, 5.99 mmol) and H_2SO_4 (few drops) in refluxing EtOH (10.0 mL) for 16 h provided the title compound (1.23 g, 5.35 mmol, 89%) as colorless liquid.

^{1}H NMR (400 MHz, CDCl$_3$): δ 8.52 (dd, *J* = 5.1, 0.8 Hz, 1H), 8.04 (dd, *J* = 1.4, 0.8 Hz, 1H), 7.80 (dd, *J* = 5.0, 1.4 Hz, 1H), 4.42 (q, *J* = 7.2 Hz, 2H), 1.41 (t, *J* = 7.1 Hz, 3H) ppm.

The chemical shifts are in agreement with previous reported values.[233]

4.10.2 Oxidations

General procedure A:

Based on reported procedure,[117] the pyridine derivative was dissolved in DCM and *m*CPBA ($w = 73\%$) was added portion-wise. After stirring at room temperature, the volatiles were removed by rotary evaporation and the residue subjected to column chromatography (SiO_2).

General procedure B:

Based on reported procedure,[117] the pyridine derivative was dissolved in AcOH

and an aqueous solution of H_2O_2 ($w = 35\%$) was added. The reaction solution was stirred under heating until complete consumption of the starting material as judged by TLC. The volatiles were removed by rotary evaporation, the residue dissolved in DCM and carefully neutralized with sat. aqueous N_2CO_3. The mixture was extracted with DCM, the combined organic layers dried with Na_2SO_4, filtered and the solvent removed from the filtrate. The pyridine *N*-oxide products were obtained in an analytically pure grade without further purification.

2-(Trifluoromethyl)pyridine *N*-oxide (27d)
[SZ 3084/FW 2020]
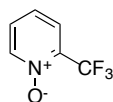
According to the general procedure A, reaction of 2-(trifluoromethyl)pyridine (1.03 g, 7.02 mmol) and *m*CPBA (2.07 g, 8.71 mmol) in DCM (15.0 mL) for 3 d provided the title compound (0.68 mg, 4.19 mmol, 60%) as pale yellow liquid after column chromatography (acetone/hexane 1:1).

^{1}H NMR (400 MHz, CDCl$_3$): δ 8.32 (ddt, J = 6.6, 1.3, 0.6 Hz, 1H), 7.70 (dd, J = 8.0, 2.1 Hz, 1H), 7.46 (td, J = 7.9, 2.1 Hz, 1H), 7.35 (t, J = 7.8 Hz, 1H) ppm.
The chemical shifts are in agreement with previous reported values.[234]
^{19}F NMR (376 MHz, DMSO-d_6): δ –69.02 ppm.

2-Cyanopyridine *N*-oxide (27e)
[SZ 3083]
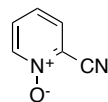
According to the general procedure A, reaction of picolinnitril (20.8 g, 0.20 mol) and *m*CPBA (57.3 g, 0.24 mol) in DCM (400 mL) for 3 d provided the title compound (22.5 g, 0.19 mol, 95%) as colorless solid after column chromatography (acetone/hexane mixtures 1:1, then 2:1, 1:0).

^{1}H NMR (400 MHz, CDCl₃): δ 8.27 (dt, *J* = 6.7, 0.8 Hz, 1H), 7.67 (ddd, *J* = 8.0, 2.1, 0.6 Hz, 1H), 7.48 (ddd, *J* = 7.7, 6.6, 2.1 Hz, 1H), 7.32 (td, *J* = 7.9, 1.1 Hz, 1H) ppm.
The chemical shifts are in agreement with previous reported values.[117]

2-(Ethoxycarbonyl)pyridine *N*-oxide (27c)

[SZ 3091]
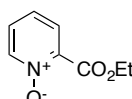
According to the general procedure A, reaction of 2-(ethoxycarbonyl)pyridine (22.7 g, 150 mmol) and *m*CPBA (43.0 g, 181 mmol) in DCM (300 mL) for 3 d provided the title compound (13.4 g, 79.9 mmol, 53%) as orange oil after column chromatography (acetone/hexane mixtures 1:2, then 1:1, 1:2).

^{1}H NMR (400 MHz, CDCl₃): δ 8.23 (dd, *J* = 6.5, 1.1 Hz, 1H), 7.57 (dd, *J* = 7.8, 2.2 Hz, 1H), 7.32 (td, *J* = 7.1, 6.5, 2.3 Hz, 1H), 7.26 (td, *J* = 7.7, 1.2 Hz, 1H), 4.46 (q, *J* = 7.2 Hz, 2H), 1.41 (t, *J* = 7.1 Hz, 3H) ppm.
The chemical shifts are in agreement with previous reported values.[117]

3-Nitropyridine *N*-oxide (27i)

[SZ 3085]
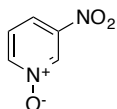
According to the general procedure B, reaction of 3-nitropyridine (4.78 g, 38.5 mmol) and H₂O₂ (4.30 mL, 46.0 mmol) in AcOH (30.0 mL) at 70 °C for 3 d provided the title compound (2.15 g, 15.3 mmol, 40%) as yellow solid after column chromatography (SiO₂, acetone/hexane mixtures 1:1, then 2:1) as yellow solid.

^{1}H NMR (400 MHz, CDCl₃): δ 9.00 (t, *J* = 1.8 Hz, 1H), 8.43 (ddt, *J* = 6.6, 1.5, 0.7 Hz, 1H), 8.03 (ddt, *J* = 8.5, 2.0, 0.7 Hz, 1H), 7.48 (dd, *J* = 8.5, 6.5 Hz, 1H) ppm.
The chemical shifts are in agreement with previous reported values.[235]

3-Methoxypyridine *N*-oxide (27f)

[SZ 3087]
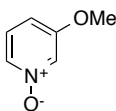
According to the general procedure B, reaction of 3-methoxyyridine (4.99 g, 45.7 mmol) and H_2O_2 (5.60 mL, 54.8 mmol) in AcOH (30.0 mL) at 70 °C for 3 d provided the title compound (5.25 g, 42.0 mmol, 92%) as colorless solid.

^{1}H NMR (400 MHz, CDCl$_3$): δ 7.96 (td, J = 2.2, 0.7 Hz, 1H), 7.88 (ddt, J = 6.3, 1.6, 0.8 Hz, 1H), 7.15 (dd, J = 8.7, 6.3 Hz, 1H), 6.86 (ddt, J = 8.7, 2.2, 0.8 Hz, 1H), 3.83 (s, 3H) ppm.

The chemical shifts are in agreement with previous reported values.[236]

4-(Ethoxycarbonyl)pyridine *N*-oxide (27l)

[SZ 2139]
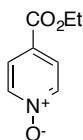
According to the general procedure B, reaction of 4-(ethoxycarbonyl)pyridine (42.6 g, 282 mmol) and H_2O_2 (35.0 mL, 343 mmol) in AcOH (215 mL) at 70 °C for 18 h provided the title compound (41.7 g, 249 mmol, 89%) as colorless solid.

^{1}H NMR (400 MHz, CDCl$_3$): δ 8.19 (d, J = 7.2 Hz, 2H), 7.85 (d, J = 7.2 Hz, 2H), 4.36 (q, J = 7.1 Hz, 2H), 1.36 (t, J = 7.1 Hz, 3H) ppm.

The chemical shifts are in agreement with previous reported values.[117]

4-(Trifluoromethyl)pyridine *N*-oxide (27m)

[SZ 2025c]
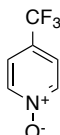
According to the general procedure A, reaction of 4-(trifluoromethyl)pyridine (4.95 g, 15.6 mmol) and *m*CPBA (9.93 g, 24.8 mmol) in DCM (40.0 mL) for 19 h provided the title compound (7.72 g, 15.6 mmol, 99%) as colorless solid after column chromatography (acetone/hexane mixtures 1:2, then 1:1, 2:1, 1:0).

^{1}H NMR (400 MHz, CDCl$_3$): δ 8.28 (d, J = 6.5 Hz, 2H), 7.51 (d, J = 6.7 Hz, 2 H) ppm.

^{19}F NMR (376 MHz, CDCl₃): δ –63.53 ppm.

The chemical shifts are in agreement with previous reported values.[117]

2-Phenylpyridine *N*-oxide (31a)

[FW 2069]
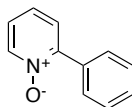
According to the general procedure B, reaction of 2-phenylpyridine (982 mg, 6.32 mmol) and H₂O₂ (0.74 mL, 7.18 mmol) in AcOH (12 mL) at 70 °C for 3 d provided the title compound (1.08 g, 6.31 mmol, quant.) as colorless solid.

^{1}H NMR (400 MHz, CDCl₃): δ 8.35 (dd, *J* = 6.4, 0.8 Hz, 1H), 7.83–7.80 (m, 2H), 7.51–7.41 (m, 4H), 7.31 (td, *J* = 7.7, 1.3 Hz, 1H), 7.23 (ddd, *J* = 7.5, 6.4, 2.2 Hz, 1H) ppm.

The chemical shifts are in agreement with previous reported values.[237]

2,2′-Bipyridine *N*-oxide (20a)

[FW 1054]
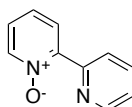
H₂O₂ (*w* = 30%, 20.0 mL, 196 mmol) was added slowly to an ice-cooled solution of 2,2-bipyridine (15.6 g, 100 mmol) in TFA (75.0 mL). The reaction solution allowed to reach room temperature and was additionally stirred for 16 h. Then DCM (200 mL) was added and the solution neutralized with an aqueous NaOH solution (6 M, 400 mL). The mixture was extracted with DCM, the combined organic layers dried with Na₂SO₄, filtered and the solvent was removed from the filtrate. The product **24a** (16.2 g, 94.3 mmol, 94%) was obtained as an analytically pure, colorless solid,

^{1}H NMR (400 MHz, CDCl₃): δ 8.89 (d, *J* = 8.1 Hz, 1H), 8.71 (ddt, *J* = 4.8, 1.7, 0.8 Hz, 1H), 8.30 (ddt, *J* = 6.5, 1.3, 0.6 Hz, 1H), 8.17 (dd, *J* = 8.0, 2.2 Hz, 1H), 7.82 (dddd, *J* = 8.3, 7.7, 1.8, 0.7 Hz, 1H), 7.40–7.29 (m, 2H), 7.30–7.21 (m, 1H) ppm.

The chemical shifts are in agreement with previous reported values.[117]

4.10.3 Palladium-catalyzed direct arylations of pyridine *N*-oxides

General procedure:

Based on reported procedure,[117] an oven-dried Schlenk flask was charged with pyridine *N*-oxide (2.0 equiv.), bromopyridine (1.0 equiv.), K_3PO_4 (2.0 equiv.), cyclometalated palladium complex **A** (2.5 mol%) and toluene (c = 1.0 M) inside the glovebox. The flask was brought outside the glovebox and placed in a pre-heated oil bath. After stirring at 120 °C for 24–48 h, the reaction mixture was cooled to room temperature and directly subjected to column chromatography.

6-Methyl-2,2′-bipyridine *N*-oxide (20b)

[CCT 1099/FW 2016]
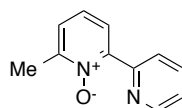
According to the general procedure, reaction of 2-picolin *N*-oxide (5.55 g, 50.9 mmol), 2-bromo-pyridine (7.80 g, 50.0 mmol), K_3PO_4 (11.0 g, 51.8 mmol), complex **A** (421 mg, 0.58 mmol) in toluene (40.0 mL) provided bipyridine *N*-oxide **20b** (711 mg, 3.82 mmol, 8%) as brown oil besides complex product mixtures after column chromatography (acetone/hexane mixtures 1:0, the 3:2, 0:1).

[SZ 2079]

Alternatively, the reaction of 2-picolin *N*-oxide (1.09 g, 10.0 mmol), 2-bromopyridine (810 mg, 5.13 mmol), K_3PO_4 (2.17 g, 10.2 mmol), Pd(OAc)$_2$ (56.4 mg, 0.25 mmol) and P^{t}Bu$_3$ (66.5 mg, 0.33 mmol) in toluene (10.0 mL) provided bipyridine *N*-oxide **20b** (197 mg, 1.06 mmol, 22%) as bright orange oil and recovered 2-picolin *N*-oxide (643 mg, 5.88 mmol, 59%) after column chromatography (MeOH in DCM mixtures: 0–10%, 1% increments).

^{1}H NMR (400 MHz, CDCl$_3$): δ 8.80 (dt, J = 8.1, 1.1 Hz, 1H), 8.71 (ddd, J = 4.8, 1.8, 0.9 Hz, 1H), 7.98 (dd, J = 7.6, 2.7 Hz, 1H), 7.80 (td, J = 7.8, 1.9 Hz, 1H), 7.32 (ddd, J = 7.5, 4.8, 1.2 Hz, 1H), 7.30–7.23 (m, 2H), 2.58 (s, 3H) ppm.

The chemical shifts are in agreement with previous reported values.[99c]

6-Ethoxycarbony-2,2′-bipyridine *N*-oxide (20c)

[FW 2005]
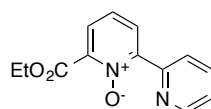
According to the general procedure, reaction of 2-(ethoxycarbonyl)pyridine *N*-oxide (12.1 g, 72.3 mmol), 2-bromopyridine (6.00 g, 38.0 mmol), K$_3$PO$_4$ (15.6 g, 73.3 mmol), complex **A** (743 mg, 1.01 mmol) in toluene (80.0 mL) provided bipyridine *N*-oxide **20c** (5.48 g, 22.4 mmol, 59%) as brown oil, bipyridine **24a** (500 mg, 3.20 mmol, 17%) and recovered 2-(ethoxycarbonyl)pyridine *N*-oxide (5.41 g, 32.4 mmol, 45%) after column chromatography (acetone/hexane mixtures 1:0, then 3:2, 0:1).

^{1}H NMR (400 MHz, CDCl$_3$): δ 8.93 (dt, *J* = 8.1, 1.1 Hz, 1H), 8.72 (ddd, *J* = 4.8, 1.9, 0.9 Hz, 1H), 8.28 (dd, *J* = 8.1, 2.2 Hz, 1H), 7.81 (ddd, *J* = 8.1, 7.6, 1.9 Hz, 1H), 7.48 (dd, *J* = 7.7, 2.2 Hz, 1H), 7.38 (t, *J* = 7.9 Hz, 1H), 7.35 (ddd, *J* = 7.6, 4.8, 1.2 Hz, 1H), 4.49 (q, *J* = 7.1 Hz, 2H), 1.42 (t, *J* = 7.2 Hz, 3H) ppm.

The chemical shifts are in agreement with previous reported values.[117]

6-Trifluoromethyl-2,2′-bipyridine *N*-oxide (20d)

[CCT 1098]
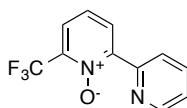
According to the general procedure, reaction of 2-(trifluoromethyl)pyridine *N*-oxide (695 mg, 4.26 mmol), 2-bromopyridine (695 mg, 4.40 mmol), K$_3$PO$_4$ (988 mg, 4.65 mmol), complex **A** (71.0 mg, 0.10 mmol) in toluene (5.00 mL) provided the bipyridine *N*-oxide **20d** (518 mg, 2.15 mmol, 49%) as yellow oil.

^{1}H NMR (400 MHz, CDCl$_3$): δ 8.85 (ddt, *J* = 8.1, 2.1, 1.1 Hz, 1H), 8.69 (dtd, *J* = 4.7, 1.9, 0.9 Hz, 1H), 8.37 (dt, *J* = 8.2, 2.1 Hz, 1H), 7.78 (ddt, *J* = 8.1, 7.5, 1.8 Hz, 1H), 7.69 (dt, *J* = 7.9, 1.9 Hz, 1H), 7.39 (tdd, *J* = 8.0, 1.7, 0.8 Hz, 1H), 7.33 (dddd, *J* = 7.7, 4.7, 1.8, 1.1 Hz, 1H) ppm.

^{13}C NMR (101 MHz, CDCl$_3$): δ 149.6, 148.4, 139.5 (q, *J* = 32.7 Hz), 136.3, 130.8, 125.7, 124.9, 124.7 (q, *J* = 4.1 Hz), 124.2, 120.2 (q, *J* = 272.1 Hz) ppm.

^{19}F NMR (376 MHz, CDCl$_3$): δ –68.62 ppm.

HRESI-MS (MeOH, +, *m/z*): [M+H]$^+$ 241.0597, calc. 241.0583, [M+Na]$^+$ 263.0442, calc. 263.0403

6-Cyano-2,2′-bipyridine *N*-oxide (20e)

[CCT 1096]
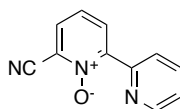
According to the general procedure, reaction of 2-cyanopyridine N-oxide (6.04 g, 50.3 mmol), 2-bromopyridine (6.39 g, 40.4 mmol), K_3PO_4 (11.0 g, 51.8 mmol), and complex **A** (423 mg, 0.58 mmol) in toluene (40.0 mL) provided bipyridine N-oxide **20e** (640 mg, 3.25 mmol, 8%) as tan solid.

^{1}H NMR (400 MHz, CDCl$_3$): δ 8.91 (dt, J = 8.1, 1.1 Hz, 1H), 8.73 (ddt, J = 4.8, 2.1, 1.0 Hz, 1H), 8.49 (ddd, J = 8.2, 2.2, 1.0 Hz, 1H), 7.86 (td, J = 8.1, 1.8 Hz, 1H), 7.69 (ddd, J = 7.8, 2.1, 0.8 Hz, 1H), 7.46–7.36 (m, 2H) ppm.

The chemical shifts are in agreement with previous reported values.[117]

5-Methoxy-2,2′-bipyridine N-oxide (20f)

[FW 2007]
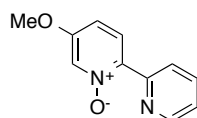
According to the general procedure, reaction of 3-methoxypyridine N-oxide (5.01 g, 40.0 mmol), 2-bromopyridine (3.18 g, 20.1 mmol), K_3PO_4 (8.54 g, 40.1 mmol), complex **A** (340 mg, 0.46 mmol) in toluene (40.0 mL) provided bipyridine N-oxide **20f** (1.42 g, 7.03 mmol, 35%) as brown solid, terpyridine N-oxide **29f** (459 mg, 1.64 mmol, 16%) as brown solid, and recovered 3-methoxypyridine N-oxid (3.27 g, 26.1 mmol, 65%) after column chromatography (acetone in hexane mixtures: 0–100%, 10% increments).

^{1}H NMR (500 MHz, CDCl$_3$): δ 8.81 (dt, J = 8.2, 1.1 Hz, 1H), 8.65 (ddd, J = 4.8, 1.9, 1.0 Hz, 1H), 8.07 (d, J = 9.1 Hz, 1H), 8.01 (d, J = 2.4 Hz, 1H), 7.76 (td, J = 7.8, 1.9 Hz, 1H), 7.26 (ddd, J = 7.6, 4.7, 1.2 Hz, 1H), 6.97 (dd, J = 9.1, 2.4 Hz, 1H), 3.85 (s, 3H) ppm.

^{13}C NMR (126 MHz, CDCl$_3$): δ 157.4, 149.7, 149.3, 141.1, 136.3, 127.9, 127.6, 125.2, 123.8, 114.1, 56.3 ppm.

IR (v/cm^{-1}): 3058 (w), 3043 (w), 2922 (m), 2852 (w), 1666 (m), 1610 (m), 1569 (m), 1514 (s), 1462 (s), 1440 (s), 1388 (s), 1312 (s), 1292 (s), 1252 (w), 1206 (s), 1185 (w), 1114 (m), 1060 (w), 1042 (m), 1022 (m), 972 (s), 942 (w), 885 (w), 863 (m), 812 (m), 776 (s), 737 (m), 717 (w).

HRESI-MS (MeOH, +, m/z): [M+H]$^+$ 203.0841, calc. 203.0815, [M+Na]$^+$ 225.0666, calc. 225.0634, [M+K]$^+$ 241.0401, calc. 241.0374

M.p.: 67 °C

5′-Methoxy-2,2′:6,2″-terpyridine N-oxide (29f)
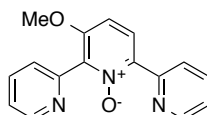
^{1}H NMR (500 MHz, CDCl$_3$): δ 8.83–8.77 (m, 2H), 8.67 (d, J = 3.9 Hz, 1H), 8.23 (d, J = 9.1 Hz, 1H), 7.83 (td, J = 7.7, 1.8 Hz, 1H), 7.71 (td, J = 7.8, 1.9 Hz, 1H), 7.51 (dt, J = 7.8, 1.1 Hz, 1H), 7.35 (ddd, J = 7.7, 4.9, 1.2 Hz, 1H), 7.30–7.21 (m, 1H), 7.11 (d, J = 9.2 Hz, 1H), 3.83 (s, 3H) ppm.

^{13}C NMR (126 MHz, CDCl$_3$): δ 156.0, 150.2, 150.0, 149.2, 141.6, 141.5, 136.6, 136.1, 127.1, 126.2, 125.5, 123.7, 123.6, 120.7, 109.9, 56.7 ppm.

IR (v/cm^{-1}): 3058 (w), 3002 (w), 2957 (w), 2922 (m), 2851 (w) 1651 (m), 1604 (m), 1585 (w), 1562 (m), 1498 (m), 1469 (m), 1454 (m), 1425 (s), 1360 (s), 1294 (m), 1270 (m), 1223 (w), 1209 (m), 1177 (w), 1150 (m), 1132 (w), 1082 (s), 1036 (m), 988 (m), 965 (w), 820 (w), 779 (s), 745 (s), 727 (m).

HRESI-MS (MeOH, +, m/z): [M+H]$^+$ 280.1116, calc. 280.1081, [M+Na]$^+$ 302.0941, calc. 302.0900, [M+K]$^+$ 318.0679, calc. 318.0639

M.p.: 143 °C

5-Methyl-2,2′-bipyridine N-oxide (20g)

[CCT 1092/FW 2018]
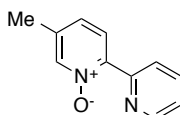
Similar to the general procedure, reaction of 3-picolin N-oxide (11.0 g, 101 mmol), 2-bromopyridine (7.90 g, 50.0 mmol), K$_3$PO$_4$ (21.0 g, 98.9 mmol), Pd(OAc)$_2$ (280 mg, 1.25 mmol), P^{t}Bu$_3$ (303 mg, 1.50 mmol) in toluene (70.0 mL) provided bipyridine N-oxide **20g** (1.85 g, 9.95 mmol, 20%) as off-white solid, and bipyridine **24a** (339 mg, 2.17 mmol, 9%) after column chromatography (acetone in hexane mixtures: 0–80%, 10% increments).

^{1}H NMR (500 MHz, CDCl$_3$): δ 8.84 (dt, J = 8.1, 1.1 Hz, 1H), 8.66 (ddd, J = 4.8, 1.9, 1.0 Hz, 1H), 8.13 (dt, J = 1.7, 0.8 Hz, 1H), 8.02 (d, J = 8.2 Hz, 1H), 7.76 (td, J = 7.8, 1.9 Hz, 1H), 7.27 (ddd, J = 7.7, 4.9, 1.3 Hz, 1H), 7.14 (ddd, J = 8.3, 1.7, 0.8 Hz, 1H), 2.29 (d, J = 0.8 Hz, 3H) ppm.

^{13}C NMR (126 MHz, CDCl$_3$): δ 149.8, 149.3, 144.7, 140.4, 136.3, 136.1, 127.3, 127.2, 125.4, 124.0, 18.1 ppm.

IR (v/cm^{-1}): 3048 (w), 2996 (w), 2921 (w), 2854 (w), 1699 (w), 1613 (w), 1580 (m), 1570 (m), 1497 (w), 1455 (m), 1435 (m), 1377 (s), 1300 (w), 1272 (s), 1236 (w), 1208 (s), 1167 (m), 1151 (m), 1137 (w), 1092 (m), 1054 (w), 1033 (m), 1019 (w), 990 (w), 953 (m), 902 (w), 859 (m), 825 (s), 783 (s), 742 (s), 729 (w), 717 (m).

HRESI-MS (MeOH, +, m/z): [M+H]$^+$ 187.0888, calc. 187.0866, [M+Na]$^+$ 209.0712, calc. 209.0685, [M+K]$^+$ 225.0602, calc. 225.0425

M.p.: 65 °C

5-(Methoxycarbonyl)-2,2′-bipyridine *N*-oxide (20h)

[FW 2009]
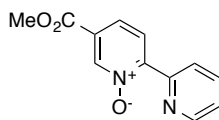
According to the general procedure, reaction of 3-(methoxycarbonyl)pyridine *N*-oxide (15.0 g, 98.2 mmol), 2-bromopyridine (7.78 g, 49.2 mmol), K$_3$PO$_4$ (20.9 g, 98.4 mmol), complex **A** (900 mg, 1.23 mmol) in toluene (100 mL) provided bipyridine *N*-oxide **20h** (8.14 g, 35.3 mmol, 72%) as off-white solid, bipyridine **24a** (463 mg, 2.97 mmol, 12%) and recovered 3-(methoxycarbonyl)pyridine *N*-oxide (7.63 g, 49.9 mmol, 51%) after column chromatography (acetone in hexane mixtures: 0–90%, 10% increments).

^{1}H NMR (400 MHz, CDCl$_3$): δ 9.00 (dt, *J* = 8.1, 1.1 Hz, 1H), 8.90 (dd, *J* = 1.6, 0.6 Hz, 1H), 8.75 (ddd, *J* = 4.8, 1.8, 0.9 Hz, 1H), 8.33 (dd, *J* = 8.4, 0.6 Hz, 1H), 7.91 (dd, *J* = 8.4, 1.6 Hz, 1H), 7.86 (ddd, *J* = 8.1, 7.6, 1.9 Hz, 1H), 7.40 (ddd, *J* = 7.6, 4.8, 1.2 Hz, 1H), 3.99 (s, 3H) ppm.

The chemical shifts are in agreement with previous reported values.[117]

5-Nitro-2,2′-bipyridine *N*-oxide (20i)

[FW 2003]
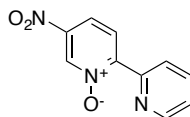
According to the general procedure, reaction of 3-nitropyridine *N*-oxide (2.05 g, 14.6 mmol), 2-bromopyridine (1.16 g, 7.34 mmol), K$_3$PO$_4$ (3.04 g, 14.3 mmol), complex **A** (285 mg, 0.39 mmol) in toluene (15.0 mL) provided bipyridine *N*-oxide **20i** (209 mg, 0.96 mmol, 13%) as yellow solid, terpyridine *N*-oxide **29i** (28.6 mg, 0.10 mmol, 3%), bipyridine **24a** (28.3 mg, 0.18 mmol, 5%) and recovered 3-nitropyridine *N*-oxide (851 mg, 6.04 mmol, 41%) after column chromatography (acetone in hexane mixtures: 0–40%, 10% increments, then pure acetone).

^{1}H NMR (500 MHz, CDCl$_3$): δ 9.10 (d, *J* = 2.2 Hz, 1H), 9.01 (dt, *J* = 7.9, 1.0 Hz, 1H), 8.75 (dt, *J* = 4.8, 1.3 Hz, 1H), 8.48 (d, *J* = 9.0 Hz, 1H), 8.04 (dd, *J* = 9.0, 2.1 Hz, 1H), 7.86 (td, *J* = 7.8, 1.8 Hz, 1H), 7.41 (ddd, *J* = 7.5, 4.7, 1.2 Hz, 1H) ppm.

^{13}C NMR (126 MHz, CDCl$_3$): δ 151.9, 149.9, 147.8, 145.6, 137.3, 136.7, 128.0, 125.8, 125.6, 119.2 ppm.

IR (ν/cm^{-1}): 3111 (w), 3053 (m), 2919 (w), 2856 (w), 1682 (w), 1610 (w), 1574 (m), 1552 (m), 1510 (s, NO$_2$), 1487 (w), 1458 (m), 1440 (w), 1385 (m), 1352 (s), 1296 (w), 1268 (s), 1239 (w), 1219 (w),

1093 (m), 1056 (w), 1031 (m), 992 (w), 965 (m), 956 (m), 900 (m), 833 (w), 820 (s), 784 (s), 736 (s), 716 (w), 678 (w).

HRESI-MS (MeOH, +, *m/z*): [M+H]$^+$ 218.0576, calc. 218.0560, [M+Na]$^+$ 240.0404, calc. 240.0380, [M+K]$^+$ 256.0128, calc. 256.0119

M.p.: 154 °C

5′-Nitro-2,2′:6,2″-terpyridine *N*-oxide (**29i**)
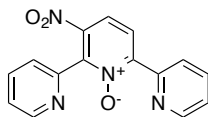
^{1}H NMR (500 MHz, CDCl$_3$): δ 8.88 (dt, *J* = 8.0, 1.0 Hz, 1H), 8.79 (ddd, *J* = 4.9, 1.8, 0.9 Hz, 1H), 8.73 (d, *J* = 5.0 Hz, 1H), 8.46 (d, *J* = 8.9 Hz, 1H), 7.98–7.87 (m, 3H), 7.84 (td, *J* = 7.8, 1.8 Hz, 1H), 7.48–7.41 (m, 2H) ppm.

^{13}C NMR (126 MHz, CDCl$_3$): δ 150.2, 149.8, 148.4, 148.3, 147.9, 145.3, 136.53, 136.52, 127.1, 126.2, 125.9, 125.7, 125.4, 124.7, 120.1 ppm.

IR (*v*/cm^{-1}): 3063 (w), 2952 (w), 2923 (w), 2856 (w) 1669 (w), 1557 (w), 1540 (s), 1455 (w), 1427 (m), 1352 (s, NO$_2$), 1271 (m), 1254 (w), 1225 (w), 1152 (m), 1092 (w), 1034 (m), 982 (m), 831 (w), 811 (m), 796 (s, NO$_2$), 784 (w), 756 (s), 746 (m), 709 (w), 672 (w).

HRESI-MS (MeOH, +, *m/z*): [M+H]$^+$ 295.0823, calc. 295.0826, [M+Na]$^+$ 317.0642, calc. 317.0645

4-Methoxy-2,2′-bipyridine *N*-oxide (20j)

[JB 0018/VA 1001]
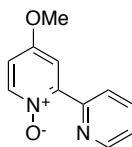
Similar to the general procedure, reaction of 4-methoxypyridine *N*-oxide (12.4 g, 99.1 mmol), 2-bromopyridine (7.77 g, 49.5 mmol), K$_3$PO$_4$ (20.0 g, 94.5 mmol), Pd(OAc)$_2$ (558, 2.49 mmol), P^{t}Bu$_3$ (622 mg, 3.07 mmol) in toluene (100 mL) provided bipyridine *N*-oxide **20j** (1.46 g, 7.20 mmol, 15%) as yellow solid, bipyridine **24a** (2.16 g, 13.8 mmol, 56%) and recovered 4-methoxypyridine *N*-oxide (4.25 g, 34.0 mmol, 34%) after column chromatography (MeOH in DCM mixtures: 0–10%, 1% increments).

^{1}H NMR (400 MHz, CDCl$_3$): δ 8.97 (dq, *J* = 8.1, 1.2 Hz, 1H), 8.68 (ddd, *J* = 4.8, 1.9, 1.0 Hz, 1H), 8.19 (dd, *J* = 7.3, 1.0 Hz, 1H), 7.80 (ddt, *J* = 8.1, 7.5, 1.5 Hz, 1H), 7.69 (dd, *J* = 3.6, 1.2 Hz, 1H), 7.33 (ddt, *J* = 7.3, 4.8, 1.2 Hz, 1H), 6.82 (ddd, *J* = 7.2, 3.6, 1.1 Hz, 1H), 3.90 (s, 3H) ppm.

The chemical shifts are in agreement with previous reported values.[169e]

4-Chloro-2,2′-bipyridine *N*-oxide (20k)

[FW 2004]
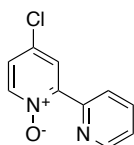
According to the general procedure, reaction of 4-chloropyridine *N*-oxide (3.89 g, 30.0 mmol), 2-bromopyridine (2.39 g, 15.1 mmol), K_3PO_4 (6.52 g, 30.6 mmol), complex **A** (275 mg, 0.37 mmol) in toluene (30.0 mL) provided bipyridine *N*-oxide **20k** (1.27 g, 6.12 mmol, 41%) as grey solid, terpyridine *N*-oxide **29k** (246 mg, 0.88 mmol, 12%), bipyridine **24a** (159 mg, 1.01 mmol, 13%) and recovered 4-chloropyridine *N*-oxide (1.62 g, 12.5 mmol, 42%) after column chromatography (acetone in hexane mixtures: 0–100%, 10% increments).

^{1}H NMR (400 MHz, CDCl₃): δ 8.96 (dt, *J* = 8.1, 1.1 Hz, 1H), 8.72 (ddd, *J* = 4.8, 1.9, 0.9 Hz, 1H), 8.26 (d, *J* = 3.1 Hz, 1H), 8.22 (d, *J* = 7.0 Hz, 1H), 7.84 (td, *J* = 7.8, 1.8 Hz, 1H), 7.37 (ddd, *J* = 7.6, 4.8, 1.2 Hz, 1H), 7.23 (dd, *J* = 7.0, 3.1 Hz, 1H) ppm.

The chemical shifts are in agreement with previous reported values.[117]

4′-Chloro-2,2′:6,2″-terpyridine *N*-oxide (**29k**)
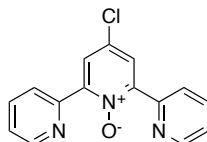
^{1}H NMR (400 MHz, CDCl₃): δ 8.77–8.74 (m, 4H), 8.13 (s, 2H), 7.84 (td, *J* = 7.9, 1.6 Hz, 2H), 7.39 (ddd, *J* = 7.6, 4.6, 1.3 Hz, 2H) ppm.

The chemical shifts are in agreement with previous reported values.[117]

4-Ethoxycarbonyl-2,2′-bipyridine *N*-oxide (20l)

[SZ 2007]
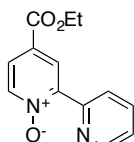
According to the general procedure, reaction of 4-(ethoxycarbonyl)pyridine *N*-oxide (974 mg, 4.00 mmol), 2-bromopyridine (0.19 mL, 2.00 mmol), K_3PO_4 (849 mg, 4.00 mmol), complex **A** (37.0 mg, 0.05 mmol) in toluene (4.00 mL) provided bipyridine *N*-oxide **20l** (326 mg, 1.34 mmol, 67%) as orange solid, terpyridine *N*-oxide **29l** (47.0 mg, 0.15 mmol, 15%) and recovered 4-

(ethoxycarbonyl)pyridine *N*-oxide (381 mg, 2.28 mmol, 39%) after column chromatography (acetone in hexane mixtures: 0–100%, 10% increments).

^{1}H NMR (400 MHz, CDCl$_3$): δ 8.82 (dd, *J* = 8.1, 1.0 Hz, 1H), 8.82–8.73 (m, 2H), 8.35 (d, *J* = 6.8 Hz, 1H), 7.92–7.79 (m, 2H), 7.38 (ddt, *J* = 7.0, 4.8, 1.1 Hz, 1H), 4.42 (q, *J* = 7.1 Hz, 2H), 1.42 (td, *J* = 7.1, 1.0 Hz, 3H) ppm.

The chemical shifts are in agreement with previous reported values.[117]

4′-Ethoxycarbonyl-2,2′:6,2″-terpyridine *N*-oxide (**29l**)
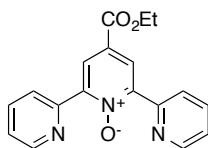
^{1}H NMR (400 MHz, CDCl$_3$): δ 8.76 (d, *J* = 4.8 Hz, 2H), 8.62 (s, 2H), 8.58 (d, *J* = 8.1 Hz, 2H), 7.80 (td, *J* = 7.7, 1.5 Hz, 2H), 7.35 (dd, *J* = 7.5, 4.8 Hz, 2H), 4.40 (q, *J* = 7.1 Hz, 2H), 1.39 (t, *J* = 7.1 Hz, 3H) ppm.

The chemical shifts are in agreement with previous reported values.[117]

4-Trifluoromethyl-2,2′-bipyridine *N*-oxide (20m)

[SZ 2038]
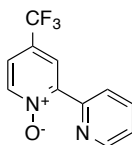
According to the general procedure, reaction of 4-(trifluoromethyl)pyridine *N*-oxide (653 mg, 4.00 mmol), 2-bromopyridine (0.19 mL, 2.00 mmol), K$_3$PO$_4$ (851 mg, 4.01 mmol), complex **A** (36.9 mg, 0.05 mmol) in toluene (4.00 mL) provided bipyridine *N*-oxide **20m** (420 mg, 1.75 mmol, 87%) as pale yellow solid, terpyridine *N*-oxide **29m** (32.0 mg, 0.10 mmol, 10%) and recovered 4-(trifluoromethyl)pyridine *N*-oxide (338 mg, 3.92 mmol, 52%) after column chromatography (acetone in hexane mixtures: 0–100%, 10% increments).

^{1}H NMR (400 MHz, CDCl$_3$): δ 8.90 (dt, *J* = 8.1, 1.0 Hz, 1H), 8.73 (ddd, *J* = 4.7, 1.7, 0.8 Hz, 1H), 8.52 (d, *J* = 2.7 Hz, 1H), 8.35 (d, *J* = 6.9 Hz, 1H), 7.83 (td, *J* = 7.8, 1.8 Hz, 1H), 7.44 (dd, *J* = 6.8, 2.8 Hz, 1H), 7.37 (ddd, *J* = 7.6, 4.7, 1.1 Hz, 1H) ppm.

The chemical shifts are in agreement with previous reported values.[117]

4′-Trifluoromethyl-2,2′:6,2″-terpyridine *N*-oxide (**29m**)
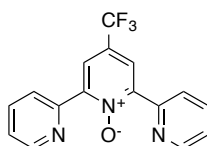
^{1}H NMR (400 MHz, CDCl$_3$): δ 8.77 (dd, *J* = 4.8, 0.9 Hz, 2H), 8.72 (d, *J* = 8.0 Hz, 2H), 8.38 (s, 2H), 7.85 (td, *J* = 7.8, 1.8 Hz, 2H), 7.40 (ddd, *J* = 7.6, 4.8, 1.2 Hz, 2H) ppm.

The chemical shifts are in agreement with previous reported values.[117]

4-Cyano-2,2′-bipyridine *N*-oxide (20n)

[CCT 1091/FW 2002]
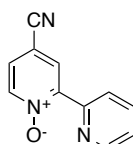
Similar to the general procedure, reaction of 4-cyanopyridine *N*-oxide (12.0 g, 100 mmol), 2-bromo-pyridine (7.90 g, 50.0 mmol), K$_3$PO$_4$ (851 mg, 4.01 mmol), Pd(OAc)$_2$ (280 mg, 1.25 mmol) and P^{t}Bu$_3$ (303 mg, 1.50 mmol) in toluene (70.0 mL) provided bipyridine *N*-oxide **20n** (2.62 g, 13.3 mmol, 27%) and terpyridine *N*-oxide **29n** (310 mg, 1.14 mmol, 5%) as yellow solids after column chromatography (acetone in hexane mixtures: 0–50%, 10% increments).

^{1}H NMR (400 MHz, CDCl$_3$): δ 8.88 (dt, *J* = 8.1, 1.1 Hz, 1H), 8.76 (ddd, *J* = 4.8, 1.8, 0.9 Hz, 1H), 8.61 (dd, *J* = 2.6, 0.6 Hz, 1H), 8.32 (dd, *J* = 6.8, 0.6 Hz, 1H), 7.87 (ddd, *J* = 8.2, 7.6, 1.8 Hz, 1H), 7.47 (dd, *J* = 6.9, 2.6 Hz, 1H), 7.42 (ddd, *J* = 7.6, 4.8, 1.1 Hz, 1H) ppm.

The chemical shifts are in agreement with previous reported values.[117]

4′-Cyano-2,2′:6,2″-terpyridine *N*-oxide (**29n**)
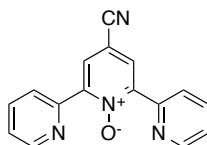
^{1}H NMR (400 MHz, CDCl$_3$): δ 8.78 (ddd, *J* = 4.8, 1.8, 1.0 Hz, 2H), 8.70 (dt, *J* = 8.1, 1.1 Hz, 2H), 8.42 (s, 2H), 7.86 (td, *J* = 7.8, 1.8 Hz, 2H), 7.42 (ddd, *J* = 7.6, 4.8, 1.2 Hz, 2H) ppm.

The chemical shifts are in agreement with previous reported values.[117]

6′-Methoxy-2,2′-bipyridine *N*-oxide (20p)

[CCT 1090]
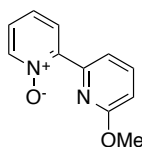
Similar to the general procedure, reaction of pyridine *N*-oxide (5.00 g, 52.6 mmol), 6-methoxy-2-bromopyridine (4.40 g, 23.4 mmol), K$_3$PO$_4$ (10.5 g, 49.5 mmol), Pd(OAc)$_2$ (270 mg, 1.20 mmol) and P^{t}Bu$_3$ (290 mg, 1.43 mmol) in toluene (40.0 mL) provided bipyridine *N*-oxide **20p** (3.05 g, 15.1 mmol, 64%) and terpyridine *N*-oxide **29p** (482 mg, 1.56 mmol, 13%) as colorless solids after column chromatography (MeOH in DCM: 0–10%, 1% increments).

^{1}H NMR (400 MHz, CDCl$_3$): δ 8.76 (dd, *J* = 7.6, 0.8 Hz, 1H), 8.35 (dd, *J* = 8.1, 2.2 Hz, 1H), 8.31 (dt, *J* = 6.5, 1.1 Hz, 1H), 7.72 (ddd, *J* = 8.3, 7.5, 0.8 Hz, 1H), 7.35 (ddt, *J* = 8.0, 7.3, 1.4 Hz, 1H), 7.23 (dddd, *J* = 7.5, 6.5, 2.3, 1.1 Hz, 1H), 6.83 (dt, *J* = 8.3, 0.8 Hz, 1H), 3.99 (d, *J* = 0.8 Hz, 3H) ppm.

^{13}C NMR (101 MHz, CDCl$_3$): δ 163.3, 147.2 146.1, 141.2, 139.4, 127.7, 125.6, 124.8, 118.9, 112.5, 53.5 ppm.

IR (*v*/cm^{-1}): 3070 (w), 2968 (w), 1583 (m), 1576 (m), 1483 (w), 1466 (m), 1424 (m), 1396 (m), 1335 (m), 1263 (m), 1229 (m), 1208 (m), 1154 (m), 118 (w), 1072 (w), 1044 (w), 1017 (m), 984 (w), 894 (w), 828 (m), 805 (m), 770 (s), 740 (m), 701 (w).

HRESI-MS (MeOH, +, *m/z*): [M+H]$^+$ 203.0803, calc. 203.0815, [M+Na]$^+$ 225.0647, calc. 225.0634

M.p.: 90–91 °C

6,6″-Dimethoxy-2,2′:6′,2″-terpyridine *N*-oxide (29p)
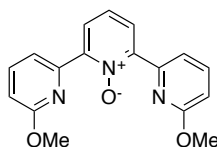
^{1}H NMR (400 MHz, CDCl$_3$): δ 8.53 (dt, *J* = 7.6, 0.8 Hz, 2H), 8.19 (dd, *J* = 8.0, 0.7 Hz, 2H), 7.71 (ddd, *J* = 8.3, 7.5, 0.7 Hz, 2H), 7.44 (td, *J* = 8.0, 0.7 Hz, 1H), 6.83 (dt, *J* = 8.3, 0.8 Hz, 2H), 4.01 (d, *J* = 0.7 Hz, 6H) ppm.

^{13}C NMR (101 MHz, CDCl$_3$): δ 163.5, 148.3, 147.2, 139.1, 127.2, 125.0, 119.0, 111.9, 53.5 ppm.

IR (*v*/cm^{-1}): 2983 (w), 2952 (w), 1577 (m), 1487 8w), 1459 (m), 1422 (m), 1407 (m), 1323 (w), 1256 (s), 1237 (s), 1152 (w), 1077 (w), 1020 (m), 986 (w), 940 (w), 878 (w), 827 (w), 796 (w), 778 (s), 729 (s).

HRESI-MS (MeOH, +, *m/z*): [M+H]$^+$ 310.1169, calc. 310.1186, [M+Na]$^+$ 332.1037, calc. 332.1006, [M+K]$^+$ 348.0723, calc. 348.0745

M.p.: 141 °C

6′-Methyl-2,2′-bipyridine *N*-oxide (20q)

[CCT 1089]
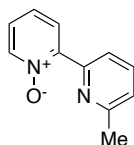
Similar to the general procedure, reaction of pyridine *N*-oxide (5.00 g, 52.6 mmol), 6-methyl-2-bromopyridine (4.30 g, 25.0 mmol), K$_3$PO$_4$ (10.5 g, 49.5 mmol), Pd(OAc)$_2$ (280 mg, 1.25 mmol) and P^{t}Bu$_3$ (305 mg, 1.51 mmol) in toluene (40.0 mL) provided bipyridine *N*-oxide **20q** (1.90 g, 10.2 mmol, 41%) as reddish oil and terpyridine *N*-oxide **29q** (176 mg, 0.63 mmol, 5%) as tan solid after column chromatography (MeOH in DCM 2%).

^{1}H NMR (400 MHz, CDCl$_3$): δ 8.65 (dt, *J* = 7.9, 0.8 Hz, 1H), 8.30 (ddd, *J* = 6.5, 1.2, 0.6 Hz, 1H), 8.17 (dd, *J* = 8.0, 2.2 Hz, 1H), 7.71 (t, *J* = 7.8 Hz, 1H), 7.35 (ddd, *J* = 8.1, 7.5, 1.3 Hz, 1H), 7.27–7.22 (m, 1H), 7.20 (ddd, *J* = 7.8, 1.1, 0.6 Hz, 1H), 2.61 (s, 3H) ppm.

^{13}C NMR (101 MHz, CDCl$_3$): δ 158.3, 149.0, 147.8, 140.8, 136.6, 128.1, 125.8, 125.1, 124.0, 122.6, 24.7 ppm.

IR (v/cm^{-1}): 3112 (w), 3061 (w), 1608 (w), 1584 (m), 1572 (m), 1486 (w), 1453 (s), 1424 (s), 1315 (w), 1247 (m), 1221 (s), 1159 (w), 1117 (w), 1082 (w), 1042 (w), 995 (w), 880 (m), 825 (m), 800 (m), 764 (s), 744 (m), 723 (w), 702 (w).

HRESI-MS (MeOH, +, *m/z*): [M+H]$^+$ 187.0885, calc. 187.0866

6,6″-Dimethyl-2,2′:6′,2″-terpyridine *N*-oxide (**29q**)
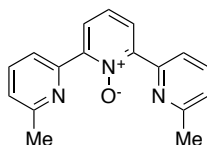
^{1}H NMR (400 MHz, CDCl$_3$): δ 8.44 (ddd, *J* = 7.9, 1.1, 0.6 Hz, 1H), 8.03 (d, *J* = 7.9 Hz, 1H), 7.69 (t, *J* = 7.8 Hz, 1H), 7.44 (t, *J* = 7.9 Hz, 1H), 7.21 (ddd, *J* = 7.6, 1.1, 0.5 Hz, 1H), 2.64 (s, 3H) ppm.

^{13}C NMR (101 MHz, CDCl$_3$): δ 158.3, 150.0, 148.6, 136.4, 127.7, 125.6, 123.8, 122.9, 24.7 ppm.

IR (v/cm^{-1}): 3054 (w), 2977 8w), 2921 (w), 1584 (m), 1573 (m), 1496 (w), 1475 (w), 1446 (m), 1369 (s), 1326 (w), 1303 (w), 1242 (s), 1218 (s), 1167 (w), 1092 (w), 1077 8w), 1032 (w), 998 (w), 944 (w), 920 (w), 889 (w), 870 (w), 810 (m), 772 (s), 733 (s), 697 (w), 677 (w).

HRESI-MS (MeOH, +, *m/z*): [M+H]$^+$ 278.1303, calc. 278.1288

M.p.: 151–155 °C

6′-(Trifluoromethyl)-2,2′-bipyridine *N*-oxide (20r)

[CCT 1093]
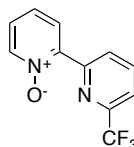
According to the general procedure, reaction of pyridine *N*-oxide (1.35 g, 14.2 mmol), 6-(trifluoromethyl)-2-bromopyridine (1.22 g, 5.40 mmol), K_3PO_4 (2.60 g, 12.3 mmol), complex **A** (80.0 mg, 0.11 mmol) in toluene (10.0 mL) provided bipyridine *N*-oxide **20r** (838 mg, 3.49 mmol, 65%) as pale yellow solid, terpyridine *N*-oxide **29r** (111 mg, 0.29 mmol, 11%) and bipyridine **24r** (87.6 mg, 0.30 mmol, 11%) after column chromatography (acetone in hexane mixtures: 0–100%, 10% increments).

^{1}H NMR (400 MHz, CDCl$_3$): δ 9.18 (dt, J = 8.2, 0.8 Hz, 1H), 8.30 (ddd, J = 6.4, 1.3, 0.6 Hz, 2H), 8.27 (dd, J = 8.1, 2.2 Hz, 1H), 7.99 (ddt, J = 8.4, 7.8, 0.7 Hz, 1H), 7.71 (dt, J = 7.7, 0.7 Hz, 1H), 7.43–7.34 (m, 1H), 7.30 (tdd, J = 7.1, 2.2, 0.6 Hz, 1H) ppm.

^{13}C NMR (101 MHz, CDCl$_3$): δ 150.1, 148.0 (q, J = 35.2 Hz), 146.1, 140.9, 138.0, 128.3, 128.1, 126.1, 126.0, 121.5 (q, J = 274.3 Hz), 120.8 (q, J = 2.7 Hz) ppm.

^{19}F NMR (376 MHz, CDCl$_3$): δ –67.96 ppm.

HRESI-MS (MeOH, +, *m/z*): [M+Na]$^+$ 263.0426, calc. 263.0403

6,6″-Bis(trifluoromethyl)-2,2′:6′,2″-terpyridine *N*-oxide (29r)
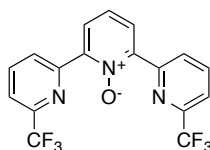
^{1}H NMR (400 MHz, CDCl$_3$): δ 8.97 (d, J = 8.1 Hz, 2H), 8.23 (d, J = 8.0 Hz, 2H), 8.01 (t, J = 7.9 Hz, 2H), 7.75 (d, J = 7.7 Hz, 2H), 7.54 (t, J = 8.0 Hz, 1H) ppm.

^{13}C NMR (101 MHz, CDCl$_3$): δ 150.7, 148.1 (q, J = 35.1 Hz), 147.1, 137.7, 128.9, 128.3, 126.0, 121.5 (q, J = 274.4 Hz), 120.8 (q, J = 2.8 Hz) ppm.

^{19}F NMR (376 MHz, CDCl$_3$): δ –67.92 ppm.

IR (v/cm^{-1}): 3082 (w), 1588 (w), 1453 (w), 1426 (w), 1375 (w), 1338 (s), 1239 (m), 1212 (s), 1173 (m), 1111 (s), 1059 (m), 994 (w), 922 (w), 890 (w), 854 (w), 834 (w), 790 (m), 743 (m), 714 (w), 695 (w), 668 (m).

HRESI-MS (MeOH, +, *m/z*): [M+H]$^+$ 386.0719, calc. 386.0723, [M+Na]$^+$ 408.0547, calc. 408.0542, [M+K]$^+$ 424.0274, calc. 424.0281

M.p.: 188–190 °C

6,6′-Bis(trifluoromethyl)-2,2′-biypridine (24r)
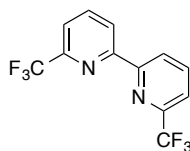
^{1}H NMR (400 MHz, CDCl$_3$): δ 8.72 (d, J = 8.0 Hz, 2H), 8.03 (td, J = 7.9, 0.8 Hz, 2H), 7.74 (dd, J = 7.8, 1.0 Hz, 2H) ppm.

The chemical shifts are in agreement with previous reported values.[238]

5′-Methyl-2,2′-bipyridine *N*-oxide (20s)

[JN 1004]
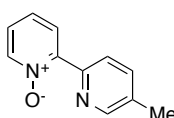
According to the general procedure, reaction of pyridine *N*-oxide (3.29 g, 34.6 mmol), 5-methyl-2-bromopyridine (2.98 g, 17.3 mmol), K$_3$PO$_4$ (7.34 g, 34.6 mmol), complex **A** (320 mg, 0.44 mmol) in toluene (35.0 mL) provided bipyridine *N*-oxide **20s** (438 mg, 2.30 mmol, 13%) as brown solid after column chromatography (MeOH in DCM mixtures: 0–3%, 1% increments).

^{1}H NMR (500 MHz, CDCl$_3$): δ 8.78 (d, J = 8.2 Hz, 1H), 8.52 (d, J = 2.1 Hz, 1H), 8.27 (dd, J = 6.5, 0.8 Hz, 1H), 8.14 (dd, J = 8.1, 2.1 Hz, 1H), 7.61 (ddd, J = 8.2, 2.3, 0.7 Hz, 1H), 7.32 (td, J = 7.8, 1.2 Hz, 1H), 7.22 (ddd, J = 7.4, 6.6, 2.2 Hz, 1H), 2.37 (s, 3H) ppm.

^{13}C NMR (126 MHz, CDCl$_3$): δ 150.0, 147.6, 147.5, 147.0, 140.8, 136.8, 134.4, 127.7, 125.8, 125.0, 18.5 ppm.

IR (v/cm^{-1}): 3384 (w), 3110 (w), 3058 (w), 1565 (w), 1466 (m), 1424 (m), 1246 (m), 1226 (m), 1026 (m), 846 (m), 767 (m), 716 (m).

HRESI-MS (MeOH, +, *m/z*): [M+H]$^+$ 187.0905, calc. 187.0871, [M+Na]$^+$ 209.0726, calc. 209.0691

M.p.: 44–45 °C

4′-Methoxy-2,2′-bipyridine *N*-oxide (20t)

[FW 2014]
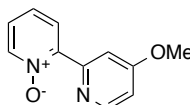
According to the general procedure, reaction of pyridine *N*-oxide (984 mg, 10.3 mmol), 4-methoxy-2-bromopyridine (941 mg, 5.00 mmol), K$_3$PO$_4$ (2.15 g, 10.1 mmol), complex **A** (97.6 mg, 0.13 mmol) in toluene (11.0 mL) provided bipyridine *N*-oxide **20t** (573 mg, 2.35 mmol, 44%), terpyridine *N*-oxide **29t** (52.8 mg, 0.17 mmol, 7%) as brown solids, and bipyridine **24t** (90.8 mg, 0.42 mmol, 17%) and

recovered pyridine *N*-oxide (515 mg, 5.42 mmol, 52%) after column chromatography (acetone in hexane mixtures: 0–90%, 10% increments).

^{1}H NMR (500 MHz, CDCl$_3$): δ 8.55 (d, *J* = 2.6 Hz, 1H), 8.47 (d, *J* = 5.7 Hz, 1H), 8.26 (ddd, *J* = 6.5, 1.3, 0.6 Hz, 1H), 8.17 (dd, *J* = 8.0, 2.2 Hz, 1H), 7.32 (ddd, *J* = 8.1, 7.5, 1.3 Hz, 1H), 7.23 (ddd, *J* = 7.5, 6.5, 2.2 Hz, 1H), 6.83 (dd, *J* = 5.7, 2.6 Hz, 1H), 3.87 (s, 3H) ppm.

^{13}C NMR (126 MHz, CDCl$_3$): δ 165.9, 151.1, 150.3, 147.3, 140.8, 128.1, 125.8, 125.3, 111.22, 111.16, 55.4 ppm.

IR (ν/cm^{-1}): 3112 (w), 3060 (w), 3000 (w), 2967 (w), 2923 (w), 2851 (w), 1701 (w), 1651 (w), 1608 (w), 1585 (m), 1565 (s), 1487 (w), 1467 (m), 1442 (m), 1405 (s), 1311 s, 1273 (m), 1256 (w), 1241 (m), 1203 (w), 1185 (w), 1160 (w), 1111 (w), 1044 (w), 1025 (s), 986 (w), 953 (w), 885 (w), 866 (s), 827 (s), 766 (s), 752 (w), 731 (m).

HRESI-MS (MeOH, +, *m/z*): [M+H]$^+$ 203.0841, calc. 203.0816, [M+Na]$^+$ 225.0666, calc. 225.0634

M.p.: 64 °C

4,4″-Dimethoxy-2,2′:6′,2″-terpyridine *N*-oxide (**29t**)
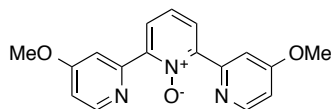
^{1}H NMR (500 MHz, CDCl$_3$): δ 8.51 (d, *J* = 5.7 Hz, 2H), 8.27 (d, *J* = 2.5 Hz, 2H), 8.04 (d, *J* = 7.9 Hz, 2H), 7.42 (t, *J* = 7.9 Hz, 1H), 6.86 (dd, *J* = 5.7, 2.5 Hz, 2H), 3.87 (s, 6H) ppm.

^{13}C NMR (126 MHz, CDCl$_3$): δ 165.8, 152.1, 150.4, 148.3, 127.9, 125.5, 111.3, 55.5 ppm.

IR (ν/cm^{-1}): 3064 (w), 3013 (w), 2923 (m), 2852 (w), 1653 (w), 1608 (w), 1584 (s), 1561 (s), 1509 (w), 1492 (w), 1461 (m), 1427 (w), 1412 (w), 1373 (m), 1320 (w), 1307 (w), 1292 (m), 1259 (w), 1239 (m), 1205 (w), 1186 (w), 1152 (w), 1128 (w), 1117 (w), 1094 (w), 1030 (s), 985 (w), 896 (w), 885 (w), 869 (w), 852 (m), 826 (w), 811 (m), 770 (w), 759 (w), 747 (w), 734 (w), 712 (w).

HRESI-MS (MeOH, +, *m/z*): [M+H]$^+$ 310.1185, calc. 310.1186, [M+Na]$^+$ 332.1005, calc. 332.1006, [M+K]$^+$ 348.0741, calc. 348.0745

M.p.: 167 °C

4,4′-Dimethoxy-2,2′-bipyridine (**24t**)
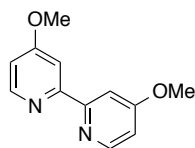
^{1}H NMR (500 MHz, CDCl$_3$): δ 8.47 (d, *J* = 5.7 Hz, 2H), 7.98 (d, *J* = 2.6 Hz, 2H), 6.85 (dd, *J* = 5.7, 2.6 Hz, 2H), 3.95 (s, 6H) ppm.

The chemical shifts are in agreement with previous reported values.[239]

4′-Methyl-2,2′-bipyridine *N*-oxide (20u)

[CCT 1100/FW 2001]
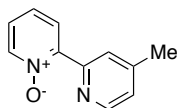
According to the general procedure, reaction of pyridine *N*-oxide (4.98 g, 52.3 mmol), 4-methyl-2-bromopyridine (4.30 g, 25.0 mmol), K$_3$PO$_4$ (11.0 g, 51.8 mmol), complex **A** (420 mg, 0.57 mmol) in toluene (40.0 mL) provided bipyridine *N*-oxide **20u** (1.46 g, 7.85 mmol, 31%) as brown solid, terpyridine *N*-oxide **29u** (135 mg, 0.49 mmol, 4%) as off-white solid after column chromatography (acetone in hexane mixtures: 0–50%, 10% increments).

^{1}H NMR (500 MHz, CDCl$_3$): δ 8.66 (s, 1H), 8.53 (dd, *J* = 4.9, 1.2 Hz, 1H), 8.27 (dt, *J* = 6.4, 1.4 Hz, 1H), 8.09 (dt, *J* = 8.1, 1.7 Hz, 1H), 7.31 (tt, *J* = 7.8, 1.3 Hz, 1H), 7.22 (ddt, *J* = 6.6, 4.4, 1.3 Hz, 1H), 7.12 (d, *J* = 4.0 Hz, 1H), 2.39 (s, 3H) ppm.

^{13}C NMR (126 MHz, CDCl$_3$): δ 149.5, 149.2, 147.5, 140.7, 128.0, 126.3, 125.8, 125.3, 125.2, 21.3 ppm.

IR (*v*/cm^{-1}): 3060 (w), 3010 (w), 2924 (w), 1613 (m), 1597 (m), 1558 (w), 1488 (w), 1470 (w), 1429 (m), 1394 (w), 1382 (w), 1291 (w), 1249 (s), 1184 (m), 1156 (w), 1112 (w), 1040 (w), 992 (w), 937 (w), 876 (m), 857 (w), 835 (m), 754 (s), 733 (w), 722 (m).

HRESI-MS (MeOH, +, *m/z*): [M+H]$^+$ 187.0881, calc. 187.0866, [M+Na]$^+$ 209.0703, calc. 209.0685, [M+K]$^+$ 225.0437, calc. 225.0425

M.p.: 72 °C

4,4″-Dimethyl-2,2′:6′,2″-terpyridine *N*-oxide (**29u**)
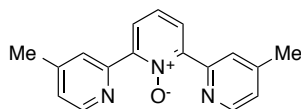
^{1}H NMR (500 MHz, CDCl$_3$): δ 8.57 (dd, *J* = 5.0, 0.8 Hz, 2H), 8.48 (dt, *J* = 1.7, 0.8 Hz, 2H), 7.99 (d, *J* = 7.9 Hz, 2H), 7.42 (t, *J* = 7.9 Hz, 1H), 7.14 (ddt, *J* = 4.4, 1.7, 0.8 Hz, 2H), 2.39 (t, *J* = 0.7 Hz, 6H) ppm.

^{13}C NMR (126 MHz, CDCl$_3$): δ 150.4, 149.3, 148.4, 147.3, 127.7, 126.5, 125.6, 125.1, 21.3 ppm.

IR (*v*/cm^{-1}): 3058 (w), 2919 (w), 1615 (w), 1592 (m), 1554 (w), 1445 (w), 1392 (w), 1366 (m), 1248 (m), 1186 (w), 1164 (w), 1123 (w), 1041 (w), 989 (w), 900 (w), 863 (m), 829 (s), 796 (s), 773 (w), 761 (m), 737 (w), 714 (w).

HRESI-MS (MeOH, +, *m/z*): [M+H]⁺ 278.1273, calc. 278.1288, [M+Na]⁺ 300.1087, calc. 300.1107, [M+K]⁺ 316.0823, calc. 316.0847

M.p.: 135 °C

4′-Fluoro-2,2′-bipyridine *N*-oxide (20v)

[FW 2087]
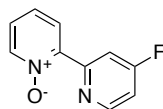
According to the general procedure, reaction of pyridine *N*-oxide (3.65 g, 38.3 mmol), 4-fluoro-2-chloropyridine (2.52 g, 19.2 mmol), K₃PO₄ (8.16 g, 38.4 mmol), complex **A** (351 mg, 0.48 mmol) in toluene (40.0 mL) provided bipyridine *N*-oxide **20v** (276 mg, 1.45 mmol, 8%) as brown solid after column chromatography (acetone in hexane mixtures: 0–60%, 10% increments).

¹H NMR (500 MHz, CDCl₃): δ 8.82 (dd, *J* = 11.0, 2.5 Hz, 1H), 8.64 (dd, *J* = 8.6, 5.5 Hz, 1H), 8.29 (dd, *J* = 6.5, 1.3 Hz, 1H), 8.25 (dd, *J* = 8.0, 2.2 Hz, 1H), 7.34 (td, *J* = 7.8, 1.3 Hz, 1H), 7.27 (ddd, *J* = 7.5, 6.5, 2.2 Hz, 1H), 7.07 (ddd, *J* = 7.9, 5.5, 2.5 Hz, 1H) ppm.

¹³C NMR (126 MHz, CDCl₃): δ 152.3 (d, *J* = 9.1 Hz), 125.8, 113.8 (d, *J* = 21.1 Hz), 112.2 (d, *J* = 16.9 Hz), 125.8 (2C), 168.7 (d, *J* = 260.9 Hz), 151.3 (d, *J* = 7.5 Hz), 146.2, 140.9, 128.0 ppm.

¹⁹F NMR (471 MHz, CDCl₃): δ –101.11 – –101.24 (m) ppm.

IR (*v*/cm⁻¹): 3060 (w), 2962 (w), 2922 (w), 1672 (w), 1594 (m), 1575 (s), 1485 (w), 1468 (m), 1431 (m), 1389 (m), 1303 (w), 1255 (s), 1218 (w), 1176 (m), 1148 (w), 988 (w), 894 (s), 841 (s), 768 (s), 729 (m), 719 (m).

HRESI-MS (MeOH, +, *m/z*): [M+H]⁺ 191.0623, calc. 191.0615, [M+Na]⁺ 213.0447, calc. 213.0435, [M+K]⁺ 229.0161, calc. 229.0174

M.p.: 94 °C

4′-(Ethoxycarbonyl)-2,2′-bipyridine *N*-oxide (20w)

[FW 2010]
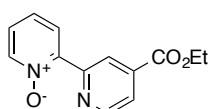
According to the general procedure, reaction of pyridine *N*-oxide (1.02 g, 10.7 mmol), 4-ethoxy-carbonyl-2-bromopyridine (1.23 g, 5.34 mmol), K₃PO₄ (2.28 g, 10.7 mmol), complex **A** (110 mg, 0.15 mmol) in toluene (11.0 mL) provided bipyridine *N*-oxide **20w** (573 mg, 2.35 mmol, 44%), terpyridine *N*-oxide **29w** (114 mg, 0.29 mmol, 11%) as brown solids, bipyridine **24w** (208 mg,

0.69 mmol, 26%) as tan solid and recovered pyridine *N*-oxide (547 mg, 5.75 mmol, 54%) after column chromatography (acetone in hexane mixtures: 0–100%, 10% increments).

^{1}H NMR (500 MHz, CDCl$_3$): δ 9.37 (dd, *J* = 1.6, 0.9 Hz, 1H), 8.82 (dd, *J* = 4.9, 0.9 Hz, 1H), 8.30 (ddd, *J* = 6.5, 1.3, 0.6 Hz, 1H), 8.13 (dd, *J* = 8.0, 2.2 Hz, 1H), 7.88 (dd, *J* = 4.9, 1.6 Hz, 1H), 7.34 (td, *J* = 7.7, 1.3 Hz, 1H), 7.27 (ddd, *J* = 7.4, 6.4, 2.3 Hz, 1H), 4.40 (q, *J* = 7.2 Hz, 3H), 1.38 (t, *J* = 7.1 Hz, 3H) ppm.

^{13}C NMR (126 MHz, CDCl$_3$): δ 165.0, 150.9, 150.0, 146.8, 140.8, 138.3, 128.0, 125.7, 124.8, 123.6, 62.0, 14.3 ppm.

IR (v/cm^{-1}): 3114 (w), 3055 (w), 3026 (w), 2978 (w), 2925 (w), 2851 (w), 1716 (s), 1668 (w), 1589 (w), 1559 (w), 1459 (w), 1426 (m), 1385 (m), 1366 (w), 1305 (w), 1294 (w), 1280 (m), 1250 (w), 1219 (m), 1202 (m), 1154 (w), 1123 (m), 1055 (w), 1024 (s), 939 (w), 897 (m), 887 (m), 781 (w), 765 (s), 715 (m), 682 (m).

HRESI-MS (MeOH, +, *m/z*): [M+H]$^+$ 245.0960, calc. 245.0921, [M+Na]$^+$ 267.0779, calc. 267.0740, [M+K]$^+$ 283.0516, calc. 283.0480

Elemental analysis (%): C 63.8, H 5.12, N 11.1, calc. C 63.9, H 4.95, N 11.5

M.p.: 68 °C

4,4″-Bis(ethoxycarbonyl)-2,2′:6′,2″-terpyridine *N*-oxide (**29w**)
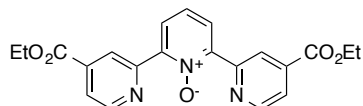
^{1}H NMR (500 MHz, CDCl$_3$): δ 9.18 (dd, *J* = 1.6, 0.9 Hz, 2H), 8.88 (dd, *J* = 5.0, 0.9 Hz, 2H), 8.07 (d, *J* = 7.9 Hz, 2H), 7.92 (dd, *J* = 5.0, 1.6 Hz, 2H), 7.48 (t, *J* = 7.9 Hz, 1H), 4.41 (q, *J* = 7.1 Hz, 4H), 1.38 (t, *J* = 7.1 Hz, 6H) ppm.

^{13}C NMR (126 MHz, CDCl$_3$): δ 165.1, 151.6, 150.2, 147.8, 138.2, 128.3, 125.5, 125.0, 123.6, 62.0, 14.4 ppm.

IR (v/cm^{-1}): 3086 (w), 2983 (w), 2935 (w), 2871 (w), 1718 (s), 1662 (s), 1590 (m), 1561 (w), 1561 (w), 1472 (w), 1457 (w), 1414 (w), 1380 (m), 1364 (m), 1330 (w), 1313 (w), 1285 (w), 1260 (m), 1243 (m), 1218 (w), 1202 (w), 1164 (w), 1133 (w), 1111 (w), 1080 (w), 1061 (w), 1018 (m), 990 (w), 928 (w), 917 (w), 894 (w), 858 (w), 843 (w), 813 (w), 760 (s), 721 (w), 682 (w).

HRESI-MS (MeOH, +, *m/z*): [M+H]$^+$ 394.1438, calc. 394.1397, [M+Na]$^+$ 416.1264, calc. 516.1217, [M+K]$^+$ 432.1000, calc. 432.0956

M.p.: 108 °C

4,4′-Bis(ethoxycarbonyl)-2,2′-bipyridine (**24w**)
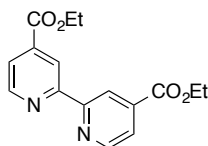
^{1}H NMR (400 MHz, CDCl$_3$): δ 8.95 (dd, J = 1.5, 0.8 Hz, 2H), 8.86 (dd, J = 5.0, 0.7 Hz, 2H), 7.91 (dd, J = 5.0, 1.6 Hz, 2H), 4.46 (q, J = 7.1 Hz, 4H), 1.44 (t, J = 7.1 Hz, 6H) ppm.

The chemical shifts are in agreement with previous reported values.[240]

4′-(Trifluoromethyl)-2,2′-bipyridine *N*-oxide (20x)

[FW 2086]
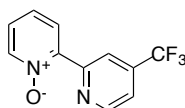
According to the general procedure, reaction of pyridine *N*-oxide (1.09 g, 11.5 mmol), 4-trifluoromethyl-2-chloropyridine (1.04 g, 5.70 mmol), K$_3$PO$_4$ (2.43 g, 11.4 mmol), complex **A** (105 mg, 0.14 mmol) in toluene (10.0 mL) provided bipyridine *N*-oxide **20x** (204 mg, 0.85 mmol, 15%) as brown oil after column chromatography (acetone in hexane mixtures: 0–60%, 10% increments).

^{1}H NMR (500 MHz, CDCl$_3$): δ 9.28 (dt, J = 1.7, 0.8 Hz, 1H), 8.88 (d, J = 5.0 Hz, 1H), 8.34 (dd, J = 6.5, 1.2 Hz, 1H), 8.24 (dd, J = 8.0, 2.2 Hz, 1H), 7.55 (ddd, J = 5.0, 1.7, 0.8 Hz, 1H), 7.39 (ddd, J = 8.0, 7.6, 1.3 Hz, 1H), 7.32 (ddd, J = 7.5, 6.5, 2.2 Hz, 1H) ppm.

^{13}C NMR (126 MHz, CDCl$_3$): δ 151.0, 150.2, 146.1, 140.9, 138.8 (q, J = 35 Hz), 136.4, 128.1, 126.09, 126.06, 122.9 (q, J = 273 Hz), 121.5 (q, J = 4.1 Hz), 120.0 (q, J = 3.5 Hz) ppm.

^{19}F NMR (471 MHz, CDCl$_3$): δ –64.6 ppm.

IR (ν/cm^{-1}): 3114 (w), 3071 (w), 1675 (w), 1626 (w), 1572 (w), 1469 (w), 1433 (m), 1394 (m), 1333 (s), 1283 (m), 1227 (m), 1205 (w), 1169 (m), 1129 (s), 1085 (m), 1057 (w), 992 (w), 909 (w), 851 (s), 814 (w), 766 (s), 666 (s).

HRESI-MS (MeOH, +, *m/z*): [M+H]$^+$ 241.0592, calc. 241.0583, [M+Na]$^+$ 263.0410, calc. 263.0403

2-(Pyridin-2-yl)quinoline *N*-oxide (20y)

[JN 1008]
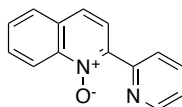
According to the general procedure, reaction of quinoline *N*-oxide (3.09 g, 21.3 mmol), 2-bromopyridine (3.37 g, 21.3 mmol), K$_3$PO$_4$ (9.03 g, 42.6 mmol), complex **A** (391 mg, 0.53 mmol) in

toluene (45.0 mL) provided pyridylquinoline *N*-oxide **20y** (896 mg, 4.00 mmol, 19%) as yellow solid after column chromatography (MeOH in DCM mixtures: 0–1%, 0.5% increments).

^{1}H NMR (500 MHz, CDCl$_3$): δ 9.12 (d, J = 8.1 Hz, 1H), 8.82 (d, J = 8.8 Hz, 1H), 8.73 (d, J = 4.1 Hz, 1H), 8.23 (d, J = 8.9 Hz, 1H), 7.86–7.77 (m, 2H), 7.77–7.69 (m, 2H), 7.61–7.56 (m, 1H), 7.31 (ddd, J = 7.4, 4.8, 0.9 Hz, 1H) ppm.

^{13}C NMR (126 MHz, CDCl$_3$): δ 150.4, 149.5, 143.4, 142.5, 136.4, 130.5, 130.0, 128.9, 128.1, 126.1, 125.2, 124.3, 123.2, 120.3 ppm.

IR (v/cm^{-1}): 3059 (w), 2968 (w), 2359 (w), 1668 (w), 1584 (m), 1563 (m), 1466 (m), 1427 (m), 1348 (s), 1254 (m), 1209 (m), 1065 (m), 992 (m), 922 (m), 892 (m) , 822 (s), 773 (s), 736 (s).

HRESI-MS (MeOH, +, *m/z*): [M+H]$^+$ 223.0898, calc. 223.0871, [M+Na]$^+$ 245.0724, calc. 245.0691

M.p.: 92–93 °C

2-(Pyridin-2-yl)pyrazine *N*-oxide

[JN 1014]
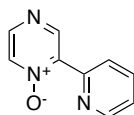
According to the general procedure, reaction of pyrazine *N*-oxide (4.24 g, 44.1 mmol), 2-bromopyridine (3.48 g, 22.1 mmol), K$_3$PO$_4$ (9.35 g, 44.1 mmol), complex **A** (404 mg, 0.55 mmol) in toluene (45.0 mL) provided pyridylpyrazine *N*-oxide (794 mg, 4.58 mmol, 21%) as colorless solid after column chromatography (acetone in hexane mixtures: 0–40%, 10% increments).

^{1}H NMR (400 MHz, DMSO-d_6): δ 9.15 (s, 1H), 8.76 (d, J = 4.1 Hz, 1H), 8.57 (d, J = 8.0 Hz, 1H), 8.52 (d, J = 4.2 Hz, 1H), 8.44 (d, J = 4.1 Hz, 1H), 7.96 (td, J = 7.9, 1.8 Hz, 1H), 7.52 (ddd, J = 7.5, 4.8, 0.9 Hz, 1H) ppm.

The chemical shifts are in agreement with previous reported values.[99c]

4.10.4 Other procedures

6-Methyl-2,2′-bipyridine *N*-oxide (20b)

[SZ 5092]
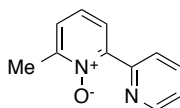
Based on the reported procedure,[99c] an oven-dried and argon-purged Schlenk flask was charged with 2-picolin N-oxide (2.49 g, 22.8 mmol), 2-bromopyridine (2.38 g, 15.1 mmol), THF (20.0 mL) and a freshly prepared TMPZnCl • LiCl solution in THF, which was made from TMP (3.71 mL, 22.0 mmol), nBuLi (2.3 M in hexane, 9.56 mL, 22.0 mmol) in THF (20.0 mL) according to the literature procedure[241] and quantitatively transferred into the reaction flask. The resulting suspension was vigorously stirred at room temperature for 10 min, before (dppf)PdCl$_2$·DCM (305 mg, 0.37 mmol) was added as solid. The reaction mixture was placed in a pre-heated oil bath and stirred at 60 °C for 16 h. After cooling to room temperature, the flask was opened to air, the reaction mixture quenched with an aqueous sat. NH$_4$Cl and the volatiles were removed by rotary evaporation. The residue was extracted with DCM, the combined organic layers dried with Na$_2$SO$_4$, filtered and solvent removed from the filtrate. The crude product was purified by column chromatography (SiO$_2$, MeOH in DCM mixtures: 0–5%, 1% increments, then 10%) providing **20b** (2.43 g, 13.0 mmol, 86%) as brown oil.

NMR Data are identical to an previous obtained sample (SZ 2079) and are agreement with previous reported values.[99c]

4-Nitro-2,2′-bipyridine N-oxide (20o)

[FW 2019/FW 2036]
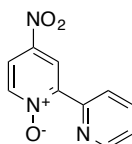
Bipyridine N-oxide **20a** (1.69 g, 9.81 mmol) and KNO$_3$ (5.39 g, 53.3 mmol) were added portion-wise to ice-cooled H$_2$SO$_4$ (13.3 mL). The mixture was warmed to 80 °C and stirred for 42 h. The resulting solution was poured into ice and neutralized with NaOH (w = 25%). The formed precipitate was filtered and washed with a lot of cold water. The solid was dissolved in DCM, the resulting solution dried with Na$_2$SO$_4$, filtered and the filtrate concentrated in vacuum. The product **20o** (601 mg, 2.77 mmol, 28%) was isolated as yellow crystals after recrystallization by overlaying the concentrated solution with hexane.

^{1}H NMR (400 MHz, CDCl$_3$): δ 9.15 (d, J = 3.3 Hz, 1H), 8.88 (dd, J = 8.1, 1.1 Hz, 1H), 8.78 (ddd, J = 4.7, 1.8, 1.0 Hz, 1H), 8.35 (dd, J = 7.2, 0.5 Hz, 1H), 8.06 (dd, J = 7.2, 3.3 Hz, 1H), 7.87 (ddd, J = 8.1, 7.6, 1.8 Hz, 1H), 7.43 (ddd, J = 7.6, 4.8, 1.2 Hz, 1H) ppm.

The chemical shifts are in agreement with previous reported values.[117]

4-Methoxy-2,2′-bipyridine *N*-oxide (20j)

[FW 2043]
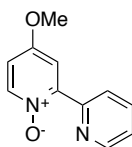
Under argon atmosphere nitrobipyridine *N*-oxide **20o** (54.8 mg, 0.25 mmol) was dissolved in dry MeOH (2.00 mL) and a solution of NaOMe in MeOH (*w* = 25%, 0.12 mL, 0.53 mmol) was added. After stirring for 4 h at 55 °C, the reaction solution was cooled to room temperature and quenched with water. The mixture was extracted with DCM, the combined organic layers dried with Na_2SO_4, filtered and the solvent removed from the filtrate. The product **20j** (52.4 mg, 0.26 mmol, quant.) was isolated as analytically pure, yellow solid.

^{1}H NMR (400 MHz, CDCl$_3$): δ 9.02 (dt, *J* = 8.1, 1.0 Hz, 1H), 8.70 (d, *J* = 4.2 Hz, 1H), 8.19 (d, *J* = 7.2 Hz, 1H), 7.82 (td, *J* = 7.8, 1.7 Hz, 1H), 7.72 (d, *J* = 3.6 Hz, 1H), 7.34 (ddd, *J* = 7.5, 4.7, 1.1 Hz, 1H), 6.83 (dd, *J* = 7.3, 3.6 Hz, 1H), 3.91 (s, 3H) ppm.

The chemical shifts are in agreement with previous reported values.[169e]

4.11 Palladium-catalyzed directed halogenations of bipyridine *N*-oxides

4.11.1 Optimization of the reaction conditions

General procedure:

A Teflon-lined green cap vial was charged with bipyridine *N*-oxide **20a**, NBS, Pd(OAc)$_2$, and solvent. The vial was sealed and placed in a pre-heated aluminum heating well plate. After 17 h, the reaction mixtures were cooled to room temperature, diluted with DCM and extracted with an aqueous, sat. Na$_2$CO$_3$ or 1 M NaOH solution. The combined organic layers were dried with Na$_2$SO$_4$, filtered and the solvent removed from the filtrate. The crude products were re-dissolved in a stock solution of TMB in CDCl$_3$ and transferred into a NMR tube. Yields were calculated by integration of the isolated and fitted signals relative to the aromatic protons of TMB.

4.11.1.1 Influence of solvent
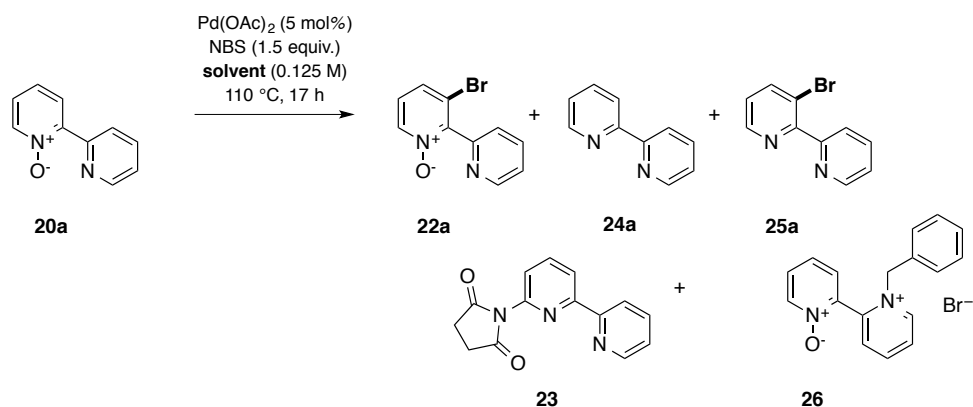
According to the general procedure, bipyridine *N*-oxide **20a** (0.25 mmol), NBS (0.38 mmol, 1.5 equiv.), Pd(OAc)$_2$ (0.012 mmol, 5 mol%), and solvent (2.00 mL, 0.125 M).

entry	Exp. No. FW 1xxx	**20a** [mg]	NBS [mg]	Pd(OAc)$_2$ [mg]	solvent	**22a** [%]	recov. **20a** [%]	**24a** [%]	**25a** [%]	**23** [%]	**26** [%]
1	055FA	43.5	66.9	2.8	AcOH	14	34	0	0	0	0
2	055FB	43.6	67.5	3.1	toluene	0	46	0	0	0	22
3	056FC	43.0	66.8	3.0	THF	0	29	17	0	0	0
4	056FD	43.3	66.7	3.1	DMA	14	17	17	10	0	0
5	056FE	43.1	66.7	2.9	MeCN	37	15	13	0	0	0
6	056FF	43.0	67.2	3.0	DME	0	31	0	0	10	0
7	056FG	43.3	66.8	2.8	DMF	0	22	21	0	0	0
8	055FH	43.4	67.2	3.0	Ac$_2$O	0	0	0	0	27	0
9	055FI	43.3	66.8	3.1	AcOH/benzene (1:1)	42	31	0	0	0	0
10	055FJ	43.4	66.8	3.2	Ac$_2$O/AcOH (1:1)	0	15	0	0	15	0
11	055FK	43.1	67.0	3.1	Ac$_2$O/benzene (1:1)	0	0	0	0	26	0
12	059FA	43.2	66.6	2.6	AcOH/benzene (3:1)	28	34	0	0	0	0
13	059FB	43.1	67.0	3.1	AcOH/benzene (1:3)	40	23	0	7	0	0
14	059FC	42.8	67.0	2.8	benzene	77	0	0	0	0	0
15	059FD	43.1	67.0	3.0	benzene^a	72	0	0	0	0	0
16	060FE	42.8	66.8	2.8	MeCN^a	22	17	24	0	0	0
17	062FF	43.1	66.4	3.0	DCE	35	10	0	0	0	0
18	061FG	42.8	67.1	3.0	DMSO	0	0	0	0	0	0
19	060FH	43.1	66.6	3.1	MeCN (5 μl AcOH)	66	62	21	0	0	0
20	060FI	43.2	66.5	2.8	MeCN (7,8 mg PivOH)	21	77	0	0	0	0
21	060FJ	42.9	66.8	3.1	MeCN (6 μl pyridine)	19	128	0	0	0	0
22	059FK	42.8	66.8	3.1	TFA	0	91	0	0	0	0
23	059FL	43.2	67.2	2.6	TFA/benzene (1:1)	0	84	0	0	0	0
24	062FM	43.2	67.0	3.0	EtOH	0	37	9	0	0	0
25	062FN	42.9	66.7	2.9	^{i}PrOH	0	29	0	0	0	0

26	061FO	43.0	66.5	3.1	hexane	0	3	14	0	0	0
27	061FP	43.1	66.9	2.8	acetone	0	0	0	0	0	0
28	061FQ	43.2	66.9	2.9	2-butanone	16	35	0	0	0	0
29	062FR	43.2	67.2	2.9	Ethylenglycol	0	40	0	0	0	0
30	062FS	43.1	66.9	2.7	MTBE	0	18	0	0	0	0
31	062FT	42.8	67.2	2.9	dioxane	2	11	0	8	1	0
32	073FJ	42.9	66.5	2.9	chlorobenzene	77	0	0	22	0	0
33	073FK	43.2	66.8	2.8	toluene (23,9 mg PTSA)	$-^b$	14	0	0	0	37
34	073FL	43.4	66.8	2.8	benzene (23,8 mg PTSA)	0	0	17	0	0	0
35	055FA	43.5	66.9	2.8	AcOH	14	34	0	0	0	0
36	2026FW	44.0	59.9	2.8	benzotrifluoride	56	0	0	0	0	0

[a]Sample was extracted with an aqueous 1N NaOH solution.
[b]Complex product mixture

Independent synthesis of

6-(2,5-Pyrrolindion-1-yl)-2,2′-bipyridine (23)

[SZ 5082A+C]
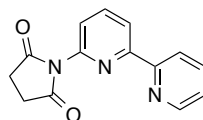
Bipyridine *N*-oxide **20a** (86.3 mg, 0.50 mmol) and succinimide (74.8 mg, 0.76 mmol) were dissolved in Ac$_2$O (4.00 mL). The reaction solution was heated at 110 °C for 9 h before MeOH (4.00 mL) was added. The volatiles were removed in vacuum and the crude product purified by column chromatography (SiO$_2$, MeOH in DCM: 3%) providing **23** (82.8 mg, 0.31 mmol, 62%) as tan solid.

Alternatively, the reaction of **20a** (87.7 mg, 0.51 mmol) and NBS (136.1 mg, 0.77 mmol) in Ac$_2$O (4.00 mL) provided **23** (49.9 mg, 0.20 mmol, 39%) following the same procedure.

^{1}H NMR (400 MHz, CDCl$_3$): δ 8.67 (dd, *J* = 4.8, 1.7 Hz, 1H, ArH-3′), 8.47 (d, *J* = 7.9 Hz, 1H, ArH-3), 8.35 (d, *J* = 7.9 Hz, 1H, ArH-5), 7.98 (td, *J* = 7.9, 0.6 Hz, 1H, ArH-4), 7.79 (td, *J* = 7.8, 1.8 Hz, 1H, ArH-5′), 7.36–7.26 (m, 2H, ArH-4′, ArH-6′), 2.95 (s, 2H, -CH$_2$-) ppm.

^{13}C NMR (101 MHz, CDCl$_3$): δ 175.8, 156.8, 155.1, 149.3, 145.8, 139.4, 137.1, 124.3, 122.1, 121.8, 121.4, 77.2, 28.8 ppm.

HRESI-MS (MeOH, +, *m/z*): [M+Na]$^+$ 276.0757, calc. 276.0743

IR (ν/cm^{-1}): (3053 (w), 2932 (w), 1769 (w), 1704 (s), 1583 (m), 1558 (m), 1452 (m), 1427 (s), 1381 (s), 1299 (w), 1173 (s), 1081 (w), 1045 (w), 993 (m), 960 (w), 819 (w), 774 (m), 743 (m), 666 (m).

M.p.: 140–150 °C

Isolation and independent synthesis of

N'-Benzyl-N-oxo-2,2′-bipyridinium bromide (26)

[SZ 5085/SZ 5089]
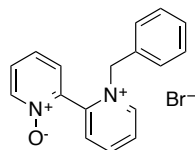
Following the general procedure, bipyridine N-oxide **20a** (346 mg, 2.01 mmol), NBS (559 mg, 3.14 mmol), and Pd(OAc)$_2$ (22.5 mg, 0.10 mmol) in toluene (16.0 mL) gave **26** (33.5 mg, 0.10 mmol, 5%) as tan oil in a very polar fraction after column chromatography (SiO$_2$, MeOH in DCM mixtures: 10%).

Alternatively, the reaction of bipyridine N-oxide **20a** (173 mg, 1.00 mmol) and benzyl bromide (0.13 mL, 1.09 mmol) in MeCN (1.00 mL) at 60 ° for 4 h provided **26** (325 mg, 0.95 mmol, 94%) after removal of the solvent, washing the residue with Et$_2$O and drying in vacuum.

^{1}H NMR (500 MHz, CDCl$_3$): δ 9.35 (d, J = 5.2 Hz, 1H, ArH-3′), 8.68 (t, J = 7.7 Hz, 1H, ArH-5′), 8.34 (d, J = 6.4 Hz, 1H, ArH-3), 8.15 (t, J = 6.8 Hz, 1H, ArH-4′), 8.06 (d, J = 7.4 Hz, 1H, ArH-6′), 7.97 (d, J = 6.9 Hz, 1H, ArH-6), 7.56 (t, J = 7.1 Hz, 1H, ArH-4), 7.42 (t, J = 7.8 Hz, 1H, ArH-5), 7.32–7.23 (m, 5H, Ph-H), 5.97 (d, J = 14.5 Hz, 1H, -CH$_2$-), 5.92 (d, J = 14.7 Hz, 1H, -CH$_2$-) ppm.

^{13}C NMR (126 MHz, CDCl$_3$): δ 146.9 (C-2′), 146.8 (C-5′), 146.6 (C-3′), 141.0 (C-2), 139.8 (C-3), 131.6 (C-6′), 131.5 (C-1″), 130.6 (C-6), 130.1 (C-4″), 129.7 (C-3″, C-5″), 129.6 (C-2″, C-6″), 129.03 (C-4′), 128.95 (C-4), 127.0 (C-5), 62.9 (-CH$_2$-) ppm.

IR (v/cm^{-1}): 3390 (s), 3044 (s), 1706 (w), 1621 (m), 1519 (w), 1480 (m), 1455 (m), 1422 (s), 1244 (s), 1154 (m), 1119 (w), 1080 (w), 1031 (m), 847 (s), 771 (s), 745 (s), 725 (s), 696 (s).

HRESI-MS (MeOH, +, m/z): [M-Br]$^+$ 263.1181, calc. 263.1179

4.11.1.2   Control experiments

According to the general procedure, bipyridine N-oxide **20a**, NBS, Pd(OAc)$_2$, and benzene.

entry	Exp. No. FW 1xxx	**20a** [mg]	NBS [mg]	Pd(OAc)₂ [mg]	conditions	**22a** [%]	recov. **20a** [%]	**24a** [%]	**25a** [%]
1	073FO	43.3	67.0 (1.5 equiv.)	2.8 (5 mol%)	inert	56	0	0	0
2	073FP	–	67.1 (1.5 equiv.)	2.8 (5 mol%)	**24a** (39.5 mg)	0	0	quant.	0
3	073FQ	42.7	67.2 (1.5 equiv.)	0.0 (0 mol%)	w/o catalyst	0	quant.	0	0
4	084FA	43.0	67.3 (1.5 equiv.)	3.0 (5 mol%)	150 °C, in PhCl	6	0	19	52
5	083FB	55.5	68.5 (1.2 equiv.)	–	150 °C, in PhCl	0	0	53	0
6	SZ 5115A	195.4	–	–	150 °C, in PhCl	0	quant.	0	0
7	SZ 5115B	171.8	36.1 (0.2 equiv.)	–	150 °C, in PhCl	0	80	20	0
8[a]	SZ 5115C	183.2	50.5 (0.5 equiv.)	–	150 °C, in PhCl	0	quant.	0	0
9	089FA	43.2	68.4 (1.5 equiv.)	3.4 (5 mol%)	95 °C, in PhCl	28	72	0	0

[a]Succinimide was used instead of NBS.

4.11.1.3   Catalyst Screening
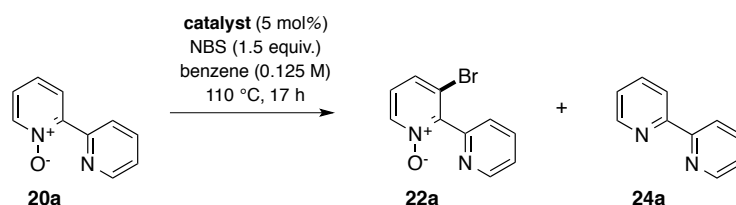
According to the general procedure, bipyridine *N*-oxide **20a** (0.25 mmol), NBS (0.38 mmol, 1.5 equiv.), transition metal catalyst (0.012 mmol, 5 mol%), and benzene (2.00 mL, 0.125 M).

entry	Exp. No. FW 1xxx	**20a** [mg]	NBS [mg]	catalyst	catalyst [mg]	**22a** [%]	recov. **20a** [%]	**24a** [%]
1	075FA	43.0	67.0	RuCl₃·H₂O	3.1	0	quant.	0
2	075FB	43.0	66.9	[(C₆H₆)RuCl₂]₂	3.1	0	0	54
3	075FC	43.0	66.7	[(*p*-cymene)RuCl₂]₂	3.7	0	0	52
4	075FD	43.0	66.7	[(*p*-cymene)Ru(OAc)₂]₂	4.6	0	0	48
5	076FE	43.0	66.9	Pd(OTf)₂	4.2	65	0	0
6	076FF	43.0	66.6	Pd(O₂CPh)₂	4.3	63	0	0
7	076FG	43.0	67.3	Pd(OPiv)₂	4.1	68	0	0
8	076FH	43.0	67.0	K₂PdCl₆	5.3	60	0	0
9	077FI	43.0	67.2	Pd(OAc)₂ + phenanthroline (1:1)	2.8 + 2.3	0	0	50
10	077FJ	43.0	66.7	Pd(OAc)₂ + dppf (1:1)	2.8 + 6.9	0	0	65
11	078FK	43.0	67.2	dimer **A**	4.5	56	0	0
12	078FL	43.0	67.0	dimer **B**	4.9	23	10	16
13	078FM	43.0	66.8	Hermann-Beller (X = OAc)	6.0	69	0	0
14	078FN	43.0	66.6	Hermann-Beller (X = Br)	6.3	56	0	0

15	079FO	43.0	66.9	(IMes)PdCl$_2$(3-ClPy)	7.4	0	0	43
16	079FP	43.0	66.3	(IPr)PdCl$_2$(3-ClPy)	8.5	0	0	48
17	079FQ	43.0	66.6	(CH$_3$CN)$_4$Pd(BF$_4$)$_2$	5.6	0	0	48
18	079FR	43.0	66.7	(CH$_3$CN)$_2$PdCl$_2$	3.2	60	0	0
19	079FS	43.0	66.9	Buchwald's pre-catalyst G1	8.6	35	11	6
				[(S-Phos)Pd(N,2(N-Me-2-(PhEt)amine))Cl]				
20	077FT	43.0	66.5	(tmeda)PdCl$_2$	3.7	0	0	0
21	077FU	43.0	66.5	(dppf)PdCl$_2$	9.1	0	0	0
22	077FV	43.0	67.0	(bipy)Pd(OAc)$_2$	4.8	0	0	46
23	077FW	43.0	66.7	PdCl$_2$	2.2	62	0	0

X = OAc dimer **A**
= Br dimer **B**

Herrmann-Beller catalysts

NHC-palladium catalysts

Buchwald's pre-catalyst G1
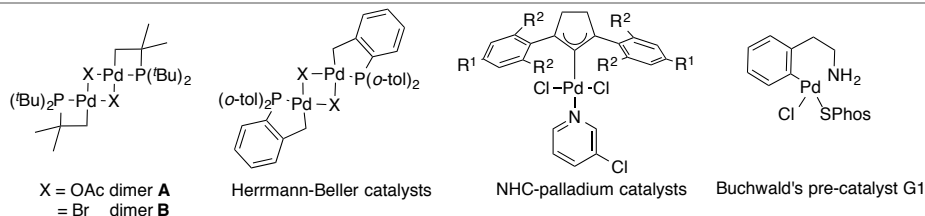
4.11.1.4   Catalyst loading, amount of NBS and concentration
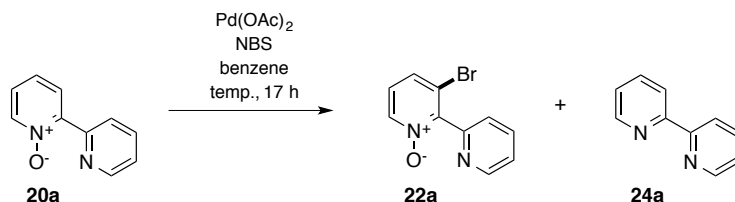
According to the general procedure, bipyridine *N*-oxide **20a**, NBS, Pd(OAc)$_2$, and benzene.

entry	Exp. No. FW 1xxx	**20a** [mg]	NBS [mg]	Pd(OAc)$_2$ [mg]	conditions	**22a** [%]	recov. **20a** [%]	**24a** [%]
1	081FZ	43.2	66.8 (1.5 equiv.)	1.6 (2.5 mol%)		59	0	0
2	105FB	43.3	66.4 (1.5 equiv.)	0.7 (1 mol%)		47	0	0
3	081Fab	43.3	53.1 (1.2 equiv.)	3.1 (5 mol%)		90	0	0
4	081Fac	43.1	45.0 (1.0 equiv.)	3.0 (5 mol%)		88	0	0
5	084FD	43.3	66.5 (1.5 equiv.)	3.1 (5 mol%)	0.063 M	quant.	0	0
6	106FA	64.8	101.2 (1.5 equiv.)	4.4 (5 mol%)	0.188 M	30	9	0
7	106FB	86.0	133.7 (1.5 equiv.)	5.6 (5 mol%)	0.250 M	23	0	30
8	105FE	107.4	166.7 (1.5 equiv.)	6.9 (5 mol%)	0.312 M	44	9	0
9	105FF	128.9	202.7 (1.5 equiv.)	8.5 (5 mol%)	0.374 M	21	0	0

4.11.1.5   *Brominating reagents*
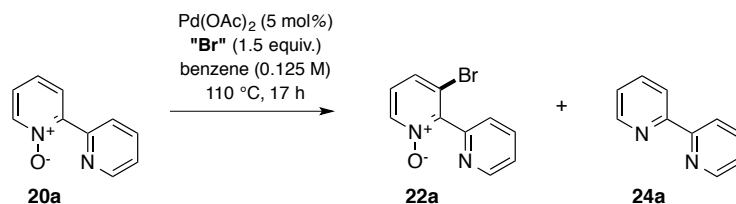
According to the general procedure, bipyridine *N*-oxide **20a** (0.25 mmol), brominating reagent (0.38 mmol, 1.5 equiv.), if applicable, oxidant (0.38 mmol, 1.5 equiv.), Pd(OAc)$_2$ (0.012 mmol, 5 mol%), and benzene (2.00 mL, 0.125 M).

entry	Exp. No. FW 1xxx	**20a** [mg]	brominating reagent	amount	oxidant	amount	**22a** [%]	recov. **20a** [%]	**24a** [%]
1	072FF	43.0	Br$_2$	19.5 μL	–	–	0	0	10
2[a]	072FG	42.9	Br$_2$	19.5 μL	PhI(OAc)$_2$	114.5 mg	0	0	15
3	072FH	42.8	LiBr	43.0 mg	oxone	115.3 mg	2	6	0
4	072FI	43.4	CuBr	77.7 mg	–	–	0	0	0
5	072FM	43.3	KBr	59.4	oxone	117.0 mg	1	7	0

[a]Unidentified *m/z* ratios in HRESI-MS spectra: 179.0608, 234.09891, 249.0044

4.11.2 Substrate scope of directed halogenations

General procedure:

A reaction vial was charged with bipyridine *N*-oxide **20** (1.0 equiv.), Pd(OAc)$_2$ (5 mol%), NXS (1.2 equiv.) and chlorobenzene (0.10 M). The vial was sealed with a Teflon-lined screw cap and placed into a pre-heated aluminum well plate. After stirring at 110 °C for 24 h and subsequent cooling to room temperature, the reaction mixture was diluted with DCM and extracted with an aqueous NaOH solution (1.0 M). The aqueous layer was extracted with DCM, the combined organic layers dried with Na$_2$SO$_4$, filtered and the solvent removed from the filtrate. In cases of incomplete conversion of the starting material additional purification by column chromatography was performed on SiO$_2$.

All brominated bipyridine *N*-oxide products are new compounds. The assignments for corresponding protons and carbons were made by evaluation of two dimensional NMR spectra (COSY, HMBC, HMQC).

4.11.2.1   Direct brominations

3-Bromo-2,2′-bipyridine *N*-oxide (22a)

[FW 1071/FW 1091/FW 2025/ SZ 5104]
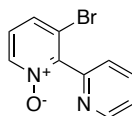
According to the general procedure, the reaction of bipyridine *N*-oxide **20a** (1.53 g, 8.90 mmol), Pd(OAc)$_2$ (102 mg, 0.46 mmol), and NBS (1.68 g, 9.46 mmol) in chlorobenzene (93.0 mL) provided **22a** (1.95 g, 7.78 mmol, 87%) as brown solid after extraction. Recrystallization from hot EtOAc yielded a colorless analytically pure sample. Single crystals for X-ray diffraction were grown by slow diffusion of pentane into a concentrated solution of **22a** in DCM. CCDC-1476436 contains the crystallographic data for **22a**.

^{1}H NMR (500 MHz, CDCl$_3$): δ 8.78 (d, J = 4.7 Hz, 1H, ArH-3′), 8.27 (d, J = 6.5Hz, 1H, ArH-4), 7.86 (td, J = 7.7, 1.7 Hz, 1H, ArH-5′), 7.56 (d, J = 8.3 Hz, 1H, ArH-6), 7.50 (d, J = 7.8 Hz, 1H, ArH-6′), 7.39 (ddd, J = 7.6, 4.9, 0.9 Hz, 1H, ArH-4′), 7.17 (dd, J = 8.2, 6.6 Hz, 1H, ArH-5) ppm.

^{13}C NMR (126 MHz, CDCl$_3$): δ 151.3 (C-2′), 150.3 (C-3′), 148.7 (C-2), 139.2 (C-4), 136.9 (C-5′), 129.9 (C-6), 125.43 (C-5), 125.35 (C-6′), 124.4 (C-4′), 122.1 (C-3′) ppm.

IR (ν/cm^{-1}): 3098 (w), 3061 (w), 3048 (w), 3012 (w), 2359 (w), 2337 (w), 1597 (m), 1581 (w), 1565 (m), 1541 (w), 1486 (w), 1454 (m), 1426 (m), 1412 (s), 1282 (w), 1253 (s, N$^+$-O$^-$), 1231 (w), 1208 (w), 1186 (w), 1152 (w), 1097 (w), 1050 (w), 1029 (m), 991 (m), 900 (s), 791 (s), 779 (s), 745 (s), 731 (s), 674 (w).

HRESI-MS (MeOH, +, *m/z*): [M+H]$^+$ 250.9846, calc. 250.9815, [M+Na]$^+$ 272.9688, calc. 272.9634

Elemental analysis (%): C 47.9, H 2.85, N 11.2, calc. C 47.8, H 2.81, N 11.2

M.p.: 142 °C

3-Bromo-6-methyl-2,2′-biypridine *N*-oxide (22b)

[FW 2071/SZ 5144]
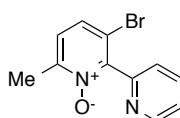
According to the general procedure, the reaction of bipyridine *N*-oxide **20b** (3.28 g, 16.2 mmol), Pd(OAc)$_2$ (207 mg, 0.92 mmol), and NBS (3.77 g, 21.2 mmol) in chlorobenzene (180 mL) provided **22b** (2.56 g, 9.68 mmol, 60%) as brown oil after purification by column chromatography (MeOH in DCM mixtures: 0%–10%, 1% increments).

^{1}H NMR (500 MHz, CDCl$_3$): δ 8.79 (ddd, J = 4.9, 1.7, 1.0 Hz, 1H, ArH-3′), 7.86 (td, J = 7.7, 1.7 Hz, 1H, ArH-5′), 7.49–7.46 (m, 2H, ArH-4, ArH-6′), 7.38 (ddd, J = 7.7, 4.9, 1.2 Hz, 1H, ArH-4′), 7.20 (dd, J = 8.4, 0.8 Hz, 1H, ArH-5), 2.48 (d, J = 0.6 Hz, 3H, -CH$_3$) ppm.

^{13}C NMR (126 MHz, CDCl$_3$): δ 152.1 (C-2′), 150.2 (C-3′), 149.1 (C-2), 148.4 (C-6), 137.0 (C-5′), 129.0 (C-4), 125.9 (C-5), 125.2 (C-6′), 124.1 (C-4′), 118.7 (C-3), 17.9 (-CH$_3$) ppm.

IR (ν/cm^{-1}): 3061 (w), 2920 (w), 1601 (m), 1585 (m), 1567 (m), 1485 (w), 1458 (m), 1443 (m), 1426 (m), 1384 (w), 1344 (s), 1256 (s, N$^+$-O$^-$), 1146 (m), 1090 (w), 1046 (w), 1001 (m), 903 (s), 871 (m), 781 (s), 745 (m), 706 (w), 652 (m).

HRESI-MS (MeOH, +, m/z): [M+H]$^+$ 264.9966, calc. 264.9971, [M+Na]$^+$ 286.9794, calc. 286.9790, [M+K]$^+$ 302.9534, calc. 302.9530

M.p.: 70–71 °C

3-Bromo-6-(ethoxycarbonyl)-2,2′-bipyridine *N*-oxide (22c)

[FW 2055]
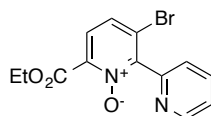
According to the general procedure, the reaction of bipyridine *N*-oxide **20c** (250 mg, 1.02 mmol), Pd(OAc)$_2$ (11.9 mg, 0.053 mmol), and NBS (214 mg, 1.20 mmol) in chlorobenzene (10.0 mL) provided **22c** (271 mg, 0.84 mmol, 82%) as brown oil after extraction.

^{1}H NMR (500 MHz, CDCl$_3$): δ 8.77 (ddd, J = 4.9, 1.8, 1.0 Hz, 1H, ArH-3′), 7.86 (td, J = 7.7, 1.7 Hz, 1H, ArH-5′), 7.58 (d, J = 8.5 Hz, 1H, ArH-4), 7.51 (dt, J = 7.8, 1.1 Hz, 1H, ArH-6′), 7.48 (d, J = 8.6 Hz, 1H, ArH-5), 7.39 (ddd, J = 7.7, 4.9, 1.2 Hz, 1H ArH-4′), 4.42 (q, J = 7.1 Hz, 2H, -CH$_2$-), 1.37 (t, J = 7.1 Hz, 3H, -CH$_3$) ppm.

^{13}C NMR (126 MHz, CDCl$_3$): δ 161.4 (C=O), 150.7 (C-2′), 150.2 (C-3′), 149.7 (C-2), 141.7 (C-6), 137.0 (C-5′), 128.8 (C-4), 125.8 (C-5), 125.6 (C-6′), 124.5 (C-4′), 123.8 (C-3), 62.9 (-CH$_2$-), 14.2 (-CH$_3$) ppm.

IR (ν/cm^{-1}): 3059 (w), 2980 (w), 1736 (s), 1581 (m), 1568 (w), 1541 (w), 1475 (w), 1454 (w), 1427 (w), 1369 (m), 1351 (s), 1316 (m), 1247 (s), 1196 (w), 1150 (s), 1097 (w), 1082 (m), 1044 (w), 1011 (m), 992 (m), 917 (s), 883 (w), 860 (w), 821 (w), 780 (s), 745 (s).

HRESI-MS (MeOH, +, m/z): [M+H]$^+$ 323.0042, calc. 323.0028, [M+Na]$^+$ 344.9851, calc. 344.9845

3-Bromo-6-(trifluoromethyl)-2,2′-bipyridine *N*-oxide (22d)

[FW 2072]
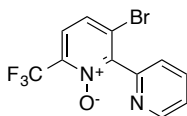
According to the general procedure, the reaction of bipyridine *N*-oxide **20d** (79.5 mg, 0.33 mmol), Pd(OAc)$_2$ (3.8 mg, 0.017 mmol), and NBS (70.8 mg, 0.40 mmol) in chlorobenzene (3.30 mL) provided **22d** (111 mg, 0.35 mmol, quant.) as colorless solid containing only traces of impurities after extraction.

^{1}H NMR (500 MHz, CDCl$_3$): δ 8.80 (d, *J* = 4.8 Hz, 1H, ArH-3′), 7.88 (td, *J* = 7.7, 1.7 Hz, 1H, ArH-5′), 7.64 (d, *J* = 8.7 Hz, 1H, ArH-4), 7.59 (d, *J* = 8.7 Hz, 1H, ArH-5), 7.52 (dt, *J* = 7.8, 1.2 Hz, 1H, ArH-6′), 7.42 (ddd, *J* = 7.6, 4.9, 1.2 Hz, 1H, ArH-4′) ppm.

^{13}C NMR (126 MHz, CDCl$_3$): δ 150.7 (C-2), 150.4 (C-3′), 150.1 (C-2′), 137.0 (C-5′), 128.5 (C-4), 125.7 (C-6), 125.6 (C-6′), 124.7 (C-4′), 124.3 (q, *J* = 3.8 Hz, C-5)), 123.1 (C-3), 119.8 (q, *J* = 273 Hz, -CF$_3$) ppm.

^{19}F NMR (471 MHz, CDCl$_3$): δ −68.8 ppm

IR (*v*/cm^{-1}): 3105 (w), 3084 (w), 1724 (w), 1597 (w), 1586 (w), 1570 (w), 1548 (w), 1451 (w), 1433 (w), 1362 (m), 1339 (m), 1270 (m), 1253 (m), 1148 (s), 1120 (m), 1097 (w), 1066 (m), 1044 (w), 996 (w), 915 (m), 838 (m), 783 (m), 748 (w), 737 (w).

HRESI-MS (MeOH, +, *m/z*): [M+H]$^+$ 318.9713, calc. 318.9688, [M+Na]$^+$ 340.9517, calc. 340.9508, [M+K]$^+$
356.9234, calc. 358.9247

M.p.: 148 °C

3-Bromo-6-cyano-2,2′-bipyridine *N*-oxide 22e)

[SZ 5048]
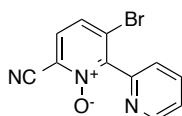
According to the general procedure, the reaction of bipyridine *N*-oxide **20e** (204 mg, 1.04 mmol), Pd(OAc)$_2$ (12.8 mg, 0.057 mmol), and NBS (228 mg, 1.21 mmol) in degassed chlorobenzene (10.0 mL) provided pure **22e** (48.4 mg, 0.18 mmol, 17%) as colorless solid, starting material **20e** (28.8 mg, 0.15 mmol, 14%) and a mixture of starting material **20e** and product **22e** (69.9 mg, 1:1.7) after purification by CombiFlash liquid chromatography (acetone/hexane mixture: 1:4).

^{1}H NMR (400 MHz, CDCl$_3$): δ 8.78 (ddd, J = 4.9, 1.5, 1.0 Hz, 1H, ArH-3′), 7.88 (td, J = 7.8, 1.8 Hz, 1H, ArH-5′), 7.62 (d, J = 8.7 Hz, 1H, ArH-4), 7.55 (d, J = 8.7 Hz, 1H, ArH-5), 7.49 (dt, J = 7.8, 0.9 Hz, 1H, ArH-6′), 7.43 (ddd, J = 7.7, 4.8, 1.0 Hz, 1H, ArH-4′) ppm.

^{13}C NMR (126 MHz, CDCl$_3$): δ 150.5 (C-3′), 149.9 (C-2), 149.6 (C-2′), 137.1 (C-5′), 130.0 (C-5), 129.0 (C-4), 126.6 (C-6), 125.7 (C-3), 125.4 (C-6′), 125.0 (C-4′), 111.5 (-CN) ppm.

IR (v/cm^{-1}): 3100 (w), 2923 (w), 2239 (w), 1579 (m), 1541 (w), 1446 (m) 1428 (m), 1347 (s), 1282 (w), 1257 (s), 1210 (m), 1128 (w), 1048 (w), 996 (m), 918 (s), 864 (w), 828 (s), 780 (s), 746 (s), 697 (m), 657 (w).

HRESI-MS (MeOH, +, m/z): [M+H]$^+$ 275.9766, calc. 275.9767, [M+Na]$^+$ 297.9586, calc. 297.9586

M.p.: 178–181 °C

3-Bromo-5-methoxy-2,2′-bipyridine *N*-oxide (22f)

[FW 2058]
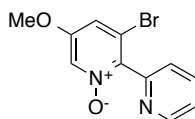
According to the general procedure, the reaction of bipyridine *N*-oxide **20f** (205 mg, 1.01 mmol), Pd(OAc)$_2$ (12.0 mg, 0.054 mmol), and NBS (217 mg, 1.22 mmol) in chlorobenzene (10.0 mL) provided **22f** (281 mg, 1.00 mmol, 99%) as brown solid after extraction. Single crystals for X-ray diffraction were grown by slow diffusion of pentane into a concentrated solution of **22f** in DCM. CCDC-1476430 contains the crystallographic data for **22f**.

^{1}H NMR (500 MHz, CDCl$_3$): δ 8.77 (ddd, J = 4.9, 1.8, 0.9 Hz, 1H, ArH-3′), 8.04 (d, J = 2.3 Hz, 1H, ArH-4), 7.83 (td, J = 7.7, 1.7 Hz, 1H, ArH-5′), 7.48 (dt, J = 7.8, 1.1 Hz, 1H, ArH-6′), 7.36 (ddd, J = 7.6, 4.9, 1.2 Hz, 1H, ArH-4′), 7.20 (d, J = 2.2 Hz, 1H, ArH-6), 3.86 (s, 3H, -OCH$_3$) ppm.

^{13}C NMR (126 MHz, CDCl$_3$): δ 156.9 (C-2), 151.2 (C-2′), 150.1 (C-3′), 142.2 (C-5), 136.8 (C-5′), 127.6 (C-4), 125.9 (C-6′), 124.1 (C-4′), 121.5 (C-3), 117.5 (C-6), 56.6 (-OCH$_3$) ppm.

IR (v/cm^{-1}): 3033 (w), 2923 (w), 2852 (w), 1594 (m), 1578 (w), 1564 (w), 1539 (s), 1493 (w), 1451 (m), 1422 (m), 1384 (m), 1313 (m), 1233 (m), 1214 (s), 1175 (w), 1159 (s), 1139 (m), 1088 (w), 1067 (w), 1040 (w), 1020 (s), 986 (w), 970 (w), 891 (m), 853 (m), 821 (m), 790 (m), 753 (m), 737 (m).

HRESI-MS (MeOH, +, m/z): [M+H]$^+$ 280.9952, calc. 280.9920, [M+Na]$^+$ 302.9773, calc. 302.9740, [M+K]$^+$ 318.9819, calc. 318.9479

M.p.: 122 °C

3-Bromo-5-methyl-2,2′-bipyridine *N*-oxide (22g)

[SZ 5054]
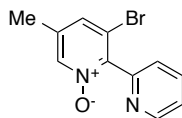
Similar to the general procedure, the reaction of bipyridine *N*-oxide **20g** (188 mg, 1.01 mmol), Pd(OAc)$_2$ (11.6 mg, 0.052 mmol), and NBS (215 mg, 1.21 mmol) in degassed chlorobenzene (10.0 mL) provided reduced product **25g** (88.9 mg, 0.36 mmol, 35%) as red oil and **22g** (107 mg, 0.40 mmol, 40%) as tan solid after purification by column chromatography (MeOH in DCM mixtures: 0%–0.5%, 0.1% increments the 1–5%, 1% increments).

^{1}H NMR (500 MHz, CDCl$_3$): δ 8.79 (d, *J* = 4.9 Hz, 1H, ArH-3′), 8.15 (s, 1H, ArH-4), 7.85 (td, *J* = 7.7, 1.7 Hz, 1H, ArH-5′), 7.50 (d, *J* = 7.8 Hz, 1H, ArH-6′), 7.42 (s, 1H, ArH-6), 7.38 (ddd, *J* = 7.6, 4.9, 1.1 Hz, 1H, ArH-4′), 2.34 (s, 3H, -CH$_3$) ppm.

^{13}C NMR (126 MHz, CDCl$_3$): δ 151.2 (C-2′), 150.0 (C-3′), 145.8 (C-2), 138.9 (C-4), 136.6 (C-5′), 136.2 (C-5), 130.9 (C-6), 125.4 (C-6′), 124.0 (C-4′), 121.1 (C-3), 18.0 (-CH$_3$) ppm.

IR (ν/cm^{-1}): 3051 (w), 2925 (w), 1708 (w), 1598 (m), 1565 (w), 1537 (m), 1460 (w), 1428 (m), 1371 (s), 1280 (s), 1212 (s), 1146 (m), 1096 (w), 1057 (w), 1020 (s), 986 (m) 898 (w), 854 (s), 789 /s), 751 (m), 731 (m).

HRESI-MS (MeOH, +, *m/z*): [M+H]$^+$ 264.9991, calc. 264.9971, [M+Na]$^+$ 286.9813, calc. 286.9790, [M+K]$^+$ 302.9560, calc. 302.9530

M.p.: 109–112 °C

3-Bromo-5-methyl-2,2′-bipyridine (**25g**)
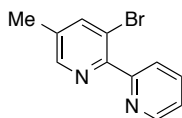
^{1}H NMR (400 MHz, CDCl$_3$): δ 8.72 (s, 1H, ArH-3′), 8.46 (s, 1H, ArH-4), 7.82 (dd, *J* = 1.8, 0.7 Hz, 1H, ArH-6), 7.77 (td, *J* = 7.7, 1.8 Hz, 1H, ArH-5′), 7.70 (d, *J* = 7.8 Hz, 1H, ArH-6′), 7.30 (ddd, *J* = 7.4, 4.8, 1.1 Hz, 1H, ArH-4′), 2.35 (s, 3H, -CH$_3$) ppm.

^{13}C NMR (126 MHz, CDCl$_3$): δ 157.1 (C-2′), 153.7 (C-2), 149.1 (C-3′), 148.5 (C-4), 141.8 (C-6), 136.2 (C-5′), 134.5 (C-5), 124.3 (C-6), 123.2 (C-4′), 119.0 (C-3), 17.7 (-CH$_3$) ppm.

IR (ν/cm^{-1}): 3042 (w), 3002 (w), 2921 (w), 1718 (m), 1584 (m), 1568 (m), 1445 (m), 1424 (s), 1377 (m), 1285 (w), 1248 (w), 1213 (w), 1184 (w), 1147 (w), 1099 (m), 1086 (m), 1047 (w), 1030 (s), 991 (m), 963 (w), 872 (s), 797 (s), 744 (s), 670 (w).

HRESI-MS (MeOH, +, *m/z*): [M+H]$^+$ 249.0040, calc. 249.0022, [M+Na]$^+$ 270.9863, calc. 270.9841

3-Bromo-5-(methoxycarbonyl)-2,2′-bipyridine *N*-oxide (22h)

[SZ 5049]
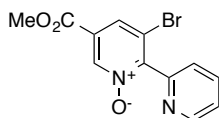
According to the general procedure, the reaction of bipyridine *N*-oxide **20h** (233 mg, 1.01 mmol), Pd(OAc)$_2$ (13.3 mg, 0.059 mmol), and NBS (218 mg, 1.22 mmol) in chlorobenzene (10.0 mL) provided **22h** (9.3 mg, 0.03 mmol, 3%) as reddish oil after purification by column chromatography (acetone in hexane mixtures: 5%–20%, 5% increments, then 50%).

^{1}H NMR (500 MHz, CDCl$_3$): δ 8.85–8.81 (m, 2H, ArH-4, ArH-3′), 8.13 (d, *J* = 1.1 Hz, 1H, ArH-6), 7.89 (td, *J* = 7.8, 1.5 Hz, 1H, ArH-5′), 7.53 (d, *J* = 7.6 Hz, 1H, ArH-6′), 7.45–7.40 (m, 1H, ArH-4′), 3.99 (s, 3H, -CH$_3$) ppm.

^{13}C NMR (126 MHz, CDCl$_3$): δ 162.6 (C=O), 151.6 (C-2), 150.7 (C-3′), 150.4 (C-2′), 140.2 (C-4), 137.0 (C-5′), 130.2 (C-6), 128.9 (C-5), 125.4 (C-6′), 124.8 (C-4′), 122.1 (C-3), 53.5 (-CH$_3$) ppm.

IR (v/cm^{-1}): 3051 (w), 2952 (w), 2924 (w), 2851 (w), 1727 (s), 1581 (m), 1538 (m), 1489 (w), 1456 (w), 1426 (m), 1364 (s), 1301 (s), 1235 (s), 1192 (m), 1106 (m), 1055 (w), 1032 (w), 928 (m), 878 (w), 850 (m), 786 (m), 760 (m), 730 (m).

HRESI-MS (MeOH, +, *m/z*): [M+H]$^+$ 308.9902, calc. 308.9869, [M+Na]$^+$ 330.9726, calc. 330.9689

3-Bromo-5-nitro-2,2′-bipyridine *N*-oxide (22i)

[FW 2092]
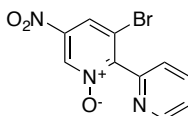
According to the general procedure, the reaction of bipyridine *N*-oxide **20i** (115 mg, 0.53 mmol), Pd(OAc)$_2$ (5.8 mg, 0.026 mmol), and NBS (114 mg, 0.64 mmol) in chlorobenzene (5.30 mL) provided a complex product mixture (101 mg) after extraction.

3-Bromo-4-chloro-2,2′-bipyridine *N*-oxide (22k)

[FW 2050]
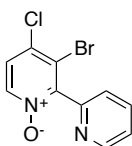
According to the general procedure, the reaction of bipyridine *N*-oxide **20k** (207 mg, 1.00 mmol), Pd(OAc)$_2$ (11.2 mg, 0.050 mmol), and NBS (214 mg, 1.20 mmol) in chlorobenzene (10.0 mL) provided a complex product mixture (254 mg) after extraction.

3-Bromo-4-(ethoxycarbonyl)-2,2′-bipyridine *N*-oxide (22l)

[FW 1090]
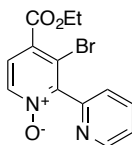
According to the general procedure, the reaction of bipyridine *N*-oxide **20l** (82.4 mg, 0.34 mmol), Pd(OAc)$_2$ (4.8 mg, 0.021 mmol), and NBS (63.9 mg, 0.36 mmol) in chlorobenzene (2.80 mL) provided starting material (89.9 mg) containing traces of impurities after extraction.

3-Bromo-4-(trifluoromethyl)-2,2′-bipyridine *N*-oxide (22m)

[FW 2074]
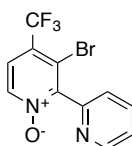
According to the general procedure, the reaction of bipyridine *N*-oxide **20m** (248 mg, 1.03 mmol), Pd(OAc)$_2$ (11.8 mg, 0.053 mmol), and NBS (222 mg, 1.25 mmol) in chlorobenzene (10.0 mL) provided (dioxopyrrolidinyl)bipyridine *N*-oxide **30m** (125 mg, 0.37 mmol, 36%) as a brown solid and starting material (133 mg, 0.55 mmol, 53%) after column chromatography (acetone in hexane mixtures: 0–40%, 10% increments).

4-(Trifluoromethyl)-6-dioxopyrrolidinyl-2,2′-bipyridine *N*-oxide (**30m**)
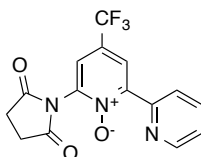
^{1}H NMR (500 MHz, CDCl$_3$): δ 8.81 (dt, *J* = 8.1, 1.1 Hz, 1H, ArH-6′), 8.75 (ddd, *J* = 4.8, 1.8, 1.0 Hz, 1H, ArH-3′), 8.65 (dd, *J* = 2.8, 0.8 Hz, 1H, ArH-5), 7.81 (td, *J* = 7.8, 1.9 Hz, 1H, ArH-5′), 7.60 (dd, *J* = 2.8, 0.7 Hz, 1H, ArH-3), 7.38 (ddd, *J* = 7.6, 4.7, 1.2 Hz, 1H, ArH-4′), 3.12–2.92 (m, 4H, -CH$_2$CH$_2$-) ppm.

^{13}C NMR (126 MHz, CDCl$_3$): δ 174.3 (C=O), 149.8 (C-3), 148.9 (C-2′), 147.9 (C-2), 140.6 (C-6), 136.6 (C-5′), 126.1 (q, *J* = 36.0 Hz, C-4), 125.5 (C-6′), 125.4 (C-4′), 125.2 (q, *J* = 4.0 Hz, C-5), 122.7 (q, *J* = 3.9 Hz, C-3), 122.3 (q, *J* = 272 Hz, CF$_3$), 29.1 (-CH$_2$CH$_2$-) ppm.

^{19}F NMR (471 MHz, CDCl$_3$): δ -63.3 ppm.

IR (*v*/cm^{-1}): 3086 (w), 3052 (w), 2938 (w), 1797 (w), 1715 (s), 1573 (w), 1475 (w), 1449 (w), 1414 (w), 1388 (m), 1327 (m), 1272 (m), 1240 (w), 1222 (w), 1150 (s), 1134 (s), 1116 (m), 1095 (w), 1047

(w), 1014 (w), 992 (w), 980 (w), 929 (w), 883 (w), 816 (w), 787 (m), 737 (m), 685 (m).

HRESI-MS (MeOH, +, *m/z*): [M+H]$^+$ 338.0749, calc. 338.0747, [M+Na]$^+$ 360.0573, calc. 360.0566, [M+K]$^+$

376.0270, calc. 376.0306

M.p.: 122 °C

3-Bromo-4-cyano-2,2′-bipyridine *N*-oxide (22n)

[FW 2049]
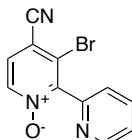
According to the general procedure, the reaction of bipyridine *N*-oxide **20n** (197 mg, 1.00 mmol), Pd(OAc)$_2$ (11.6 mg, 0.052 mmol), and NBS (214 mg, 1.20 mmol) in chlorobenzene (10.0 mL) provided **22n** (102 mg, 0.37 mmol, 37%) as red solid and starting material (62.1 mg, 0.32 mmol, 32%) after column chromatography (acetone in hexane mixtures: 0–100%, 10% increments). Single crystals for X-ray diffraction were grown by slow diffusion of pentane into a concentrated solution of **22n** in DCM. CCDC-1476429 contains the crystallographic data for **22n**.

^{1}H NMR (500 MHz, CDCl$_3$): δ 8.80 (ddd, *J* = 4.9, 1.7, 1.0 Hz, 1H, ArH-3′), 8.28 (d, *J* = 7.0 Hz, 1H, ArH-5), 7.91 (td, *J* = 7.7, 1.7 Hz, 1H, ArH-5′), 7.53 (d, *J* = 6.9 Hz, 1H, ArH-6), 7.48–7.43 (m, 2H, ArH-4′, ArH-6′) ppm.

^{13}C NMR (126 MHz, CDCl$_3$): δ 150.6 (C-3′), 150.5 (C-2′), 150.0 (C-2), 139.7 (C-5), 137.3 (C-5′), 128.3 (C-6), 125.4 (C-3), 125.3 (C-6′), 125.0 (C-4′), 115.2 (C-4), 112.2 (-CN) ppm.

IR (*v*/cm^{-1}): 3103 (w), 3059 (w), 2956 (w), 2922 (w), 2852 (w), 2228 (m), 1731 (w), 1597 (w), 1583 (w), 1569 (w), 1444 (w), 1428 (m), 1403 (m), 1303 (w), 1288 (m), 1267 (s), 1233 (w), 1194 (w), 1149 (w), 1096 (w), 1080 (m), 1046 (w), 993 (w), 844 (w), 821 (s), 768 (w), 738 (s), 727 (s), 678 (w).

HRESI-MS (MeOH, +, *m/z*): [M+H]$^+$ 275.9788, calc. 275.9767, [M+Na]$^+$ 297.9609, calc. 297.9586

M.p.: 157 °C

3-Bromo-4-nitro-2,2′-bipyridine *N*-oxide (22o)

[FW 2048]

According to the general procedure, the reaction of bipyridine *N*-oxide **20o** (217 mg, 1.00 mmol), Pd(OAc)$_2$ (11.1 mg, 0.051 mmol), and NBS (216 mg, 1.21 mmol) in chlorobenzene (10.0 mL)

provided pure starting material (120 mg, 0.55 mmol, 55%) and a mixture of starting material and presumably (dioxopyrrolidinyl)bipyridine *N*-oxide **30o** (75.3 mg, 1:1.4) after column chromatography (acetone in hexane mixtures: 0–100%, 10% increments).

4-Nitro-6-dioxopyrrolidinyl-2,2′-bipyridine *N*-oxide (**30o**)
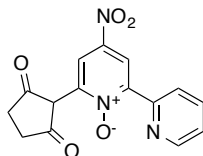
^{1}H NMR (500 MHz, CDCl$_3$): δ 9.23 (d, J = 3.3 Hz, 1H), 8.80–8.73 (m, 2H), 8.20 (d, J = 3.3 Hz, 1H), 7.82 (td, J = 7.8, 2.0 Hz, 1H), 7.41 (ddd, J = 7.4, 4.7, 1.1 Hz, 1H), 3.16–2.92 (m, 4H) ppm.

3′-Bromo-6′-methoxy-2,2′-bipyridine *N*-oxide (22p)

[FW 2046]
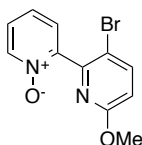
According to the general procedure, the reaction of bipyridine *N*-oxide **20p** (203 mg, 1.00 mmol), Pd(OAc)$_2$ (11.2 mg, 0.050 mmol), and NBS (216 mg, 1.21 mmol) in chlorobenzene (10.0 mL) provided **22p** (276 mg, 0.98 mmol, 98%) as brown solid after extraction.

^{1}H NMR (500 MHz, CDCl$_3$): δ 8.32–8.28 (m, 1H, ArH-3), 7.78 (d, J = 8.8 Hz, 1H, ArH-5′), 7.37 (dd, J = 5.5, 4.4 Hz, 1H, ArH-4), 7.34–7.30 (m, 2H, ArH-5, ArH-6), 6.72 (d, J = 8.8 Hz, 1H, ArH-4′), 3.87 (s, 3H, -OCH$_3$) ppm.

^{13}C NMR (126 MHz, CDCl$_3$): δ 163.1 (C-5′), 148.5 (C-2), 148.2 (C-2′), 142.8 (C-6′), 139.9 (C-3), 127.5 (C-4), 126.0 and 125.1 (C-5, C-6), 113.4 (C-4′), 113.1 (C-3′), 54.1 (-CH$_3$) ppm.

IR (v/cm^{-1}): 3065 (w), 3054 (w), 3013 (w), 2988 (w), 2970 (w), 2937 (w), 1579 (m), 1493 (w), 1456 (m), 1423 (s), 1408 (s), 1320 (s), 1276 (w), 1247 (s), 1219 (m), 1176 (w), 1155 (w), 1128 (m), 1119 (m), 1093 (w), 1046 (w), 1020 (s), 1011 (s), 893 (s), 835 (m), 823 (s), 783 (m), 764 (s), 741 (w), 700 (w), 653 (s).

HRESI-MS (MeOH, +, *m/z*): [M+H]$^+$ 280.9930, calc. 280.9920, [M+Na]$^+$ 302.9755, calc. 302.9740, [M+K]$^+$ 318.9490, calc. 318.9479

M.p.: 142 °C

3′-Bromo-6′-methyl-2,2′-bipyridine *N*-oxide (22q)

[SZ 5055]
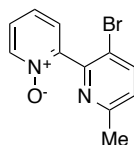
Similar to the general procedure, the reaction of bipyridine *N*-oxide **20q** (177.3 mg, 0.95 mmol), Pd(OAc)$_2$ (12.1 mg, 0.054 mmol), and NBS (227 mg, 1.27 mmol) in degassed chlorobenzene (10.0 mL) provided reduced product **25b** (30.9 mg, 0.12 mmol, 13%) as orange oil, and a complex product fraction after purification by column chromatography (MeOH in DCM mixtures: 0.5%).

3-Bromo-6-methyl-2,2′-bipyridine (**25b**)
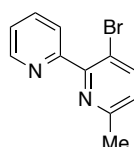
^{1}H NMR (500 MHz, CDCl$_3$): δ 8.74 (d, *J* = 4.8 Hz, 1H, ArH-3′), 7.86 (d, *J* = 8.2 Hz, 1H, ArH-4), 7.79 (td, *J* = 7.7, 1.8 Hz, 1H, ArH-,)), 7.67 (d, *J* = 7.8 Hz, 1H, ArH-6′), 7.32 (ddd, *J* = 7.6, 4.9, 1.2 Hz, 1H, ArH-4′), 7.06 (d, *J* = 8.2 Hz, 1H, ArH-5), 2.57 (s, 3H, -CH$_3$) ppm.

^{13}C NMR (126 MHz, CDCl$_3$): δ 157.5 and 157.4(C-6, C2′), 155.8 (C-2), 149.3 (C-3′), 141.6 (C-4), 136.4 (C-5′), 124.5 (C-5), 124.4 (C-6′), 123.4 (C-4′), 116.5 (C-3), 24.2 (-CH$_3$) ppm.

IR (v/cm^{-1}): 3054 (w), 2922 (w), 1714 (m), 1588 (w), 1561 (m), 1474 (w), 1446 (w), 1417 (s), 1378 (w), 1283 (w), 1233 (w), 1134 (w), 1112 (w), 1014 (s), 993 (w), 876 (w), 820 (m), 796 (m), 757 (s).

HRESI-MS (MeOH, +, *m/z*): [M+H]$^+$ 249.0042, calc. 249.0022, [M+Na]$^+$ 270.9863, calc. 270.9841

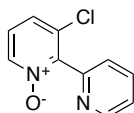### 3′-Bromo-6′-(trifluoromethyl)-2,2′-bipyridine *N*-oxide (22r)

[FW 2045]
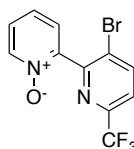
According to the general procedure, the reaction of bipyridine *N*-oxide **20r** (241 mg, 1.00 mmol), Pd(OAc)$_2$ (11.4 mg, 0.051 mmol), and NBS (216 mg, 1.21 mmol) in chlorobenzene (10.0 mL) provided **22r** (23.4 mg, 0.07 mmol, 7%) as tan solid, reduced **25d** (75.8 mg, 0.25 mmol, 25%) as yellow solid, and a mixture of **22r** and starting material (130 mg, 1:1.24) after column chromatography (acetone in hexane mixtures: 1–60%, 10% increments).

^{1}H NMR (500 MHz, CDCl$_3$): δ 8.31 (d, J = 5.7 Hz, 1H, ArH-3), 8.18 (dt, J = 8.2, 0.7 Hz, 1H, ArH-4′), 7.65 (d, J = 8.3 Hz, 1H, ArH-5′), 7.47 (dd, J = 7.0, 2.8 Hz, 1H, ArH-5), 7.43–7.36 (m, 2H, ArH-4, ArH-6) ppm.

^{13}C NMR (126 MHz, CDCl$_3$): δ 152.5 (C-2′), 147.3 (q, J = 36 Hz, C-6′), 146.9 (C-2), 142.1 (C-4′), 139.9 (C-3), 127.6 (C-5), 126.8 (C-4), 126.1 (C-3′), 125.7 (C-6), 122.0 (q, J = 3.0 Hz, C-5′), 121.2 (q, J = 274 Hz, -CF$_3$) ppm.

^{19}F NMR (471 MHz, CDCl$_3$): δ –67.5 ppm.

IR (v/cm^{-1}): 3122 (w), 3074 (w), 2960 (w), 2922 (m), 2852 (w), 1458 (w), 1434 (w), 1421 (w), 1397 (w), 1337 (m), 1289 (w), 1258 (m), 1230 (w), 1173 (w), 1159 (w), 1133 (w), 1119 (w), 1106 (s), 1069 (w), 1042 (w), 1022 (s), 862 (w), 849 (w), 820 (w), 795 (m), 772 (s), 741 (w), 730 (w).

HRESI-MS (MeOH, +, m/z): [M+H]$^+$ 318.9639, calc. 318.9688, [M+Na]$^+$ 340.9513, calc. 340.9508

3-Bromo-6-(trifluoromethyl)-2,2′-bipyridine (**25d**)
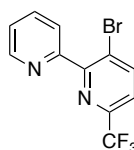
^{1}H NMR (400 MHz, CDCl$_3$): δ 8.75 (d, J = 4.8 Hz, 1H, ArH-3′), 8.21 (d, J = 8.2 Hz, 1H, ArH-4), 7.86 (td, J = 7.7, 1.7 Hz, 1H, ArH-5′), 7.77 (d, J = 7.8 Hz, 1H, ArH-6′), 7.58 (d, J = 8.3 Hz, 1H, ArH-5), 7.40 (ddd, J = 7.5, 4.9, 1.2 Hz, 1H, ArH-4′) ppm.

^{13}C NMR (126 MHz, CDCl$_3$): δ 155.5, 155.2, 149.2, 146.1 (q, J = 35.6 Hz), 140.0, 136.9, 133.8, 124.8, 124.1, 121.3 (d, J = 274.3 Hz) 121.0 (q, J = 2.3 Hz) ppm.

^{19}F NMR (376 MHz, CDCl$_3$): δ –67.5 ppm.

IR (v/cm^{-1}): 2924 (w), 2853 (w), 1590 (w), 1574 (w), 1479 (w), 1449 (w), 1424 (w), 1394 (m), 1335 (m), 1273 (w), 1225 (w), 1185 (m), 1121 (s), 1097 (m), 1082 (m), 1032 (m), 1019 (m), 993 (w), 845 (m), 797 (m), 770 (w), 742 (m), 684 (w).

HRESI-MS (MeOH, +, m/z): [M+H]$^+$ 302.9769, calc. 302.9739, [M+Na]$^+$ 324.9588, calc. 324.9559

M.p.: 54 °C

3-Bromo-5′-methyl-2,2′-bipyridine *N*-oxide (22s)

[FW 2073]
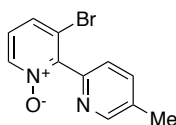
According to the general procedure, the reaction of bipyridine *N*-oxide **20s** (112 mg, 0.60 mmol), Pd(OAc)$_2$ (8.4 mg, 0.038 mmol), and NBS (129 mg, 0.72 mmol) in chlorobenzene (6.00 mL) provided **22s** (11.6 mg, 0.04 mmol, 7%) as brown solid, reduced **25s** (11.1 mg, 0.05 mmol, 8%) as brown oil,

and starting material (16.6 mg, 0.09 mmol, 15%) after column chromatography (acetone in hexane mixtures: 1–100%, 10% increments).

^{1}H NMR (500 MHz, CDCl$_3$): δ 8.62 (dt, J = 1.9, 0.8 Hz, 1H, ArH-6′), 8.27 (dd, J = 6.6, 1.1 Hz, 1H, ArH-4), 7.67 (ddd, J = 7.9, 2.2, 0.9 Hz, 1H, ArH-4′), 7.56 (dd, J = 8.3, 1.0 Hz, 1H, ArH-6), 7.41 (dd, J = 7.9, 0.8 Hz, 1H, ArH-3′), 7.15 (dd, J = 8.3, 6.6 Hz, 1H, ArH-5), 2.42 (s, 3H, -CH$_3$) ppm.

^{13}C NMR (126 MHz, CDCl$_3$): δ 150.8 (C-6′), 148.5 (C-2), 139.2 (C-4), 137.4 (C-4′), 134.3 (C-5′), 129.8 (C-6), 125.3 (C-5), 124.8 (C-3′), 122.3 (C-3), 18.7 (-CH$_3$) ppm.

IR (v/cm^{-1}): 3041 (w), 2922 (w), 2852 (w), 1713 (w), 160 (w), 1588 (w), 1566 (w), 1536 (w), 1451 (m), 1408 (s), 1371 (w), 1252 (s), 1231 (w), 1205 (w), 1181 (w), 1082 (w), 1037 (w), 1026 (s), 903 (s), 842 (w), 828 (m), 797 (s), 741 (w), 732 (w).

HRESI-MS (MeOH, +, m/z): [M+H]$^+$ 264.9977, calc. 264.9971, [M+Na]$^+$ 286.9801, calc. 286.9790, [M+K]$^+$ 302.9540, calc. 302.9530

M.p.: 138 °C

3-Bromo-5′-methyl-2,2′-bipyridine (**25s**)
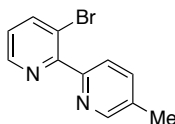
^{1}H NMR (500 MHz, CDCl$_3$): δ 8.64 (dd, J = 4.5, 1.5 Hz, 1H, ArH-4), 8.58 (s, 1H, ArH-6′), 8.01 (dd, J = 8.1, 1.5 Hz, 1H, ArH-6), 7.66–7.61 (m, 2H, ArH-3′, ArH-4′), 7.19 (dd, J = 8.1, 4.6 Hz, 1H, ArH-5), 2.42 (s, 3H, -CH$_3$) ppm.

^{13}C NMR (126 MHz, CDCl$_3$): δ 156.7 (C-2), 154.6 (C-2′), 149.7 (C-6′), 148.2 (C-4), 141.7 (C-6), 137.0 and 124.0 (C-3′, C-4′), 132.2 (C-5′), 124.2 (C-5), 119.8 (C-3), 18.5 (-CH$_3$) ppm.

IR (v/cm^{-1}): 3040 (w), 3002 (w), 2922 (w), 2861 (w), 1715 (w), 1589 (w), 1567 (m) 1548 (w), 1489 (w), 1459 (m), 1429 (s), 1374 (m), 1274 (w), 1247 (w), 1218 (w), 1122 (w), 1093 (m), 1015 (s), 838 (m), 791 (s), 774 (w), 743 (s).

HRESI-MS (MeOH, +, m/z): [M+H]$^+$ 249.0030, calc. 249.0022, [M+Na]$^+$ 270.9852, calc. 270.9841

3-Bromo-4′-methoxy-2,2′-bipyridine *N*-oxide (22t)

[FW 2068]
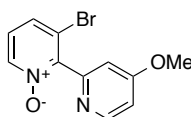
According to the general procedure, the reaction of bipyridine *N*-oxide **20t** (204 mg, 1.01 mmol), Pd(OAc)$_2$ (11.5 mg, 0.051 mmol), and NBS (215 mg, 1.21 mmol) in chlorobenzene (10.0 mL) provided **22t** (152.2 mg, 0.54 mmol, 54%) as yellow oil after column chromatography (MeOH in

DCM mixtures: 1–10%, 1% increments).

^{1}H NMR (500 MHz, CDCl$_3$): δ 8.57 (d, J = 5.8 Hz, 1H, ArH-4), 8.24 (dd, J = 6.6, 1.1 Hz, 1H, ArH-6), 7.53 (dd, J = 8.3, 1.0 Hz, 1H, ArH-6′), 7.15 (dd, J = 8.3, 6.5 Hz, 1H, ArH-5), 6.99 (d, J = 2.5 Hz, 1H, ArH-5′), 6.89 (dd, J = 5.7, 2.5 Hz, 1H, ArH-3′), 3.86 (s, 3H, -OCH$_3$) ppm.

^{13}C NMR (126 MHz, CDCl$_3$): δ 166.3 (C-2′), 152.6 (C-2), 151.5 (C-6′), 148.8 (C-4′), 139.1 (C-4), 129.7 (C-6), 125.3 (C-5), 122.0 (C-3′), 111.4 (C-3), 110.6 (C-5′), 55.5 (-OCH$_3$) ppm.

IR (v/cm^{-1}): 3106 (w), 3079 (w), 2964 (w), 1602 (m), 1584 (w), 1563 (m), 1542 (w), 1473 (m), 1442 (w), 1410 (s), 1312 (m), 1256 (s), 1245 (m), 1215 (w), 1186 (w), 1140 (w), 1046 (w), 1029 (s), 988 (w), 903 (s), 862 (m), 845 (m), 783 (s), 744 (w), 726 (s).

HRESI-MS (MeOH, +, m/z): [M+H]$^+$ 280.9934, calc. 280.9920, [M+Na]$^+$ 302.9757, calc. 302.9740, [M+K]$^+$ 318.9489, calc. 318.9479

3-Bromo-4′-methyl-2,2′-bipyridine N-oxide (22u)

[FW 2066]
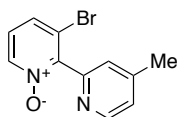
According to the general procedure, the reaction of bipyridine N-oxide **20u** (188 mg, 1.01 mmol), Pd(OAc)$_2$ (11.5 mg, 0.051 mmol), and NBS (215 mg, 1.21 mmol) in chlorobenzene (10.0 mL) provided **22u** (282 mg, 1.06 mmol, quant.) as brown solid containing traces of impurities after extraction.

^{1}H NMR (500 MHz, CDCl$_3$): δ 8.63 (dd, J = 5.1, 0.8 Hz, 1H, ArH-6′), 8.26 (dd, J = 6.5, 1.0 Hz, 1H, ArH-4), 7.55 (dd, J = 8.3, 1.0 Hz, 1H, ArH-6), 7.31 (d, J = 0.8 Hz, 1H, ArH-3′), 7.20 (d, J = 5.0 Hz, 1H, ArH-5′), 7.15 (dd, J = 8.3, 6.5 Hz, 1H, ArH-5), 2.42 (s, 3H, -CH$_3$) ppm.

^{13}C NMR (126 MHz, CDCl$_3$): δ 151.1 (C-2), 150.0 (C-6′), 148.3 (C-2′), 139.2 (C-4), 129.8 (C-6), 128.7 (C-4′), 126.0 (C-3′), 125.4 (C-5′), 125.3 (C-5), 122.1 (C-3), 21.3 (-CH$_3$) ppm.

IR (v/cm^{-1}): 3056 (w), 2922 (w), 1711 (m), 1605 (m), 1586 (w), 1557 (w), 1441 (w), 1407 (s), 1287 (w), 1256 (s), 1182 (m), 1121 (w), 1052 (w), 1041 (w), 1019 (w), 991 (w), 904 (s), 871 (w), 829 (m), 779 (s), 754 (w), 720 (s), 680 (w).

HRESI-MS (MeOH, +, m/z): [M+H]$^+$ 264.9991, calc. 264.9971, [M+Na]$^+$ 286.9813, calc. 286.9790, [M+K]$^+$ 302.9556, calc. 302.9530

M.p.: 79 °C

3-Bromo-4′-(ethoxycarbonyl)-2,2′-bipyridine *N*-oxide (22w)

[FW 2065]
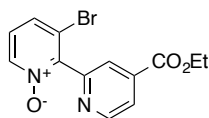
According to the general procedure, the reaction of bipyridine *N*-oxide **20w** (247 mg, 1.01 mmol), Pd(OAc)$_2$ (11.5 mg, 0.051 mmol), and NBS (214 mg, 1.20 mmol) in chlorobenzene (10.0 mL) provided **22w** (272 mg, 0.84 mmol, 83%) as brown solid after extraction.

^{1}H NMR (500 MHz, CDCl$_3$): δ 8.94 (dd, J = 5.0, 0.9 Hz, 1H, ArH-6′), 8.29 (dd, J = 6.6, 1.0 Hz, 1H, ArH-4), 8.07 (dd, J = 1.6, 0.9 Hz, 1H, ArH-3′), 7.96 (dd, J = 5.1, 1.6 Hz, 1H, ArH-5′), 7.59 (dd, J = 8.3, 1.0 Hz, 1H, ArH-6), 7.21 (dd, J = 8.3, 6.6 Hz, 1H, ArH-5), 4.42 (q, J = 7.2 Hz, 2H, -CH$_2$-), 1.40 (t, J = 7.1 Hz, 3H, -CH$_3$) ppm.

^{13}C NMR (126 MHz, CDCl$_3$): δ 164.6 (C=O), 152.2 (C-2′), 151.1 (C-6′), 148.2 (C-2), 139.2 (C-4), 138.9 (C-4′), 129.9 (C-6), 125.7 (C-5), 124.9 (C-3′), 123.6 (C-5′), 122.1 (C-3), 62.2 (-CH$_2$-), 14.3 (-CH$_3$) ppm.

IR (v/cm^{-1}): 3061 (w), 2980 (w), 2927 (w), 1722 (s), 1604 (w), 1557 (w), 1463 (w), 1408 (m), 1367 (w), 1303 (m), 1289 (m), 1236 (s), 1116 (m), 1101 (m), 1049 (w), 1014 (m), 896 (s), 859 (w), 784 (m), 760 (s), 731 (w), 687 (w), 674 (w).

HRESI-MS (MeOH, +, *m/z*): [M+H]$^+$ 323.0057, calc. 323.0026, [M+Na]$^+$ 344.9882, calc. 344.9845, [M+K]$^+$ 360.9701, calc. 360.9585

M.p.: 68 °C

3-Bromo-2-(pyridin-2-yl)quinoline *N*-oxide (22y)

[FW 2063]
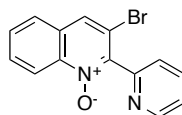
According to the general procedure, the reaction of pyridylquinoline *N*-oxide **20y** (214 mg, 0.96 mmol), Pd(OAc)$_2$ (11.4 mg, 0.051 mmol), and NBS (218 mg, 1.23 mmol) in chlorobenzene (10.0 mL) provided **22y** (143 mg, 0.48 mmol, 49%), reduced **25y** (23.6 mg, 0.08 mmol, 9%), and dioxopyrrolidinylisoqinoline *N*-oxide **30y** (29.4 mg, 0.07 mmol, 8%) as brown solids after column chromatography (acetone in hexane mixtures: 0–80%, 10% increments).

^{1}H NMR (500 MHz, CDCl$_3$): δ 8.82 (d, J = 4.4 Hz, 1H, ArH-6′), 8.66 (d, J = 8.9 Hz, 1H, ArH-9), 8.06 (s, 1H, ArH-4), 7.89 (td, J = 7.8, 1.7 Hz, 1H, ArH-4′), 7.80 (d, J = 8.0 Hz, 1H, ArH-6), 7.75 (ddd, J =

8.6, 7.0, 1.4 Hz, 1H, ArH-8), 7.66 (ddd, J = 8.2, 6.9, 1.2 Hz, 1H, ArH-7), 7.58 (d, J = 7.8 Hz, 1H, ArH-3′), 7.42 (ddd, J = 7.6, 4.9, 1.2 Hz, 1H, ArH-5′) ppm.

^{13}C NMR (126 MHz, CDCl$_3$): δ 152.2 (C-2′), 150.2 (C-6′), 144.4 (C-2), 141.3 (C-10), 136.9 (C-4′), 130.8 (C-8), 129.9 (C-7), 129.7 (C-5), 128.5 (C-4), 127.3 (C-6), 125.4 (C-3′), 124.2 (C-5′), 120.4 (C-9), 116.2 (C-3) ppm.

IR (ν/cm^{-1}): 3087 (w), 3070 (w), 3058 (w), 3010 (w), 1715 (w), 1592 (w), 1565 (w), 1551 (w), 1496 (w), 1473 (w), 1446 (w), 1425 (w), 1412 (w), 1324 (s), 1294 (w), 1267 (w), 1205 (m), 1140 (w), 1123 (w), 1077 (w), 1051 (w), 994 (w), 962 (w), 918 (s), 890 (w), 873 (w), 846 (m), 811 (w), 768 (s), 750 (m), 742 (m).

HRESI-MS (MeOH, +, m/z): [M+H]$^+$ 300.9979, calc. 300.9971, [M+Na]$^+$ 322.9803, calc. 322.9790, [M+K]$^+$ 338.9535, calc. 338.9530

M.p.: 158 °C

3-Bromo-2-(pyridin-2-yl)quinoline (**25y**)
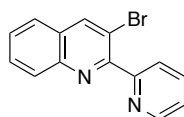
^{1}H NMR (400 MHz, CDCl$_3$): δ 8.79 (d, J = 4.8 Hz, 1H, ArH-6′), 8.52 (s, 1H ArH-4), 8.15 (d, J = 8.5 Hz, 1H ArH-9), 7.86 (td, J = 7.7, 1.7 Hz, 1H, ArH-4′), 7.29 (d, J = 7.9 Hz, 2H, ArH-6, ArH-3′), 7.74 (ddd, J = 8.4, 7.0, 1.4 Hz, 1H, ArH-8), 7.59 (t, J = 7.5 Hz, 1H, ArH-7), 7.39 (ddd, J = 7.5, 4.9, 1.2 Hz, 1H, ArH-5′) ppm.

^{13}C NMR (126 MHz, CDCl$_3$): δ 157.6 (C-2′), 156.4 (C-2), 149.2 (C-6′), 146.5 (C-10), 140.4 (C-4), 136.6 (C-4′), 130.3 (C-8), 129.8 (C-6), 128.8 (C-5), 128.0 (C-7), 126.7 (C-6), 124.5 (C-3′), 123.6 (C-5′), 116.2 (C-3′) ppm.

IR (ν/cm^{-1}): 3053 (w), 2922 (w), 2851 (w), 1578 (w), 1564 (w), 1545 (w), 1476 (m), 1434 (m), 1396 (m), 1369 (w), 1331 (w), 1306 (w), 1276 (w), 1238 (w), 1193 (w), 1147 (w), 1125 (w), 1085 (m), 1046 (w), 1022 (w), 992 (w), 857 (s), 900 (m), 883 (w), 862 (w), 799 (w), 775 (s), 752 (s), 742 (s), 708 (m).

HRESI-MS (MeOH, +, m/z): [M+H]$^+$ 285.0044, calc. 285.0022, [M+Na]$^+$ 306.9865, calc. 306.9841

M.p.: 86–88 °C

3-Bromo-4-(dioxopyrrolidinyl)-2-(pyridin-2-yl)quinoline *N*-oxide (**30y**)
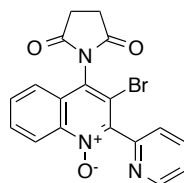
^{1}H NMR (500 MHz, CDCl$_3$): δ 8.83 (d, J = 3.8 Hz, 1H, ArH-6′), 8.72 (d, J = 8.5 Hz, 1H, ArH-6), 7.90 (td, J = 7.7, 1.6 Hz, 1H, ArH-4′), 7.80 (ddd, J = 8.6, 7.0, 1.3 Hz, 1H, ArH-7), 7.69 (ddd, J = 8.2, 6.9, 1.2 Hz, 1H, ArH-8), 7.61–7.54 (m, 2H, ArH-9, ArH-3′), 7.42 (t, J = 6.3 Hz, 1H, ArH-5′), 3.15–3.02 (m, 4H, -CH$_2$CH$_2$-) ppm.

^{13}C NMR (126 MHz, CDCl$_3$): δ 174.8 (C=O), 151.9 (C-2′), 150.4 (C-6′), 144.9 (C-2), 142.2 (C-4), 137.0 (C-4′), 131.3 (C-7), 130.9 (C-8), 126.8 (C-10), 126.6 (C-5), 125.5 (C-3′), 124.5 (C-5′), 123.1 (C-9), 121.2 (C-6), 118.9 (C-3), 29.1 (-CH$_2$CH$_2$-) ppm.

IR (v/cm^{-1}): 3050 (w), 2923 (w), 2852 (w), 1783 (w), 1716 (s), 1588 (w), 1567 (w), 1543 (w), 1498 (w), 1472 (w), 1429 (w), 1411 (m), 1367 (w), 1320 (s), 1212 (w), 1169 (s), 1150 (s), 1079 (m), 1042 (w), 1001 (w), 991 (w), 921 (w), 882 (w), 812 (w), 771 (m), 762 (m), 749 (w), 724 (w), 695 (w), 680 (w), 666 (w).

HRESI-MS (MeOH, +, m/z): [M+H]$^+$ 398.0165, calc. 398.0135, [M+Na]$^+$ 419.9985, calc. 419.9954

M.p.: 116–120 °C (decomp.)

2-(2-Bromophenyl)pyridine *N*-oxide (32a)

[FW 2081]
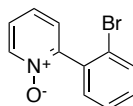
According to the general procedure, the reaction of phenylpyridine *N*-oxide **31a** (172 mg, 1.00 mmol), Pd(OAc)$_2$ (11.8 mg, 0.053 mmol), and NBS (214 mg, 1.21 mmol) in chlorobenzene (10.0 mL) provided **32a** (165 mg, 0.66 mmol, 66%) as colorless solid, and dibrominated product **33a** (32.1 mg, 0.10 mmol, 10%) as brown solid after column chromatography (acetone in hexane mixtures: 0–70%, 10% increments).

^{1}H NMR (500 MHz, CDCl$_3$): δ 8.31 (dp, J = 6.9, 2.3 Hz, 1H), 7.67 (dd, J = 8.1, 1.2 Hz, 1H), 7.42–7.39 (m, 1H), 7.37 (dd, J = 7.6, 2.0 Hz, 1H), 7.33–7.27 (m, 4H) ppm.

^{13}C NMR (126 MHz, CDCl$_3$): δ 149.3, 140.1, 134.5, 133.0, 131.1, 130.9, 128.1, 127.6, 125.6, 125.2, 123.6 ppm.

IR (v/cm^{-1}): 3057 (w), 3033 (w), 2923 (w), 1561 (w), 1496 (w), 1475 (w), 1458 (m), 1411 (s), 1308 (w), 1254 (s), 1241 (s), 1230 (s), 1147 (w), 1109 (w), 1047 (w), 1044 (w), 1007 (m), 841 (s), 756 (s), 737 (m), 696 (w), 662 (w).

HRESI-MS (MeOH, +, m/z): [M+H]$^+$ 249.9870, calc. 249.9862, [M+Na]$^+$ 271.9691, calc. 271.9681, [M+K]$^+$ 287.9454, calc. 287.9421

M.p.: 113 °C

2-(3,6-Dibromophenyl)pyridine *N*-oxide (**33a**)
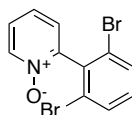
^{1}H NMR (500 MHz, CDCl$_3$): δ 8.37 (dd, J = 5.2, 2.4 Hz, 1H, ArH-3), 7.64 (d, J = 8.0 Hz, 2H, ArH-3′, ArH-5′), 7.36–7.32 (m, 2H, ArH-4, ArH-5), 7.30–7.26 (m, 1H, ArH-6), 7.19 (t, J = 8.1 Hz, 1H, ArH-4′) ppm.

^{13}C NMR (126 MHz, CDCl$_3$): δ 149.2 (C-2), 140.1 (C-3), 135.5 (C-1′), 132.0 (C-4′, C-5′), 131.8 (C-4′), 128.2 (C-6), 126.1 and 125.2 (C-4, C-5), 124.6 (C-2′) ppm.

IR (v/cm^{-1}): 3070 (w), 2918 (m), 2849 (m), 1725 (w), 1569 (w), 1546 (w), 1496 (w), 1465 (w), 1433 (w), 1419 (s), 1378 (w), 1291 (w), 1245 (s), 1186 (m), 1157 (w), 1115 (w), 1085 (w), 903 (w), 862 (w), 847 (s), 783 (s), 764 (s), 718 (s).

HRESI-MS (MeOH, +, *m/z*): [M+H]$^+$ 327.8975, calc. 327.8967, [M+Na]$^+$ 349.8797, calc. 349.8787, [M+K]$^+$ 365.8583, calc. 365.8526

M.p.: 154 °C

2-(2-Bromophenyl)pyridine

[FW 2061]
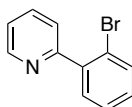
According to the general procedure, the reaction of phenylpyridine (160 mg, 1.03 mmol), Pd(OAc)$_2$ (11.6 mg, 0.052 mmol), and NBS (212 mg, 1.19 mmol) in chlorobenzene (10.0 mL) provided the title compound (119 mg, 0.51 mmol, 49%) as pale yellow oil, and 2-(3,6-dibromophenyl)pyridine (41.2 mg, 0.13 mmol, 13%) as pale yellow solid after column chromatography (EtOAc in hexane mixtures: 0–100%, 10% increments).

^{1}H NMR (500 MHz, CDCl$_3$): δ 8.71 (ddd, J = 4.9, 1.8, 1.0 Hz, 1H), 7.75 (td, J = 7.7, 1.8 Hz, 1H), 7.67 (dd, J = 8.0, 1.2 Hz, 1H), 7.59 (dt, J = 7.9, 1.1 Hz, 1H), 7.53 (dd, J = 7.6, 1.7 Hz, 1H), 7.40 (td, J = 7.5, 1.2 Hz, 1H), 7.30–7.22 (m, 2H) ppm.

The chemical shifts are in agreement with previous reported values.[242]

2-(3,6-Dibromophenyl)pyridine
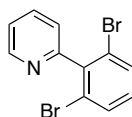
^{1}H NMR (500 MHz, CDCl$_3$): δ 8.75 (ddd, J = 4.9, 1.8, 1.0 Hz, 1H), 7.81 (td, J = 7.7, 1.8 Hz, 1H), 7.63 (d, J = 8.0 Hz, 2H), 7.34 (ddd, J = 7.6, 4.9, 1.2 Hz, 1H), 7.30 (dt, J = 7.8, 1.1 Hz, 1H), 7.12 (t, J = 8.1 Hz, 1H) ppm.

The chemical shifts are in agreement with previous reported values.[242]

3-Bromo-2-(pyridin-2-yl)pyrazine *N*-oxide

[FW 2062]
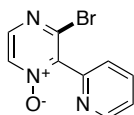
According to the general procedure, the reaction of pyridylpyrazine *N*-oxide (176 mg, 1.02 mmol), Pd(OAc)$_2$ (11.7 mg, 0.052 mmol), and NBS (216 mg, 1.21 mmol) in chlorobenzene (10.0 mL) provided starting material (138 mg, 0.80 mmol, 78%) after extraction.

4.11.2.2   *Direct chlorinations*

3-Chloro-2,2′-bipyridine *N*-oxide (21a)

[FW 2039]

According to the general procedure, the reaction of bipyridine *N*-oxide **20a** (3.44 g, 20.0 mmol), Pd(OAc)$_2$ (229 mg, 1.02 mmol), and NCS (3.23 g, 24.2 mmol) in chlorobenzene (200 mL) provided **21a** (3.93 g, 19.0 mmol, 95%) as brown solid after extraction.

^{1}H NMR (500 MHz, CDCl$_3$): δ 8.79 (ddd, J = 4.9, 1.7, 1.0 Hz, 1H, ArH-6′), 8.24 (dd, J = 6.6, 1.0 Hz, 1H, ArH-4), 7.87 (td, J = 7.8, 1.7 Hz, 1H, ArH-4′), 7.53 (dd, J = 8.5, 1.0 Hz, 1H, ArH-6), 7.42–7.38 (m, 2H, ArH-3′, ArH-5′), 7.23 (dd, J = 8.4, 6.5 Hz, 1H, ArH-5) ppm.

^{13}C NMR (126 MHz, CDCl$_3$): δ 149.6 (C-6′), 148.8 (C-2), 146.8 (C-2′), 138.4 (C-4), 137.4 (C-3), 133.7 (C-4′), 128.5 (C-6), 125.6 (C-5), 125.5 (C-3′), 124.6 (C-5′) ppm.

IR (ν/cm^{-1}): 3092 (w), 3068 (w), 3057 (w), 3040 (w), 1716 (w), 1595 (w), 1582 (w), 1542 (w), 1454 (w), 1415 (s), 1266 (m), 1247 (s), 1208 (w), 1185 (w), 1145 (w), 1031 (m), 990 (w), 926 (s), 792 (s), 780 (s), 750 (m), 725 (s).

HRESI-MS (MeOH, +, m/z): [M+H]$^+$ 207.0325, calc. 207.0320, [M+Na]$^+$ 229.0147, calc. 229.0139, [M+K]$^+$ 244.9869, calc. 244.9878

M.p.: 105 °C

3-Chloro-6-methyl-2,2′-bipyridine *N*-oxide (21b)

[SZ 5097/SZ 5103]
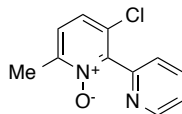
According to the general procedure, the reaction of bipyridine *N*-oxide **20b** (91.9 mg, 0.49 mmol), Pd(OAc)$_2$ (5.7 mg, 0.025 mmol), and NCS (86.0 mg, 0.64 mmol) in chlorobenzene (5.00 mL) provided **21b** (75.1 mg, 0.34 mmol, 68%) as tan oil containing traces of brominated analogue **22b** (1:11 for **22b**:**21b**) after column chromatography (MeOH in DCM mixtures: 1%, then 2%, 5%).

^{1}H NMR (500 MHz, CDCl$_3$): δ 8.77 (d, *J* = 4.8 Hz, 1H, ArH-6′), 7.83 (td, *J* = 7.8, 1.8 Hz, 1H, ArH-4′), 7.47 (d, *J* = 7.8 Hz, 1H, ArH-3′), 7.36 (ddd, *J* = 7.7, 4.9, 1.1 Hz, 1H, ArH-5′), 7.30 (d, *J* = 8.5 Hz, 1H, ArH-4), 7.24 (d, *J* = 8.5 Hz, 1H, ArH-5), 2.47 (s, 3H, -CH$_3$) ppm.

^{13}C NMR (126 MHz, CDCl$_3$): δ 150.5 (C-2′), 150.2 (C-6′), 148.5 (C-2), 147.2 (C-6), 136.8 (C-4′), 130.5 (C-3), 126.0 (C-4), 125.41 (C-5), 125.36 (C-3′), 124.0 (C-5′), 17.8 (-CH$_3$ ppm.

IR (ν/cm^{-1}): 3062 (w), 2920 (w), 1604 (w), 1586 (w), 1567 (w), 1487 (w), 1459 (m), 1443 (m), 1426 (m), 1347 (s), 1260 (s), 1147 (w), 1117 (w), 1091 (w), 1048 (w), 1002 (m), 928 (s), 873 (w), 782 (m), 745 (m), 708 (w), 671 (w).

HRESI-MS (MeOH, +, *m/z*): [M+H]$^+$ 221.0524, calc. 221.0476, [M+Na]$^+$ 243.0351, calc. 243.0296

3-Chloro-6-(ethoxycarbonyl)-2,2′-bipyridine *N*-oxide (21c)

[FW 2084/SZ 5047]
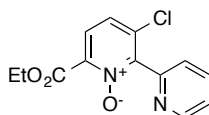
According to the general procedure, the reaction of bipyridine *N*-oxide **20c** (243 mg, 0.99 mmol), Pd(OAc)$_2$ (11.2 mg, 0.050 mmol), and NCS (162 mg, 1.22 mmol) in chlorobenzene (10.0 mL) provided **21c** (252 mg, 0.90 mmol, 91%) as brown oil after extraction.

^{1}H NMR (500 MHz, CDCl$_3$): δ 8.77 (ddd, *J* = 4.9, 1.8, 1.0 Hz, 1H, ArH-6′), 7.84 (td, *J* = 7.7, 1.8 Hz, 1H, ArH-4′), 7.57–7.51 (m, 2H, ArH-5, ArH-3′), 7.40 (d, *J* = 8.7 Hz, 1H, ArH-4), 7.37 (dd, *J* = 4.9, 1.1 Hz, 1H, ArH-5′), 4.42 (q, *J* = 7.1 Hz, 2H, -CH$_2$-), 1.37 (t, *J* = 7.1 Hz, 3H, -CH$_3$) ppm.

^{13}C NMR (126 MHz, CDCl$_3$): δ 161.3 (C=O), 150.3 (C-6′), 149.2 (C-2′), 148.6 (C-2), 141.2 (C-6), 136.8 (C-4′), 135.2 (C-3), 125.9 (C-3′), 125.8 (C-4), 125.5 (C-5), 124.4 (C-5′), 62.9 (-CH$_2$-), 14.1 (-CH$_3$) ppm.

IR (v/cm^{-1}): 3062 (w), 2981 (w), 1736 (s), 1596 (w), 1583 (m) 1568 (w), 1546 (w), 1477 (w), 1457 (w), 1428 (w), 1413 (w), 1391 (w), 1383 (s), 1318 (m), 1248 (s), 1202 (w), 1158 (m), 1133 (w), 1099 (m), 1084 (m), 1045 (w), 1012 (m), 992 (w), 940 (s), 886 (w), 861 (w), 821 (w), 782 (m), 745 (m), 700 (w), 684 (w).

HRESI-MS (MeOH, +, m/z): [M+H]$^+$ 279.0562, calc. 279.0531, [M+Na]$^+$ 301.0387, calc. 301.0350, [M+K]$^+$ 317.0125, calc. 317.0090

3-Chloro-6-cyano-2,2′-bipyridine *N*-oxide (21e)

[SZ 5050]
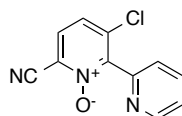
According to the general procedure, the reaction of bipyridine *N*-oxide **20e** (195 mg, 0.99 mmol), Pd(OAc)$_2$ (12.0 mg, 0.053 mmol), and NCS (171 mg, 1.28 mmol) in chlorobenzene (10.0 mL) starting material (168 mg, 0.85 mmol, 85%) after purification by column chromatography (MeOH in DCM mixtures: 0%–10%, 1% increments).

3-Chloro-5-methoxy-2,2′-bipyridine *N*-oxide (21f)

[FW 2079]
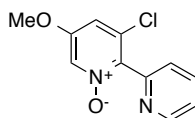
According to the general procedure, the reaction of bipyridine *N*-oxide **20f** (204 mg, 1.01 mmol), Pd(OAc)$_2$ (11.2 mg, 0.050 mmol), and NCS (160 mg, 1.20 mmol) in chlorobenzene (10.0 mL) provided **21f** (230 mg, 0.97 mmol, 97%) as brown solid after extraction.

^{1}H NMR (500 MHz, CDCl$_3$): δ 8.76 (ddd, J = 4.9, 1.8, 1.0 Hz, 1H, ArH-6′)), 8.01 (d, J = 2.2 Hz, 1H, ArH-4), 7.82 (td, J = 7.7, 1.8 Hz, 1H, ArH-4′), 7.50 (dt, J = 7.8, 1.1 Hz, 1H, ArH-3′), 7.35 (ddd, J = 7.7, 4.9, 1.2 Hz, 1H, ArH-5′), 7.02 (d, J = 2.2 Hz, 1H, ArH-6), 3.85 (s, 3H, -CH$_3$) ppm.

^{13}C NMR (126 MHz, CDCl$_3$): δ 156.7 (C-5), 150.1 (C-6′), 149.8 (C-2′), 141.1 (C-2), 136.7 (C-4′), 133.3 (C-3), 127.1 (C-4), 126.1 (C-3′), 124.1 (C-5′), 114.5 (C-6), 56.6 (-CH$_3$) ppm.

IR (v/cm^{-1}): 3086 (w), 3039 (w), 3012 (w), 2923 (w), 2852 (w), 1711 (w), 1668 (w), 1603 (m), 1564 (w), 1545 (m), 1504 (w), 1460 (m), 1449 (m), 1427 (m), 1376 (m), 1314 (w), 1281 (w), 1237 (w), 1225 (w), 1200 (w), 1190 (w), 1165 (s), 1118 (w), 1097 (w), 1068 (w), 1045 (w), 1018 (s), 986 (w), 967 (w), 893 (m), 865 (m), 836 (m), 787 (m), 748 (m), 733 (w).

HRESI-MS (MeOH, +, m/z): [M+H]$^+$ 237.0449, calc. 237.0425, [M+Na]$^+$ 259.0274, calc. 259.0245, [M+K]$^+$ 275.0009, calc. 274.9984

M.p.: 145 °C

3-Chloro-5-methyl-2,2′-bipyridine *N*-oxide (21g)

[FW 2094]
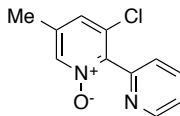
According to the general procedure, the reaction of bipyridine *N*-oxide **20g** (186 mg, 1.00 mmol), Pd(OAc)$_2$ (11.5 mg, 0.051 mmol), and NCS (161 g, 1.20 mmol) in chlorobenzene (10.0 mL) provided **21g** (198 mg, 0.90 mmol, 90%) as brown solid after extraction.

^{1}H NMR (500 MHz, CDCl$_3$): δ 8.78 (d, *J* = 4.6 Hz, 1H, ArH-6′), 8.11 (s, 1H, ArH-4), 7.85 (td, *J* = 7.7, 1.7 Hz, 1H, ArH-4′), 7.52 (dt, *J* = 7.9, 1.1 Hz, 1H, ArH-3′), 7.38 (ddd, *J* = 7.5, 4.9, 1.2 Hz, 1H, ArH-5′), 7.24 (s, 1H, ArH-6), 2.33 (s, 3H, -CH$_3$) ppm.

^{13}C NMR (126 MHz, CDCl$_3$): δ 150.2 (C-6′), 149.9 (C-2′), 144.9 (C-2), 138.7 (C-4), 136.8 (C-4′), 136.0 (C-5), 132.9 (C-3), 128.1 (C-6), 125.9 (C-3′), 124.2 (C-5′), 18.3 (-CH$_3$) ppm.

IR (*v*/cm^{-1}): 3052 (w), 2956 (w), 2925 (w), 2868 (w), 1710 (m), 1599 (m), 1566 (m), 1539 (m), 1460 (w), 1440 (w), 1427 (m), 1374 (s), 1283 (s), 1217 (s), 1146 (m), 1096 (w), 1059 (w), 1022 (s), 991 (m), 892 (s), 845 (m), 789 (s), 750 (s), 732 (m).

HRESI-MS (MeOH, +, *m/z*): [M+H]$^+$ 221.0488, calc. 221.0476, [M+Na]$^+$ 243.0313, calc. 243.0296, [M+K]$^+$ 259.0319, calc. 259.0035

M.p.: 113 °C

3-Chloro-5-(methoxycarbonyl)-2,2′-bipyridine *N*-oxide (21h)

[FW 2077]
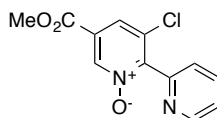
According to the general procedure, the reaction of bipyridine *N*-oxide **20h** (231 mg, 1.00 mmol), Pd(OAc)$_2$ (11.0 mg, 0.049 mmol), and NCS (160 mg, 1.20 mmol) in chlorobenzene (10.0 mL) provided **21h** (170 mg, 0.64 mmol, 64%) as brown solid after extraction.

^{1}H NMR (500 MHz, CDCl$_3$): δ 8.80 (dd, *J* = 5.8, 1.1 Hz, 1H, ArH-6′), 8.79 (s, *J* = 1.3 Hz, 1H, ArH-4), 7.95 (d, *J* = 1.4 Hz, 1H, ArH-6), 7.88 (td, *J* = 7.8, 1.8 Hz, 1H, ArH-4′), 7.55 (dt, *J* = 7.8, 1.1 Hz, 1H, ArH-3′), 7.42 (ddd, *J* = 7.7, 4.9, 1.2 Hz, 1H, ArH-5′), 3.98 (s, 3H, -OCH$_3$) ppm.

^{13}C NMR (126 MHz, CDCl$_3$): δ 162.6 (C=O), 150.3 (C-2), 149.1 (C-2′), 139.7 (C-4), 137.0 (C-4′), 133.8 (C-3), 128.7 (C-5), 128.6 (C-6′), 127.1 (C-6), 125.6 (C-3′), 124.7 (C-5′), 53.5 (-OCH$_3$) ppm.

IR (v/cm^{-1}): 3102 (w), 3066 (w), 3011 (w), 2957 (w), 2922 (w), 2850 (w), 1724 (s), 1597 (w), 1582 (w), 1566 (w), 1547 (w), 1459 (w), 1439 (w), 1427 (m), 1372 (s), 1318 (s), 1231 (s), 1156 (w), 1110 (m), 1031 (w), 1008 (m), 992 (w), 958 (m), 898 (w), 879 (m), 784 (w), 772 (w), 757 (m), 744 (m), 728 (m), 713 (w).

HRESI-MS (MeOH, +, m/z): [M+H]$^+$ 265.0379, calc. 265.0374, [M+Na]$^+$ 287.0199, calc. 287.0194, [M+K]$^+$ 302.9945, calc. 302.9933

M.p.: 96 °C

3-Chloro-5-nitro-2,2′-bipyridine N-oxide (21i)

[SZ 5051]
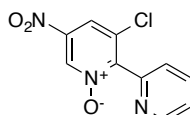
According to the general procedure, the reaction of bipyridine N-oxide **20i** (71.8 mg, 0.33 mmol), Pd(OAc)$_2$ (4.1 mg, 0.018 mmol), and NCS (53.3 mg, 0.40 mmol) in chlorobenzene (3.30 mL) provided **21** (26.0 mg, 0.10 mmol, 31%) as yellow solid, and starting material (24.0 mg, 0.11 mmol, 33%) after purification by column chromatography (MeOH in DCM mixtures: 0%, then 0.1%, 0.5% and 10%).

^{1}H NMR (400 MHz, CDCl$_3$): 9.05 (d, J = 2.0 Hz, 1H, ArH-4), 8.83 (d, J = 4.5 Hz, 1H, ArH-3′), 8.15 (d, J = 2.0 Hz, 1H, ArH-6), 7.92 (td, J = 7.8, 1.7 Hz, 1H, ArH-5′), 7.56 (d, J = 7.8 Hz, 1H, ArH-6′), 7.47 (ddd, J = 7.7, 4.9, 1.1 Hz, 1H, ArH-4′) ppm.

^{13}C NMR (126 MHz, CDCl$_3$): δ 152.2 (C-2), 150.6 (C-3′), 148.1 (C-2′), 145.2 (C-5), 137.1 (C-5′), 135.1 (C-4), 134.4 (C-3), 125.6 (C-6′), 125.2 (C-4′), 120.9 (C-6) ppm.

IR (v/cm^{-1}): 3029 (w), 2924 (w), 1586 (w), 1558 (w), 1514 (s), 1455 (w), 1424 (m), 1374 (m), 1351 (s), 1268 (s), 1186 (m), 1150 (w), 1101 (m), 1055 (w), 994 (s), 916 (w), 778 (s), 743 (s), 717 (w).

HRESI-MS (MeOH, +, m/z): [M+H]$^+$ 252.0166, calc. 252.0170, [M+Na]$^+$ 273.9990, calc. 273.9990

M.p.: 165–168 °C (decomp.)

3,4-Dichloro-2,2′-bipyridine N-oxide (21k)

[FW 2101]
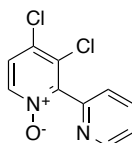
According to the general procedure, the reaction of bipyridine N-oxide **20k** (209 mg, 1.01 mmol), Pd(OAc)$_2$ (11.3 mg, 0.050 mmol), and NCS (161 mg, 1.21 mmol) in chlorobenzene (10.0 mL) provided starting material (220 mg, 1.06 mmol, quant.) containing traces of impurities after extraction.

3-Chloro-4-cyano-2,2′-bipyridine *N*-oxide (21n)

[FW 2102]
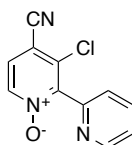
According to the general procedure, the reaction of bipyridine *N*-oxide **20n** (162 mg, 0.82 mmol), Pd(OAc)$_2$ (9.7 mg, 0.043 mmol), and NCS (132 mg, 0.99 mmol) in chlorobenzene (10.0 mL) provided starting material (147 mg, 0.75 mmol, 91%) after extraction.

3′-Chloro-6′-methoxy-2,2′-bipyridine *N*-oxide (21p)

[FW 2078]
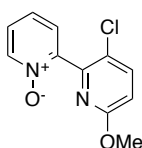
According to the general procedure, the reaction of bipyridine *N*-oxide **20p** (202 mg, 1.00 mmol), Pd(OAc)$_2$ (11.2 mg, 0.050 mmol), and NCS (160 mg, 1.20 mmol) in chlorobenzene (10.0 mL) provided **21p** (227 mg, 0.96 mmol, 96%) as yellow solid after extraction.

^{1}H NMR (500 MHz, CDCl$_3$): δ 8.29 (dd, *J* = 4.9, 2.8 Hz, 1H, ArH-3), 7.62 (d, *J* = 8.7 Hz, 1H, ArH-5′), 7.37 (dd, *J* = 5.5, 4.4 Hz, 1H, ArH-5), 7.32–7.28 (m, 2H, ArH-4, ArH-6), 6.77 (d, *J* = 8.7 Hz, 1H, ArH-), 3.87 (s, 3H, -OCH$_3$) ppm.

^{13}C NMR (126 MHz, CDCl$_3$): δ 162.5 (C-6′), 148.5 (C-2′), 148.2 (C-2), 142.8 (C-5′), 139.9 (C-3), 127.6 (C-5), 126.0 and 125.0 (C-4, C-6), 113.4 (C-3′), 113.0 (C-4′), 54.1 (-OCH$_3$) ppm.

IR (v/cm^{-1}): 3072 (w), 3014 (w), 2947 (w), 2853 (w), 1713 (w), 1584 (m), 1572 (w), 1460 (s), 1410 (s), 1324 (s), 1272 (w), 1251 (s), 1226 (m), 1184 (w), 1146 (w), 1119 (w), 1023 (s), 986 (w), 930 (m), 893 (m), 831 (m), 766 (m), 678 (m).

HRESI-MS (MeOH, +, *m/z*): [M+H]$^+$ 237.0451, calc. 237.0425, [M+Na]$^+$ 259.0276, calc. 259.0245

M.p.: 134 °C

3′-Chloro-6′-methyl-2,2′-bipyridine *N*-oxide (21q)

[SZ 5056]
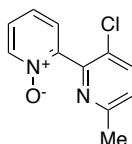
According to the general procedure, the reaction of bipyridine *N*-oxide **20q** (187 mg, 1.01 mmol), Pd(OAc)$_2$ (11.5 mg, 0.051 mmol), and NCS (162 mg, 1.21 mmol) in chlorobenzene (10.0 mL)

provided starting material (192 mg, 1.03 mmol, quant.) containing traces of impurities after extraction.

3′-Chloro-6′-(trifluoromethyl)-2,2′-bipyridine *N*-oxide (21r)

[FW 2103]
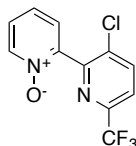
According to the general procedure, the reaction of bipyridine *N*-oxide **20r** (228 mg, 0.95 mmol), Pd(OAc)$_2$ (11.2 mg, 0.050 mmol), and NCS (151 mg, 1.13 mmol) in chlorobenzene (10.0 mL) provided **21r** (234 mg, 0.85 mmol, 90%) as colorless solid after extraction.

^{1}H NMR (500 MHz, CDCl$_3$): δ 8.32 (dd, *J* = 5.6, 2.0, 1H, ArH-3), 8.01 (dt, *J* = 8.3, 0.7 Hz, 1H, ArH-4′), 7.74 (d, *J* = 8.4 Hz, 1H, ArH-5′), 7.50 (dd, *J* = 7.3, 2.6 Hz, 1H, ArH-6), 7.43–7.36 (m, 2H, ArH-4, ArH-5) ppm.

^{13}C NMR (126 MHz, CDCl$_3$): δ 150.8 (C-2), 146.5 (q, *J* = 36 Hz, C-6′), 146.6 (C-2′), 139.9 (C-3), 138.8 (C-4′), 136.5 (C-3′), 127.8 (C-6), 126.8 and 125.4 (C-4, C-5), 122.0 (q, *J* = 2.4 Hz, C-5′), 121.2 (q, *J* = 275 Hz, -CF$_3$) ppm.

^{19}F NMR (471 MHz, CDCl$_3$): δ –67.4 ppm.

IR (*v*/cm^{-1}): 3130 (w), 3079 (w), 3061 (w), 2958 (w), 2925 (w), 2871 (w), 1717 (w), 1598 (w), 1577 (w), 1567 (w), 1458 (w), 1436 (w), 1422 (m), 1402 (w), 1336 (s), 1291 (w), 1251 (m), 1233 (w), 1221 (w), 1173 (m), 1160 (m), 1135 (s), 1119 (s), 1105 (s), 1075 (w), 1033 (m), 975 (w), 949 (w), 865 (w), 850 (m), 823 (m), 770 (s), 743 (w), 732 (w).

HRESI-MS (MeOH, +, *m/z*): [M+H]$^+$ 275.0198, calc. 275.0194, [M+Na]$^+$ 297.0025, calc. 297.0013

M.p.: 146 °C

3-Chloro-4′-methyl-2,2′-bipyridine *N*-oxide (21u)

[FW 2082]
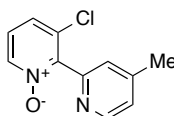
According to the general procedure, the reaction of bipyridine *N*-oxide **20u** (187 mg, 1.00 mmol), Pd(OAc)$_2$ (11.3 mg, 0.050 mmol), and NCS (161 mg, 1.20 mmol) in chlorobenzene (10.0 mL) provided **21u** (216 mg, 0.98 mmol, 98%) as brown solid after extraction.

¹H NMR (500 MHz, CDCl₃): δ 8.63 (dd, *J* = 5.0, 0.8 Hz, 1H, ArH-4), 8.23 (dd, *J* = 6.6, 1.1 Hz, 1H, ArH-6), 7.38 (dd, *J* = 8.4, 1.1 Hz, 1H, ArH-6′), 7.33 (dt, *J* = 1.7, 0.8 Hz, 1H, ArH-3′), 7.21 (dd, *J* = 8.3, 6.6 Hz, 1H, ArH-5′), 7.20 (ddd, *J* = 5.0, 1.6, 0.7 Hz, 1H, ArH-5), 2.42 (s, 3H, -CH₃) ppm.

¹³C NMR (126 MHz, CDCl₃): δ 150.0 (C-2), 149.6 (C-2′), 148.2 (C-4), 147.8 (C-4′), 138.7 (C-6), 133.7 (C-3), 126.8 (C-6′), 126.2 (C-3′), 125.4 (C-5), 124.9 (C-5′), 21.2 (-CH₃) ppm.

¹⁹F NMR (376 MHz, CDCl₃): δ -67.4 ppm.

IR (*v*/cm⁻¹): 3116 (w), 3104 (w), 2980 (w), 1712 (w), 1605 (m), 1587 (w), 1555 (w), 1463 (w), 1446 (w), 1404 (m), 1386 (w), 1252 (m), 1208 (w), 1177 (w), 1117 (w), 1048 (w), 991 (w), 927 (s), 890 (w), 874 (w), 835 (m), 788 (m), 754 (w), 723 (m).

HRESI-MS (MeOH, +, *m/z*): [M+H]⁺ 221.0473 calcd. 221.0476, [M+Na]⁺ 243.0317 calcd. 243.0296, [M+K]⁺ 259.0030, calc. 259.0035

M.p.: 129 °C

3-Chloro-4′-fluoro-2,2′-bipyridine *N*-oxide (21v)

[FW 2099]
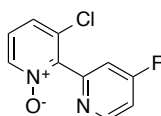
According to the general procedure, the reaction of bipyridine *N*-oxide **20v** (193 mg, 1.01 mmol), Pd(OAc)₂ (11.5 mg, 0.051 mmol), and NCS (161 mg, 1.20 mmol) in chlorobenzene (10.0 mL) provided **21v** (204 mg, 0.91 mmol, 90%) as brown solid after extraction.

¹H NMR (500 MHz, CDCl₃): δ 8.77 (dd, *J* = 8.3, 5.7 Hz, 1H), 8.26 (dd, *J* = 6.6, 1.0 Hz, 1H), 7.42 (dd, *J* = 8.4, 1.0 Hz, 1H), 7.31 (dd, *J* = 9.0, 2.4 Hz, 1H), 7.27 (dd, *J* = 8.4, 6.6 Hz, 1H), 7.15 (ddd, *J* = 8.2, 5.7, 2.5 Hz, 1H) ppm.

¹³C NMR (126 MHz, CDCl₃): δ 169.0 (d, *J* = 264 Hz, C-4′), 152.8 (d, *J* = 7.5 Hz, C-6′), 152.4 (d, *J* = 8.0 Hz, C-2′), 146.7 (C-2), 138.8 (C-4), 133.7 (C-3), 126.9 (C-6), 125.4 (C-5), 114.2 (d, *J* = 18 Hz, C-3′), 112.5 (d, *J* = 16 Hz, C-5′) ppm.

¹⁹F NMR (471 MHz, CDCl₃): δ –100.7 ppm.

IR (*v*/cm⁻¹): 3114 (w), 3045 (w), 2959 (w), 2924 (w), 2854 (w), 1712 (w), 1672 (w), 1637 (w), 1600 (m), 1575 (s), 1467 (m), 1414 (s), 1395 (m), 1300 (w), 1267 (s), 1184 (m), 1148 (w), 1101 (w), 1046 (m), 900 (m), 932 (s), 894 (s), 839 (m), 829 (m), 783 (s), 724 (s).

HRESI-MS (MeOH, +, *m/z*): [M+H]⁺ 225.0259, calc. 225.0225, [M+Na]⁺ 247.0051, calc. 247.0045, [M+K]⁺ 262.9766, calc. 262.9784

M.p.: 125 °C

3-Chloro-4′-(ethoxycarbonyl)-2,2′-bipyridine _N_-oxide (21w)

[FW 2096]
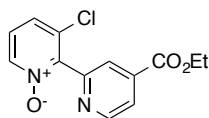
According to the general procedure, the reaction of bipyridine _N_-oxide **20w** (145 mg, 0.59 mmol), Pd(OAc)$_2$ (7.0 mg, 0.031 mmol), and NCS (95.3 mg, 0.71 mmol) in chlorobenzene (6.00 mL) provided **21w** (124 mg, 0.53 mmol, 90%) as brown oil after extraction.

^{1}H NMR (500 MHz, CDCl$_3$): δ 8.97 (d, _J_ = 5.0 Hz, 1H, ArH-6), 8.28 (d, _J_ = 6.5 Hz, 1H, ArH-4), 8.13 (t, _J_ = 1.2 Hz, 1H, ArH-3′), 8.00 (dd, _J_ = 5.0, 1.6 Hz, 1H, ArH-5′), 7.46 (d, _J_ = 8.3 Hz, 1H, ArH-6), 7.31 (dd, _J_ = 8.6, 6.7 Hz, 1H, ArH-5), 4.45 (q, _J_ = 7.1 Hz, 2H, -CH$_2$-), 1.43 (t, _J_ = 7.1 Hz, 3H, -CH$_3$) ppm.

^{13}C NMR (126 MHz, CDCl$_3$): δ 164.6 (C=O), 151.1 (C-6′), 150.7 (C-2′), 146.8 (C-2), 139.0 (C-4), 138.8 (C-4′), 133.8 (C-3), 127.1 (C-6), 125.3 (C-5), 125.2 (C-3′), 123.7 (C-5′), 62.2 (-CH$_2$-), 14.3 (-CH$_3$) ppm.

IR (_v_/cm^{-1}): 3101 (w), 3062 (w), 2981 (w), 2936 (w), 1722 (s), 1604 (w), 1586 (w), 1557 (w), 1464 (w), 1412 (m), 1396 (w), 1387 (w), 1367 (w), 1303 (m), 1236 (s), 1185 (w), 1116 (m), 1100 (m), 1049 (w), 1014 (m), 930 (s), 896 (w), 861 (w), 787 (m), 762 (s), 727 (w), 695 (w), 676 (m).

HRESI-MS (MeOH, +, _m/z_): [M+H]$^+$ 279.0537, calc. 279.0531, [M+Na]$^+$ 301.0359, calc. 301.0350, [M+K]$^+$ 317.0094, calc. 317.0090

M.p.: 129 °C

3-Chloro-4′-(trifluoromethyl)-2,2′-bipyridine _N_-oxide (21x)

[FW 2098]
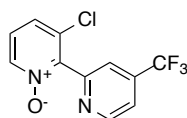
According to the general procedure, the reaction of bipyridine _N_-oxide **20x** (139 mg, 0.58 mmol), Pd(OAc)$_2$ (7.0 mg, 0.031 mmol), and NCS (93.4 mg, 0.70 mmol) in chlorobenzene (6.00 mL) provided **21x** (155 mg, 0.56 mmol, 97%) as brown oil after extraction.

^{1}H NMR (500 MHz, CDCl$_3$): δ 8.98 (d, _J_ = 5.3 Hz, 1H, ArH-6), 8.27 (dd, _J_ = 6.6, 1.1 Hz, 1H, ArH-4), 7.80 (s, 1H, ArH-3′), 7.62 (dd, _J_ = 5.1, 0.9 Hz, 1H, ArH-5′), 7.44 (dd, _J_ = 8.4, 1.1 Hz, 1H, ArH-6), 7.29 (dd, _J_ = 8.4, 6.5 Hz, 1H, ArH-5) ppm.

^{13}C NMR (126 MHz, CDCl$_3$): δ 151.3 (C-6′), 151.1 (C-2′), 146.4 (C-2), 139.2 (q, J = 35 Hz, C-4′), 138.8 (C-4), 133.7 (C-3), 127.0 (C-6), 125.5 (C-5), 122.7 (q, J = 274 Hz, -CF$_3$), 121.9 (q, J = 3.7 Hz, C-3′), 120.1 (q, J = 3.5 Hz, C-5′) ppm.

^{19}F NMR (376 MHz, CDCl$_3$): δ –64.6 ppm.

IR (v/cm^{-1}): 3102 (w), 3062 (w), 2926 (w), 1615 (w), 1587 (w), 1570 (w), 1470 (w), 1414 (m), 1395 (m), 1333 (s), 1270 (w), 1244 (m), 1214 (w), 1169 (m), 1133 (s), 1083 (m), 1046 (m), 991 (w), 931 (s), 894 (w), 850 (m), 833 (m), 787 (m), 751 (w), 728 (w), 691 (w), 664 (s).

HRESI-MS (MeOH, +, m/z): [M+H]$^+$ 275.0192, calc. 275.0194, [M+Na]$^+$ 297.0013, calc. 297.0013, [M+K]$^+$ 312.9748, calc. 312.9752

M.p.: 129 °C

3-Chloro-2-(pyridin-2-yl)-quinoline *N*-oxide (4s)

[SZ 5052]
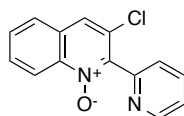
According to the general procedure, the reaction of quinoline *N*-oxide **20y** (234 mg, 1.05 mmol), Pd(OAc)$_2$ (11.9 mg, 0.053 mmol), and NCS (161 mg, 1.21 mmol) in chlorobenzene (10.0 mL) provided **21y** (236 mg, 0.92 mmol, 87%) as brown solid after extraction.

^{1}H NMR (500 MHz, CDCl$_3$): δ 8.83 (ddd, J = 4.9, 1.6, 0.9 Hz, 1H, ArH-6′), 8.69 (d, J = 8.7 Hz, 1H, ArH-9), 7.89 (td, J = 7.8, 1.8 Hz, 1H, ArH-4′), 7.87 (s, 1H, ArH-4), 7.81 (dd, J = 8.1, 1.2 Hz, 1H, ArH-6), 7.75 (ddd, J = 8.6, 7.0, 1.4 Hz, 1H, ArH-8), 7.67 (ddd, J = 8.1, 7.0, 1.2 Hz, 1H, ArH-7), 7.61 (dt, J = 7.8, 1.0 Hz, 1H, ArH-3′), 7.42 (ddd, J = 7.7, 4.9, 1.1 Hz, 1H, ArH-5′) ppm.

^{13}C NMR (126 MHz, CDCl$_3$): δ 150.8 (C-2), 150.3 (C-6′), 143.7 (C-2′), 141.2 (C-10), 136.8 (C-4′), 130.6 (C-8), 129.9 (C-7), 129.1 (C-3), 128.2 (C-5), 127.5 (C-6), 125.7 (C-3′), 125.1 (C-4), 124.2 (C-5′, 120.5 (C-9) ppm.

IR (v/cm^{-1}): 3059 (w), 2924 (w), 2853 (w), 1713 (m), 1672 (w), 1634 (w), 1589 (m), 1556 (m), 1472 (m), 1428 (m), 1370 (w), 1328 (s), 1270 (w), 1243 (w), 1208 (w), 1141 (w), 1078 (w), 1049 (w), 994 (w), 938 (s), 873 (w), 847 (m), 821 (m), 769 (s), 741 (m), 672 (m).

HRESI-MS (MeOH, +, m/z): [M+H]$^+$ 257.0499, calc. 257.0476, [M+Na]$^+$ 279.0326, calc. 279.0296

M.p.: 127–130 °C

3-Chloro-2-(pyridin-2yl)pyrazine *N*-oxide

[FW 2097]
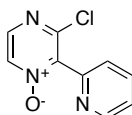
According to the general procedure, the reaction of pyridylpyrazine *N*-oxide (171 mg, 1.00 mmol), Pd(OAc)$_2$ (11.3 mg, 0.050 mmol), and NCS (160 mg, 1.20 mmol) in chlorobenzene (10.0 mL) provided starting material (160 mg, 0.92 mmol, 92%) after extraction.

4.11.3 Deoxygenation of halogenated bipyridine *N*-oxides

General procedure:

A reaction vial was loaded with halogenated bipyridine *N*-oxide **21** or **22** (1.0 equiv.) and CHCl$_3$ (0.10 M). The solution was cooled to 0 °C and PX$_3$ (4.0 equiv.) was added. The reaction vial was sealed with a Teflon-lined screw cap and the reaction mixture stirred at 80 °C for 3 h. After cooling to room temperature, the reaction was quenched and neutralized with sat. NaHCO$_3$. The aqueous layer was extracted with DCM, the combined organic layers dried with Na$_2$SO$_4$, filtered and the volatiles removed from the filtrate. If necessary, Flash column chromatography (SiO$_2$, acetone/hexane 1:9) provides analytically pure products **25** or **34**.

4.11.3.1   Reduction of brominated products

3-Bromo-2,2′-bipyridine (25a)

[SZ 5101/FW 1101]
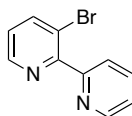
According to the general procedure, bipyridine *N*-oxide **22a** (63.0 mg, 0.25 mmol) and PBr$_3$ (0.16 mL, 1.65 mmol) in CHCl$_3$ (1.20 mL) provided **25a** (44.3 mg, 0.19 mmol, 76%) as pale yellow oil after extraction.

^{1}H NMR (500 MHz, CDCl$_3$): δ 8.74 (d, *J* = 4.4 Hz, 1H), 8.64 (d, *J* = 3.7 Hz, 1H), 8.00 (dd, *J* = 8.1, 1.5 Hz, 1H), 7.80 (td, *J* = 7.7, 1.8 Hz, 1H), 7.71 (d, *J* = 7.8 Hz, 1H), 7.33 (ddd, *J* = 7.5, 4.9, 1.2 Hz, 1H), 7.19 (dd, *J* = 8.1, 4.6 Hz, 1H) ppm.

^{13}C NMR (126 MHz, CDCl$_3$): δ 157.3 (C-2), 156.7 (C-2′), 149.3 (C-6′), 148.1 (C-6), 141.7 (C-4), 136.4 (C-4′), 124.4 (C-5), 124.3 (C-5′), 123.5 (C-3′), 119.7 (C-3) ppm.

IR (v/cm^{-1}): 3051 (w), 1587 (w), 1567 (m), 1547 (w), 1476 (w), 1410 (s), 1285 (w), 1228 (w), 1204 (w), 1148 (w), 1124 (w), 1101 (m), 1051 (w), 1037 (w), 1014 (s), 991 (m), 894 (w), 792 (s), 744 (s), 681 (m).

HRESI-MS (MeOH, +, m/z): [M+H]$^+$ 234.9890, calc. 234.9865, [M+Na]$^+$ 256.9713, calc. 256.9685

[SZ 5084A]

Bipyridine N-oxide **22a** (63.6 mg, 0.25 mmol) was dissolved in MeOH (1.30 mL) and NH$_4$CO$_2$H (188 mg, 2.99 mmol) and Pd/C (w = 10%, 26.5 mg, 0.025 mmol) were added as solids. The reaction solution was stirred at room temperature for 5 h, the volatiles removed and the residue extracted with DCM. After removal of the solvent from the extracted solution, bipyridine **24a** (35.5 mg, 0.25 mmol, quant.) was obtained.

3-Bromo-6-methyl-2,2′-bipyridine (25b)

[SZ 5071]
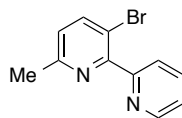
According to the general procedure, bipyridine N-oxide **22b** (51.3 mg, 0.19 mmol) and PBr$_3$ (0.15 mL, 1.58 mmol) in CHCl$_3$ (5.00 mL) provided **25b** (38.3 mg, 0.15 mmol, 79%) as orange oil after extraction.

NMR data are identical to previous obtained sample (SZ 5055).

3-Bromo-6-(ethoxycarbonyl)-2,2′-bipyridine (25c)

[SZ 5078]
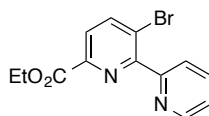
According to the general procedure, bipyridine N-oxide **22c** (102 mg, 0.31 mmol) and PBr$_3$ (0.15 mL, 1.58 mmol) in CHCl$_3$ (5.00 mL) provided **25c** (58.8 mg, 0.19 mmol, 61%) as colorless oil after extraction.

^{1}H NMR (400 MHz, CDCl$_3$): δ 8.73 (d, J = 4.6 Hz, 1H), 8.16 (d, J = 8.3 Hz, 1H), 7.98 (d, J = 8.3 Hz, 1H), 7.83 (td, J = 7.7, 1.7 Hz, 1H), 7.77 (d, J = 7.7 Hz, 1H), 7.36 (ddd, J = 7.4, 4.9, 1.2 Hz, 1H), 4.46 (q, J = 7.1 Hz, 2H), 1.41 (t, J = 7.1 Hz, 3H) ppm.

^{13}C NMR (126 MHz, CDCl$_3$): δ 164.7, 156.7, 149.0, 146.9, 142.7, 136.7, 125.5, 124.7, 123.8, 123.7, 62.3, 14.4 ppm.

IR (ν/cm^{-1}): 3060 (w), 2979 (w), 1739 (m), 1715 (s), 1587 (w), 1562 (m), 1474 (w), 1443 (w), 1417 (m), 1392 (m), 1367 (m), 1311 (s), 1281 (m), 1136 (s), 1105 (m), 1046 (w), 1015 (s), 992 (m), 893 (w), 856 (m), 798 (m), 785 (m), 744 (s), 695 (w).

HRESI-MS (MeOH, +, m/z): [M+H]$^+$ 307.0107, calc. 307.007, [M+Na]$^+$ 328.9937, calc. 328.9896, [M+K]$^+$ 344.9666, calc. 344.9635

3-Bromo-6-(trifluoromethyl)-2,2′-bipyridine (25d)

[SZ 5072]
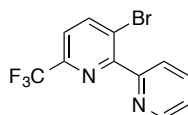
According to the general procedure, bipyridine N-oxide **22d** (86.3 mg, 0.27 mmol) and PBr$_3$ (0.15 mL, 1.58 mmol) in CHCl$_3$ (5.00 mL) provided **25d** (34.8 mg, 0.11 mmol, 43%) as colorless solid after column chromatography.

NMR data are identical to previous obtained sample (FW 2045).

3-Bromo-5-methoxy-2,2′-bipyridine (25f)

[SZ 5070]
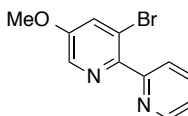
According to the general procedure, bipyridine N-oxide **22f** (150 mg, 0.53 mmol) and PBr$_3$ (0.15 mL, 1.58 mmol) in CHCl$_3$ (5.00 mL) did not provide **25f**, instead dibrominated bipyridine **35f** (83.4 mg, 0.24 mmol, 45%) was obtained as pale yellow solid after column chromatography.

3,6-Dibromo-5-methoxy-2,2′-bipyridine (**35f**)
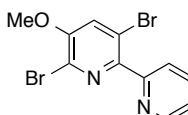
^{1}H NMR (400 MHz, CDCl$_3$): δ 8.72 (d, J = 4.8 Hz, 1H), 7.80 (td, J = 7.8, 1.7 Hz, 1H), 7.73 (d, J = 7.8 Hz, 1H), 7.43 (s, 1H), 7.32 (ddd, J = 7.5, 4.9, 1.3 Hz, 1H), 3.98 (s, 3 H) ppm.

^{13}C NMR (126 MHz, CDCl$_3$): δ 155.9, 152.9, 149.1, 148.3, 136.6, 130.7, 124.6, 123.9, 123.5, 118.5, 56.9 ppm.

IR (v/cm^{-1}): 2923 (m), 2853 (w), 1584 (w), 1562 (m), 1526 (w), 1460 (m), 1410 (s), 1354 (w), 1316 (m), 1281 (w), 1232 (w), 1211 (m), 1182 (w), 1119 (m), 1091 (w), 1065 (m), 1043 (w), 1011 (m), 991 (w), 889 (w), 873 (m), 797 (m), 744 (s), 687 (w), 657 (w).

HRESI-MS (MeOH, +, m/z): [M+H]$^+$ 344.9078, calc. 344.9056, [M+Na]$^+$ 366.8899, calc. 366.8875

M.p.: 93–96 °C

3-Bromo-6-methoxy-2,2′-bipyridine (25p)

[SZ 5075]
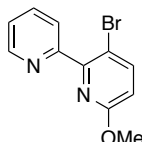
According to the general procedure, bipyridine N-oxide **22p** (99.1 mg, 0.35 mmol) and PBr$_3$ (0.15 mL, 1.58 mmol) in CHCl$_3$ (5.00 mL) provided **25p** (7.9 mg, 0.03 mmol, 8%) as pale yellow oil after column chromatography.

^{1}H NMR (400 MHz, CDCl$_3$): δ 8.74 (d, J = 4.1 Hz, 1H), 7.87–7.77 (m, 2H), 7.73 (dt, J = 7.9, 1.0 Hz, 1H), 7.34 (ddd, J = 7.6, 4.9, 1.2 Hz, 1H), 6.68 (d, J = 8.7 Hz, 1H), 3.95 (s, 3H) ppm.

^{13}C NMR (126 MHz, CDCl$_3$): δ 162.7, 157.4, 153.1, 148.9, 144.1, 136.5, 124.5, 123.4, 112.4, 110.3, 77.2, 54.0 ppm.

IR (v/cm^{-1}): 2946 (w), 2923 (w), 2852 (w), 1564 (s), 1458 (s), 1408 (s), 1382 (w), 1318 (s), 1284 (w), 1120 (w), 1046 (w), 1011 (m), 992 (m), 891 (w), 823 (m), 795 (m), 744 (m), 717 (w), 670 (w) 655 (m).

HRESI-MS (MeOH, +, m/z): [M+H]$^+$ 265.0012, calc. 264.9971, [M+Na]$^+$ 286.9833, calc. 286.9790

3-Bromo-4′-methyl-2,2′-bipyridine (25u)

[SZ 5076]
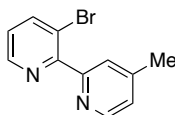
According to the general procedure, bipyridine N-oxide **22u** (156 mg, 0.59 mmol) and PBr$_3$ (0.15 mL, 1.58 mmol) in CHCl$_3$ (5.00 mL) provided **25u** (65.8 mg, 0.26 mmol, 45%) as pale yellow solid after column chromatography.

^{1}H NMR (400 MHz, CDCl$_3$): δ 8.59 (d, J = 4.6 Hz, 1H), 8.56 (d, J = 5.0 Hz, 1H), 7.97 (dt, J = 8.1, 1.6 Hz, 1H), 7.50 (s, 1H), 7.18–7.11 (m, 2H), 2.39 (s, 3H) ppm.

^{13}C NMR (126 MHz, CDCl$_3$): δ 157.1, 156.7, 148.9, 147.9, 147.6, 141.6, 125.1, 124.4, 124.2, 119.6, 21.2 ppm.

IR (v/cm^{-1}): 3036 (w), 2960 (w), 2924 (w), 2854 (w), 1603 (m), 1568 (m), 1476 (w), 1437 (m), 1384 (m), 1286 (w), 1133 (w), 1115 (w), 1099 (w), 1018 (s), 994 (m), 894 (w), 878 (w), 797 (s), 772 (m), 755 (w), 743 (m), 689 (w).

HRESI-MS (MeOH, +, m/z): [M+H]$^+$ 249.0053, calc. 249.0022, [M+Na]$^+$ 270.9853, calc. 270.9841

M.p.: 50–52 °C

3-Bromo-4′-(ethoxycarbonyl)-2,2′-bipyridine (25w)

[SZ 5077]
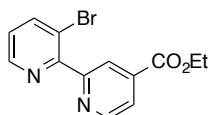
According to the general procedure, bipyridine N-oxide **22w** (157 mg, 0.49 mmol) and PBr$_3$ (0.15 mL, 1.58 mmol) in CHCl$_3$ (5.00 mL) provided **25w** (128 mg, 0.42 mmol, 86%) as brown solid after extraction.

^{1}H NMR (400 MHz, CDCl$_3$): δ 8.87 (d, J = 5.0 Hz, 1H), 8.65 (dd, J = 4.6, 1.3 Hz, 1H), 8.28 (s, 1H), 8.02 (dd, J = 8.1, 1.4 Hz, 1H), 7.90 (dd, J = 5.0, 1.5 Hz, 1H), 7.22 (dd, J = 8.1, 4.6 Hz, 1H), 4.41 (q, J = 7.1 Hz, 2H), 1.39 (t, J = 7.1 Hz, 3H) ppm.

^{13}C NMR (126 MHz, CDCl$_3$): δ 164.9, 158.2, 155.8, 149.9, 148.2, 141.8, 138.3, 124.6, 123.7, 122.6, 119.7, 62.0, 14.3 ppm.

IR (v/cm^{-1}): 3044 (w), 2984 (w), 2924 (w), 2852 (w), 1721 (s), 1561 (w), 1471 (w), 1440 (w), 1395 (w), 1374 (m), 1307 (m), 1293 (s), 1249 (s), 1232 (m), 1203 (m), 1128 (m), 1101 (w), 1090 (w), 1015 (s), 899 (m), 856 (w), 912 (m), 794 (w), 778 (w), 750 (s), 733 (m), 693 (m), 680 (m).

HRESI-MS (MeOH, +, m/z): [M+Na]$^+$ 328.9928, calc. 328.9896

M.p.: 78–80 °C

3-Bromo-2-(pyridin-2-yl)quinoline (7s)

[SZ 5079]
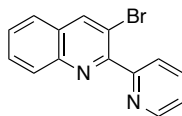
According to the general procedure, pyridylquinoline N-oxide **22y** (110 mg, 0.37 mmol) and PBr$_3$ (0.15 mL, 1.58 mmol) in CHCl$_3$ (5.00 mL) provided **25y** (39.6 mg, 0.14 mmol, 38%) as colorless solid after column chromatography.

Data are identical to previous obtained sample (FW 2063).

4.11.3.2   Reduction of chlorinated products

3-Chloro-2,2′-bipyridine (34a)

[SZ 5056]
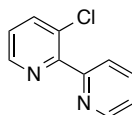
According to the general procedure, bipyridine *N*-oxide **21a** (102 mg, 0.49 mmol) and PCl$_3$ (0.17 mL, 1.94 mmol) in CHCl$_3$ (5.00 mL) provided **34a** (34.9 mg, 0.18 mmol, 37%) as pale orange oil after extraction.

^{1}H NMR (400 MHz, CDCl$_3$): δ 8.72 (d, *J* = 3.2 Hz, 1H), 8.58 (d, *J* = 3.9 Hz, 1H), 7.78 (dd, *J* = 8.0, 1.2 Hz, 2H), 7.72 (d, *J* = 7.8 Hz, 1H), 7.30 (ddd, *J* = 7.2, 4.9, 1.2 Hz, 1H), 7.25 (dd, *J* = 8.1, 4.6 Hz, 1H) ppm.

^{13}C NMR (126 MHz, CDCl$_3$): δ 156.1, 155.0, 149.3, 147.6, 138.4, 136.4, 130.5, 124.5, 124.2, 123.5 ppm.

IR (*v*/cm^{-1}): 3055 (w), 1587 (w), 1569 (m), 1553 (w), 1476 (w), 1412 (s), 1287 (w), 1234 (w), 1135 (w), 1104 (m), 1090 (w), 1030 (s), 991 (m), 796 (s), 746 (s), 695 (w).

HRESI-MS (MeOH, +, *m/z*): [M+H]$^+$ 191.0384, calc. 191.0371, [M+Na]$^+$ 213.0208, calc. 213.0190, [M+K]$^+$ 228.9958, calc. 228.9929

[SZ 5084B]

Bipyridine *N*-oxide **21a** (51.7 mg, 0.25 mmol) was dissolved in MeOH (1.30 mL) and NH$_4$CO$_2$H (158 mg, 2.51 mmol) and Pd/C (*w* = 10%, 26.0 mg, 0.024 mmol) were added as solids. The reaction solution was stirred at room temperature for 5 h, the volatiles removed and the residue extracted with DCM. After removal of the solvent from the extracted solution, only starting material **21a** (53.4 mg, 0.26 mmol, quant.) was recovered.

3-Chloro-6-methyl-2,2′-bipyridine (34b)

[SZ 5109]
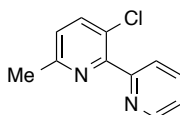
According to the general procedure, bipyridine N-oxide **21b** (85.7 mg, 0.36 mmol) and PCl$_3$ (0.15 mL, 1.71 mmol) in CHCl$_3$ (5.00 mL) provided **34b** (46.4 mg, 0.21 mmol, 58%) containing traces of brominated **25b** (1:10 for **25b:34b**) as pale yellow oil after column chromatography.

^{1}H NMR (400 MHz, CDCl$_3$): δ 8.73 (d, J = 4.5 Hz, 1H), 7.77 (td, J = 7.7, 1.8 Hz, 1H), 7.68 (d, J = 7.9 Hz, 1H), 7.65 (d, J = 8.2 Hz, 1H), 7.30 (ddd, J = 7.5, 4.9, 1.2 Hz, 1H), 7.11 (d, J = 8.2 Hz, 1H), 2.57 (s, 3H) ppm.

^{13}C NMR (126 MHz, CDCl$_3$): δ 156.8, 156.3, 154.2, 149.4, 138.4, 136.3, 127.5, 124.6, 124.0, 123.3, 24.1 ppm.

IR (v/cm^{-1}): 3055 (w), 3010 (w), 2923 (w), 2855 (w), 1588 (w), 1562 (m), 1474 (w), 1448 (m), 1418 (s), 1474 (m), 1282 (w), 1234 (m), 1206 (w), 1141 (m), 1118 (m), 1091 (w), 1027 (s), 992 (m) 962 (w), 879 (w), 821 (m), 797 (m), 745 (s), 660 (m).

HRESI-MS (MeOH, +, m/z): [M+H]$^+$ 205.0549, calc. 205.0527

3-Chloro-6-(ethoxycarbonyl)-2,2′-bipyridine (34c)

[SZ 5057]
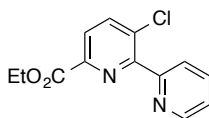
According to the general procedure, bipyridine N-oxide **21c** (134 mg, 0.48 mmol) and PCl$_3$ (0.17 mL, 1.94 mmol) in MeOH (5.00 mL) provided **34c** (104 mg, 0.40 mmol, 82%) as orange oil after extraction.

^{1}H NMR (400 MHz, CDCl$_3$): δ 8.71 (d, J = 4.4 Hz, 1H), 8.06 (d, J = 8.3 Hz, 1H), 7.93 (d, J = 8.3 Hz, 1H), 7.83–7.75 (m, 2H), 7.33 (ddd, J = 6.7, 4.8, 1.8 Hz, 1H), 4.43 (q, J = 7.1 Hz, 1H), 1.38 (t, J = 7.1 Hz, 3H) ppm.

^{13}C NMR (126 MHz, CDCl$_3$): δ 164.5, 155.7, 155.2, 149.1, 146.3, 139.4, 136.7, 134.3, 125.4, 124.9, 123.8, 62.3, 14.3 ppm.

IR (v/cm^{-1}): 2980 (w), 2934 (w), 1739 (m), 1716 (s), 1588 (w), 1568 (m), 1474 (w), 1445 (w), 1418 (m), 1392 (m), 1368 (m), 1313 (s), 1282 (m), 1246 (w), 1221 (m), 1171 (w), 1140 (s), 1109 (m), 1092 (w), 1030 (s), 993 (w), 897 (w), 857 (m), 800 (m), 787 (m), 745 (s), 705 (w).

HRESI-MS (MeOH, +, m/z): [M+H]$^+$ 263.0588, calc. 263.0582, [M+Na]$^+$ 285.0409, calc. 285.0401

3-Chloro-5-methoxy-2,2′-bipyridine (34f)

[SZ 5061]
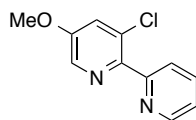
According to the general procedure, bipyridine *N*-oxide **21f** (85.7 mg, 0.36 mmol) and PCl$_3$ (0.15 mL, 1.71 mmol) in CHCl$_3$ (5.00 mL) provided **34f** (46.4 mg, 0.21 mmol, 58%) as colorless solid, and dichlorinated product **36f** (12.5 mg, 0.05 mmol, 14%) as pale yellow solid after column chromatography.

^{1}H NMR (500 MHz, CDCl$_3$): δ 8.73 (br s, 1H), 8.33 (br s, 1H), 7.76 (td, *J* = 7.6, 1.6 Hz, 1H), 7.72 (br d, *J* = 7.0 Hz, 1H), 7.31 (d, *J* = 2.5 Hz, 1H), 7.30–7.27 (m, 1H), 3.87 (s, 1H) ppm.

^{13}C NMR (126 MHz, CDCl$_3$): δ 156.0, 155.7, 149.2, 147.3, 136.3, 136.0, 130.5, 124.5, 123.1, 122.3, 56.1 ppm.

IR (v/cm^{-1}): 3075 (w), 3006 (w), 2923 (m), 2839 (w), 1583 (s), 1541 (w), 1489 (w), 1455 (s) 1424 (m), 1316 (w), 1273 (s), 1239 (m), 1206 (m), 1177 (m), 1142 (m), 1097 (m), 1032 (s), 991 (m), 888 (w), 871 (m), 801 (m), 747 (m).

HRESI-MS (MeOH, +, *m/z*): [M+H]$^+$ 221.0512, calc. 221.0476, [M+Na]$^+$ 243.0335, calc. 243.0296

M.p.: 63 °C

3,6-Dichloro-5-methoxy-2,2′-bipyridine (36f)
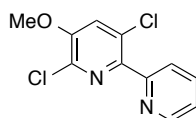
^{1}H NMR (500 MHz, CDCl$_3$): δ 8.73 (d, *J* = 4.4 Hz, 1H), 7.80 (td, *J* = 7.5, 1.5 Hz, 1H), 7.75 (dt, *J* = 7.9, 1.1 Hz, 1H), 7.32 (ddd, *J* = 7.4, 4.8, 1.4 Hz, 1H), 7.33 (s, 1H), 3.98 (s, 3H) ppm.

^{13}C NMR (126 MHz, CDCl$_3$): δ 155.0, 151.6, 149.2, 145.9, 138.4, 136.6, 129.5, 124.7, 123.4, 121.5, 56.8 ppm.

IR (v/cm^{-1}): 3063 (w), 2924 (m), 2853 (w), 1568 (m), 1456 (m), 1413 (s), 1362 (w), 1324 (m), 1287 (w), 1213 (m), 1123 (m), 1081 (m), 1047 (w), 1016 (m), 921 (w), 867 (m), 798 (m), 745 (m), 697 (w), 666 (m).

HRESI-MS (MeOH, +, *m/z*): [M+H]$^+$ 255.0129, calc. 255.0086, [M+Na]$^+$ 276.9950, calc. 276.9906

M.p.: 66–68 °C

3-Chloro-5-methyl-2,2′-bipyridine (34g)

[SZ 5062]
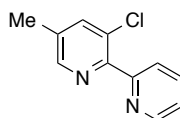
According to the general procedure, bipyridine *N*-oxide **21g** (70.2 mg, 0.32 mmol) and PCl$_3$ (0.15 mL, 1.71 mmol) in CHCl$_3$ (5.00 mL) provided **34g** (59.8 mg, 0.27 mmol, 85%) as brown oil after extraction.

^{1}H NMR (400 MHz, CDCl$_3$): δ 8.74 (d, *J* = 4.7 Hz, 1H), 8.43 (s, 1H), 7.81 (td, *J* = 7.6, 1.7 Hz, 1H), 7.75 (d, *J* = 7.8 Hz, 1H), 7.63 (s, 1H), 7.33 (ddd, *J* = 7.2, 4.9, 1.3 Hz, 1H), 2.37 (s, 3H) ppm.

^{13}C NMR (126 MHz, CDCl$_3$): δ 155.8, 151.8, 149.0, 148.3, 138.8, 136.7, 134.7, 130.0, 124.7, 123.4, 17.9 ppm.

IR (v/cm^{-1}): 3044 (w), 3004 (w), 2923 (w), 1585 (m), 1568 (w), 1542 (w), 1446 (m), 1426 (m), 1380 (m), 1287 (w), 1253 (w), 1217 (w), 1193 (w), 1148 (w), 1105 (m), 1089 (w), 1049 (w), 1034 (m), 991 (w), 898 (m), 799 (m), 746 (s), 683 (w).

HRESI-MS (MeOH, +, *m/z*): [M+H]$^+$ 205.0542, calc. 205.0527

3-Chloro-5-(methoxycarbonyl)-2,2′-bipyridine (34h)

[SZ 5063]
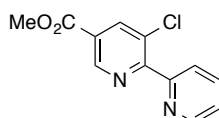
According to the general procedure, bipyridine *N*-oxide **21h** (77.0 mg, 0.29 mmol) and PCl$_3$ (0.15 mL, 1.71 mmol) in CHCl$_3$ (5.00 mL) provided **34h** (66.4 mg, 0.27 mmol, 93%) as tan solid after extraction.

^{1}H NMR (400 MHz, CDCl$_3$): δ 9.17 (d, *J* = 1.8 Hz, 1H), 8.79 (d, *J* = 4.3 Hz, 1H), 8.42 (dd, *J* = 1.8, 0.8 Hz, 1H,), 7.88 (td, *J* = 7.8, 1.7 Hz, 1H), 7.83 (d, *J* = 7.8 Hz, 1H), 7.42 (ddd, *J* = 7.0, 4.9, 1.3 Hz, 1H), 3.98 (s, 3H) ppm.

^{13}C NMR (126 MHz, CDCl$_3$): δ 164.5, 157.7, 154.9, 149.1, 148.4, 139.6, 137.1, 130.6, 126.7, 125.0, 124.2, 52.9 ppm.

IR (v/cm^{-1}): 3072 (w), 3005 (w), 2954 (w), 2924 (w), 2851 (w), 1726 (s), 1584 (m), 1536 (w), 1477 (w), 1424 (m), 1377 (m), 1279 (s), 1244 (), 1227 (w), 1212 (w), 1196 (w), 1119 (m), 1104 (m), 1088 (m), 1050 (w), 1033 (m), 992 (m), 958 (m), 929 (w), 806 (w), 783 (w), 761 (s), 742 (s), 712 (w).

HRESI-MS (MeOH, +, *m/z*): [M+H]$^+$ 249.0440, calc. 249.0425, [M+Na]$^+$ 271.0261, calc. 271.0245

M.p.: 52 °C

3-Chloro-6-methoxy-2,2′-bipyridine (34p)

[SZ 5068]
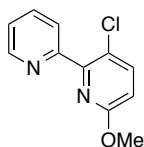
According to the general procedure, bipyridine *N*-oxide **21p** (57.1 mg, 0.24 mmol) and PCl$_3$ (0.15 mL, 1.71 mmol) in CHCl$_3$ (5.00 mL) provided **34p** (35.0 mg, 0.16 mmol, 66%) as colorless oil after column chromatography.

^{1}H NMR (400 MHz, CDCl$_3$): δ 8.74 (d, *J* = 4.8 Hz, 1H), 7.80 (td, *J* = 7.5, 1.6 Hz, 1H), 7.75 (d, *J* = 7.9 Hz, 1H), 7.65 (d, *J* = 8.7 Hz, 1H), 7.32 (ddd, *J* = 6.9, 4.8, 1.1 Hz, 1H), 6.74 (d, *J* = 8.7 Hz, 1H), 3.95 (s, 3H) ppm.

^{13}C NMR (126 MHz, CDCl$_3$): δ 162.1, 156.5, 151.4, 149.0, 141.14, 141.12, 136.4, 124.6, 123.3, 122.3, 112.10, 112.08, 54.0 ppm.

IR (*v*/cm^{-1}): 3061 (w), 2980 (w), 2947 (w), 1583 (m), 1567 (m), 1460 (s), 1408 (s), 1322 (s), 1284 (w), 1252 (s), 1181 (w), 1129 (m), 1092 (w), 895 (w), 823 (m), 797 (m), 745 (m), 718 (w), 688 (m), 658 (w).

HRESI-MS (MeOH, +, *m/z*): [M+H]$^+$ 221.0489, calc. 221.0476, [M+Na]$^+$ 243.0308

3-Chloro-6-(trifluoromethyl)-2,2′-bipyridine (34r)

[SZ 5069]
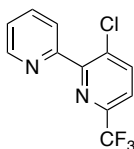
According to the general procedure, bipyridine *N*-oxide **21r** (84.9 mg, 0.31 mmol) and PCl$_3$ (0.15 mL, 1.71 mmol) in CHCl$_3$ (5.00 mL) provided **34r** (67.8 mg, 0.26 mmol, 85%) as yellow solid after extraction.

^{1}H NMR (400 MHz, CDCl$_3$): δ 8.76 (d, *J* = 4.9 Hz, 1H), 8.01 (d, *J* = 8.3 Hz, 1H), 7.86 (td, *J* = 7.7, 1.8 Hz, 1H), 7.81 (dt, *J* = 7.9, 1.0 Hz, 1H), 7.67 (d, *J* = 8.3 Hz, 1H), 7.40 (ddd, *J* = 7.3, 4.8, 1.3 Hz, 1H) ppm.

^{13}C NMR (126 MHz, CDCl$_3$): δ 155.6, 155.3, 149.2, 146.1 (q, *J* = 35.7 Hz), 140.0, 136.9, 133.8, 124.8, 124.1, 121.3 (q, *J* = 274.3 Hz), 121.0 (q, *J* = 2.6 Hz) ppm.

^{19}F NMR (376 MHz, CDCl$_3$): δ -67.47 ppm.

IR (v/cm^{-1}): 2955 (w), 1733 (w), 1576 (w), 1479 (w), 1451 (w), 1425 (w), 1395 (m), 1334 (s), 1293 (w), 1276 (w), 1224 (w), 1185 (m), 1122 (s), 1097 (m), 1032 (m), 993 (w), 845 (m), 797 (w), 770 (w), 742 (m), 684 (w).

HRESI-MS (MeOH, +, *m/z*): [M+H]$^+$ 259.0266, calc. 259.0244, [M+Na]$^+$ 281.0083, calc. 281.0064

M.p.: 51–53 °C

3-Chloro-4′-methyl-2,2′-bipyridine (34u)

[SZ 5064]
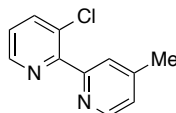
According to the general procedure, bipyridine *N*-oxide **21u** (125 mg, 0.57 mmol) and PCl$_3$ (0.15 mL, 1.71 mmol) in CHCl$_3$ (5.00 mL) provided **34u** (110 mg, 0.54 mmol, 95%) as tan solid after extraction.

^{1}H NMR (400 MHz, CDCl$_3$): δ 8.57 (br s, 2H), 7.78 (dd, *J* = 8.1, 1.4 Hz, 1H), 7.54 (s, 1H), 7.24 (dd, *J* = 8.1, 4.6 Hz, 1H), 7.14 (d, *J* = 5.0 Hz, 1H), 2.38 (s, 3H) ppm.

^{13}C NMR (126 MHz, CDCl$_3$): δ 155.8, 155.0, 148.8, 147.9, 147.5, 138.4, 130.5, 125.3, 124.5, 124.1, 21.2 ppm.

IR (v/cm^{-1}): 3040 (w), 2924 (w), 1709 (w), 1604 (m), 1568 (m), 1476 (w), 1433 (m), 1385 (m), 1287 (w), 1232 (w), 1141 (m), 1117 (m), 1099 (m), 1035 (s), 993 (m), 896 (w), 880 (w), 835 (m), 800 (s), 774 (m), 762 (m), 743 (w), 702 (w).

HRESI-MS (MeOH, +, *m/z*): [M+H]$^+$ 205.0532, calc. 205.0527, [M+Na]$^+$ 227.0355, calc. 227.0346

M.p.: 61 °C

3-Chloro-4′-fluoro-2,2′-bipyridine (34v)

[SZ 5065]
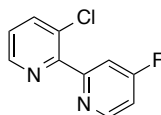
According to the general procedure, bipyridine *N*-oxide **21v** (74.3 mg, 0.33 mmol) and PCl$_3$ (0.15 mL, 1.71 mmol) in CHCl$_3$ (5.00 mL) provided **34v** (42.7 mg, 0.21 mmol, 62%) as colorless solid after column chromatography.

^{1}H NMR (400 MHz, CDCl$_3$): δ 8.72 (dd, *J* = 8.5, 5.7 Hz, 1H), 8.62 (d, *J* = 4.6 Hz, 1H), 7.84 (dd, *J* = 8.1, 1.4 Hz, 1H), 7.53 (dd, *J* = 9.6, 2.5 Hz, 1H), 7.32 (dd, *J* = 8.1, 4.6 Hz, 1H), 7.10 (ddd, *J* = 8.2, 5.6, 2.5 Hz, 1H) ppm.

^{13}C NMR (126 MHz, CDCl$_3$): δ 168.8 (d, J = 262.7 Hz), 159.2 (d, J = 7.1 Hz), 153.9 (d, J = 3.7 Hz), 151.7 (d, J = 7.1 Hz), 147.7, 138.8, 130.7, 124.7, 112.7 (d, J = 18.0 Hz), 111.5 (d, J = 16.2 Hz) ppm.

^{19}F NMR (376 MHz, CDCl$_3$): δ –101.74 (q, J = 8.8 Hz) ppm.

IR (v/cm^{-1}): 3071 (w), 2923 (m), 2853 (w), 1594 (w), 1579 (m), 1476 (w), 1448 (m), 1388 (m), 1309 (w), 1285 (w), 1218 (w), 1188 (m), 1146 w), 1104 (w), 1080 (w), 1038 (m), 995 (w), 973 (w), 905 (m), 874 (m), 845 (m), 812 (s), 766 (m), 737 (w), 699 (w).

HRESI-MS (MeOH, +, m/z): [M+H]$^+$ 209.0293, calc. 209.0276, [M+Na]$^+$ 231.0113, calc. 231.0096, [M+K]$^+$ 246.9817, calc. 246.9817

M.p.: 74–76 °C

3-Chloro-4′-(ethoxycarbonyl)-2,2′-bipyridine (34w)

[SZ 5067]
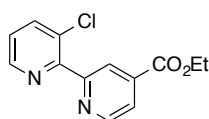
According to the general procedure, bipyridine N-oxide **21w** (93.5 mg, 0.34 mmol) and PCl$_3$ (0.15 mL, 1.71 mmol) in CHCl$_3$ (5.00 mL) provided **34w** (61.2 mg, 0.23 mmol, 70%) as orange solid after extraction.

^{1}H NMR (400 MHz, CDCl$_3$): δ 8.91 (br s, 1H), 8.65 (br s, 1H), 8.34 (s, 1H), 7.92 (dd, J = 5.0, 1.3 Hz, 1H), 7.86 (dd, J = 8.1, 1.4 Hz, 1H), 7.33 (dd, J = 8.1, 4.6 Hz, 1H), 4.43 (q, J = 7.1 Hz, 2H), 1.41 (t, J = 7.1 Hz, 3H) ppm.

^{13}C NMR (126 MHz, CDCl$_3$): δ 164.9, 157.1, 154.2, 150.0, 147.8, 138.7, 138.5, 124.6, 124.0, 122.8, 62.1, 14.3 ppm.

IR (v/cm^{-1}): 3062 (w), 2996 (w), 2901 (w), 1720 (s), 1562 (w), 1474 (w), 1442 (m), 1394 (w), 1376 (m), 1308 (m), 1295 (s), 1251 (s), 1228 (m), 1207 (w), 1146 (w), 1129 (m), 1101 (w), 1038 (w), 1020 (m), 895 (w), 865 (w), 813 (m), 780 (w), 750 (s), 733 (w), 709 (w), 683 (m).

HRESI-MS (MeOH, +, m/z): [M+H]$^+$ 263.0598, calc. 263.0582, [M+Na]$^+$ 285.0432, calc. 285.0401

M.p.: 99–102 °C

3-Chloro-4′-(trifluoromethyl)-2,2′-bipyridine (34x)

[SZ 5066]
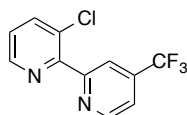
According to the general procedure, bipyridine *N*-oxide **21x** (63.3 mg, 0.23 mmol) and PCl$_3$ (0.15 mL, 1.71 mmol) in CHCl$_3$ (5.00 mL) provided **34x** (22.3 mg, 0.09 mmol, 37%) as colorless solid after column chromatography.

^{1}H NMR (400 MHz, CDCl$_3$): δ 8.94 (d, *J* = 5.0 Hz, 1H), 8.65 (d, *J* = 4.6 Hz, 1H), 8.05 (s, 1H), 7.87 (dd, *J* = 8.1, 1.5 Hz, 1H), 7.58 (dd, *J* = 5.1, 1.0 Hz, 1H), 7.35 (dd, *J* = 8.1, 4.6 Hz, 1H) ppm.

^{13}C NMR (126 MHz, CDCl$_3$): δ 157.6, 153.7, 150.2, 147.8, 139.0 (q, *J* = 34.3 Hz), 138.9, 130.8, 124.9, 122.9 (q, *J* = 273.4 Hz) 120.5 (d, *J* = 3.6 Hz), 119.1 (d, *J* = 3.4 Hz) ppm.

^{19}F NMR (376 MHz, CDCl$_3$): δ –64.63 ppm.

IR (*v*/cm^{-1}): 3066 (w), 3046 (w), 1559 (w), 1475 (w), 1426 (w), 1397 (m), 1334 (s), 1277 (m), 1232 (w), 1164 (s), 1131 (s), 1086 (m), 1050 (w), 1033 (s), 986 (w), 947 (w), 909 (w), 870 (m), 838 (m), 798 (s), 779 (m), 764 (w), 749 (w), 703 (w), 665 (s).

HRESI-MS (MeOH, +, *m/z*): [M+H]$^+$ 259.0282, calc. 259.0244, [M+Na]$^+$ 281.0104

M.p.: 49–50 °C

3-Chloro-2-(pyridin-2yl)quinoline (34y)

[SZ 5059]
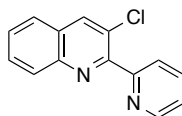
According to the general procedure, pyridylquinoline *N*-oxide **21y** (122 mg, 0.47 mmol) and PCl$_3$ (0.17 mL, 1.94 mmol) in MeOH (5.00 mL) provided **34y** (64.9 mg, 0.27 mmol, 57%), and dichlorinated product **36y** (17.2 mg, 0.06 mmol, 13%) as pale yellow solids after column chromatography.

^{1}H NMR (400 MHz, CDCl$_3$): δ 8.78 (d, *J* = 4.7 Hz, 1H), 8.28 (s, 1H), 8.16 (d, *J* = 8.3 Hz, 1H), 7.87–7.78 (m, 2H), 7.76 (d, *J* = 8.2 Hz, 1H), 7.71 (ddd, *J* = 8.4, 7.0, 1.4 Hz, 1H), 7.56 (td, *J* = 7.6, 7.1, 1.0 Hz, 1H), 7.37 (ddd, *J* = 6.8, 4.9, 1.7 Hz, 1H) ppm.

^{13}C NMR (126 MHz, CDCl$_3$): δ 156.5, 155.4, 149.3, 146.1, 136.7, 136.5, 130.0, 129.8, 128.3, 128.0, 127.2, 126.6, 124.7, 123.6 ppm.

IR (*v*/cm^{-1}): 3053 (w), 2923 (w), 2853 (w), 1582 (m), 1568 (m), 1550 (w), 1479 (m), 1434 (m), 1400 (m), 1370 (m), 1333 (w), 1310 (m), 1284 (w), 1240 (w), 1194 (w), 1151 (w), 1128 (w), 1092 (s), 1047 (m), 994 (m), 971 (s), 952 (m), 900 (s), 860 (m), 804 (w), 772 (s), 750 (s), 734 (s), 711 (s).

HRESI-MS (MeOH, +, *m/z*): [M+H]$^+$ 241.0564, calc. 241.0527, [M+Na]$^+$ 263.0389

M.p.: 87–88 °C

3,4-Dichloro-2-(pyridin-2yl)quinoline (**36y**)
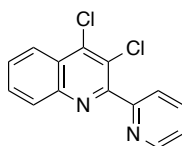
^{1}H NMR (400 MHz, CDCl$_3$): δ 8.80 (d, J = 4.1 Hz, 1H), 8.25 (dd, J = 8.4, 0.7 Hz, 1H), 8.18 (d, J = 8.4 Hz, 1H), 7.88 (td, J = 7.7, 1.8 Hz, 1H), 7.81–7.76 (m, 2H), 7.70 (ddd, J = 7.9, 7.0, 0.8 Hz, 1H), 7.42 (dd, J = 7.6, 4.9 Hz, 1H, ArH-4$'$) ppm.

^{13}C NMR (126 MHz, CDCl$_3$): δ 156.7, 156.0, 149.4, 146.2, 141.4, 136.7, 130.7, 130.3, 128.9, 126.8, 126.4, 124.6, 124.5, 123.9 ppm.

IR (v/cm^{-1}): 3059 (w), 2924 (w), 1585 (w), 1564 (m), 1545 (w), 1476 (m), 1432 (w), 1410 (w), 1380 (m), 1351 (m), 1335 (m), 1310 (m), 1285 (w), 1258 (w), 1238 (w), 1168 (w), 1146 (w), 1111 (m), 1091 (w), 993 (w), 958 (w), 905 (m), 851 (m), 792 (m), 760 (s), 736 (s), 711 (m), 669 (m).

HRESI-MS (MeOH, +, m/z): [M+H]$^+$ 275.0182, calc. 275.0137, [M+Na]$^+$ 297.0005, calc. 296.9957

M.p.: 101–103 °C

4.11.4 Mechanistic experiments and isolation of catalyst intermediates

4.11.4.1   *Synthesis of possible catalyst intermediates*

(2,2$'$-Bipyridin-3-yl-*N*-oxide)palladium acetate dimer (D)
[SZ 4085/SZ 4114/SZ 5095]
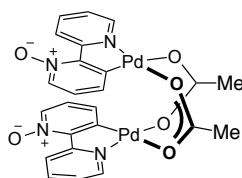
An argon-purged Schlenk flask was charged with Pd$_2$dba$_3$ $\cdot$ CHCl$_3$ (1.01 g, 0.98 mmol), brominated bipyridine *N*-oxide **22a** (508 mg, 2.02 mmol) and dry toluene (20.0 mL). The mixture was stirred at 50 °C for 1 h and cooled to room temperature before the flask was opened to air and the solvent removed in vacuum. The solid residue was re-dissolved in DCM (20.0 mL) and AgOAc (1.01 g, 6.06 mmol) was added as solid. The resulting mixture was stirred at room temperature for 2.5 h and subsequently filtered through Celite. The filtrate was concentrated in vacuum and Et$_2$O was added resulting in the formation of a yellow solid. The clear yellow supernatant solution was decanted and the solid washed with Et$_2$O and dried in vacuum providing complex **D** (624 mg, 0.93 mmol, 95%) as yellow solid.

Single crystals for X-ray diffraction were grown by slow diffusion of Et$_2$O into a concentrated solution of **D** in DCM. CCDC-1476427 contains the crystallographic data for **D**.

^{1}H NMR (400 MHz, CDCl$_3$, major isomer): δ 9.07 (ddd, J = 8.3, 1.6, 0.7 Hz, 2H), 7.99 (ddd, J = 5.6, 1.7, 0.7 Hz, 2H), 7.75–7.69 (m, 4H), 6.83 (dd, J = 7.7, 1.2 Hz, 2H), 6.76 (ddd, J = 7.4, 5.5, 1.5 Hz, 2H), 6.74 (dd, J = 7.7, 6.4 Hz, 2H), 2.24 (s, 8H) ppm.

^{13}C NMR (126 MHz, CDCl$_3$): δ 182.6, 157.6, 149.7, 148.7, 147.6, 139.6, 136.8, 125.5, 123.3, 122.4, 24.8 ppm.

IR (v/cm^{-1}): 3112 (w), 3081 (w), 3056 (w), 3046 (w), 2922 (w), 2851 (w), 1595 (w), 1559 (m), 1524 (m), 1473 (w), 1401 (s), 1347 (w), 1290 (w), 1253 (m), 1244 (m), 1205 (m), 1179 (w), 1155 (w), 1110 (w), 1073 (w), 1038 (w), 1025 (w), 1007 (w), 902 (s), 782 (s), 746 (m), 706 (s).

HRESI-MS (MeOH, +, m/z): [(BiPyNox)$_2$Pd$_2$(OAc)]$^+$ 614.9368, calc. 614.9324, [(BiPyNox)$_2$Pd$_2$(OAc)$_2$+Na]$^+$ 696.9401, calc. 696.9354

Elemental analysis (%): C 42.8, H 3.34, N 8.36, calc. C 42.8, H 2.99, N 8.32

M.p.: 204 °C (decomp.)

(2,2′-Bipyridin-3-yl-N-oxide)palladium succinate dimer (E)

[SZ 5096]
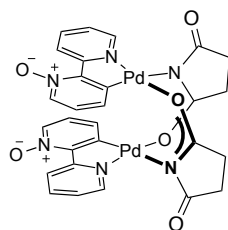
A mixture of palladium acetate dimer **D** (336 mg, 0.5 mmol) and succinimide (101 mg, 1.02 mmol) in MeCN (20.0 mL) was stirred at 40 °C for 1.5 h. The volatiles were removed and re-dissolved in CHCl$_3$ (20.0 mL) and the resulting solution stirred at 40 °C for additional 1.5 h. The reaction solution was concentrated in vacuum, and Et$_2$O was added resulting in the formation of a yellow precipitate. The supernatant liquid was decanted, the solid washed with Et$_2$O and dried in vacuum. The dimer **E** (372 mg, 0.50 mmol, quant.) was obtained as yellow solid.

^{1}H NMR (400 MHz, CDCl$_3$): δ 9.21 (d, J = 8.3 Hz, 2H), 7.94 (d, J = 5.4 Hz, 2H), 7.78–7.70 (m, 4H), 6.83 (t, J = 6.6 Hz, 2H), 6.61 (dd, J = 7.6, 6.6 Hz, 2H), 6.43 (d, J = 7.7 Hz, 2H), 2.91–2.79 (m, 8H) ppm.

^{13}C NMR (126 MHz, CDCl$_3$): δ 195.7, 188.2, 157.1, 149.3, 148.4, 146.7, 140.0, 136.9, 130.5, 125.6, 123.8, 122.8, 32.2, 32.1 ppm.

IR (v/cm^{-1}): 1717 (w), 1589 (s), 1530 (w), 1474 (w), 1407 (w), 1379 (m), 1283 (w), 1244 (m), 1215 (m), 1079 (w), 1039 (w), 1005 (w), 897 (m), 823 (w), 789 (m), 747 (m), 706 (m), 668 (m).

HRESI-MS (MeOH, +, m/z): [(BiPyNox)$_2$Pd$_2$(succinate)$_2$+Na]$^+$ 774.9609, calc. 774.9563, [(BiPyNox)Pd(succinate) +Na]$^+$ 397.9751, calc. 397.9727

Elemental analysis ($\%$): C 44.0, H 3.66, N 10.5 calc. C 44.8, H 3.95, N 11.2

A better elemental analysis could not be obtained.

M.p.: > 250 °C

(2,2-Bipyridine-N-oxide)palladium(II) acetate (C1)

[SZ 2032A/SZ 5123A]
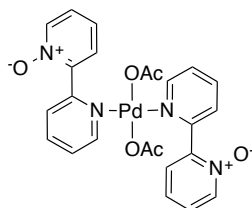
A mixture of Pd(OAc)$_2$ (62.7 mg, 0.28 mmol) and bipyridine N-oxide **20a** (97.1 mg, 0.56 mmol) was dissolved in DCM (3.00 mL) under vigorous stirring. A precipitate was formed within the first 2 min. The mixture was additionally stirred at room temperature for 12 h, before Et$_2$O (3.00 mL) was added. The supernatant liquid was decanted, the solid was washed with Et$_2$O and dried in vacuum. The monomer complex **C1** (149 mg, 0.262 mmol, 94%) was obtained as pale tan almost insoluble solid.

IR (v/cm^{-1}): 3057 (w), 1624 (m), 1601 (m), 1503 (w), 1470 (w), 1445 (w), 1419 (w), 1376 (w), 1357 (m), 1305 (s), 1245 (s), 1158 (w), 1044 (w), 1014 (w), 957 (w), 927 (w), 845 (m), 784 (m), 762 (s), 727 (m), 695 (m), 655 (w).

HRESI-MS (MeOH, +, m/z): [(BiPyNox)Pd(OAc)]$^+$ 336.9892, calc. 336.9799

Elemental analysis ($\%$): C 49.4, H 4.04, N 9.88 calc. C 50.7, H 3.90, N 9.85

A better elemental analysis could not be obtained.

M.p.: 173 °C (decomp.)

(4-Ethoxycarbonayl-2,2-bipyridine-N-oxide)palladium(II) acetate (C2)

[SZ 2027A/SZ 5123B]

A mixture of Pd(OAc)$_2$ (56.3 mg, 0.25 mmol) and bipyridine *N*-oxide **20l** (122 mg, 0.50 mmol) was dissolved in DCM (3.00 mL) under vigorous stirring. A precipitate was formed within the first 2 min. The mixture was additionally stirred at room temperature for 12 h, before Et$_2$O (3.00 mL) was added. The supernatant liquid was decanted, the solid was washed with Et$_2$O and dried in vacuum. The monomer complex **C2** was obtained as a 2:1 mixture with bipyridine *N*-oxide **20ll** (190 mg). Single crystals for X-ray diffraction were grown by slow diffusion of Et$_2$O into a concentrated solution of **C2** in CDCl$_3$. CCDC-1476437 contains the crystallographic data for **C2**.

^{1}H NMR (400 MHz, CDCl$_3$): δ 10.57 (d, *J* = 1.9 Hz, 2H), 8.71 (d, *J* = 5.2 Hz, 2H), 8.25 (d, *J* = 6.8 Hz, 2H), 8.02 (dd, *J* = 6.8, 2.5 Hz, 2H), 7.89 (dd, *J* = 8.0, 0.9 Hz, 2H), 7.87–7.79 (m, 2H, overlapping with **10l**), 7.30 (ddd, *J* = 7.5, 5.8, 1.6 Hz, 2H), 4.49 (q, *J* = 7.1 Hz, 4H), 1.57 (s, 6H), 1.46–1.37 (m, 6H, overlapping with **20l**) ppm.

IR (v/cm^{-1}): 1718 (m), 1624 (m), 1458 (w), 1421 (w), 1361 (m), 1304 (s), 1246 (s), 1206 (m), 1124 (w), 1017 (w), 776 (m), 696 (m).

HRESI-MS (MeOH, +, *m/z*): [(4-EtO$_2$CBiPyNox)$_2$Pd(OAc)]$^+$ 653.0964, calc. 653.0858, [(4-EtO$_2$CBiPyNox)$_2$Pd(OMe)]$^+$ 625.1013, calc. 625.0909, [(4-EtO$_2$CBiPyNox)Pd(OAc)]$^+$ 409.0008, calc. 409.0010

M.p.: 154 °C (decomp.)

4.11.4.2   *Catalytic reactions in palladium*

General procedure:

8-mL reaction vials were charged with bipyridine *N*-oxide **20a** (0.25 mmol), NBS (0.30 mmol), palladium source (5 mol% based on Pd), chlorobenzene (2.50 mL), and if applicable the additive. NBu$_4$OAc (0.025 mmol, 10 mol%) was directly weighted out together with the substrate, the liquids were added using Hamilton syringe. Pyridine (20 μL, 0.25 mmol) was added neat and AcOH was added as stock solution in chlorobenzene (0.25 M, 100 μL, 0.025 mmol, 10 mol%). The reaction vials were sealed with a Teflon-lined screw cap and placed in a pre-heated aluminum well-plate at 110 °C at the same time. After 1 h stirring at this temperature, the vials were cooled to room temperature, the reaction solutions/mixtures were transferred into round-bottom flasks and the solvent removed by

rotary evaporation. The solid residues were additionally dried in high vacuum for several hours, before being redissolved in CDCl₃. The solutions were directly filtered through a short plug of Celite (pipette) and the filtrate transferred into NMR tubes and analyzed by ¹H NMR. Only isolated peaks of **20a** and **22a** were used for integration. The average of 3–4 integrals for each compound was used to calculate the ratio **22a** to **20a**.

entry	Exp. No. SZ 51xx	**20a** [mg]	NBS [mg]	[Pd] [mg]	additive	ratio **22a:20a**	est. yield[a] **22a**
1	17A	43.0	53.4	Pd(OAc)₂ (2.7)	–	1.90	66%
3	22C	43.1	53.4	Pd(OAc)₂ (2.8)	pyridine	n.c.[b]	0
4	17B	43.1	53.4	Dimer **D** (4.2)	–	13.1	93%
5	11C	43.5	55.1	Dimer **E** (4.8)	–	0.71	41%
6	17E	43.8	53.5	Dimer **E** (4.6)	AcOH	18.4	95%
7	17D	43.1	53.3	Dimer **E** (4.6)	NBu₄OAc	0.33	25%

[a]The estimated yield was calculated using following equation: (1+ratio)·100/ratio

[b]Only starting material was recovered. n.c. = no conversion

4.11.4.3   *Stoichiometric reactions in palladium*
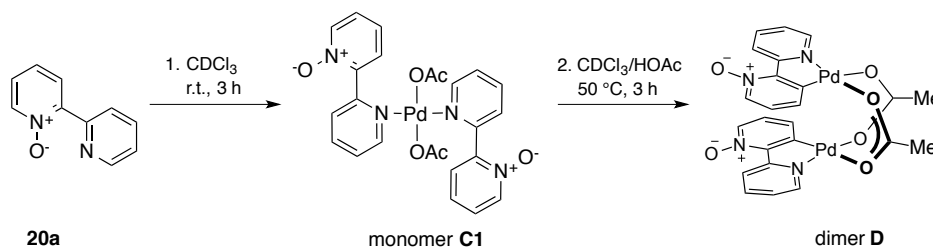
[SZ 5118A]

A 8-mL reaction vial was charged with bipyridine *N*-oxide **20a** (51.5 mg, 0.30 mmol), Pd(OAc)₂ (68.4 mg, 0.30 mmol) and CDCl₃ (0.60 mL) and sealed. After stirring at room temperature for 3 h a precipitate was formed, which was allowed to settle and the supernatant solution was transferred into a NMR tube and measured by ¹H NMR, showing a species corresponding with the structure of monomeric complex **C1**.

¹H NMR (400 MHz, CDCl₃): δ 9.13 (dd, *J* = 8.1, 1.6 Hz, 2H), 8.79 (td, *J* = 7.9, 1.3 Hz, 2H), 8.54 (dd, *J* = 6.4, 1.2 Hz, 2H), 8.43 (dd, *J* = 5.7, 1.1 Hz, 2H), 8.12 (d, *J* = 7.3 Hz, 2H), 7.87 (td, *J* = 7.8, 1.6 Hz, 2H), 7.65 (ddd, *J* = 8.0, 6.4, 1.7 Hz, 2H), 7.48 (ddd, *J* = 7.6, 5.7, 1.4 Hz, 2H), 1.98 (s, 6H) ppm.

Then, the reaction mixture was treated with one drop of AcOH resulting in formation of a clear solution. The solution was stirred under heating at 50 °C for additional 3 h before again being measured by ^{1}H NMR. The spectrum showed besides the formation of dimer **D** an additional set of signals.
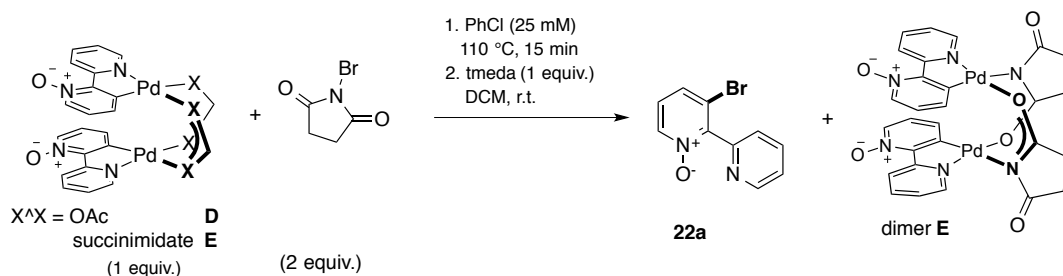
General procedure:

20-mL reaction vials were charged with dimer **D** or **E** (0.075 mmol), NBS (0.15 mmol) and chlorobenzene (3.00 mL). The reaction vials were sealed with Teflon-lined scerw cap and placed in a pre-heated aluminum well-plate at 110 °C. After 10 min stirring at this temperature, the vials were cooled to room temperature, the reaction solutions/mixtures were transferred into round-bottom flasks and the solvent removed by rotary evaporation. The solid residues were additionally dried in high vacuum for several hours, before a stock solution of TMB in CDCl$_3$ (35 mM, 1.00 mL, 0.035 mmol) was added. The resulting solutions were directly transferred into NMR tubes and analyzed by ^{1}H NMR spectroscopy (sample X1). Only isolated peaks were used integration. The average values of several integrals for the quantified compound were used to estimate the yields. Then, the ^{1}H sample solutions were quantitatively transferred back to the corresponding flasks, the solvent was removed and DCM (2.00 mL) and tmeda (22 μL, 0.15 mmol) was added. After 15 min stirring, the volatiles were removed and CDCl$_3$ was added and ^{1}H NMR spectra were recorded (sample X2).

entry	Exp. No. SZ 5112	dimer [mg]	NBS [mg]	additive	yield **22a**	yield dimer **E**
1	A1	**D** 50.2	27.4	–	0%	28%
2	A2	**D** 50.2	27.4	tmeda	16%	28%
3	B1	**E** 56.2	29.3	–	0%	16%
4	B2	**E** 56.2	29.3	tmeda	11%	16%
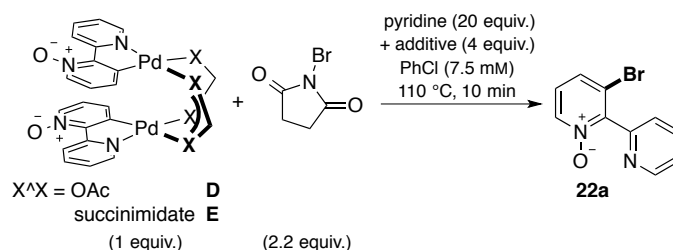
General procedure:

20-mL reaction vials were charged with dimers **D** or **E** (0.075 mmol), NBS (0.17 mmol), pyridine (120 μL, 1.50 mmol) and chlorobenzene (7.5 mM, based on palladium dimer). NBu$_4$OAc (22.9 mg, 0.075 mmol) was directly weighted out together with the palladium dimer and NBS. AcOH was added as stock solution in chlorobenzene (0.25 M, 1.20 mL, 0.30 mmol). The reaction vials were sealed with a Teflon-lined screw cap and placed in a pre-heated aluminum well-plate at 110 °C. After 10 min stirring at this temperature, the vials were cooled to room temperature, the reaction solutions/mixtures were transferred into round-bottom flasks and the solvent removed by rotary evaporation. The solid residues were additionally dried in high vacuum for several hours, before a stock solution of TCB in CDCl$_3$ (0.17 M, 0.25 mL, 0.042 mmol) was added. The mixtures were directly filtered through a short plug of Celite (pipette) and the filtrate transferred into NMR tubes and analyzed by ^{1}H NMR spectroscopy. Only isolated peaks were used integration. The average values of several integrals for each compound were used to calculate the yields.

entry	Exp. No. SZ 5119	dimer [mg]	NBS [mg]	additive	yield 22a	yield dimer E
1	C	**D** 50.5	31.1	–	66%	–
2	E	**D** 50.5	39.6	AcOH	71%	–
2	B	**E** 56.6	31.3	–	20%	46%
3	A	**E** 55.9	30.4	AcOH	51%	–
4	D	**E** 56.4	34.3	NBu$_4$OAc	81%	–

4.12 Synthesis of C3-substituted Caerulomycines

3-Methoxy-2,2′-bipyridine *N*-oxide (41a)

[FW 2051/SZ 5138]
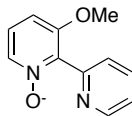
In an oven-dried, argon-filled Schlenk flask was charged with chlorobipyridine *N*-oxide **21a** (1.65 g, 7.98 mmol), dry MeOH (20.0 mL) and a solution of NaOMe in MeOH (≈ 2.9 M, 3.30 mL, 9.57 mmol). After the reaction solution has been stirred at 85 °C for 24 h, water was added and the resulting mixture exhaustively extracted with DCM. The combined organic layers were dried with Na_2SO_4, filtered and he solvent removed from the filtrate. The residue was purified by column chromatography (MeOH in DCM mixtures: 0–10%, 1% increments) providing **41a** (1.38 g, 6.80 mmol, 85%) as pale tan solid.

^{1}H NMR (500 MHz, CDCl$_3$): δ 8.76 (d, *J* = 4.2 Hz, 1H), 8.00 (dd, *J* = 6.5, 0.7 Hz, 1H), 7.82 (td, *J* = 7.7, 1.8 Hz, 1H), 7.52 (dd, *J* = 7.8, 1.0 Hz, 1H), 7.34 (ddd, *J* = 7.6, 4.9, 1.1 Hz, 1H), 7.22 (dd, *J* = 8.7, 6.5 Hz, 1H), 6.93 (d, *J* = 8.7 Hz, 1H), 3.77 (s, 3H) ppm.

^{13}C NMR (126 MHz, CDCl$_3$): δ 156.5, 150.0, 149.2, 139.7, 136.6, 133.2, 126.2, 124.7, 123.8, 109.0, 56.7 ppm.

IR (v/cm^{-1}): 3084 (w), 3063 (w), 2986 (w), 1601 (w), 1586 (w), 1558 (m), 1493 (w), 1461 (m), 1447 (w), 1420 (s), 1305 (w), 1285 (w), 1248 (m), 1222 (s), 1173 (w), 1153 (w), 1107 (w), 1078 (s), 1031 (m), 990 (w), 954 (w), 906 (w), 784 (s), 752 (w), 732 (m).

HRESI-MS (MeOH, +, *m/z*): [M+H]$^+$ 203.0810, calc. 203.0815

M.p.: 106 °C

3-Methoxy-4-nitro-2,2′-bipyridine *N*-oxide (42a)

[FW 2059C]
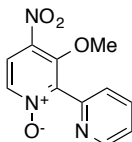
Bipyridine *N*-oxide **14a** (103 mg, 0.51 mmol) and KNO$_3$ (278 mg, 2.75 mmol) were dissolved in conc. H$_2$SO$_4$ (0.70 mL) at 0 °C. The reaction solution was stirred at 80 °C for 39 h, then cooled to room temperature and quenched with ice. The yellow solution was basified with NaOH (*w* = 25%) to pH = 12. The aqueous solution was extracted with DCM, the combined organic layers dried with Na$_2$SO$_4$, filtered and the solvent removed from the filtrate. Initially attempted column chromatography (MeOH

in DCM: 0–5%, 1% increments) failed and provided only product mixtures. The fractions were combined, and preparative TLC (acetone/hexane 1:1) provided pure **42a** (31.1 mg, 0.13 mmol, 25%), its isomer **42a′** (29.9 mg, 0.12 mmol, 24%), and the deoxygenated product **44a** (14.5 mg, 0.06 mmol, 12%), and starting material **42a** (9.8 mg, 0.05 mmol, 10%).

^{1}H NMR (500 MHz, CDCl_3): δ 8.82 (ddd, J = 4.9, 1.8, 1.0 Hz, 1H), 8.16 (d, J = 7.3 Hz, 1H), 7.93 (d, J = 7.3 Hz, 1H), 7.90 (td, J = 7.8, 1.8 Hz, 1H), 7.55 (dt, J = 7.9, 1.1 Hz, 1H), 7.45 (ddd, J = 7.7, 4.9, 1.2 Hz, 1H), 3.73 (s, 3H) ppm.

HRESI-MS (MeOH, +, m/z): [M+H]+ 248.0675, calc. 248.0666, [M+Na]+ 270.0499, calc. 270.0485, [M+K]+ 286.0092, calc. 286.0225.

3-methoxy-6-nitro-2,2′-bipyridine *N*-oxide (**42a′**)
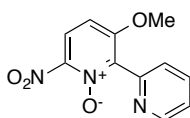
^{1}H NMR (500 MHz, CDCl_3): δ 8.80 (dt, J = 4.9, 1.3 Hz, 1H), 8.36 (d, J = 8.9 Hz, 1H), 7.92 (d, J = 7.9 Hz, 1H), 7.87 (td, J = 7.7, 1.7 Hz, 1H), 7.55 (d, J = 8.9 Hz, 1H), 7.40 (ddd, J = 7.4, 4.9, 1.3 Hz, 1H), 4.03 (s, 3H) ppm.

HRESI-MS (MeOH, +, m/z): [M+H]+ 232.0742, calc. 232.0717, [M+Na]+ 254.0563, calc. 254.0536 [M+K]+ 270.0294, calc. 270.0275.

3-methoxy-4-nitro-2,2′-bipyridine (**44a**)
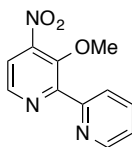
^{1}H NMR (500 MHz, CDCl_3): δ 8.79 (ddd, J = 4.9, 1.7, 0.9 Hz, 1H), 7.87 (td, J = 7.7, 1.7 Hz, 1H), 7.80 (d, J = 9.3 Hz, 1H), 7.56 (dt, J = 7.8, 1.1 Hz, 1H), 7.41 (ddd, J = 7.7, 4.9, 1.2 Hz, 1H), 7.02 (d, J = 9.3 Hz, 1H), 3.89 (s, 3H) ppm.

HRESI-MS (MeOH, +, m/z): [M+H]+ 248.0670, calc. 248.0666, [M+Na]+ 270.0495, calc. 270.0485, [M+K]+ 286.0224, calc. 286.0225.

3-Methoxy-6-methoxycarbonyl-2,2′-bipyridine *N*-oxide (41c)

[SZ 5080]
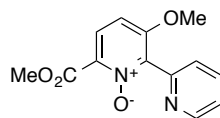
An oven-dried Schlenk flask was charged with bipyridine *N*-oxide **21c** (275 mg, 0.99 mmol) and set under argon atmosphere. Then, MeOH (10.0 mL) and a solution of NaOMe in MeOH (1.9 M, 2.50 mL, 4.75 mmol) was added. After stirring at 60 °C for 6 h, the reaction was allowed to cool to room temperature, the flask was opened to air and H_2SO_4 (1.00 mL, 18.8 mmol) was added. After additional stirring at room temperature for 2 d, the solvent was removed and the residue dissolved in DCM and basified with sat. Na_2CO_3. The aqueous layer was extracted with DCM, the combined organic layers dried with Na_2SO_4, filtered and the solvent removed from the filtrate. The crude product was purified by column chromatography (SiO_2, acetone in hexane mixtures: 20%, 50%, then pure acetone) providing **41c** (78.9 mg, 0.30 mmol, 31%) as colorless solid, and starting material **21c** (25.9 mg, 0.10 mmol, 10%) as methyl ester as pale orange oil.

^{1}H NMR (400 MHz, CDCl$_3$): δ 8.73 (d, J = 4.9 Hz, 1H), 7.79 (td, J = 7.8, 1.7 Hz, 1H), 7.69 (d, J = 9.0 Hz, 1H), 7.50 (d, J = 7.8 Hz, 1H), 7.32 (dd, J = 7.6, 4.9 Hz, 1H), 6.95 (d, J = 9.1 Hz, 1H), 3.91 (s, 3H), 3.80 (s, 3H) ppm.

^{13}C NMR (101 MHz, CDCl$_3$): δ 162.3, 157.8, 149.9, 148.7, 140.6, 136.4, 135.1, 127.1, 126.3, 123.8, 108.2, 56.8, 53.0 ppm.

HRESI-MS (MeOH, +, *m/z*): [M+H]$^+$ 261.0869, calc. 261.0870, [M+Na]$^+$ 283.0717, calc. 283.0683

IR (v/cm^{-1}): 3031 (w), 2951 (w), 1733 (s), 1584 (w), 1558 (m), 1496 (m), 1461 (m), 1427 (m), 1365 (m), 1265 (m), 1330 (w), 1291 (m), 1257 (s), 1240 (s), 1222 (s), 1190 (w), 1146 (m), 1099 (m), 1072 (s), 1044 (w), 983 (m), 947 (w), 851 (w), 812 (m), 776 (s), 755 (m), 736 (m), 717 (m).

M.p.: 105–109 °C

3-Chloro-6-methoxycarbonyl-2,2′-bipyridine *N*-oxide
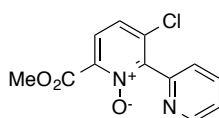
^{1}H NMR (400 MHz, CDCl$_3$): δ 8.77 (d, J = 4.3 Hz, 1H), 7.85 (td, J = 7.7, 1.7 Hz, 1H), 7.59 (d, J = 8.6 Hz, 1H), 7.53 (d, J = 7.8 Hz, 1H), 7.41 (d, J = 8.7 Hz, 1H), 7.40–7.36 (m, 1H), 3.95 (s, 3H) ppm.

^{13}C NMR (101 MHz, CDCl$_3$): δ 161.8, 150.3, 149.2, 148.8, 140.9, 136.8, 135.4, 126.0, 125.8, 124.5, 53.4 ppm.

HRESI-MS (MeOH, +, *m/z*): [M+H]$^+$ 265.0399, calc. 265.0374, [M+Na]$^+$ 287.0226, calc. 287.0194

IR (v/cm^{-1}): 3064 (w), 2954 (w), 2851 (w), 1742 (s), 1583 (w), 1544 (w), 1458 (w), 1429 (m), 1358 (s), 1323 (m), 1252 (s), 1204 (m), 1160 (m), 1134 (w), 1100 (w), 1085 (w), 993 (w), 935 (s), 821 (w), 781 (m), 748 (w).

3-Methoxy-6-methyl-2,2′-bipyridine *N*-oxide (41b)

[SZ 5108/SZ 5145]
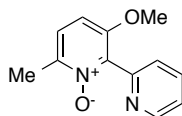
Test scale:

An oven-dried and argon-purged Schlenk flask was charged with 3-bromobiypridine *N*-oxide **22b** (241 mg, 0.91 mmol), CuBr (23.0 mg, 0.16 mmol), a solution of NaOMe in MeOH ($\approx$ 4.8 M, 2.00 mL, 9.6 mmol), prepared by dissolution of sodium (2.45 g, 107 mmol) in MeOH (22.0 mL), and EtOAc (60 μL, 0.61 mmol). The mixture was stirred at 100 °C for 3 h, quenched with water and extracted with DCM. The combined organic layers were dried with Na$_2$SO$_4$, the desiccant filtered and the filtrates concentrated in vacuum. The crude product was purified by column chromatography (MeOH in DCM mixtures: 2–4%, 1% increments) providing **41b** (140 mg, 0.65 mmol, 71%) as orange oil.

Large scale:

Following the same procedure, a mixture of 3-bromobiypridine *N*-oxide **22b** (2.05 g, 7.73 mmol), CuBr (215 mg, 1.5 mmol), NaOMe solution ($\approx$ 5.0 M, 16.0 mL, 80.0 mmol), and EtOAc (0.90 mL, 9.16 mmol) was stirred at 100 °C for 2 h providing **41b** (1.06 g, 4.91 mmol, 63%).

^{1}H NMR (400 MHz, CDCl$_3$): δ 8.76 (ddd, J = 4.9, 1.7, 0.9 Hz, 1H, ArH-3′), 7.80 (td, J = 7.7, 1.8 Hz, 1H, ArH-5′), 7.48 (dt, J = 7.8, 1.0 Hz, 1H, ArH-6′), 7.32 (ddd, J = 7.6, 4.9, 1.2 Hz, 1H, ArH-4′), 7.22 (d, J = 8.8 Hz, 1H, ArH-5), 6.90 (d, J = 8.8 Hz, 1H, ArH-4), 3.75 (s, 3H, -OCH$_3$), 2.46 (s, 3H, -CH$_3$) ppm.

^{13}C NMR (126 MHz, CDCl$_3$): δ 154.5, 150.2, 150.0, 142.3, 139.6, 136.5, 126.1, 124.8, 123.6, 109.2, 56.5, 17.3 ppm.

IR (v/cm^{-1}): 3048 (w), 2923 (w), 2844 (w), 1615 (w), 1588 (w), 1566 (m), 1500 (m), 1465 (m), 1450 (m), 1427 (m), 1361 (m), 1292 (m), 1257 (m), 1215 (m), 1173 (m), 1126 (m), 1075 (s), 1047 (m), 991 (w), 874 (w), 782 (m), 747 (m), 727 (m).

HRESI-MS (MeOH, +, *m/z*): [M+H]$^+$ 217.1049, calc. 217.0972, [M+Na]$^+$ 239.0879, calc. 239.0791

3-Methoxy-4-nitro-6-methyl-2,2′-bipyridine *N*-oxide (42b)

[SZ 5110/SZ 5146]
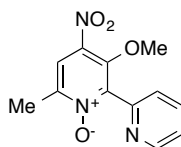
Test scale:

A mixture of bipyridine *N*-oxide **41b** (128 mg, 0.59 mmol), KNO$_3$ (1.21 g, 12.0 mmol) and H$_2$SO$_4$ (4.00 mL) was stirred at 80 °C for 19 h. After cooling to room temperature, ice was added and the resulting solution basified with an aqueous sat. Na$_2$CO$_3$. The solution was exhaustively extracted with DCM, the combined organic layers dried with Na$_2$SO$_4$, the desiccant filtered and the solvent removed from the filtrate. The crude product was purified by column chromatography (SiO$_2$, MeOH in DCM mixtures: 0–2%, 1% increments) providing the product **42b** (39.6 mg, 0.15 mmol, 26%) and alcohol **45** (21.3 mg, 0.08 mmol, 13%) as yellow solids.

Large scale:

Following the same procedure, a mixture of bipyridine *N*-oxide **41b** (792 mg, 4.90 mmol), conc. HNO$_3$ (1.30 mL, 31.2 mmol) and H$_2$SO$_4$ (2.80 mL) was stirred at 80 °C for 2 h providing **42b** (550 mg, 2.10 mmol, 43%) besides starting material (114 mg, 0.53 mmol, 11%).

^{1}H NMR (400 MHz, CDCl$_3$): δ 8.80 (d, *J* = 4.4 Hz, 1H), 7.94 (s, 1H), 7.87 (td, *J* = 7.8, 1.7 Hz, 1H), 7.49 (d, *J* = 7.8 Hz, 1H), 7.47–7.37 (m, 1H), 3.67 (s, 2H), 2.50 (s, 1H) ppm.

^{13}C NMR (126 MHz, CDCl$_3$): δ 150.3, 149.0, 148.4, 146.7, 146.6, 138.2, 136.9, 125.9, 124.5, 120.5, 63.7, 17.6 ppm.

IR (*v*/cm^{-1}): 3035 (w), 2923 (w), 2848 (w), 1608 (w), 1588 (w), 1566 (m), 1520 (s), 1486 (w), 1461 (m), 1418 (m) 1344 (s), 1296 (s), 1238 (s), 1194 (m), 1154 (w), 1097 (s), 1042 (m), 1009 (w), 976 (s), 917 (w), 791 (m), 774 (m), 749 (s), 715 (m).

HRESI-MS (MeOH, +, *m/z*): [M+H]$^+$ 262.0861, calc. 262.0822, [M+Na]$^+$ 284.0682, calc. 284.0642

M.p.: 126–128 °C

3-Methoxy-4-nitro-6-hydroxymethyl-2,2′-bipyridine *N*-oxide (45)
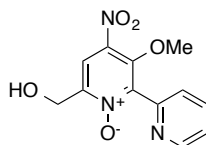
^{1}H NMR (500 MHz, CDCl$_3$): δ 8.83 (ddd, *J* = 4.8, 1.7, 1.1 Hz, 1H), 8.04 (s, 1H), 7.94 (td, *J* = 7.8, 1.8 Hz, 1H), 7.50 (m, 2H), 4.73 (s, 2H), 3.73 (s, 3H) ppm.

^{13}C NMR (126 MHz, CDCl$_3$): δ 150.2, 149.6, 149.1, 147.6, 146.3, 139.2, 137.6, 126.3, 125.0, 118.5, 63.8, 59.7 ppm.

IR (v/cm^{-1}): 3098 (w), 3063 (w), 2923 (w), 2851 (w), 1612 (w), 1596 (w), 1568 (m), 1524 (m), 1468 (w), 1419 (w), 1364 (w), 1331 (s), 1298 (s), 1283 (s), 1212 (m), 1154 (w), 1145 (w), 1084 (s), 1066 (m), 1003 (m), 969 (m), 907 (w), 894 (w), 871 (w), 793 (m), 776 (w), 754 (m), 726 (w), 695 (w), 668 (w).

HRESI-MS (MeOH, +, m/z): [M+H]$^+$ 278.0796, calc. 278.0771, [M+Na]$^+$ 300.0619, calc. 300.0591

M.p.: 128–131 °C

3,4-Dimethoxy-6-methyl-2,2′-bipyridine *N*-oxide (43b)

[SZ 5116/ SZ 5147]
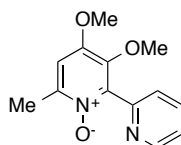
Test scale:

An oven-dried and argon-purged Schlenk flask was charged with bipyridine *N*-oxide **42b** (39.6 mg, 0.15 mmol), MeOH (1.50 mL) and a solution of NaOMe in MeOH ($c \approx 4.8$ M, 40 μL, 0.18 mmol). The reaction solution was stirred at 85 °C for 1 h, the quenched with water and extracted with DCM. The combined organic layers were dried with Na$_2$SO$_4$, the desiccant filtered and the solvent removed from the filtrate. The crude product was purified by column chromatography (SiO$_2$, 5% MeOH in DCM) providing the product **43b** (32.9 mg, 0.13 mmol, 88%) as colorless solid.

Large scale:

Following the same procedure, a solution of bipyridine *N*-oxide **42b** (405 mg, 1.55 mmol), MeOH (12.0 mL), and a solution of NaOMe in MeOH (≈ 2.8 M, 0.66 mL, 1.85 mmol) was stirred at 85 °C for 1h providing **43b** (381 mg, 1.55 mmol, quant.).

^{1}H NMR (500 MHz, CDCl$_3$): δ 8.73 (d, J = 4.2 Hz, 1H, ArH-3′), 7.78 (td, J = 7.7, 1.8 Hz, 1H, ArH-5′), 7.50 (d, J = 7.8 Hz, 1H, ArH-6′), 7.31 (ddd, J = 7.6, 4.9, 1.1 Hz, 1H, ArH-4′), 6.81 (s, 1H, ArH-5), 3.91 (s, 3H, -pOCH$_3$), 3.67 (s, 3H, -mOCH$_3$), 2.49 (s, 3H, -CH$_3$) ppm.

^{13}C NMR (126 MHz, CDCl$_3$): δ 151.6 (C-4), 150.1 (C-2′), 149.8 (C-3′), 145.5 (C-6), 144.5 (C-2), 144.1 (C-3), 136.2 (C-5′), 125.9 (C-6′), 123.5 (C-4′), 108.6 (C-5), 61.7 (-mOCH$_3$), 56.3 (-pOCH$_3$), 18.2 (-CH$_3$) ppm.

IR (v/cm^{-1}): 2925 (w), 1615 (w), 1588 (m), 1566 (w), 1497 (m), 1481 (m), 1466 (m), 1447 (w), 1434 (w), 1421 (w), 1397 (m), 1379 (m), 1351 (w), 1284 (w),1219 (m), 1200 (m), 1172 (w), 1156 (w), 1125 (s), 1092 (w), 1125 (s), 1032 (s), 985 (s), 903 (m), 886 (w), 861 (m), 788 m), 758 (m), 743 (m), 719 (w), 675 (m).

HRESI-MS (MeOH, +, m/z): [M+H]$^+$ 247.1088, calc. 247.1077, [M+Na]$^+$ 269.0906, calc. 269.0897, [M+K]$^+$ 285.0643, calc. 285.0636

M.p.: 130–132 °C

3,4-Dimethoxy-6-(hydroxymethyl)-2,2′-bipyridine (40), Caerulomycin G

[SZ 5134/ SZ 5149]
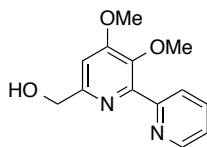
Test scale:

Bipyridine N-oxide **43b** (32.2 mg, 0.13 mmol) was dissolved in Ac$_2$O (0.60 mL) and the solution stirred at 110 °C for 2h. The volatiles were removed providing 3,4-dimethoxy-6-(acetoxymethyl)-2,2′-bipyridine as orange oil, which was converted without further purification. A solution of 3,4-dimethoxy-6-(acetoxymethyl)-2,2′-bipyridine in MeOH (2.00 mL) and a few drops of H$_2$SO$_4$ was refluxed for 15 h. The volatiles were removed, the residue diluted with DCM, and neutralized with an aqueous sat. NaHCO$_3$. The aqueous layer was extracted with DCM, the organic layers combined, dried with Na$_2$SO$_4$ and the desiccant filtered. The filtrate was concentrated in vacuum and the residue subjected to column chromatography (10% MeOH in DCM), which provided **40** (24.9 mg, 0.10 mmol, 77%) as colorless solid.

Large scale:

Following the same procedure, a solution of bipyridine **43b** (381 mg, 1.55 mmol) in Ac$_2$O (7.00 mL) was stirred at 110 °C for 1.5 h providing 3,4-dimethoxy-6-(acetoxymethyl)-2,2′-bipyridine, which was further converted in a solution of MeOH (7.00 mL) and H$_2$SO$_4$ (1.00 mL) at reflux for 21 h. Work-up provided **40** (365 mg, 1.48 mmol, 96%).

^{1}H NMR (500 MHz, CDCl$_3$): δ 8.70 (ddd, J = 4.9, 1.7, 1.0 Hz, 1H, ArH-3′), 7.79–7.73 (m, 2H, ArH-5′, ArH-6′), 7.27 (ddd, J = 7.0, 5.0, 1.9 Hz, 1H, ArH-4′), 6.95 (s, 1H, ArH-5), 4.82 (br s, 1H, OH), 4.71 (s, 2H, -CH$_2$-), 3.89 (s, 3H, -pOCH$_3$), 3.69 (s, 3H, -mOCH$_3$) ppm.

^{13}C NMR (126 MHz, CDCl$_3$): δ 160.1 (C-4), 157.3 (C-6), 155.5 (C-2′), 149.6 (C-2), 149.5 (C-3′), 143.1 (C-3), 136.4 (C-5′), 124.8 (C-6′), 123.1 (C-4′), 104.2 (C-5), 64.7 (C-OH), 61.4 (-mOCH$_3$), 56.0 (-pOCH$_3$) ppm.

IR (v/cm^{-1}): 3266 (br m), 2918 (m), 2849 (w), 1580 (m), 1563 (m), 1468 (m), 1419 (m) 1394 (m), 1364 (m), 1329 (w), 1243 (s), 1191 (m), 1154 (m), 1055 (s), 1039 (s), 992 (s), 951 (w), 863 (m), 804 (m), 786 (m), 753 (m), 687 (s).

HRESI-MS (MeOH, +, m/z): [M+H]$^+$ 247.1100, calc. 247.1077, [M+Na]$^+$ 269.0919, calc. 269.0897

Elemental analysis (%): C 63.6, H 5.98, N 11.4 calc. C 63.4, H 5.73, N 11.4

M.p.: 111–113 °C (lit. 127 °C)[97a]

3,4-Dimethoxy-6-acetoxymethyl-2,2′-bipyridine
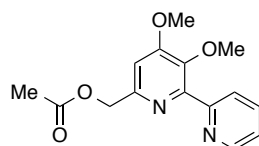
^{1}H NMR (400 MHz, CDCl$_3$): δ 8.76 (d, J = 5.1 Hz, 1H), 7.82–7.71 (m, 2H), 7.29 (ddd, J = 6.8, 4.8, 2.0 Hz, 1H), 6.97 (s, 1H), 5.21 (s, 2H), 3.95 (s, 3H), 3.69 (s, 3H), 2.13 (s, 13H) ppm

^{13}C NMR (101 MHz, CDCl$_3$): δ 170.7, 160.0, 155.3, 152.3, 150.7, 149.5, 143.8, 136.4, 124.8, 123.1, 106.2, 67.3, 61.4, 56.0, 21.1 ppm.

3,4-Dimethoxy-2,2′-bipyridine-6-carboxaldehyde (46)

[SZ 5148/SZ 5152]
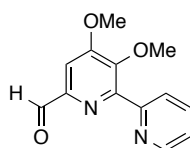
Test scale:

A mixture of bipyridine **40** (24.9 mg, 0.10 mmol) and MnO$_2$ (88.5 mg, 1.02 mmol) in CHCl$_3$ (0.20 mL) was stirred at room temperature for 3 h. The reaction mixture was filtered through Celite, the filtrate concentrated and the residue directly subjected to column chromatography (1% MeOH in DCM) providing **46** (12.5 mg, 0.05 mmol, 51%) as colorless solid.

Large scale:

Following the same procedure, bipyridine **40** (280 mg, 1.14 mmol) and MnO$_2$ (978 mg, 11.2 mmol) in CHCl$_3$ was stirred at room temperature for 13 h providing **46** (162 mg, 0.66 mmol, 58%).

^{1}H NMR (400 MHz, CDCl$_3$): δ 10.03 (s, 1H), 8.78 (ddd, J = 4.9, 1.8, 1.0 Hz, 1H), 7.85–7.74 (m, 2H), 7.57 (s, 1H), 7.32 (ddd, J = 7.3, 4.8, 1.6 Hz, 1H), 3.99 (s, 3H), 3.81 (s, 3H) ppm.

The chemical shifts are in agreement with previous reports.[98d]

^{13}C NMR (126 MHz, CDCl$_3$): δ 192.9 160.1, 154.9, 151.6, 149.8, 149.4, 147.8, 136.5, 124.8, 123.4, 105.1, 61.5, 56.4 ppm.

Elemental analysis (%): C 64.0, H 5.10, N 11.5 calc. C 63.9, H 4.95, N 11.5

3,4-Dimethoxy-2,2′-bipyridine-6-carboxaldehyde *O*-methyloxime (38), Caerulomycin C

[SZ 5154]
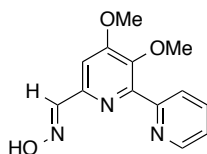
A solution of bipyridine **46** (82.6 mg, 0.34 mmol), NH$_2$OH·HCl (117 mg, 1.67 mmol), and pyridine (0.14 mL, 1.73 mmol) in EtOH (5.50 mL) was refluxed under stirring for 1 h. The reaction solution was concentrated, diluted with few water (1.00 mL) and extracted with EtOAc. The combined organic layers were dried with Na$_2$SO$_4$, filtered and the solvent removed from the filtrate. The solid residue was washed with Et$_2$O and dried in vacuum providing **38** (77.6 mg, 0.30 mmol, 89%) as colorless solid.

^{1}H NMR (500 MHz, DMSO-d_6): δ 11.64 (s, 1H, NOH), 8.69 (d, J = 4.7 Hz, 1H, ArH-6′), 8.04 (s, 1H, HC=N), 7.96 (td, J = 7.7, 1.7 Hz, 1H, ArH-4′), 7.75 (d, J = 7.9 Hz, 1H, ArH-3′), 7.50–7.46 (m, 2H, ArH-5, ArH-5′), 3.98 (s, 3H, -*p*OCH$_3$), 3.76 (s, 3H-*m*OCH$_3$) ppm.

^{13}C NMR (126 MHz, CDCl$_3$): δ 159.5 (C-4), 155.2 (C-2′), 150.1 (C-2), 148.4 (C-6′), 148.3 (C-7), 148.2 (C-6), 144.0 (C-3), 137.2 (C-4′), 124.2 (C-3′), 123.5 (C-5′), 103.7 (C-5), 61.0 (-*m*OCH$_3$), 56.1 (-*p*OCH$_3$) ppm.

The chemical shifts are in agreement with previously reported values.[168]

IR (v/cm^{-1}): 3328 (w), 3151 (w), 3048 (w), 2983 (w), 2833 (w), 1584 (m), 1563 (m), 1522 (w), 1490 (m), 1459 (m), 1420 (m), 1393 (m), 1361 (m), 1243 (m), 1199 (m), 1149 (w), 1103 (w), 1059 (s), 988 (s), 949 (m), 847 (m), 796 (m), 752 (m), 707 (m), 673 (m).

HRESI-MS (MeOH, +, m/z): [M+H]$^+$ 260.1038, calc. 260.1030, [M+Na]$^+$ 282.0869, calc. 282.0849

Elemental analysis (%): C 58.9, H 5.15, N 15.5 calc. C 60.2, H 5.05, N 16.2

A better elemental analysis could not be obtained.

M.p.: 180 °C (lit. 208–210 °C)[168]

3,4-Dimethoxy-6-cyano-2,2′-bipyridine (39), Caerulomycinonitrile C

[SZ 5156]
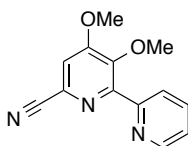
To a mixture of bipyridine **46** (30.4 mg, 0.12 mmol) and NaN$_3$ (15.2 mg, 0.23 mmol) in CH$_3$CN (0.30 mL) TfOH (100 μL, 1.13 mmol) was added dropwise. After stirring at room temperature for 30 min, the reaction solution was quenched with aqueous sat. Na$_2$CO$_3$. The mixture was extracted with DCM, the combined organic layers dried with Na$_2$SO$_4$, filtered and the volatiles removed from the

filtrate. The residue was directly subjected to column chromatography (1% MeOH in DCM) providing **39** (18.4 mg, 0.08 mmol, 62%) as colorless solid.

^{1}H NMR (500 MHz, CDCl$_3$): δ 8.76 (d, J = 4.5 Hz, 1H, ArH-3′), 7.83–7.76 (m, 2H, ArH-5′, ArH-6′), 7.35 (ddt, J = 6.2, 4.9, 1.5 Hz, 1H, ArH-4′), 7.29 (s, 1H, ArH-5), 4.00 (s, 3H, -mOCH$_3$), 3.84 (s, 3H, -pOCH$_3$) ppm.

^{13}C NMR (126 MHz, CDCl$_3$): δ 159.8 (C-3), 154.4 (C-2′), 153.0 (C-2), 149.5 (C-3′), 147.1 (C-4), 136.7 (C-5′), 129.3 (C-6), 124.8 (C-6′), 123.8 (C-4′), 117.2 (CN), 112.8 (C-5), 61.8 (-pOCH$_3$), 56.6 (-mOCH$_3$) ppm.

IR (v/cm^{-1}): 3072 (w), 3006 (w), 2949 (w), 2848 (w), 2231 (w), 1568 (m), 1477 (m), 1435 (w), 1415 (m), 1388 (w), 1350 (m), 1258 (m), 1203 (w), 1148 (w), 1044 (s), 994 (s), 944 (w), 858 (m), 807 (m), 781 (w), 739 (s), 675 (m), 665 (m).

HRESI-MS (MeOH, +, m/z): [M+H]$^+$ 242.0931, calc. 242.0924, [M+Na]$^+$ 264.0752, calc. 264.0743

Elemental analysis (%): C 64.8, H 4.69, N 17.5 calc. C 64.7, H 4.60, N 17.4

M.p.: 106–108 °C (lit. 114–116 °C)[168]

4.13 Investigations of direct arylations of pyridine *N*-oxides

4.13.1 Kinetic measurements by ReactIR and isolations of products and side products

General procedure:

In an argon-filled glovebox, pyridine *N*-oxide **27** (4.00 mmol), K$_3$PO$_4$ (4.00 mmol), dimer **A** (0.05 mmol) were weighted in a 10-mL-Schlenk tube and toluene (4.00 mL) was added. The flask was brought outside the glovebox and under a counter flow of argon, the aryl halide **28** or **47** (2.00 mmol) was syringed to the mixture and the IR probe was inserted into the reaction mixture. After placing the flask in a stirred oil bath at 120 °C, the recording of the IR spectra was immediately started. Upon the conversion stopped as judged by monitoring characteristic IR bands, the reaction mixture was cooled to room temperature and subjected to a silica gel filled column.
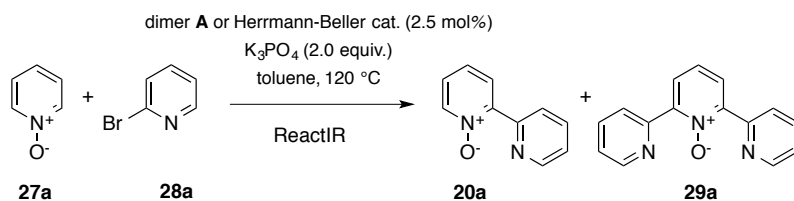
[SZ 1087b]

According to the general procedure, pyridine *N*-oxide **27a** (381 mg, 4.00 mmol), K$_3$PO$_4$ (850 mg, 4.00 mmol), dimer **A** (36.8 mg, 0.05 mmol) and bromopyridine **28a** (0.19 mL, 2.00 mmol). Purification by column chromatography (MeOH in DCM: 0%–10%, 1% increments per 100 mL) gave bipyridine *N*-oxide **20a** (150 mg, 0.87 mmol, 44%) as the major product, complex **F**(Br) (35 mg, 0.06 mmol) as colorless solid and pyridine *N*-oxide **27a** (180 mg, 1.90 mmol, recov. 69%).
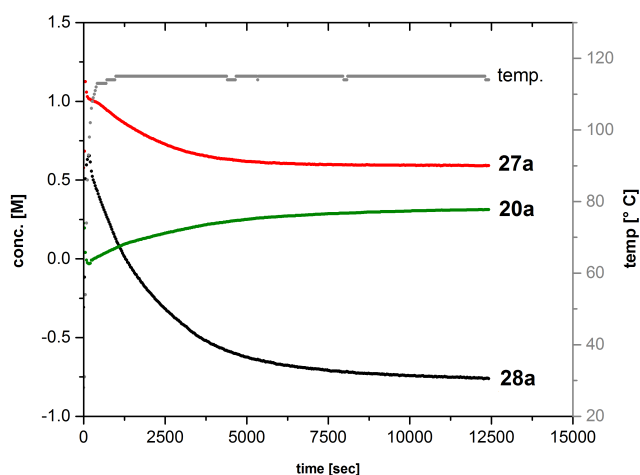
	k_{obs} [mM/min]	R^2
SZ 1087b		
27a	−4.55 ± 0.07	0.986
28a	−11.5 ± 0.2	0.993
20a	+2.81 ± 0.02	0.997

[SZ 2010a]

According to the general procedure, pyridine *N*-oxide **27a** (380 mg, 4.00 mmol), K₃PO₄ (849 mg, 4.00 mmol), Herrmann-Beller catalyst (46.8 mg, 0.05 mmol) and bromopyridine **28a** (0.19 mL, 2.00 mmol).
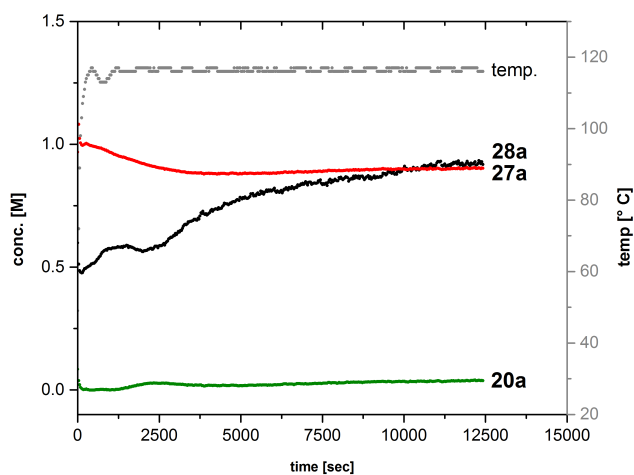

	k_{obs} [mM/min]	R^2
SZ 2010a		
27a	−1.56 ± 0.04	0.972
28a	+4.8 ± 0.2	0.931
20a	−0.13 ± 0.04	0.133

2,2′-Bipyridine *N*-oxide (**20a**)
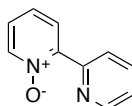
^{1}H NMR (400 MHz, CDCl₃): δ 8.79 (d, *J* = 8.1 Hz, 1H), 8.63 (dd, *J* = 4.8, 0.8 Hz, 1H), 8.23 (dd, *J* = 6.5, 0.7 Hz, 1H), 8.08 (dd, *J* = 8.0, 2.1 Hz, 1H), 7.74 (td, *J* = 7.8, 1.8 Hz, 1H), 7.31–7.23 (m, 2H), 7.18 (td, *J* = 7.5, 7.0, 2.2 Hz, 1H) ppm.

The chemical shifts are in agreement with previous reported values.[117]

[(Bipy)Pd(X)(^{t}Bu$_2$P(CH$_3$)(CH$_2$)], complex **F**(X)
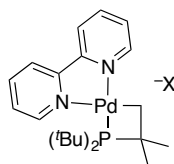
^{1}H NMR (400 MHz, CDCl$_3$): δ 8.98 (d, J = 8.1 Hz, 2H), 8.28 (t, J = 7.9 Hz, 2H), 7.66 (m, 2H), 1.59 (d, J = 13.9 Hz, 18H), 1.57 (d, J = 13.6 Hz, 6H), 1.29 (d, J = 3.5 Hz, 2H) ppm.

^{31}P NMR (162 MHz, CDCl$_3$, r.t.): δ = –12.60 ppm.

^{1}H NMR (500 MHz, CDCl$_3$, –45 °C): δ 8.82 (t, J = 7.2 Hz, 2H), 8.53 (d, J = 5.2 Hz, 1H), 8.23 (d, J = 4.7 Hz, 1H), 8.19 (q, J = 7.7 Hz, 2H), 7.62 (t, J = 6.5 Hz, 1H), 7.58 (t, J = 6.4 Hz, 1H), 1.54–1.44 (m, 24 H), 1.18 (d, J = 3.7 Hz, 2H) ppm.

^{13}C NMR (126 MHz, CDCl$_3$, –45 °C): δ 154.85, 153.67, 151.35, 147.49, 140.85, 140.39, 127.24, 126.84, 124.42, 124.29, 48.60, 48.42, 37.08, 37.00, 30.92 ppm.

IR (v_{max}/cm^{-1}): 3065 (w), 3041 (w), 3025 (w), 2991 (w), 2960 (w), 2901 (w), 2864 (w), 1601 (m), 1560 (w), 1539 (w), 1492 (w), 1473 (m), 1142 (m), 1421 (w), 1390 (w), 1380 (w), 1365 (w), 1315 (m), 1250 (w), 1225 (w), 1172 (m), 1154 (m), 1104 (w), 1067 (w), 1020 (m), 971 (w), 930 (w), 912 (w), 812 (w), 778 (s), 735 (m), 719 (w).

HRESI-MS (+, m/z): [(Bipy)Pd(^{t}Bu$_2$P(CH$_3$)(CH$_2$)]$^+$ 463.1462, calc. 463.1494.

Elemental analysis (%): C 48.7 H 6.63 N 5.21 calc. C 48.6 H 6.30 N 5.15

M.p.: 184 °C (decomp.)

Independent synthesis of complexes **F** (Br):

[SZ 2030a/SZ 2169a]

X = Br: A NMR tube was loaded with dimer **B** (40.2 mg, 0.10 mmol), bipyridine **24a** (16.2 mg, 0.10 mmol) and CDCl$_3$ (0.60 mL). The reaction solution was allowed to stand at room temperature for 16 h before being measured by NMR. Removal of solvent provided complex **F** (Br).

[FW 1006/FW 1036]

X = BF$_4$: Dimer **B** (28.8 mg, 0.04 mmol), bipyridine **24a** (11.7 mg, 0.08 mmol) and AgOTf (19.2 mg, 0.08 mmol) were mixed in DCM (1.00 mL) and stirred for 1 h at room temperature. After filtration over Celite, the solvent was removed from the filtrate providing the complex **F** (BF$_4$) (46.2 mg, 0.08 mmol, quant.) as colorless solid. Crystals suitable for X-ray diffraction were grown by slow diffusion of Et$_2$O into a solution of **F** (BF$_4$) in DCM.

^{1}H NMR (500 MHz, CDCl$_3$, –30 °C): δ 8.64 (d, J = 5.3 Hz, 1H), 8.57 (dd, J = 8.1, 2.3 Hz, 2H), 8.32 (d, J = 5.3 Hz, 1H), 8.25–8.19 (m, 2H), 7.65 (dt, J = 7.7, 4.1 Hz, 2H), 1.59 (d, J = 14.0 Hz, 18H), 1.57 (d, J = 14.0 Hz, 6H), 1.28 (d, J = 3.9 Hz, 2H) ppm.

^{13}C NMR (126 MHz, CDCl$_3$, –30 °C): δ 155.3, 154.1, 151.9, 147.9, 141.2, 140.7, 127.6, 127.1, 124.1, 124.0, 48.9 (d, J = 22.3 Hz), 37.4 (d, J = 9.7 Hz), 32.4, 31.3, 16.7, 16.4 ppm.

^{31}B NMR (128 MHz, CDCl$_3$): δ –1.70 (quin, J = 0.9 Hz) ppm.

^{19}F NMR (376 MHz, CDCl$_3$): δ –153.24 (1F), –153.3 (3F) ppm.

^{31}P NMR (162 MHz, CDCl$_3$): δ –12.56 ppm.

IR (ν_{max}/cm^{-1}): 2992 (w), 2963 (w), 2895 (w), 2359 (w), 2341 (w), 1598 (w), 1469 (w), 1442 (w), 1390 (w), 1378 (w), 1314 (w), 1249 (w), 1173 (w), 1053 (s), 1025 (m), 931 (w), 807 (w), 775 (s), 733(w).

HRESI-MS (+, m/z): [(Bipy)Pd(^{t}Bu$_2$P(CH$_3$)(CH$_2$)]$^+$ 463.1503, calc. 463.1494.

Elemental analysis (%): C C 45.21, H 5.48, N 4.43, calc. C 48.0, H 6.22, N 5.09

M.p.: 167 °C (decomp.)
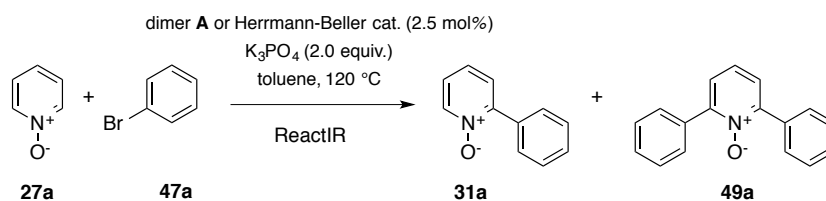
[SZ 2004a]

According to the general procedure, pyridine N-oxide **27a** (381 mg, 4.00 mmol), K$_3$PO$_4$ (850 mg, 4.00 mmol), dimer **A** (36.7 mg, 0.05 mmol) and bromobenzene **47a** (0.21 mL, 2.00 mmol). Purification by column chromatography (MeOH in DCM: 0%–10%, 1% increments per 100 mL) gave phenylpyridine N-oxide **31a** (244 mg, 1.42 mmol, 71%) as the major product, diphenylpyridine N-oxide **49a** (81 mg, 0.33 mmol, 33%) as the minor product and recovered pyridine N-oxide **27a** (203 mg, 2.14 mmol, 97%).
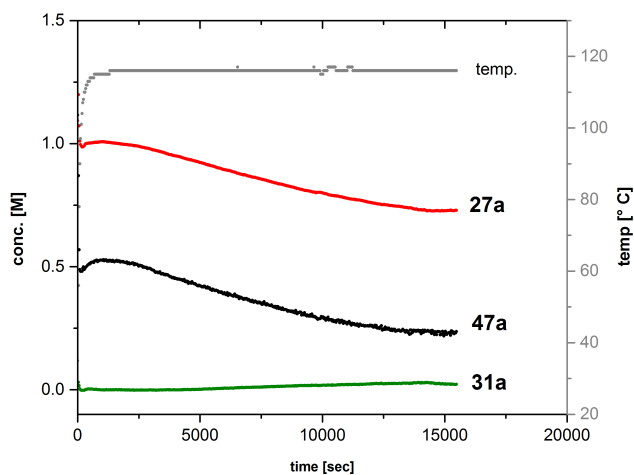
	k_{obs} [mM/min]	R^2
SZ 2004a		
27a	–1.26 ± 0.03	0.980
47a	–1.87 ± 0.05	0.970
31a	-0.004 ± 0.007	0.007

[SZ 2011a]

According to the general procedure, pyridine *N*-oxide **27a** (380 mg, 4.00 mmol), K_3PO_4 (849 mg, 4.00 mmol), Herrmann-Beller catalyst (47.0 mg, 0.05 mmol) and bromobenzene **47a** (0.21 mL, 2.00 mmol).
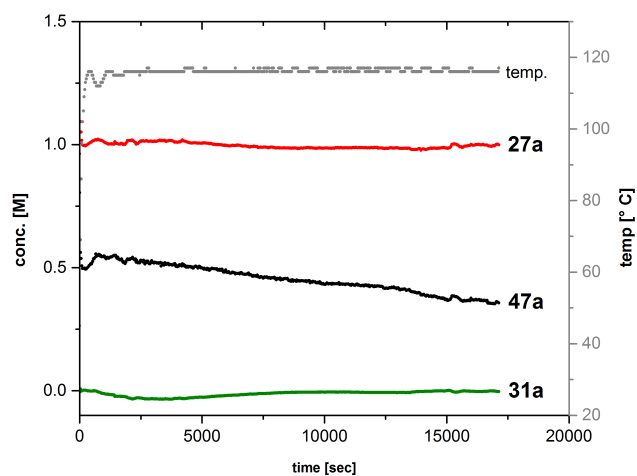
	k_{obs} [mM/min]	R^2
SZ 2011a		
27a	+0.24 ± 0.06	0.223
47a	−0.58 ± 0.09	0.446
31a	−0.23 ± 0.03	0.556

2-Phenylpyridine *N*-oxide (**31a**)
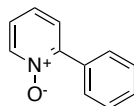
^{1}H NMR (400 MHz, CDCl$_3$): δ 8.33 (d, J = 6.5 Hz, 1H), 7.80 (dd, J = 8.0, 1.6 Hz, 2 H), 7.53–7.37 (m, 4 H), 7.30 (td, J = 7.7, 1.1 Hz, 1H), 7.22 (ddd, J = 7.6, 6.5, 2.1 Hz, 1H) ppm.

The chemical shifts are in agreement with previous reported values.[163a]

2,6-Diphenylpyridine *N*-oxide (**49a**)
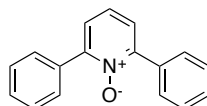
^{1}H NMR (400 MHz, CDCl$_3$): δ 7.85 (d, J = 8.1 Hz, 4H), 7.52–7.38 (m, 8H), 7.38–7.30 (m, 1H) ppm.

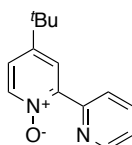The chemical shifts are in agreement with previous reported values.[163a]
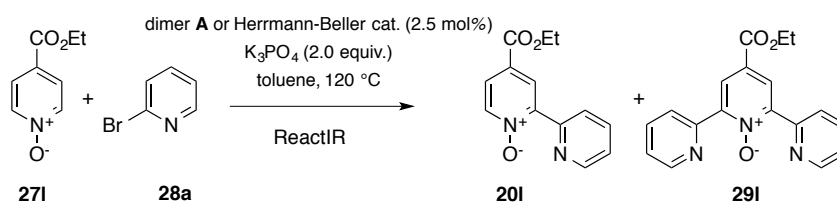
[SZ 2007a]

According to the general procedure, ester pyridine *N*-oxide **27l** (974 mg, 4.00 mmol), K$_3$PO$_4$ (849 mg, 4.00 mmol), dimer **A** (37.0 mg, 0.05 mmol) and bromopyridine **28a** (0.19 mL, 2.00 mmol). Purification by column chromatography (acetone in hexane: 0%–100%, 10% increments per 100 mL) gave ester bipyridine *N*-oxide **20l** (326 mg, 1.34 mmol, 67%) as the major product, terpyridine *N*-oxide **29l** (47 mg, 0.15 mmol, 15%), bipyridine *N*-dioxides **51l** (19 mg, 0.06 mmol, 3%), and **52l** (30 mg, 0.07 mmol, 4%) as the minor products as pale orange oil, as well as recovered ester pyridine *N*-oxide **27l** (381 mg, 2.28 mmol, 99%).
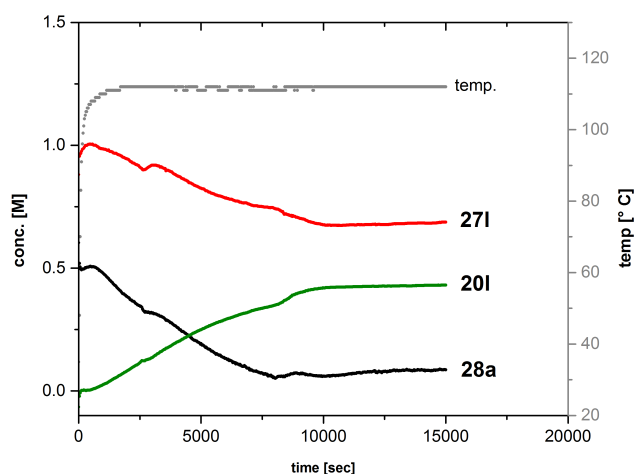

	k_{obs} [mM/min]	R^2
SZ 2007a		
27l	−1.27 ± 0.2	0.582
28a	−3.50 ± 0.09	0.964
20l	+3.34 ± 0.04	0.994

[SZ 2008a]

According to the general procedure, pyridine *N*-oxide **27l** (669 mg, 4.00 mmol), K$_3$PO$_4$ (850 mg, 4.00 mmol), Herrmann-Beller catalyst (46.8 mg, 0.05 mmol) and bromopyridine **28a** (0.19 mL, 2.00 mmol).
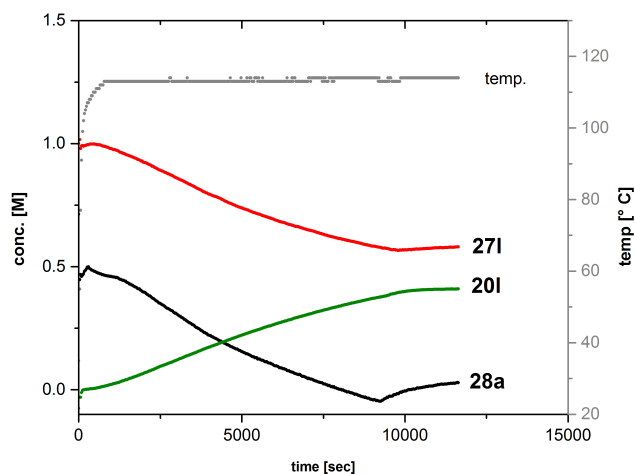
	k_{obs} [mM/min]	R^2
SZ 2008a		
27l	−3.85 ± 0.01	0.9995
28a	−5.30 ± 0.02	0.9995
20l	+3.184 ± 0.005	0.9999

4-Ethoxycarbony-2,2′-bipyridine *N*-oxide (**20l**)

^{1}H NMR (400 MHz, CDCl$_3$): δ 8.82 (dd, *J* = 8.1, 1.0 Hz, 1H), 8.82–8.73 (m, 2H), 8.35 (d, *J* = 6.8 Hz, 1H), 7.92–7.79 (m, 2H), 7.38 (ddt, *J* = 7.0, 4.8, 1.1 Hz, 1H), 4.42 (q, *J* = 7.1 Hz, 2H), 1.42 (td, *J* = 7.1, 1.0 Hz, 3H) ppm.

The chemical shifts are in agreement with previous reported values.[117]

4′-Ethoxycarbonyl-2,2′:6,2″-terpyridine *N*-oxide (**29l**)
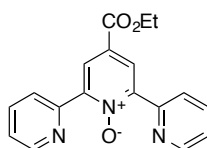
^{1}H NMR (400 MHz, CDCl$_3$): δ 8.76 (d, *J* = 4.8 Hz, 2H), 8.62 (s, 2H), 8.58 (d, *J* = 8.1 Hz, 2H), 7.80 (td, *J* = 7.7, 1.5 Hz, 2H), 7.35 (dd, *J* = 7.5, 4.8 Hz, 2H), 4.40 (q, *J* = 7.1 Hz, 2H), 1.39 (t, *J* = 7.1 Hz, 3H) ppm.

The chemical shifts are in agreement with previous reported values.[117]

4,4′-Dicarboxyethyl-*N,N′*-2,2′-bipyridine dioxide (**51l**)
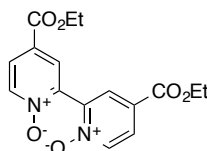
^{1}H NMR (400 MHz, CDCl$_3$): δ 8.33 (d, *J* = 6.8 Hz, 2H), 8.14 (d, *J* = 2.5 Hz, 2H), 7.96 (dd, *J* = 6.8, 2.5 Hz, 2H), 4.39 (q, *J* = 7.1 Hz, 4H), 1.37 (t, *J* = 7.1 Hz, 6H) ppm.

The chemical shifts are in agreement with previous reported values.[118]

4,4′-Bis(ethoxycarbonyl)-2-(pyridin-2-yl)-2,2′-bipyridine *N,N′*-dioxide (**52l**)
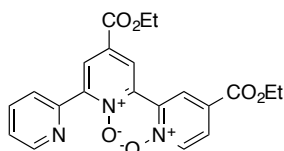
^{1}H NMR (400 MHz, CDCl$_3$): δ 8.93 (d, *J* = 2.7 Hz, 1H), 8.81 (d, *J* = 8.1 Hz, 1H), 8.78 (dt, *J* = 4.5, 1.1 Hz, 1H), 8.37 (d, *J* = 6.8 Hz, 1H), 8.14 (d, *J* = 2.5 Hz, 1H), 8.11 (dd, *J* = 2.7, 0.8 Hz, 1H), 7.99 (ddd, *J* = 6.8, 2.5, 0.9 Hz, 1H), 7.80 (td, *J* = 7.8, 1.8 Hz, 1H), 7.37 (ddd, *J* = 7.5, 4.7, 1.1 Hz, 1H), 4.46–4.36 (m, 4H), 1.45–1.33 (m, 6H) ppm.

^{13}C NMR (101 MHz, CDCl$_3$): δ 163.56, 163.28, 149.70, 148.81, 148.13, 143.87, 143.44, 140.22, 136.38, 129.13, 128.58, 127.42, 126.86, 126.23, 126.13, 125.73, 124.87, 62.24, 62.22, 14.43, 14.37 ppm.

HRESI-MS (+, m/z): [M+Na]$^+$ 432.1192 (100%) calc. 432.1166, [M+K]$^+$ 448.0928 calc. 448.0905.
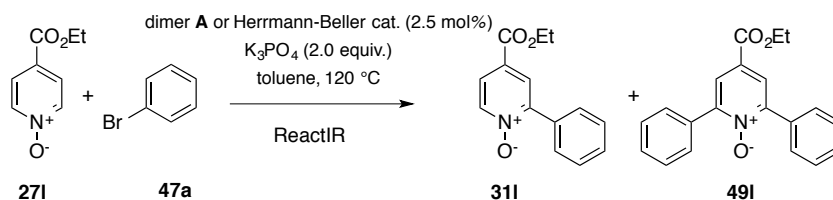
[SZ 1089b]

According to the general procedure, ester pyridine N-oxide **27l** (669 mg, 4.00 mmol), K$_3$PO$_4$ (850 mg, 4.00 mmol), dimer **A** (36.8 mg, 0.05 mmol) and bromobenzene **47a** (0.21 mL, 2.00 mmol). Purification by column chromatography (acetone in hexane: 0%–100%, 10% increments per 100 mL) gave phenylpyridine N-oxide **31l** (248 mg, 1.43 mmol, 71%) as the major product, diphenylpyridine N-oxide **49l** (61 mg, 0.19 mmol, 19%), biphenyl **17aa** (11 mg, 0.07 mmol, 7%), bipyridine N,N'-dioxides **51l** (0.03 mmol, 3%), and **33l** (0.04 mmol, 4%) as the minor product, as well as recovered ester pyridine N-oxide **27l** (203 mg, 2.19 mmol, 98%).
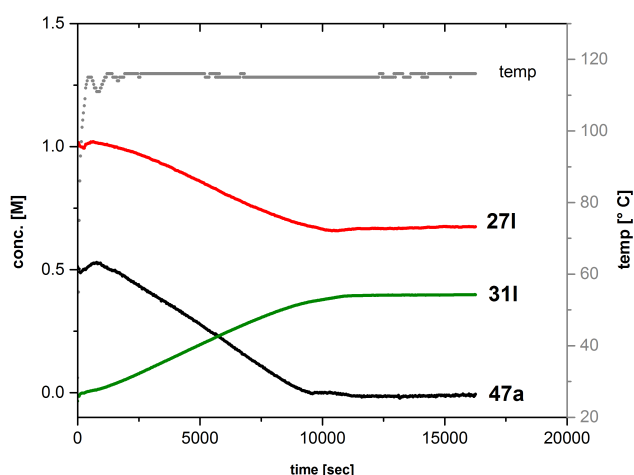
	k_{obs} [mM/min]	R^2
SZ 1089b		
27l	-2.26 ± 0.03	0.994
47a	-3.73 ± 0.03	0.997
31l	$+2.747 \pm 0.007$	0.9997

[SZ 2009a]

According to the general procedure, pyridine N-oxide **27l** (669 mg, 4.00 mmol), K$_3$PO$_4$ (850 mg, 4.00 mmol), Herrmann-Beller catalyst (46.5 mg, 0.05 mmol) and bromobenzene **47a** (0.19 mL, 2.00 mmol).
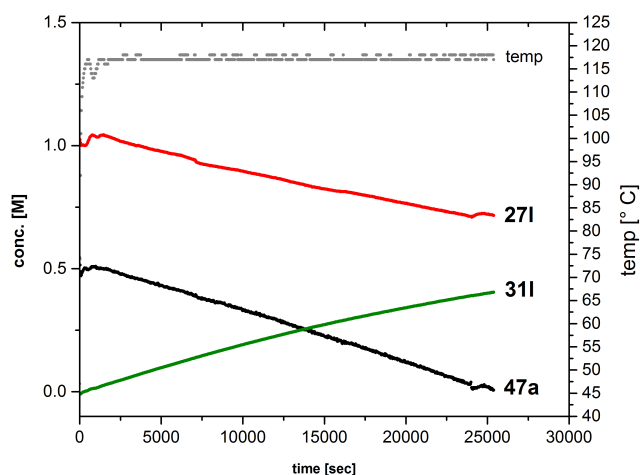
	k_{obs} [mM/min]	R^2
SZ 2009a		
27l	−1.23 ± 0.02	0.989
47a	−1.27 ± 0.03	0.980
31l	+1.227 ± 0.005	0.9997

4-Ethoxycarbonly-2-phenylpyridine *N*-oxide (**31l**)
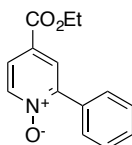
^{1}H NMR (400 MHz, CDCl$_3$): δ 8.32 (d, *J* = 6.8 Hz, 1H), 8.02 (d, *J* = 2.5 Hz, 1H), 7.82 –7.76 (m, 3H), 7.51–41 (m, 3H), 4.38 (q, *J* = 7.1 Hz, 2H), 1.38 (t, *J* = 7.1 Hz, 2H) ppm.

The chemical shifts are in agreement with previous reported values.[118]

4-Ethoxycarbonly-2,6-diphenylpyridine *N*-oxide (**49l**)
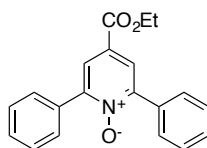
^{1}H NMR (400 MHz, CDCl$_3$): δ 8.02 (s, 2H), 7.85–7.81 (m, 4H), 7.52–7.44 (m, 6H), 4.42 (q, *J* = 7.1 Hz, 2H), 1.41 (t, *J* = 7.1 Hz, 3H) ppm.

The chemical shifts are in agreement with previous reported values.[118]

4,4′-Bis(ethoxycarbonyl)-2-phenyl-2,2′-bipyridine *N,N′*-dioxide (**53l**)
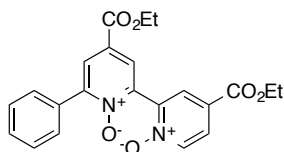
^{1}H NMR (400 MHz, CDCl$_3$): δ 8.35 (d, *J* = 6.8 Hz, 1H), 8.17 (dd, *J* = 5.5, 2.5 Hz, 1H), 8.09 (d, *J* = 2.5 Hz, 1H), 7.97 (dd, *J* = 6.9, 2.5 Hz, 1H), 7.84 (dd, *J* = 7.1, 2.7 Hz, 2H), 7.51–7.44 (m, 3H), 4.45–4.36 (m, 4H), 1.43–1.35 (m, 6H) ppm.

The chemical shifts are in agreement with previous reported values.[118]
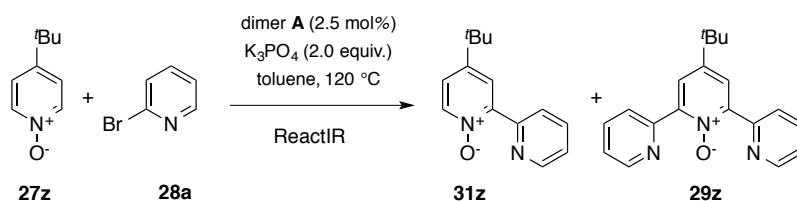

[SZ 2036]

According to the general procedure, *tert*-butylpyridine *N*-oxide **27z** (605 mg, 4.00 mmol), K$_3$PO$_4$ (852 mg, 4.01 mmol), dimer **A** (37.4 mg, 0.05 mmol) and bromopyridine **28a** (0.19 mL, 2.00 mmol). Purification by column chromatography (MeOH in DCM: 0%–10%, 1% increments per 100 mL) gave bipyridine *N*-oxide **20z** (131 mg, 0.57 mmol, 29%) as the major product, terpyridine *N*-oxide **29z** (14 mg, 0.05 mmol, 5%) as brown oil, and bipyridine **24a** (36 mg, 0.23 mmol, 23%) as the minor products, as well as recovered *tert*-pyridine *N*-oxide **27z** (447 mg, 2.95 mmol, 89%).
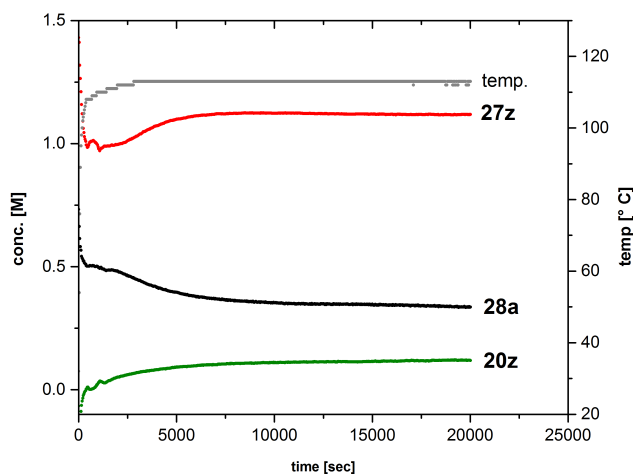
	k_{obs} [mM/min]	R^2
SZ 2036		
27z	+2.31 ± 0.04	0.984
28a	−2.36 ± 0.01	0.997
20z	+1.04 ± 0.02	0.988

4-*tert*-Butyl-2,2′-bipyridine *N*-oxide (**20z**)

^{1}H NMR (400 MHz, CDCl$_3$): δ 8.84 (d, *J* = 8.1 Hz, 1H), 8.73 (d, *J* = 4.8 Hz, 1H), 8.26 (d, *J* = 6.9 Hz, 1H), 8.10 (d, *J* = 2.9 Hz, 1H), 7.82 (td, *J* = 7.8, 1.8 Hz, 1H), 7.35 (ddd, *J* = 7.5, 4.8, 1.1 Hz, 1H), 7.28 (dd, *J* = 6.9, 2.9 Hz, 1H), 1.36 (s, 9H) ppm.

The chemical shifts are in agreement with previous reported values.[117]

4′-*tert*-Butyl-2,2′:6,2″-terpyridine *N*-oxide (**29z**)
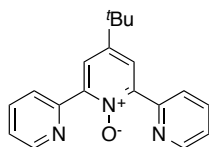
^{1}H NMR (400 MHz, CDCl$_3$): δ 8.75 (ddd, *J* = 4.9, 1.8, 0.9 Hz, 2H), 8.64 (dt, *J* = 8.1, 1.0 Hz, 2H), 8.01 (s, 1H), 7.80 (td, *J* = 7.8, 1.8 Hz, 2H), 7.35 (ddd, *J* = 7.5, 4.9, 1.1 Hz, 2H), 1.42 (s, 9H) ppm.

^{13}C NMR (101 MHz, CDCl$_3$): δ 151.10, 149.99, 149.51, 147.31, 136.04, 126.01, 125.04, 124.08, 35.02, 30.74 ppm.

IR (v_{max}/cm^{-1}): 3059 (w), 2957 (s), 2923 (s), 2854 (s), 1740 (m), 1672 (m), 1585 (m), 1570 (m), 1539 (w), 1464 (m), 1433 (w), 1399 (m), 1365 (w), 1250 (s, R$_3$N$^+$-O$^-$), 1151 (w), 1094 (w), 1045 (w), 1024 (w), 989 (w), 930 (w9, 890 (w), 834 (w), 791 (s), 747 (s), 679 (w).

HRESI-MS (+, *m/z*): [M+H]$^+$ 306.1590 calc. 306.1601, [M+Na]$^+$ 328.1412 calc. 328.1420
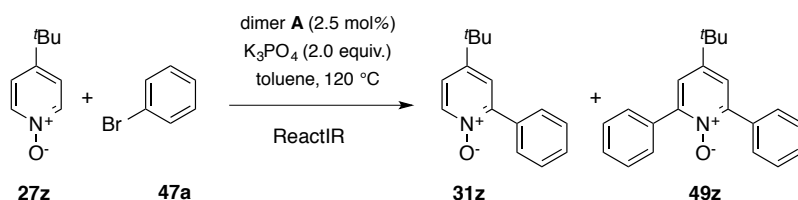
[SZ 2037]

According to the general procedure, *tert*-butylpyridine *N*-oxide **27z** (607 mg, 4.01 mmol), K$_3$PO$_4$ (849 mg, 4.00 mmol), dimer **A** (36.9 mg, 0.05 mmol) and bromobenzene **47a** (0.21 mL, 2.00 mmol). Purification by column chromatography (MeOH in DCM: 0%–10%, 1% increments per 100 mL) gave phenylpyridine *N*-oxide **31z** (222 mg, 0.98 mmol, 49%) as the major product and diphenylpyridine *N*-oxide **49z** (40 mg, 0.13 mmol, 13%) as orange oils, as well as biphenyl **17aa** (20 mg, 0.13 mmol, 13%) as the minor products, and recovered *tert*-pyridine *N*-oxide **27z** (481 mg, 3.18 mmol, 107%).
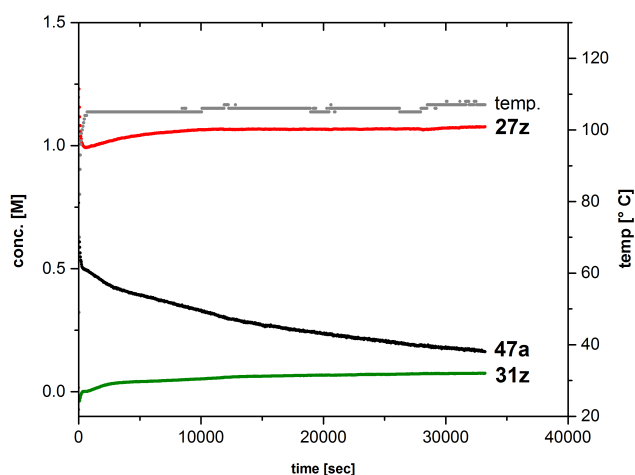
	k_{obs} [mM/min]	R^2
SZ 2037		
27z	+0.78 ± 0.01	0.993
47a	−1.44 ± 0.04	0.972
31z	+0.52 ± 0.02	0.951

4-*tert*-Butyl-2-phenylpyridine *N*-oxide (**31z**)
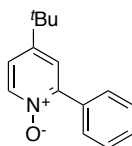
^{1}H NMR (400 MHz, CDCl$_3$): δ 8.25 (d, J = 6.9 Hz, 1H), 7.79 (dd, J = 8.0, 1.6 Hz, 2H), 7.50–7.42 (m, 3H), 7.36 (d, J = 2.9 Hz, 1H), 7.21 (dd, J = 6.9, 2.8 Hz, 1H), 1.33 (s, 9H) ppm.

^{13}C NMR (101 MHz, CDCl$_3$): δ 151.1, 148.4, 139.78, 133.1, 129.6, 129.5, 128.4, 124.5, 122.0, 34.7, 30.6 ppm.

IR (v_{max}/cm^{-1}): 3059 (w), 3037 (w), 2960 (m), 2907 (m), 2870 (m), 1616 (w), 1579 (w), 1545 (w), 1467 (m), 1405 (m), 1368 (m), 1241 (s), 1191 (m), 1132 (m), 1076 (w), 1020 (w), 890 (w), 825 8s), 775 (m), 757 (m), 732 (m), 695 (s).

HRESI-MS (+, *m/z*): [M+H]$^+$ 228.1367 calc. 228.1383, [M+Na]$^+$ 250.1191 calc. 250.1202.

4-*tert*-Butyl-2,6-phenylpyridine *N*-oxide (**49z**)
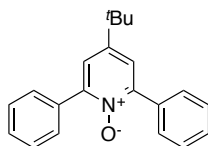
^{1}H NMR (400 MHz, CDCl$_3$): δ 7.86–7.82 (m, 4H), 7.50–7.42 (m, 6H), 7.38 (s, 2H), 1.38 (s, 9H) ppm.

^{13}C NMR (101 MHz, CDCl$_3$): δ 149.0, 133.9, 129.8, 129.4, 128.2, 123.5, 122.4, 30.8, 30.4 ppm.

IR (v_{max}/cm^{-1}): 3059 (w), 3034 (w), 2960 (m), 2907 (w), 2870 (w), 1616 (w), 1548 (w), 1495 (w), 1477 (w), 1455 (w), 1424 (w), 1402 (m), 1365 (w), 1337 (w), 1312 (w), 1244 (s), 1073 8w), 1030 (w), 924 (w), 884 (w), 831 (m), 778 (m), 738 (m), 691 (s).

HRESI-MS (+, *m/z*): [M+H]$^+$ 304.1685 calc. 304.1696, [M+Na]$^+$ 326.1507 calc. 326.1515.
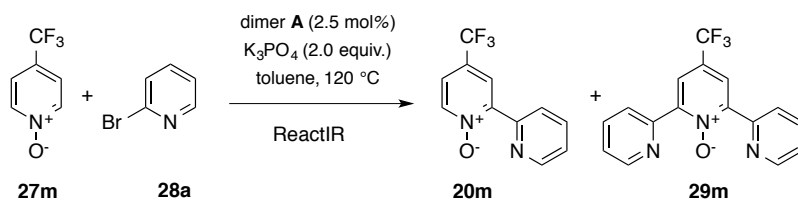
[SZ 2038]

According to the general procedure, trifluoromethylpyridine *N*-oxide **27m** (653 mg, 4.00 mmol), K$_3$PO$_4$ (851 mg, 4.01 mmol), dimer **A** (36.9 mg, 0.05 mmol) and bromopyridine **28a** (0.19 mL, 2.00 mmol). Purification by column chromatography (acetone in hexane: 0%–100%, 10% increments per 100 mL) gave bipyridine *N*-oxide **20m** (420 mg, 1.75 mmol, 87%) as the major product, terpyridine *N*-oxide **29m** (32 mg, 0.10 mmol, 10%) as the minor product, and recovered trifluoromethylpyridine *N*-oxide **27m** (338 mg, 3.92 mmol, 98%).
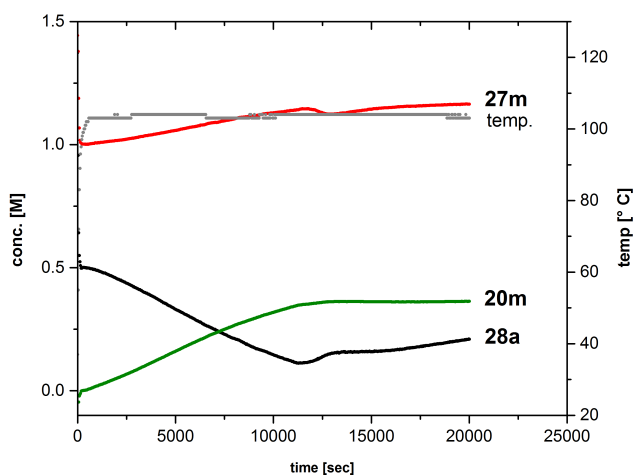
	k_{obs} [mM/min]	R^2
SZ 2038		
27m	+0.78 ± 0.01	0.992
28a	−2.36 ± 0.01	0.999
20m	+2.096 ± 0.009	0.9989

4-(Trifluoromethyl)-2,2′-bipyridine *N*-oxide (**20m**)
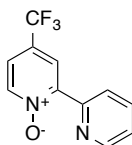
^{1}H NMR (400 MHz, CDCl$_3$): δ 8.90 (dt, J = 8.1, 1.0 Hz, 1H), 8.73 (ddd, J = 4.7, 1.7, 0.8 Hz, 1H), 8.52 (d, J = 2.7 Hz, 1H), 8.35 (d, J = 6.9 Hz, 1H), 7.83 (td, J = 7.8, 1.8 Hz, 1H), 7.44 (dd, J = 6.8, 2.8 Hz, 1H), 7.37 (ddd, J = 7.6, 4.7, 1.1 Hz, 1H) ppm.

The chemical shifts are in agreement with previous reported values.[117]

2′-(Trifluoromethyl)-2,2′:6,2″-terpyridine *N*-oxide (**29m**)
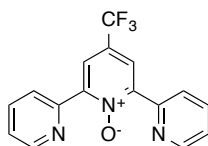
^{1}H NMR (400 MHz, CDCl$_3$): δ 8.77 (dd, J = 4.8, 0.9 Hz, 2H), 8.72 (d, J = 8.0 Hz, 2H), 8.38 (s, 2H), 7.85 (td, J = 7.8, 1.8 Hz, 2H), 7.40 (ddd, J = 7.6, 4.8, 1.2 Hz, 2H) ppm.

The chemical shifts are in agreement with previous reported values.[117]
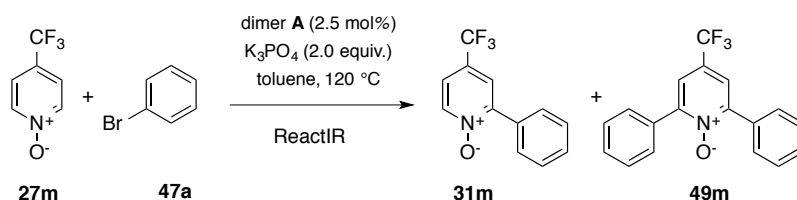
[SZ 2039]

According to the general procedure, trifluoromethylpyridine *N*-oxide **27m** (655 mg, 4.02 mmol), K$_3$PO$_4$ (850 mg, 4.00 mmol), dimer **A** (36.7 mg, 0.05 mmol) and bromobenzene **47a** (0.21 mL, 2.00 mmol). Purification by column chromatography (acetone in hexane: 0%–100%, 10% increments per 100 mL) gave phenylpyridine *N*-oxide **31m** (450 mg, 1.88 mmol, 94%) as the major product and diphenylpyridine *N*-oxide **49m** (44 mg, 0.14 mmol, 14%) as the minor product each as pale yellow solids.
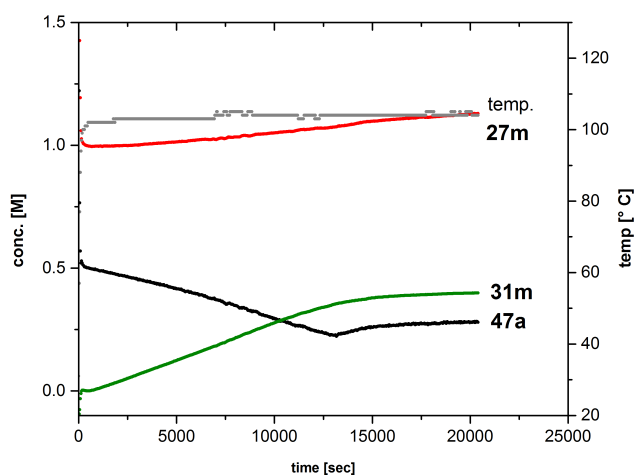
	k_{obs} [mM/min]	R^2
SZ 2039		
27m	$+0.25 \pm 0.02$	0.904
47a	-1.10 ± 0.02	0.991
31m	$+1.765 \pm 0.005$	0.9996

4-(Trifluoromethyl)-2-phenylpyridine *N*-oxide (**31m**)
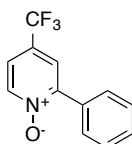
^{1}H NMR (400 MHz, CDCl$_3$): δ 8.39 (d, *J* = 6.8 Hz, 1H), 7.82–7.77 (m, 2H), 7.65 (d, *J* = 2.7 Hz, 1H), 7.53 –7.46 (m, 3H), 7.43 (dd, *J* = 6.8, 2.7 Hz, 1H) ppm.

^{13}C NMR (101 MHz, CDCl$_3$): δ 149.93, 141.11, 131.37, 130.37, 129.18, 128.55, 126.62 (q, *J* = 35 Hz) 124.05 (q, *J* = 3.8 Hz) 122.59 (q, *J* = 272 Hz), 120.99 (q, *J* = 3.9 Hz) ppm.

^{19}F NMR (471 MHz, CDCl$_3$): δ –63.37 ppm.

IR (v_{max}/cm^{-1}): 3059 (w), 3044 (w), 2926 (w), 2864 (w), 1629 (w), 1560 (w), 1477 (w), 1455 (m), 1424 (m), 1328 (s), 1259 8s), 1210 (w), 1169 (m), 1120 (s), 1079 (s), 899 (m), 865 (w), 837 (m), 766 (m), 732 (w), 688 (m).

HRESI-MS (+, *m/z*): [M+H]$^+$ 240.0613 calc. 240.0631, [M+Na]$^+$ 262.0439 calc. 262.0450.

M.p. 55–57 °C.

4-(Trifluoromethyl)-2,6-diphenylpyridine *N*-oxide (**49m**)
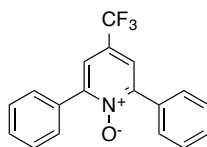
^{1}H NMR (400 MHz, CDCl$_3$): δ 7.85–7.79 (m, 4H), 7.63 (s, 2H), 7.54–7.46 (m, 6H) ppm.

^{13}C NMR (101 MHz, CDCl$_3$): δ 150.92, 132.27, 130.23, 129.54, 128.49, 122.47 (q, *J* = 3.8 Hz) ppm.

^{19}F NMR (471 MHz, CDCl$_3$): δ –63.30 ppm.

IR (v_{max}/cm^{-1}): 3062 (w), 2960 (w), 2929 (w), 2857 (w), 1734 (w), 1629 (w), 1560 (w), 1458 (m), 1430 (m), 1340 (m), 1306 (m), 1262 (s, R$_3$N$^+$-O$^-$), 1179 (s), 1123 (s), 1107 (s), 1048 (w), 1030 (w), 1002 (w), 924 (w), 884 (m), 800 8w), 772 (m), 741 (m), 695 (s).

HRESI-MS (+, *m/z*): [M+H]$^+$ 316.0930 calc. 316.0994, [M+Na]$^+$ 338.0752 calc. 338.0763.
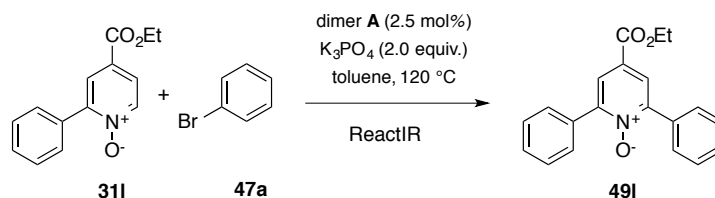
M.p. 89–91 °C.
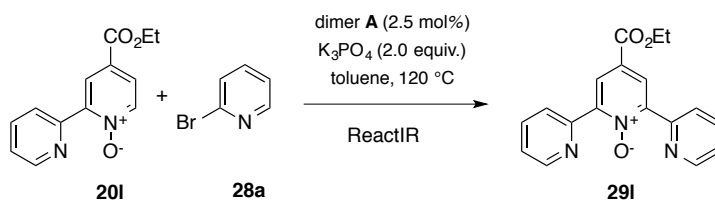
[SZ 1091a]

According to the general procedure, bipyridine *N*-oxide **20l** (977 mg, 4.00 mmol), K_3PO_4 (850 mg, 4.00 mmol), dimer **A** (37.0 mg, 0.05 mmol) and bromopyridine **28a** (0.19 mL, 2.00 mmol) in toluene (4.00 mL). Purification by column chromatography (acetone in hexane: 0%–100%, 10% increments per 100 mL) gave terpyridine *N*-oxide **29l** (591 mg, 1.84 mmol, 92%), bipyridine **24l** (21.9 mg, 0.10 mmol, 2%), bipyridine **24a** (6.2 mg, 0.04 mmol, 4%) and starting material **20l** (540 mg, 2.21 mmol, recov. 96%).
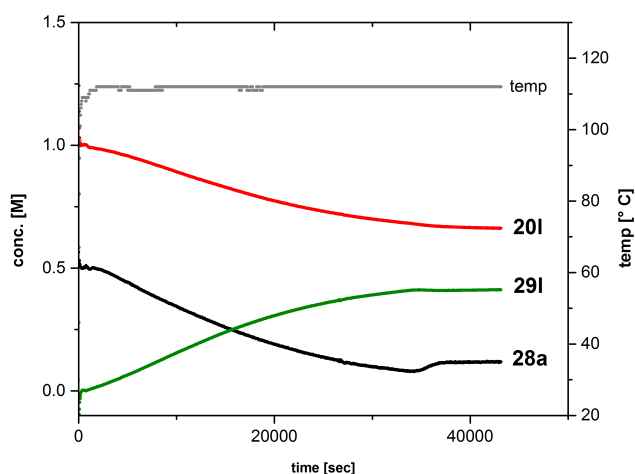
	k_{obs} [mM/min]	R^2
SZ 1091b		
20l	-0.497 ± 0.006	0.993
28a	-0.94 ± 0.02	0.981
29l	$+0.898 \pm 0.006$	0.998

4-Ethoxycarbonyl-2,2′-bipyridine (**24l**)
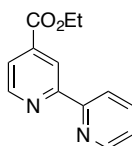
^{1}H NMR (400 MHz, CDCl$_3$): δ 8.93 (d, J = 0.7 Hz, 1H), 8.82 (d, J = 5.0 Hz, 1H), 8.73 (d, J = 4.8 Hz, 1H), 8.42 (dd, J = 8.0, 1.0 Hz, 1H), 7.88 (dd, J = 5.0, 1.6 Hz, 1H), 7.84 (td, J = 7.8, 1.8 Hz, 1H), 7.35–7.33 (m, 1H), 4.45 (q, J = 7.1 Hz, 2H), 1.44 (t, J = 7.1 Hz, 3H) ppm.

The chemical shifts are in agreement with previous reported values.[117]
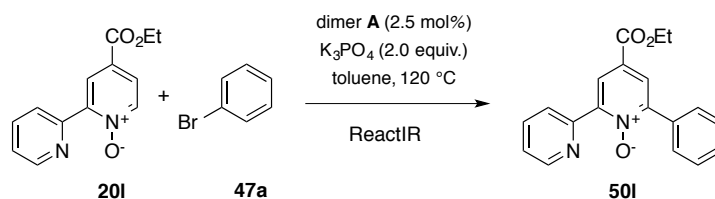
[SZ 2001b]

According to the general procedure, bipyridine *N*-oxide **20l** (977 mg, 4.00 mmol), K_3PO_4 (850 mg, 4.00 mmol), dimer **A** (36.8 mg, 0.05 mmol) and bromobenzene **47a** (0.21 mL, 2.00 mmol) in toluene

(4.00 mL). Purification by column chromatography (acetone in hexane: 0%–100%, 10% increments per 100 mL) gave teraryl *N*-oxide **50l** (415 mg, 1.30 mmol, 65%), ester-substituted bipyridine **24l** (17.0 mg, 0.07 mmol, 2%), ester-substituted teraryl **55l** (17 mg, 0.06 mmol, 3%), and starting material **20l** (612 mg, 2.50 mmol, recov. 98%).
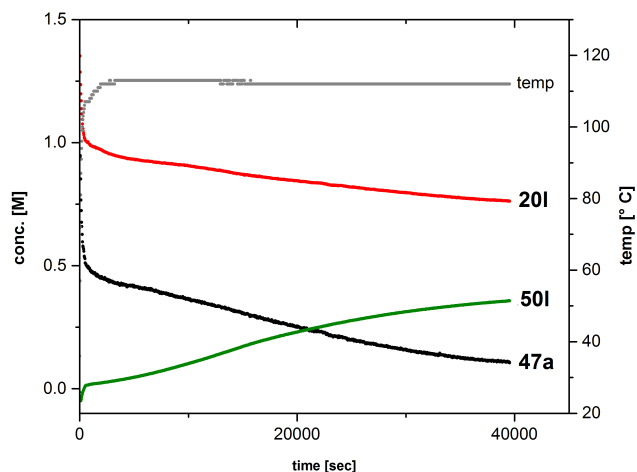
	k_{obs} [mM/min]	R^2
SZ 2001b		
20l	-1.04 ± 0.02	0.981
47a	-1.00 ± 0.04	0.941
50l	$+0.411 \pm 0.004$	0.995

4-Ethoxycarbonyl-6-phenyl-2,2′-bipyridine *N*-oxide (**55l**)
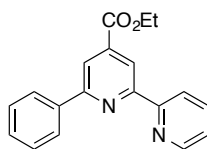
^{1}H NMR (400 MHz, CDCl₃): δ 8.91 (d, *J* = 1.1 Hz, 1H), 8.75 (d, *J* = 4.7 Hz, 1H), 8.65 (d, *J* = 8.0 Hz, 1H), 8.36 (d, *J* = 1.2 Hz, 1H), 8.27–8.15 (m, 2H), 7.89 (td, *J* = 7.7, 1.6 Hz, 1H), 7.54 (t, *J* = 7.3 Hz, 2H), 7.47 (t, *J* = 7.3 Hz, 1H), 7.38 (dd, *J* = 6.8, 5.4 Hz, 1H), 4.49 (q, *J* = 7.2 Hz, 2H), 1.47 (t, *J* = 7.1 Hz, 3H) ppm.

The chemical shifts are in agreement with previous reported values.[118]
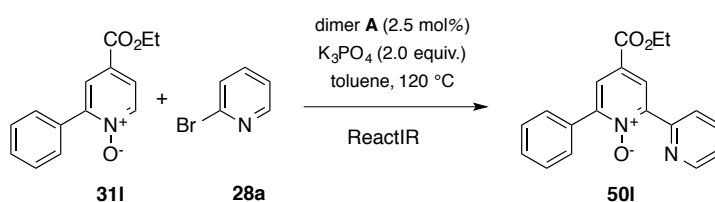
[SZ 2002a]

According to the general procedure, phenylpyridine *N*-oxide **31l** (974 mg, 4.00 mmol), K₃PO₄ (849 mg, 4.00 mmol), dimer **A** (37.0 mg, 0.05 mmol) and bromopyridine **28a** (0.19 mL, 2.00 mmol) in toluene (4.00 mL). Purification by column chromatography (acetone in hexane: 0%–100%, 10%

increments per 100 mL) gave teraryl *N*-oxide **50l** (538 mg, 1.68 mmol, 84%), ester-substituted teraryl **55l** (33.5 mg, 0.11 mmol, 6%), bipyridine **24a** (17.7 mg, 0.11 mmol, 11%), and starting material **31l** (506 mg, 2.08 mmol, recov. 97%).
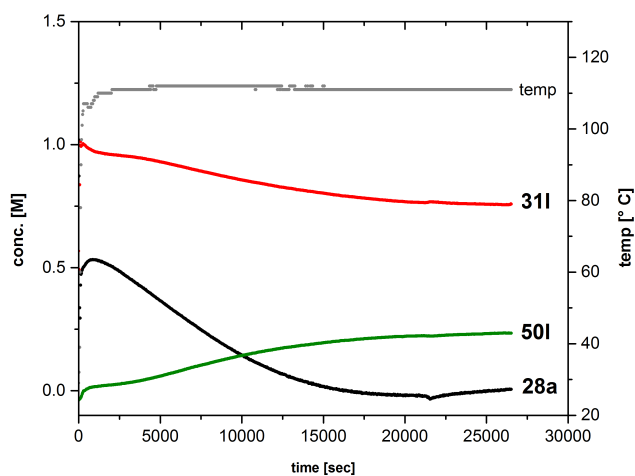
	k_{obs} [mM/min]	R^2
SZ 2002a		
31l	−0.44 ± 0.01	0.993
28a	−2.68 ± 0.02	0.997
50l	+0.542 ± 0.008	0.988

[SZ 2003b]

According to the general procedure, phenylpyridine *N*-oxide **31l** (973 mg, 4.00 mmol), K$_3$PO$_4$ (850 mg, 4.00 mmol), dimer **A** (36.7 mg, 0.05 mmol) and bromobenzene **47a** (0.21 mL, 2.00 mmol) in toluene (4.00 mL). Purification by column chromatography (acetone in hexane: 0%–100%, 10% increments per 100 mL) gave teraryl *N*-oxide **49l** (295 mg, 0.92 mmol, 46%), biphenyl **17aa** (16.7 mg, 0.11 mmol, 11%), and starting material **31l** (737 mg, 3.03 mmol, recov. 99%).
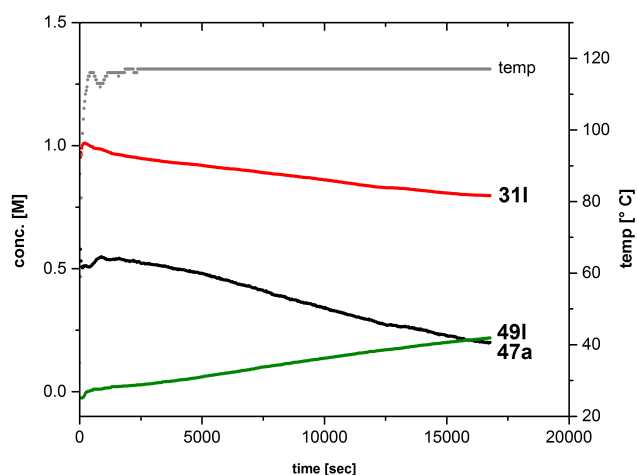
	k_{obs} [mM/min]	R^2
SZ 2003b		
31l	-0.852 ± 0.007	0.981
47a	-0.93 ± 0.03	0.968
49l	$+0.64 \pm 0.02$	0.980

4.13.2 Competition experiments

General procedure A:

In a glovebox, pyridine *N*-oxides **27** (each 4.00 mmol), K$_3$PO$_4$ (4.00 mmol), aryl halide **28** or **47** (2.00 mmol), and dimer **A** (0.05 mmol) were weighted in a Schlenk tube and toluene (4.00 mL) was added. After the reaction mixture has been stirred for 13–16 h at 120 °C, the Schlenk tube was cooled to room temperature and the reaction mixture directly subjected to a silica gel filled columned and purified by using acetone in hexane mixtures (0–100%, 10% increments per 150 mL).

General procedure B:

In a glovebox, pyridine *N*-oxides **27** (each 0.40 mmol), K$_3$PO$_4$ (0.40 mmol), aryl halide **28** or **47** (0.20 mmol), and dimer **A** (0.05 mmol) were weighted in a reaction vial and toluene (0.50 mL) was added. After the reaction mixture has been stirred for 16 h at 120 °C, the vials were cooled to room temperature. The reaction mixtures were then diluted with DCM and filtered over a short plug of celite. The solvent was removed from the filtrate, the resulting solid was dissolved in CDCl$_3$ and the ^{1}H NMR spectrum was recorded.

[SZ 2018a]

According to the general procedure A, reaction of pyridine *N*-oxides **27a** (381 mg, 4.01 mmol) and **27l** (669 mg, 4.00 mmol), K$_3$PO$_4$ (845 mg, 4.00 mmol), dimer **A** (37.2 mg, 0.05 mmol), and bromopyridine **28a** (0.19 mL, 2.00 mmol) gave bipyridine *N*-oxide **20l** (257 mg, 1.06 mmol, 53%), terpyridine *N*-oxide **29l** (29 mg, 0.09 mmol, 9%), bipyridine **24a** (19 mg, 0.12 mmol, 12%), recovered starting materials **27a** (383 mg, 4.03 mmol, 100%), and **27l** (492 mg, 2.94 mmol, 102%).

[SZ 2047a]

According to the general procedure B, reaction of pyridine *N*-oxides **27a** (39 mg, 0.41 mmol) and **27l** (68 mg, 0.41 mmol), K$_3$PO$_4$ (86 mg, 0.41 mmol), dimer **A** (3.7 mg, 0.005 mmol), and bromopyridine **28a** (31 mg, 0.20 mmol) provided a product ratio calculated from ^{1}H NMR of 1 to 1.86 (**27a** to **27l**).

[SZ 2018b]

According to the general procedure A, reaction of pyridine *N*-oxides **27a** (382 mg, 4.01 mmol) and **27l** (673 mg, 4.02 mmol), K$_3$PO$_4$ (851 mg, 4.01 mmol), dimer **A** (37.2 mg, 0.05 mmol), and bromobenzene **47a** (0.21 mL, 2.00 mmol) gave phenylpyridine *N*-oxide **31l** (282 mg, 1.16 mmol, 58%), diphenylpyridine *N*-oxide **49l** (24 mg, 0.08 mmol, 8%), biphenyl **17aa** (8.3 mg, 0.05 mmol, 5%), recovered starting materials **27a** (295 mg, 3.10 mmol, 77%), and **27l** (563 mg, 3.37 mmol, 115%).

[SZ 2047b]

According to the general procedure B, reaction of pyridine *N*-oxides **27a** (39 mg, 0.41 mmol) and **27l** (67 mg, 0.40 mmol), K$_3$PO$_4$ (85 mg, 0.40 mmol), dimer **A** (3.8 mg, 0.005 mmol), and bromobenzene **47a** (31 mg, 0.20 mmol) provided a product ratio calculated from ^{1}H NMR of 1 to 1.02 (**31a** to **31l**).


[SZ 2020a]

According to the general procedure A, reaction of pyridine *N*-oxides **27a** (192 mg, 2.02 mmol) and **27m** (327 mg, 2.00 mmol), K$_3$PO$_4$ (424 mg, 2.00 mmol), dimer **A** (18.5 mg, 0.025 mmol), and

bromopyridine **28a** (163.1 mg, 1.03 mmol) gave bipyridine *N*-oxides **20a** (16 mg, 0.09 mmol, 9%), **20m** (143 mg, 0.60 mmol, 58%), terpyridine *N*-oxide **29m** (21 mg, 0.07 mmol, 14%), reduced terpyridine **54m** (3 mg, 0.01 mmol, 2%), recovered starting materials **27a** (179 mg, 1.87 mmol, 98%), and **27m** (197 mg, 1.21 mmol, 96%).

4′-Trifluoromethyl-2,2′:6,2″-terpyridine (**54m**)
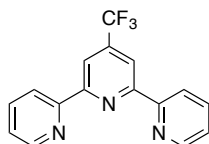
^{1}H NMR (400 MHz, CDCl$_3$): δ 8.75 (ddd, *J* 4.7, 1.7, 09 Hz, 2H), 8.73 (s, 2H), 8.66 (dt, *J* = 8.0, 1.0 Hz, 2H), 7.92 (td, *J* = 7.8, 1.8 Hz, 2H), 7.41 (ddd, *J* = 7.5, 4.8, 1.1 Hz, 2H) ppm.

Chemical shifts are in agreement with previously reported values.[243]

[SZ 2046a]

According to the general procedure B, reaction of pyridine *N*-oxides **27a** (38 mg, 0.40 mmol) and **27m** (65 mg, 0.40 mmol), K$_3$PO$_4$ (87 mg, 0.41 mmol), dimer **A** (3.7 mg, 0.005 mmol), and bromopyridine **28a** (33 mg, 0.21 mmol) provided a product ratio calculated from ^{1}H NMR of 1 to 3.85 (**20a** to **20m**)
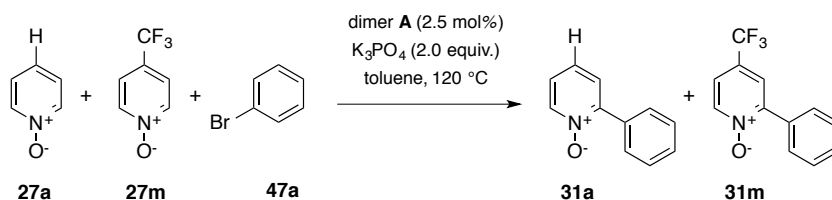

[SZ 2020b]

According to the general procedure A, reaction of pyridine *N*-oxides **27a** (192 mg, 2.02 mmol) and **27m** (327 mg, 2.00 mmol), K$_3$PO$_4$ (427 mg, 2.01 mmol), dimer **A** (18.8 mg, 0.026 mmol), and bromobenzene **47a** (158 mg, 1.01 mmol) gave phenylpyridine *N*-oxides **31m** (133 mg, 0.56 mmol, 55%), **31a** (26 mg, 0.15 mmol, 15%), diphenylpyridine *N*-oxide **49m** (19 mg, 0.06 mmol, 12%), recovered starting materials **27a** (245 mg, 5.58 mmol, 128%), and **27m** (197 mg, 1.21 mmol, 91%).

[SZ 2046b]

According to the general procedure B, reaction of pyridine *N*-oxides **27a** (38 mg, 0.40 mmol) and **27m** (66 mg, 0.40 mmol), K$_3$PO$_4$ (86 mg, 0.40 mmol), dimer **A** (3.7 mg, 0.005 mmol), and bromobenzene **47a** (33 mg, 0.21 mmol) provided a product ratio calculated from ^{1}H NMR of 1 to 1.89 (**31a** to **31m**)
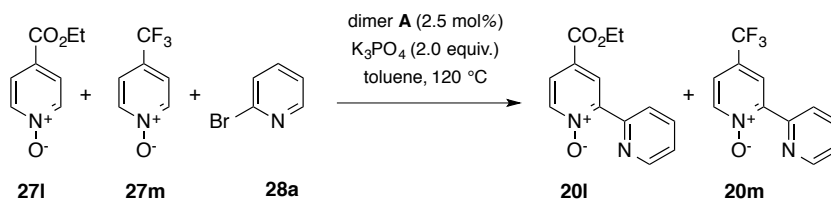
[SZ 2033a]

According to the general procedure B, reaction of pyridine *N*-oxides **27l** (67 mg, 0.40 mmol) and **27m** (66 mg, 0.40 mmol), K_3PO_4 (85 mg, 0.40 mmol), dimer **A** (3.8 mg, 0.005 mmol), and bromopyridine **28a** (31 mg, 0.20 mmol) provided a product ratio calculated from ^{1}H NMR of 1 to 1.80 (**20l** to **20m**).
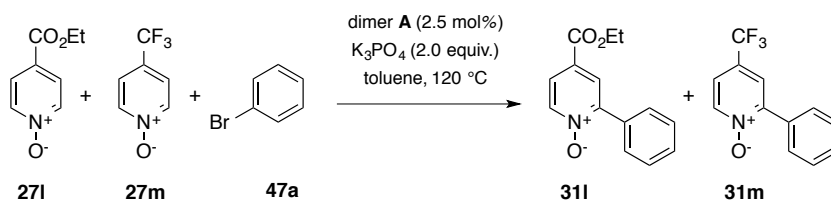

[SZ 2033b]

According to the general procedure B, reaction of pyridine *N*-oxides **27l** (67 mg, 0.40 mmol) and **27m** (65 mg, 0.40 mmol), K_3PO_4 (86 mg, 0.41 mmol), dimer **A** (3.9 mg, 0.005 mmol), and bromobenzene **47a** (32 mg, 0.20 mmol) provided a product ratio calculated from ^{1}H NMR of 1 to 1.71 (**31l** to **31m**).
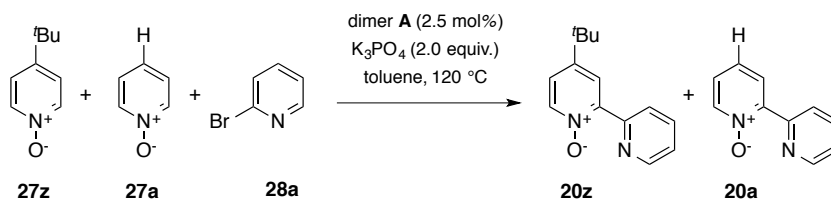
[SZ 2040]

According to the general procedure B, reaction of pyridine *N*-oxides **27a** (40 mg, 0.42 mmol) and **27z** (61 mg, 0.41 mmol), K_3PO_4 (85 mg, 0.40 mmol), dimer **A** (3.9 mg, 0.005 mmol), and bromopyridine **28a** (37 mg, 0.24 mmol) provided a product ratio calculated from ^{1}H NMR of 1 to 0.88 (**20z** to **20a**).
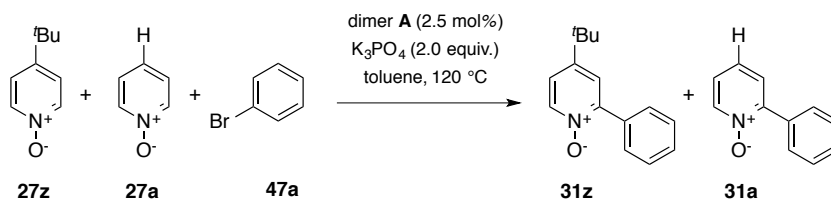
[SZ 2041]

According to the general procedure B, reaction of pyridine *N*-oxides **27a** (38 mg, 0.40 mmol) and **27z** (63 mg, 0.42 mmol), K_3PO_4 (85 mg, 0.40 mmol), dimer **A** (3.7 mg, 0.005 mmol), and bromobenzene **47a** (31 mg, 0.20 mmol) provided a product ratio calculated from ^{1}H NMR of 1 to 0.82 (**31z** to **31a**).

433
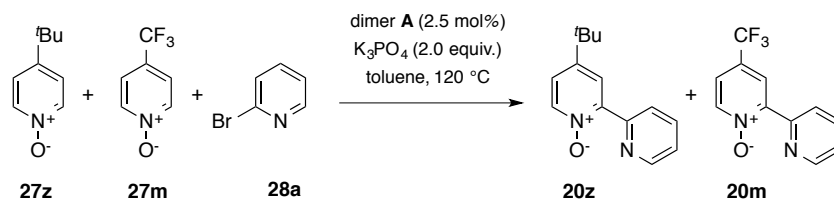
[SZ 2042]

According to the general procedure B, reaction of pyridine *N*-oxides **27m** (66 mg, 0.41 mmol) and **27z** (62 mg, 0.41 mmol), K_3PO_4 (85 mg, 0.40 mmol), dimer **A** (3.9 mg, 0.005 mmol), and bromopyridine **28a** (33 mg, 0.21 mmol) provided a product ratio calculated from ^{1}H NMR of 1 to 3.33 (**20z** to **20m**).
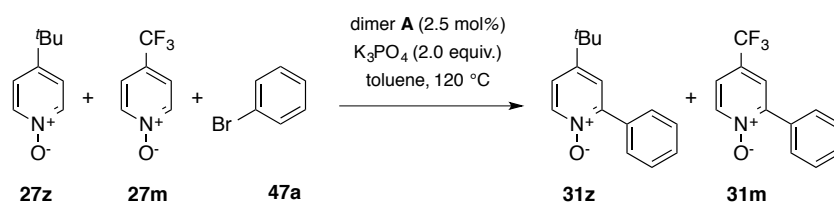
[SZ 2043]

According to the general procedure B, reaction of pyridine *N*-oxides **27m** (66 mg, 0.41 mmol) and **27z** (60 mg, 0.40 mmol), K_3PO_4 (86 mg, 0.40 mmol), dimer **A** (3.7 mg, 0.005 mmol), and bromobenzene **47a** (33 mg, 0.21 mmol) provided a product ratio calculated from ^{1}H NMR of 1 to >10 (**31z** to **31m**).
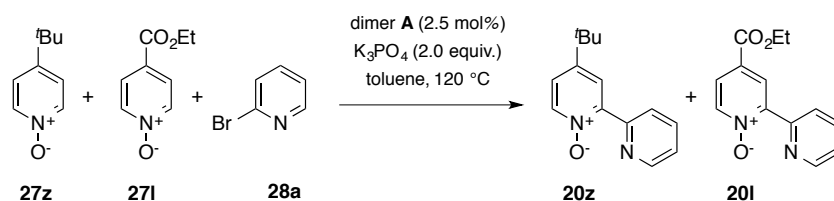
[SZ 2044]

According to the general procedure B, reaction of pyridine *N*-oxides **27l** (67 mg, 0.40 mmol) and **27z** (62 mg, 0.41 mmol), K_3PO_4 (85 mg, 0.40 mmol), dimer **A** (3.8 mg, 0.005 mmol), and bromopyridine **28a** (36 mg, 0.23 mmol) provided a product ratio calculated from ^{1}H NMR of 1 to 5.88 (**20z** to **20l**).
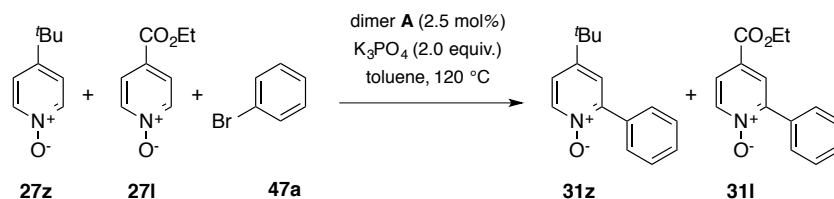
[SZ 2045]

According to the general procedure B, reaction of pyridine *N*-oxides **27l** (67 mg, 0.40 mmol) and **27z** (61 mg, 0.40 mmol), K_3PO_4 (86 mg, 0.40 mmol), dimer **A** (3.7 mg, 0.005 mmol), and bromobenzene **47a** (32 mg, 0.20 mmol) provided a product ratio calculated from ^{1}H NMR of 1 to 0.76 (**31z** to **31l**).

4.13.3 Electronic influence of aryl halides

General procedure:

In a glovebox, the reaction vials of the same batch equipped with a stirring bar were loaded with K_3PO_4 (106 mg, 0.50 mmol), bromoarene derivatives **28** or **47** (1.00 mmol), a stock solution (0.30 mL, 0.50 mmol) of ester-substituted pyridine *N*-oxide **27l** (2.79 g, 16.7 mmol) in toluene (10.0 mL) and another stock solution (0.20 mL, 6.25 μmol) of dimer **A** (229.5 mg, 0.31 mmol) in toluene (10.0 mL). The reaction vials were sealed with a Teflon-lined screw cap and brought outside the glovebox. After heating on an aluminum well plate at 120 °C for 50 min, the reaction vials were immediately transferred into another pre-cooled aluminum well plate under and further cooled in an ice bath. Then, the solvent was removed by rotary evaporation and dried under high vacuum. 0.50 mL of a stock solution of TMB (257 mg, 1.53 mmol) as internal standard in $CDCl_3$ (10.0 mL) was added to the dried samples and the filtered through a short plug of Celite directly into a NMR tube. Quantifications were done by integration of product signals relative to the aromatic protons of the internal standard.

[SZ 2133/2137]
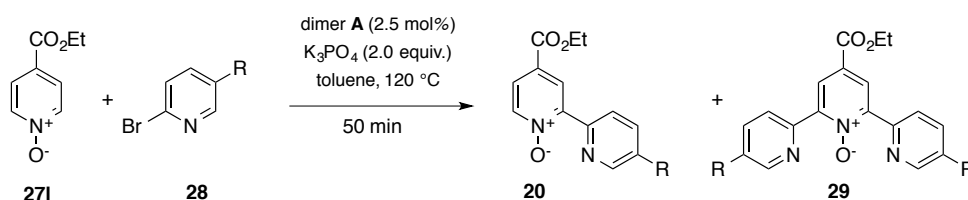
entry	R		28 [mg]	28 [mmol]	20 [mmol]	20 [%]	29 [mmol]	29 [%]
1	OMe	**28b**	50	0.27	0.072	27	0	0
2	Me	**28c**	43	0.25	0.110	44	0	0
3	H	**28a**	41	0.26	0.143	55	0.011	8
4	CF_3	**28d**	57	0.25	0.096	38	0	0
5	NO_2	**28e**	52	0.26	0	0	0	0

[SZ 2136]
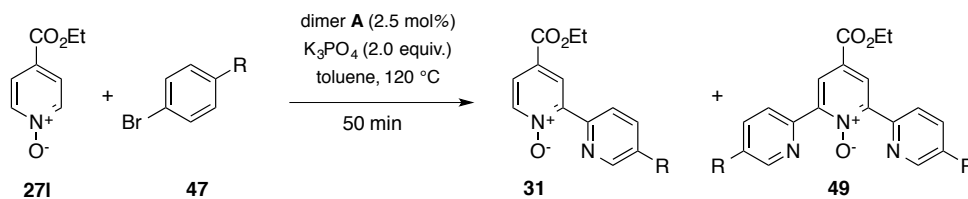
entry	R		31 [mg]	31 [mmol]	49 [mmol]	49 [%]
1	OMe	**47b**	48	0.26	0.082	32
2	^tBu	**47c**	56	0.26	0.104	40
3	H	**47a**	42	0.27	0.102	38
4	F	**47d**	45	0.26	0.092	35

435

5	CO$_2$Me	**47e**	55	0.25	0.091	36
6	CF$_3$	**47f**	58	0.26	0.094	36
7	CN	**47g**	47	0.26	0.095	37

Independent Syntheses and characterization of the bi- and teraryl N-oxides:

General procedure:

In a glovebox under inert atmosphere, reaction vials were loaded with pyridine *N*-oxide **27l** (1.00 mmol), aryl halide **28** or **47** (0.50 mmol), K$_3$PO$_4$ (1.00 mol), toluene (0.60 mL) and 0.40 mL (12.5 μmol) of a stock solution of dimer **A** (229.5 mg, 0.31 mmol) in toluene (10.0 mL). The reaction vials were sealed with a Teflon-lined screw cap, brought outside the glovebox and heated under stirring at 120 °C for 24 h. After cooling to room temperature, the crude reaction mixtures directly subjected to column chromatography (silica gel, acetone/hexane mixtures 0–100%, 10% increments per 150 mL).

4-Ethoxycarbonyl-5-methoxy-2,2′-biypridine *N*-oxide (20lb)

[SZ 2170a]
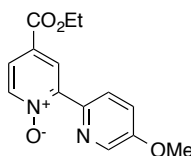
 According tot he general procedure, pyridine *N*-oxide **27l** (167 mg, 1.00 mmol), 2-bromo-5-methoxy-pyridine (**28b**) (96.3 mg, 0.51 mmol), K$_3$PO$_4$ (212 mg, 1.00 mmol), and dimer **A** (9.9 mg, 0.014 mmol) in toluene (1.00 mL). Column chromatography provided bipyridine *N*-oxide **20lb** (84.2 mg, 0.31 mmol, 60%), terpyridine *N*-oxide **29lb** (11.5 mg, 0.03 mmol, 12%) as brownish solid, and recovered starting material **27l** (79.9 mg, 0.48 mmol, recov. 81%).

^{1}H NMR (400 MHz, CDCl$_3$): δ 8.90 (d, *J* = 9.0 Hz, 1H), 8.77 (d, *J* = 2.6 Hz, 1H), 8.42 (dd, *J* = 3.0, 0.8 Hz, 1H), 8.27 (dd, *J* = 6.8, 0.6 Hz, 1H), 7.77 (dd, *J* = 6.8, 2.6 Hz, 1H), 7.28 (dd, *J* = 9.0, 3.0 Hz, 1H), 4.39 (q, *J* = 7.0 Hz, 2H), 3.91 (s, 3H), 1.39 (t, *J* = 7.3 Hz, 3H) ppm.

The chemical shifts are in agreement with previous reported values.[117]

4′-Ethoxycarbonyl-5,5″-dimethoxy-2,2′:6,2″-terpyridine *N*-oxide (29lb)
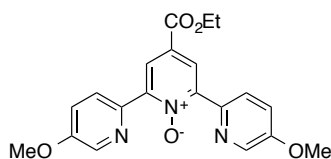
^{1}H NMR (400 MHz, CDCl$_3$): δ 8.69 (dd, *J* = 8.9, 0.5 Hz, 2H), 8.61 (s, 2H), 8.46 (dt, *J* = 3.0, 0.5 Hz, 2H), 7.30 (dd, *J* = 8.9, 3.0 Hz, 2H), 4.42 (q, *J* = 7.1 Hz, 2H), 3.93 (s, 6H), 1.41 (t, *J* = 7.2 Hz, 3H) ppm.

^{13}C NMR (101 MHz, CDCl$_3$): δ 164.2, 156.2, 148.4, 142.3, 137.9, 126.6, 126.3, 119.6, 61.9, 33.9, 14.5 ppm.

IR (v_{max}/cm^{-1}): 3096 (w), 3067 (w), 2993 (w), 2925 (w), 2842 (w), 1719 (s), 1619 (w), 1574 (m), 15558 (m), 1474 (m), 1448 (m), 1394 (w), 1362 (w), 1342 (w), 1304 (w), 1252 (s), 1220 (s), 118 (w), 1127 (w), 1111 (w), 1072 (w), 1017 (s), 905 (m), 824 (m), 760 (m), 734 (w), 708 (w).

HRESI-MS (+, m/z): [M+H]$^+$ 382.1421 calc. 382.1377, [M+Na]$^+$ 404.1245 calc. 404.1217, [M+K]$^+$ 420.0984 calc. 420.0956.

M.p.: 124–126 °C (decomp.)

4-Ethoxycarbonyl-5-methyl-2,2′-biypridine *N*-oxide (20lc)

[SZ 2170b]
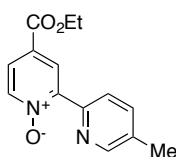
According to the general procedure, pyridine *N*-oxide **27l** (168 mg, 1.00 mmol), 2-bromo-5-methyl-pyridine (**28c**) (85.9 mg, 0.50 mmol), K$_3$PO$_4$ (221 mg, 1.04 mmol) and dimer **A** (9.5 mg, 0.013 mmol) in toluene (1.00 mL). Column chromatography provided bipyridine *N*-oxide **20lc** (69.4 mg, 0.27 mmol, 54%), terpyridine *N*-oxide **29lc** (7.9 mg, 0.023 mmol, 9%) as brownish solid, and starting material **27l** (93.3 mg, 0.56 mmol, recov. 85%).

^{1}H NMR (400 MHz, CDCl$_3$): δ 8.74 (dd, J = 2.7, 0.6 Hz, 1H), 8.69 (d, J = 8.2 Hz, 2H), 8.57 (dt, J = 2.3, 0.8 Hz, 1H), 8.29 (dt, J = 6.8, 0.6 Hz, 1H), 7.81 (ddd, J = 6.8, 2.6, 0.5 Hz, 1H), 7.62 (ddt, J = 8.2, 2.2, 0.7 Hz, 1H), 4.39 (q, J = 7.1 Hz, 2H), 2.40 (s, 3H), 1.39 (t, J = 7.1 Hz, 3H) ppm.

The chemical shifts are in agreement with previous reported values.[117]

4′-Ethoxycarbonyl-5,5″-dimethyl-2,2′:6,2″-terpyridine *N*-oxide (**29lc**)
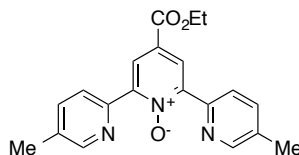
^{1}H NMR (400 MHz, CDCl$_3$): δ 8.62–8.59 (m, 4H), 8.51 (d, J = 8.1 Hz, 2H), 7.63 (dd, J = 8.2, 2.3 Hz, 2H), 4.42 (q, J = 7.1 Hz, 2H), 2.42 (s, 6H), 1.41 (t, J = 7.1 Hz, 3H) ppm.

^{13}C NMR (101 MHz, CDCl$_3$): δ 164.11, 150.21, 148.79, 147.40, 136.64, 134.47, 127.24, 126.67, 125.05, 61.93, 18.62, 14.46 ppm.

IR (v_{max}/cm^{-1}): 3095 (w), 3027 (w), 3007 (w), 2959 (w), 2925 (w), 2854 (w), 1729 (s), 1623 (w), 1562 (w), 1480 (m), 1463 (m), 1335 (m), 1253 (s), 1128 (w), 1112 (w), 1066 (w), 1020 (m), 905 (w), 865 (w), 826 (m), 767 (m), 767 (m), 741 (w), 708 (m).

HRESI-MS (+, m/z): [M+H]$^+$ 350.1509 calc. 350.1499, [M+Na]$^+$ 372.1324 calc. 372.1324.

M.p.: 118–120 °C (decomp.)

4-Ethoxycarbonyl-5-trifluromethyl-2,2′-biypridine *N*-oxide (20ld)

[SZ 2170c]
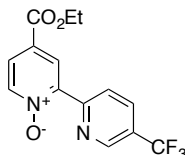
According to the general procedure, pyridine *N*-oxide **27l** (171 mg, 1.03 mmol), 2-bromo-5-trifluoro-methylpyridine (**28d**) (113 mg, 0.50 mmol), K$_3$PO$_4$ (213 mg, 1.00 mmol), and dimer **A** (9.9 mg, 0.014 mmol) in toluene (1.00 mL). Column chromatography provided bipyridine *N*-oxide **20ld** (43.3 mg, 0.14 mmol, 28%), and starting material **27l** (93.7 mg, 0.56 mmol, recov. 83%).

^{1}H NMR (400 MHz, CDCl$_3$): δ 9.02–8.96 (m, 2H), 8.82 (d, J = 2.6 Hz, 1H), 8.32 (d, J = 6.8 Hz, 1H), 8.06 (dd, J = 8.4, 2.4 Hz, 1H), 7.90 (dd, J = 6.8, 2.6 Hz, 1H), 4.42 (q, J = 7.1 Hz, 2H), 1.41 (t, J = 7.1 Hz, 3H) ppm.

^{19}F NMR (471 MHz, CDCl$_3$): δ –62.49 ppm

The chemical shifts are in agreement with previous reported values.[117]

4-Ethoxycarbonyl-5-trifluromethyl-2,2′-biypridine *N*-oxide (20le)

[SZ 2166]
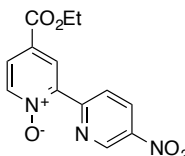
According to the general procedure, pyridine *N*-oxide **27l** (169 mg, 1.01 mmol), 5-nitro-2-bromo-pyridine (**28e**) (109 mg, 0.54 mmol), K$_3$PO$_4$ (216 mg, 1.02 mmol), and dimer **A** (9.2 mg, 0.025 mmol) in toluene (1.00 mL). Column chromatography did not provide **20le**, but recovered starting material **27l** (159 mg, 0.95 mmol, recov. 98%).

4-Ethoxycarbonyl-2-(4-methoxyphenyl)pyridine *N*-oxide (31lb)

[SZ 2167b]
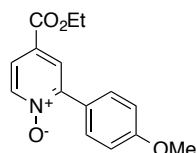
According to the general procedure, pyridine *N*-oxide **27l** (184 mg, 1.11 mmol), 4-methoxybromo-benzene (**47b**) (95.2 mg, 0.51 mmol), K_3PO_4 (219 mg, 1.03 mmol), and dimer **A** (9.2 mg, 0.025 mmol) in toluene (1.00 mL). Column chromatography provided biaryl *N*-oxide **31lb** (94.2 mg, 0.35 mmol, 68%) as a pale yellow solid, and teraryl *N*-oxide **49lb** (12.1 mg, 0.032 mmol, 3%) as orange solid and starting material **27l** (99.3 mg, 0.59 mmol, recov. 87%).

^{1}H NMR (400 MHz, CDCl$_3$): δ 8.28 (d, *J* = 6.8 Hz, 1H), 8.00 (d, *J* = 2.3 Hz, 1H), 7.80 (dt, *J* = 9.8, 2.1 Hz, 2H), 7.73 (dd, *J* = 6.8, 2.5 Hz, 1H), 6.98 (dt, *J* = 9.8, 2.3 Hz, 2H), 4.37 (q, *J* = 7.2 Hz, 2H), 3.83 (s, 3H), 1.37 (t, *J* = 7.1 Hz, 3H) ppm.

^{13}C NMR (101 MHz, CDCl$_3$): δ 163.8, 160.8, 149.1, 140.7, 130.8, 130.6, 127.2, 126.6, 124.1, 124.0, 123.7, 113.8, 61.9, 55.4, 14.3 ppm.

IR (ν_{max}/cm^{-1}): 3044 (w), 2982 (w), 2935 (w), 1716 (s), 1604 (s), 1514 (m), 1464 (m), 1433 (m), 1408 (w), 1390 (w), 1365 (w), 1303 (m), 1256 (s), 1241 (s), 1182 (m), 1126 (m), 1114 (m), 1045 (w), 1014 (m), 902 (m), 862 (w), 852 (w), 829 (m), 800 (w), 766 (m), 738 (m), 727 (m), 709 (w).

HRESI-MS (+, *m/z*): [M+H]$^+$ 274.1074 calc. 274.1083, [M+Na]$^+$ 296.0907 calc. 296.0893, [M+K]$^+$ 312.0643 calc. 312.0633.

M.p.: 79–81 °C

4-Ethoxycarbonyl-2,6-bis(4-methoxyphenyl)pyridine *N*-oxide (**49lb**)
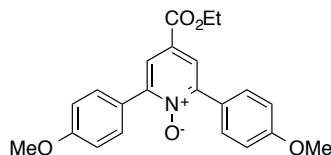
^{1}H NMR (400 MHz, CDCl$_3$): δ 7.96 (s, 2H), 7.83 (d, *J* = 8.6 Hz, 4H), 7.00 (d, *J* = 8.7 Hz, 4H), 4.42 (q, *J* = 7.1 Hz, 2H), 3.86 (s, 6H), 1.41 (t, *J* = 7.1 Hz, 3H) ppm.

^{13}C NMR (101 MHz, CDCl$_3$): δ 164.3, 160.8, 150.0, 131.2, 126.0, 125.2, 125.1, 113.8, 62.0, 55.5, 14.4 ppm.
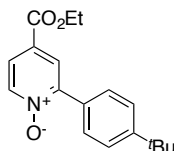
IR (ν_{max}/cm^{-1}): 2986 (w), 2925 (w), 2851 (w), 2832 (w), 1723 (s), 1609 (s), 1514 (s), 1444 (m), 1330 (w), 1291 (w), 1235 (s), 1179 (s), 1126 (m), 1112 (m), 1022 (s), 910 (w), 901 (w), 873 (w), 820 (m), 759 (m), 729 (w), 701 (w), 666 (w).

HRESI-MS (+, *m/z*): [M+H]$^+$ 380.1517 calc. 380.1492, [M+Na]$^+$ 402.1334 calc. 402.1312, [M+K]$^+$ 418.1070 calc. 418.1051.

M.p.: 137 °C

4-Ethoxycarbonyl-2-(4-*tert*-butylphenyl)pyridine *N*-oxide (31lc)

[SZ 2167a]

According to the general procedure, pyridine *N*-oxide **27l** (247 mg, 1.48 mmol), 4-*tert*-butyl-1-bromobenzene (**47c**) (108 mg, 0.51 mmol), K$_3$PO$_4$ (218 mg, 1.03 mmol) and dimer **A** (9.2 mg, 0.025 mmol) in toluene (1.00 mL). Column chromatography provided biaryl *N*-oxide **31lc** (111 mg, 0.37 mmol, 73%), teraryl *N*-oxide **49lc** (12.5 mg, 0.029 mmol, 3%) as pale yellow solids and recovered starting material **27l** (126 mg, 0.76 mmol, recov. 104%).

^{1}H NMR (400 MHz, CDCl$_3$): δ 8.31 (d, *J* = 6.7 Hz, 1H), 8.04 (d, *J* = 2.6 Hz, 1H), 7.82–7.71 (m, 3H), 7.50 (d, *J* = 8.6 Hz, 1H), 4.38 (q, *J* = 7.1 Hz, 2H), 1.38 (t, *J* = 7.1 Hz, 3H), 1.34 (s, 9H) ppm.

^{13}C NMR (101 MHz, CDCl$_3$): δ 163.7, 153.3, 149.4, 140.6, 128.9, 127.5, 126.6, 125.5, 124.1, 61.9, 34.9, 31.2, 14.3 ppm.

IR (v_{max}/cm^{-1}): 3058 (w), 2960 (m), 2904 (w), 2870 (w), 1719 (s), 1619 (w), 1473 (m), 1436 (m), 1393 (w), 1365 (w), 1300 (w), 1238 (s), 1138 (m), 1110 (m), 921 (w), 909 (w), 856 (m), 828 (m), 769 (m), 726 (m), 685 (w).

HRESI-MS (+, *m/z*): [M+H]$^+$ 300.1596 calc. 300.1594, [M+Na]$^+$ 322.1419 calc. 322.1413, [M+K]$^+$ 338.1150 calc. 338.1153.

M.p.: 96–97 °C

4-Ethoxycarbonyl-2,6-bis(4-*tert*-butylphenyl)pyridine *N*-oxide (**49lc**)
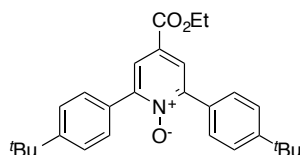
^{1}H NMR (400 MHz, CDCl$_3$): δ 8.01 (s, 2H), 7.80 (d, *J* = 8.4 Hz, 4H), 7.50 (d, *J* 0 8.4 Hz, 4H), 4.41 (q, *J* = 7.1 Hz, 2H), 1.40 (t, *J* = 7.1 Hz, 3H), 1.36 (s, 18H) ppm.

^{13}C NMR (101 MHz, CDCl$_3$): δ 164.3, 153.1, 150.2, 129.8, 129.4, 125.9, 125.7, 125.4, 61.9, 35.0, 31.4, 14.4 ppm.
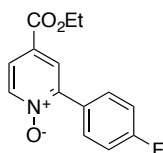
HRESI-MS (+, *m/z*): [M+H]$^+$ 432.2543 calc. 432.2533, [M+Na]$^+$ 454.2355 calc. 454.2353, [M+K]$^+$ 470.2090 calc. 470.2092.

IR (ν_{max}/cm^{-1}): 3065 (w), 2960 (s), 2907 (w), 2870 (w), 1719 (s), 1604 (w), 1554 (w), 1514 (w), 1461 (m), 1442 (m), 1387 (w), 1365 (m), 1328 (m), 1269 (m), 1241 (s), 1173 (w), 1104 (m), 1051 (w), 1011 (m), 912 (w), 844 (m), 834 (m), 769 (m), 738 (w), 688 (m).

M.p.: 141–145 °C

4-Ethoxycarbonyl-2-(4-fluorophenyl)pyridine *N*-oxide (31ld)

[SZ 2167d]

According to the general procedure, pyridine *N*-oxide **27l** (198 mg, 1.19 mmol), 4-fluorobromo-benzene (**47d**) (96.9 mg, 0.55 mmol), K$_3$PO$_4$ (242 mg, 1.14 mmol) and dimer **A** (9.2 mg, 0.025 mmol) in toluene (1.00 mL). Column chromatography provided biaryl *N*-oxide **31ld** (90.0 mg, 0.34 mmol, 63%) as a colorless solid, teraryl *N*-oxide **49ld** (13.4 mg, 0.038 mmol, 3%), and recovered starting material **27l** (107 mg, 0.64 mmol, recov. 86%).

^{1}H NMR (400 MHz, CDCl$_3$): δ 8.33 (d, *J* = 6.8 Hz, 1H), 8.03 (d, *J* = 2.4 Hz, 1H), 7.92 (d, *J* = 8.2 Hz, 2H), 7.85 (dt, *J* = 6.8, 1.7 Hz, 1H), 7.73 (d, *J* = 8.1 Hz, 2H), 4.39 (q, *J* = 7.1 Hz, 2H), 1.38 (t, *J* = 7.3 Hz, 3H) ppm.

^{13}C NMR (101 MHz, CDCl$_3$): δ 163.6, 163.5 (d, *J* = 251 Hz), 148.4, 140.7, 131.5 (d, *J* = 8.5 Hz), 127.8 (d, *J* = 3.4 Hz), 127.4, 126.7, 124.5, 115.6 (d, *J* = 22 Hz), 62.0, 14.3 ppm.
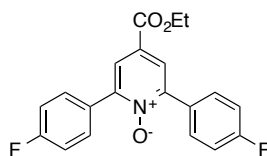
^{19}F NMR (471 MHz, CDCl$_3$): δ –109.71 ppm.

IR (ν_{max}/cm^{-1}): 3126 (w), 3058 (w), 2984 (w), 2935 (w), 1709 (s), 1598 (m), 1509 (m), 1466 (m), 1438 (m), 1392 (m), 1367 (m), 1271 (s), 1234 (s), 1163 (m), 1135 (w), 1105 (m), 1018 (m), 913 (w), 901 (w), 867 (w), 830 (s), 814 (m), 765 (m), 731 (m), 703 (w).

HRESI-MS (+, *m/z*): [M+H]$^+$ 262.0857 calc. 262.0874, [M+Na]$^+$ 284.0680 calc. 284.0693, [M+K]$^+$ 300.0411 calc. 300.0433.

M.p.: 104–106 °C

4-Ethoxycarbonyl-2,6-bis(4-fluorophenyl)pyridine *N*-oxide (**49ld**)

^{1}H NMR (400 MHz, CDCl$_3$): δ 8.00 (s, 2H), 7.83 (dd, J = 8.9, 5.4 Hz, 4H), 7.18 (t, J = 8.7 Hz, 4H), 4.43 (q, J = 7.1 Hz, 1H), 1.42 (t, J = 7.1 Hz, 1H) ppm.

^{13}C NMR (101 MHz, CDCl$_3$): δ 163.9, 163.5 (d, J = 250 Hz), 149.4, 131.8 (d, J = 7.9 Hz), 128.6, 126.2, 1266.0, 115.6 (d, J = 22 Hz), 62.2, 14.4 ppm.
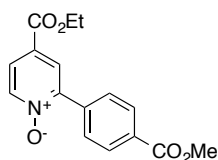
^{19}F NMR (471 MHz, CDCl$_3$): δ –110.0 ppm.

IR (v_{max}/cm^{-1}): 3044 (w), 2997 (w), 2954 (w), 1719 (s), 1604 (m), 1508 (m), 1473 (w), 1436 (m), 1396 (w), 1365 (w), 1247 (s, R$_3$N$^+$-O$^-$), 1163 (w), 1129 (w), 1107 (m), 1042 (w), 1014 (m), 971 (w), 902 (w), 828 (m), 766 (m), 729 (m), 701 (m) .

HRESI-MS (+, m/z): [M+H]$^+$ 356.1071 calc. 356.1093, [M+Na]$^+$ 378.0895 calc. 378.0912, [M+K]$^+$ 394.0630 calc. 394.0652.

M.p.: 194 °C

4-Ethoxycarbonyl-2-(4-methoxycarbonylphenyl)pyridine *N*-oxide (31le)

[SZ 2167f]

According to the general procedure, pyridine *N*-oxide **27l** (211 mg, 1.26 mmol), 4-methoxycarbonyl-bromobenzene (**47e**) (112 mg, 0.52 mmol), K$_3$PO$_4$ (226 mg, 1.07 mmol) and dimer **A** (9.2 mg, 0.025 mmol) in toluene (1.00 mL). Column chromatography provided biaryl *N*-oxide **31le** (80.1 mg, 0.29 mmol, 56%), teraryl *N*-oxide **49le** (6.3 mg, 0.014 mmol, 1%) as colorless solids, and starting material **27l** (126 mg, 0.76 mmol, recov. 84%).

^{1}H NMR (400 MHz, CDCl$_3$): δ 8.33 (d, J = 6.8 Hz, 1H), 8.14 (d, J = 8.2 Hz, 2H), 8.05 (d, J = 2.5 Hz, 1H), 7.88 (d, J = 8.2 Hz, 2H), 7.84 (dd, J = 6.6, 2.3 Hz, 1H), 4.40 (q, J = 7.1 Hz, 2H), 3.93 (s, 3H), 1.39 (t, J = 7.4 Hz, 3H) ppm.

^{13}C NMR (101 MHz, CDCl$_3$): δ 166.5, 163.5, 148.5, 140.8, 136.1, 131.3, 129.7, 129.4, 127.7, 126.8, 125.1, 62.2, 52.4, 14.3 ppm.

IR (v_{max}/cm^{-1}): 3096 (w), 3047 (w), 2994 (w), 2954 (w), 1716 (s), 1626 (w), 1610 (w), 1573 (w), 1548 (w), 1514 (w), 1470 (w), 1436 (s), 1399 (w), 1374 (w), 1269 (m), 1244 (s), 1182 (w), 1132 (w), 1107 (s), 1039 (m), 1020 (m), 968 (w), 939 (w), 902 (w), 859 (w), 769 (m), 750 (w), 729 (m), 701 (m).

HRESI-MS (+, m/z): [M+H]$^+$ 302.1036 calc. 302.1023, [M+Na]$^+$ 324.0855 calc. 324.0842, [M+K]$^+$ 340.0582 calc. 340.0582.

M.p.: 112–113 °C

4-Ethoxycarbonyl-2,6-bis(4-methoxycarbonylphenyl)pyridine *N*-oxide (**49le**)
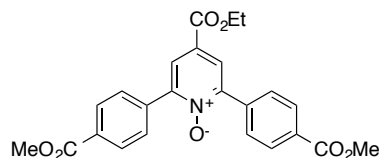
^{1}H NMR (400 MHz, CDCl$_3$): δ 8.16 (d, J = 7.6 Hz, 4H), 8.06 (s, 2H), 7.91 (d, J = 7.7 Hz, 4H), 4.44 (q, J = 7.1 Hz, 2H), 3.96 (s, 6H), 1.42 (t, J = 7.1 Hz, 3H) ppm.

^{13}C NMR (101 MHz, CDCl$_3$): δ 166.6, 163.8, 149.6, 136.7, 131.4, 129.7, 126.7, 126.3, 62.3, 52.5, 14.4 ppm.

IR (v_{max}/cm^{-1}): 3073 (w), 2990 (w), 2954 (w), 2922 (w), 2851 (w), 1719 (s), 1613 (w), 1558 (w), 1515 (w), 1439 (m), 1387 (w), 1365 (w), 1313 (m), 1271 (s), 1243 (s, R$_3$N$^+$-O$^-$), 1185 (m), 1110 (s), 1049 (w), 1017 (m), 966 (w), 911 (w), 856 (w), 831 (w), 805 (w), 766 (w), 750 (w), 728 (m), 699 (m).

HRESI-MS (+, *m/z*): [M+Na]$^+$ 458.1172 calc. 458.1210.

M.p.: 194–196 °C (decomp.)

4-Ethoxycarbonyl-2-(4-trifluoromethylphenyl)pyridine *N*-oxide (31lf)

[SZ 2167c]
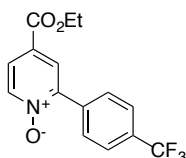
According to the general procedure, pyridine *N*-oxide **27l** (181 mg, 1.08 mmol), 4-trifluoromethyl-bromobenzene (**47f**) (113 mg, 0.50 mmol), K$_3$PO$_4$ (243 mg, 1.14 mmol) and dmer **A** (9.2 mg, 0.025 mmol) in toluene (1.00 mL). Column chromatography provided biaryl *N*-oxide **31lf** (82.2 mg, 0.26 mmol, 53%) as a colorless solid, teraryl *N*-oxide **49lf** (24.0 mg, 0.053 mmol, 5%) as pale yellow solid, and starting material **27l** (85.4 mg, 0.51 mmol, recov. 77%).

^{1}H NMR (400 MHz, CDCl$_3$): δ 8.33 (d, J = 6.8 Hz, 1H), 8.03 (d, J = 2.4 Hz, 1H), 7.92 (d, J = 8.2 Hz, 2H), 7.85 (dt, J = 6.8, 1.7 Hz, 1H), 7.73 (d, J = 8.1 Hz, 2H), 4.39 (q, J = 7.1 Hz, 2H), 1.38 (t, J = 7.3 Hz, 3H) ppm.

^{13}C NMR (101 MHz, CDCl$_3$): δ 163.5, 148.0, 140.8, 135.4, 131.7 (q, J = 33 Hz), 129.8, 127.7, 126.9, 125.4 (q, J = 3.7 Hz), 125.2, 122.5, 62.1, 14.3 ppm.
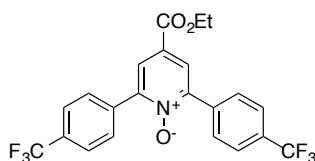
^{19}F NMR (471 MHz, CDCl$_3$): δ –62.85 ppm.

IR (v_{max}/cm^{-1}): 3124 (w), 3068 (w), 2997 (w), 1712 (s), 1616 (m), 1545 (w), 1520 (w), 1473 (m), 1442 (m), 1396 (m), 1368 (m), 1321 (s), 1300 (m), 1269 (m), 1244 (s), 1207 (w), 1166 (m), 1110 (s), 1070 (m), 1014 (m), 918 (w), 902 (w), 850 (m), 834 (m), 769 (m), 750 (w), 732 (w), 713 (w).

HRESI-MS (+, *m/z*): [M+H]+ 312.0823 calc. 312.0842, [M+Na]+ 334.0645 calc. 334.0661, [M+K]+ 350.0379 calc. 350.0401.

M.p.: 108–110 °C

4-Ethoxycarbonyl-2,6-bis(4-trifluoromethylphenyl)pyridine *N*-oxide (**49lf**)

^{1}H NMR (400 MHz, CDCl$_3$): δ 8.08 (s, 2H), 7.95 (d, *J* = 8.1 Hz, 4H), 7.76 (d, *J* = 8.6 Hz, 4H), 4.45 (q, *J* = 7.2 Hz, 2H), 1.42 (t, *J* = 7.1 Hz, 3H) ppm.

^{13}C NMR (101 MHz, CDCl$_3$): δ 163.6, 149.2, 135.8, 131.9 (q, *J* = 33 Hz), 126.8, 126.5, 125.5 (q, *J* = 3.6 Hz), 125.3, 122.6, 62.4, 14.4 ppm.

^{19}F NMR (471 MHz, CDCl$_3$): δ −62.83 ppm.

IR (v_{max}/cm^{-1}): 3071 (w), 2994 (w), 2935 (w), 1719 (s), 1619 (w), 1560 (w), 1321 (s), 1247 (s), 1163 (m), 1104 (s), 1070 (s), 1014 (m), 909 (w), 847 (w), 825 (m), 760 (m), 732 (m), 716 (m) .

HRESI-MS (+, *m/z*): [M+H]+ 456.0997 calc. 456.1029, [M+Na]+ 478.0821 calc. 478.0848, [M+K]+ 494.0552 calc. 494.0588.

M.p.: 117–118 °C

4-Ethoxycarbonyl-2-(4-cyanophenyl)pyridine *N*-oxide (31lg)

[SZ 2167e]
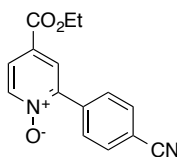
According to the general procedure, pyridine *N*-oxide **27l** (183 mg, 1.09 mmol), 4-cyano-bromobenzene (**47g**) (95.6 mg, 0.53 mmol), K$_3$PO$_4$ (218 mg, 1.03 mmol) and dimer **A** (9.2 mg, 0.025 mmol) in toluene (1.00 mL). Column chromatography provided biaryl *N*-oxide **31lg** (75.1 mg, 0.28 mmol, 53%) as a pale yellow solid, teraryl *N*-oxide **49lg** (20.3 mg, 0.055 mmol, 5%) as as yellow solid, and starting material **27l** (106 mg, 0.63 mmol, recov. 89%).

^{1}H NMR (400 MHz, CDCl$_3$): δ 8.33 (d, *J* = 6.8 Hz, 1H), 8.03 (d, *J* = 2.4 Hz, 1H), 7.92 (d, *J* = 8.2 Hz, 2H), 7.85 (dt, *J* = 6.8, 1.7 Hz, 1H), 7.73 (d, *J* = 8.1 Hz, 2H), 4.39 (q, *J* = 7.1 Hz, 2H), 1.38 (t, *J* = 7.3 Hz, 3H) ppm.

^{13}C NMR (101 MHz, CDCl$_3$): δ 163.3, 147.5, 140.9, 136.2, 132.2, 130.1, 127.6, 127.0, 125.5, 118.3, 113.6, 62.2, 14.3 ppm.

IR (v_{max}/cm^{-1}): 3140 (w), 3050 (w), 2997 (w), 2228 (m), 1712 (s), 1616 (w), 1470 (m), 1436 (m), 1390 (m), 1359 (m), 1306 (m), 1244 (s), 1114 (m), 1014 (m), 909 (w), 868 (w), 847 (w), 828 (m), 772 (m), 738 (m), 716 (w), 701 (w).

HRESI-MS (+, m/z): [M+H]$^+$ 269.0923 calc. 269.0921, [M+Na]$^+$ 291.0752 calc. 291.0740, [M+K]$^+$ 307.0489 calc. 307.0480.

M.p.: 136–139 °C

4-Ethoxycarbonyl-2,6-bis(4-cyanophenyl)pyridine *N*-oxide (**49lg**)
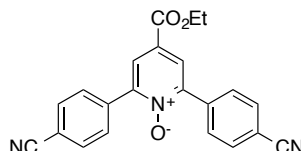
^{1}H NMR (400 MHz, CDCl$_3$): δ 8.07 (s, 2H), 7.94 (d, J = 8.4 Hz, 4H), 7.79 (d, J = 8.5 Hz, 4H), 4.45 (q, J = 7.1 Hz, 2H), 1.42 (t, J = 7.1 Hz, 3H) ppm.

^{13}C NMR (101 MHz, CDCl$_3$): δ 163.3, 148.7, 136.5, 132.2, 130.3, 127.0, 126.6, 118.3, 113.8, 62.5, 14.4 ppm.

IR (v_{max}/cm^{-1}): 3070 (w), 3048 (w), 2990 (w), 2961 (w), 2925 (w), 2855 (w), 2224 (m), 1712 (s), 1622 (w), 1606 (w), 1558 (w), 1510 (w), 1445 (w), 1365 (w), 1329 (w), 1252 (s), 1130 (m), 1114 (m), 1053 (w), 1017 (m), 921 (w), 827 (m), 770 (m), 760 (m), 728 (m), 695 (m).

HRESI-MS (+, m/z): [M+H]$^+$ 370.1191 calc. 370.1189, [M+Na]$^+$ 392.1009 calc. 392.1006, [M+K]$^+$ 408.0747 calc. 408.0745.

M.p.: 251 °C (decomp.)

## 4.13.4 Monitoring by ^{31}P NMR spectroscopy under catalytic conditions

General procedure A:

In a glovebox, K$_3$PO$_4$ (106 mg, 0.50 mmol, 2.0 equiv.) was weighted in reaction vials equipped with a stirring bar and 0.75 mL of a stock solution containing the aryl halide **28a** or **47a** (0.50 M), pyridine *N*-oxide **27** (1.00 M), and dimer **A** (0.0125 M) in C$_6$D$_6$ was added to each vial. After sealing the reaction vials with a Teflon-lined screw cap, the vials were heated outside the glovebox by a pre-heated aluminum well plate at 120 °C. The reactions were aborted at different time points (t = 0 min, 10 min, 30 min, 60 min, 120 min, 16 h) by immediate cooling in another pre-cooled aluminum well plate at 0 °C. The reaction vials were again brought inside the glovebox, and the reaction solutions were pipetted into NMR tubes, containing a capillary standard with P(OMe)$_3$ in C$_6$D$_6$. Equipped with a

Swagelok adapter, the NMR tubes were sealed by ablating and ^{31}P, and ^{1}H NMR were subsequently recorded. Yields were calculated as percentage of the sum of integrals of all phosphor species.
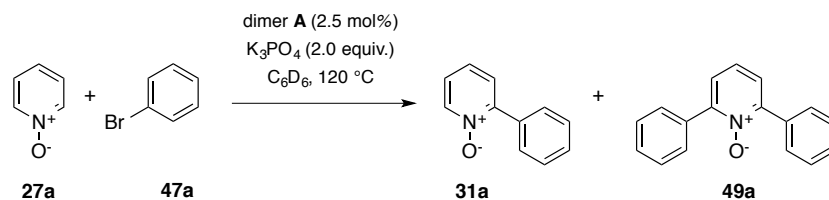
General procedure B:

Similar to general procedure A, with the modification that the reactions were directly carried out in NMR tubes, heated in an oil bath and cooled in an ice bath.
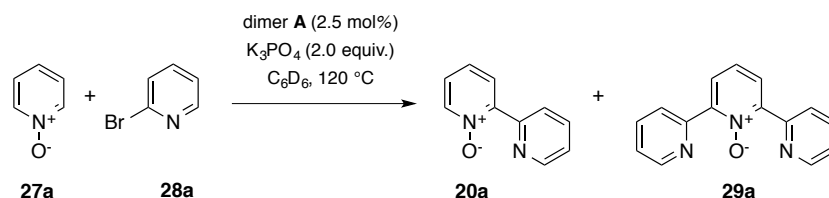
[SZ 2143]

According to procedure A, a stock solution was prepared of pyridine N-oxide **27a** (428 mg, 4.50 mmol), bromopyridine **28a** (366 mg, 2.31 mmol) and dimer **A** (41.0 mg, 0.056 mmol) in C$_6$D$_6$ (4.50 mL).
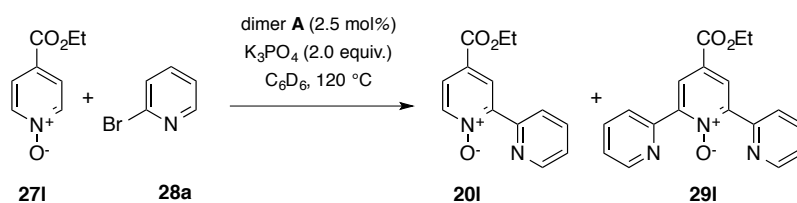
entry	shift δ [ppm]	percentage of P in [%] at t =				
		0 min	10 min	30 min	120 min	960 min
1	85.0					54
2	66.0			8	23	14
3	62.0					4
4	47.8				13	3
5	45.0					7
6	62.3			13	13	
7	62.6			17	26	
8	9.6			5	3	2
9	8.8			24	22	
10	3.2					14
11	−8.1	100				
12	−9.2		100	35		

[SZ 2144]

According to procedure A, a stock solution was prepared of pyridine N-oxide **27a** (754 mg, 4.51 mmol), bromobenzene **47a** (369 mg, 2.24 mmol) and dimer **A** (41.7 mg, 0.057 mmol) in C$_6$D$_6$ (4.50 mL).
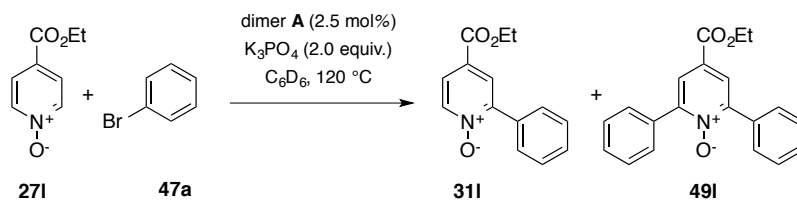
entry	shift δ	percentage of P in [%] at t =					
	[ppm]	0 min	10 min	30 min	60 min	120 min	960 min
1	85.0						7
2	61.9						18
3	60.9						15
4	62.3						22
5	9.7						9
6	3.2						29
7	−8.2	100					
8	−9.2		100	100	100	100	

27l   **28a**   **20l**   **29l**

[SZ 2141]

According to procedure A, a stock solution was prepared of pyridine *N*-oxide **27l** (428 mg, 4.50 mmol), bromopyridine **28a** (366 mg, 2.31 mmol) and dimer **A** (41.0 mg, 0.056 mmol) in C_6D_6 (4.50 mL).

entry	shift δ	percentage of P in [%] at t =				
	[ppm]	0 min	10 min	60 min	120 min	960 min
1	−8.28	100				
2	9.7			8	3	
3	3.2					19
4	−9.2		100	68		
5	62.5			15	9	11
6	85.0				76	44
7	66.0			10	12	14
8	62.2					12

27l   **47a**   **31l**   **49l**

[SZ 2142]

According to procedure A, a stock solution was prepared of pyridine *N*-oxide **27l** (753 mg, 4.50 mmol), bromobenzene **47a** (356 mg, 2.27 mmol) and dimer **A** (41.3 mg, 0.057 mmol) in C_6D_6 (4.50 mL).

447

entry	shift δ	percentage of P in [%] at $t =$				
	[ppm]	0 min	10 min	30 min	60 min	960 min
1	–8.40	100				
2	–9.3		100	100	100	
3	85.0					91

R = CO$_2$Et **27l**
^{t}Bu **27z**

R = CO$_2$Et **51l**
^{t}Bu **51z**
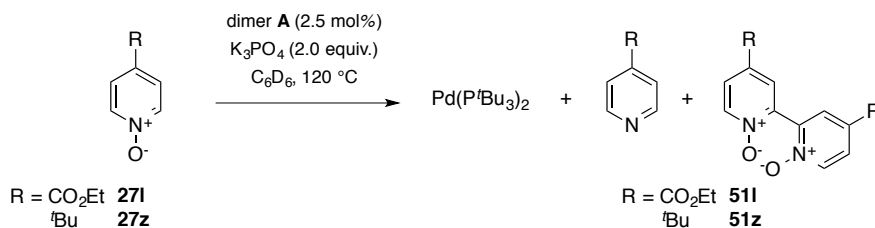
[SZ 2147/SZ 2150]

According to the general procedure B, an NMR tube was loaded with K$_3$PO$_4$ (106 mg, 0.50 mol) and a stock solution of ester pyridine N-oxide **27l** (501 mg, 3.00 mmol), dimer **A** (27.5 mg, 0.075 mmol) in C$_6$D$_6$ (3.00 mL) or with *tert*-butylpyridine N-oxide **27z** (454 mg, 3.00 mmol), dimer **A** (27.5 mg, 0.075 mmol) in C$_6$D$_6$ (3.00 mL).

entry	shift δ	R = CO$_2$Et (**27l**)		R = ^{t}Bu (**27z**)^a	
	[ppm]	10 min	30 min	10 min	30 min
1	124.7				6
2	104.2			6	8
3	102.6				1
4	85.0	95	92	65	74
5	62.3		2		
6	61.9	3	4	1	
7	9.7	3	2	2	3
8	3.2		1		2
9	0.8			8	2
10	–0.7			18	5

^{a}Formation of **51z** confirmed by ^{1}H NMR and HRESI-MS; formation of 4-*tert*-butylpyridine confirmed by GC-MS.

R = CO$_2$Et **27l**
^{t}Bu **27z**
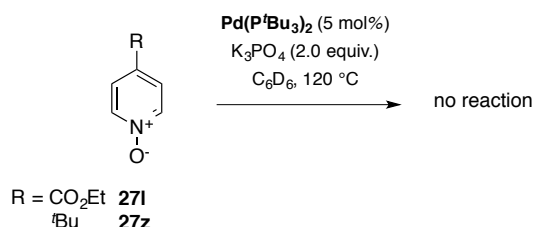
[SZ 2151/SZ 2152]

According to the general procedure B, solutions of ester pyridine N-oxide **27l** (168 mg, 1.00 mmol) and Pd(P^{t}Bu$_3$)$_2$ (12.4 mg, 0.024 mmol), or *tert*-butylpyridine N-oxide **27z** (151 mg, 1.00 mmol) and Pd(P^{t}Bu$_3$)$_2$ (12.4 mg, 0.024 mmol) each in C$_6$D$_6$ (1.00 mL) were prepared.

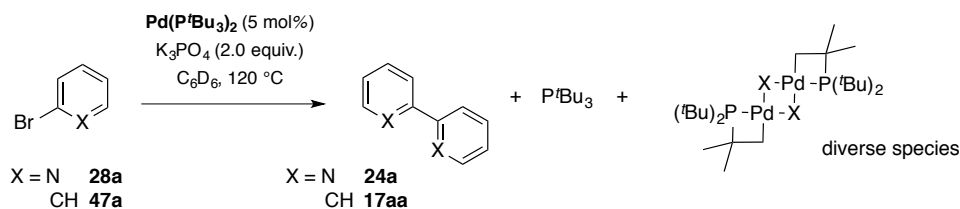| entry	shift δ	R = CO$_2$Et (27l)		R = ^{t}Bu (27z)	
	[ppm]	10 min	30 min	10 min	30 min
1	85.0	100	97	98	97
2	62.3		2	2	1
3	29.4		<1		
4	9.7		<1		<1
5	3.2		<1		<1
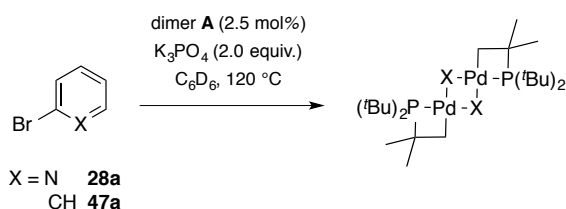
[SZ 2157/SZ 2158]

According to the general procedure B, stock solutions of bromopyridine 28a (79 mg, 0.50 mmol) and dimer A (9.7 mg, 0.026 mmol), or bromobenzene 47a (81 mg, 0.52 mmol) and dimer A (9.4 mg, 0.026 mmol) each in C$_6$D$_6$ (1.00 mL) were prepared.

| entry	shift δ	X = N (28a)		X = CH (47a)	
	[ppm]	10 min	60 min	10 min	60 min
1	130.6	9			
2	127.2	3			
3	106.5		4		
4	66.0		4		
5	49.0				11
6	−8.0 (m)	88		100	
7	−9.2		81		48
8	−9.7				41

[SZ 2159/2160]

According to the general procedure B, solutions of bromopyridine 28a (80 mg, 0.51 mmol) and Pd(P^{t}Bu$_3$)$_2$ (12.8 mg, 0.025 mmol), or bromobenzene 47a (82 mg, 0.52 mmol) and Pd(P^{t}Bu$_3$)$_2$ (12.7 mg, 0.025 mmol) each in C$_6$D$_6$ (1.00 mL).

entry	shift δ [ppm]	X = N (**28a**)				
		0 min	2 min	10 min	30 min	960 min
1	106.6					3
2	101.1					12
3	85.0	100	48			
4	62.3		52	100	67	26
5	47.7					12
6	3.2				10	12
7	−9.2				23	35
8	approx. yield[b] of **24a** [%]	0	<1	3	7	21

entry	shift δ [ppm]	X = CH (**47a**)				
		0 min	2 min	10 min	30 min	960 min[b]
1	85.0	100	36	5		
2	62.3		37	44	52	13
3	55.4[c]					17
4	3.2		9	3	7	3
5	−9.2		10	28	58	15
6	−9.7		7	20	35	16
7	−14.8[c]					21
8	approx. yield[a] of **17aa** [%]	0	<1	3	3	6

[a]Yields are calculated from the ratio of **28a/24a** and **47a/17aa**. [b]Formation of another unidentified species observed in ^{1}H NMR spectrum. [c]Doublet $J = 392$ Hz.
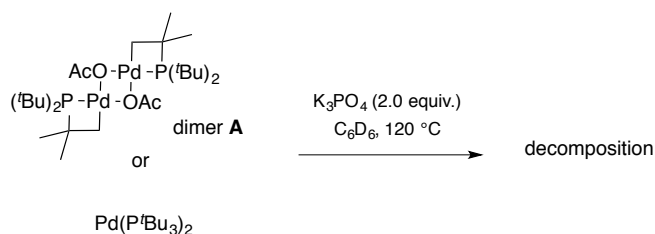

[SZ 2161/SZ 21062]

According to procedure B, dimer **A** (5.5 mg, 0.015 mmol) or Pd(P^{t}Bu$_3$)$_2$ (6.7 mg, 0.013 mmol) and C$_6$D$_6$ were added to the NMR tube containing K$_3$PO$_4$.

entry	shift δ [ppm]	with dimer **A** 10 min	with Pd(P^{t}Bu$_3$)$_2$ 10 min
1	132.8	3	
2	124.1	7	
3	85.0	6	97
4	65.8	1	
5	61.6	3	
6	38.2	3	
7	6.6	14	
8	3.2		3
9	−7.3	27	
10	−8.6	34	

[SZ 2162/SZ 2163]

According to the general procedure B, P^{t}Bu$_3$ (2.5 mg, 0.0125 mmol) bromopyridine **28a** (39.4 mg, 0.25 mmol) or bromobenzene **47a** (39.1 mg, 0.25 mmol) were weighted in NMR tubes containing K$_3$PO$_4$. Then a stock solution of pyridine *N*-oxide **27z** (151 mg, 1.00 mmol) in C$_6$D$_6$ (1.00 mL) was divided to the both NMR tubes. After heating for 16 h at 120 °C, ^{1}H- and ^{31}P NMR spectra were recorded showing no conversions.

4.13.5 Isolation of palladium(II) intermediates

[SZ 2073]

In a glovebox under inert atmosphere, a NMR tube was loaded with K$_3$PO$_4$ (9.6 mg, 0.05 mmol), bromopyridine **28a** (15.8 mg, 0.10 mmol), Pd(P^{t}Bu$_3$)$_2$ (25.6 mg, 0.05 mmol), and C$_6$D$_6$ (0.60 mL). The NMR tube was sealed, and the reaction mixture analyzed by ^{1}H NMR spectroscopy, which showed bromopyridine **28a**. The corresponidng ^{31}P NMR spectrum showed one single peak at 84.9 ppm (Pd(P^{t}Bu$_3$)$_2$). Then the reaction mixture was heated at 100 °C for 1 h, during which a yellow precipitate and palladium(0) were formed. Analysis by ^{1}H NMR spectroscopy still showed only one set of signals, which belong to bromopyridine **28a**. The ^{31}P NMR spectrum showed, besides the peak 85.3 ppm (Pd(P^{t}Bu$_3$)$_2$), an additional one at 62.4 ppm (P^{t}Bu$_3$) in a ratio 1.5:1. Heating the reaction mixture over night, the reulting ^{1}H NMR exhibited one single set of aromatic signals identified as bipyridine **24a**. The ^{31}P NMR spectrum showed the peak at 62.4 ppm (P^{t}Bu$_3$) as a single signal.

[SZ 2081c]

In a glovebox under inert atmosphere, an NMR tube was loaded with 3-methyl-2-bromopyridine (**28f**) (37.3 mg, 0.22 mmol), Pd(P^{t}Bu$_3$)$_2$ (26.8 mg, 0.05 mmol), and toluene (0.60 mL). The NMR tube was sealed and allowed to stand at room temperature. After 2 weeks crystals suitable for X-ray analysis were formed of an insoluble complex with the structure of complex **I**.
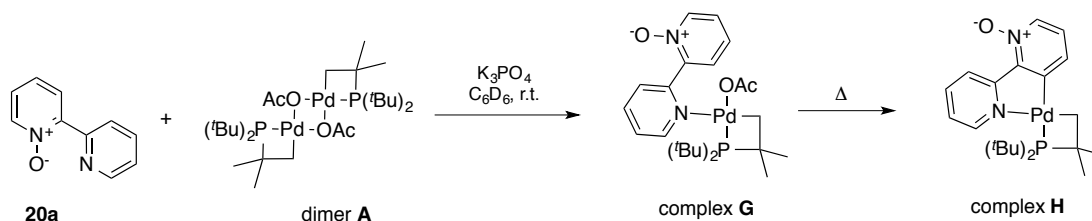
[SZ 2084b–85b, SZ 2089]

In a glovebox under inert atmosphere, an NMR tube was loaded with K$_3$PO$_4$ (10.8 mg, 0.05 mmol), bipyridine *N*-oxide **20a** (8.6 mg, 0.05 mmol), dimer **A** (18.1 mg, 0.025 mmol) and C$_6$D$_6$ (0.60 mL). The NMR tube was sealed and ^{1}H NMR and ^{31}P NMR spectra were recorded. The ^{1}H NMR spectrum showed a new set of signals, which belong to complex **G**. Heating the reaction mixture at 80 °C for 16.5 h led to a color change from colorless to bright yellow and provided a new set of signals in the aromatic region. This new set of signals might be assigned a structure of complex **H**.

^{1}H NMR (400 MHz, C$_6$D$_6$): δ 9.38 (br s, 1H), 8.60 (br s, 1H), 8.47 (br s, 1H), 7.93 (d, J = 6.6 Hz, 1H), 6.63 (t, J = 6.2 Hz, 1H), 6.49 (t, J = 7.8 Hz, 1H), 6.20 (t, J = 7.2 Hz, 1H), 2.14 (s, 2H), 1.44 (d, J = 13.5 Hz, 18H), 1.44 (d, J = 11.6 Hz, 6H, overlapping) ppm.

^{31}P NMR (162 MHz, C$_6$D$_6$): δ 9.48 ppm.

HRESI-MS (+, *m/z*): [M-OAc]$^+$ 479.1466, calc. 479.1438.

Independent synthesis of complex **G**:
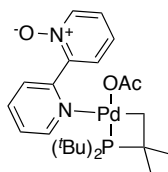
[SZ 2032]

Bipyridine *N*-oxide **20a** (17.5 mg, 0.10 mmol) and dimer **A** (37.2 mg, 0.51 mmol) were dissolved in CDCl$_3$ (0.70 mL). Slow diffusion of Et$_2$O into this solution provided crystals, which were measured by X-ray diffraction.

^{1}H NMR (400 MHz, CDCl$_3$, r.t.): δ 8.86 (br s, 1H), 8.73 (br s, 1H), 8.55 (br s, 1H), 8.27 (dd, J = 6.5, 0.7 Hz, 1H), 7.60 (td, J = 7.9, 1.7 Hz, 1H), 7.43 (t, J = 7.5 Hz, 1H), 7.34 (t, J = 6.5 Hz, 1H), 7.28 (t, J = 7.1 Hz, 1H), 1.89 (s, 3H), 1.48 (d, J = 13.6 Hz, 18H), 1.34 (br s, 6H) ppm.

^{31}P NMR (162 MHz, CDCl$_3$): δ = –12.60 ppm.

^{1}H NMR (500 MHz, CDCl$_3$, –45 °C): δ 8.98 (d, J = 8.1 Hz, 2H), 8.28 (t, J = 7.9 Hz, 2H), 7.66 (m, 2H), 1.59 (d, J = 13.9 Hz, 18H), 1.57 (d, J = 13.6 Hz, 6H), 1.29 (d, J = 3.5 Hz, 2H) ppm.

^{31}P NMR (202 MHz, CDCl$_3$, –70 °C): δ = –12.60 ppm

^{1}H NMR (400 MHz, C$_6$D$_6$, r.t.): δ 9.37 (br s, 1H), 8.60 (br s, 1H), 8.47 (br s, 1 H), 7.93 (d, J = 6.5 Hz, 1H), 6.64–6.61 (m, 1H), 6.49 (br s, 1H), 6.20 (t, J = 6.3 Hz, 1H), 2.14 (s, 3H), 1.43 (d, J = 13.4 Hz, + overlaying br s, 26H) ppm.

^{31}P NMR (162 MHz, C$_6$D$_6$, r.t): δ –8.08 ppm.

HRESI-MS (+, m/z): [M]$^+$ 479.1466 calc. 463.1449.

4.13.6 Optimization of the reaction conditions

General procedure A:

In a glovebox under inert atmosphere, K$_3$PO$_4$ (2.0 equiv.), pyridine N-oxide **27a** (2.0 equiv.), catalyst (5 mol%[Pd]), additives and pyridyl pseudo(halide) **28** were weighted ot in an oven-dired Schlenk flask. After Addition of toluene (1 M in N-oxide **27a**) the flask was brought outside the glovebox and heated under stirring for 16 h. After cooling to room temperature, the reaction mixture was subjected to column chromatography (MeOH in DCM mixtures: 0–10%, 1% increments).

General procedure B:

Samples were prepared analogous to the general procedure A, with the exception that after cooling to room temperature the solvent was removed, TMB (internal standard) and CDCl$_3$ were added. The resulting mixtures were filtered, and the filtrate was analyzed by ^{1}H NMR spectroscopy. Quantification of the products was done from integration of the product signals relative to the peak of aromatic protons of the internal standard.
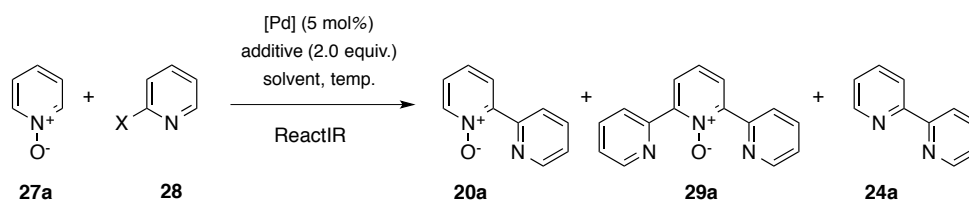
entry	X	additive (equiv.)	solvent	temp.	catalyst	method	20a [%]	29a [%]	24a [%]
1	Br	–	toluene	120 °C	dimer A	isolated	44	–	10
2	Br	–	toluene	120 °C	dimer A	^{1}H NMR	45	5	28
3[a]	Br	–	toluene	120 °C	dimer A	isolated	33	9	14
4[b]	Br	–	toluene	120 °C	dimer A	isolated	34	8	20
5[c]	Br	–	toluene	120 °C	dimer A	isolated	38	6	8
6[d]	Br	–	toluene	100 °C	dimer A	isolated	44	6	26
7[d]	Br	–	toluene	80 °C	dimer A	isolated	51	11	14
6[d]	Br		toluene	80 °C	dimer A	^{1}H NMR	53	–	16
8	Br	AgOAc (2.0)	toluene	80 °C	dimer A	^{1}H NMR	10	–	–
9	Br	AgOTf (1.0)	toluene	80 °C	dimer A	^{1}H NMR	25	–	–
10	Br	Ag$_2$CO$_3$ (2.0)	toluene	80 °C	dimer A	isolated	27	8	–
11[d]	Br	Ag$_2$CO$_3$ (2.0)	THF	70 °C	dimer A	isolated	3	–	–
12	Br	–	THF	120 °C	dimer A	isolated	46	6	
13[d]	Br		THF	80 °C	dimer A	isolated	54	13	
14	Br	–	benzene	120 °C	dimer A	isolated	47	7	
15	Br	–	DME	120 °C	dimer A	isolated	44	7	
16[d]	Br		DME	80 °C	dimer A	isolated	53	11	
17	Br	–	DMF	120 °C	dimer A	isolated	42	7	
18	Br	–	dioxane	120 °C	dimer A	isolated	38	4	
19	Cl	–	toluene	120 °C	dimer A	isolated	28		
20	Cl	–	toluene	120 °C	dimer A	^{1}H NMR	34	8	38
21	OTf	–	toluene	120 °C	dimer A	isolated	16		
22	OTs	–	toluene	120 °C	dimer A	isolated	4		
23	Br	–	toluene	120 °C	Herrmann-Beller	isolated	18	–	–
24	Br	–	toluene	120 °C	Pd(OAc)$_2$/ CataCXiumA	isolated	< 1	–	–
25	Br	AgOAc (0.1)	toluene	120 °C	(IPr)PdCl$_2$(3-ClPy)	^{1}H NMR	8	–	24
26	Br	AgOAc (0.1)	toluene	120 °C	(IMes)PdCl$_2$(3-ClPy)	^{1}H NMR	23	–	24
27	Br	AgOAc (0.1)	toluene	80 °C	(IMes)PdCl$_2$(3-ClPy)	^{1}H NMR	10	–	–
28	Br	–	toluene	120 °C	complex F(BF$_4$)	^{1}H NMR	30	6	
29	Br	ZnCl$_2$ (x.x)	toluene	120 °C	dimer A	isolated	0	0	–
30	Br	ZnCl$_2$ (x.x)	THF	120 °C	dimer A	isolated	0	0	–
31	Cl	ZnCl$_2$ (x.x)	toluene	120 °C	dimer A	isolated	0	0	–
32	Cl	ZnCl$_2$ (x.x)	THF	120 °C	dimer A	isolated	0	0	–
33	Br	MgCl$_2$ (x.x)	toluene	120 °C	dimer A	isolated	0	0	–
34	Br	MgCl$_2$ (x.x)	THF	120 °C	dimer A	isolated	0	0	–
35	Br	MS 4Å	toluene	120 °C	dimer A	isolated	29	3	–
36[e]	Br	MS 4Å	toluene	120 °C	dimer A	isolated	12	3	–

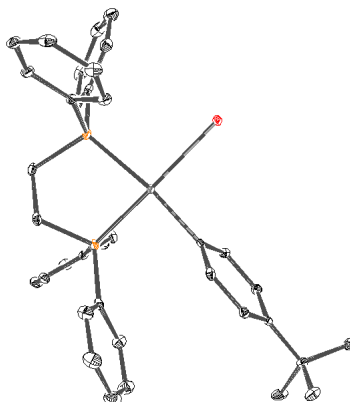[a]28a was added via syringe pump; addition rate 2.1 mM/min. [b]28a was added via syringe pump; addition 1.1 mM/min. [c]Half-molar reaction solution. [d]Reaction time was 2 days. [e]K$_2$CO$_3$ instead of K$_3$PO$_4$.

AcO-Pd-P(^{t}Bu)$_2$
(^{t}Bu)$_2$P-Pd-OAc

dimer A

Br Pd -P(o-tol)$_2$
(o-tol)$_2$P -Pd -Br

Herrmann-Beller catalyst

R^2 R^2
R^1 — R^2 R^2 — R^1
Cl—Pd-Cl
N
Cl

NHC-palladium catalysts

Pd
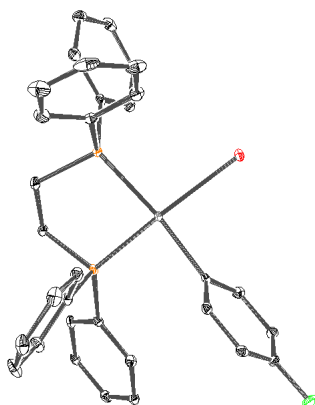
CataCXium A

454
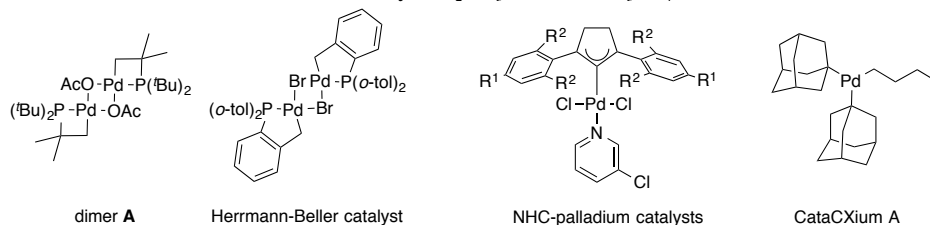
5 Crystallographic Data

Structure determinations were done by Manuela Weber or Prof. Dieter Lentz and were carried out by single-crystal X-ray diffraction by selecting an appropriate crystal under a stream of cold nitrogen and transferring it to the nitrogen cooled goniometer. Reflections were measured by using a *D8 Venture, Bruker Photon CMOS Detector* (MoKα radiation; λ = 0.71073 Å or CuKα radiation; λ = 1.54178 Å) The structures were solved with SHELXS-2013[244] by using direct methods and refined with SHELXL-2014/7 on $F2$ for all reflections.[244] Non-hydrogen atoms were refined by using anisotropic displacement parameters. The positions of the hydrogen atoms were calculated for idealized positions. Geometry calculations and checks for higher symmetry were performed with the PLATON program.[245] Molecular graphics were obtained with ORTEP. Atomic coordinates and displacement parameters can be found in the Appendix.

***cis*-(dppe)Pd(*p*-*t*BuC₆H₄)I (2e)**

Sample number	SZAC4117
Emperical formula	C36 H37 I P2 Pd
Formula weight	764.96
Temperature	100(2) K
Wavelength	0.71073 Å
Crystal system	monoclinic
Space group	P 21/n
Unit cell dimensions	a = 13.2093(2) Å α = 90 °
	b = 16.5319(3) Å β = 112.5710(10) °
	c = 16.1163(3) Å γ = 90 °
Volume	3249.82(10) Å³
Crystal color	yellow
Z	4
Density	1.563 g/cm³
Absorption coefficient	1.643
F(000)	1528
Crystal size	0.320 x 0.23 x 0.08 mm³
Theta range for data collection	2.46 to 26.40 °C
Reflection collected	50661
Completeness to theta = 26.40 °	99.8%
Absorption correction type	multi-scan

Max. and min. transmission	0.6198 and 0.5375
Data / restraints / parameters	6680 / 0 / 364
Goodness-to-fit on F^2	1.154
R (all data)	0.0249

cis-(dppe)Pd(*p*-FC$_6$H$_4$)I (2g)

Sample number	AC4119B1
Emperical formula	C32 H28 F I P2 Pd
Formula weight	726.78
Temperature	100(2) K
Wavelength	0.71073 Å
Crystal system	triclinic
Space group	P –1
Unit cell dimensions	a = 9.3773(2) Å α = 90.4140(7) °
	b = 13.5357(2) Å β = 92.0483(7) °
	c = 22.2975(4) Å γ = 93.2614 °
Volume	2823.67(9) Å^3
Crystal color	yellow
Z	4
Density	1.710 g/cm^3
Absorption coefficient	1.891
F(000)	1432
Crystal size	0.55 x 0.13 x 0.13 mm^3
Theta range for data collection	2.33 to 26.42 °C
Reflection collected	101494
Completeness to theta = 26.42 °	99.6%
Absorption correction type	multi-scan
Max. and min. transmission	0.4974 and 0.4070
Data / restraints / parameters	11609 / 0 / 667
Goodness-to-fit on F^2	1.165
R (all data)	0.0445

cis-(dppf)Pd(*p*-FC$_6$H$_4$)I (3g)
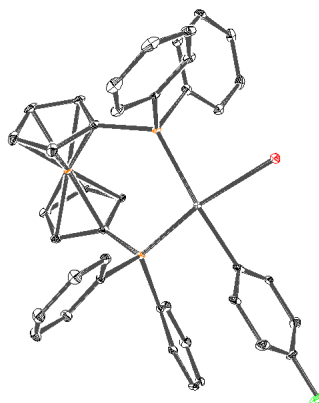
Sample number	SZ4028
Emperical formula	C40 H32 F Fe I P2 Pd
Formula weight	882.74
Temperature	100(2) K
Wavelength	0.71073 Å
Crystal system	monoclinic
Space group	P 21/n
Unit cell dimensions	a = 13.3506(2) Å α = 90 °
	b = 17.3421(3) Å β = 101.5610(10) °
	c = 14.9224(3) Å γ = 90 °
Volume	3384.85(10) Å^3
Crystal color	orange
Z	4
Density	1.732 g/cm^3
Absorption coefficient	2.001
F(000)	1744
Crystal size	0.37 x 0.33 x 0.15 mm^3
Theta range for data collection	2.288 to 26.428 °C
Reflection collected	43003
Completeness to theta = 26.428 °	99.8%
Absorption correction type	multi-scan
Max. and min. transmission	0.7454 and 0.607
Data / restraints / parameters	6950 / 0 / 409
Goodness-to-fit on F^2	1.026
R (all data)	0.0350

cis-(dppf)Pd(*p*-FC₆H₄)Br (7g)
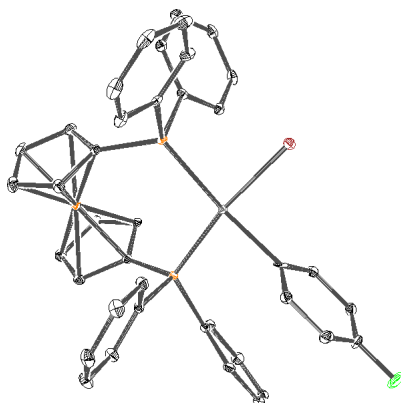
Sample number	SZ4032
Emperical formula	C40 H32 Br F Fe P2 Pd
Formula weight	835.75
Temperature	100(2) K
Wavelength	0.71073 Å
Crystal system	monoclinic
Space group	P 21/n
Unit cell dimensions	a = 13.3250(3) Å $\quad\quad$ α = 90 °
	b = 17.1103(3) Å $\quad\quad$ β = 102.4350(10) °
	c = 14.9691(3) Å $\quad\quad$ γ = 90 °
Volume	3332.81(12) Å³
Crystal color	yellow
Z	4
Density	1.666 g/cm³
Absorption coefficient	2.305
F(000)	1672
Crystal size	0.48 x 0.31 x 0.18 mm³
Theta range for data collection	2.309 to 26.443 °C
Reflection collected	55504
Completeness to theta = 26.443 °	99.6%
Absorption correction type	multi-scan
Max. and min. transmission	0.7454 and 0.4717
Data / restraints / parameters	6842 / 0 / 415
Goodness-to-fit on F²	1.060
R (all data)	0.0368

trans-(PPh₃)₂Pd(_p_-MeC₆H₄)Br (9f)

$\mathbf{\mathit{trans}\text{-}(PPh_3)_2Pd(\mathit{p}\text{-}MeC_6H_4)Br}$ **(9f)**
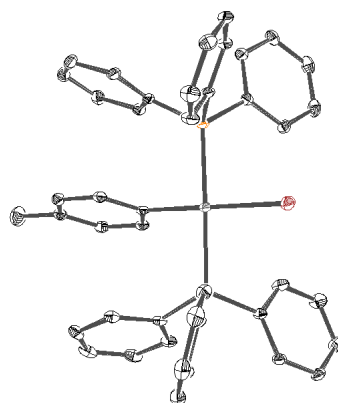
Sample number	SZ3020	
Emperical formula	C43 H37 Br P2 Pd	
Formula weight	801.98	
Temperature	145(2) K	
Wavelength	0.71073 Å	
Crystal system	monoclinic	
Space group	I2/a	
Unit cell dimensions	a = 11.481(2) Å	$\alpha = 90\ °$
	b = 12.895(2) Å	$\beta = 93.855(4)\ °$
	c = 23.574(5) Å	$\gamma = 90\ °$
Volume	3482.4(12) Å^3	
Crystal color	yellow	
Z	4	
Density	1.530 g/cm^3	
Absorption coefficient	1.803	
F(000)	1624	
Crystal size	0.50 x 0.31 x 0.25 mm^3	
Theta range for data collection	2.4 to 30.5 °C	
Reflection collected	20384	
Absorption correction type	multi-scan	
Data / restraints / parameters	5282 / 0 / 216	
Goodness-to-fit on F^2	1.086	
R (all data)	0.0354	

***trans*-(PPh₃)₂Pd(*p*-FC₆H₄)Br (9g)**
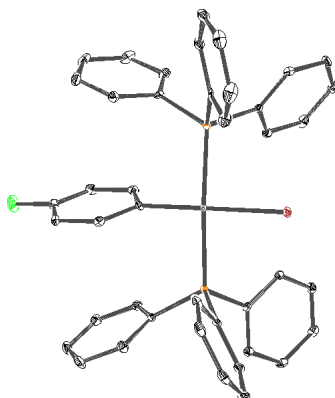
Sample number	SZ3021
Emperical formula	C42 H34 Br F P2 Pd
Formula weight	805.94
Tmeperature	100(2) K
Crystal system	triclinic
Space group	P –1
Unit cell dimensions	a = 11.3757(7) Å α = 67.608(2) °
	b = 12.0559(7) Å β = 87.652(2) °
	c = 13.8051(9) Å γ = 88.783(2) °
Volume	1749.03(19) Å³
Crystal color	clolorless
Z	2
Density	1.530 g/cm³
Absorption coefficient	1.799
F(000)	812
Crystal size	0.35 x 0.11 x 0.10 mm³
Theta range for data collection	2.57 to 33.18 °C
Reflection collected	45792
Completeness to theta = 33.18 °	99.6%
Absorption correction type	multi-scan
Data / restraints / parameters	45792 / 0 / 426
Goodness-to-fit on F²	1.080
R (all data)	0.0356

trans-(py)₂Pd(_p_-Et₂OCC₆H₄)Br (11i)
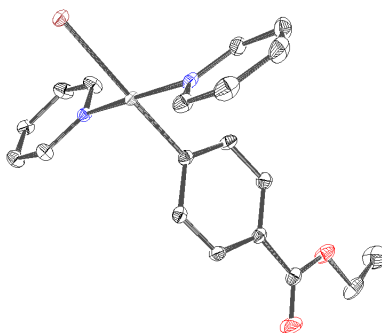
Sample number	SZ4127a
Emperical formula	C19 H19 Br N2 O2 Pd
Formula weight	493.67
Temperature	99(2) K
Wavelength	1.54178 Å
Crystal system	monoclinic
Space group	P 21/c
Unit cell dimensions	a = 14.5291(13) Å α = 90 °
	b = 8.1088(7) Å β = 90.422(3) °
	c = 16.2314(15) Å γ = 90 °
Volume	1912.2(3) Å³
Crystal color	colorless
Z	4
Density	1.715 g/cm³
Absorption coefficient	10.391
F(000)	976
Crystal size	0.37 x 0.22 x 0.07 mm³
Theta range for data collection	3.04 to 74.55 °C
Reflection collected	36316
Completeness to theta = 74.55 °	99.4%
Absorption correction type	multi-scan
Data / restraints / parameters	3910 / 0 / 226
Goodness-to-fit on F²	1.144
R (all data)	0.0325

N-Methyl-2-aminobiphenylpalladium methanesulfonate, Buchwald pre-catalyst G4
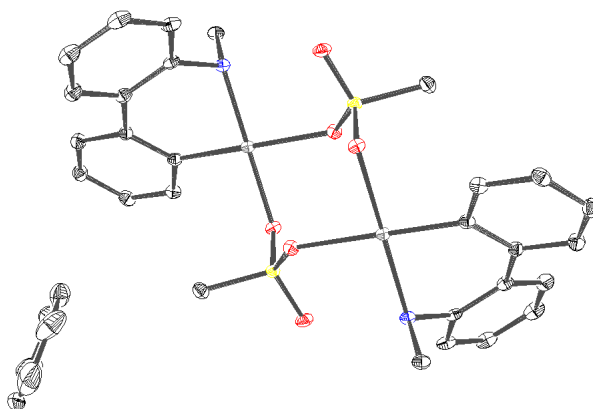
Selected bond distances (Å) and angles (deg): Pd–N 2.046, Pd–C 1.959, Pd–O1 2.182, Pd–O2 2.089, N–Pd–C 87.4, dihedral angle 32.2.

Sample number	SZ1028BA	
Emperical formula	C40 H42 N2 O6 Pd2 S2	
Formula weight	923.68	
Temperature	133(2) K	
Wavelength	0.71073 Å	
Crystal system	monoclinic	
Space group	P2(1)/c	
Unit cell dimensions	a = 17.111(3) Å	$\alpha = 90\,°$
	b = 10.291(2) Å	$\beta = 102.092(4)\,°$
	c = 11.195(2) Å	$\gamma = 90\,°$
Volume	1927.7(7) Å^3	
Crystal color	colorless	
Z	2	
Density	1.591 g/cm^3	
Absorption coefficient	1.090	
F(000)	936	
Crystal size	0.36 x 0.20 x 0.10 mm^3	
Theta range for data collection	3.13 to 30.4 °C	
Reflection collected	18870	
Absorption correction type	multi-scan	
Data / restraints / parameters	5874 / 0 / 237	
Goodness-to-fit on F^2	1.118	
R (all data)	0.0542	

3-Bromo-2,2′-bipyridine *N*-oxide (22a)
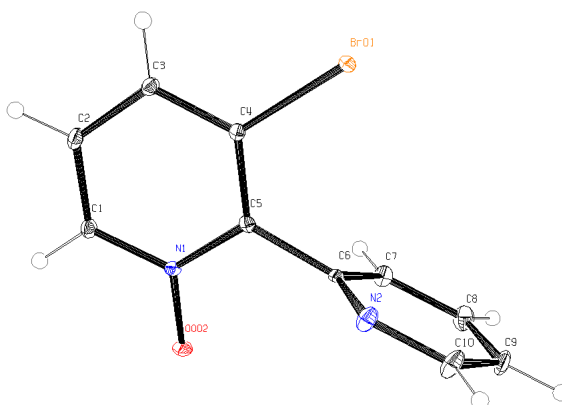
Sample number	FW46a
Emperical formula	C10 H7 Br N2 O
Formula weight	251.09
Temperature	100(2) K
Wavelength	0.71073 Å
Crystal system	orthorhombic
Space group	P 21 21 21
Unit cell dimensions	a = 7.8537(2) Å $\quad$ α = 90 °
	b = 9.5726(3) Å $\quad$ β = 90 °
	c = 12.6431(3) Å $\quad$ γ = 90 °
Volume	950.51(4) Å^3
Crystal color	colorless
Z	4
Density	1.755 g/cm^3
Absorption coefficient	4.289
F(000)	496
Crystal size	0.22 x 0.10 x 0.08 mm^3
Theta range for data collection	2.64 to 26.4 °C
Reflection collected	14604
Completeness to theta = 26.4 °	100%
Absorption correction type	multi-scan
Data / restraints / parameters	1933 / 0 / 127
Goodness-to-fit on F^2	1.065
R (all data)	0.0144

CCDC-1476436 contains the crystallographic data for **22a**.

3-Bromo-5-methoxy-2,2′-bipyridine *N*-oxide (22f)
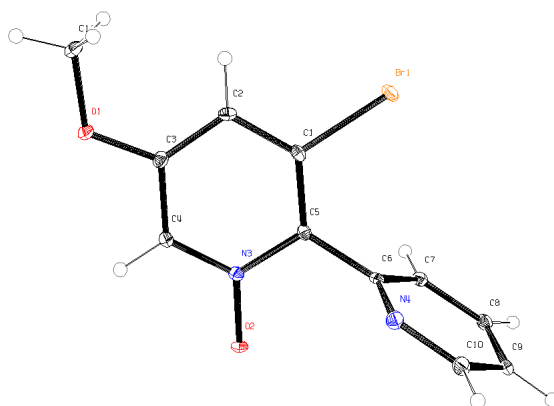
Sample number	FW2058
Emperical formula	C11 H9 Br N2 O2
Formula weight	281.11
Temperature	100(2) K
Wavelength	0.71073 Å
Crystal system	monoclinic
Space group	P 21/c
Unit cell dimensions	a = 10.8711(2) Å α = 90 °
	b = 8.8580(2) Å β = 98.6919(8) °
	c = 11.1022(3) Å γ = 90 °
Volume	1056.82(4) Å^3
Crystal color	yellow
Z	4
Density	1.767 g/cm^3
Absorption coefficient	3.874
F(000)	560
Crystal size	0.33 x 0.26 x 0.14 mm^3
Theta range for data collection	2.96 to 26.41 °C
Reflection collected	12520
Completeness to theta = 26.41 °	99.1%
Absorption correction type	multi-scan
Max. and min. transmission	0.5111 and 0.3764
Data / restraints / parameters	2151 / 0 / 146
Goodness-to-fit on F^2	1.054
R (all data)	0.0321

CCDC-1476430 contains the crystallographic data for **22f**.

3-Bromo-4-cyano-2,2′-bipyridine *N*-oxide (22n)
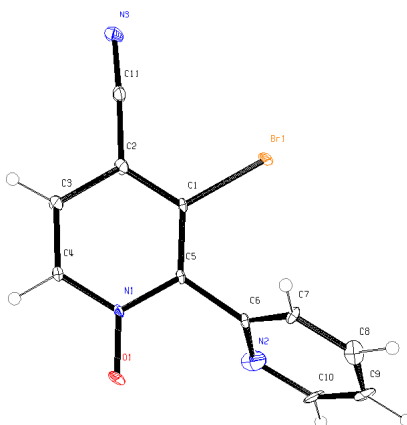
Sample number	FW2049F4
Emperical formula	C11 H6 Br N3 O
Formula weight	276.10
Temperature	100(2) K
Wavelength	0.71073 Å
Crystal system	monoclinic
Space group	P 21/c
Unit cell dimensions	a = 15.0501(7) Å $\quad$ α = 90 °
	b = 17.1801(7) Å $\quad$ β = 95.692(2) °
	c = 7.8219(3) Å $\quad$ γ = 90 °
Volume	2012.48(15) Å^3
Crystal color	orange
Z	8
Density	1.823 g/cm^3
Absorption coefficient	4.063
F(000)	1088
Crystal size	0.27 x 0.27 x 0.05 mm^3
Theta range for data collection	2.37 to 26.29 °C
Reflection collected	20601
Completeness to theta = 26.29 °	99.0%
Absorption correction type	multi-scan
Max. and min. transmission	0.5624 and 0.3566
Data / restraints / parameters	4104 / 0 / 241
Goodness-to-fit on F^2	1.225
R (all data)	0.1861

CCDC-1476429 contains the crystallographic data for **22n**.

(4-Ethoxycarbonayl-2,2′-bipyridine-*N*-oxide)palladium(II) acetate (C2)
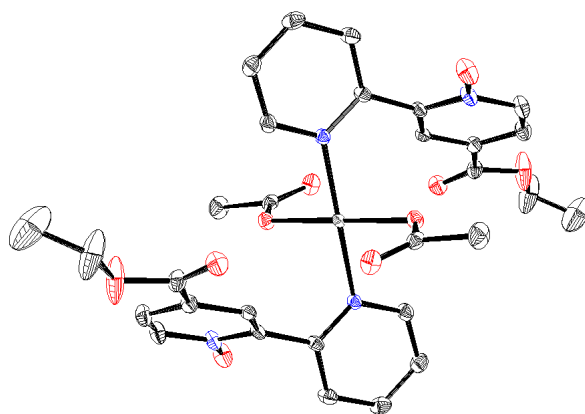
Sample number	SZ2027a
Emperical formula	C15 H15 N2 O5 Pd0.5
Formula weight	356.49
Temperature	120(2) K
Wavelength	0.71073 Å
Crystal system	monoclinic
Space group	P 21/c
Unit cell dimensions	a = 8.6046(17) Å α = 90 °
	b = 12.288(2) Å β = 103.226(4) °
	c = 17.865(4) Å γ = 90°
Volume	1838.8(6) Å^3
Crystal color	yellow
Z	4
Density	1.288 g/cm^3
Absorption coefficient	0.558
F(000)	728
Crystal size	0.30 x 0.11 x 0.09 mm^3
Theta range for data collection	2.34 to 30.48 °C
Reflection collected	24142
Completeness to theta = 30.48 °	99.8%
Absorption correction type	none
Data / restraints / parameters	5622 / 0 / 207
Goodness-to-fit on F^2	1.079
R (all data)	0.0632

CCDC-1476437 contains the crystallographic data for **C2**.

(2,2′-Bipyridin-3-yl-*N*-oxide)palladium acetate dimer (D)
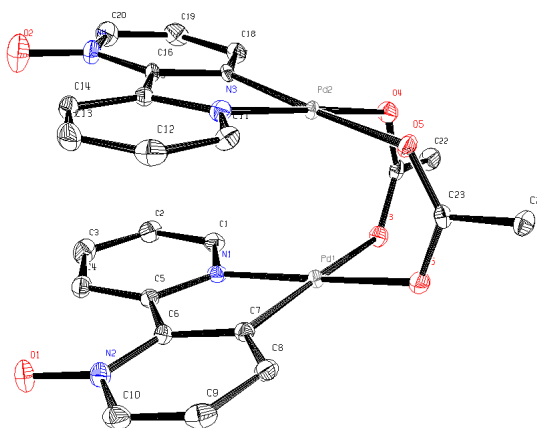
Sample number	SZ4085
Emperical formula	$C_{24}H_{20}N_4O_6Pd_2$
Formula weight	673.24
Temperature	100(2) K
Wavelength	0.71073 Å
Crystal system	monoclinic
Space group	P 21/n
Unit cell dimensions	a = 14.5855(3) Å α = 90 °
	b = 9.6821(2) Å β = 100.7190(7) °
	c = 16.1879(3) Å γ = 90 °
Volume	2246.14(8) Å³
Crystal color	yellow
Z	4
Density	1.991 g/cm³
Absorption coefficient	1.653
F(000)	1328
Crystal size	0.38 x 0.28 x 0.08 mm³
Theta range for data collection	2.54 to 26.44 °C
Reflection collected	24445
Completeness to theta = 26.42 °	99.5%
Absorption correction type	multi-scan
Max. and min. transmission	0.7347 and 0.4774
Data / restraints / parameters	4620 / 0 / 327
Goodness-to-fit on F²	1.023
R (all data)	0.0533

CCDC-1476427 contains the crystallographic data for **D**.

[(2,2′-Bipyridine)Pd(X)(^{t}Bu$_2$P(CH$_3$)(CH$_2$)], complex F(BF$_4$)
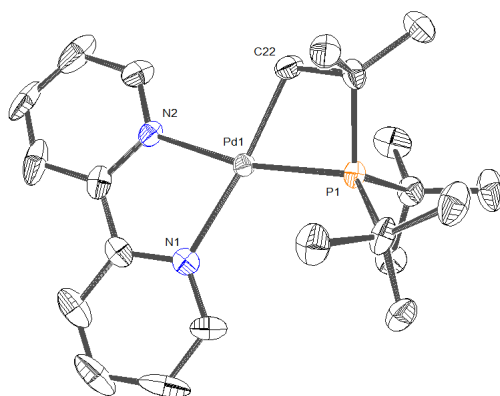
Sample number	FW1006
Emperical formula	C22 H34 B F4 N2 P Pd
Formula weight	550.69
Temperature	200(2) K
Wavelength	0.71073 Å
Crystal system	monoclinic
Space group	P 21/c
Unit cell dimensions	a = 11.0660(10) Å α = 90 °
	b = 12.1000(10) Å β = 95.330(10) °
	c = 18.223(2) Å γ = 90 °
Volume	2429.5(4) Å^3
Crystal color	colorless
Z	4
Density	1.506 g/cm^3
Absorption coefficient	0.872
F(000)	1128
Crystal size	0.35 x 0.21 x 0.13 mm^3
Theta range for data collection	3.24 to 29.43 °C
Reflection collected	11720
Completeness to theta = 29.43 °	99.6%
Absorption correction type	none
Data / restraints / parameters	4246 / 0 / 280
Goodness-to-fit on F^2	1.008
R (all data)	0.0999

Complex G
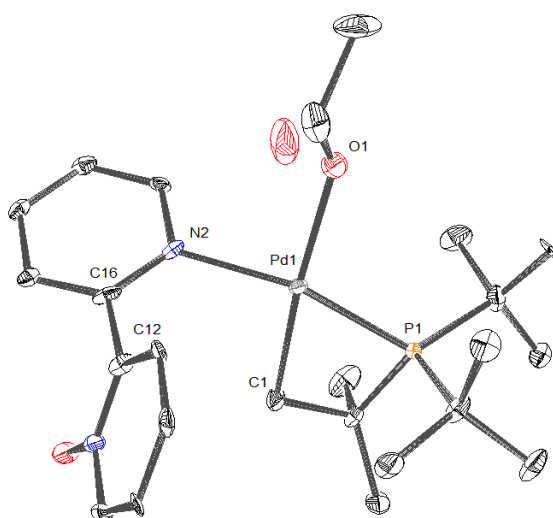
Sample number	SZ2032b
Emperical formula	C24 H37 N2 O3 P Pd
Formula weight	538.96
Crystal system	monoclinic
Space group	P 21/c
Unit cell dimensions	a = 15.226(4) Å $\alpha = 90°$
	b = 10.863(2) Å $\beta = 97.166(8)°$
	c = 16.303(4) Å $\gamma = 90°$
Volume	2675.4 Å^3
Crystal color	colorless

Structural refinements of the crystal structure of complex **G** is currently in process.

Complex I
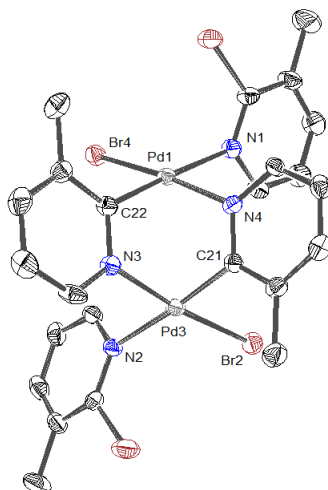
Sample number	SZ2081c
Emperical formula	C24 H24 Br4 N4 Pd2
Formula weight	900.91
Temperature	293(2) K
Wavelength	0.71073 Å
Crystal system	monoclinic
Space group	P 21/c

Unit cell dimensions		
	a = 11.391(3) Å	$\alpha = 90\ °$
	b = 14.658(4) Å	$\beta = 101.840(5)\ °$
	c = 17.260(5) Å	$\gamma = 90\ °$

Volume	2820.6(14) Å^3
Crystal color	orange
Z	4
Density	2.122 g/cm^3
Absorption coefficient	6.962
F(000)	1712
Crystal size	unknown
Theta range for data collection	1.83 to 25.16 °C
Reflection collected	18105
Completeness to theta = 25.16 °	99.6%
Absorption correction type	unknown
Data / restraints / parameters	5048 / 0 / 307
Goodness-to-fit on F^2	1.034
R (all data)	0.0684

6 Computational Section

6.1 Computational details

DFT calculations were performed using the Gaussian09 program package[246] with the hybrid meta exchange-correlation M06 functional.[88] LanL2DZ effective core pseudo potentials and basis sets for Pd, Zn, I and Cl and 6-31G(d,p) basis set for C, H, O and P were used. Geometry optimizations were performed without any symmetry constraints at 298.15 K using the polarizable continuum model (PCM).[90] Stationary points were checked by frequency calculations, which showed exclusively positive frequencies for ground state structures. The relative Gibbs energies ΔG^0 in kcal/mol for ground states are based on the sum of electronic and thermal free energies E (in a.u.). Cartesian coordinates of the calculated structures can be found in the Appendix.
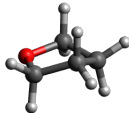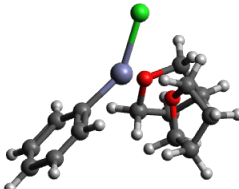
If not otherwise state the following route sections were used for geometry optimizations and frequency calculation:
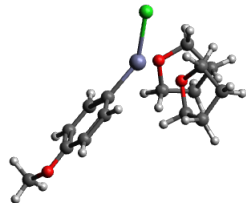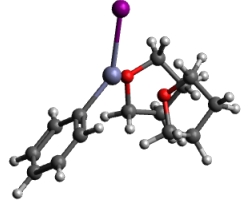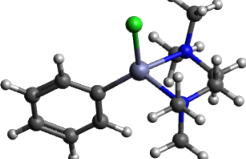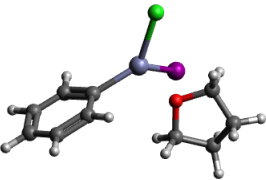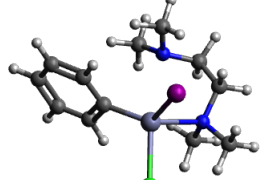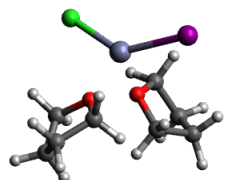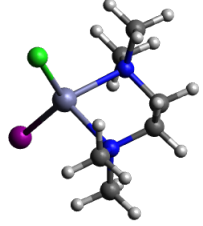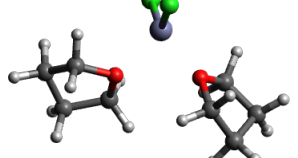
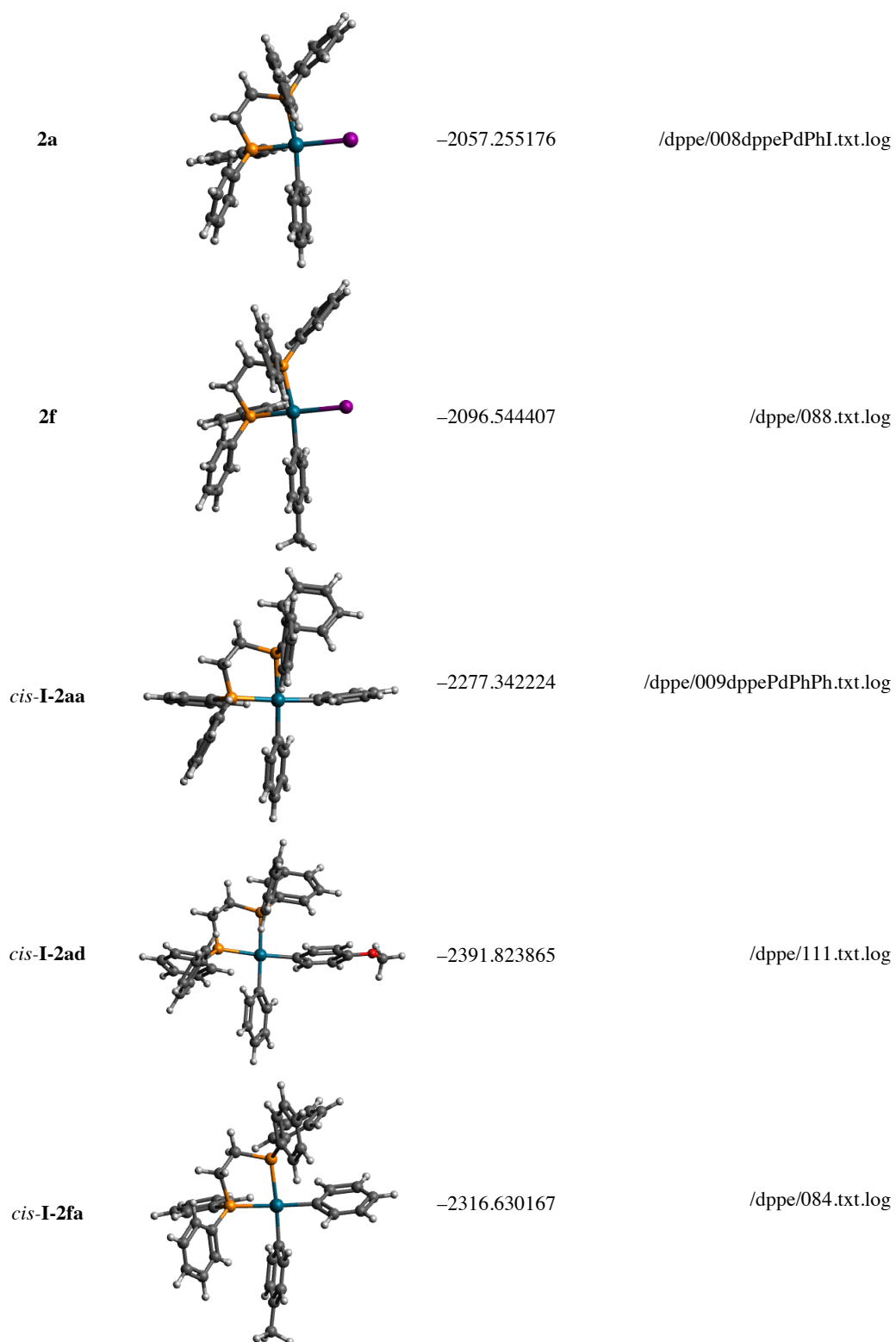M06L/GenECP 5D gfinput IOP(6/7=3) Opt SCRF=(solvent=TetraHydroFuran) Freq symm=loose
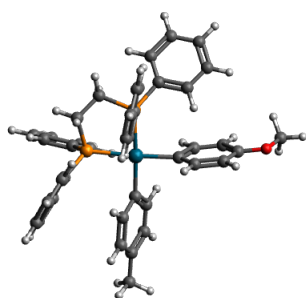
or

M06L/Def2QZVP 5D gfinput IOP(6/7=3) Opt SCRF=(solvent=TetraHydroFuran) Freq symm=loose

6.2 Reactants and products

Compound	Structure	sum of electronic and thermal Free Energies [a.u.]	Directory
THF		–232.332237 –232.432293	/LanL2DZ/005THF.txt.log /def2QZVP/022freq.txt.log
iodide		–11.559450 –298.062917	/LanL2DZ/007iodide.txt.log /def2QZVP/023freq.txt.log
16a(thf)$_2$		–776.371177 –2936.192759	/dppe/001cPhZnCl.txt.log /dppe/001cfreq.txt.log

16d(thf)$_2$	−890.854630	/dppe/108.txt.log
19a(thf)$_2$	−772.788479	/dppe/002b.txt.log
16a(tmeda)	−659.245756 −2819.013491	/dppe/112.txt.log /dppe/112def.txt.log
[**16a**I(thf)]⁻	−555.706460 −555.699951 −3001.833687	/LanL2DZ/006PhZnClI.txt.log /LanL2DZ/counterpoise/006ct.txt.log /def2QZVP/026freq.txt.log
[**16a**I(tmeda)]⁻	−670.793391 −3117.063819	/dppe/120b.txt.log /dppe/120bdefdef.txt.log
ZnClI(thf)$_2$	−556.284001	/dppe/003bZnClI.txt.log
ZnClI(tmeda)	−439.162590	/dppe/115a.txt.log
ZnCl$_2$(thf)$_2$	−559.867025	/LanL2DZ/031ZnCl2.txt.log

2a		–2057.255176	/dppe/008dppePdPhI.txt.log
2f		–2096.544407	/dppe/088.txt.log
cis-**I-2aa**		–2277.342224	/dppe/009dppePdPhPh.txt.log
cis-**I-2ad**		–2391.823865	/dppe/111.txt.log
cis-**I-2fa**		–2316.630167	/dppe/084.txt.log
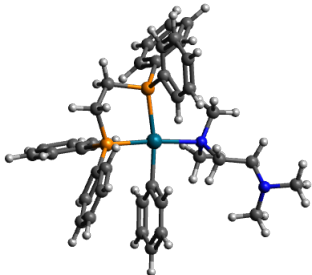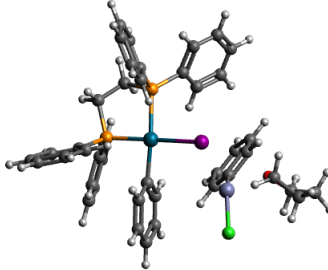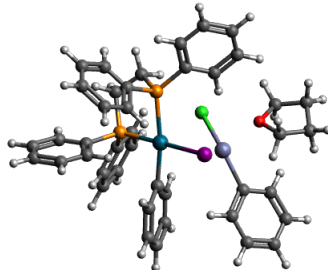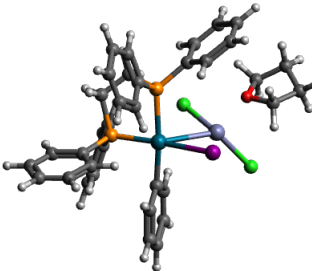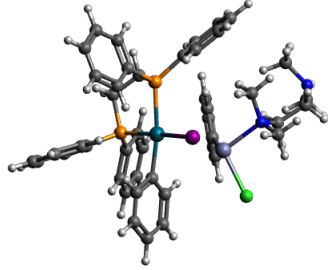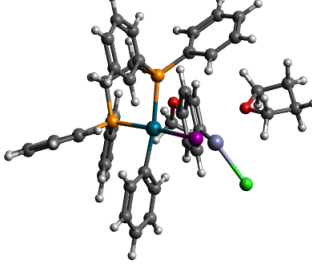
cis-**I-2fd**		–2431.114336	/dppe/116.txt.log

6.3   Intermediates

	Structure	sum of electronic and thermal Free Energies [a.u.]	Directory
2a(thf)		–2289.582597	/dppe/035.txt.log
[**2a**(thf)]⁺		–2278.003068	/dppe/010dppePdPh.txt.log
[**2f**(thf)]⁺		–2317.293713	/dppe/089.txt.log

[**2a**(tmeda)]⁺		–2393.19672	/dppe/119.txt.log
[**2a**–**16a**(thf)]		–2601.292435	/dppe/043b.txt.log
[**2a**–**16a**(thf)′]		–2601.292956	/dppe/098.txt.log
[**2a**–ZnCl₂(thf)]		–2384.793388	/dppe/090.txt.log
[**2a**–**16a**(tmeda)]		–2716.476287	/dppe/113.txt.log
[**2a**–**16d**(thf)]		–2715.777053	/dppe/109.txt.log
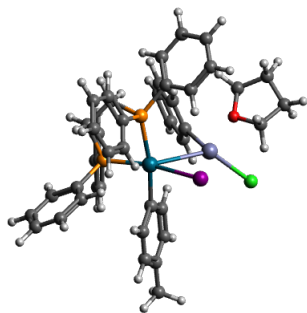
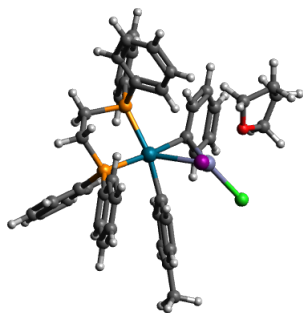|			
[**2f**–**16a**(thf)]		−2640.582452	/dppe/096.txt.log
[**2f**–**16d**(thf)]		−2755.066803	/dppe/118.txt.log
[**2a**–**19a**(thf)]		−2597.707819	/dppe/050.txt.log
[**I-2aa**–ZnCII(thf)]		−2601.298064	/dppe/017a.txt.log
[**I-2ad**–ZnCII(thf)]		−2715.782257	/dppe/110.txt.log
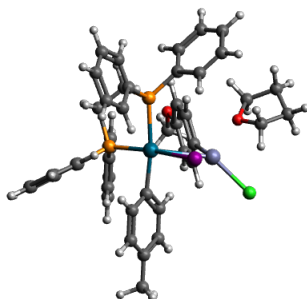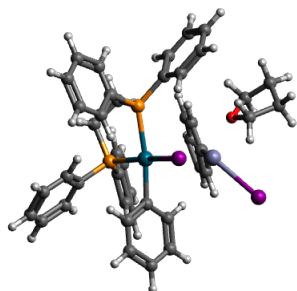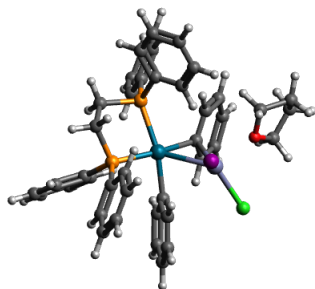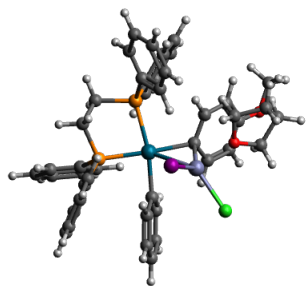
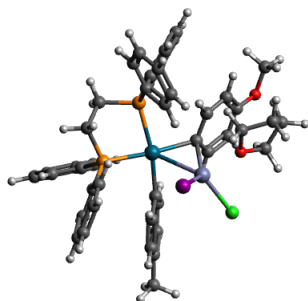**[I-2fa**–ZnClI(thf)]   –2640.586083   /dppe/087.txt.log
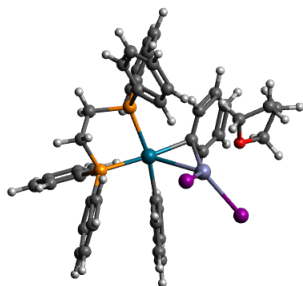
[I-2fd–ZnClI(thf)]   –2755.071745   /dppe/117.txt.log
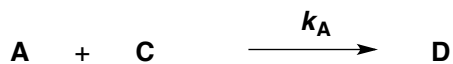
[I-2aa–ZnI$_2$(thf)]   –2597.714212   /dppe/107.txt.log

7 Mathematical Section

7.1 Calculation of relative reaction rates

Based on the reaction equations:

$$A + C \xrightarrow{k_A} D$$

$$B + C \xrightarrow{k_B} E$$

The rate laws for the decay of the concentration of the differently substituted competing reagents **A** and **B** in the reaction with reagent **C**, where k_A and k_B are the observed rate constants, are as follows:

(eq. 14)
$$\frac{d[\mathbf{A}]}{dt} = -k_A[\mathbf{A}][\mathbf{C}]$$

(eq. 15)
$$\frac{d[\mathbf{B}]}{dt} = -k_B[\mathbf{B}][\mathbf{C}]$$

Derived from the law of mass action, the concentration of the reagent $[\mathbf{C}]_t$ at the time t is:

(eq. 16)
$$[\mathbf{C}]_t = [\mathbf{C}]_0 - [\mathbf{A}]_0 + [\mathbf{A}]_t - [\mathbf{B}]_0 + [\mathbf{B}]_t$$

The ratio of the rate constants k_{rel}, which was previously described as competition constant κ,[7h] is:

(eq. 17)
$$k_{rel} = \frac{k_A}{k_B}$$

(eq. 18)
$$k_A = k_{rel} \cdot k_B$$

Insertion of equation 18 into equation 14 gives:

(eq. 19)
$$\frac{d[\mathbf{A}]}{dt} = -k_{rel} \cdot k_B \cdot [\mathbf{A}][\mathbf{C}]$$

Equation 14 devided by equation 15 gives:

(eq. 20)
$$\frac{d[\mathbf{A}]}{d[\mathbf{B}]} = \frac{k_A \cdot [\mathbf{A}]}{k_B[\mathbf{B}]} = k_{rel}\frac{[\mathbf{A}]}{[\mathbf{B}]}$$

Separation of variables and integration:

(eq. 21)
$$\frac{1}{[\mathbf{A}]}d[\mathbf{A}] = \frac{k_{rel}}{[\mathbf{B}]}d[\mathbf{B}]$$

(eq. 22)
$$\int_0^t \frac{1}{[\mathbf{A}]} d[\mathbf{A}] = \int_0^t \frac{k_{rel}}{[\mathbf{B}]} d[\mathbf{B}]$$

(eq. 23)
$$ln([\mathbf{A}]_t) - ln([\mathbf{A}]_0) = k_{rel} \cdot \left(ln([\mathbf{B}]_t) - ln([\mathbf{B}]_0)\right)$$

(eq. 24)
$$k_{rel} = \frac{ln([\mathbf{A}]_t) - ln([\mathbf{A}]_0)}{ln([\mathbf{B}]_t) - ln([\mathbf{B}]_0)}$$

The concentrations of the reactants [**A**] and [**B**] at the time *t* can be expressed as the concentration of the of the corresponding products [**D**] and [**E**]:

(eq. 25)
$$[\mathbf{A}]_t = [\mathbf{A}]_0 - [\mathbf{D}]$$

(eq. 26)
$$[\mathbf{B}]_t = [\mathbf{B}]_0 - [\mathbf{E}]$$

Substitution and insertion in equation 24 gives:

(eq. 27)
$$k_{rel} = \frac{ln([\mathbf{A}]_0 - [\mathbf{D}]) - ln([\mathbf{A}]_0)}{ln([\mathbf{B}]_0 - [\mathbf{E}]) - ln([\mathbf{B}]_0)}$$

The Hammett diagrams are plots of the logarithm of the relative rate constant k_{rel} as function of the Hammett parameters σ_{para}. To obtain the logarithm of the relative rate constants $k_{R,H}$ of a substituted reactant **A** or **B** relative to the unsubstituted reactant **H** from competition experiments, where only substituted reactants were applied, the linear regression of the Hammett plot, resulting from combinations **A** or **B** with **B** the same, was parallel shifted along the y-axes towards the origin of the ordinates. This transformation can be mathematically expressed by subtraction of the interception q_B from k_{rel}:

(eq. 28)
$$ln\left(k_{R,H}\right) = ln(k_{rel}) - q_B$$

7.2   Derivation of observed Hammett constants

7.2.1   Derivatives of the Hammett equation

The first derivative of the Hammett equation (equation 1) to the Hammett substituent parameter σ corresponds to the slope, which is the Hammett reaction constant ρ:

(eq. 1)
$$log\left(\frac{k^R}{k^H}\right) = \rho \cdot \sigma$$

(eq. 29)
$$\frac{d}{d\sigma} log\left(\frac{k^R}{k^H}\right) = \rho$$

The Hammett equation 1 can be also expressed as exponential function with its derivate:

(eq. 30)
$$\frac{k^R}{k^H} = 10^{\rho\sigma}$$

(eq. 31)
$$k^R = k^H \cdot 10^{\rho\sigma}$$

It can be shown, that the derivative of the logarithmic rate constant results is equal to the Hammett constant ρ:

(eq. 32)
$$\frac{d}{d\sigma} k^R = k^H \cdot \rho 10^{\rho\sigma} \cdot ln(10) = k^R \cdot \rho \cdot ln(10)$$

(eq. 33)
$$\frac{d}{d\sigma} log(k^R) = \frac{k^R \cdot \rho \cdot ln(10)}{k^R \cdot ln(10)} = \rho$$

For the following derivations of the observed Hammett constants ρ_{obs}, some general derivatives were used. For the derivatives of the logarithm of products or quotients of rate constants $k_{\pm i}$:

(eq. 34)
$$\frac{d}{d\sigma} log(K_{\pm i}) = \frac{d}{d\sigma} log\left(\frac{k_{+i}}{k_{-i}}\right) = K_{\pm i}(\rho_i - \rho_{-i})$$

(eq. 35)
$$\frac{d}{d\sigma} k_j K_{\pm i} = k_j K_{\pm i}(\rho_j + \rho_i - \rho_{-i})$$

In addition, it can be shown, that derivative of the rate law of a reaction provides the Hammett constant ρ:

(eq. 36)
$$v^R = \frac{d[C^R]}{dt} = k^R \cdot [A^R] \cdot [B^R]$$

(eq. 37)
$$log(v^R) = log(k^R) + log([A^R]) + log([B^R])$$

(eq. 38)
$$\frac{d}{d\sigma} log(v^R) = \frac{d}{d\sigma} log(k^R) + \frac{d}{d\sigma} log([A^R]) + \frac{d}{d\sigma} log([B^R])$$

(eq. 39)
$$\frac{d}{d\sigma} log(v^R) = \rho + \frac{d}{d\sigma} log([A^R]) + \frac{d}{d\sigma} log([B^R])$$

In a competition experiment, where the two reagents A^R and A^H compete for the reagent B, the concentrations of $[A^R]$ and $[A^H]$ have to be in large excess with respect to B, so that the ratio of the competing reagents does not change significantly during the course of the reaction. Therefore, the concentration of reagent $[A^R]$ is independent of the Hammett substituent parameter σ.

(eq. 40)
$$\frac{d}{d\sigma} log([A^R]) = 0$$

481

The concentration of reagent $[B]$ is also independent of σ:

(eq. 41)
$$\frac{d}{d\sigma} log([B^R]) = 0$$

Because, the derivatives of $log([A^R])$ and $log([B])$ are zero:

(eq. 42)
$$\frac{d}{d\sigma} log(v^R) = \frac{d}{d\sigma} log([k^R]) = \rho_{obs}$$

Therefore, the Hammett reaction constant ρ_{obs} can be interpreted more generally as the sensitivity of the (relative) rate of reaction towards a change in σ under otherwise identical conditions.

For reason of legibility, the indices R and H were omitted from the further calculations, unless otherwise noted:

(eq. 43) $$[A^R] = [A]$$
(eq. 44) $$[B^R] = [B]$$
(eq. 45) $$[C^R] = [C]$$
(eq. 46) $$k^R = k$$

7.2.2 Dissociative mechanism A

(eq. 47)
$$\frac{d[C]}{dt} = k_2[A^+][X][B]$$

Applying the steady-state approximation:

(eq. 48)
$$\frac{d[A^+]}{dt} = k_1[A] - k_{-1}[A^+][X] - k_2[A^+][X][B] \approx 0$$

(eq. 49)
$$[A^+][X] = \frac{k_1[A]}{k_{-1} + k_2[B]}$$

(eq. 50)
$$v = \frac{d[C]}{dt} = \frac{k_1 k_2 [A][B]}{k_{-1} + k_2[B]}$$

$$\frac{d}{d\sigma} log(v) = \rho_{obs}$$

(eq. 51)
$$= \frac{d}{d\sigma} log(k_1) + \frac{d}{d\sigma} log(k_2) + \frac{d}{d\sigma} log([A]) + \frac{d}{d\sigma} log([B])$$
$$- \frac{d}{d\sigma} log(k_{-1} + k_2[B])$$
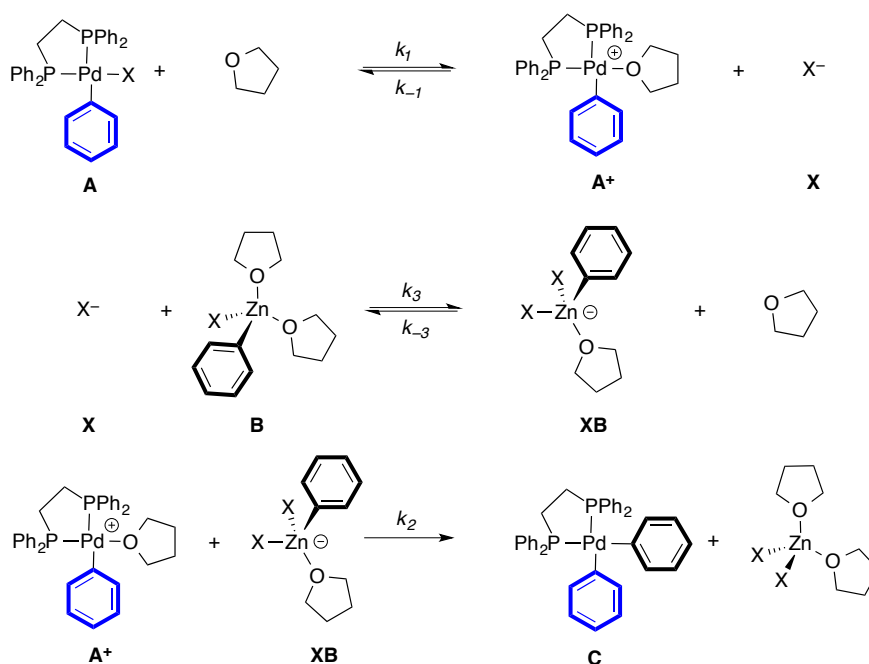
With respect to competing arylpalladium(II) complexes A:

(eq. 52)
$$\rho_{obs} = \rho_1 + \rho_2 - \frac{k_{-1}\rho_{-1} + k_2\rho_2[B]}{k_{-1} + k_2[B]}$$

With respect to competing arylzinc reagent B (with $\rho_1 = \rho_{-1} = 0$):

(eq. 53)
$$\rho_{obs} = \rho_2 - \frac{k_2\rho_2[B]}{k_{-1} + k_2[B]}$$

7.2.3   Dissociative mechanism B

(eq. 54)
$$\frac{d[C]}{dt} = k_2[A^+][XB]$$

(eq. 55)
$$\frac{d[A^+]}{dt} = k_1[A] - k_{-1}[A^+][X] - k_2[A^+][XB] \approx 0$$

If the equilibrium between X and XB is fast, then:

(eq. 56)
$$[X] = \frac{k_{-3}[XB]}{k_3[B]}$$

(eq. 57)
$$\frac{d[A^+]}{dt} = k_1[A] - \frac{k_{-1}k_{-3}}{k_3[B]}[A^+][XB] - k_2[A^+][XB] \approx 0$$

(eq. 58)
$$[A^+][XB] = \frac{k_1[A]}{\dfrac{k_{-1}k_{-3}}{k_3[B]} + k_2}$$

(eq. 59)
$$[A^+][XB] = \frac{k_1k_3[A][B]}{k_{-1}k_{-3} + k_2k_3[B]}$$

(eq. 60)
$$[A^+][XB] = \frac{k_1K_{\pm3}[A][B]}{k_{-1} + k_2K_{\pm3}[B]}$$

(eq. 61)
$$v = \frac{d[C]}{dt} = \frac{k_1k_2K_{\pm3}[A][B]}{k_{-1} + k_2K_{\pm3}[B]}$$

(eq. 62)
$$v = \frac{d[C]}{dt} = \frac{k_1k_2[A][B]}{\dfrac{k_{-1}}{K_{\pm3}} + k_2[B]}$$
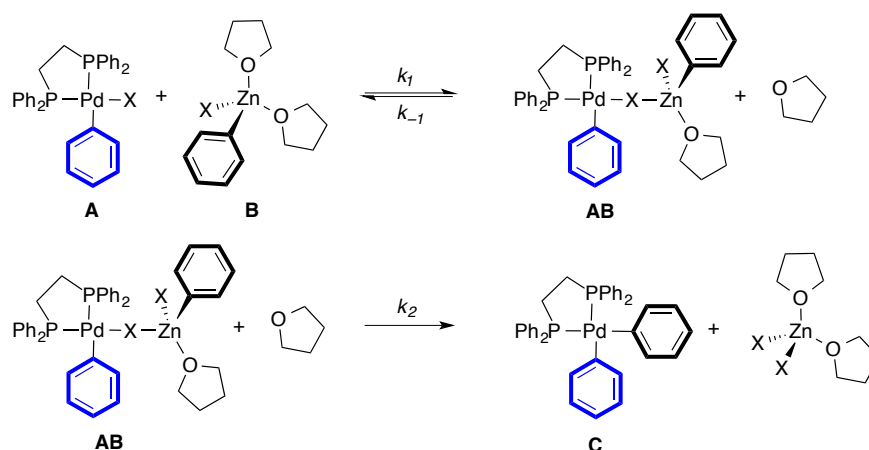
With respect to competing arylpalladium(II) complex A (with $\rho_{\pm3} = 0$):

(eq. 63)
$$\frac{d}{d\sigma}log(v) = \rho_{obs} = \rho_1 + \rho_2 - \frac{k_{-1}\rho_{-1} + k_2K_{\pm3}\rho_2[B]}{k_{-1} + k_2K_{\pm3}[B]}$$

With respect to competing arylzinc reagent B (with $\rho_{\pm1} = 0$):

(eq. 64)
$$\frac{d}{d\sigma}log(v) = \rho_{obs} = \rho_2 + \rho_3 - \rho_{-3} - \frac{k_2K_{\pm3}(\rho_2 + \rho_3 - \rho_{-3})[B]}{k_{-1} + k_2K_{\pm3}[B]}$$

7.2.4 Associative mechanism C

(eq. 65)
$$\frac{d[C]}{dt} = k_2[AB]$$

(eq. 66)
$$\frac{d[AB]}{dt} = k_1[A][B] - k_{-1}[AB] - k_2[AB] \approx 0$$

(eq. 67)
$$[AB] = \frac{k_1[A][B]}{k_{-1} + k_2}$$

(eq. 68)
$$v = \frac{d[C]}{dt} = \frac{k_1 k_2[A][B]}{k_{-1} + k_2}$$

With respect to arylpalladium(II) complex A and with respect to arylzinc reagent B:

(eq. 69)
$$\frac{d}{d\sigma} log(v) = \rho_{obs} = \rho_1 + \rho_2 - \frac{k_{-1}\rho_{-1} + k_2 \cdot \rho_2}{k_{-1} + k_2}$$

7.2.5 Associative mechanism D
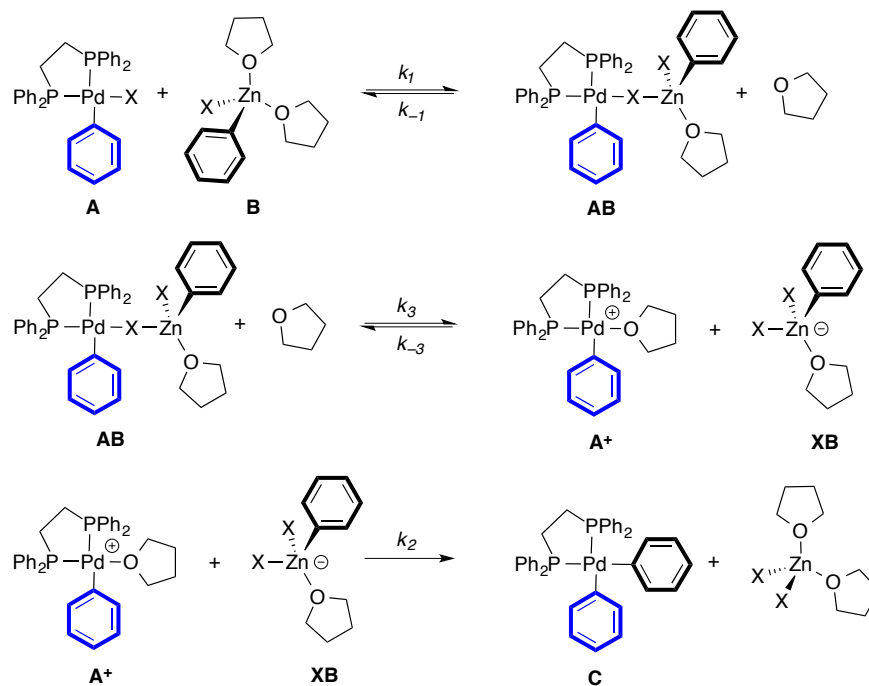
(eq. 70)
$$\frac{d[C]}{dt} = k_2[A^+][XB]$$

(eq. 71)
$$\frac{d[A^+]}{dt} = k_3[AB] - k_{-3}[A^+][XB] - k_2[A^+][XB] \approx 0$$

(eq. 72)
$$[A^+][XB] = \frac{k_3[AB]}{k_2 + k_{-3}}$$

If the equilibrium between A, B and AB is fast, then:

(eq. 73)
$$[AB] = \frac{k_1[A][B]}{k_{-1}}$$

(eq. 74)
$$[A^+][XB] = \frac{k_1 k_2[A][B]}{k_{-1}(k_2 + k_{-3})}$$

(eq. 75)
$$v = \frac{d[C]}{dt} = \frac{k_1 k_2 k_3[A][B]}{k_{-1}(k_2 + k_{-3})}$$

With respect to arylpalladium(II) complex A and with respect to arylzinc reagent B:

(eq. 76)
$$\frac{d}{d\sigma} log(v) = \rho_{obs} = \rho_1 - \rho_{-1} + \rho_2 + \rho_3 - \frac{k_2\rho_2 + k_{-3}\rho_{-3}}{k_2 + k_{-3}}$$

7.2.6   Addition of ZnCl₂
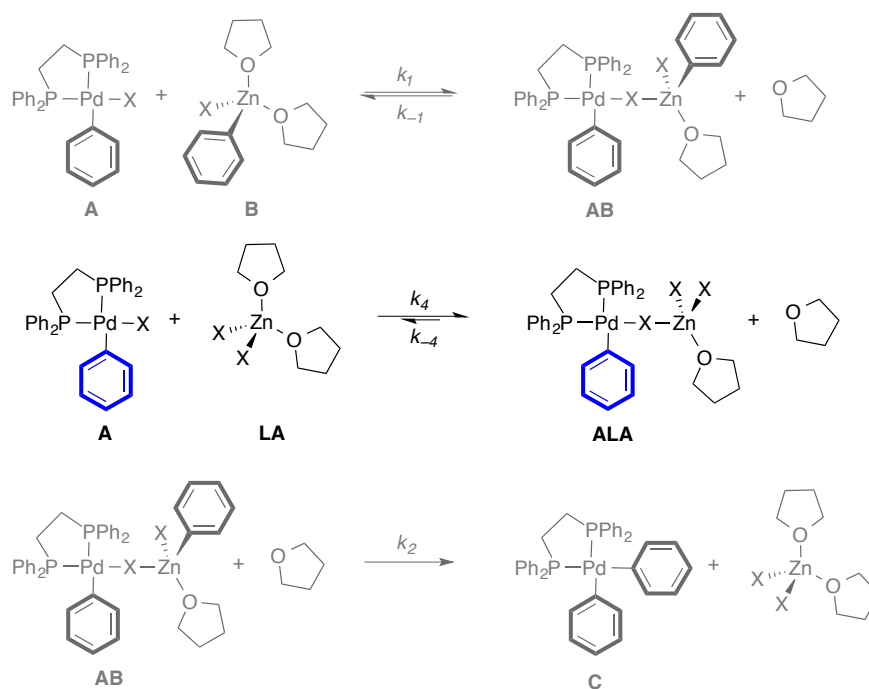
In case large amounts of a Lewis acid, such as ZnCl$_2$ is added to the reaction, and the complexes A form unproductive adduct ALA, the derivative if the logarithm of the concentration of [A] is not zero anymore (*cf.* eq 40).

(eq. 77)
$$\rho_{obs}^{LA} = \rho_{obs}^{w/o} + \frac{d}{d\sigma} log([A])$$

(eq. 78)
$$\frac{d}{d\sigma} log([A]) \neq 0$$

In this case, the concentration of [A] has an influence of the observed Hammett constant ρ_{obs}. The concentration of [A] can be calculated from equilibrium constant $K_{\pm 4}$ and the law of mass action:

(eq. 79)
$$K_{\pm 4} = \frac{k_4}{k_{-4}} = \frac{[ALA]}{[A][LA]}$$

(eq. 80)
$$0 = k_4[A][LA] - k_{-4}[ALA]$$

With

(eq. 81)
$$[ALA] = [A]_0 - [A]$$

(eq. 82)
$$[LA] = [LA]_0 - [ALA] = [LA]_0 - [A]_0 + [A]$$

Insertion into equation 80:

(eq. 83)
$$0 = k_4[A]([LA]_0 - [A]_0 + [A]) - k_{-4}([A]_0 - [A])$$

(eq. 84)
$$0 = k_4[A]^2 + k_4[A][LA]_0 - k_4[A][A]_0 - k_{-4}[A]_0 + k_{-4}[A]$$

(eq. 85)
$$0 = k_4[A]^2 + [A](k_4[LA]_0 - k_4[A]_0 + k_{-4}) - k_{-4}[A]_0$$

(eq. 86)
$$0 = [A]^2 + [A]\left(\frac{k_{-4}}{k_4} + [LA]_0 - [A]_0\right) - \frac{k_{-4}}{k_4}[A]_0$$

(eq. 87)
$$0 = [A]^2 + [A]\left(\frac{1}{K_{\pm 4}} + [LA]_0 - [A]_0\right) - \frac{1}{K_{\pm 4}}[A]_0$$

With the substitutions:

(eq. 88)
$$[A] = \alpha[A]_0$$

(eq. 89)
$$[LA]_0 = b[A]_0$$

The factor α describes the proportion of the concentration $[A]$ relative to the initial concentration $[A]_0$ and the factor b describes the equivalents of the added Lewis acid $[LA]$ relative to the initial concentration of $[A]_0$.

(eq. 90)
$$0 = \alpha^2 \cdot [A]_0^2 + \alpha[A]_0\left(\frac{1}{K_{\pm 4}} + b[A]_0 - [A]_0\right) - \frac{1}{K_{\pm 4}}[A]_0$$

(eq. 91)
$$0 = \alpha^2 + \alpha\left(\frac{1}{K_{\pm 4}[A]_0} + b - 1\right) - \frac{1}{K_{\pm 4}[A]_0}$$

Solving the equation 91 with the pq-formula:

(eq. 92)
$$\alpha = -\frac{1}{2} \cdot \left(\frac{1}{K_{\pm 4}[A]_0} + b - 1\right) \pm \sqrt{\frac{1}{4}\left(\frac{1}{K_{\pm 4}[A]_0} + b - 1\right)^2 + \frac{1}{K_{\pm 4}[A]_0}}$$

However with b ≥ 1, only the addition of the square root would lead to a physically sensible result:

(eq. 93)
$$\alpha = -\frac{1}{2} \cdot \left(\frac{1}{K_{\pm 4}[A]_0} + b - 1\right) + \sqrt{\frac{1}{4}\left(\frac{1}{K_{\pm 4}[A]_0} + b - 1\right)^2 + \frac{1}{K_{\pm 4}[A]_0}}$$

(eq. 94)
$$\alpha = -\frac{1}{2} \cdot \left(\frac{1}{K_{\pm 4}[A]_0} + b - 1\right) + \sqrt{\frac{1}{4K_{\pm 4}^2[A]_0^2} + \frac{(b-1)}{2K_{\pm 4}[A]_0} + \frac{1}{K_{\pm 4}[A]_0} + \frac{(b-1)^2}{4}}$$

(eq. 95)
$$\alpha = -\frac{1}{2} \cdot \left(\frac{1}{K_{\pm 4}[A]_0} + b - 1\right) + \sqrt{\frac{1}{4K_{\pm 4}^2[A]_0^2} + \frac{(b+1)}{2K_{\pm 4}[A]_0} + \frac{(b-1)^2}{4}}$$

To derive the logarithm of α, the derivative of equation 95 has to be formed:

(eq. 96)
$$\frac{d}{d\sigma} log(\alpha) = \frac{\alpha'}{\alpha \cdot ln(10)}$$

where

(eq. 97)
$$\alpha' = \frac{d}{d\sigma}\alpha$$

And with:

(eq. 98)
$$\frac{d}{d\sigma}\frac{1}{K} = -\frac{\rho}{K} \cdot ln(10)$$

(eq. 99)
$$\frac{d}{d\sigma}\frac{1}{(K)^2} = -\frac{2\rho}{(K)^2} \cdot ln(10)$$

The derivative of equation 95 is:

(eq. 100)
$$\alpha' = +\frac{\rho_{\pm4}}{2K_{\pm4}[A]_0} \cdot ln(10) - \frac{\left(\frac{\rho_{\pm4}}{2K_{\pm4}^2[A]_0^2} + \frac{\rho_{\pm4}(b+1)}{2K_{\pm4}[A]_0}\right) \cdot ln(10)}{2\sqrt{\frac{1}{4}\left(\frac{1}{K_{\pm4}[A]_0} + b - 1\right)^2 + \frac{1}{K_{\pm4}[A]_0}}}$$

(eq. 101)
$$\alpha' = +\frac{\rho_{\pm4}}{K_{\pm4}[A]_0} \cdot ln(10)\left[\frac{1}{2} - \frac{\left(\frac{1}{2K_{\pm4}[A]_0} + \frac{(b+1)}{2}\right)}{2\sqrt{\frac{1}{4}\left(\frac{1}{K_{\pm4}[A]_0} + b - 1\right)^2 + \frac{1}{K_{\pm4}[A]_0}}}\right]$$

(eq. 102)
$$\alpha' = +\frac{\rho_{\pm4}}{K_{\pm4}[A]_0} \cdot ln(10)\left[\frac{1}{2} - \frac{(1 + (b+1)K_{\pm4}[A]_0)}{4K_{\pm4}[A]_0\sqrt{\frac{1}{4}\left(\frac{1}{K_{\pm4}[A]_0} + b - 1\right)^2 + \frac{1}{K_{\pm4}[A]_0}}}\right]$$

(eq. 103)
$$\frac{d}{d\sigma} log(\alpha) = \frac{\frac{\rho_{\pm4}}{K_{\pm4}[A]_0}\left[\frac{1}{2} - \frac{1 + (b+1)K_{\pm4}[A]_0}{4K_{\pm4}[A]_0\sqrt{\frac{1}{4}\left(\frac{1}{K_{\pm4}[A]_0} + b - 1\right)^2 + \frac{1}{K_{\pm4}[A]_0}}}\right]}{-\frac{1}{2} \cdot \left(\frac{1}{K_{\pm4}[A]_0} + b - 1\right) + \sqrt{\frac{1}{4}\left(\frac{1}{K_{\pm4}[A]_0} + b - 1\right)^2 + \frac{1}{K_{\pm4}[A]_0}}}$$

The long mathematical term can be considered as a factor f, with which the Hammett constant $\rho_{\pm4}$ contributes to the observed Hammett constant ρ_{obs}. This factor f becomes zero if no Lewis acid is added and reaches -1 for large amounts of Lewis acid (see graph below).

(eq. 104)

$$f = \cfrac{\cfrac{1}{K_{\pm4}[A]_0}\left[+\cfrac{1}{2}-\cfrac{1+(b+1)K_{\pm4}[A]_0}{4K_{\pm4}[A]_0\sqrt{\cfrac{1}{4}\left(\cfrac{1}{K_{\pm4}[A]_0}+b-1\right)^2+\cfrac{1}{K_{\pm4}[A]_0}}}\right]}{-\cfrac{1}{2}\cdot\left(\cfrac{1}{K_{\pm4}[A]_0}+b-1\right)+\sqrt{\cfrac{1}{4}\left(\cfrac{1}{K_{\pm4}[A]_0}+b-1\right)^2+\cfrac{1}{K_{\pm4}[A]_0}}}$$

With $\rho_{\pm4} = \rho_{-4} - \rho_4$

(eq. 105)

$$\rho_{obs}^{LA} = \rho_{obs}^{w/o} + (\rho_{-4} - \rho_4) \cdot f$$

With $\rho_{\pm4} < 0$, $\rho_{obs}^{LA} > \rho_{obs}^{w/o}$ upon addition of Lewis acid LA.
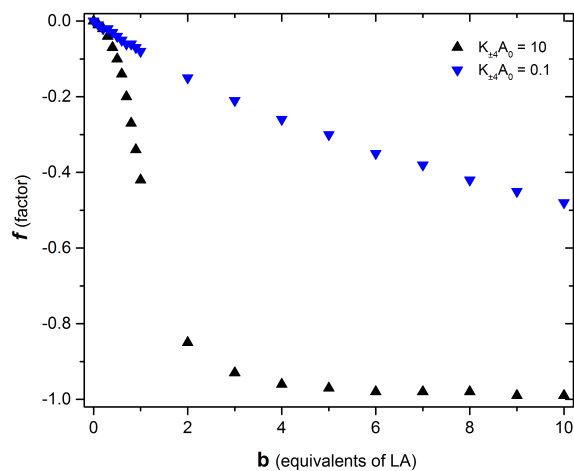
8 References

[1]   (a) M. H. Pérez-Temprano, J. A. Casares, P. Espinet, *Chem. Eur. J.* **2012**, *18*, 1864; (b) S. Tamke, J. Paradies, *Nachr. Chem.* **2013**, *61*, 536.

[2]   A. J. J. Lennox, G. C. Lloyd-Jones, *Angew. Chem. Int. Ed.* **2013**, *52*, 7362.

[3]   (a) P. Espinet, A. M. Echavarren, *Angew. Chem. Int. Ed.* **2004**, *43*, 4704; (b) C. Cordovilla, C. Bartolomé, J. M. Martínez-Ilarduya, P. Espinet, *ACS Catalysis* **2015**, *5*, 3040.

[4]   S. E. Denmark, R. F. Sweis, in *Metal-Catalyzed Cross-Coupling Reactions and More*, Wiley-VCH Verlag GmbH & Co. KGaA, **2014**, pp. 475.

[5]   C. He, J. Ke, H. Xu, A. Lei, *Angew. Chem.* **2013**, *125*, 1567.

[6]   L. Jin, A. Lei, *Org. Biomol. Chem.* **2012**, *10*, 6817.

[7]   (a) V. Farina, B. Krishnan, D. R. Marshall, G. P. Roth, *J. Org. Chem.* **1993**, *58*, 5434; (b) V. R. Lando, A. L. Monteiro, *Org. Lett.* **2003**, *5*, 2891; (c) C. M. Nunes, A. L. Monteiro, *J. Brazil. Chem. Soc.* **2007**, *18*, 1443; (d) D. Zim, S. M. Nobre, A. L. Monteiro, *J. Mol. Catal. A: Chem.* **2008**, *287*, 16; (e) S. E. Denmark, R. C. Smith, W.-T. T. Chang, *Tetrahedron* **2011**, *67*, 4391; (f) J. Li, L. Jin, C. Liu, A. Lei, *Org. Chem. Front.* **2014**, *1*, 50; (g) J. Li, L. Jin, C. Liu, A. Lei, *Chem. Commun.* **2013**, *49*, 9615; (h) Z.-B. Dong, G. Manolikakes, L. Shi, P. Knochel, H. Mayr, *Chem. Eur. J.* **2010**, *16*, 248.

[8]   (a) L. P. Hammett, *Chem. Rev.* **1935**, *17*, 125; (b) L. P. Hammett, *J. Am. Chem. Soc.* **1937**, *59*, 96.

[9]   C. Hansch, A. Leo, R. W. Taft, *Chem. Rev.* **1991**, *91*, 165.

[10]   H. H. Jaffé, *Chem. Rev.* **1953**, *53*, 191.

[11]   (a) J. Catalán, C. Díaz, F. García-Blanco, *J. Org. Chem.* **1999**, *64*, 6512; (b) A. H. Fainberg, S. Winstein, *J. Am. Chem. Soc.* **1956**, *78*, 2770; (c) S. Winstein, E. Grunwald, H. W. Jones, *J. Am. Chem. Soc.* **1951**, *73*, 2700; (d) E. Grunwald, S. Winstein, *J. Am. Chem. Soc.* **1948**, *70*, 846.

[12]   J. O. Schreck, *J. Chem. Educ.* **1971**, *48*, 103.

[13]   (a) L. M. Stock, H. C. Brown, in *Advances in Physical Organic Chemistry, Vol. Volume 1* (Ed.: V. Gold), Academic Press, **1963**, pp. 35; (b) H. C. Brown, Y. Okamoto, *J. Am. Chem. Soc.* **1957**, *79*, 1913.

[14]   (a) R. J. Cross, *Chem. Soc. Rev.* **1985**, *14*, 197; (b) R. Romeo, *Comment. Inorg. Chem.* **1990**, *11*, 21; (c) D. T. Richens, *Chem. Rev.* **2005**, *105*, 1961; (d) B. Fred, in *Mechanisms of Inorganic Reactions, Vol. 49*, American Chemical Society, **1965**, pp. 81.

[15]   (a) C. Bartolomé, P. Espinet, Jose M. Martín-Álvarez, F. Villafañe, *Eur. J. Inorg. Chem.* **2004**, *2004*, 2326; (b) R. Romeo, A. Grassi, L. Monsu Scolaro, *Inorg. Chem.* **1992**, *31*, 4383; (c) U.

Frey, L. Helm, A. E. Merbach, R. Romeo, *J. Am. Chem. Soc.* **1989**, *111*, 8161; (d) J. A. Casares, S. Coco, P. Espinet, Y.-S. Lin, *Organometallics* **1995**, *14*, 3058.

[16]   A. L. Casado, P. Espinet, *Organometallics* **1998**, *17*, 954.

[17]   J. Vicente, A. Arcas, D. Bautista, P. G. Jones, *Organometallics* **1997**, *16*, 2127.

[18]   A. W. Verstuyft, J. H. Nelson, *Inorg. Chem.* **1975**, *14*, 1501.

[19]   (a) J. M. Brown, N. A. Cooley, *Chem. Rev.* **1988**, *88*, 1031; (b) A. Gillie, J. K. Stille, *J. Am. Chem. Soc.* **1980**, *102*, 4933.

[20]   (a) B. Martín-Matute, K. J. Szabó, T. N. Mitchell, in *Metal-Catalyzed Cross-Coupling Reactions and More*, Wiley-VCH Verlag GmbH & Co. KGaA, **2014**, pp. 423; (b) A. M. Echavarren, A. Homs, in *Metal-Catalyzed Cross-Coupling Reactions and More*, Wiley-VCH Verlag GmbH & Co. KGaA, **2014**, pp. 1.

[21]   (a) J. W. Labadie, J. K. Stille, *J. Am. Chem. Soc.* **1983**, *105*, 6129; (b) E. C. Swift, E. R. Jarvo, *Tetrahedron* **2013**, *69*, 5799.

[22]   (a) R. Á. O. N. Faza, A. R. de Lera, D. J. Cárdenas, *Adv. Synth. Catal.* **2007**, *349*, 887; (b) R. Álvarez, O. N. Faza, C. S. López, Á. R. de Lera, *Org. Lett.* **2006**, *8*, 35; (c) M. García-Melchor, A. A. C. Braga, A. Lledós, G. Ujaque, F. Maseras, *Acc. Chem. Res.* **2013**, *46*, 2626; (d) A. L. Casado, P. Espinet, *J. Am. Chem. Soc.* **1998**, *120*, 8978.

[23]   V. Farina, *Pure Appl. Chem.* **1996**, *68*, 73.

[24]   (a) V. Farina, B. Krishnan, *J. Am. Chem. Soc.* **1991**, *113*, 9585; (b) J. Louie, J. F. Hartwig, *J. Am. Chem. Soc.* **1995**, *117*, 11598; (c) A. Ariafard, B. F. Yates, *J. Am. Chem. Soc.* **2009**, *131*, 13981.

[25]   V. Farina, S. Kapadia, B. Krishnan, C. Wang, L. S. Liebeskind, *J. Org. Chem.* **1994**, *59*, 5905.

[26]   A. Ariafard, Z. Lin, I. J. S. Fairlamb, *Organometallics* **2006**, *25*, 5788.

[27]   J. C. H. Lee, D. G. Hall, in *Metal-Catalyzed Cross-Coupling Reactions and More*, Wiley-VCH Verlag GmbH & Co. KGaA, **2014**, pp. 65.

[28]   A. A. Thomas, S. E. Denmark, *Science* **2016**, *352*, 329.

[29]   D. Leonori, V. K. Aggarwal, *Angew. Chem. Int. Ed.* **2015**, *54*, 1082.

[30]   (a) C. Amatore, A. Jutand, G. Le Duc, *Chem. Eur. J.* **2011**, *17*, 2492; (b) C. Amatore, A. Jutand, G. Le Duc, *Angew. Chem. Int. Ed.* **2012**, *51*, 1379.

[31]   (a) K. Matos, J. A. Soderquist, *J. Org. Chem.* **1998**, *63*, 461; (b) C. F. R. A. C. Lima, A. S. M. C. Rodrigues, V. L. M. Silva, A. M. S. Silva, L. M. N. B. F. Santos, *ChemCatChem* **2014**, *6*, 1291.

[32]   T. Moriya, N. Miyaura, A. Suzuki, *Synlett* **1994**, *1994*, 149.

[33]   Y. Nakao, T. Hiyama, *Chem. Soc. Rev.* **2011**, *40*, 4893.

[34]   (a) S. A. Tymonko, R. C. Smith, A. Ambrosi, S. E. Denmark, *J. Am. Chem. Soc.* **2015**, *137*, 6192; (b) S. E. Denmark, R. F. Sweis, *J. Am. Chem. Soc.* **2004**, *126*, 4876; (c) S. E. Denmark,

N. S. Werner, *J. Am. Chem. Soc.* **2010**, *132*, 3612; (d) S. E. Denmark, R. C. Smith, *J. Am. Chem. Soc.* **2010**, *132*, 1243.

[35] (a) M. R. an der Heiden, H. Plenio, S. Immel, E. Burello, G. Rothenberg, H. C. J. Hoefsloot, *Chem. Eur. J.* **2008**, *14*, 2857; (b) M. an der Heiden, H. Plenio, *Chem. Commun.* **2007**, 972.

[36] (a) K. Sonogashira, *J. Organomet. Chem.* **2002**, *653*, 46; (b) R. Chinchilla, C. Nájera, *Chem. Rev.* **2007**, *107*, 874; (c) R. Chinchilla, C. Najera, *Chem. Soc. Rev.* **2011**, *40*, 5084; (d) M. Karak, L. C. A. Barbosa, G. C. Hargaden, *RSC Adv.* **2014**, *4*, 53442.

[37] A. Ricci, F. Angelucci, M. Bassetti, C. Lo Sterzo, *J. Am. Chem. Soc.* **2002**, *124*, 1060.

[38] (a) R. J. Oeschger, D. H. Ringger, P. Chen, *Organometallics* **2015**, *34*, 3888; (b) I. Meana, P. Espinet, A. C. Albéniz, *Organometallics* **2014**, *33*, 1.

[39] (a) K. Koszinowski, P. Böhrer, *Organometallics* **2009**, *28*, 100; (b) K. Koszinowski, P. Böhrer, *Organometallics* **2009**, *28*, 771; (c) T. D. Bluemke, W. Clegg, P. Garcia-Alvarez, A. R. Kennedy, K. Koszinowski, M. D. McCall, L. Russo, E. Hevia, *Chem. Sci.* **2014**, *5*, 3552; (d) Z. Zhu, M. Brynda, R. J. Wright, R. C. Fischer, W. A. Merrill, E. Rivard, R. Wolf, J. C. Fettinger, M. M. Olmstead, P. P. Power, *J. Am. Chem. Soc.* **2007**, *129*, 10847; (e) Y. Wang, B. Quillian, C. S. Wannere, P. Wei, P. v. R. Schleyer, G. H. Robinson, *Organometallics* **2007**, *26*, 3054; (f) L. Jin, C. Liu, J. Liu, F. Hu, Y. Lan, A. S. Batsanov, J. A. K. Howard, T. B. Marder, A. Lei, *J. Am. Chem. Soc.* **2009**, *131*, 16656; (g) J. J. Dunsford, E. R. Clark, M. J. Ingleson, *Angew. Chem. Int. Ed.* **2015**, *54*, 5688; (h) H. N. Hunter, N. Hadei, V. Blagojevic, P. Patschinski, G. T. Achonduh, S. Avola, D. K. Bohme, M. G. Organ, *Chem. Eur. J.* **2011**, *17*, 7845.

[40] (a) A. Krasovskiy, V. Malakhov, A. Gavryushin, P. Knochel, *Angew. Chem. Int. Ed.* **2006**, *45*, 6040; (b) H. Ren, G. Dunet, P. Mayer, P. Knochel, *J. Am. Chem. Soc.* **2007**, *129*, 5376; (c) N. Boudet, S. Sase, P. Sinha, C.-Y. Liu, A. Krasovskiy, P. Knochel, *J. Am. Chem. Soc.* **2007**, *129*, 12358; (d) A. Metzger, M. A. Schade, P. Knochel, *Org. Lett.* **2008**, *10*, 1107.

[41] L. C. McCann, M. G. Organ, *Angew. Chem. Int. Ed.* **2014**, *53*, 4386.

[42] C. J. OBrien, E. A. B. Kantchev, C. Valente, N. Hadei, G. A. Chass, A. Lough, A. C. Hopkinson, M. G. Organ, *Chem. Eur. J.* **2006**, *12*, 4743.

[43] (a) N. Hadei, E. A. B. Kantchev, C. J. O'Brie, M. G. Organ, *J. Org. Chem.* **2005**, *70*, 8503; (b) N. Hadei, E. A. B. Kantchev, C. J. O'Brie, M. G. Organ, *Org. Lett.* **2005**, *7*, 3805; (c) M. G. Organ, S. Avola, I. Dubovyk, N. Hadei, E. A. B. Kantchev, C. J. O'Brien, C. Valente, *Chem. Eur. J.* **2006**, *12*, 4749; (d) C. Valente, M. E. Belowich, N. Hadei, M. G. Organ, *Eur. J. Org. Chem.* **2010**, *2010*, 4343; (e) M. Pompeo, R. D. J. Froese, N. Hadei, M. G. Organ, *Angew. Chem. Int. Ed.* **2012**, *51*, 11354; (f) S. Calimsiz, M. G. Organ, *Chem. Commun.* **2011**, *47*, 5181; (g) S. Çalimsiz, M. Sayah, D. Mallik, M. G. Organ, *Angew. Chem. Int. Ed.* **2010**, *49*, 2014.

[44]   G. T. Achonduh, N. Hadei, C. Valente, S. Avola, C. J. O'Brien, M. G. Organ, *Chem. Commun.* **2010**, *46*, 4109.

[45]   N. Hadei, G. T. Achonduh, C. Valente, C. J. O'Brien, M. G. Organ, *Angew. Chem. Int. Ed.* **2011**, *50*, 3896.

[46]   (a) J. A. Casares, P. Espinet, B. Fuentes, G. Salas, *J. Am. Chem. Soc.* **2007**, *129*, 3508; (b) B. Fuentes, M. García-Melchor, A. Lledós, F. Maseras, J. A. Casares, G. Ujaque, P. Espinet, *Chem. Eur. J.* **2010**, *16*, 8596; (c) M. García-Melchor, B. Fuentes, A. Lledós, J. A. Casares, G. Ujaque, P. Espinet, *J. Am. Chem. Soc.* **2011**, *133*, 13519; (d) J. delPozo, E. Gioria, J. A. Casares, R. Álvarez, P. Espinet, *Organometallics* **2015**, *34*, 3120.

[47]   M. L. Clarke, M. Heydt, *Organometallics* **2005**, *24*, 6475.

[48]   P. Ribagnac, M. Blug, J. Villa-Uribe, X.-F. Le Goff, C. Gosmini, N. Mézailles, *Chem. Eur. J.* **2011**, *17*, 14389.

[49]   A. B. González-Pérez, R. Álvarez, O. N. Faza, Á. R. de Lera, J. M. Aurrecoechea, *Organometallics* **2012**, *31*, 2053.

[50]   K. Böck, J. E. Feil, K. Karaghiosoff, K. Koszinowski, *Chem. Eur. J.* **2015**, *21*, 5548.

[51]   (a) G. A. Chass, C. J. O'Brien, N. Hadei, E. A. B. Kantchev, W.-H. Mu, D.-C. Fang, A. C. Hopkinson, I. G. Csizmadia, M. G. Organ, *Chem. Eur. J.* **2009**, *15*, 4281; (b) Q. Liu, Y. Lan, J. Liu, G. Li, Y.-D. Wu, A. Lei, *J. Am. Chem. Soc.* **2009**, *131*, 10201.

[52]   (a) U. Christmann, R. Vilar, *Angew. Chem. Int. Ed.* **2005**, *44*, 366; (b) P. G. Gildner, T. J. Colacot, *Organometallics* **2015**, *34*, 5497.

[53]   (a) M. Ludwig, S. Strömberg, M. Svensson, B. Åkermark, *Organometallics* **1999**, *18*, 970; (b) G. Mann, D. Baranano, J. F. Hartwig, A. L. Rheingold, I. A. Guzei, *J. Am. Chem. Soc.* **1998**, *120*, 9205; (c) T. I. Wallow, F. E. Goodson, B. M. Novak, *Organometallics* **1996**, *15*, 3708; (d) B. A. Markies, A. J. Canty, W. de Graaf, J. Boersma, M. D. Janssen, M. P. Hogerheide, W. J. J. Smeets, A. L. Spek, G. van Koten, *J. Organomet. Chem.* **1994**, *482*, 191; (e) T. Ogata, J. F. Hartwig, *J. Am. Chem. Soc.* **2008**, *130*, 13848; (f) C. Czauderna, H. Wurziger, Y. Sun, W. R. Thiel, *Z. Anorg. Allg. Chem.* **2008**, *634*, 2380.

[54]   (a) N. D. Ball, J. B. Gary, Y. Ye, M. S. Sanford, *J. Am. Chem. Soc.* **2011**, *133*, 7577; (b) M. Yamashita, J. V. Cuevas Vicario, J. F. Hartwig, *J. Am. Chem. Soc.* **2003**, *125*, 16347.

[55]   N. D. Ball, J. W. Kampf, M. S. Sanford, *J. Am. Chem. Soc.* **2010**, *132*, 2878.

[56]   J. L. Hoare, K. Lorenz, N. J. Hovestad, W. J. J. Smeets, A. L. Spek, A. J. Canty, H. Frey, G. van Koten, *Organometallics* **1997**, *16*, 4167.

[57]   M. S. Driver, J. F. Hartwig, *J. Am. Chem. Soc.* **1997**, *119*, 8232.

[58]   F. Paul, J. Patt, J. F. Hartwig, *J. Am. Chem. Soc.* **1994**, *116*, 5969.

[59]   (a) J. P. Stambuli, C. D. Incarvito, M. Bühl, J. F. Hartwig, *J. Am. Chem. Soc.* **2004**, *126*, 1184; (b) J. P. Stambuli, M. Bühl, J. F. Hartwig, *J. Am. Chem. Soc.* **2002**, *124*, 9346.

[60]   (a) P. Larini, C. E. Kefalidis, R. Jazzar, A. Renaudat, E. Clot, O. Baudoin, *Chem. Eur. J.* **2012**, *18*, 1932; (b) M. A. Düfert, K. L. Billingsley, S. L. Buchwald, *J. Am. Chem. Soc.* **2013**, *135*, 12877; (c) T. E. Barder, M. R. Biscoe, S. L. Buchwald, *Organometallics* **2007**, *26*, 2183.

[61]   (a) A. J. DeAngelis, P. G. Gildner, R. Chow, T. J. Colacot, *J. Org. Chem.* **2015**, *80*, 6794; (b) H. G. Lee, P. J. Milner, M. T. Colvin, L. Andreas, S. L. Buchwald, *Inorg. Chim. Acta* **2014**, *422*, 188; (c) P. J. Milner, T. J. Maimone, M. Su, J. Chen, P. Müller, S. L. Buchwald, *J. Am. Chem. Soc.* **2012**, *134*, 19922; (d) M. Su, S. L. Buchwald, *Angew. Chem. Int. Ed.* **2012**, *51*, 4710; (e) E. V. Vinogradova, B. P. Fors, S. L. Buchwald, *J. Am. Chem. Soc.* **2012**, *134*, 11132.

[62]   R. A. Widenhoefer, H. A. Zhong, S. L. Buchwald, *Organometallics* **1996**, *15*, 2745.

[63]   F. Paul, J. Patt, J. F. Hartwig, *Organometallics* **1995**, *14*, 3030.

[64]   J. D. Neukom, N. S. Perch, J. P. Wolfe, *Organometallics* **2011**, *30*, 1269.

[65]   M. Yamashita, J. F. Hartwig, *J. Am. Chem. Soc.* **2004**, *126*, 5344.

[66]   L. M. Alcazar-Roman, J. F. Hartwig, A. L. Rheingold, L. M. Liable-Sands, I. A. Guzei, *J. Am. Chem. Soc.* **2000**, *122*, 4618.

[67]   (a) V. V. Grushin, W. J. Marshall, *J. Am. Chem. Soc.* **2006**, *128*, 4632; (b) J. R. Moncarz, T. J. Brunker, J. C. Jewett, M. Orchowski, D. S. Glueck, R. D. Sommer, K.-C. Lam, C. D. Incarvito, T. E. Concolino, C. Ceccarelli, L. N. Zakharov, A. L. Rheingold, *Organometallics* **2003**, *22*, 3205.

[68]   (a) J.-F. Ma, Y. Yamamoto, *Inorg. Chim. Acta* **2000**, *299*, 164; (b) J. M. Brown, J. J. Perez-Torrente, N. W. Alcock, H. J. Clase, *Organometallics* **1995**, *14*, 207; (c) I. R. Butler, L. J. Hobson, S. J. Coles, M. B. Hursthouse, K. M. A. Malik, *J. Organomet. Chem.* **1997**, *540*, 27.

[69]   J. P. Flemming, M. C. Pilon, O. Y. Borbulevitch, M. Y. Antipin, V. V. Grushin, *Inorg. Chim. Acta* **1998**, *280*, 87.

[70]   (a) P. Fitton, E. A. Rick, *J. Organomet. Chem.* **1971**, *28*, 287; (b) P. E. Garrou, R. F. Heck, *J. Am. Chem. Soc.* **1976**, *98*, 4115; (c) C. Amatore, A. Jutand, F. Khalil, M. F. Nielsen, *J. Am. Chem. Soc.* **1992**, *114*, 7076; (d) A. H. Roy, J. F. Hartwig, *Organometallics* **2004**, *23*, 1533; (e) W. R. Moser, A. W. Wang, N. K. Kildahl, *J. Am. Chem. Soc.* **1988**, *110*, 2816; (f) A. Jutand, S. Négri, A. Principaud, *Eur. J. Inorg. Chem.* **2005**, *2005*, 631.

[71]   (a) F. E. Goodson, T. I. Wallow, B. M. Novak, *J. Am. Chem. Soc.* **1997**, *119*, 12441; (b) B. E. Segelstein, T. W. Butler, B. L. Chenard, *J. Org. Chem.* **1995**, *60*, 12; (c) D. Marcoux, A. B. Charette, *J. Org. Chem.* **2008**, *73*, 590.

[72]   M. Sundermeier, S. Mutyala, A. Zapf, A. Spannenberg, M. Beller, *J. Organomet. Chem.* **2003**, *684*, 50.

[73]   M. R. Biscoe, B. P. Fors, S. L. Buchwald, *J. Am. Chem. Soc.* **2008**, *130*, 6686.

[74]   N. C. Bruno, N. Niljianskul, S. L. Buchwald, *J. Org. Chem.* **2014**, *79*, 4161.

[75]   F. Barrios-Landeros, B. P. Carrow, J. F. Hartwig, *J. Am. Chem. Soc.* **2009**, *131*, 8141.

[76]   (a) V. V. Grushin, W. J. Marshall, *J. Am. Chem. Soc.* **2009**, *131*, 918; (b) A. Maleckis, M. S. Sanford, *Organometallics* **2011**, *30*, 6617.

[77]   (a) B. P. Carrow, J. F. Hartwig, *J. Am. Chem. Soc.* **2010**, *132*, 79; (b) A. G. Sergeev, A. Spannenberg, M. Beller, *J. Am. Chem. Soc.* **2008**, *130*, 15549.

[78]   F. Barrios-Landeros, B. P. Carrow, J. F. Hartwig, *J. Am. Chem. Soc.* **2008**, *130*, 5842.

[79]   T. Klatt, J. T. Markiewicz, C. Sämann, P. Knochel, *J. Org. Chem.* **2014**, *79*, 4253.

[80]   H. K. Hofstee, J. Boersma, G. J. M. Van Der Kerk, *J. Organomet. Chem.* **1978**, *144*, 255.

[81]   P. Knochel, S. Bernhardt, G. Manolikakes, Google Patents, **2014**.

[82]   A. Côté, A. B. Charette, *J. Am. Chem. Soc.* **2008**, *130*, 2771.

[83]   R. Li-Yuan Bao, R. Zhao, L. Shi, *Chem. Commun.* **2015**, *51*, 6884.

[84]   D. Villemin, B. Nechab, *J. Chem. Res.* **2000**, *2000*, 432.

[85]   (a) G. A. Olah, B. G. B. Gupta, R. Malhotra, S. C. Narang, *J. Org. Chem.* **1980**, *45*, 1638; (b) A. R. Bassindale, T. Stout, *Tetrahedron Lett.* **1985**, *26*, 3403; (c) M. G. Voronkov, E. I. Dubinskaya, *J. Organomet. Chem.* **1991**, *410*, 13; (d) M. E. Jung, P. L. Ornstein, *Tetrahedron Lett.* **1977**, *18*, 2659.

[86]   (a) S. Ram, R. E. Ehrenkaufer, *Synthesis* **1988**, *1988*, 91; (b) N. A. Cortese, R. F. Heck, *J. Org. Chem.* **1977**, *42*, 3491; (c) S. Cacchi, P. G. Ciattini, E. Morera, G. Ortar, *Tetrahedron Lett.* **1986**, *27*, 5541.

[87]   G. Hilt, F. Pünner, J. Möbus, V. Naseri, M. A. Bohn, *Eur. J. Org. Chem.* **2011**, *2011*, 5962.

[88]   Y. Zhao, D. G. Truhlar, *Theor. Chem. Acc.* **2008**, *120*, 215.

[89]   M. Weidenbruch, M. Herrndorf, A. Schäfer, S. Pohl, W. Saak, *J. Organomet. Chem.* **1989**, *361*, 139.

[90]   J. Tomasi, B. Mennucci, R. Cammi, *Chem. Rev.* **2005**, *105*, 2999.

[91]   C. A. Tolman, *Chem. Rev.* **1977**, *77*, 313.

[92]   Y. Tan, F. Barrios-Landeros, J. F. Hartwig, *J. Am. Chem. Soc.* **2012**, *134*, 3683.

[93]   G. T. L. Broadwood-Strong, P. A. Chaloner, P. B. Hitchcock, *Polyhedron* **1993**, *12*, 721.

[94]   (a) G. Bringmann, Y. Reichert, V. V. Kane, *Tetrahedron* **2004**, *60*, 3539; (b) Q.-Y. Li, Y.-G. Zu, R.-Z. Shi, L.-P. Yao, *Curr. Med. Chem.* **2006**, *13*, 2021.

[95]   A. D. Bolzán, M. S. Bianchi, *Mutat. Res.* **2001**, *488*, 25.

[96]   E. V. Dehmlow, H.-J. Schulz, *Liebigs Ann. Chem.* **1987**, *1987*, 857.

[97]   (a) P. Fu, S. Wang, K. Hong, X. Li, P. Liu, Y. Wang, W. Zhu, *J. Nat. Prod.* **2011**, *74*, 1751; (b) A. Funk, P. V. Divekar, *Can. J. Microbiol.* **1959**, *5*, 317; (c) S. Kaur, G. Srivastava, A. N. Sharma, R. S. Jolly, *Brit. J. Pharmacol.* **2015**, *172*, 2286; (d) W. Kujur, R. K. Gurram, N. Haleem, S. K. Maurya, J. N. Agrewala, *Sci. Rep.* **2015**, *5*, 15396; (e) D. K. Chatterjee, W. Raether, N. Iyer, B. N. Ganguli, *Z. Parasitenk.* **1984**, *70*, 569; (f) A. K. Singla, R. K. Gurram, A. Chauhan, N. Khatri, R. M. Vohra, R. S. Jolly, J. N. Agrewala, *PLoS ONE* **2014**, *9*, e107051.

[98]   (a) George R. Newkome, Anil K. Patri, E. Holder, Ulrich S. Schubert, *Eur. J. Org. Chem.* **2004**, *2004*, 235; (b) F. Mongin, F. Trécourt, B. Gervais, O. Mongin, G. Quéguiner, *J. Org. Chem.* **2002**, *67*, 3272; (c) T. Sammakia, E. L. Stangeland, M. C. Whitcomb, *Org. Lett.* **2002**, *4*, 2385; (d) F. Trécourt, B. Gervais, M. Mallet, G. Quéguiner, *J. Org. Chem.* **1996**, *61*, 1673.

[99]   (a) P. Pierrat, P. Gros, Y. Fort, *Org. Lett.* **2005**, *7*, 697; (b) P. Rocca, F. Marsais, A. Godard, G. Quéguiner, *Tetrahedron Lett.* **1993**, *34*, 2937; (c) F. Gosselin, S. J. Savage, N. Blaquiere, S. T. Staben, *Org. Lett.* **2012**, *14*, 862.

[100]   (a) J. A. Zoltewicz, C. D. Dill, *Tetrahedron* **1996**, *52*, 14469; (b) A. Takahashi, Y. Hirose, H. Kusama, N. Iwasawa, *Chem. Commun.* **2008**, 609.

[101]   (a) T. W. Lyons, M. S. Sanford, *Chem. Rev.* **2010**, *110*, 1147; (b) A. R. Dick, M. S. Sanford, *Tetrahedron* **2006**, *62*, 2439; (c) D. Kalyani, M. Sanford, in *Directed Metallation, Vol. 24* (Ed.: N. Chatani), Springer Berlin Heidelberg, **2007**, pp. 85.

[102]   (a) D. Kalyani, A. R. Dick, W. Q. Anani, M. S. Sanford, *Org. Lett.* **2006**, *8*, 2523; (b) A. R. Dick, K. L. Hull, M. S. Sanford, *J. Am. Chem. Soc.* **2004**, *126*, 2300; (c) A. S. Dudnik, N. Chernyak, C. Huang, V. Gevorgyan, *Angew. Chem. Int. Ed.* **2010**, *49*, 8729; (d) C. Huang, N. Chernyak, A. S. Dudnik, V. Gevorgyan, *Adv. Synth. Catal.* **2011**, *353*, 1285; (e) S. Korwar, K. Brinkley, A. R. Siamaki, B. F. Gupton, K. C. Ellis, *Org. Lett.* **2015**, *17*, 1782; (f) P. Zhang, L. Hong, G. Li, R. Wang, *Adv. Synth. Catal.* **2015**, *357*, 345; (g) Y. Lu, R. Wang, X. Qiao, Z. Shen, *Synlett* **2011**, *2011*, 1038; (h) S. Mo, Y. Zhu, Z. Shen, *Org. Biomol. Chem.* **2013**, *11*, 2756; (i) X. Jia, D. Yang, W. Wang, F. Luo, J. Cheng, *J. Org. Chem.* **2009**, *74*, 9470; (j) X. Jia, D. Yang, S. Zhang, J. Cheng, *Org. Lett.* **2009**, *11*, 4716; (k) F. Jafarpour, H. Hazrati, S. Zarei, S. Izadidana, *Synthesis* **2014**, *46*, 1224; (l) X. Zhao, E. Dimitrijević, V. M. Dong, *J. Am. Chem. Soc.* **2009**, *131*, 3466; (m) W. Wang, C. Pan, F. Chen, J. Cheng, *Chem. Commun.* **2011**, *47*, 3978; (n) G. Zhang, S. Sun, F. Yang, Q. Zhang, J. Kang, Y. Wu, Y. Wu, *Adv. Synth. Catal.* **2015**, *357*, 443; (o) H. Aiso, T. Kochi, H. Mutsutani, T. Tanabe, S. Nishiyama, F. Kakiuchi, *J. Org. Chem.* **2012**, *77*, 7718; (p) F. Kakiuchi, T. Kochi, H. Mutsutani, N. Kobayashi, S. Urano, M. Sato, S. Nishiyama, T. Tanabe, *J. Am. Chem. Soc.* **2009**, *131*, 11310.

[103]   (a) B. Butschke, H. Schwarz, *Chem. Sci.* **2012**, *3*, 308; (b) M. Lersch, M. Tilset, *Chem. Rev.* **2005**, *105*, 2471.

[104]   (a) K. J. H. Young, O. A. Mironov, R. A. Periana, *Organometallics* **2007**, *26*, 2137; (b) K. J. H. Young, M. Yousufuddin, D. H. Ess, R. A. Periana, *Organometallics* **2009**, *28*, 3395; (c) F. O. Garces, R. J. Watts, *Inorg. Chem.* **1990**, *29*, 582; (d) P. Alam, G. Kaur, S. Chakraborty, A. Roy Choudhury, I. R. Laskar, *Dalton Trans.* **2015**, *44*, 6581.

[105]   M. Zuber, F. P. Pruchnik, *Polyhedron* **2006**, *25*, 2773.

[106]   (a) G. Minghetti, S. Stoccoro, M. A. Cinellu, B. Soro, A. Zucca, *Organometallics* **2003**, *22*, 4770; (b) B. Butschke, M. Schlangen, D. Schröder, H. Schwarz, *Chem. Eur. J.* **2008**, *14*, 11050; (c) S. H. Crosby, G. J. Clarkson, J. P. Rourke, *Organometallics* **2011**, *30*, 3603; (d) G.

J. P. Britovsek, R. A. Taylor, G. J. Sunley, D. J. Law, A. J. P. White, *Organometallics* **2006**, *25*, 2074; (e) A. Doppiu, G. Minghetti, M. A. Cinellu, S. Stoccoro, A. Zucca, M. Manassero, *Organometallics* **2001**, *20*, 1148; (f) L. Maidich, G. Zuri, S. Stoccoro, M. A. Cinellu, A. Zucca, *Dalton Trans*. **2014**, *43*, 14806; (g) A. C. Skapski, V. F. Sutcliffe, G. B. Young, *J. Chem. Soc., Chem. Commun*. **1985**, 609; (h) A. Zucca, D. Cordeschi, L. Maidich, M. I. Pilo, E. Masolo, S. Stoccoro, M. A. Cinellu, S. Galli, *Inorg. Chem*. **2013**, *52*, 7717.

[107]   F. Cocco, M. A. Cinellu, G. Minghetti, A. Zucca, S. Stoccoro, L. Maiore, M. Manassero, *Organometallics* **2010**, *29*, 1064.

[108]   (a) G. Minghetti, A. Doppiu, A. Zucca, S. Stoccoro, M. Cinellu, M. Manassero, M. Sansoni, *Chem. Heterocycl. Compd*. **1999**, *35*, 992; (b) G. L. Petretto, A. Zucca, S. Stoccoro, M. A. Cinellu, G. Minghetti, *J. Organomet. Chem*. **2010**, *695*, 256; (c) G. L. Petretto, J. P. Rourke, L. Maidich, S. Stoccoro, M. A. Cinellu, G. Minghetti, G. J. Clarkson, A. Zucca, *Organometallics* **2012**, *31*, 2971; (d) F. Cocco, A. Zucca, S. Stoccoro, M. Serratrice, A. Guerri, M. A. Cinellu, *Organometallics* **2014**, *33*, 3414.

[109]   J. Kwak, Y. Ohk, Y. Jung, S. Chang, *J. Am. Chem. Soc*. **2012**, *134*, 17778.

[110]   T. Katagiri, T. Mukai, T. Satoh, K. Hirano, M. Miura, *Chem. Lett*. **2009**, *38*, 118.

[111]   M. E. Moustafa, P. D. Boyle, R. J. Puddephatt, *Organometallics* **2014**, *33*, 5402.

[112]   (a) F. M. Romero, R. Ziessel, *Tetrahedron Lett*. **1995**, *36*, 6471; (b) D. M. DSouza, D. A. Leigh, M. Papmeyer, S. L. Woltering, *Nat. Protocols* **2012**, *7*, 2022.

[113]   F. Trécourt, B. Gervais, O. Mongin, C. Le Gal, F. Mongin, G. Quéguiner, *J. Org. Chem*. **1998**, *63*, 2892.

[114]   (a) M. Hapke, L. Brandt, A. Lutzen, *Chem. Soc. Rev*. **2008**, *37*, 2782; (b) L.-Y. Liao, X.-R. Kong, X.-F. Duan, *J. Org. Chem*. **2014**, *79*, 777.

[115]   (a) M. L. Hlavinka, J. R. Hagadorn, *Organometallics* **2007**, *26*, 4105; (b) S. E. Denmark, Y. Fan, *Tetrahedron: Asymmetr* **2006**, *17*, 687; (c) R. A. Abramovitch, E. M. Smith, E. E. Knaus, M. Saha, *J. Org. Chem*. **1972**, *37*, 1690.

[116]   X.-F. Duan, Z.-Q. Ma, F. Zhang, Z.-B. Zhang, *J. Org. Chem*. **2009**, *74*, 939.

[117]   S. Duric, C. C. Tzschucke, *Org. Lett*. **2011**, *13*, 2310.

[118]   S. Duric, F. D. Sypaseuth, S. Hoof, E. Svensson, C. C. Tzschucke, *Chem. Eur. J*. **2013**, *19*, 17456.

[119]   (a) A. Petit, J. Flygare, A. T. Miller, G. Winkel, D. H. Ess, *Org. Lett*. **2012**, *14*, 3680; (b) L. Ackermann, *Chem. Rev*. **2011**, *111*, 1315; (c) S. I. Gorelsky, *Organometallics* **2012**, *31*, 4631.

[120]   (a) L. V. Desai, K. J. Stowers, M. S. Sanford, *J. Am. Chem. Soc*. **2008**, *130*, 13285; (b) M. Zhang, Y. Zhang, X. Jie, H. Zhao, G. Li, W. Su, *Org. Chem. Front*. **2014**, *1*, 843.

[121]   (a) Q. Ding, X. Zhou, S. Pu, B. Cao, *Tetrahedron* **2015**, *71*, 2376; (b) N. Schröder, F. Lied, F. Glorius, *J. Am. Chem. Soc*. **2015**, *137*, 1448; (c) N. Schröder, J. Wencel-Delord, F. Glorius, *J.*

Am. Chem. Soc. **2012**, *134*, 8298; (d) G. Qian, X. Hong, B. Liu, H. Mao, B. Xu, *Org. Lett.* **2014**, *16*, 5294.

[122] D.-G. Yu, T. Gensch, F. de Azambuja, S. Vásquez-Céspedes, F. Glorius, *J. Am. Chem. Soc.* **2014**, *136*, 17722.

[123] (a) A. T. Higgs, P. J. Zinn, S. J. Simmons, M. S. Sanford, *Organometallics* **2009**, *28*, 6142; (b) A. T. Higgs, P. J. Zinn, M. S. Sanford, *Organometallics* **2010**, *29*, 5446.

[124] (a) B. Li, B. Liu, B.-F. Shi, *Chem. Commun.* **2015**, *51*, 5093; (b) B. Urones, A. M. Martinez, N. Rodriguez, R. G. Arrayas, J. C. Carretero, *Chem. Commun.* **2013**, *49*, 11044; (c) Z.-J. Du, L.-X. Gao, Y.-J. Lin, F.-S. Han, *ChemCatChem* **2014**, *6*, 123.

[125] A. Corma, A. Leyva-Pérez, M. J. Sabater, *Chem. Rev.* **2011**, *111*, 1657.

[126] D. Kalyani, A. R. Dick, W. Q. Anani, M. S. Sanford, *Tetrahedron* **2006**, *62*, 11483.

[127] (a) S. K. Santra, A. Banerjee, N. Khatun, A. Samanta, B. K. Patel, *RSC Adv.* **2015**, *5*, 11960; (b) A. Carrër, J.-D. Brion, S. Messaoudi, M. Alami, *Org. Lett.* **2013**, *15*, 5606.

[128] V. B. Purohit, S. C. Karad, K. H. Patel, D. K. Raval, *Catal. Sci. Tech.* **2015**, *5*, 3113.

[129] Q. Tian, X. Chen, W. Liu, Z. Wang, S. Shi, C. Kuang, *Org. Biomol. Chem.* **2013**, *11*, 7830.

[130] (a) B. T. Bhattarai, S. Adhikari, E. A. Kimball, J. N. Moore, K. H. Shaughnessy, T. S. Snowden, F. R. Fronczek, D. D. Dolliver, *Tetrahedron Lett.* **2014**, *55*, 4801; (b) E. Dubost, C. Fossey, T. Cailly, S. Rault, F. Fabis, *J. Org. Chem.* **2011**, *76*, 6414; (c) J. J. P. Kramer, C. Yildiz, M. Nieger, S. Bräse, *Eur. J. Org. Chem.* **2014**, *2014*, 1287.

[131] (a) X. Sun, Y. Sun, C. Zhang, Y. Rao, *Chem. Commun.* **2014**, *50*, 1262; (b) A. John, K. M. Nicholas, *J. Org. Chem.* **2012**, *77*, 5600.

[132] (a) R. B. Bedford, M. F. Haddow, C. J. Mitchell, R. L. Webster, *Angew. Chem. Int. Ed.* **2011**, *50*, 5524; (b) F. Péron, C. Fossey, J. Sopkova-de Oliveira Santos, T. Cailly, F. Fabis, *Chem. Eur. J.* **2014**, *20*, 7507.

[133] B. Du, X. Jiang, P. Sun, *J. Org. Chem.* **2013**, *78*, 2786.

[134] X.-T. Ma, S.-K. Tian, *Adv. Synth. Catal.* **2013**, *355*, 337.

[135] X. Sun, G. Shan, Y. Sun, Y. Rao, *Angew. Chem. Int. Ed.* **2013**, *52*, 4440.

[136] C. J. Teskey, A. Y. W. Lui, M. F. Greaney, *Angew. Chem. Int. Ed.* **2015**, *54*, 11677.

[137] Q. Yu, L. a. Hu, Y. Wang, S. Zheng, J. Huang, *Angew. Chem. Int. Ed.* **2015**, *54*, 15284.

[138] (a) X. Zheng, B. Song, G. Li, B. Liu, H. Deng, B. Xu, *Tetrahedron Lett.* **2010**, *51*, 6641; (b) B. Song, X. Zheng, J. Mo, B. Xu, *Adv. Synth. Catal.* **2010**, *352*, 329.

[139] (a) J. Dupont, C. S. Consorti, J. Spencer, *Chem. Rev.* **2005**, *105*, 2527; (b) D. L. Davies, S. M. A. Donald, S. A. Macgregor, *J. Am. Chem. Soc.* **2005**, *127*, 13754.

[140] (a) P. Sehnal, R. J. K. Taylor, I. J. S. Fairlamb, *Chem. Rev.* **2010**, *110*, 824; (b) L.-M. Xu, B.-J. Li, Z. Yang, Z.-J. Shi, *Chem. Soc. Rev.* **2010**, *39*, 712; (c) K. Muñiz, *Angew. Chem. Int. Ed.* **2009**, *48*, 9412.

[141]   (a) T. Yoneyama, R. H. Crabtree, *J. Mol. Catal. A: Chem.* **1996**, *108*, 35; (b) A. J. Canty, *Acc. Chem. Res.* **1992**, *25*, 83.

[142]   (a) A. R. Dick, J. W. Kampf, M. S. Sanford, *J. Am. Chem. Soc.* **2005**, *127*, 12790; (b) S. R. Whitfield, M. S. Sanford, *J. Am. Chem. Soc.* **2007**, *129*, 15142.

[143]   Y. Fu, Z. Li, S. Liang, Q.-X. Guo, L. Liu, *Organometallics* **2008**, *27*, 3736.

[144]   L. Guo, Y. Xu, X. Wang, W. Liu, D. Lu, *Organometallics* **2013**, *32*, 3780.

[145]   D. C. Powers, M. A. L. Geibel, J. E. M. N. Klein, T. Ritter, *J. Am. Chem. Soc.* **2009**, *131*, 17050.

[146]   (a) D. C. Powers, T. Ritter, *Nat Chem* **2009**, *1*, 302; (b) D. C. Powers, D. Y. Xiao, M. A. L. Geibel, T. Ritter, *J. Am. Chem. Soc.* **2010**, *132*, 14530; (c) D. Powers, T. Ritter, in *Higher Oxidation State Organopalladium and Platinum Chemistry, Vol. 35* (Ed.: A. J. Canty), Springer Berlin Heidelberg, **2011**, pp. 129.

[147]   (a) M. A. Gutierrez, G. R. Newkome, J. Selbin, *J. Organomet. Chem.* **1980**, *202*, 341; (b) A. D. Ryabov, *Synthesis* **1985**, *1985*, 233; (c) A. C. Cope, R. W. Siekman, *J. Am. Chem. Soc.* **1965**, *87*, 3272; (d) E. Laga, A. García-Montero, F. J. Sayago, T. Soler, S. Moncho, C. Cativiela, M. Martínez, E. P. Urriolabeitia, *Chem. Eur. J.* **2013**, *19*, 17398.

[148]   N. R. Deprez, M. S. Sanford, *J. Am. Chem. Soc.* **2009**, *131*, 11234.

[149]   (a) A. R. Dick, J. W. Kampf, M. S. Sanford, *Organometallics* **2005**, *24*, 482; (b) S. R. Whitfield, M. S. Sanford, *Organometallics* **2008**, *27*, 1683.

[150]   D. C. Powers, D. Benitez, E. Tkatchouk, W. A. Goddard, T. Ritter, *J. Am. Chem. Soc.* **2010**, *132*, 14092.

[151]   I. Fabre, N. von Wolff, G. Le Duc, E. Ferrer Flegeau, C. Bruneau, P. H. Dixneuf, A. Jutand, *Chem. Eur. J.* **2013**, *19*, 7595.

[152]   J. R. Bowers, G. W. Hopkins, G. P. A. Yap, K. A. Wheeler, *Cryst. Growth Des.* **2005**, *5*, 727.

[153]   M. G. Hutchinson, W. E. Lynch, C. W. Padgett, *Acta Crystallogr., Sect. E* **2015**, *71*, o869.

[154]   (a) J. Yin, B. Xiang, M. A. Huffman, C. E. Raab, I. W. Davies, *J. Org. Chem.* **2007**, *72*, 4554; (b) W. J. Lominac, M. L. D'Angelo, M. D. Smith, D. A. Ollison, J. M. Hanna Jr, *Tetrahedron Lett.* **2012**, *53*, 906; (c) R. P. Farrell, M. V. Silva Elipe, M. D. Bartberger, J. S. Tedrow, F. Vounatsos, *Org. Lett.* **2013**, *15*, 168.

[155]   S. Shimizu, Y. Imamura, T. Ueki, *Org. Proc. Res. Dev.* **2014**, *18*, 354.

[156]   P. B. Arockiam, C. Bruneau, P. H. Dixneuf, *Chem. Rev.* **2012**, *112*, 5879.

[157]   (a) L.-C. Campeau, S. Rousseaux, K. Fagnou, *J. Am. Chem. Soc.* **2005**, *127*, 18020; (b) H.-Y. Sun, S. I. Gorelsky, D. R. Stuart, L.-C. Campeau, K. Fagnou, *J. Org. Chem.* **2010**, *75*, 8180.

[158]   F. W. Joachim Demnitz, M. B. D'Heni, *Org. Prep. Proc. Int.* **1998**, *30*, 467.

[159]   M. Zalas, B. Gierczyk, M. Cegłowski, G. Schroeder, *Chem. Pap.* **2012**, *66*, 733.

[160]   D. P. White, J. C. Anthony, A. O. Oyefeso, *J. Org. Chem.* **1999**, *64*, 7707.

[161] R. Moreno-Fuquen, F. Cano, M. Martinez-Ripoll, A. Montano, J. Zukerman-Schpector, *Acta Crystallogr., Sect. E* **2001**, *57*, o712.

[162] R. Moreno-Fuquen, C. Arana, C. A. De Simone, *Acta Crystallogr., Sect. E* **2012**, *68*, o2805.

[163] (a) S. H. Cho, S. J. Hwang, S. Chang, *J. Am. Chem. Soc.* **2008**, *130*, 9254; (b) E. Kianmehr, N. Faghih, K. M. Khan, *Org. Lett.* **2015**, *17*, 414.

[164] D. Wenkert, R. B. Woodward, *J. Org. Chem.* **1983**, *48*, 283.

[165] (a) H. Yamanaka, T. Araki, T. Sakamoto, *Chem. Pharm. Bull.* **1988**, *36*, 2244; (b) S. Okuda, M. M. Robison, *J. Am. Chem. Soc.* **1959**, *81*, 740; (c) R. B. Clark, M. He, C. Fyfe, D. Lofland, W. J. O'Brien, L. Plamondon, J. A. Sutcliffe, X.-Y. Xiao, *J. Med. Chem.* **2011**, *54*, 1511; (d) W. Lumeras, F. Caturla, L. Vidal, C. Esteve, C. Balagué, A. Orellana, M. Domínguez, R. Roca, J. M. Huerta, N. Godessart, B. Vidal, *J. Med. Chem.* **2009**, *52*, 5531.

[166] S. V. Kravtsova, I. P. Romm, A. I. Stash, V. K. Belsky, *Acta Crystallogr., Sect. C* **1996**, *52*, 2201.

[167] J. F. Berry, F. A. Cotton, S. A. Ibragimov, C. A. Murillo, X. Wang, *Inorg. Chem.* **2005**, *44*, 6129.

[168] A. G. McInnes, D. G. Smith, J. L. C. Wright, L. C. Vining, *Can. J. Chem.* **1977**, *55*, 4159.

[169] (a) S. Ranganathan, B. B. Singh, P. V. Divekar, *Can. J. Chem.* **1969**, *47*, 165; (b) J. Dash, H.-U. Reissig, *Chem. Eur. J.* **2009**, *15*, 6811; (c) D. N. Bobrov, V. I. Tyvorskii, *Tetrahedron* **2010**, *66*, 5432; (d) F. Zhang, X.-F. Duan, *Org. Lett.* **2011**, *13*, 6102; (e) J. López-Ogalla, G. Saiz, F. E. Palomo, *Org. Proc. Res. Dev.* **2013**, *17*, 120.

[170] (a) J. Beerhues, Bachelor Thesis thesis, Freie Universität Berlin (Berlin), **2014**; (b) L. Tepper, Bachelor Thesis thesis, Freie Universität Berlin (Berlin), **2015**.

[171] B. V. Rokade, K. R. Prabhu, *J. Org. Chem.* **2012**, *77*, 5364.

[172] (a) F. Bellina, R. Rossi, *Tetrahedron* **2009**, *65*, 10269; (b) I. V. Seregin, V. Gevorgyan, *Chem. Soc. Rev.* **2007**, *36*, 1173; (c) R. Rossi, F. Bellina, M. Lessi, C. Manzini, L. A. Perego, *Synthesis* **2014**, *46*, 2833; (d) R. Rossi, F. Bellina, M. Lessi, C. Manzini, *Adv. Synth. Catal.* **2014**, *356*, 17; (e) Y.-X. Su, L.-P. Sun, *Mini Rev. Org. Chem.* **2012**, *9*, 87.

[173] D. E. Stephens, O. V. Larionov, *Tetrahedron* **2015**, *71*, 8683.

[174] G. Yan, A. J. Borah, M. Yang, *Adv. Synth. Catal.* **2014**, *356*, 2375.

[175] J.-P. Leclerc, K. Fagnou, *Angew. Chem.* **2006**, *118*, 7945.

[176] L.-C. Campeau, D. R. Stuart, J.-P. Leclerc, M. Bertrand-Laperle, E. Villemure, H.-Y. Sun, S. Lasserre, N. Guimond, M. Lecavallier, K. Fagnou, *J. Am. Chem. Soc.* **2009**, *131*, 3291.

[177] M. P. Huestis, K. Fagnou, *Org. Lett.* **2009**, *11*, 1357.

[178] (a) L.-C. Campeau, D. J. Schipper, K. Fagnou, *J. Am. Chem. Soc.* **2008**, *130*, 3266; (b) D. J. Schipper, L.-C. Campeau, K. Fagnou, *Tetrahedron* **2009**, *65*, 3155.

[179] D. J. Schipper, M. El-Salfiti, C. J. Whipp, K. Fagnou, *Tetrahedron* **2009**, *65*, 4977.

[180] L. Ackermann, S. Fenner, *Chem. Commun.* **2011**, *47*, 430.

[181] D. Lapointe, K. Fagnou, *Chem. Lett.* **2010**, *39*, 1119.

[182] S. I. Gorelsky, D. Lapointe, K. Fagnou, *J. Am. Chem. Soc.* **2008**, *130*, 10848.

[183] (a) H. Werner, H. J. Kraus, *J. Organomet. Chem.* **1981**, *204*, 415; (b) H. C. Clark, A. B. Goel, R. G. Goel, S. Goel, W. O. Ogini, *Inorg. Chim. Acta* **1978**, *31*, L441; (c) W. H. Henderson, J. M. Alvarez, C. C. Eichman, J. P. Stambuli, *Organometallics* **2011**, *30*, 5038.

[184] Y. Tan, J. F. Hartwig, *J. Am. Chem. Soc.* **2011**, *133*, 3308.

[185] E. Svensson, Freie Universität Berlin

[186] A. B. Goel, S. Goel, *Inorg. Chim. Acta* **1985**, *98*, 67.

[187] (a) D. F. Mullica, E. L. Sappenfield, *J. Appl. Crystallogr.* **1986**, *19*, 142; (b) D. F. Mullica, E. L. Sappenfield, D. H. Leschnitzer, *J. Crystallogr. Spectrosc. Res.*, *21*, 675; (c) V. Dura-Vila, D. M. P. Mingos, R. Vilar, A. J. P. White, D. J. Williams, *Chem. Commun.* **2000**, 1525.

[188] A. Bowden, S. J. Coles, M. B. Pitak, A. W. G. Platt, *Inorg. Chem.* **2012**, *51*, 4379.

[189] H. Schmidbaur, G. Blaschke, *Z. Naturforsch., B: Chem. Sci.* **1978**, *33*, 1556.

[190] E. Rémond, A. Tessier, F. R. Leroux, J. Bayardon, S. Jugé, *Org. Lett.* **2010**, *12*, 1568.

[191] C. Sicre, A. A. C. Braga, F. Maseras, M. M. Cid, *Tetrahedron* **2008**, *64*, 7437.

[192] N. C. Bruno, M. T. Tudge, S. L. Buchwald, *Chem. Sci.* **2013**, *4*, 916.

[193] C. D. Borgmann, A. P. D. Börner, D. D. Hess, R. D. Kadyrov, D. D. Röttger, D. D. Selent, K. D. D. Wiese, Google Patents, **2003**.

[194] C. R. Conrad, M. A. Dolliver, *Org. Synth.* **1932**, *12*, 22.

[195] C. B. Ziegler, R. F. Heck, *J. Org. Chem.* **1978**, *43*, 2941.

[196] R. A. Zelonka, M. C. Baird, *Can. J. Chem.* **1972**, *50*, 3063.

[197] W. De Graaf, J. Boersma, W. J. J. Smeets, A. L. Spek, G. Van Koten, *Organometallics* **1989**, *8*, 2907.

[198] (a) S. S. Zalesskiy, V. P. Ananikov, *Organometallics* **2012**, *31*, 2302; (b) Y. Ishii, *Ann. N. Y. Acad. Sci.* **1974**, *239*, 114.

[199] A. F. Littke, G. C. Fu, in *Org. Synth.*, John Wiley & Sons, Inc., **2003**.

[200] H. Geissler, P. Gross, B. Guckes, Google Patents, **2000**.

[201] W. A. Herrmann, C. Brossmer, C.-P. Reisinger, T. H. Riermeier, K. Öfele, M. Beller, *Chem. Eur. J.* **1997**, *3*, 1357.

[202] R. Shang, Y. Fu, J.-B. Li, S.-L. Zhang, Q.-X. Guo, L. Liu, *J. Am. Chem. Soc.* **2009**, *131*, 5738.

[203] M. D. Eastgate, F. G. Buono, *Angew. Chem. Int. Ed.* **2009**, *48*, 5958.

[204] F. Ragaini, M. Gasperini, S. Cenini, L. Arnera, A. Caselli, P. Macchi, N. Casati, *Chem. Eur. J.* **2009**, *15*, 8064.

[205] D. A. Tocher, R. O. Gould, T. A. Stephenson, M. A. Bennett, J. P. Ennett, T. W. Matheson, L. Sawyer, V. K. Shah, *J. Chem. Soc., Dalton Trans.* **1983**, 1571.

[206] B. E. Love, E. G. Jones, *J. Org. Chem.* **1999**, *64*, 3755.

[207] H. Gilman, F. Schulze, *J. Am. Chem. Soc.* **1925**, *47*, 2002.

[208] X.-F. Wu, C. Darcel, *Eur. J. Org. Chem.* **2009**, *2009*, 1144.

[209] S.-Y. Cheung, H.-F. Chow, T. Ngai, X. Wei, *Chem. Eur. J.* **2009**, *15*, 2278.

[210] Y. Zhu, Y. Wei, *Eur. J. Org. Chem.* **2013**, *2013*, 4503.

[211] K. Tahara, Y. Yamamoto, D. E. Gross, H. Kozuma, Y. Arikuma, K. Ohta, Y. Koizumi, Y. Gao, Y. Shimizu, S. Seki, K. Kamada, J. S. Moore, Y. Tobe, *Chem. Eur. J.* **2013**, *19*, 11251.

[212] A. Klapars, S. L. Buchwald, *J. Am. Chem. Soc.* **2002**, *124*, 14844.

[213] A. P. Sarkate, S. S. Bahekar, V. M. Wadhai, G. N. Ghandge, P. S. Wakte, D. B. Shinde, *Synlett* **2013**, *24*, 1513.

[214] E. Kolvari, A. Amoozadeh, N. Koukabi, S. Otokesh, M. Isari, *Tetrahedron Lett.* **2014**, *55*, 3648.

[215] J. R. White, G. J. Price, S. Schiffers, P. R. Raithby, P. K. Plucinski, C. G. Frost, *Tetrahedron Lett.* **2010**, *51*, 3913.

[216] T. Leermann, F. R. Leroux, F. Colobert, *Org. Lett.* **2011**, *13*, 4479.

[217] T. Ueda, H. Konishi, K. Manabe, *Org. Lett.* **2013**, *15*, 5370.

[218] M. Amatore, C. Gosmini, *Angew. Chem. Int. Ed.* **2008**, *47*, 2089.

[219] T. Noël, S. Kuhn, A. J. Musacchio, K. F. Jensen, S. L. Buchwald, *Angew. Chem. Int. Ed.* **2011**, *50*, 5943.

[220] R. Shintani, T. Hayashi, *Nat. Protocols* **2007**, *2*, 2903.

[221] Y. Yang, N. J. Oldenhuis, S. L. Buchwald, *Angew. Chem. Int. Ed.* **2013**, *52*, 615.

[222] Y. Cheng, X. Gu, P. Li, *Org. Lett.* **2013**, *15*, 2664.

[223] S. A. R. Mulla, S. M. Inamdar, M. Y. Pathan, S. S. Chavan, *RSC Adv.* **2012**, *2*, 12818.

[224] L. Bai, J.-X. Wang, *Adv. Synth. Catal.* **2008**, *350*, 315.

[225] C. M. So, H. W. Lee, C. P. Lau, F. Y. Kwong, *Org. Lett.* **2009**, *11*, 317.

[226] D. Toummini, F. Ouazzani, M. Taillefer, *Org. Lett.* **2013**, *15*, 4690.

[227] X.-J. Li, J.-L. Zhang, Y. Geng, Z. Jin, *J. Org. Chem.* **2013**, *78*, 5078.

[228] S. K. Gurung, S. Thapa, A. Kafle, D. A. Dickie, R. Giri, *Org. Lett.* **2014**, *16*, 1264.

[229] L. Liu, Y. Zhang, B. Xin, *J. Org. Chem.* **2006**, *71*, 3994.

[230] T. Iwai, R. Tanaka, T. Harada, M. Sawamura, *Chem. Eur. J.* **2014**, *20*, 1057.

[231] F. Zhu, Z.-X. Wang, *J. Org. Chem.* **2014**, *79*, 4285.

[232] Q. Liang, P. Xing, Z. Huang, J. Dong, K. B. Sharpless, X. Li, B. Jiang, *Org. Lett.* **2015**, *17*, 1942.

[233] P. E. Joos, E. L. Esmans, R. A. Dommisse, W. V. Dongen, J. A. Lepoivre, F. C. Alderweireldt, J. Balzarini, E. D. Clercq, *Nucleosides* **1991**, *10*, 883.

[234] Y. Oguro, N. Miyamoto, T. Takagi, K. Okada, Y. Awazu, H. Miki, A. Hori, K. Kamiyama, S. Imamura, *Bioorg. Med. Chem.* **2010**, *18*, 7150.

[235] M. Vamos, N. D. P. Cosford, *J. Org. Chem.* **2014**, *79*, 2274.

[236] J. M. Keith, *J. Org. Chem.* **2008**, *73*, 327.

[237]   J.-B. Rouchet, C. Schneider, C. Spitz, J. Lefèvre, G. Dupas, C. Fruit, C. Hoarau, *Chem. Eur. J.* **2014**, *20*, 3610.

[238]   T. D. Nelson, R. D. Crouch, in *Organic Reactions*, John Wiley & Sons, Inc., **2004**.

[239]   G.-J. ten Brink, I. W. C. E. Arends, M. Hoogenraad, G. Verspui, R. A. Sheldon, *Adv. Synth. Catal.* **2003**, *345*, 497.

[240]   A. Kopecky, G. Liu, A. Agushi, A. G. Agrios, E. Galoppini, *Tetrahedron* **2014**, *70*, 6271.

[241]   M. Mosrin, P. Knochel, *Org. Lett.* **2009**, *11*, 1837.

[242]   X. Chen, X.-S. Hao, C. E. Goodhue, J.-Q. Yu, *J. Am. Chem. Soc.* **2006**, *128*, 6790.

[243]   A. Joshi-Pangu, M. Ganesh, M. R. Biscoe, *Org. Lett.* **2011**, *13*, 1218.

[244]   G. M. Sheldrick, *Acta Crystallogr., Sect. A* **2008**, *64*, 112.

[245]   A. L. Spek, *Acta Crystallogr., Sect. D* **2009**, *65*, 148.

[246]   M. J. Frisch, G. W. Trucks, H. B. Schlegel, G. E. Scuseria, M. A. Robb, J. R. Cheeseman, G. Scalmani, V. Barone, B. Mennucci, G. A. Petersson, H. Nakatsuji, M. Caricato, X. Li, H. P. Hratchian, A. F. Izmaylov, J. Bloino, G. Zheng, J. L. Sonnenberg, M. Hada, M. Ehara, K. Toyota, R. Fukuda, J. Hasegawa, M. Ishida, T. Nakajima, Y. Honda, O. Kitao, H. Nakai, T. Vreven, J. A. Montgomery Jr., J. E. Peralta, F. Ogliaro, M. J. Bearpark, J. Heyd, E. N. Brothers, K. N. Kudin, V. N. Staroverov, R. Kobayashi, J. Normand, K. Raghavachari, A. P. Rendell, J. C. Burant, S. S. Iyengar, J. Tomasi, M. Cossi, N. Rega, N. J. Millam, M. Klene, J. E. Knox, J. B. Cross, V. Bakken, C. Adamo, J. Jaramillo, R. Gomperts, R. E. Stratmann, O. Yazyev, A. J. Austin, R. Cammi, C. Pomelli, J. W. Ochterski, R. L. Martin, K. Morokuma, V. G. Zakrzewski, G. A. Voth, P. Salvador, J. J. Dannenberg, S. Dapprich, A. D. Daniels, Ö. Farkas, J. B. Foresman, J. V. Ortiz, J. Cioslowski, D. J. Fox, Gaussian, Inc., Wallingford, CT, USA, **2009**.

9 Curriculum Vitae

The Curriculum Vitae is not included for reasons of data protection.